

Prakash Kumar Sarangi · Sonil Nanda
Pravakar Mohanty *Editors*

Recent Advancements in Biofuels and Bioenergy Utilization

 Springer

Recent Advancements in Biofuels and Bioenergy Utilization

Prakash Kumar Sarangi • Sonil Nanda
Pravakar Mohanty
Editors

Recent Advancements in Biofuels and Bioenergy Utilization

 Springer

Editors

Prakash Kumar Sarangi
Directorate of Research
Central Agricultural University
Imphal, Manipur, India

Sonil Nanda
Department of Chemical and Biochemical
Engineering
University of Western Ontario
London, Ontario, Canada

Pravakar Mohanty
Science and Engineering Research Board
Department of Science and Technology
Government of India
New Delhi, India

ISBN 978-981-13-1306-6 ISBN 978-981-13-1307-3 (eBook)
<https://doi.org/10.1007/978-981-13-1307-3>

Library of Congress Control Number: 2018953340

© Springer Nature Singapore Pte Ltd. 2018

This work is subject to copyright. All rights are reserved by the Publisher, whether the whole or part of the material is concerned, specifically the rights of translation, reprinting, reuse of illustrations, recitation, broadcasting, reproduction on microfilms or in any other physical way, and transmission or information storage and retrieval, electronic adaptation, computer software, or by similar or dissimilar methodology now known or hereafter developed.

The use of general descriptive names, registered names, trademarks, service marks, etc. in this publication does not imply, even in the absence of a specific statement, that such names are exempt from the relevant protective laws and regulations and therefore free for general use.

The publisher, the author, and the editors are safe to assume that the advice and information in this book are believed to be true and accurate at the date of publication. Neither the publisher nor the authors or the editors give a warranty, express or implied, with respect to the material contained herein or for any errors or omissions that may have been made. The publisher remains neutral with regard to jurisdictional claims in published maps and institutional affiliations.

This Springer imprint is published by the registered company Springer Nature Singapore Pte Ltd. The registered company address is: 152 Beach Road, #21-01/04 Gateway East, Singapore 189721, Singapore

Preface

According to the United States Census Bureau, the world population as of January 2018 is 7.4 billion with China, India, and the United States being the most populous countries. The world population is projected to amplify over 8 billion by 2030. In addition to food, water, and oxygen as the basic needs of survival, the human civilization also requires supplementary energy sources such as electricity and fuel for sustenance and livelihood. Fossil fuels have fast-tracked the global industrialization and are the preferred source of energy for transportation, household, and industrial sectors. Fossil fuels in the form of crude oil, petroleum, diesel, coal and natural gas have dominated the worldwide energy sector since the industrial revolution. However, the deleterious impacts of fossil fuels on the ecosystem and the environment cannot be repudiated. The direct effects of the exploiting use of fossil fuels can be evidenced by the increasing atmospheric concentration of greenhouse gases (especially CO₂), which cause air pollution and smog in urban areas. Conversely, the indirect effects of fossil fuels include, but are not restricted to, global warming, climate change, acid rain, ozone layer depletion, and other extreme weather conditions. There is a direct correlation between the emissions of greenhouse gases and the consumption of fossil fuels. Therefore, there is a global momentum in shifting the paradigm from fossil-based energy to alternative and more renewable forms of energy.

As an approach to mitigate the global warming and to realize an enduring economic sustainability in transportation and industrial sectors, the adoption of wide-ranging renewable fuels are indispensable. Nevertheless, the generation and utilization of such fuels should be socially acceptable, industrially profitable, environmentally friendly and engine-compatible and also have insignificant impact on the ecosystem, environment, food web, water resources, and land-use pattern. Most of the alternative energy resources such as solar, wind, tidal, geothermal and nuclear are capable of producing heat and power, whereas plant-based waste biomass can potentially generate usable forms of gaseous or liquid transportation fuels.

Biomass-based energy or biofuels are highly promising due to many perceptible environmental and socio-economic advantages. In a joint alliance through fundamental academic research and advanced industrial product development, biofuels have tremendous scope for implementation on a global scale and reduce the greenhouse gas emissions that are otherwise produced by fossil fuels. The prime focus of

this book is to throw light on the various technologies to recover the chemical energy from plant-based non-edible biomass and other organic wastes in the form of solid, liquid and gaseous biofuels. The opportunities and challenges of different biomass conversion technologies such as biomass-to-liquid, biomass-to-gas and gas-to-liquid, as well as biomass pretreatments, densification, anaerobic digestion, reforming, transesterification, supercritical fluid extraction, microalgal carbon sequestration, life-cycle assessment and techno-economic analysis have been discussed in this book.

This book is dedicated to advancing new developments and approaches in biomass processing and characterization, conversion technologies, fuel upgrading and utilization. This book consists of 15 chapters, as described below. Chapter 1 by Nanda et al. introduce biomass and its multifaceted significances for transformation to hydrocarbon fuels. This chapter systematically focuses on several first-, second- and third-generation biofuels with importance on the biomass resources, fuel properties and applications. This chapter comprehensively describes many biofuels such as bioethanol, biobutanol, bio-oil, biodiesel, algal oil, hydrogen, biomethane, and aviation fuel.

Chapter 2 by Azargohar et al. is focused on densification of lignocellulosic biomass as a technology to solid fuel pellets that could be used as an industrial commodity product in the fuel market. Biomass densification is described to overcome specific biomass handling limitations such as low density, non-uniformity of particle size and shape and the high cost of transportation. This chapter provides an extensive overview of the parameters affecting the quality of biomass fuel pellets, their pre-treatment and post-treatment as well as safety aspects related to their transportation and storage.

Chapter 3 by Zabed et al. throws light on lignocellulosic biomass pretreatment technologies. Pretreatment is a vital step in the upstream processing of biomass to degrade the intricate framework of cellulose, hemicellulose and lignin for producing alcohol-based biofuels through biochemical conversion. This chapter gives an overview of different ligninolytic microorganisms (e.g. fungi and bacteria) and their enzymes for biological pretreatment of biomass. The different factors affecting the biochemical pretreatment of biomass are described, which include biomass composition, type of microorganism, the concentration of enzymes and/or microbial inoculum, residence time, incubation temperature, pH, moisture content, aeration rate and other process conditions.

Chapter 4 by Sharma and Kumar presents Natural Deep Eutectic Solvents also referred to as NADES as advanced green solvents entirely made up of natural compounds to deconstruct the recalcitrance framework of lignocellulosic biomass into fuels and chemical products. The chapter comprehensively described the applicability of NADES as an effective biological agent of lignocellulosic biomass pretreatment and bioconversion.

Chapter 5 by Sarangi and Nanda accounts the recent advancements and technical challenges in acetone-butanol-ethanol fermentation. The chapter discusses the benefits of biobutanol as a superior biofuel over ethanol due to greater energy

density, better fuel properties, engine compatibility and less hygroscopic nature. Product inhibition, butanol toxicity, low butanol titer level and bacteriophage infections are a few process limitations that are explained in this chapter.

Chapter 6 by Nair et al. is focused on biomethanation as a bipartite process for producing biofuel and for bioremediation of organic wastes. The chapter is projected on bioremediation through methanotrophy by using methane-oxidizing bacteria during biomethanation. The factors affecting methanotrophy, different stages of biomethanation (pretreatment, digestion and gas purification), biogas composition as well as the advantages and disadvantages of anaerobic digestion have been systematically reviewed.

Chapter 7 by Thakkar et al. is an overview of gasification, which is a primary technology for biomass-to-gas conversion. The chapter is an assessment of different fundamental process parameters such as reactor temperature, equivalence ratio, biomass particle size, bed material as well as their individual and combined impacts on the gasification process and product distribution. The chapter also discussed on various producer gas cleaning technologies available to deliver a syngas that is suitable for power generation applications.

Chapter 8 by Fayaz et al. is a research-based synopsis of hydrogen-rich syngas generation using ethanol dry reforming approach over rare-earth metal-supported cobalt catalysts. The influence of operating conditions, especially different ratios of carbon dioxide-to-ethanol and temperature, is thoroughly investigated. Different physicochemical techniques for the preparation of cobalt-based catalysts for ethanol reforming are comprehensively demonstrated.

Chapter 9 by Galli et al. is a broad review article of several chemical and thermal processes applied for transformation of triglycerides into fuels. The high-temperature conversion of triglycerides to biofuels is illustrated through mature technologies such as cracking, gasification, esterification and transesterification.

Chapter 10 by Varma et al. reviews pyrolysis as a thermochemical technology used for the conversion of biomass-to-liquid fuels. This chapter summarizes the influence of different process parameters on pyrolysis products yield, quality and upgrading. The major operating conditions described in this chapter include temperature, heating rate, sweeping gas flow rate and biomass particle size.

Chapter 11 by Reddy et al. highlights supercritical fluids as an attractive green solvent for biodiesel production. This chapter presents some key background on the application of enzymatic transesterification, supercritical carbon dioxide and ionic liquids in biodiesel production. The prospects and challenges involved in enzymatic and noncatalytic supercritical processes both in terms of operation and economics are discussed in this chapter.

Chapter 12 by Pradhan and Das centres on the utilization of microalgae for carbon dioxide sequestration and wastewater treatment. The physicochemical functionalities of algae in the uptake of carbon dioxide from flue gas, as well as recovery of nitrogen and heavy metal from wastewater, are described. The chapter also elaborates a few biosystems and pilot-scale studies where different algal species are used in conjunction with bacterial species for increasing the efficiency of waste removal.

Chapter 13 by Saikia et al. is focused on the diverse application of fuel cells and some recent advancement in fuel cell technologies. Different types of fuel cells along with their electrolyte, operating conditions, efficiency and applications are expansively summarized. The applications of fuel cells in transportation, portable and stationary electronic devices, as well as space research, are discussed.

Chapter 14 by Patra and Sheth is a review of different thermochemical biomass conversion technologies and their techno-economic analysis. The thermochemical technologies discussed in this chapter include combustion, pyrolysis, gasification, liquefaction, carbonization and co-firing. Different process modelling tools and cost estimation methods are discussed in this chapter along with some case studies on fast pyrolysis and gasification of biomass.

Chapter 15 by Mishra and Mohanty is the final chapter of this book, which is a distinct review of the techno-economic and life-cycle assessment of thermochemical technologies for biomass conversion to fuels and chemicals. Different case studies for pyrolysis, gasification, liquefaction, combustion and cofiring have been illustrated for comparative techno-economic assessment. The life-cycle assessment along with environmental impact assessment is also explained in this chapter.

This book is an amalgamation of different chapters each with distinctive investigations but a common focus, which is related to the transition from fossil fuels towards alternative carbon-neutral renewable energy sources. To realize the real promises of biofuels and bioenergy, this book makes an attempt to assess their potentials, biorefining, applicability and sustainability.

We thank all the authors and scholars who contributed their chapters to this book. We are indebted to their efforts without which this book would not have been possible. Our sincere thanks go to Springer Nature for providing the opportunity for publication of this edited book. We appreciate the efforts by the Springer publishing team for the editorial assistance and assembling the scholarly materials in the most presentable format.

Imphal, Manipur, India
London, Ontario, Canada
New Delhi, India

Prakash Kumar Sarangi
Sonil Nanda
Pravakar Mohanty

Contents

1	A Broad Introduction to First-, Second-, and Third-Generation Biofuels	1
	Sonil Nanda, Rachita Rana, Prakash K. Sarangi, Ajay K. Dalai, and Janusz A. Kozinski	
2	Densification of Agricultural Wastes and Forest Residues: A Review on Influential Parameters and Treatments	27
	Ramin Azargohar, Sonil Nanda, and Ajay K. Dalai	
3	An Overview on the Application of Ligninolytic Microorganisms and Enzymes for Pretreatment of Lignocellulosic Biomass	53
	Hossain Zabed, Shakila Sultana, Jaya Narayan Sahu, and Xianghui Qi	
4	Role of Natural Deep Eutectic Solvents (NADES) in the Pretreatment of Lignocellulosic Biomass for an Integrated Biorefinery and Bioprocessing Concept	73
	Shaishav Sharma and Adepu Kiran Kumar	
5	Recent Developments and Challenges of Acetone-Butanol-Ethanol Fermentation	111
	Prakash K. Sarangi and Sonil Nanda	
6	Current Advancements, Prospects and Challenges in Biomethanation	125
	Soumya Nair, Anushree Suresh, and Jayanthi Abraham	
7	An Overview of Biomass Gasification	147
	Maharshi Thakkar, Pravakar Mohanty, Mitesh Shah, and Vishal Singh	
8	Hydrogen-Rich Syngas Production via Ethanol Dry Reforming over Rare-Earth Metal-Promoted Co-based Catalysts	177
	Fahim Fayaz, Mahadi B. Bahari, Thong L. M. Pham, Chinh Nguyen-Huy, Herma Dina Setiabudi, Bawadi Abdullah, and Dai-Viet N. Vo	

9	High-Temperature Conversion of Fats: Cracking, Gasification, Esterification, and Transesterification	205
	Federico Galli, Nicolas A. Patience, and Daria C. Boffito	
10	A Review on Pyrolysis of Biomass and the Impacts of Operating Conditions on Product Yield, Quality, and Upgradation	227
	Anil Kumar Varma, Ravi Shankar, and Prasenjit Mondal	
11	Applications of Supercritical Fluids for Biodiesel Production	261
	Sivamohan N. Reddy, Sonil Nanda, and Prakash K. Sarangi	
12	Application of Microalgae for CO₂ Sequestration and Wastewater Treatment	285
	Nilotpala Pradhan and Biswaranjan Das	
13	Current Advances and Applications of Fuel Cell Technologies	303
	Kaustav Saikia, Biraj Kumar Kakati, Bibha Boro, and Anil Verma	
14	Techno-economic Assessment of Thermochemical Biomass Conversion Technologies	339
	Tapas Kumar Patra and Pratik N. Sheth	
15	An Overview of Techno-economic Analysis and Life-Cycle Assessment of Thermochemical Conversion of Lignocellulosic Biomass	363
	Ranjeet Kumar Mishra and Kaustubha Mohanty	

Contributors

Bawadi Abdullah Chemical Engineering Department, Universiti Teknologi Petronas, Seri Iskandar, Perak, Malaysia

Jayanthi Abraham Microbial Biotechnology Laboratory, School of Biosciences and Technology, VIT University, Vellore, Tamil Nadu, India

Ramin Azargohar Department of Chemical and Biological Engineering, University of Saskatchewan, Saskatoon, Saskatchewan, Canada

Mahadi B. Bahari Faculty of Chemical & Natural Resources Engineering, Universiti Malaysia Pahang, Kuantan, Pahang, Malaysia

Daria C. Boffito Department of Chemical Engineering, Polytechnique Montréal, Montréal, Québec, Canada

Bibha Boro Department of Energy, Tezpur University, Tezpur, Assam, India

Ajay K. Dalai Department of Chemical and Biological Engineering, University of Saskatchewan, Saskatoon, Saskatchewan, Canada

Biswaranjan Das Environment & Sustainability Department, CSIR-Institute of Minerals and Materials Technology, Bhubaneswar, Odisha, India

Fahim Fayaz Faculty of Chemical & Natural Resources Engineering, Universiti Malaysia Pahang, Kuantan, Pahang, Malaysia

Federico Galli Department of Chemical Engineering, Polytechnique Montréal, Montréal, Québec, Canada

Biraj Kumar Kakati Department of Energy, Tezpur University, Tezpur, Assam, India

Janusz A. Kozinski New Model in Technology & Engineering, Hereford, Herefordshire, United Kingdom

Adepu Kiran Kumar Bioconversion Technology Division, Sardar Patel Renewable Energy Research Institute, Vallabh Vidyanagar, Gujarat, India

Ranjeet Kumar Mishra Department of Chemical Engineering, Indian Institute of Technology Guwahati, Guwahati, Assam, India

Kaustubha Mohanty Department of Chemical Engineering, Indian Institute of Technology Guwahati, Guwahati, Assam, India

Pravakar Mohanty Science and Engineering Research Board, Department of Science and Technology, Government of India, New Delhi, India

Prasenjit Mondal Department of Chemical Engineering, Indian Institute of Technology Roorkee, Roorkee, Uttarakhand, India

Soumya Nair Microbial Biotechnology Laboratory, School of Biosciences and Technology, VIT University, Vellore, Tamil Nadu, India

Sonil Nanda Department of Chemical and Biochemical Engineering, University of Western Ontario, London, Ontario, Canada

Chinh Nguyen-Huy School of Energy & Chemical Engineering, Ulsan National Institute of Science and Technology, Ulju-gun, Ulsan, South Korea

Nicolas A. Patience Department of Chemical Engineering, Polytechnique Montréal, Montréal, Québec, Canada

Tapas Kumar Patra Department of Chemical Engineering, Birla Institute of Technology and Science, Pilani, Rajasthan, India

Thong L. M. Pham Institute of Research and Development, Duy Tan University, Quang Trung, Danang, Vietnam

Nilotpala Pradhan Environment & Sustainability Department, CSIR-Institute of Minerals and Materials Technology, Bhubaneswar, Odisha, India

Xianghui Qi School of Food & Biological Engineering, Jiangsu University, Zhenjiang, Jiangsu, China

Rachita Rana Department of Chemical and Biological Engineering, University of Saskatchewan, Saskatoon, Saskatchewan, Canada

Sivamohan N. Reddy Department of Chemical Engineering, Indian Institute of Technology Roorkee, Roorkee, Uttarakhand, India

Jaya Narayan Sahu Institute of Chemical Technology, Faculty of Chemistry, University of Stuttgart, Stuttgart, Germany

Kaustav Saikia Department of Energy, Tezpur University, Tezpur, Assam, India

Prakash K. Sarangi Directorate of Research, Central Agricultural University, Imphal, Manipur, India

Herma Dina Setiabudi Faculty of Chemical & Natural Resources Engineering, Universiti Malaysia Pahang, Kuantan, Pahang, Malaysia

Mitesh Shah Department of Mechanical Engineering, A. D. Patel Institute of Technology, Anand, Gujarat, India

Ravi Shankar Department of Chemical Engineering, Madan Mohan Malaviya University of Technology, Gorakhpur, Uttar Pradesh, India

Shaishav Sharma Bioconversion Technology Division, Sardar Patel Renewable Energy Research Institute, Vallabh Vidyanagar, Gujarat, India

Pratik N. Sheth Department of Chemical Engineering, Birla Institute of Technology and Science, Pilani, Rajasthan, India

Vishal Singh Department of Mechanical Engineering, A. D. Patel Institute of Technology, Anand, Gujarat, India

Shakila Sultana Department of Microbiology, Primeasia University, Banani, Dhaka, Bangladesh

Anushree Suresh Microbial Biotechnology Laboratory, School of Biosciences and Technology, VIT University, Vellore, Tamil Nadu, India

Maharshi Thakkar Department of Mechanical Engineering, A. D. Patel Institute of Technology, Anand, Gujarat, India

Anil Kumar Varma Department of Chemical Engineering, Indian Institute of Technology Roorkee, Roorkee, Uttarakhand, India

Anil Verma Department of Chemical Engineering, Indian Institute of Technology Delhi, New Delhi, India

Dai-Viet N. Vo Faculty of Chemical & Natural Resources Engineering, Universiti Malaysia Pahang, Kuantan, Pahang, Malaysia

Hossain Zabed School of Food & Biological Engineering, Jiangsu University, Zhenjiang, Jiangsu, China

About the Editors



Dr. Prakash Kumar Sarangi is a scientist with a specialization in food microbiology at Central Agricultural University in Imphal, India. He received his Ph.D. degree in microbial biotechnology from the Department of Botany, Ravenshaw University, Cuttack, India; M.Tech. degree in applied botany from Indian Institute of Technology Kharagpur, India; and M.Sc. degree in botany from Ravenshaw University, Cuttack, India. Dr. Sarangi's current research is focused on bioprocess engineering, renewable energy, second-generation biofuels, biochemicals, biomaterials, fermentation technology and postharvest engineering and technology. He has a profound research experience in bioconversion of crop residues and agro wastes into value-added phenolic compounds. He has more than 10 years of teaching and research experience in biochemical engineering, microbial biotechnology, downstream processing, food microbiology and molecular biology. He has served as a reviewer for many international journals and has published more than 40 research articles in peer-reviewed international and national journal and authored more than 15 book chapters. He has presented his research work in number of national and international conferences. He is associated with many scientific societies as a fellow member (Society for Applied Biotechnology) and life member (Biotech Research Society of India; Society for Biotechnologists of India; Association of Microbiologists of India; Orissa Botanical Society; Medicinal and Aromatic Plants Association of India; Indian Science Congress Association; Forum of Scientists, Engineers & Technologists; and International Association of Academicians and Researchers.



Dr. Sonil Nanda is a research fellow at the University of Western Ontario in London, Ontario, Canada. He received his Ph.D. degree in biology from York University, Canada; M.Sc. degree in applied microbiology from Vellore Institute of Technology (VIT) University, India; and B.Sc. degree in microbiology from Orissa University of Agriculture and Technology, India. Dr. Nanda's research interests are focused on the production of advanced biofuels and biochemicals through thermochemical and biochemical conversion technologies such as gasification, pyrolysis and fermentation. He is an expert researcher in hydrothermal gasification of a wide variety of organic wastes and biomass including agricultural and forestry residues, industrial effluents, municipal solid wastes, cattle manure, sewage sludge and food wastes to produce hydrogen fuel. His parallel interests are also in the generation of hydrothermal flames for treatment of hazardous wastes, agronomic applications of biochar, phytoremediation of heavy metal-contaminated soils as well as carbon capture and sequestration. Dr. Nanda has published over 60 peer-reviewed journal articles, 12 book chapters, and has presented his work at many international conferences. His research works have gained wide interest through his highly cited research publications, book chapters, conference presentations and workshop lectures. Dr. Nanda serves as a fellow member of the Society for Applied Biotechnology in India as well as a life member of the Indian Institute of Chemical Engineers, Association of Microbiologists of India, Indian Science Congress Association and Biotech Research Society of India. He is also a member of several chemical engineering societies across North America such as the American Institute of Chemical Engineers, the Chemical Institute of Canada and the Combustion Institute-Canadian Section.



Dr. Pravakar Mohanty is a scientist at the Science and Engineering Research Board established through an Act of Parliament (SERB Act 2008), in the Department of Science and Technology (DST), Government of India, New Delhi, India. Dr. Mohanty has a Ph.D. degree in chemical engineering from the Indian Institute of Technology Delhi, India. He was the recipient of Commonwealth Scholarship by the Commonwealth Scholarship Commission of Canada to conduct research at the University of Saskatchewan, Canada. Dr. Mohanty has also worked at the European Bioenergy Research Institute (EBRI) at Aston University, Birmingham, United Kingdom. He has received the prestigious HOAP Research Award on Renewable Energy (Young Scientist Award 2014) and Dr. A.V. Rama Rao Foundation's Best Ph.D. Thesis and Research Award in Chemical Engineering and Technology (2015) from the Indian Institute of Chemical Engineers (IChE). He has more than 35 peer-reviewed international journal articles and 5 book chapters to his credit. He has more than 15 years of research experience in research and development, technology transfer, knowledge translation, implementation and management of different projects related to the development of fuel products, bulk and fine chemicals, active pharmaceutical ingredients, food processing agents and materials. Dr. Mohanty is an expert researcher in different biomass-to-liquid, biomass-to-gas and gas-to-liquid conversion technologies including pyrolysis, gasification, Fischer-Tropsch synthesis, syngas production, natural gas processing and other processes relating to clean energy concept.



A Broad Introduction to First-, Second-, and Third-Generation Biofuels

1

Sonil Nanda, Rachita Rana, Prakash K. Sarangi, Ajay K. Dalai, and Janusz A. Kozinski

Abstract

The aggregating usage of fossil fuels, rising demand for energy, fluctuating fuel prices, and increasing emissions of greenhouse gases are some of the concerning factors contributing to a shift in the interest from fossil fuels to biofuels. Biofuels are carbon-neutral sources of energy as the CO₂ emissions resulting from their combustion is utilized by the plants during photosynthesis leading to no net increase in atmospheric CO₂ levels. It is indispensable to focus on the new approaches to the research, development, and production of biofuels and their processing technologies to reshape a sustainable bioeconomy. Biofuels can be categorized into first, second, and third generation depending on the feedstock used for their production. The product range for first-generation biofuels is largely limited to ethanol produced from corn and distillers grains. In contrast, the second-generation biofuels are produced from non-food residues or lignocellulosic biomass such as agricultural biomass and forestry refuse, as well as energy crops. The third-generation biofuels are produced from algae, sewage sludge, and municipal solid wastes. This chapter comprehensively focuses on various first-, second-, and third-generation biofuels with emphasis on their biomass sources,

S. Nanda (✉)

Department of Chemical and Biochemical Engineering, University of Western Ontario, London, Ontario, Canada

e-mail: sonil.nanda@uwo.ca

R. Rana · A. K. Dalai

Department of Chemical and Biological Engineering, University of Saskatchewan, Saskatoon, Saskatchewan, Canada

P. K. Sarangi

Directorate of Research, Central Agricultural University, Imphal, Manipur, India

J. A. Kozinski

New Model in Technology & Engineering, Hereford, Herefordshire, United Kingdom

© Springer Nature Singapore Pte Ltd. 2018

P. K. Sarangi et al. (eds.), *Recent Advancements in Biofuels and Bioenergy Utilization*, https://doi.org/10.1007/978-981-13-1307-3_1

1

fuel properties, and applications. The fuel products broadly discussed in this chapter are ethanol, butanol, bio-oil, biodiesel, algal oil, hydrogen, biomethane, and aviation fuel.

Keywords

Biofuel · Biomass · Bioethanol · Biobutanol · Bio-oil · Biodiesel · Algal oil · Hydrogen · Biomethane · Aviation fuel

1.1 Introduction

Today, almost every field is being explored for a better energy usability and productivity. The worldwide economy is drastically driven by fossil fuels, especially gasoline, natural gas, and coal. These fossil energy sources are the primary fuels to generate electricity and power for domestic and industrial purposes. Rapid industrialization at a global scale is the leading cause of the momentous consumption of fossil fuels. However, a sustainable economic and industrial development necessitates the utilization of a safer form of energy that would not generate any environmental pollutants or emissions.

The global energy consumption in 2008 was 533 EJ. However, with the increasing demand, the projection likely to increase to 653 EJ in 2020 and 812 EJ in 2030 (USEIA 2011). Figure 1.1 illustrates the worldwide production of petroleum and other liquid fuels. The top ten countries with the highest production of petroleum and other liquid fuels include the United States, Saudi Arabia, Russia, China, Canada, Iraq, the United Arab Emirates, and Brazil (USEIA 2017). The exploiting

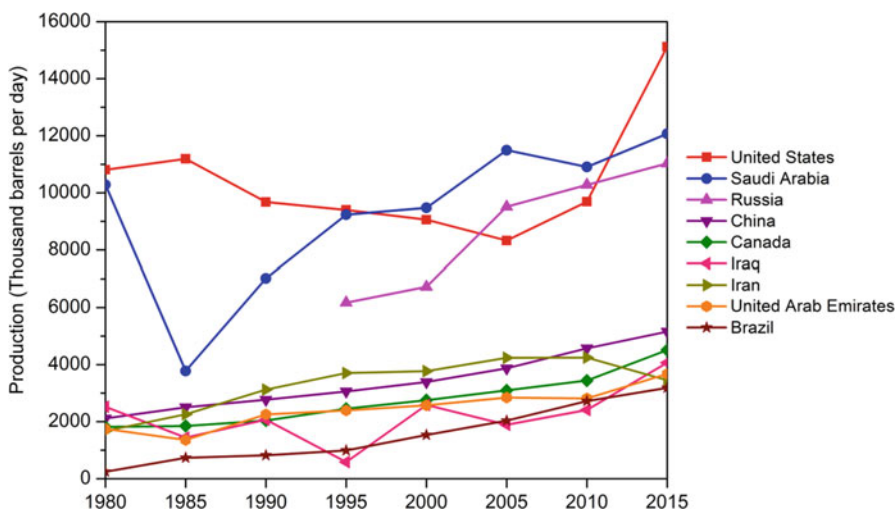


Fig. 1.1 Worldwide production of petroleum and other liquid fuels. (Data source: USEIA 2017)

consumption of fossil fuels is leading to an unparalleled increase in the greenhouse gas emissions and consequently global warming. The total CO₂ emission by the burning of fossil fuels in 2008 was 32,083 million metric tons (MMT) which increased from 5977 MMT in 1950 and 1958 MMT in 1990 (Boden et al. 2009). The worldwide energy-related CO₂ emissions are illustrated in Fig. 1.2. The non-OECD countries demonstrated a relatively higher CO₂ emissions compared to that of OECD countries. Particularly in 2015, the energy-related CO₂ emissions by the non-OECD and OECD countries were 18,517 MMT and 12,942 MMT, respectively. At a global scale, the CO₂ emissions rose from 21,536 MMT in 1990 to 31,459 MMT in 2015. However, the CO₂ emission is projected for increasing to 36,376 MMT in 2025 and 42,386 MMT in 2035.

The use of biofuels produced from renewable and biogenic materials has the tendency to mitigate greenhouse gas emissions, supplement the growing energy needs, improve the overall energy efficiency of existing fuel systems, and invigorate employment in bio-based sectors (Nanda et al. 2015). The large focus on biofuel production could replace the use of gasoline and other fossil fuels in the near future. Several developed and developing nations are emphasizing on developing their bioenergy market and established intergovernmental strategies for the use of biofuels.

Biofuels can be produced from a variety of feedstocks including agricultural crop residues, forestry biomass, energy crops, livestock manure, municipal solid waste, sewage sludge, industrial effluents, and other organic waste streams. These waste materials are rich in organic matter that could be recovered for conversion to biofuels through a variety of thermochemical and biochemical technologies. The purpose of

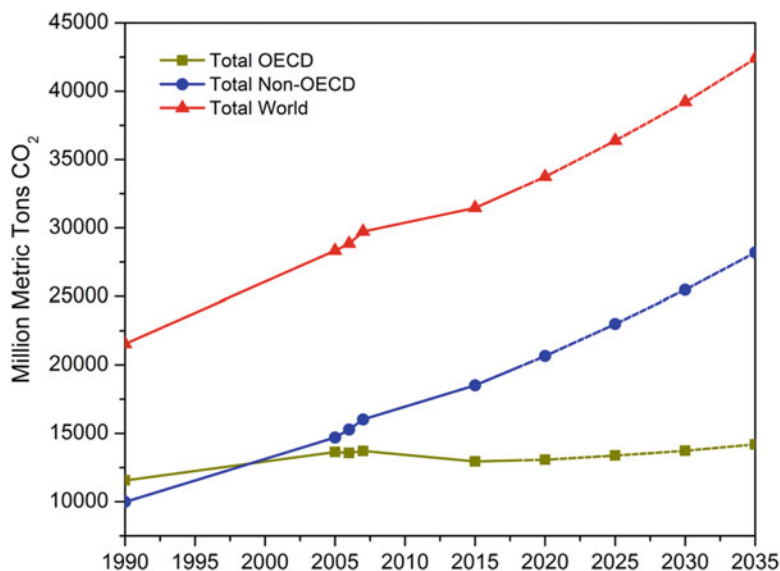


Fig. 1.2 Worldwide energy-related emission of CO₂. (Data source: IEO 2010)

this chapter is to give an introductory overview of different biomass sources and the classification of biofuels produced from them. This chapter aims to discuss different first-, second-, and third-generation biofuels along with their composition and properties. With this knowledge on the perspective of different classes of biofuels, the discussion is made on production and environmentally benign application of each of the fuels such as ethanol, butanol, bio-oil, biodiesel, algal oil, hydrogen, biomethane, and aviation fuel.

1.2 First-, Second-, and Third-Generation Biomass Sources

In a biorefinery perspective, biomass refers to a generic term for all organic material that could be potentially converted to fuels and chemicals. Biomass is a renewable and non-fossil composite biogenic organic material formed by natural or anthropogenic processes. It is obtained as a result of photosynthesis in plants, algae, and some bacteria via the conversion of solar energy to carbohydrates and lipids. In chlorophyll-containing living organisms, CO₂ reacts with water in the presence of sunlight to produce carbohydrates as the building blocks of biomass. Biomass broadly includes agricultural residues, forest residues, wood processing wastes, dedicated energy crops, animal manure, poultry litter, municipal solid wastes, industrial effluents, sewage sludge, and any other biogenic waste. It is indispensable to categorize the diversity of biomass sources to better understand the type of biofuels they produce. Figure 1.3 shows a schematic of different feedstocks and the resultant biofuels.

The first-generation biomass mostly includes food crops; hence, they appear unjustifiable for commercial use because of the food-versus-fuel controversies. The first-generation biomass includes edible plant materials and crops such as corn, wheat, sugarcane, and food grains (distillers grains). The second-generation biomass includes nonedible plant residues such as straw, wood, grasses, etc. Unlike first-generation biomass (starch-based feedstocks) that can be directly used in biorefineries for fuel production, the second-generation biomass requires a series of pretreatment to recover the fermentable sugars. Therefore, the utilization of second-generation biomass requires additional processing steps and operational cost for biofuel production.

Tremendous amounts of agricultural crop residues are obtained throughout the world as a result of agricultural and farming practices. Some commonly available agricultural biomasses include wheat straw, barley straw, flax straw, paddy straw, corncob, corn stover, cotton stalk, mustard stalk, canola meal, canola hull, flax fiber, jute bast, coconut coir, coconut shell, palm seeds, rice husk, walnut shell, almond shell, cashew nut shell, hazelnut shell, peanut shell, peach pits, plum pits, olive pits, apricot pits, sugarcane bagasse, etc.

The forest residues from softwood and hardwood species include stems, barks, twigs, cones, and needles. On the other hand, wood processing facilities generate biomass in the form of sawdust, wood chips, lumps, bales, pellets, and briquettes.

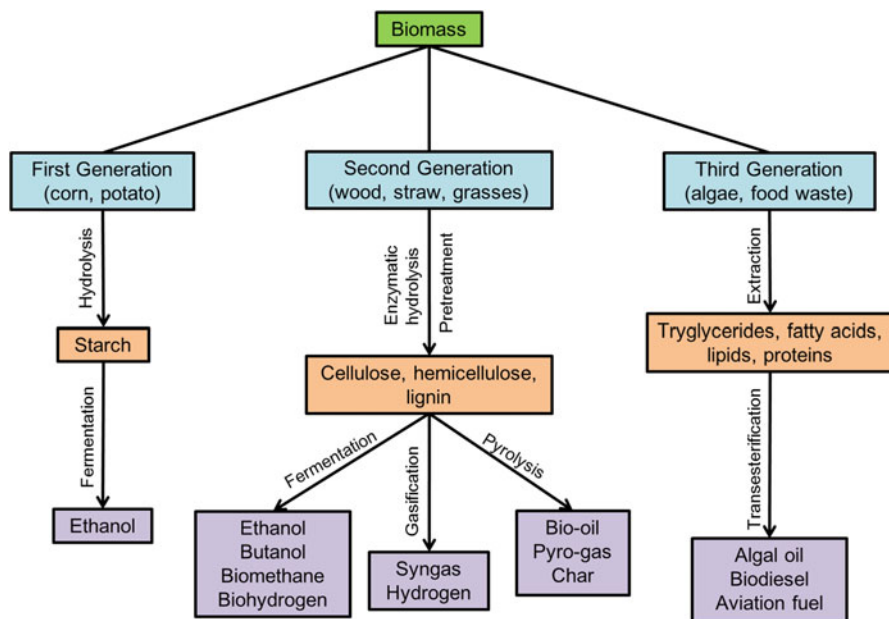


Fig. 1.3 A schematic overview of the basic steps in the production of first-, second-, and third-generation biofuels

Wood processing facilities generate fuel wood, char, and black liquor, which are chief sources of electricity in the United States, Brazil, Canada, Finland, and Sweden (FAO 2008).

Energy crops are considered as a second-generation feedstock due to their lignocellulosic composition and as third-generation feedstock owing to their fast-growing properties and less maintenance/nutrient requirement. Energy crops or dedicated energy crops are specifically cultivated for the purpose of converting them into fuel and energy. The energy crops can be both herbaceous (temperate grasses) and woody in nature. A few examples of energy crops are switchgrass, timothy grass, elephant grass, reed canary grass, ryegrass, *Miscanthus*, alfalfa, bamboo, hybrid poplar, and short rotation coppice. Perennial grasses are ideal energy crops because of high yield of biomass, round-the-year availability, fast growth, less farming needs, low nutrient requirements, low cost of production, tendency to regenerate in less fertile soil, and resistance to extreme weather conditions.

The third-generation biomass includes microalgae and macroalgae. Marine biomasses such as seaweed, hyacinth, caltrop diatoms, duckweed, kelp, and salvinia have candidacy for the production of biofuels, especially biodiesel (Vassilev et al. 2012). Aquatic biomass is considered third-generation biomass and advanced biofuel feedstock due to their perennial and inherent growth, high growth rate, as

well as no competency with arable land and crops for space, sunlight, and nutrients. While soybean and canola produce 200–450 l of biodiesel, algae are capable of producing 61,000 l/ha of biodiesel (Savage 2011). Algae can produce different types of biofuels including bioethanol, biodiesel, syngas, and biohydrogen (Demirbas 2010). Another category of biomass includes animal manure (e.g., poultry litter, dairy manure, and swine manure), municipal solid waste, industrial effluent (textile effluents, paper and pulp industry wastes, tannery effluents, pharmaceutical wastes, etc.), and sewage sludge.

Among all the categories of biomass, the major interest of biorefineries is on second-generation and third-generation biomass. The second-generation biomasses are mostly lignocellulosic materials comprised of cellulose, hemicellulose, and lignin. These components have the candidacy for being transformed into energy-dense hydrocarbons and fine chemicals. The conversion routes involve thermochemical and biochemical pathways and technologies such as biomass-to-liquid (e.g., pyrolysis, liquefaction, and fermentation), biomass-to-gas (gasification and methanation), and gas-to-liquid (Fischer-Tropsch synthesis and syngas fermentation) (Nanda et al. 2014b).

Lignocellulosic biomass typically consists of 30–60% cellulose, 20–40% hemicellulose, and 15–25% lignin (Nanda et al. 2013). Cellulose is a linear and crystalline homopolymer of repeating D-glucose subunits linked by β -1,4 glycosidic bonds. Hemicellulose is an amorphous short-chain heteropolymer containing pentose sugar (β -D-xylose, α -L-arabinose), hexose sugar (β -D-mannose, β -D-glucose, α -D-galactose), and sugar acids (α -D-glucuronic, α -D-4-O-methylgalacturonic, and α -D-galacturonic acids). Lignin is an amorphous, hydrophobic, and aromatic polymer of *p*-hydroxyphenylpropanoid units linked via C–C and C–O–C bonds. It is a result of oxidative polymerization of three monolignols, namely, *p*-coumaryl, coniferyl, and sinapyl alcohols. Lignin, present in plant cell wall, covalently binds with cellulose and hemicellulose, thus giving mechanical strength to the plant and recalcitrance to microbial and insect attack.

Corn ethanol, one of the first-generation biofuels, is profitably and commercially produced from food crops such as corn, wheat, and sugarcane. However, first-generation biofuels have many drawbacks such as: (1) social unacceptance and ethical concerns due to diversion of food crops as feedstocks, (2) lack of diversity in feedstock selection, and (3) competition for arable lands for cultivation of biofuel crops rather than harvesting food crops (Nanda et al. 2015). In contrast, second-generation biofuels such as bioethanol (cellulosic ethanol) and biobutanol do not pose any threat to the food supply or competition to arable lands. This is because second-generation biofuels are derived from nonedible plant biomass, especially lignocellulosic feedstocks. The use of second-generation biofuels can reduce the demand for first-generation biofuels and avoid the direct competition with agricultural crop harvests. Additionally, second-generation biofuels have considerably lower greenhouse gas emissions during their life cycle (Wang et al. 2007). Table 1.1 summarizes the properties and benefits of some first-, second-, and third-generation biofuels, namely, bioethanol, biobutanol, bio-oil, algal oil, biodiesel, biohydrogen, biomethane, and aviation fuel.

Table 1.1 Typical properties of some first-, second-, and third-generation biofuels

Biofuel	Feedstock	Fuel properties and advantages
Ethanol	Corn, distillers grains, molasses, straw, bagasse, woody biomass, and other lignocellulosic biomasses	Oxygenated fuel
		Blended with gasoline at flexible ratios
		High fuel concentrations require vehicle engine modification
Butanol	Corn cobs, straw, woody biomass, grasses, and other lignocellulosic biomass	Superior fuel properties than ethanol and comparable with gasoline
		No blends with gasoline required
		Compatible with the current vehicle engines at high concentrations
Bio-oil	Lignocellulosic biomass, waste organic materials, and waste rubber	Energy-dense fuel source
		Can be used directly to generate power in-house refinery
		Precursor of fine chemicals and industrially relevant bio-products
Algal oil	Microalgae and macroalgae	Cultivation of algae can lead to CO ₂ capture in parallel with oil production
		Algal oil is rich with triglycerides and fatty acids
		De-oiled algae can be used a nutrient-rich diet for livestock
Biodiesel	Vegetable oil, algal oil, and animal fats	Improves lubricity compared to that of conventional diesel
		Produced through transesterification of nonedible oil and waste edible oil
		High energy density compared to alcohol-based fuels
Hydrogen	Lignocellulose biomass, algae, water, sewage sludge, and industrial effluents	Superior heating value of 140 MJ/kg
		Energy carrier and vector
		Feedstock for fuel cells
		It's a clean fuel as its burning produces only water and no emission of pollutant and particulates
Biomethane	Waste organic materials and lignocellulosic materials	Production of biomethane requires less maintenance and capital investment
		Invigorates rural livelihood and employment
		Independent on seasonal and geographical variations
		Biomethane can be used as a domestic cooking fuel and in household heating and electricity generation
Aviation fuel	Halophytes, lignocellulosic biomass, sewage sludge, algae, <i>Camelina</i> , <i>Jatropha</i> , and oilseed crops	Its utilization decreases the dependence on fossil resources
		Reduces environmental impacts from aviation-related emissions
		Uses cheaply available feedstocks
		Blends of biokerosene and conventional aviation fuels can reduce the fuel cost

1.3 Bioethanol

Some low molecular weight alcohols that have pronounced potential to replace fossil fuels include methanol (CH_3OH), ethanol ($\text{C}_2\text{H}_5\text{OH}$), propanol ($\text{C}_3\text{H}_7\text{OH}$), and butanol ($\text{C}_4\text{H}_9\text{OH}$). Recently, ethanol has emerged as a biofuel with a great deal of interest in its production and utilization. Among the several alternative renewable fuel sources, bioethanol has proven efficient by a mass-scale production and usage. Bioethanol is produced through fermentation of starchy materials (first-generation biomass) and lignocellulosic substrates (second-generation biomass) using the widely known *Saccharomyces cerevisiae*. Bioethanol barely covers the fuel industry as it is majorly dedicated toward the alcohol and beverage industry. Ethanol that is produced for nonconsumable applications is made unfit for human intake by adding small amounts of toxic and unpleasant substances such as traces of methanol or gasoline (Gnansounou and Dauriat 2005; Balat and Balat 2009a, b). Ethanol is an oxygenated fuel containing 35% oxygen, which exhibits clean burning characteristics such as reduction in greenhouse gas emissions and particulate matters along with the benefits of low vapor pressure (Nanda et al. 2014b).

The application of ethanol as an alternative fuel source has a significant historical background. The first internal combustion engines capable of using ethanol as the fuel were designed by Samuel Morey in 1826, and the following notable ones were designed in 1876 by Nicholas Otto (Demirbas and Balat 2006). The first successful car that could run on pure ethanol was produced by Henry Ford in 1896. This led to the manufacturing of the Ford Model T car series in 1908 that were flexible in using ethanol or a gasoline-ethanol blend as the fuel (Solomon et al. 2007). Europe and the United States had a widespread use of ethanol as fuel until the 1900s. However, after the First World War, the demand for ethanol diminished as its production became more expensive than the processing of petroleum-based fuels. Nonetheless, there was still an interest subsisting in industries like General Motors and DuPont to use ethanol as an anti-knock agent and as a possible replacement of the conventional fossil fuels (Mussatto et al. 2010).

Ethanol has already captured a large-scale production market in the countries like Brazil and the United States and some European nation. It is expected to become a dominating biofuel for the transport industry within the next 20 years. Ethanol can either be blended with gasoline or used in its pure form for some newly developed advanced flex-fuel hybrid vehicles (Gnansounou and Dauriat 2005; von Blottnitz and Ann 2007). Ethanol has several advantages over the conventional fuels owing to its higher octane number, high heat of vaporization, and sustainability. The use of bioethanol as an octane enhancer in unleaded gasoline could replace methyl tert-butyl ether (MTBE). Ethanol could also be used as an oxygenated compound for the clean combustion of gasoline for an improved air quality (Gnansounou and Dauriat 2005). The other benefits of bioethanol are its lower emissions of greenhouse gases. Ethanol has an ability to replace 32% of gasoline usage when used as an E85 blend (i.e., 85% ethanol and 15% gasoline).

Brazil and the United States supply 90% of the world's total ethanol production (Nanda et al. 2014b). Currently, sugarcane (in Brazil) and corn (in the United States)

are widely being used for ethanol production with major application in the fuel industry at competitive prices. It is necessary to understand here that these raw materials for ethanol production cannot be sustained in the long term as they are first-generation biomass (food materials). Furthermore, another challenge is that the emission of greenhouse gases resulting from the consumption of ethanol obtained from sugar or starch as fuel is not as low as desired. Thus, there is an immediate need for exploring lignocellulosic feedstocks in the form of agricultural residues and forest residues for the production of ethanol.

The substrates for bioethanol production include directly fermentable sugars (pentose and hexose), starch-based materials, and lignocellulosic feedstocks. The established process for ethanol production from sugarcane and starch-based feedstocks involves the conversion of starch to ethanol through liquefaction step (to enhance the solubility of starch), followed by the hydrolysis step that results in the production of glucose. The next step involves the fermentation of glucose to ethanol using solventogenic fungi and bacteria. The bioconversion of lignocellulosic biomass involves biomass pretreatment (acid, alkali, ionic, or mechanical), delignification, enzymatic hydrolysis, and fermentation (Nanda et al. 2014a). The pathway for ethanol production from lignocellulosic biomass is not entirely similar to starch-based process because of the requirement of biomass pretreatment. Additionally, the technical and economic challenges in producing ethanol from lignocelluloses are yet to be addressed (Gnansounou and Dauriat 2005; Demirbas and Balat 2006; Mussatto et al. 2010).

Hahn-Hägerdal et al. (2006) have reviewed the current developments in the bioconversion processes that targeted ethanol production as a fuel with emphasis on the improvement and development of process integration. The cost of feedstock for ethanol production varies considerably from US \$22 to 61 per metric ton of dry matter. This makes the total cost rely on the plant capacity, making it a major contributor to the total production cost. The cost of hydrolysis specifically for the enzymatic process contributes majorly to the production cost (Hahn-Hägerdal et al. 2006).

Certain drawbacks of ethanol prevent its widespread use at the commercial level. Firstly, it takes more volume (1.5 times) of ethanol to produce the same energy as gasoline. Secondly, ethanol is corrosive to the rubbers used in the gaskets and fuel lines of older vehicles. However, this problem has been addressed in the newer vehicles that run entirely on ethanol. Lastly, ethanol tends to absorb water from the atmosphere, which dilutes it and makes its transportation through pipelines a challenging task. Biobutanol emerges as a suitable alternative to ethanol in addressing these challenges.

1.4 Biobutanol

Biobutanol is another alcohol fuel that enlists itself in the list of potential second-generation biofuels. It was traditionally used as a solvent in various products such as cosmetics, detergents, hydraulic fluids, antibiotics, and drugs, as well as an

intermediate in the manufacturing of methacrylate and butyl acrylate. It is also used as an extractant in the synthesis of many pharmaceutical products. However, the exploitation of butanol as a biofuel is a relatively new application in the fuel market. Butanol, when compared to ethanol, is less volatile and explosive. In addition, butanol has a lower vapor pressure (0.3 psi) and higher flash point (35 °C), which makes it safer to handle. The heating value of butanol (29.2 MJ/L) is higher than that of ethanol (21.2 MJ/L). Moreover, the air-to-fuel ratio (11.2) and octane ratings (96) of butanol are almost comparable to gasoline, which gives it an edge over other alcohol-based fuels. It is less hygroscopic unlike ethanol (that absorbs water from the atmosphere) and is miscible with gasoline in any proportion (Nanda et al. 2017). Butanol can be directly used as a drop-in fuel or as blends with gasoline or diesel and can be easily supplied using the existing pipelines (García et al. 2011).

Louis Pasteur in 1861 was the first to report the production of butanol using microbial fermentation. Later, Albert Fitz progressively worked on extracting butanol from glycerol using two strains of bacteria. Additionally, researchers like Beijerinck, Bredemann Sharding, and Pringsheim made significant contributions to this field. Biobutanol was industrially synthesized in a large scale during 1912–1914 by the well-known acetone-butanol-ethanol (ABE) fermentation from molasses and cereals with the help of strains like *Clostridium acetobutylicum* (Dürre 2008). It is during the First and Second World War that sugar and cereals were the main substrates for ABE fermentation. Due to the increased food demand during the war, these feedstocks became too expensive and scarce in supply, which led to a shrinking interest in ABE fermentation. Thus, there is a lot of scope for exploring different low-cost raw materials for fermentative butanol production that can lead to its cost-effective biosynthesis. Abundantly available and inexpensive lignocellulosic biomass such as agricultural waste (barley straw, corn stover, corn fiber, wheat straw, switch grass, timothy grass) and wood residues can be used for an efficient and economical ABE fermentation (Nanda et al. 2014a). Until recently, the use of butanol was primarily limited to industrial solvent or precursor for fine chemical production. Recently, DuPont and British Petroleum have announced a joint initiative to commercialize the production of biobutanol through ABE fermentation (Kumar and Gayen 2011).

Butanol production can be through either petrochemical pathways or fermentative pathway. The commonly used chemical synthesis route for butanol production is the oxo process. This process involves the catalytic reaction of propylene with carbon monoxide and hydrogen. The intermediate products formed are *n*-butyraldehyde and isobutyraldehyde, which are hydrogenated to produce *n*-butanol and iso-butanol, respectively (García et al. 2011). The biological pathway involves batch, fed-batch, and continuous production of butanol through ABE fermentation. ABE fermentation is carried out by *Clostridium* species, mostly *Clostridium acetobutylicum* and *Clostridium beijerinckii* in two phases. In the first phase of fermentation, monomeric sugars are converted to acetate and butyrate, which in the next phase are converted to acetone and butanol, respectively (Qureshi and Ezeji 2008). The typical products of ABE fermentation are acetone, butanol, and ethanol in the mass ratio of 3:6:1. Various feedstocks and microbial strains are used to obtain

better butanol yields at lower production costs. Different metabolic engineering and genetic engineering approaches have been applied to butanol-producing *Clostridium* to enhance butanol production and suppress the product inhibition (Nanda et al. 2017). Kumar and Gayen (2011) have discussed the available strains for the production of biobutanol and the different fermentative pathways involved in detail along with some recent developments in the field of biobutanol production.

Green (2011) has elaborately discussed the industrial perspective for the fermentative production route of biobutanol. It is reported that China stands top in the list of leading countries that invest in the re-commercialization of ABE fermentation. It is believed that more than US \$200 million has been invested by China to increase its annual butanol production from 0.21 to 1.0 million tons. Only a few plants in China majorly produce butanol (30,000 tons per annum) by using cornstarch as the feedstock in semicontinuous fermentation (Green 2011). China is foreseeing to retrofit its existing conventional starch-based refineries to use cheaper cellulosic materials as feedstock for butanol production. This approach of retrofitting old refineries as well as pulp and paper industries seems to be an attractive alternative to accelerate the production of biobutanol in developed countries like Brazil and the United States.

Several studies prove that blending butanol with diesel and other fuels can also be a promising attribute. Yilmaz et al. (2014) studied the effect of different blends of butanol-biodiesel on the performance and emission on the indirect injection engine. It was found that in comparison with biodiesel, the blended fuel showed lower rates of emission of nitrogen oxides with higher greenhouse gases and hydrocarbons emissions. Giakoumis et al. (2013) reviewed the exhaust emissions of *n*-butanol blends with diesel on engines working under transient conditions. The essential mechanisms of exhaust emissions during transient operation of the engine were discussed on the basis of fundamentals such as transient operation and properties of butanol in comparison with diesel.

Jin et al. (2011) reviewed the properties of butanol that make it a better biofuel than ethanol and biodiesel along with the developmental strategies in butanol production. Several methods that involved advanced fermentative techniques and metabolic engineering application on the strains were discussed. It was reported that butanol is a potential fuel as compared with gasoline or diesel fuel on the basis of its combustive properties, engine performance, and emissions from the exhaust (Jin et al. 2011). Butanol as a fuel has several advantages; however, it is important to understand the drawbacks associated with it. Butanol contributes to the formation of photochemical smog on its reaction with volatile organics present in the atmosphere. Butanol causes irritation to the human eyes, throat, and nose, and it is highly flammable. Most importantly, *Clostridium* suffers from inhibition of butanol as 2% butanol in the fermentation medium initiates microbial inhibition. Owing to the low butanol yields, its separation becomes a tedious and expensive process, unlike ethanol. These limitations though significant cannot overshadow the benefits of using butanol as a second-generation biofuel; hence there is a huge scope for research in its prospective production and utilization as an advanced biofuel.

1.5 Bio-oil

Biomass has been identified as a prominent renewable energy source to compensate the depleting fossil fuels. The major constituents of biomass are carbohydrates, which are rich in carbon, hydrogen, and oxygen with possibly high energy content. Bio-oil also termed as pyrolysis oil is mostly produced through biomass pyrolysis. It contains numerous aromatic compounds such as alkanes, phenol derivatives, and aromatic hydrocarbons and trace amounts of esters, ketones, ethers, amines, sugars, and alcohols with a H/C molar ratio usually higher than 1.5. It is produced in the oxygen- or air-deprived environment during biomass pyrolysis at high temperatures. Bio-oil is portable to be used as direct fuel in boilers, or it can be further upgraded to produce fuel or other industrial chemicals by using advanced methods such as catalytic or zeolite cracking, hydrogenation, and processing the aqueous phase (Isahak et al. 2012).

The two major techniques used for biomass conversion to bio-oil can be broadly categorized as the fast pyrolysis and hydrothermal liquefaction. Pyrolysis is the rapid decomposition of organic compounds at high temperatures in an inert atmosphere to produce bio-oil, pyro-gas, and char. Hydrothermal liquefaction, on the other hand, involves the treatment of biomass at high temperatures and pressure in the presence of water and a suitable catalyst. The effects of fast and slow pyrolysis of lignocellulosic biomass on the production of bio-oil, char, and gases have been discussed by several authors (Nanda et al. 2014c; Mohanty et al. 2013; Mohan et al. 2006). Fast pyrolysis featured by its high heating rates and short vapor residence time results in greater yields of bio-oil, whereas slow pyrolysis characterized by its slow heating rate and longer residence time leads to higher yields of char.

Moisture-free biomass is preferred in the case of pyrolysis, but for hydrothermal liquefaction, a relatively moist biomass is suitable. The presence of moisture in biomass renders hydroxyl and carboxyl groups to the bio-oil derived through pyrolysis, which reduces its heating value and compromises the fuel properties. Although there have been significant contributions to explore the technique of fast pyrolysis for the production of bio-oil, the hydrothermal liquefaction technology remains in its natal state (Xiu and Shahbazi 2012).

Along with the existing techniques of fast pyrolysis and hydrothermal liquefaction, hydrotreating is a budding process that can potentially convert the biomass into petroleum-compatible products. Out of the various reactions taking place during hydrotreating is hydrodeoxygenation to remove oxygen-containing functional groups (carboxyl and hydroxyl) from the bio-oil. The steps involved in bio-oil upgrading through hydrotreating route include purification of the bio-oil, modification of the bio-oil through chemical processing, removal of heteroatoms, breaking of the long hydrocarbon chains, and separation. However, it is critically significant to recognize these elements as multiple unit procedures or as a single unit in order to obtain a fuel product that can be either a part of the bio-oil production route or as a part of petroleum processing or conversion (Zacher et al. 2014).

The catalytic upgrading route for bio-oil purification is established over the same application of hydrotreating. However, in its crude form, bio-oil has a high content

of oxygen, which gives it low stability and poor heating value. The widely used hydrotreating catalyst $\text{Co-MoS}_2/\text{Al}_2\text{O}_3$ or other metal catalysts can be used for this purpose. The major challenge in this process is catalyst fouling due to high carbon deposition that gives the catalyst a lifetime as short as 200 h. Zeolites have been found to be a promising alternative. Zeolite cracking can be used for deoxygenation with the catalyst like HZSM-5. As deoxygenation reaction does not require hydrogen, the processing can be completed under atmospheric pressures. Furthermore, the bio-oil produced is low in hydrogen content, which leads to a low H/C ratio. Thus, it can be inferred that bio-oil produced over zeolites is of poor grade, with heating values that are almost 25% lower than the crude oil. Zhang et al. (2006) studied the upgrading of bio-oil using different solid catalysts. The study involved a comparative analysis of the effects of using solid acid catalyst $40\text{SiO}_2/\text{TiO}_2\text{-SO}_4^{2-}$ and solid base catalyst $30\text{K}_2\text{CO}_3/\text{Al}_2\text{O}_3\text{-NaOH}$ on the upgrading of bio-oil, and the properties of the product from both the processes were analyzed and discussed in detail.

There are several other studies that discuss the progress in the field of bio-oil production, upgrading, and commercialization from various sources (Jacobson et al. 2013). Hydrodeoxygenation seems to be the best route for bio-oil upgrading as deoxygenation through zeolites does not produce bio-oil of acceptable grades to compete with crude oil. A few technical advances can be contributed through catalyst synthesis for demonstrating better activities, enhanced kinetics, mechanism of carbon formation, prediction of appropriate hydrogen pressure, and understanding the deactivation caused by sulfur (Mortensen et al. 2011). Though the use of bio-oil is promising, there is a long way to trace toward its complete commercialization as a finished product that can compete with the crude oil.

1.6 Algal Oil

The past few years have gained further advancement in the field of biofuels with different alternatives being tried as the feedstock for biofuel generation. In this respect, algae have been an option of immense interest. The benefit of using algae as a source of biofuel is that higher productivities as compared to terrestrial plants. Some algal species are capable of accumulating large amounts of triacylglycerides, which form the major precursor for biodiesel production. Moreover, owing to its aquatic nature, there is no requirement for highly fertile agricultural land to cultivate algae as a third-generation biofuel feedstock. Algae produce more oil than most other agricultural biomass used. It is reported that algae are capable of producing 250 times more oil as soybean grown per acre (Hossain et al. 2008). A few of the algal strains used for the production of algal oil are cyanobacteria (*Chloroxybacteria*) and eukaryotic microalgae, e.g., green algae (*Chlorophyta*), red algae (*Rhodophyta*), and diatoms (*Bacillariophyta*) (Brennan and Owende 2010).

In biological terms, algae are one of the oldest plants that belong to the family of thallophytes that lack roots, stems, and leaves and have an uncovered reproductive cell. The major photosynthetic pigment present in algae is chlorophyll. The simple cell structure of algae makes them efficient solar energy harvesters and adaptable to

prevailing environmental situations in the long run (Brennan and Owende 2010). Several biofuels that can be derived from algae include methanol (produced from anaerobic digestion of algae), biodiesel (produced by processing of algal oil), and biohydrogen (photobiologically produced by algae).

Unicellular green algae majorly contribute to the production of biodiesel. It is a photosynthetic eukaryote with high population density and high growth rates. In favorable conditions, it can replicate its biomass to double in less than a day. In addition, it is capable of having high cell density with high lipid content. The biodiesel produced from algae has energy density similar to conventional diesel fuel. The heating value for algal oil (biodiesel) is dependent on the biomass source and comparable to the high values of the conventional diesel. The heating value for algal oil (41 MJ/kg) is more than that of oils produced from other biomass such as for rapeseed (39.5 MJ/kg). This further improves the heating values for the biodiesel derived from algal oil as compared to the biodiesel from other biomass. Although the agricultural biomass is a common feedstock for the production of biodiesel, algal oil stands strong in competing to make its place in the list at a commercial level (Demirbas 2011).

The most common methods to extract oil from algae are the expeller or pressing method, an extraction process with hexane as a solvent and supercritical fluid extraction. Biodiesel from algae contains mono-saturated and saturated fatty acids. Typically, an algal oil contains 36% oleic acid, 15% palmitic acid, 11% stearic acid, 8.4% iso-linoleic, and 7.4% linoleic acid (Demirbas and Demirbas 2011). The benefit of algal oil is that the fuel polymerization during combustion is less due to mono-saturated and saturated fatty acids as compared to fuels with polyunsaturated acids. When the algal oil is extracted, refused biomass can be used as a protein-rich feed for livestock. This adds to the relevance of this process with less strain on waste handling. The process of biodiesel production from algae is similar to the biodiesel production from vegetable oil. However, the benefits of less competition for arable land as compared to agricultural biomass and more efficiency of the products are magnificent (Demirbas and Demirbas 2011; Greenwell et al. 2010; Scott et al. 2010).

Some of the challenges of algal oil cannot be overlooked. The commercial and sustainable production of algal oil at optimized conditions is yet to be established. In particular, the optimization of algal biomass production and the triacylglyceride content need more research attention. The limitation of light penetration in the cultured algae can be a concern for low biomass production. The high water content of the algae biomass needs more energy for its drying, which makes the process expensive. The overall capital cost of the production of algal biomass is higher than the production of agricultural biomass, especially for the regions with less sunlight. All these challenges question the use of algae for biodiesel production, but the benefits of the process are much more. This calls for further intensive research in this field for an optimum and efficient utilization of algae as a third-generation biomass for biodiesel production.

1.7 Biodiesel

Rudolf Diesel became the first person to use vegetable oil for his diesel fuel engine (Shay 1993). During 1930–1940, initial use of biodiesel (vegetable oils) as fuel for diesel engines was witnessed. Biodiesel is an unconventional fuel source for the internal combustion engines and can be chemically categorized as a combination of monoalkyl esters with long-chain fatty acids extracted from biomass. The typical alkyl fatty acid chain in biodiesel ranges from C_{14} to C_{22} esters of ethanol or methanol. This chemical nature makes biodiesel a suitable substitute for the conventional diesel fuel.

There are various sources of vegetable oils that contain glycerides as a potential fuel source replacing the conventional diesel fuel. The high heating power and sulfur-free exhaust gases from vegetable oil-derived fuel combustion make it suitable for biodiesel production. Since plants are the essential source of vegetable oils, their consumption as the fuel produces CO_2 that is biologically recyclable. It is only due to the high viscosity of the biodiesel from vegetable oils that a modification in the commercial diesel engine is required, as the rest of the properties remain compatible. The kinematic viscosity of vegetable oil ranges from 30 to 40 cSt at 38 °C. This viscosity is almost 20 times higher than the viscosity of diesel fuel. The cetane number for vegetable oil varies from 32 to 40, which makes it a better fuel. Another option to enhance the performance of biodiesel as a direct engine fuel is to blend it with the conventional diesel as they are both miscible.

The reaction for biodiesel production occurs in the presence of a suitable catalyst (usually a strong base, e.g., NaOH or KOH) that leads to the production of methyl esters. These methyl esters are termed as biodiesel. The major challenges for swapping diesel fuel with biodiesel are due to the high viscosity, polyunsaturated nature, and low volatility of the biodiesel. Thus, the vegetable oils undergo processing to produce a suitable biodiesel that has comparable properties to that of the commercial diesel. The three main processes observed to achieve the target properties of biodiesel are pyrolysis, transesterification, and microemulsions. Dedicated research has been conducted on the use of biodiesel as diesel engine fuel. The divergent feedstock materials have been tested for the production of biodiesel, which includes palm oil, sunflower oil, soybean oil, rapeseed oil, coconut oil, and tung oil. Animal fat has also been explored as an alternative source of biodiesel, but it lacks detailed study as the vegetable oil.

Fukuda et al. (2001) reported that enzymatic transesterification has a great contribution toward biodiesel production. The technologies related to biodiesel upgrading were reviewed focusing on transesterification using a catalyst (acid or alkali), supercritical fluid, and lipase enzyme with an industrial viewpoint. Marchetti et al. (2005) highlighted the alternative technologies that could be employed to produce biodiesel. Various studies with different oils, catalysts, and alcohols have been conducted to produce biodiesel. Transesterification is dominated by factors like reaction conditions, alcohol-to-oil molar ratio, water contents of oils or fats, purity of reactants, and amount/type of catalyst. Murugesan et al. (2009) attempted to compile the methods of biodiesel production, its quality analysis, its performance for internal

combustion engines, and its resource availability. Recommendations for developmental strategies for biodiesel, economic aspects, and environmental considerations are also detailed.

Although it is possible to use vegetable oil as fuel in the diesel engine in the form of biodiesel, there are certain challenges that cannot be overlooked. A few of these problems are the inefficient mixing of air with biodiesel that leads to high smoke emissions. The high flash point also attributes to lower volatility of biodiesel. High carbon deposition and failure of the injection nozzle in the diesel engine are other common drawbacks. These problems bring a scope for chemical modification of biodiesel to make it compatible and efficient for use in a diesel engine.

1.8 Hydrogen

Hydrogen is one of the most promising alternatives to the conventional fuels due to its most superior heating value of 141.8 MJ/kg. It is the secondary energy source that needs to be derived from renewable and nonrenewable hydrocarbon-based materials. Hydrogen is referred to as an energy carrier and vector. It is believed to have a great role as an energy carrier in the global energy sector of the future. Hydrogen is considered as a clean fuel as it emits only water and no CO₂ upon combustion. It is widely used in fuel cells for the generation of electricity.

Hydrogen has found application in combustion engines along with fuel cells in electric vehicles. Hydrogen is in its gaseous state at ambient temperatures and pressures, which exhibits a great challenge in its transportation and storage as compared to other liquid fuels. Since it is the second lightest element and highly flammable, it needs to have special and safe storage options. It can be stored physicochemically and chemically in different states or in the form of liquid compounds such as metal hydrides, alanates, methanol, or light hydrocarbons (Balat and Kirtay 2010).

Mostly, the engines are found to be specific to the fuel properties for efficient operation. However, hydrogen can be obtained from any of the conventional feedstock, and hence the engine can be easily modified for hydrogen use. This attribute makes hydrogen a universal fuel. Recently, many nations around the globe are focusing on the development of new technologies for hydrogen production with solutions to the energy security. Countries like the United States have initiated a multiyear plan with an entire focus on improving the infrastructure of hydrogen generation, its use as an energy source, and its storage techniques (Holladay et al. 2009).

The economy of hydrogen production depends on the availability of an economic and environment-friendly source. Current scenario witnesses hydrogen production from fossil fuels through steam and dry reforming of methane and natural gas. However, fossil fuels have a very limited supply and also emit harmful greenhouse gases during hydrogen production. Bartels et al. (2010) compared the production cost of hydrogen from fossils and alternative energy sources. The analysis of the study showed that the most economical route for hydrogen production was through

coal and natural gas, with an estimated cost of hydrogen to be 0.36–1.83 \$/kg and 2.48–3.17 \$/kg, respectively. Balat and Kirtay (2010) reported that hydrogen production from steam methane reforming costs in the range of 1.5–3.7 \$/kg (natural gas price around 7 \$/GJ), whereas hydrogen production from biomass costs around 10–14 \$/GJ. The increasing cost of fossil fuels might eventually lead to higher production costs of hydrogen; hence alternative energy sources might be a prospective source for hydrogen production.

Levin and Chahine (2010) reported the production of hydrogen from renewable feedstocks such as agricultural waste and other waste streams that contributed in minimizing the emission of greenhouse gases. This increases the flexibility and improves the economics of the production and distribution of hydrogen. Few of the processes that can be taken into account for hydrogen production from alternate energy routes are electrolysis, biological production, and thermocatalytic processes. These processes can be adapted to on-site hydrogen production avoiding the need to establish an expensive and large distribution infrastructure. Nonetheless, each of the alternate routes mentioned has its technical challenge in hydrogen production such as conversion efficiencies, purification of hydrogen, feedstock selection, and storage (Levin and Chahine 2010).

Hydrogen generation from biomass through gasification is certainly an essential route; however, this technology needs more development. Kirtay (2011) reviewed the recent advances in different hydrogen production technologies. It was reported that an efficient production of hydrogen requires a coproduct pathway to compete with hydrogen production from conventional crude processes such as steam reforming of natural gas. A potential route from biomass to hydrogen is through activated carbon, which involves a coproduct that is commercially practicable. Hydrogen production from biomass has several benefits with a major challenge that targets the economical production of hydrogen (Kirtay 2011).

It is known that the most cost-efficient method of hydrogen production that currently subsists is through steam reforming of methane and this process is commercially established. As discussed earlier, this process uses nonrenewable sources for hydrogen production and does not stand the test of sustainability. It is suggested that the cost of hydrogen production is predominantly dependent on the cost of feedstock. Thus, a cost-efficient energy generation process for hydrogen production from biomass should be established. Government policy interest in switching to hydrogen-based infrastructure is rising as hydrogen conversion to useable energy is more efficient than conventional fuels. Additionally, hydrogen produces only water as a by-product during its consumption as an energy source, unlike the fossil fuels that release greenhouse gases along with obnoxious nitrogen and sulfur compounds. To achieve a large-scale global production and utilization of hydrogen, strategic planning and cooperation among developed and developing nations are required (Balat and Balat 2009a, b).

1.9 Biomethane

Attempts to minimizing the dependency on land resources are progressively made for the sustainable production of second-generation biofuels. Biomethane is produced from the high moisture-containing biogenic wastes and biogas upgrading. It can also be produced from specific agricultural feedstocks such as grasses and maize, which have huge benefits but are overshadowed due to the limitations of the agricultural land use for other significant applications like food crop cultivation. To produce biomethane at a commercial scale, it is essential to develop and utilize the gasification techniques of woody biomass (Åhman 2010). A few of methanogenic bacteria are *Methanobacterium*, *Methanobacillus*, *Methanococcus*, and *Methanosarcina* (Molino et al. 2013).

Methane has high energy density (55.5 MJ/kg). Thus, it is of interest to the energy sector. The extraction of methane from biogas is usually employed through anaerobic digestion of the biomass. The primary product, i.e., the biogas, consists of CH₄ and CO₂, which is further purified to obtain clean methane. Apart from the main components, water vapor, siloxanes, ammonia, hydrogen sulfide, carbon monoxide, oxygen, and nitrogen are present in trace amounts in the biogas. For the purification of biogas to methane, there are two primary steps involved. The first step is to clean biogas for removing any trace impurities, and the second step involves upgrading to the clean biomethane for improving its physical properties like calorific value. Upgrading makes biomethane ready for use as a vehicular fuel meeting the stringent environmental standards.

There are several methods employed in obtaining clean methane, which depend on the properties of the feed gas such as fuel efficiency, operational properties, etc. A few of the methods employed are the condensation methods and drying methods. Different impurities are removed from biogas through specific techniques to obtain clean methane (Ryckebosch et al. 2011). The processing of the biogas also depends on the type of feedstock used. Nizami et al. (2009) discussed the various processes that could be used for biomethane production using grass as the feedstock.

There are several studies that deal with the production of biomethane using anaerobic digestion of the wet biomass from different sources such as land energy crops, ocean energy crops and organic wastes (Chynoweth 2005; Molino et al. 2013), grasses (Nizami et al. 2009), and starchy and lignocellulosic materials (Frigon and Guiot 2010). There have been several attempts to identify the best feedstocks for biomethane production from biogas. Patterson et al. (2013) compared the environmental constraints for the production and use of biomethane and its blends with biohydrogen from food waste and wheat feedstock on the basis of data from two separate laboratory runs. In the case of food waste, a two-step batch process gave higher hydrogen yields, but the overall energy efficiency was lower than the single-step process. Food wastes from landfill aided in reducing the burden on the environment as compared to diesel fuel, which posed several environmental damages. In the case of wheat feedstock, the overall energy outputs were high with low hydrogen yields in a two-stage semicontinuous stage. The significance of

outlining and optimizing biofuel production variables was highlighted (Patterson et al. 2013).

Countries like Italy and Ireland have made great efforts toward residue-based biofuel production. There are studies that evidently present the constant efforts of these nations toward waste usage from various industries for the production of biomethane (Patrizio et al. 2015; Thamsiriroj and Murphy 2011). The benefits of using biomethane as an alternative fuel source are many, and that forms the reason for the revival of this biofuel for the energy market utility. However, there are certain constraints of using biomethane which cannot be neglected. With the use of biomethane, there are high greenhouse gas emissions in the environment, and the properties of biomethane are similar to the properties of methane from fossil fuels. With high energy densities and other fuel properties, biomethane is competent, but there are certain environmental constraints that cannot be overlooked when using biomethane as a biofuel. This highlights the need for some serious efforts to improve the environmental properties of biomethane.

1.10 Aviation Fuel

The requirement for fossil fuel is forecasted to grow 1.3% each year up to 2030, whereas the carbon emission from the transport system would likely increase to 80% (Hari et al. 2015). There have been several studies in the field of gaseous and liquid biofuels that can be used to run the land-based transportation. However, air transportation as a contributor to the exhaust emissions and fuel consumption cannot be ignored. During 2005–2010 the total diesel and jet fuel consumptions were between 5 and 6 million barrels per day. The average cost for jet fuels increased from US \$320 per ton in 2004 to US \$1005 per ton in 2011 (Hari et al. 2015). Aviation biofuels have strongly held on to the industry ever since 2008. The first flight run by Virgin Atlantic was fueled by 20% of biofuel along with jet fuel. Blends, as high as 50–50, have been used so far, and in October 2012, 100% biofuel was used in a flight of Dassault Falcon 20 powered by the National Research Council of Canada.

Aviation fuels comprise of both the jet fuel that is used for the turbine engine and the aviation gasoline used for the piston engines. Out of the two, jet fuel that originates from the crude oil is the dominant one used in most of the large aircrafts. The kerosene fraction of the crude oil is used for the extraction of jet fuel, which distills between the gasoline and the diesel fractions (Nygren et al. 2009). The chemical composition of jet fuels can be specified as roughly 60% paraffin (alkanes), 20% aromatic compounds (monocyclic and polycyclic hydrocarbons), and 20% naphthenes (cycloparaffins or cycloalkanes) (Hileman et al. 2010). Olefins or alkenes occur in jet fuels in trace amounts. Sulfur contained in the jet fuel is present in its molecular form with hydrogen and carbon along with traces of oxygen and nitrogen termed as heterocyclics. This sulfur present in jet fuel has some impacts on the air quality standards and fuel lubricity.

Aviation biofuels can be categorized by its fuel quality, ultralow sulfur jet fuel, and hydrocarbon jet fuels with reduced or zero aromatic compound and fatty acid methyl esters (biodiesel or biokerosene). Another ground of categorizing aviation biofuels can be by feedstocks such as vegetable oil, food wastes, and animal fat. Llamas et al. (2012) used transesterified coconut and palm kernel oils with methanol using homogeneous catalysts that resulted in good yields. The fatty acid methyl esters were subjected to vacuum fractional distillation, and the fractions with low boiling point were blended with two varieties of fossil kerosene, one was hydrotreated cut from atmospheric distillation and a commercial JetA1. Various fuel properties for the two blends were tested such as flash point, viscosity, smoke point, etc. From this study, it was concluded that it is feasible to blend up to 10 vol% coconut and palm kernel biokerosene with commercial JetA1 if there are few relaxations in the quality standards set (Llamas et al. 2012).

Chiaromonti et al. (2014) explored the possible routes for sustainable aviation biofuel production from biomass feedstock through either biochemical or thermochemical processes. The possible option for the industrial paraffinic biofuel production is large, which can diversify from biochemical to thermochemical or hybrid routes. It is reported that ITAKA group in Europe is working to develop sustainable synthetic paraffinic kerosene (SPK), which is regarded as environmentally, economically, and socially viable for production at commercial scale. Thus, attempts are being made to use this biofuel in the current aviation industry in Europe. The pre-processing of waste cooking oil is being investigated to make it compatible for standard hydroprocessing including esterification and thermal-catalytic processing at pilot scale. In this study, the initial samples of feedstock oils were characterized to further investigate the conversion of these oils to biokerosene through hydrotreatment route (Chiaromonti et al. 2014).

In the past decade, the fate of aviation biofuel has transformed from an uncertain alternative to a testified and fully certified sustainable alternative for commercial use in 50% blends with the jet fuel. Regardless of the constant efforts and success stories, aviation biofuels have to go a long way to be widely commercialized. Gegg et al. (2014) reviewed the concerns of leading global aviation biofuel industries along with the identification and examination of the factors that dictate the aviation biofuel market globally. Though the future of aviation biofuel seems promising, the way to its commercialization is constrained due to high production costs, limited feedstock and biomass availability, lack of national and international policy support through political sources, and the uncertainties that surround the sustainable production of aviation biofuel at a commercial level. Furthermore, the requirements for establishing a global market to support the commercial production of aviation biofuel is discussed (Gegg et al. 2014). This calls for an international effort to produce and commercialize the use of biofuel in the aviation industry.

1.11 Conclusions

The utilization of biomass as an energy source is becoming essential to alleviate the global warming caused by burning fossil fuels. Environmental concerns such as global warming and climatic changes and the diminishing oil resources and its increasing prices make it essential to explore all kinds of possible biofuels that are sustainable and environment-friendly. The modern era is witnessing a revolution in the energy sector with the advanced processing of the alternative fuel sources. Biofuels from biomass are commonly discussed since a long time and are widely being explored, be it ethanol, butanol, bio-oil, hydrogen, biomethane, biodiesel, or aviation biofuel. However, there are a few limitations over the sustainability of these biofuels. Two of these major limitations are the availability of the feedstock for a mass production of the biofuel at a commercial level to meet global energy demand and the efficient use of the energy derived from these biofuels which need to be transformed from theoretical predictions to practical yields.

The continued use of fossil fuels to meet the increasing energy demands poses a threat to the atmosphere due to increased greenhouse gas emissions and concerns related to the global warming. Additionally, the finite petroleum reserves are depleting and are becoming more expensive. Thus, the economic, environmental, and political limitations are driving the interest in exploring biofuels. Biofuel, a collective term, used for liquid and gaseous fuel sources are primarily derived from biomass through many thermochemical and biochemical pathways.

The reasons for using biofuels are realized to address the global environmental concerns due to greenhouse gas emission, nitrous oxides and volatiles that the fossil fuels release into the environment. However, there are serious sustainability issues related to the use of the liquid biofuels such as ethanol and biodiesel. The feedstock that is used for the production of these liquid biofuels majorly comes from agricultural material (first-generation feedstocks) that competes with the food demands of the world. However, second-generation (lignocellulosic materials) and third-generation feedstocks (algae, municipal solid wastes, sewage sludge, etc.) pose no threat to the food supply and are hence sustainable alternatives to produce advanced biofuels.

The rapid alternations in the global energy scenario have brought to light several alternative fuels that have potential to replace the conventional fossil fuels. An alternative to the conventional petroleum-based fuel is biodiesel that is derived from vegetable oils or used or waste cooking oil that contains triglycerides and animal fats. The huge strain on the depleting petroleum sources and their skyrocketing prices have made it essential for the energy industries to explore alternative fuel sources that are environment-friendly and sustainable. These factors have derived the industries to take a keen interest in sources like vegetable oil or waste cooking oil as a substitute for the petroleum-based fuel. Although holding many promises, the liquid and gaseous biofuels in the current day have a questionable existence on the grounds of economic and commercial prospective. Nevertheless, thorough research and development will lead to a better understanding of the production and utilization of these biofuels for a greener and cleaner future.

Acknowledgments The authors would like to thank the Natural Sciences and Engineering Research Council of Canada (NSERC) for funding this bioenergy research.

References

- Åhman M (2010) Biomethane in the transport sector – an appraisal of the forgotten option. *Energy Policy* 38:208–217. <https://doi.org/10.1016/j.enpol.2009.09.007>
- Balat M, Balat H (2009a) Recent trends in global production and utilization of bio-ethanol fuel. *Appl Energy* 86:2273–2282. <https://doi.org/10.1016/j.apenergy.2009.03.015>
- Balat M, Balat M (2009b) Political, economic and environmental impacts of biomass-based hydrogen. *Int J Hydrogen Energy* 34:3589–3603. <https://doi.org/10.1016/j.ijhydene.2009.02.067>
- Balat H, Kırtay E (2010) Hydrogen from biomass – present scenario and future prospects. *Int J Hydrogen Energy* 35:7416–7426. <https://doi.org/10.1016/j.ijhydene.2010.04.137>
- Bartels JR, Pate MB, Olson NK (2010) An economic survey of hydrogen production from conventional and alternative energy sources. *Int J Hydrogen Energy* 35:8371–8384. <https://doi.org/10.1016/j.ijhydene.2010.04.035>
- Boden TA, Marland G, Andres RJ (2009) Global, regional, and national fossil-fuel CO₂ emissions. Carbon Dioxide Information Analysis Center, Oak Ridge National Laboratory, US Department of Energy, Oak Ridge http://cdiac.ornl.gov/trends/emis/overview_2007.html. Accessed 3 May 2017
- Brennan L, Owende P (2010) Biofuels from microalgae – a review of technologies for production, processing, and extractions of biofuels and co-products. *Renew Sust Energy Rev* 14:557–577. <https://doi.org/10.1016/j.rser.2009.10.009>
- Chiaromonti D, Prussi M, Buffi M, Tacconi D (2014) Sustainable bio kerosene: process routes and industrial demonstration activities in aviation biofuels. *Appl Energy* 136:767–774. <https://doi.org/10.1016/j.apenergy.2014.08.065>
- Chynoweth DP (2005) Renewable biomethane from land and ocean energy crops and organic wastes. *Hortscience* 40:283–286
- Demirbas A (2010) Use of algae as biofuel sources. *Energy Convers Manag* 51:2738–2749. <https://doi.org/10.1016/j.enconman.2010.06.010>
- Demirbas A (2011) Competitive liquid biofuels from biomass. *Appl Energy* 88:17–28. <https://doi.org/10.1016/j.apenergy.2010.07.016>
- Demirbas MF, Balat M (2006) Recent advances on the production and utilization trends of bio-fuels: a global perspective. *Energy Convers Manag* 47:2371–2381. <https://doi.org/10.1016/j.enconman.2005.11.014>
- Demirbas A, Demirbas MF (2011) Importance of algae oil as a source of biodiesel. *Energy Convers Manag* 52:163–170. <https://doi.org/10.1016/j.enconman.2010.06.055>
- Dürre P (2008) Fermentative butanol production bulk chemical and biofuel. *Ann NY Acad Sci* 1125:353–362. <https://doi.org/10.1196/annals.1419.009>
- Food and Agriculture Organization of the United Nations, FAO (2008) The state of food and agriculture. Biofuels: prospects, risks, and opportunities. FOA, Rome
- Frigon JC, Guiot SR (2010) Biomethane production from starch and lignocellulosic crops: a comparative review. *Biofuels Bioprod Biorefin* 4:447–458. <https://doi.org/10.1002/bbb.229>
- Fukuda H, Konda A, Noda N (2001) Biodiesel fuel production by transesterification of oils. *J Biosci Bioeng* 92:405–416. [https://doi.org/10.1016/S1389-1723\(01\)80288-7](https://doi.org/10.1016/S1389-1723(01)80288-7)
- García V, Pääkkilä J, Ojamo H, Muurinen E, Keiski RL (2011) Challenges in biobutanol production: how to improve the efficiency? *Renew Sustain Energy Rev* 15:964–980. <https://doi.org/10.1016/j.rser.2010.11.008>
- Gegg P, Budd L, Ison S (2014) The market development of aviation biofuel: drivers and constraints. *J Air Transp Manag* 39:34–40. <https://doi.org/10.1016/j.jairtraman.2014.03.003>

- Giakoumis EG, Rakopoulos CD, Dimaratos AM, Rakopoulos DC (2013) Exhaust emissions with ethanol or *n*-butanol diesel fuel blends during transient operation: a review. *Renew Sust Energy Rev* 17:170–190. <https://doi.org/10.1016/j.rser.2012.09.017>
- Gnansounou E, Dauriat A (2005) Ethanol fuel from biomass: a review. *J Sci Ind Res* 64:809–821
- Green EM (2011) Fermentative production of butanol – the industrial perspective. *Curr Opin Biotechnol* 22:337–343. <https://doi.org/10.1016/j.copbio.2011.02.004>
- Greenwell HC, Laurens LM, Shields RJ, Lovitt RW, Flynn KJ (2010) Placing microalgae on the biofuels priority list: a review of the technological challenges. *J R Soc Interface* 7:703–726. <https://doi.org/10.1098/rsif.2009.0322>
- Hahn-Hägerdal B, Galbe M, Gorwa-Grauslund MF, Lidén G, Zacchi G (2006) Bio-ethanol – the fuel of tomorrow from the residues of today. *Trends Biotechnol* 24:549–556. <https://doi.org/10.1016/j.tibtech.2006.10.004>
- Hari TK, Yaakob Z, Biniha NN (2015) Aviation biofuel from renewable resources: routes, opportunities and challenges. *Renew Sust Energy Rev* 42:1234–1244. <https://doi.org/10.1016/j.rser.2014.10.095>
- Hileman JI, Stratton RW, Donohoo PE (2010) Energy content and alternative jet fuel viability. *J Propuls Power* 26:1184–1196. <https://doi.org/10.2514/1.46232>
- Holladay JD, Hu J, King DL, Wang Y (2009) An overview of hydrogen production technologies. *Catal Today* 139:244–260. <https://doi.org/10.1016/j.cattod.2008.08.039>
- Hossain ABMS, Salleh A, Boyce AN, Chowdhury P, Naquiddin M (2008) Biodiesel fuel production from algae as renewable energy. *Am J Biochem Biotechnol* 4:250–254
- International Energy Outlook, IEO (2010) U.S. Energy Information Administration. Report #: DOE/EIA-0484(2010), Washington, DC
- Isahak WNRW, Hisham MWM, Yarmo MA, Hin TYY (2012) A review on bio-oil production from biomass by using pyrolysis method. *Renew Sust Energy Rev* 16:5910–5923. <https://doi.org/10.1016/j.rser.2012.05.039>
- Jacobson K, Maheria KC, Dalai AK (2013) Bio-oil valorization: a review. *Renew Sust Energy Rev* 23:91–106. <https://doi.org/10.1016/j.rser.2013.02.036>
- Jin C, Yao M, Liu H, Lee CF, Ji J (2011) Progress in the production and application of *n*-butanol as a biofuel. *Renew Sust Energy Rev* 15:4080–4106. <https://doi.org/10.1016/j.rser.2011.06.001>
- Kirtay E (2011) Recent advances in production of hydrogen from biomass. *Energy Convers Manag* 52:1778–1789. <https://doi.org/10.1016/j.enconman.2010.11.010>
- Kumar M, Gayen K (2011) Developments in biobutanol production: new insights. *Appl Energy* 88:1999–2012. <https://doi.org/10.1016/j.apenergy.2010.12.055>
- Levin DB, Chahine R (2010) Challenges for renewable hydrogen production from biomass. *Int J Hydrogen Energy* 35:4962–4969. <https://doi.org/10.1016/j.ijhydene.2009.08.067>
- Llamas A, García-Martínez MJ, Al-Lal AM, Canoira L, Lapuerta M (2012) Biokerosene from coconut and palm kernel oils: production and properties of their blends with fossil kerosene. *Fuel* 102:483–490. <https://doi.org/10.1016/j.fuel.2012.06.108>
- Marchetti JM, Miguel VU, Errazu AF (2005) Possible methods for biodiesel production. *Renew Sust Energy Rev* 11:1300–1311. <https://doi.org/10.1016/j.rser.2005.08.006>
- Mohan D, Pittman CU Jr, Steele PH (2006) Pyrolysis of wood/biomass for bio-oil: a critical review. *Energy Fuel* 20:848–889. <https://doi.org/10.1021/ef0502397>
- Mohanty P, Nanda S, Pant KK, Naik S, Kozinski JA, Dalai AK (2013) Evaluation of the physiochemical development of biochars obtained from pyrolysis of wheat straw, timothy grass and pinewood: effects of heating rate. *J Anal Appl Pyrolysis* 104:485–493. <https://doi.org/10.1016/j.jaap.2013.05.022>
- Molino A, Nanna F, Ding Y, Bikson B, Braccio G (2013) Biomethane production by anaerobic digestion of organic waste. *Fuel* 103:1003–1009. <https://doi.org/10.1016/j.fuel.2012.07.070>
- Mortensen PM, Grunwaldt J, Jensen PA, Knudsen KG, Jensen AD (2011) A review of catalytic upgrading of bio-oil to engine fuels. *Appl Catal A Gen* 407:1–19. <https://doi.org/10.1016/j.apcata.2011.08.046>

- Murugesan A, Umarani C, Subramanian R, Nedunchezian N (2009) Bio-diesel as an alternative fuel for diesel engines – a review. *Renew Sust Energ Rev* 13:653–662. <https://doi.org/10.1016/j.rser.2007.10.007>
- Mussatto SI, Dragone G, Guimarães PM, Silva JP, Carneiro LM, Roberto IC, Vicente A, Domingues L, Teixeira JA (2010) Technological trends, global market, and challenges of bio-ethanol production. *Biotechnol Adv* 28:817–830. <https://doi.org/10.1016/j.biotechadv.2010.07.001>
- Nanda S, Mohanty P, Pant KK, Naik S, Kozinski JA, Dalai AK (2013) Characterization of North American lignocellulosic biomass and biochars in terms of their candidacy for alternate renewable fuels. *Bioenergy Res* 6:663–677. <https://doi.org/10.1007/s12155-012-9281-4>
- Nanda S, Dalai AK, Kozinski JA (2014a) Butanol and ethanol production from lignocellulosic feedstock: biomass pretreatment and bioconversion. *Energy Sci Eng* 2:138–148. <https://doi.org/10.1002/ese3.41>
- Nanda S, Mohammad J, Reddy SN, Kozinski JA, Dalai AK (2014b) Pathways of lignocellulosic biomass conversion to renewable fuels. *Biomass Convers Biorefinery* 4:157–191. <https://doi.org/10.1007/s13399-013-0097-z>
- Nanda S, Mohanty P, Kozinski JA, Dalai AK (2014c) Physico-chemical properties of bio-oils from pyrolysis of lignocellulosic biomass with high and slow heating rate. *Energy Environ Res* 4:21–32. <https://doi.org/10.5539/eer.v4n3p21>
- Nanda S, Azargohar R, Dalai AK, Kozinski JA (2015) An assessment on the sustainability of lignocellulosic biomass for biorefining. *Renew Sust Energ Rev* 50:925–941. <https://doi.org/10.1016/j.rser.2015.05.058>
- Nanda S, Golemi-Kotra D, McDermott JC, Dalai AK, Gökalp I, Kozinski JA (2017) Fermentative production of butanol: perspectives on synthetic biology. *New Biotechnol* 37:210–221. <https://doi.org/10.1016/j.nbt.2017.02.006>
- Nizami AS, Korres NE, Murphy JD (2009) Review of the integrated process for the production of grass biomethane. *Environ Sci Technol* 43:8496–8508. <https://doi.org/10.1021/es901533j>
- Nygren E, Aleklett K, Höök M (2009) Aviation fuel and future oil production scenario. *Energy Policy* 37:4003–4010. <https://doi.org/10.1016/j.enpol.2009.04.048>
- Patrizio P, Leduc S, Chinese D, Dotzauer E, Kraxner F (2015) Biomethane as transport fuel – a comparison with other biogas utilization pathways in northern Italy. *Appl Energy* 157:25–34. <https://doi.org/10.1016/j.apenergy.2015.07.074>
- Patterson T, Esteves S, Dinsdale R, Guwy A, Maddy J (2013) Life cycle assessment of biohydrogen and biomethane production and utilisation as a vehicle fuel. *Bioresour Technol* 131:235–245. <https://doi.org/10.1016/j.biortech.2012.12.109>
- Qureshi N, Ezeji TC (2008) Butanol, ‘a superior biofuel’ production from agricultural residues (renewable biomass): recent progress in technology. *Biofuels Bioprod Biorefin* 2:319–330. <https://doi.org/10.1002/bbb>
- Ryckeboesch E, Drouillon M, Vervaeren H (2011) Techniques for transformation of biogas to biomethane. *Biomass Bioenergy* 35:1633–1645. <https://doi.org/10.1016/j.biombioe.2011.02.033>
- Savage N (2011) Algae: the scum solution. *Nature* 474:S15–S16. <https://doi.org/10.1038/474S015a>
- Scott SA, Davey MP, Dennis JS, Horst I, Howe CJ, Lea-Smith DJ, Smith AG (2010) Biodiesel from algae: challenges and prospects. *Curr Opin Biotechnol* 21:277–286. <https://doi.org/10.1016/j.copbio.2010.03.005>
- Shay EG (1993) Diesel fuel from vegetable oils: status and opportunities. *Biomass Bioenergy* 4:227–242. [https://doi.org/10.1016/0961-9534\(93\)90080-N](https://doi.org/10.1016/0961-9534(93)90080-N)
- Solomon BD, Barnes JR, Halvorsen KE (2007) Grain and cellulosic ethanol: history, economics, and energy policy. *Biomass Bioenergy* 31:416–425. <https://doi.org/10.1016/j.biombioe.2007.01.023>
- Thamsirirot T, Murphy JD (2011) A critical review of the applicability of biodiesel and grass biomethane as biofuels to satisfy both biofuel targets and sustainability criteria. *Appl Energy* 88:1008–1019. <https://doi.org/10.1016/j.apenergy.2010.10.026>

- United States Energy Information Administration, USEIA (2011) International Energy Outlook 2011. Accessed from: [http://www.eia.gov/forecasts/ieo/pdf/0484\(2011\).pdf](http://www.eia.gov/forecasts/ieo/pdf/0484(2011).pdf). Accessed 3 Jan 2012
- United States Energy Information Administration, USEIA (2017) Total petroleum and other liquids production 2014. <https://www.eia.gov/beta/international/data/browser/>. Accessed 3 May 2017
- Vassilev SV, Baxter D, Andersen LK, Vassileva CG, Morgan TJ (2012) An overview of the organic and inorganic phase composition of biomass. *Fuel* 94:1–33. <https://doi.org/10.1016/j.fuel.2011.09.030>
- von Blottnitz H, Ann M (2007) A review of assessments conducted on bio-ethanol as a transportation fuel from a net energy, greenhouse gas, and environmental life cycle perspective. *J Clean Prod* 15:607–619. <https://doi.org/10.1016/j.jclepro.2006.03.002>
- Wang M, Wu M, Huo H (2007) Life-cycle energy and greenhouse gas emission impacts of different corn ethanol plant types. *Environ Res Lett* 2:1–13. <https://doi.org/10.1088/1748-9326/2/2/024001>
- Xiu S, Shahbazi A (2012) Bio-oil production and upgrading research: a review. *Renew Sust Energ Rev* 16:4406–4414. <https://doi.org/10.1016/j.rser.2012.04.028>
- Yilmaz N, Vigil FM, Benalil K, Davis SM, Calva A (2014) Effect of biodiesel–butanol fuel blends on emissions and performance characteristics of a diesel engine. *Fuel* 135:46–50. <https://doi.org/10.1016/j.fuel.2014.06.022>
- Zacher AH, Olarte MV, Santosa DM, Elliott DC, Jones SB (2014) A review and perspective of recent bio-oil hydrotreating research. *Green Chem* 16:491–515. <https://doi.org/10.1039/C3GC41382A>
- Zhang Q, Chang J, Jun T, Xu Y (2006) Upgrading bio-oil over different solid catalysts. *Energy Fuel* 20:2717–2720. <https://doi.org/10.1021/ef060224o>



Densification of Agricultural Wastes and Forest Residues: A Review on Influential Parameters and Treatments

2

Ramin Azargohar, Sonil Nanda, and Ajay K. Dalai

Abstract

Biomass densification is an effective process to overcome specific biomass application limitations such as low density, nonuniform particle size and shape, and cost of transportation. Lignocellulosic materials (e.g. agricultural wastes and forest residues) are the main precursors used for pelletization. The quality of fuel pellets is determined based on their mechanical strength, hydrophobicity, heating value, and density. These properties are influential in handling, transportation, storage, and fuel applications of this product. There are several parameters affecting the quality of fuel pellets: precursor chemical structure, pelletization operating conditions, precursor pre-treatments, and pellet posttreatments. Formation of a strong binding structure in biomass pellet depends on the internal structure of precursors (e.g. lignin, cellulose, hemicellulose, extractives, moisture), particle size range of precursor, additives (e.g. binders, lubricants, plasticizers, and moisture), and pelletization operating conditions. Pre-treatments such as steam explosion and torrefaction can be used to facilitate the pelletization process or improve some precursor properties such as energy content or hydrophobicity. Post-treatments such as coating and torrefaction are applied to biomass pellets to improve their hydrophobicity or heating value. This chapter provides an overview of the parameters affecting the quality of biomass fuel pellets, biomass pre-treatments, and pellet post-treatments, as well as safety aspects related to transportation and storage of fuel pellets.

R. Azargohar · A. K. Dalai (✉)

Department of Chemical and Biological Engineering, University of Saskatchewan, Saskatoon, Saskatchewan, Canada

e-mail: ajay.dalai@usask.ca

S. Nanda

Department of Chemical and Biochemical Engineering, University of Western Ontario, London, Ontario, Canada

KeywordsBiomass · Binder · Densification · Torrefaction · Steam-treatment · Fuel pellet

2.1 Introduction

Production of value-added products from low-value agricultural wastes and forest residues certainly improves agriculture industry, reduces waste, helps to develop the national/rural economy, and is an effective step to mitigate climate change. Considering the continuous increase in world population, waste biomass is one of the main energy resources for increasing demand for economy and modern life. The estimated world annual available biomass is in the range of ~220 billion dry tons (Torres et al. 2007). Biomass resources are renewable and sustainable and have a great effect on the reduction of carbon emissions as compared to fossil fuels (Tumuluru et al. 2010). Biomass utilization, storage, and transportation are limited because of low density as well as nonuniform shape and size (Gilbert et al. 2009, Bowyer and Stockmann 2001, Sokhansanj et al. 2006). The densification process is critical for producing a solid fuel (pellet) material that could be used and marketed as a commodity product. Biomass densification increases its density up to four times which resulted in the lower transportation cost, smaller required storage area, and less fine particle formation (Gilbert et al. 2009). More uniform and stable size and shape make biomass pellets useable for production of fuel and energy processes such as gasification, combustion, and pyrolysis (Kaliyan and Morey 2009). Densification improves biomass handling and transportation efficiencies throughout the supply chain until the feeding phase in a biorefinery (Tumuluru et al. 2011). Other advantages of biomass densification are simplified mechanical handling and feeding of fuel pellets, uniform combustion in boilers, lower chances of spontaneous combustion in storage, streamlined storage and handling infrastructures, relatively less capital requirement at the biorefinery related to feeding and conversion, reduced chances of feed loss compared to pulverized biomass, and reduced cost of logistics due to improved energy density (Clarke and Preto 2011). The issues which negatively impact the densification process are related to pellet quality and hygroscopic properties of pellets.

To evaluate the quality of fuel pellets, different properties such as density, mechanical strength (hardness, compaction force, etc.), heating value, and moisture uptake (adsorption) are considered and tested. The quality of a fuel pellet is a function of different parameters such as precursor composition, additive concentration and properties, pelletization operating conditions, pre-treatment techniques used for the precursor, moisture content, particle size distribution, type of pelletizer, post-treatments for pellets, etc.

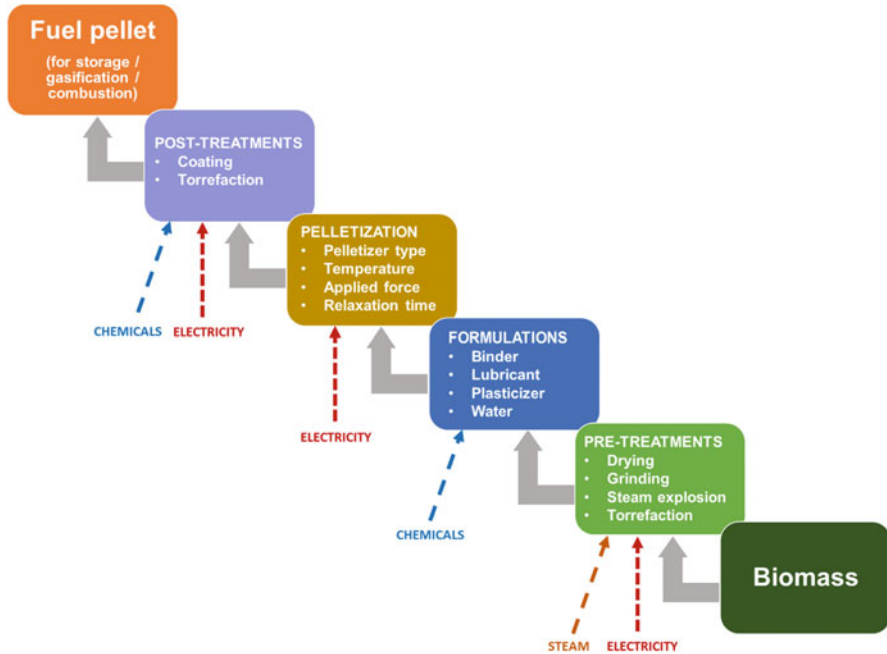


Fig. 2.1 Different steps in the production of durable biomass fuel pellets

These parameters affect the pellet-binding structure and pellet properties. There are different mechanisms involved in densification. Rumpf (1962), for the first time, categorized the mechanisms and forces involved in biomass densification as follows:

- Short-range attraction forces applied between solid particles (such as van der Waals force and hydrogen bond)
- Forces between liquid and particles such as capillary pressure and interfacial forces
- Attraction between molecules of particles (cohesion and adhesion)
- Formation of solid bridges which depend on operating conditions of pelletization (pressure and temperature) and properties of material (precursor and additives)
- Mechanical interlocking between particles, which form closed bonds

Biomass fuel pellet production, as shown in Fig. 2.1, includes different steps. In this figure, these steps and some influential parameters on them, as well as some treatments, are shown. The objective of this chapter is to provide an overview about this production process including biomass pelletization, precursor pre-treatments, most influential parameters on these processes, pellet post-treatments, and risk factors involved in handling and storage of fuel pellets.

2.2 Effects of Moisture Content

Moisture content is one of the most important parameters affecting pellet mechanical properties and stability. Details of some research work on the effects of this parameter are given in Table 2.1. Moisture can act as a binder and develop binding forces (Samuelsson et al. 2012). In addition, the presence of water in the feed facilitates activation of inherent/internal binder and added/external binders (Kaliyan and Morey 2009). Water also acts as a lubricant, which reduces the energy required for the pelletization (Samuelsson et al. 2012). It is reported that by an increase in the contact area between particles, water improves van der Waals forces (Grover and Mishra 1996). Biomass moisture has positive effects on pellet density by reduction of friction between particles that resulted in lower void space in the pellet (Faborode 1989). However, it has also shown that high moisture content (~15 wt%) had negative effects on the corn stover briquette, which could be due to the lubricant characteristics of water resulting in a weak binding structure in densified material and therefore, a decrease in mechanical durability of products (Mani et al. 2006a).

It has been observed that there is an optimum value for moisture content in pellets beyond which pellet's mechanical strength reduces (Kaliyan and Morey 2009; Samuelsson et al. 2012; Turner 1995). It is due to trapping moisture between particles, which causes interference in binder functions, and function of other binding forces (Pickard et al. 1961). For woody material, the hydrogen bond between water molecules and wood polymer units replaces hydrogen bonds between wood polymer units. It makes the material softer and more flexible resulting in less friction in pelletization process. It was observed that for the presence of >20 wt% water in the feedstock, the pelletization failed. It can be due to the drastic reduction in the hydrogen bond between wood polymer units, which reduces the material strength and pellet integrity (Stelte et al. 2011a).

Although moisture content has shown a great effect on the binding mechanism in pellets, no direct effect has been observed for it on pellet heating value (Poddar et al. 2014). Heating value, as a function of pellet internal bonds and ingredient's chemical composition, is not directly related to the moisture content.

2.3 Effects of Pelletization Temperature

Temperature is an influential factor in the deformation and flowability of external or inherent binders in biomass pelletization. Binders, extractives, or other additives, at the optimum range of temperature, go through deformation which results in better binding function for them (Kaliyan and Morey 2009). This phenomenon causes higher mechanical durability for pellets. Details of some research work on the effects of this parameter are given in Table 2.2.

As a typical example, lignin melts at a temperature higher than its glass transition temperature (T_g), flows as a viscous material, participates in the particles' binding structure, and is re-polymerized after cooling down. Choosing the right range of temperature for this process is crucial. Lower temperatures cause no melting of

Table 2.1 Research work on the effects of moisture content on fuel pellets

Raw material	Operating conditions	Pelletizer	Observations	Reference
Norway spruce	Moisture: 0–25 wt%	Single pellet press (SPP) unit	With an increase in moisture content:	Stelte et al. (2011a)
European beech	Temperature: 20 and 180 °C		For woody samples, the pelletizing pressure dropped	
Wheat straw			For wheat straw, this pressure increased	
Eight species of wood sawdust	Moisture: 11–41 wt%	Universal testing machine	No direct effect of moisture content on pellet heating value	Poddar et al. (2014)
	Pressure: 6–20 kN			
	Temperature: 25 °C			
Blends of poplar and pine sawdust	60 g/min, as the feeder flow rate for pelletization of poplar and pine sawdust blends	Pellet mill	An increase in pellet density with increase in inlet moisture in the range of 10–20 wt%	Monedero et al. (2015)
			Higher moisture content caused a decrease in die temperature in the pellet mill	
<i>Miscanthus</i>	Die preheating temperature: 90 °C	Pilot-scale flat ring die pellet mill	For miscanthus, switchgrass, and wheat straw: direct relationship of moisture content with pellet production rate and durability	Jackson et al. (2016)
Corn stover				
Switchgrass			No change in pellet production rate for corn stover with moisture content larger than 15 wt %	
Wheat straw				
Scots pine	Moisture: 8–14 wt%	Pilot mill	With an increase in moisture content:	Samuelsson et al. (2012)
			A decrease in bulk density was noticed	
			A decrease in motor energy consumption was noticed	
Oak	Moisture: 1–16 wt%	Punch-and-die process	5–12 wt% moisture is suitable range for good-quality pellets	Li and Liu (2000)
Oak bark	Pressure: 34–138 MPa		~8 wt% was the optimum moisture content	
Pine	Room temperature			
Cottonwood				

(continued)

Table 2.1 (continued)

Raw material	Operating conditions	Pelletizer	Observations	Reference
Scots pine and bark	Moisture: 11–14 wt%	Hammer mill	An increase in durability with an increase in moisture content was observed	Filbakk et al. (2011)
	Temperature: 90 and 120 °C			
Corn stover briquette	Moisture: 5–15 wt%	Hydraulic press	Lower density at moisture content >10 wt%	Mani et al. (2006a)
	Pressure: 5–15 MPa			

Table 2.2 Research work on the effects of pelletization temperature on fuel pellets

Raw material	Operating conditions	Pelletizer	Observations	Reference
Norway spruce	Moisture: 0–25 wt%	Single pellet press (SPP) unit	With an increase in pelletization temperature:	Stelte et al. (2011a)
European beech	Temperature: 20 and 180 °C		Pressure required for pelletization decreased	
Wheat straw				
Norway spruce	Temperature: 20 and 100 °C	Single pellet press (SPP) unit	At higher pelletization temperature:	Stelte et al. (2011b)
European beech	Moisture: 10 wt%		Higher compression strengths of the pellets were observed	
Wheat straw			Stronger pellets from hardwood comparing with that from softwood were generated	
Canola meal	Temperature: 60–90 °C	Lab-scale single-pelleting unit	An increase in pelletization temperature:	Tilay et al. (2015)
	Pressure: 75–120 MPa		Increased pellet density and decreased pellet expansion for pelletization load up to 105 MPa were found	
Olive tree pruning residues	Temperature: 60–150 °C	Lab-scale pellet press	Temperature was the most influencing parameter	Carone et al. (2011)
	Pressure: 71–176 MPa		At temperature >100 °C, pellet mass loss was observed due to the moisture evaporation	
	Moisture: 5–20 wt%		Compressive modulus of elasticity (E) for pellets was directly related to temperature	

binder, and higher temperatures can result in decomposition of other constituents of biomass, such as pyrolysis of cellulose (Yang et al. 2007). Stelte et al. (2011a, b) have shown that to produce a pellet with suitable mechanical strength, an increase in temperature decreases the pressure required for pelletization, in a single pellet press (SPP) unit, for beech, spruce, and straw precursors. This trend is due to the lower friction at higher temperatures in the press channel of the pelletizer. This change in

friction is more pronounced in hardwoods compared with softwoods (Nielsen et al. 2009) and can be related to the softening and migration of biomass extractives and biopolymers (Finell et al. 2009; Stelte et al. 2011b). Pellets made from hardwood material (beech) were stronger than those made from softwood material (spruce), which can be related to the lower glass transition point of lignin in hardwoods (Stelte et al. 2011b).

Tilay et al. (2015) studied the effect of pelletization operating conditions on the pellets produced from canola meal using a binder, a lubricant, and moisture. They found that an increase of temperature up to 90 °C increased the pellet density. However, this trend is valid for the pelletization force up to 3500 N. For higher pelletization forces, a part of feedstock came out of the die and weakened the binding structure, which can be related to extractives present in canola meal.

There can also be interactions between the temperature and moisture affecting the pellet quality. Carone et al. (2011) observed the determinant effect of pelletization temperature (60–150 °C) on pellet quality produced from olive tree pruning residues in a lab-scale pellet press. There was a reduction in pellet mass for pelletization temperature >100 °C, due to the water evaporation. This decrease was higher for samples with more initial moisture contents. Pellet-specific rigidity (compressive modulus of elasticity) and pellet density showed a direct relationship with temperature. They suggested that the effects of temperature on pellets' properties are due to changes in biomass-building material (such as lignin, starch, and protein) with temperature.

2.4 Effects of Pelletization Pressure (Applied Force)

The compressive pressure used for densification can provide more compact structure in the pellets. Its effect is studied mostly in interactions with other parameters. This pressure can have positive and negative effects on the pellet properties. Details of some research work on the effects of this parameter are given in Table 2.3. Stelte et al. (2011a) studied the relationship between pelletization operating conditions and pellet properties with the pressure built up in the channel of a pellet mill for beech and spruce precursors. At the steady-state condition, effects of pressure in the range of 50–550 MPa on the pellet density were measured. It showed that up to 250 MPa, density increased with an increase in pressure, but after that, increase in pellet density was not significant. They related this phenomenon to the approach of pellet density obtained by this process to the density of plant cell wall (1,420–1,500 kg/m³).

Poddar et al. (2014) observed mass loss during pelletization. They related this fact to the removal of water from pellet by increasing pressure resulting in an increase in friction and temperature in the die. In addition, pellet density increased significantly with an increase in pressure at the beginning, but for the higher pressures, it was minor. Pressure showed no clear effect on the higher heating value of pellets. It shows that atomic-level bonding structure of biomass has a determinant effect on higher heating value (HHV).

Table 2.3 Research work on the effects of pelletization pressure on fuel pellets

Raw material	Operating conditions	Pelletizer	Observations	Reference
Corn stover briquette	Pressure: 5–15 MPa	Hydraulic press	With an increase in pressure:	Mani et al. (2006a)
	Moisture: 5–15 wt%		Durability and density increased for moisture content ≤ 10 wt%	
			Consumption energy increased	
Norway spruce	Moisture: 0–25 wt%	Single pellet press (SPP) unit	With an increase in pressure (≤ 250 MPa), pellet density increased	Stelte et al. (2011a)
European beech	Temperature: 20 and 180 °C		For $P > 250$ MPa, only minor change in density was observed	
Wheat straw	Compaction pressure: 50–550 MPa			
Eight species of wood sawdust	Moisture: 11–41 wt%	Universal testing machine	There was an increase in density, but it became minor at higher pressures	Poddar et al. (2014)
	Pressure: 6–20 kN		No relationship between pressure and HHV	
	Temperature: 25 °C			
Canola meal	Temperature: 60–90 °C	Lab-scale single- pelleting unit	With an increase in applied force:	Tilay et al. (2015)
	Pressure: 75–120 MPa		Relaxed density and mechanical strength of pellets decreased	
Barley straw	Particle size: 3.2, 1.6, and 0.8 mm	Single pelleting unit	With an increase in compressive pressure, pellet density increased and approached particle density	Mani et al. (2006b)
Corn stover	Moisture: 12 wt% and 15 wt%			
Wheat straw	Compressive pressure: 35–155 MPa			

Mani et al. (2006a) observed an interaction between pelletizer pressure and initial moisture content of feed (corn stover) on the briquette density and durability. With an increase in pressure, density increased for moisture content up to 10 wt%. For larger moisture content (15 wt%), a decrease in density was observed. The same trend was shown for durability of products. They also found that there is a direct relationship between energy consumption for briquetting process and applied pressure. Tilay et al. (2015) investigated the effects of pressure (3,500–4,500 N) on the canola meal pellets prepared at 60 °C. With an increase in pressure, relaxed density and mechanical strength (hardness and durability) of pellets decreased. They related

this observation to the plastic deformation of the material, which makes it more flowable and results in weak binding structure.

Mani et al. (2006b) investigated the effects of pelletization operating conditions on the quality of pellets made from grasses. They found that with an increase in compressive pressure (35–155 MPa), pellet density increased for all precursors (wheat straw, barley straw, corn stover, and switchgrass). The only precursor, which could approach its particle density at lower pressure (~70 MPa), was corn stover. It was due to the protein portion of this precursor, which melted at pelletization temperature and acted as a binder. Therefore, at pressures >70 MPa, only gradual changes in pellet durability were observed for this precursor.

2.5 Effects of Particle Size

Better mechanical interlocking for particles and fibers can be expected for smaller particle size in densification process (Kirsten et al. 2016). This effect is observed and interpreted by different researchers in different ways. Details of some research work on the effects of this parameter are given in Table 2.4. Arzola et al. (2012) showed that smaller particle size of precursor (oil palm shell) provided higher pellet density. They found that the effect of particle size on pellet density was more important than the effect of binding agent (molasses) concentration. They observed that particle size after binder concentration was the most influential parameter on the mechanical durability of pellets. With an increase in the particle size, durability decreased. They concluded that for larger particle size range, the connection between particles on the pellet surface is more difficult resulting in a decrease in adhesion area, increase in friction, and development of a rough surface. All these parameters lead to lower mechanical durability.

Haruna and Afzal (2016), who worked on the blending agricultural biomass with woody biomass, showed that density of biomass precursor and blended biomass, both, increased with a decrease in feed particle size. In addition, they observed that stronger pellets could be produced from the precursor with smaller particle size range. They related these observations with filling the gaps in each layer of the pellet with particles from neighboring layers during densification, which can be performed better using smaller particles.

Mani et al. (2006b) investigated the effects of different pelletization parameters on the mechanical strength of grass biomass pellets. They found that hammer mill screen size (0.8–3.2 mm) was an effective parameter on the density of pellets made from barley straw, corn stover, and switchgrass, but not for wheat straw. Wang et al. (2018) studied the effects of particle size (1.8–15 mm) on rice straw briquette. They showed that the effect of particle size on density and mechanical strength is more pronounced for milled material (1.8 mm) compared with that for chopped material (5–15 mm). They related that to better flow of biomass natural binders through smaller particles.

Table 2.4 Research work on the effects of precursor particle size on fuel pellets

Raw material	Operating conditions	Pelletizer	Observations	Reference
Oil palm shell	Particle size: 160–570 μm	In-house built cylindrical pelletizer unit	With an increase in particle size, density and mechanical durability decreased	Arzola et al. (2012)
	Temperature: 75–85 $^{\circ}\text{C}$			
	Pressure: 100 MPa			
	Binder (molasses): 15–25 wt%			
Agricultural and wood biomass blends	Particle size: 150–300, 300–425, and 425–600 μm	In-house built single unit pelletizer	Mechanical strength and density increased with a decrease in particle size	Haruna and Afzal (2016)
	Temperature: 80–85 $^{\circ}\text{C}$			
Barley straw	Particle size: 3.2, 1.6, and 0.8 mm	Single-pelleting unit	Particle size had significant effect on density of pellets made of all precursors except wheat straw	Mani et al. (2006b)
Corn stover	Moisture: 12% and 15% wt basis			
Switchgrass	Compressive forces: 1,000–4,400 N			
Wheat straw				
Rice straw	Particle size: 1.8–15 mm	Self-designed single-pelleting unit	Particle size effects were more visible for milled material compared with chopped material	Wang et al. (2018)
	Temperature: 120 $^{\circ}\text{C}$			
	Pressure: 30 kN			
	Moisture: 15 wt %			

2.6 Effects of Binders and Extractives

To improve pellet quality and reduce the energy required for pelletization, binders can be used for densification (Peng et al. 2015). Some natural binders present in the structure of biomass are lignin, protein, starch, water, and fat. In addition, different types of external binders are used for pelletization.

Stelte et al. (2011b) studied the effects of lignin, hemicellulose, and extractives (mainly waxes) in the binding structure of pellets made of beech (hardwood), spruce (softwood), and straw (grass) at 100 $^{\circ}\text{C}$. T_g value is lower for lignin in hardwood compared with that in softwood. Therefore, they concluded, for beech pellets, probably voids and gaps in pellet structure can be filled with solid bridges made

by lignin flow, which increases interparticle contact area. However, in the case of spruce, the temperature was not enough to pass T_g of inherent lignin, as shown by lacking solid bridges between particles in SEM micrographs. They stated that solid bridges can be made by hemicelluloses also, but due to their low molecular weight, comparing with lignin, their cohesive strength is weak. The voids between particles of straw pellet were larger than those for other two precursors' pellets. It was due to the lack of plastic flow from biomass polymers. In addition, particle surface area and hydrogen bonding structure were weak due to the larger extractive (wax) content of straw.

Using SEM micrographs, Tumuluru (2014) showed that inherent lignin in corn stover, after reaching T_g , can either develop cross-links with other components in feedstock or agglomerate in ball form instead of building bridges between particles. He suggested that denaturation and gelatinization of protein and starch at high temperatures resulted in the formation of complexes which participate in binding structure. The effects of protein as one of the constituents of biomass are not described well yet. Some positive effects are observed regarding its role in densification process (Kaliyan and Morey 2010).

Extractives in wood include a broad range of chemicals such as waxes, fatty acids, sterols, and resin compounds (Finell et al. 2009). Stelte et al. (2011a) showed that extractives decreased friction between biomass and die due to their lubricating properties. They found that easier pelletization (lower pressure required) of softwood material (spruce) compared with hardwood (beech) is related to its higher extractive content.

Peng et al. (2015) used raw biomass (pine sawdust) as a binder to pelletize torrefied sawdust. This work showed that sawdust binder works well for all treated samples prepared using torrefaction up to 300 °C. Addition of sawdust (0–30 wt%) caused a slight increase in the density of pellets. They related it to the fact that this binder (sawdust), at the low pelletization temperature (110 °C), can only fill the pores in the range of micrometers. These gaps are created during torrefaction process by removal of volatiles. To cover the gaps in the range of nanometers, higher temperatures (~220 °C) are required to activate high melting point lignin. The Meyer hardness of pellets made using binder showed an improvement. The HHVs of pellets (20.4–22.3 MJ/kg) were smaller than that for torrefied precursor (22–23 MJ/kg) due to the low value of HHV for sawdust. The energy required for pelletization decreased with an increase in the binder concentration.

In their research, Peng et al. (2015) also used lignin and starch as a binder. These binders showed an improvement in mechanical durability of pellets due to adhesion forces and solid bridges between particles of starch and lignin, respectively. However, these binders, at ~110 °C as pelletization temperature, could not fill the pores in the range of nanometers. Finney et al. (2009) used starch (organic binder) and caustic soda (inorganic binder) for pelletization of spent mushroom compost and coal tailing. They found that up to 1 wt% of both binders can improve the tensile strength of pellets but more concentrations weakened the pellets. The starch binding function is suggested to be related to its solubilization and crystallization in biomass, which develops cohesion binding between particles (Thomas et al. 1998).

Soleimani et al. (2017) used carbohydrate with low molecular weight (including molasses, fructose, maltodextrin, sucrose, and glucose) as a binder (4–12 wt%) for pelletization of spruce wood shavings and wheat straw. The main advantage of this family of binders is that they include no ash, nitrogen, and sulfur. Therefore, during gasification process, their respective pellets will generate less amount of toxic and corrosive material. In addition, they studied the effects of four lubricants (including crude glycerol, canola oil, mineral oil, and pure glycerol), with 5 wt% concentration, on the pellet quality. For spruce wood, use of fructose (binder) and canola oil (lubricant) showed the best performance. For wheat straw, use of molasses or fructose (as the binder) and crude glycerol or canola oil (as the lubricant) showed convincing quality for pellets. For both precursors, an increase in the binder content caused an increase in pellet durability. They tried their formulations in a pilot-scale pelletizer too. Pure glycerol as lubricant did not work for this system, and pelletization failed. They found that pure glycerol mostly acts as a binder rather than a lubricant. An increase in binder content increased the energy consumption for pelletization, but an increase in lubricant content showed a reverse trend. Addition of crude glycerol as lubricant slightly increased HHV of the pellet, which is related to the presence of fatty acids and biodiesel in crude glycerol.

Carboxymethyl cellulose (CMC) was used as a binder by Si et al. (2016) for pelletization of agricultural wastes. Its binding property comes from its source, which is a polyelectrolyte material and is able to improve electrostatic forces and hydrogen bonds on the particle surface. It worked for biomass feedstock with a low amount of extractives (≤ 5 wt%). It could improve mechanical durability, relaxed density, and compressive strength. In addition, it decreased the energy required for compression during densification. This function is related to light hydrocarbons present in wax and oil, which can be repelled by CMC and ended up at the surface of the pellet. This layer can decrease friction between material and mold. For the feedstocks with a high percentage of extractive, especially waxes, CMC showed opposite effects due to its oleophobic characteristic.

Emadi et al. (2017) used polymer plastic binder (linear low-density polyethylene, LLDPE) for improving the quality of pellets produced from torrefied wheat and barley straws. LLDPE is extracted from municipal solid waste. It has a greater HHV (42 MJ/kg) and tensile strength (17.8 MPa). About 6 wt % of LLDPE was the optimum value of binder for both precursors to achieve the maximum relaxed density. Addition of this binder (up to 10 wt%) increased the HHV, fracture load, and tensile strength of pellets. The addition of the binder decreased the ash content of pellets. An increase in the HHV and mechanical strength can be directly related to the high value of these properties for the plastic binder. Miao et al. (2013) showed that binder (steep water) slightly increased the compression energy. They suggested it could be because of converting biomass particle to stiffer and harder material by applying binder.

2.7 Biomass Pre-treatments

Different types of pre-treatments are used for biomass precursors before densification process. The main objective of pre-treatment is the structural change in biomass feedstock to make it more suitable for pelletization of switchgrass. The two most known pre-treatments are steam treatment and torrefaction.

2.7.1 Steam Explosion

Steam explosion, also known as autohydrolysis, deals with exposing biomass with steam (typically at 140–260 °C) and then a sudden drop in the pressure to atmospheric pressure. It affects the main components of biomass (Biswas et al. 2011). During the pressurization step, the hydrolysis of hemicellulose and activation of lignin occur, and after pressure drop, biomass fragmentation/mechanical disruption happens (Kumar et al. 2009; Ramos 2003). It breaks down the biomass original structure, makes biomass-building polymers more accessible, and increases the brittleness of material (Martín-Sampedro et al. 2011; Pu et al. 2008). This treatment is found specifically effective for agricultural residues and hardwoods (Sun and Cheng 2002). It is reported that pellet made of treated precursor showed higher mechanical strength due to activation of inherent lignin. Steam treatment affects lignin and cellulosic structure of biomass (Zandersons et al. 2004). Activated lignin, at temperatures higher than its glass transition point, can flow and form bonds between particles as an effective binder (Kaliyan and Morey 2010). This process has increased the portion of particles with lower particle size. In some cases, it resulted in an increase in HHV due to the removal of volatiles. However, for some precursors, this treatment increased the total energy required for pelletization of precursor.

Lam et al. (2015) used steam treatment (5 min and 220 °C) on oil palm residues as a pre-treatment before densification. This process increased mechanical strength (Meyer hardness and maximum breaking strength) of pellets made from both precursors: empty fruit bunch (EFB) and palm kernel shell (PKS). In addition, it improved dimensional stability for these pellets. On the other side, this pre-treatment increased the compression energy required for densification and ash content of treated pellets. Removal of volatiles and moisture using this process increased HHV of FEB pellets for 21%, but there was not a significant change in HHV for PKS. They observed no significant change in density for treated samples at the severe process conditions they used for the process compared with other researchers. For treated FEB, the required extrusion and total energy were larger than that for an untreated sample, which is related to the rougher surface and monosaccharide presence on the pellet surface resulting in more friction during densification.

The more dimensional stability of the pellets produced from treated samples is due to hydrolysis of hemicellulose resulting in the formation of the cellulose-lignin matrix with a strong structure. The large extractive amount in the precursor can cause diffusion resistance for penetration of steam into the biomass structure, and it reduces the effects of the process on lignin activation (Lam et al. 2015). Tooyserkani et al. (2012) studied steam treatment (5 min and 220 °C) of three softwood species which were pine, spruce, and Douglas fir and one sample of bark from Douglas fir. This process made samples' color darker. The particle size of softwood species reduced after steam treatment. In addition, they observed a slight decrease in density of treated softwood pellets and larger mechanical strength for these pellets. This treatment increased the compression and extrusion energy required for densification of these pellets.

The lower particle size of steam-treated samples is more pronounced for wood-based samples. It is related to the explosion on the wood surface, after decreasing the pressure at the end of the process, which produces smaller particles (Lam 2011). The larger portion of small particle size after steam treatment results in fewer voids in pellet and increases the hardness (Tooyserkani et al. 2012).

Increase in energy required for densification of steam-treated pellets can be related to the removal of extractives observed during steam treatment (Tooyserkani et al. 2012). Lubrication and plasticization effects of volatiles (Nielsen et al. 2009) play an important role in the reduction of pellet densification energy requirements. Lam (2011) investigated the effects of steam treatment operating conditions (residence time and temperature) on the pellet quality. Pellets prepared from treated samples showed higher mechanical strength, less moisture adsorption rate, and less expansion after densification. Treated biomass/pellets showed higher cellulose crystallinity compared with untreated biomass/pellet. However, the energy required for densification of steam-treated pellets was more than that for untreated pellets.

Biswas et al. (2011) studied the effects of steam treatment on the precursor (*Salix*) and pellets produced from it. It was observed that the process increased carbon content and decreased oxygen content, while there was no significant change in hydrogen content. In addition, the ash content of precursor decreased by this process. They showed an enhancement in pellet density and its abrasive and impact resistance. They observed a mild reduction in volatile content and increase in fixed carbon content due to the steam treatment. They found that ash content of the treated sample was less than the original precursor. After damage to biomass cell structure by steam treatment, these mineral compounds can be removed by water leaching. In addition, they realized alkali metal content, such as potassium, decreased by this treatment. Considering the corrosive effects of potassium in pellet combustion in boilers, it is an industrially attracting point for application of treated samples. They observed a decrease in contents of some heavy metals (e.g., Ba, B, Co, Zn, and Cd), which is environmentally beneficial. Pellets produced from treated sample showed larger density and durability. The larger mechanical resistances observed for pellet can be attributed to the formation of lignin layer on the surface (Angles et al. 2001).

Adapa et al. (2010) worked on the effects of steam treatment on barley, canola, oat, and wheat straws. They observed an increase in cellulose content and a decrease

in lignin content for all precursors after the treatment. Ash content also increased except for canola straw. A slight increase in HHV was observed for all precursors after the treatment. During pelletization, with an increase in pressure at high values (≥ 94.7 MPa), no significant increase in pellet density was observed due to the approaching density values to particle density for each precursor.

2.7.2 Biomass Torrefaction

Torrefaction is a thermochemical treatment, which can be applied to the biomass feedstock. It is performed in the absence of oxygen or with a very low oxygen content (< 6 vol% O_2) and at a temperature range of 200–300 °C (Stelte et al. 2011a, b; Mei et al. 2015). It degrades the biomass polymers, especially hemicellulose, and removes moisture and volatiles (van der Stelt et al. 2011; Rudolfsson et al. 2015) but increases the energy density of the material. In general, this process results in more brittle (grindable) material, higher energy density, more homogeneous material, more thermally stable material, and more hydrophobic characteristic. Better grindability is related to the decrease of viscoelastic properties of biomass (Ohliger et al. 2013). It is reported that torrefied material needs more energy for pelletization due to the excess friction in die channel (Li et al. 2012). This process makes precursor's color darker, with an increase in temperature, which is related to the changes in the acid-insoluble lignin portion of biomass (González-Peña and Hale 2009).

Bergman et al. (2005) have categorized the torrefaction steps into the following four steps: moisture evaporation, hemicellulose decomposition, lignin decomposition, and cellulose decomposition. At ~ 200 °C, decomposition of hemicellulose starts, and from ~ 250 to 260 °C, slight decomposition of lignin and cellulose starts (van der Stelt et al. 2011). Phanphanich and Mani (2011) showed that there was a linear decrease in the grinding energy with an increase in the torrefaction temperature for forest biomass. In addition, HHV of the torrefied sample was higher than that for the original precursor. Elemental and proximate analyses of the torrefied sample showed coal-like characteristics for them.

For Norway spruce, Rudolfsson et al. (2015) have shown that torrefaction changes the chemical composition of material including an increase in carbon content, decrease in the oxygen content, mild decrease in hydrogen content, and an increase in ash content. It means a reduction in O/C and H/C atomic ratios, which on the van Krevelen diagram shows more coal-like characteristic for treated biomass/pellet. Rudolfsson et al. (2017) studied the effects of different parameters in an industrial setup including torrefaction and pelletization, for wood chips of Scots pine. They found that torrefaction temperature was an influential factor in the pellet density, durability, and power required for pelletization, but no effects were observed from torrefaction time on these parameters. The screen sizes (sieve) used for grinding torrefied material showed no effects on the pellet quality. A higher degree of torrefaction resulted in larger brittleness for torrefied material.

The pellet quality is a function of biomass precursor, torrefaction operating conditions, and pelletization operating conditions. Stelte et al. (2011a) have shown that, for spruce, with an increase in the torrefaction temperature (250–300 °C), there was a decrease in the compression strength of pellets produced from torrefied spruce compared with that prepared from raw spruce. They related it to the degradation of carbohydrates (especially hemicellulose), the removal of extractives, and a decrease in the number of hydrogen bonding sites with an increase in the torrefaction temperature. They concluded that there was a need for adjusting the torrefaction operating conditions to achieve a controlled material degradation in biomass. It results in a balance between mechanical strength and other properties (such as hydrophobicity, heating value, grindability) of produced pellets. Wang et al. (2013) showed that making pellets from sawdust torrefied under oxidative torrefaction (3–6% O₂) atmosphere needed higher die temperature for achieving the same mechanical strength of pellets made from untreated sawdust.

Co-pelletization has been investigated as a solution to increase the mechanical strength and decrease the energy required for pelletization of torrefied biomass. Cao et al. (2015) used oil cake as an additive for pelletization of two forest residues. Oil cake reduced negative effects of torrefaction such as high-energy consumption and mechanical strength. Oil cake is a lubricant, which decreases the energy required for pelletization. In addition, protein and starch present in oil cake can act as a binder and enhance pellet mechanical strength.

Another parameter, which can affect the quality of pellets produced from the torrefied precursor, is particle size of feedstock. Peng et al. (2012) showed that with a decrease in particle size (0–1000 µm), pellets from torrefied sawdust needed less energy for pelletization and had larger Meyer hardness as well as hydrophobicity. In addition, they showed that a higher degree of torrefaction (temperature and time) increased the energy required for pelletization, while it improved hydrophobicity and hardness of pellets.

Wet torrefaction has also been tried, at the hot compressed water (175–225 °C and 15–250 bar), for Norway spruce and birch (Bach et al. 2013). With an increase in process temperature and/or residence time, yield decreased but fuel properties such as HHV, hydrophobicity, and grindability improved. A reduction in the particle size decreased the solid yield. This process decreased the ash content of torrefied material compared with raw biomass due to the water leaching effect.

Kumar et al. (2017) reviewed the effects of torrefaction integration in a wood pelletization unit. For upstream integration of torrefaction unit, they stated the following benefits: large durability and density for final pellets and lower energy requirements for grinding torrefied biomass. However, they emphasized on the following drawbacks of this arrangement: more difficult pelletization and possible need for binder for effective pelletization of torrefied biomass, more fine production from the torrefied precursor and possibility of dust explosion, as well as higher capital cost for torrefaction unit considering larger torrefaction unit needed due to lower bulk density of torrefied biomass.

2.8 Pellet Post-treatments

2.8.1 Pellet Coating

During transportation and storage, the pellets absorb moisture, which results in a decrease in its density, lower mechanical strength, and finally disintegration. In addition, this increase in moisture content increases the biological activities in pellets and decreases its heating value. Hydrophobic coatings can be applied to the pellets to make them water-resistant.

Craven et al. (2015) used oils (paraffin oil, castor oil, mineral oil, and linseed oil) for hydrophobic coating of wood pellets. These treated pellets after submerging in water could remain integrated up to 1800 s. However, the untreated pellet lost its integrity after 300 s. This treatment increased the volumetric energy content of treated pellets in average $\sim 11.8\%$ compared with the untreated pellet. The proximate analysis showed that this post-treatment increased the volatile content of pellet and decreased the fixed carbon and moisture content. However, they estimated this treatment would increase CO_2 formation from pellets during combustion by 3.1% per unit mass of combusted pellet. In addition, this treatment probably decreases the self-heating temperature of pellets in storage condition due to the lower self-heating temperature for mineral oils.

Tilay et al. (2015) applied an industrial coating, with the concentration of 4 wt% in $\sim 85\%$ isopropyl alcohol, on the canola meal pellets. After drying, the pellets were exposed to the ambient temperature. After 8 weeks, these pellets adsorbed no moisture, and their durability ($\sim 98\%$) and hardness (~ 168 N) did not change. However, uncoated pellets, at the same conditions, had 1.1% water adsorption, and there was a significant decrease in their durability ($\sim 48\%$) and hardness (~ 117 N), which can be related to the moisture adsorption.

2.8.2 Pellet Torrefaction

Torrefaction has been used as a post-treatment for fuel pellets to increase its heating value and hydrophobicity. In addition, it converts different biomass precursors to a more uniform material whose properties are closer to those for coal (Ghiasi et al. 2014). To overcome the problems of making pellet from torrefied biomass (such as high friction in the die channel) and low dimensional (especially longitudinal) stability of these pellets, some efforts are performed to study the effects of torrefaction after pelletization of precursor. Optimization of the torrefaction operating conditions can result in a suitable combination of properties for pellets, which can satisfy thermal and mechanical requirements. For example, mass loss occurred by torrefaction process can be compensated by the increase in the heating value of the material, and an optimum value of process temperature can be determined using the result of experiments (Shang et al. 2012).

Ghiasi et al. (2014) studied the energy efficiency and pellet quality for two schemes of fuel pellet production from wood chips. For Scheme I, first they torrefied

the precursor and then pelletized this treated precursor. In Scheme II, the untreated precursor was pelletized, and then, these pellets were torrefied. Due to problems for pelletization of torrefied sample in Scheme I, they added 7 wt% of wheat flour, as a binder, to the torrefied sample before pelletization. This binder helped in making strong pellets from the torrefied material. Without a binder, the pelletization of torrefied material was difficult and needed a large amount of energy (~1,164 kJ/kg). Pelletization using binder needed only ~40% of the energy consumed for pelletization of torrefied material. In total, use of binder decreased the total energy required for Scheme I by ~15%. They also observed that dry matter loss and energy consumption for torrefaction step in both schemes were very close. Nearly 79% of original feedstock was converted to pellets for Scheme I (when binder was used for the process), but this yield for Scheme II was 81%. The main weight loss for Scheme I was for pelletization process, but for Scheme II, the weight loss was caused by torrefaction. A final moisture content of pellets for Scheme I was ~8 wt%, but that for Scheme II was lower (~3%). The lower moisture content of pellets obtained by Scheme II is an advantage for their transportation and storage. Torrefaction decreased the density of pellets by ~11%, and these pellets produced by Scheme II had a lower density (~15%) than pellets obtained from Scheme I. There was not a significant difference in durability of pellets produced from both schemes. The pellets produced from Scheme II showed much better integrity in water compared with Scheme I pellets. Scheme II pellet showed higher HHV (~6%) and larger carbon content (51.2 wt% vs 49.5 wt%) too. Finally, they concluded that Scheme II is a promising pathway compared with the first pathway.

Shang et al. (2012) performed thermochemical torrefaction on pellets made of Scots pine at temperatures of 230–270 °C with the residence time of 1 h. With an increase in temperature, pellets become darker, the pellets were not shiny, and smoothness of the pellet decreased. HHV of pellets increased by ~32% at the highest torrefaction temperature compared with that for the untreated pellet. For temperature >250 °C, a sharp decrease in mass and energy (on a mass basis) of treated pellets was observed. They related this decrease to strong decomposition of hemicellulose and partial decomposition of cellulose at this range of temperature. The mechanical strength of pellets decreased with an increase in temperature. Based on their observations, they recommended a torrefaction temperature ≤250 °C, which makes a balance between mechanical strength reduction and increase in energy content as well as the hydrophobicity of treated pellets. They also observed no significant dimensional changes in pellets due to lack of springback effect.

Some researchers have used microwave torrefaction for this step. They found this method to be efficient in the increase of energy density of pellet and its hydrophobicity. However, this process, depending on the operating conditions used, can lower mechanical strength of pellets. This method needs no drying for pellets due to the positive effect of moisture in the absorption of microwaves (Thostenson and Chou 1999; Ren et al. 2012).

Ren et al. (2012) used microwave torrefaction for Douglas fir sawdust pellets at a temperature range of 250–300 °C and residence time of 10–20 min. The yield of pellet obtained from the process decreased with an increase in temperature or

residence time. They observed a reverse trend for the yield of bio-oil and non-condensable gases obtained from the process. At temperatures $<250\text{ }^{\circ}\text{C}$, hemicellulose degradation is a source of mass loss, but at temperatures $>270\text{ }^{\circ}\text{C}$, deformation of cellulose and lignin happens (Chen and Kuo 2011; Prins et al. 2006; Ren et al. 2012). Non-condensable gases released were CO_2 for $250\text{ }^{\circ}\text{C}$ and CO , CO_2 , and low amount of light hydrocarbons for higher temperatures. HHV of the pellets increased with an increase in temperature and residence time. The maximum increase in HHV was $\sim 30\%$ compared with that for the untreated pellet. The density of treated pellets was 8–28% less than that for untreated pellet depending on the operating conditions used. The energy yield (calculated based on HHV and density) of the treated pellets decreased significantly with an increase in temperature, but the effect of residence time on energy yield was weaker.

In their review on the effects of torrefaction integration in a wood pelletization unit for downstream integration of torrefaction unit, Kumar et al. (2017) emphasized on the following benefits: (i) more hydrophobicity of final pellets, (ii) lower capital cost required for torrefaction unit due to larger density of pellets compared with that for torrefied precursor, and (iii) no changes required in the existing grinding and pelletization units. They also highlighted the following drawbacks for this arrangement: (i) lower mechanical durability and density for final pellets compared with those for untreated pellets, (ii) careful design needed for torrefaction reactor to prevent damage to pellets and increase the mass loss, and (iii) possible mass loss during transportation and storage due to the production of fines and dust.

2.9 General Risk Evaluation for Handling and Storage of Biomass Pellets

Similar to untreated biomass that is often connected to major problems such as dust formation, self-heating, off-gassing, and biological decomposition, biomass pellets are also subject to risk evaluation. A few factors should be considered during safety handling and storage of large amounts of biomass pellets. The quality of biomass pellets could largely vary depending on the source and origin of biomass, biomass particle size and shape, biomass pore volume, biochemical composition, moisture content, pellet size and shape, etc. Biomass pellets are sensitive to physical wear and tear during transportation and storage. Poor-quality biomass pellets occur as a result of either poor-quality manufacturing or transfer of moisture during transportation, handling, or storage. Some general factors that should be considered during handling and storage of biomass pellets are comprehensively described by Stelte (2012) and also summarized in this section.

2.9.1 Dust Formation

Health and safety are important concerns with the formation of fine particles from biomass handling, which can result in dust explosions and the spontaneous

combustion of pellets during storage and transportation. Handling of poor-quality and less durable biomass pellets can liberate a significant amount of dust. Chopped or pulverized biomass particles can release significant amount of dust due to low density. The high drag coefficient of biomass dust particles leads to their easy dispersion in the air. If inhaled, the airborne biomass dust particles pose a significant health risk, especially to the lungs, nasal canal, and respiratory system. Excessive and repeated exposure to biomass dust particles can cause severe allergies (rashes, soreness, and conjunctivitis), coughing, and other respiratory illness. Apart from health hazards, the risk of explosion and fire is also associated with dust arising from biomass pellets. Biomass dust is more flammable than the biomass pellet due to its relatively high surface area. The accumulation of biomass dust can be ignited through electrostatic discharges, sparks generated by metal pieces, heat generated through friction, overheating of motors and conveyer belts, and flammable materials at the storage area. In British Columbia, Canada, three consecutive fatality cases in sawmills were reported in 2012, which were due to biomass dust explosion (Zeeuwen 2012). Dry and fine biomass dust particles create dust cloud, which when ignited can lead to a violent explosion.

In the cases of fire and explosion in the flat storage area or silos, water is not the preferred fire extinguisher. This is due to the fact the biomass pellets can absorb water and swell to more than four times their original size and/or form slurry often difficult to remove from the silos. Therefore, inert gases such as N_2 and CO_2 and inflammable foams are desired fire extinguishers in pellet silos.

2.9.2 Self-Ignition and Self-Heating

As discussed in the previous subsection, fine dust particles and dust cloud arising from poor-quality biomass pellets can cause fire and explosion. However, fire can also occur by self-heating and self-ignition of biomass pellets due to oxidation and microbial decay. The main factors affecting the self-heating in a pellet storage silo are temperature, moisture, size of the biomass pellet, and particle density. Fresh and high moisture-containing biomass is prone to self-heating and self-ignition by oxidation reactions (Saidur et al. 2011). The oxidation rate of the biomass pellets decreases with their storage time. With the aging of biomass, oxygen starts to deplete posing a potential threat to pellet-handling personnel.

The moisture content and surface area of biomass pellet can lead to microbial decomposition and self-heating as the decaying process is enhanced at high temperatures. Moisture in biomass can be inherent or from external sources such as rain or water leakage at poor storage areas. Depending on the type of microorganism, decomposition of biomass pellets can increase their temperature up to 80 °C, unlike chemical degradation, which raises the temperature up to 40 °C (Stelte 2012). Due to the insulating properties of biomass and its poor heat transfer, the heat is usually accumulated inside the bulk, thus leading to self-ignition. The microbial decomposition of biomass pellets is also contagious to the handling personnel. Airborne spores of fungi and bacteria, predominantly found on biomass, can cause

severe allergic reactions and infection when inhaled or injected through other sources of exposure. Fungi and molds also produce mycotoxins during biomass decomposition that have fatal health hazards.

The temperature inside a pellet storage silo should be routinely monitored using sensors and thermocouples embedded in the pellet mass stored in bulk. Oxidation of pellets can also occur at low temperatures resulting in the formation of CO, CO₂, and CH₄ at the expense of oxygen that is consumed during oxidation. The pellet storage silo should be ventilated and maintained at low temperatures even lower than the ambient outside temperature at all times. Low temperatures could not only lessen the chances of self-heating and self-ignition of biomass pellets but also reduce the activity of microorganisms during decaying. The acceptable temperature in a pellet silo should be below 45 °C (Stelte 2012). In the situation that there is a rise in temperature above the acceptable limits, the pellet bulk should be shuffled and relocated to cooler places to breakdown the hotspots. Nevertheless, proper emergency protocols, evacuation procedures, and safety measures should be in place in the case of high-temperature (> 60 °C) scenarios inside the pellet storage silos.

2.9.3 Formation of Off-Gases

As mentioned earlier, oxygen depletes from the biomass pellets with aging and consumption in the chemical oxidation and microbial decaying processes. The gases resulting from these processes are CO and CO₂. Therefore, a closed pellet silo could be obnoxious and suffocating for handling personnel due to the presence of CO and CO₂. Moreover, since these gases are odorless, even their presence in low concentration could be highly lethal. Since CO and CO₂ are heavier than air, they tend to settle at higher concentrations at the bottom of the storage room, i.e., in the working space for handling personnel. Therefore, proper ventilation should be established along with CO and CO₂ gas monitors. The best practice is to avoid entering a closed biomass storage silo without ventilation with fresh air. Biomass contains extractives (i.e., terpenes, terpenoids, esters, ethers, aldehydes, ketones, and resins) along with cellulose, hemicellulose, and lignin (Nanda et al. 2013). The chemical oxidation of these extractives and other volatile components could also produce CO and CO₂.

2.10 Conclusions

Woody and agricultural biomasses, as a renewable resource of energy, are the main feedstocks for fuel pellet production, which are being deployed as a new global biorefining business. These pellets have great potential to be used for generation of heat and power. Biomass structure and composition are important factors in the development of binding structure during densification. Some constituents of biomass can be considered as potential binders such as lignin and protein. Some extractives in biomass can have negative effects on the pellet quality. Additives (binder, lubricant, plasticizer, moisture, etc.) are used in the formulation of the pellet to enhance the

quality and fuel properties of the pellet. Optimization of pelletization operating conditions (temperature and applied force) is important in the production of high-quality pellets. These conditions have shown some interactions with the biomass components and additives used for pelletization. Steam explosion is an effective pre-treatment to activate inherent lignin, as a binder for pelletization. Torrefaction can enhance the hydrophobicity and energy content of precursor before pelletization. Pellet can be coated to make them more moisture resistance and also to decrease the fine production from them during transportation and storage. Torrefaction can also be applied to pellets to improve their heating value and hydrophobicity. Dust formation, self-ignition, and production of off-gases are possible challenging items in postproduction steps of fuel pellet applications.

References

- Adapa P, Tabil L, Schoenau G, Opoku A (2010) Pelleting characteristics of selected biomass with and without steam explosion pretreatment. *Int J Agric & Biol Eng* 3:62–79
- Angles MN, Ferrandob F, Farriola X, Salvad J (2001) Suitability of steam exploded residual softwood for the production of binderless panels. Effect of the pre-treatment severity and lignin addition. *Biomass Bioenergy* 21:211–224
- Arzola N, Gómez A, Rincón S (2012) The effects of moisture content, particle size and binding agent content on oil palm shell pellet quality parameters. *Ing Investig* 32:24–29
- Bach QV, Tran KQ, Khalil RA, Skreiberg Ø, Seisenbaeva G (2013) Comparative assessment of wet torrefaction. *Energy Fuel* 27:6743–6753
- Bergman PCA, Boersma AR, Zwart RWR, Kiel JHA (2005) Torrefaction for biomass co-firing in existing coal-fired power stations “biocoal”, Report ECN-C-05-013. ECN, Petten
- Biswas AK, Yang W, Blasiak W (2011) Steam pretreatment of Salix to upgrade biomass fuel for wood pellet production. *Fuel Process Technol* 92:1711–1717
- Bowyer JL, Stockmann VE (2001) Agricultural residues: an exciting bio-based raw material for the global panel industry. *Forest Prod J* 51:10–21
- Cao L, Yuan X, Li H, Li C, Xiao Z, Jiang L, Huang B, Xiao Z, Chen X, Wang H, Zeng G (2015) Complementary effects of torrefaction and co-pelletization: energy consumption and characteristics of pellets. *Bioresour Technol* 185:254–262
- Carone MT, Pantaleo A, Pellerano A (2011) Influence of process parameters and biomass characteristics on the durability of pellets from the pruning residues of *Olea europaea* L. *Biomass Bioenergy* 35:402–410
- Chen P, Kuo C (2011) Torrefaction and co-torrefaction characterization of hemicellulose, cellulose and lignin as well as torrefaction of some basic constituents in biomass. *Energy* 36:803–811
- Clarke S, Preto F (2011) Biomass densification for energy production, Factsheet order no. 11-035. Ontario Ministry of Agriculture, Food and Rural Affairs, Ontario
- Craven JM, Swithenbank J, Sharifi VN, Peralta-Solorio D, Kelsall G, Sage P (2015) Hydrophobic coatings for moisture stable wood pellets. *Biomass Bioenergy* 80:278–285
- Emadi B, Iroba KL, Tabil LG (2017) Effect of polymer plastic binder on mechanical, storage and combustion characteristics of torrefied and pelletized herbaceous biomass. *Appl Energy* 198:312–319
- Faborode MO (1989) Moisture effects in the compaction of fibrous agricultural residues. *Biological Wastes* 28:61–71
- Filbakk T, Jirjis R, Nurmi J, Hoibo O (2011) Effect of bark content on quality parameters of Scots pine (*Pinus sylvestris* L.) pellets. *Biomass Bioenergy* 35:3342–3349

- Finell M, Arshadi M, Gref R, Scherzer T, Knolle W, Lestander T (2009) Laboratory-scale production of biofuel pellets from electron beam treated Scots pine (*Pinus silvestris* L.) sawdust. *Radiat Phys Chem* 78:281–287
- Finney KN, Sharifi VN, Swithenbank J (2009) Fuel pelletization with a binder: part I-identification of a suitable binder for spent mushroom compost-coal tailing pellets. *Energy Fuel* 23:3195–3202
- Ghiasi B, Kumar L, Furubayashi T, Lim CJ, Bi X, Kim CS, Sokhansanj S (2014) Densified biocoal from woodchips: is it better to do torrefaction before or after densification? *Appl Energy* 134:133–142
- Gilbert P, Ryu C, Sharifi V, Swithenbank J (2009) Effect of process parameters on pelletization of herbaceous crops. *Fuel* 88:1491–1497
- González-Peña MM, Hale MDC (2009) Colour in thermally modified wood of beech, Norway spruce and Scots pine. Part 1: colour evolution and colour changes. *Holzforschung* 63:385–393
- Grover PD, Mishra SK (1996) Biomass briquetting: technology and practices. Regional wood energy development program in Asia, field document no. 46. Food and Agriculture Organization of the United Nations, Bangkok
- Haruna NY, Afzal MT (2016) Effect of particle size on mechanical properties of pellets made from biomass blends. *Procedia Eng* 148:93–99
- Jackson J, Turner A, Mark T, Montross M (2016) Densification of biomass using a pilot scale flat ring roller pellet mill. *Fuel Process Technol* 148:43–49
- Kaliyan N, Morey RV (2009) Factors affecting strength and durability of densified biomass products. *Biomass Bioenergy* 33:337–359
- Kaliyan N, Morey RV (2010) Natural binders and solid bridge type binding mechanisms in briquettes and pellets made from corn stover and switchgrass. *Bioresour Technol* 101:1082–1090
- Kirsten C, Lenz V, Schroder HW, Repke JU (2016) Hay pellets and the influence of particle size reduction on their physical mechanical quality and energy demand during production. *Fuel Process Technol* 148:163–174
- Kumar P, Barrett DM, Delwiche MJ, Stroeve P (2009) Methods for pretreatment of lignocellulosic biomass for efficient hydrolysis and biofuel production. *Ind Eng Chem Res* 48:3713–3729
- Kumar L, Koukoulas AA, Mani S, Satyavolu J (2017) Integrating torrefaction in the wood pellet industry: a critical review. *Energy Fuel* 31:37–54
- Lam PS (2011) Steam explosion of biomass to produce wood pellets. PhD dissertation. University of British Columbia, Department of Chemical and Biological Engineering, Vancouver, BC, Canada
- Lam PS, Lam PY, Sokhansanj S, Lim CJ, Bi XT, Stephen JD, Pribowo A, Mabee WE (2015) Steam explosion of oil palm residues for the production of durable pellets. *Appl Energy* 141:160–166
- Li Y, Liu H (2000) High-pressure densification of wood residues to form an upgraded fuel. *Biomass Bioenergy* 19:177–186
- Li H, Liu X, Legros R, Bi XT, Lim C, Sokhansanj S (2012) Pelletization of torrefied sawdust and properties of torrefied pellets. *Appl Energy* 93:680–685
- Mani S, Tabil LG, Sokhansanj S (2006a) Specific energy requirement for compacting corn stover. *Bioresour Technol* 97:1420–1426
- Mani S, Tabil LG, Sokhansanj S (2006b) Effects of compressive force, particle size and moisture content on mechanical properties of biomass pellets from grasses. *Biomass Bioenergy* 30:648–654
- Martín-Sampedro R, Eugenio ME, Revilla E, Martín JA, Villar JC (2011) Integration of the kraft pulping on a forest biorefinery by the addition of a steam explosion pretreatment. *Bioresources* 6:513
- Mei Y, Liu R, Yang Q, Yang H, Shao J, Draper C, Zhang S, Chen H (2015) Torrefaction of cedarwood in a pilot scale rotary kiln and the influence of industrial flue gas. *Bioresour Technol* 177:355–360

- Miao Z, Grift TE, Hansen AC, Ting K (2013) Energy requirement for lignocellulosic feedstock densifications in relation to particle physical properties, preheating, and binding agents. *Energy Fuel* 27:588–595
- Monedero E, Portero H, Lapuerta M (2015) Pellet blends of poplar and pine sawdust: effects of material composition, additive, moisture content and compression die on pellet quality. *Fuel Process Technol* 132:15–23
- Nanda S, Mohanty P, Pant KK, Naik S, Kozinski JA, Dalai AK (2013) Characterization of North American lignocellulosic biomass and biochars in terms of their candidacy for alternate renewable fuels. *Bioenergy Res* 6:663–677
- Nielsen NPK, Holm JK, Felby C (2009) Effect of fiber orientation on compression and frictional properties of sawdust particles in fuel pellet production. *Energy Fuel* 23:3211–3216
- Ohliger A, Foerster M, Kneer R (2013) Torrefaction of beechwood: a parametric study including heat of reaction and grindability. *Fuel* 104:607–613
- Peng JH, Bi HT, Sokhansanj S, Lim JC (2012) A study of particle size effect on biomass torrefaction and densification. *Energy Fuel* 26:3826–3839
- Peng JH, Bi HT, Lim JC, Peng H, Kim CS, Jia D, Zuo H (2015) Sawdust as an effective binder for making torrefied pellets. *Appl Energy* 157:491–498
- Phanphanich M, Mani S (2011) Impact of torrefaction on the grindability and fuel characteristics of forest biomass. *Bioresour Technol* 102:1246–1253
- Pickard GE, Roll WM, Ramser JH (1961) Fundamentals of hay wafering. *Trans ASAE* 4:65–68
- Poddar S, Kamruzzaman M, Sujana SMA, Hossain M, Jamal MS, Gafur MA, Khanam M (2014) Effect of compression pressure on lignocellulosic biomass pellet to improve fuel properties: higher heating value. *Fuel* 131:43–48
- Prins MJ, Ptasiński KJ, Janssen FJJG (2006) Torrefaction of wood: part 1. Weight loss kinetics. *J Anal Appl Pyrolysis* 77:28–34
- Pu Y, Zhang D, Singh PM, Ragauskas AJ (2008) The new forestry biofuels sector. *Biofuels Bioprod Biorefin* 2:58–73
- Ramos LP (2003) The chemistry involved in the steam treatment of lignocellulosic materials. *Quim Nova* 26:863–871
- Ren S, Lei H, Wang L, Bu Q, Wei Y, Liang J, Liu Y, Julson J, Chen S, Wu J, Ruan R (2012) Microwave torrefaction of douglas fir sawdust pellets. *Energy Fuel* 26:5936–5943
- Rudolfsson M, Stelte W, Lestander TA (2015) Process optimization of combined biomass torrefaction and palletization for fuel pellet production – a parametric study. *Appl Energy* 140:378–384
- Rudolfsson M, Borén E, Pommer L, Nordin A, Lestander TA (2017) Combined effects of torrefaction and pelletization parameters on the quality of pellets produced from torrefied biomass. *Appl Energy* 191:414–424
- Rumpf H (1962) The strength of granules and agglomerates. In: Knepper WA (ed) *Agglomeration*. Interscience, New York, pp 379–418
- Saidur R, Abdelaziz EA, Demirbas A, Hossain MS, Mekhilef S (2011) A review on biomass as a fuel for boilers. *Renew Sust Energy Rev* 15:2262–2289
- Samuelsson R, Larsson SH, Thyrel M, Lestander TA (2012) Moisture content and storage time influence the binding mechanisms in biofuel wood pellets. *Appl Energy* 99:109–115
- Shang L, Nielsen NPK, Dahl J, Stelte W, Ahrenfeldt J, Holm JK, Thomsen T, Henriksen UB (2012) Quality effects caused by torrefaction of pellets made from Scots pine. *Fuel Process Technol* 101:23–28
- Si Y, Hu J, Wang X, Yang H, Chen Y, Shao J, Chen H (2016) Effect of carboxymethyl cellulose binder on the quality of biomass pellets. *Energy Fuel* 30:5799–5808
- Sokhansanj S, Mani S, Stumborg M, Samson R, Fenton J (2006) Production and distribution of cereal straw on the Canadian prairies. *Can Biosyst Eng* 48:3.39–3.46
- Soleimani M, Tabil XL, Grewal R, Tabil LG (2017) Carbohydrates as binders in biomass densification for biochemical and thermochemical processes. *Fuel* 193:134–141

- Stelte W (2012) Guideline: storage and handling of wood pellets. Resultat Kontrakt (RK) report. Danish Technological Institute. www.teknologisk.dk
- Stelte W, Holm JK, Sanadi AR, Barsberg S, Ahrenfeldt J, Henriksen UB (2011a) Fuel pellets from biomass: the importance of the pelletizing pressure and its dependency on the processing conditions. *Fuel* 90:3285–3290
- Stelte W, Holm JK, Sanadi AR, Barsberg S, Ahrenfeldt J, Henriksen UB (2011b) A study of bonding and failure mechanisms in fuel pellets made from different biomass resources. *Biomass Bioenergy* 35:910–918
- Sun Y, Cheng J (2002) Hydrolysis of lignocellulosic materials for ethanol production: a review. *Bioresour Technol* 83:1–11
- Thomas M, van Vliet T, van der Poel AFB (1998) Physical quality of pelleted animal feed 3. Contribution of feedstuff components. *Anim Feed Sci Technol* 70:59–78
- Thostenson T, Chou W (1999) Microwave processing: fundamentals and applications. *Compos Part A* 30:1055–1071
- Tilay A, Azargohar R, Drisdelle M, Dalai AK, Kozinski JA (2015) Canola meal moisture-resistant fuel pellets: study on the effects of process variables and additives on the pellet quality and compression characteristics. *J Ind Crop Prod* 63:337–348
- Tooyserkani Z, Sokhansanj S, Bi X, Lim CJ, Saddler J, Lau A, Melin S, Lam PS, Kumar L (2012) Effect of steam treatment on pellet strength and the energy input in pelleting of softwood particles. *ASABE* 55:2265–2272
- Torres W, Pansare SS, Goodwin JG Jr (2007) Hot gas removal of tars, ammonia, and hydrogen sulphide from biomass gasification gas. *Catal Rev* 49:407–456
- Tumuluru JS (2014) Effect of process variables on the density and durability of the pellets made from high moisture corn stover. *Biosyst Eng*:11944–11957
- Tumuluru JS, Christopher TW, Kevin LK, Hess JR (2010) A technical review on biomass processing: densification, preprocessing, modeling and optimization. *ASABE Meeting Presentation Paper Number*: 1009401
- Tumuluru JS, Wright CT, Hess JR, Kenney KL (2011) A review of biomass densification systems to develop uniform feedstock commodities for bioenergy application. *Biofuels Bioprod Biorefin* 5:683–707
- Turner R (1995) Bottomline in feed processing: achieving optimum pellet quality. *Feed Manage* 46:30–33
- van der Stelt MJC, Gerhauser H, Kiel JHA, Ptasinski KJ (2011) Biomass upgrading by torrefaction for the production of biofuels: a review. *Biomass Bioenergy* 35:3748–3762
- Wang C, Peng J, Li H, Bi XT, Legros R, Lim CJ, Sokhansanj S (2013) Oxidative torrefaction of biomass residues and densification of torrefied sawdust to pellets. *Bioresour Technol* 127:318–325
- Wang Y, Wu K, Sun Y (2018) Effects of raw material particle size on the briquetting process of rice straw. *J Energy Inst* 91:153–162
- Yang H, Yan R, Chen H, Lee DH, Zheng C (2007) Characteristics of hemicellulose, cellulose and lignin pyrolysis. *Fuel* 86:1781–1788
- Zandersons J, Gravitis J, Zhurins A, Kokorevics A, Kallavus U, Suzuki CK (2004) Carbon materials obtained from self-binding sugar cane bagasse and deciduous wood residues plastics. *Biomass Bioenergy* 26:345–360
- Zeeuwen P (2012) Hazardous material that lead to dust explosions. *Canadian Biomass Magazine*. <https://www.canadianbiomassmagazine.ca/safety-fire/hazardous-material-6351>. Accessed 8 Sept 2017



An Overview on the Application of Ligninolytic Microorganisms and Enzymes for Pretreatment of Lignocellulosic Biomass

Hossain Zabed, Shakila Sultana, Jaya Narayan Sahu, and Xianghui Qi

Abstract

Generation of biofuels from lignocellulosic biomass has received much interest in recent times to achieve an alternative energy source over conventional fossil fuels. Pretreatment is a vital step in the bioconversion of lignocellulosic biomass into biofuels, which is required to break down the lignocellulosic network of biomass. It is necessarily applied prior to the production of bioalcohols (bioethanol and biobutanol), biohydrogen, and biogas through fermentation. Delignification is the main objective of pretreatment that releases polysaccharides from the lignocellulosic matrix and increases enzymatic digestibility of cellulose. Although pretreatment can be done by using different physical, chemical, physicochemical, and biological methods, the latter is considered more promising as it is less expensive and eco-friendly, generates low or no inhibitors, and consumes relatively lower energy (steam and electricity). Many naturally occurring ligninolytic microorganisms and enzymes are used for delignification of biomass biologically. The aim of this chapter is to present an overview of different ligninolytic microorganisms (fungi and bacteria) and their enzymes for biological pretreatment of lignocellulosic biomass.

H. Zabed · X. Qi

School of Food & Biological Engineering, Jiangsu University, Zhenjiang, Jiangsu, China

S. Sultana

Department of Microbiology, Primeasia University, Banani, Dhaka, Bangladesh

J. N. Sahu (✉)

Institute of Chemical Technology, Faculty of Chemistry, University of Stuttgart, Stuttgart, Germany

e-mail: jaya.sahu@itc.uni-stuttgart.de

Keywords

Biofuels · Biological pretreatment · Lignocellulosic biomass · Delignification · Ligninolytic enzymes · White rot fungi · Bacterial pretreatment · Laccase · Fungal pretreatment

3.1 Introduction

The growing concerns about the energy crisis and global warming as a result of our dependence on fossil fuels have led to generate alternative energy from renewable sources, in which biofuels are considered most promising options. Despite the extensive research efforts of producing different biofuels, only a few are produced commercially (Zabed et al. 2014). Among the biofuels, bioethanol has drawn much attention in recent times. It is produced and used in several countries, where the USA, Brazil, China, Canada, and France are the top five bioethanol-producing countries (Lu et al. 2012; Nanda et al. 2014).

Biofuels can be generated from various biological sources that can broadly be classified into sugars, starch, lignocellulosic biomass, and algae. Almost all the current bioethanol is generated from sugars and starchy materials commercially (Zabed et al. 2016b, c). Nevertheless, sugar and starch-based sources are not adequate to replace nearly one trillion gallons of liquid fuels currently required each year in the world (Bell and Atfield 2009). Furthermore, commercial exploitation of biofuels from nonfood sources is necessary over food-based feedstocks to avoid the criticism of “food versus fuel” as the latter compete with the limited agricultural lands used for food and fiber production. The high costs of raw materials, as estimated to around 40–70% of the total capital investments, also limit the sustainability of biofuel production from sugars and starchy raw materials (Claassen et al. 1999; Zabed et al. 2016a). Although algae could have the potential to be a promising source of biofuels, they are still far away from commercial exploitation (Chen et al. 2013). As a result, current research efforts are being more focused on lignocellulosic biomass (Zabed et al. 2017b). Moreover, conversion of lignocellulose into biofuels generates a lower net greenhouse gas emission compared with those occurring during the conversion of biofuels from sugar and starch, thereby reducing overall environmental pollution (Hahn-Hägerdal et al. 2006; Zabed et al. 2017a).

Biochemical conversion of biomass into biofuels (bioalcohols, biohydrogen, and biogas) primarily includes pretreatment and/or detoxification, hydrolysis, fermentation, and downstream processing. Among these basic steps, pretreatment is the most crucial and costly step, which is required to overcome the recalcitrance of lignocellulosic matrix and the crystallinity of cellulose. In general, pretreatment works on biomass by altering its macroscopic, submicroscopic, and microscopic structure that results in the removal of lignin, increased surface area, and improvement of the accessibility of cellulose to hydrolytic enzymes (Zabed et al. 2016d). An ideal pretreatment method should avoid the requirements of biomass size reduction, enhance biomass digestibility for fast hydrolysis with high sugar yield, and minimize

the generation of inhibitors, energy consumption, and operational costs (Gupta and Verma 2015). The efficiency of a pretreatment process relies on the treatment conditions and the nature of biomass, particularly its physical structure and chemical composition (Sindhu et al. 2016).

In the last several years, many pretreatment methods studied have been classified as physical, chemical, and biological. Physical and chemical pretreatment methods require extensive energy input and corrosion resistant high-pressure reactors. Chemical and thermochemical pretreatments also produce various hydrolysis and/or fermentation inhibitors that affect subsequent hydrolysis and fermentation processes. On the other hand, biological pretreatments use natural microorganisms or their metabolites (such as enzymes) that have potential advantages over other pretreatment methods. This method produces low inhibitors due to the less biomass degradation, is cost-effective and environmentally friendly, and do not require detoxification and recycling of chemicals prior to hydrolysis and fermentation (Sindhu et al. 2016). The current chapter focuses on the utilization of different ligninolytic fungi and bacteria along with their enzymes for biological pretreatment of lignocellulosic biomass in light of the recent advances in this technology.

3.2 Composition of Biomass

The major biochemical components of biomass are carbohydrates (holocellulose) and lignin, where holocellulose comprises of cellulose and hemicellulose. The quantity of different biochemical components in biomass varies greatly that ranges 30–35% in cellulose, 25–30% in hemicellulose, and 10–20% in lignin (Achinis and Euverink 2016). Cellulose and hemicellulose are linked with lignin by covalent cross-linkages and non-covalent forces, forming a complex lignocellulosic network that causes the recalcitrance of biomass (Fig. 3.1).

Cellulose is a linear glucose polymer where its units are joined together by $\beta\rightarrow 1,4$ -glycosidic linkages (Fig. 3.2a). Cellulose molecules form a crystalline and rigid structure called microfibrils due to extensive hydrogen bonding among the hydroxyl groups of different molecules, which results in the water insolubility of cellulose and resistance to enzymatic digestibility (Zabed et al. 2017c). As shown in Fig. 3.2b, hemicellulose comprises short, linear, and extensively branched chains of hexoses, pentoses, and sugar acids (Saxena et al. 2009; Gírio et al. 2010).

Lignin is a vigorously cross-linked heterogeneous polymer of 4-hydroxyphenylpropanoid monomers called monolignols that are polymerized by C-O-C and C-C linkages. The phenolic parts of the monomers consist of three basic units such as guaiacyl (G), syringyl (S), and *p*-hydroxyphenyl (H). Lignin is formed by the action of peroxidases and/or laccases. The monolignols can be coupled *via* a

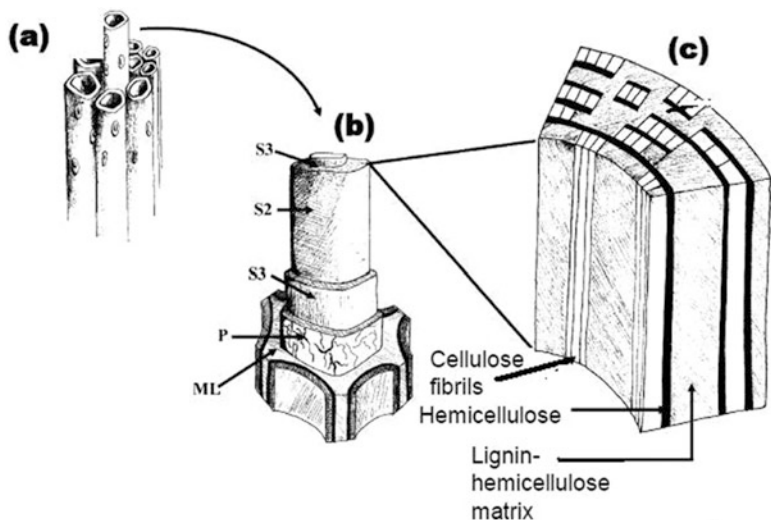


Fig. 3.1 Structure of a typical lignocellulosic biomass: (a) adjacent cells; (b) cell wall layers, where S1, S2, and S3 are 2° layers, P is the 1° layer, and ML is the middle lamella; and (c) arrangement of components in the lignocellulosic contents in the 2° wall. (Adapted from Pérez et al. 2002)

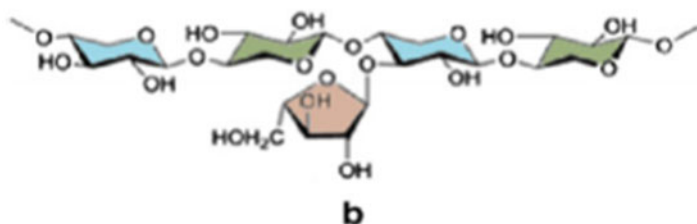
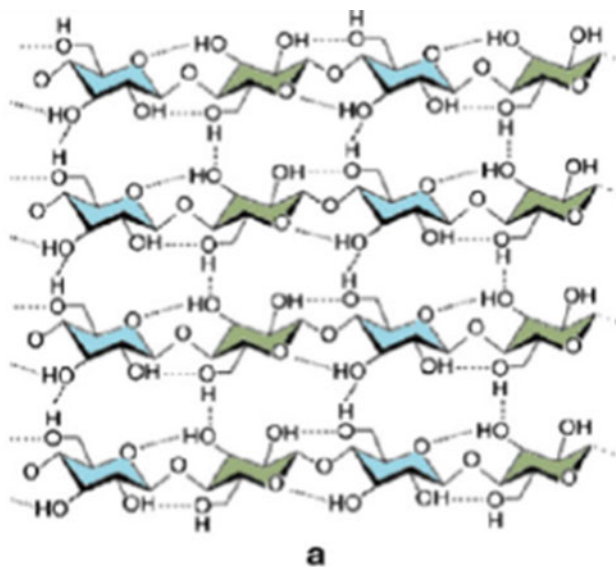


Fig. 3.2 Chemical structures of (a) cellulose and (b) hemicellulose. (Adapted from Nanda et al. 2014)

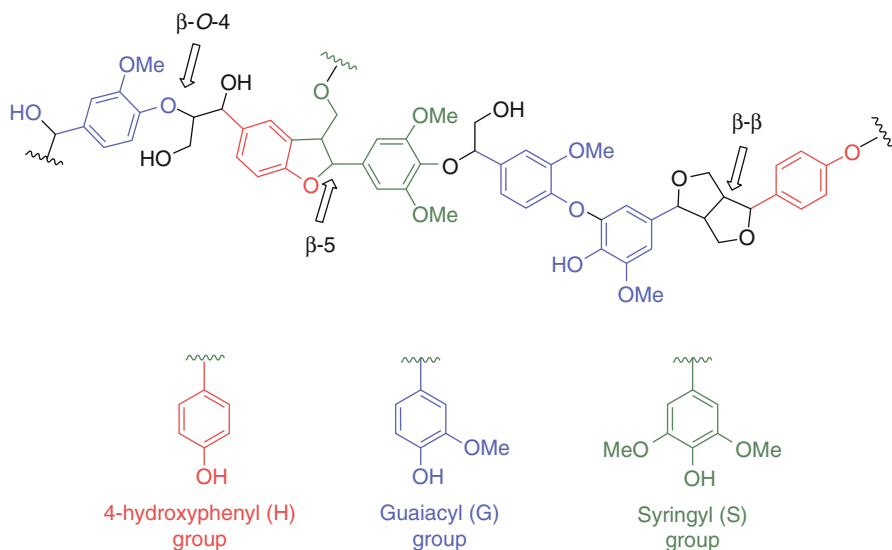


Fig. 3.3 Basic structure of lignin showing the most common linkages and relevant monomers. (Adapted from de Gonzalo et al. 2016)

number of linkages where coupling through the β -carbon is preferred (de Gonzalo et al. 2016). The most commonly found linkages in lignin are β - β , β -O-4, and β -5 linkages (Fig. 3.3).

3.3 Biological Pretreatment of Biomass: An Overview

Biological pretreatment can be done either by using ligninolytic microorganisms or enzymes. In particular, four distinct techniques have been reported thus far for biological pretreatment of biomass such as (i) microbial pretreatment (e.g., fungal and bacterial), (ii) use of microbial consortium, (iii) ensilaging, and (iv) enzymatic pretreatment (Table 3.1). Biological agents can be applied in a single pretreatment method or in combination with other pretreatment techniques (Rodriguez et al. 2017).

In nature, certain fungi, particularly white rot fungi, can degrade lignin completely with the production of carbon dioxide and water, while other fungi and ruminant bacteria apparently degrade lignin incompletely (Crawford and Crawford 1980). The characteristic of naturally occurring microorganisms to degrade lignin has been exploited in the delignification of biomass for sustainable and eco-friendly biofuel production. Although there are some reports of bacterial involvement in biological delignification, some selected fungal species are the best lignin degraders. For this reason, fungal pretreatment has been considered widely and extensively for biological pretreatment of biomass (Wan and Li 2012).

Microorganisms usually secrete several extracellular ligninolytic enzymes while growing on the biomass that catalyzes various biochemical reactions and thus lignin degradation takes place. Currently, most of the biological delignification is

Table 3.1 Technological approaches of biological pretreatment of biomass

Approach	Major sources of biological agents	Temperature (°C)	Incubation time	Advantages	Disadvantages	References
Microbial pretreatment	Fungi and bacteria	28–37	Weeks to months	<ul style="list-style-type: none"> Simple techniques Need less inputs Need less energy No or less waste streams Low costs for downstream processing No or less inhibitors formation 	<ul style="list-style-type: none"> Loss of carbohydrates Long pretreatment time 	Zheng et al. (2014), Rouches et al. (2016), and Wan and Li (2012)
Microbial consortium	Mixture of fungi, yeasts, and bacteria	20–55	Hours to days	<ul style="list-style-type: none"> Relatively lower incubation time compared to fungal pretreatment Complex microbial communities accelerate organic hydrolysis which in turn facilitate the accessibility of enzymes in lignocelluloses Can produce required components stably and continuously to degrade lignocellulosic content in biomass 	<ul style="list-style-type: none"> May need to maintain strictly anaerobic condition Pure cultures may not adapt to environmental fluctuations 	Zheng et al. (2014), Zhang et al. (2011), Poszytek et al. (2016), and Wongwilaiwain et al. (2010)

Enzymatic pretreatment	Fungal ligninolytic enzymes	35–37	Hours to days	Relatively lower incubation time compared to other biological approaches No or reduced inhibitors formation Operated at mild conditions Enzyme recycling can effectively increase the rate and yield of the hydrolysis. Can be done under ambient and mild conditions No or less waste production	Enzyme production and extraction can be costly Poor stability of ligninolytic enzymes in industrial processes	Zheng et al. (2014) and Rouches et al. (2016)
	Bacterial ligninolytic enzymes					
Ensiling	Mixtures of homo- and heterofermentative bacteria and enzymes	Ambient temperature	Weeks to months		Long time High loss of carbohydrates	Zheng et al. (2014) and Rouches et al. (2016)

conducted by inoculating microbial inoculum (either single or mixed microorganisms) on the biomass that subsequently grows and metabolize, resulting in the degradation of lignin. However, it takes unusually long incubation time as ranged from weeks to months. In an alternative approach, ligninolytic enzymes are extracted from the fungal or bacterial cultures, and purified enzymes are then used or pretreatment purposes. Although enzymatic pretreatment can decrease overall incubation time significantly, there is a further challenge with this technology as enzyme purification requires an additional cost, thus increasing the net capital costs of the process.

Another promising approach for reducing pretreatment time is the utilization of unique microbial consortia, where lignin degradation occurs by the synergistic action of various bacteria and fungi. The utilization of microbial consortium offers some advantages over single microbial treatment, such as increased adaptability, improved hydrolysis efficiency and productivity, controlled pH in the system, and increased substrate utilization (Kalyani et al. 2013). In nature, ligninolytic microorganisms can be found in many ecosystems, where they usually develop particular consortia to break down lignocellulose. While individual strains can be involved in industrial practices, studies have reported that application of microbial consortia is more effective for delignification of biomass (Poszytek et al. 2016).

Ensiling, typically used in forage crop preservation, is considered as an advanced technology for biological pretreatment. It incorporates fermentation by lactic acid bacteria in the absence of oxygen that prevents microbial contamination and breakdown of the structure of macromolecules through producing different organic acids. Dewar et al. (1963) first reported that hemicellulose in rye grass was hydrolyzed during ensiling due to enzyme secretion of the grass at the early stage and during long storage (7–28 days) as a result of carbohydrate hydrolysis under the acidic condition at a pH around 4. These findings recommend that this technique can be utilized for biological pretreatment for lignocellulosic biomass for generation of biofuels. However, three major factors may affect the yield of ensiling, which are the composition of biomass, dry matter content, and microbial community (Ambye-Jensen et al. 2013).

3.4 Application of Lignin-Degrading Microorganisms for Pretreatment of Biomass

A good number of microorganisms have been reported for their delignification potential using a wide range of biomass (Table 3.2). Two groups of fungi, especially ascomycetes (*Trichoderma reesei*) and basidiomycetes (*Pleurotus ostreatus*), are worth mentioning due to their ability to break down the lignocellulosic network in the biomass (Mustafa et al. 2016). In an alternative classification, fungal lignin degraders are grouped into brown rot, white rot, and soft rot fungi. Several ascomycetes can break down hemicellulose with a low capability of lignin degradation, while white rot fungi are renowned for lignin breakdown (Liers et al. 2010).

Table 3.2 Application of microorganisms in biological pretreatment of biomass

Microorganism	Group	Feedstock	Process conditions	Major effects on biomass	References
<i>Phanerochaete chrysosporium</i>	White rot fungus	Cotton stalk	Submerged and solid-state cultivation; oxygen-enriched conditions; 14 days; 39 °C	Significant lignin degradation of 19.38% for submerged and 35.53% for solid state Cellulose conversion was not observed (10.98% and 3.04%) for submerged and solid-state samples, respectively	Shi et al. (2009)
<i>Irpex lacteus</i>	White rot fungus	Non-sterile corn stover	28 °C; 42 days	Around 43.8% lignin loss Enhanced efficiency of saccharification (seven-fold)	Song et al. (2013)
<i>Punctularia</i> sp. TUF20056	White rot fungus	Bamboo culms (<i>Phyllostachys pubescens</i>)	12 weeks	Good lignin breakdown (>50%) A high ratio of lignin to holocellulose (>6)	Suhara et al. (2012)
<i>Coniophora puteana</i>	Brown rot fungus	Scots pine (<i>Pinus sylvestris</i>)	22 °C; 20 days	Improved downstream glucose yields Four- to five-fold higher than the yield of untreated biomass	Ray et al. (2010)
<i>Positia placenta</i>	Brown rot fungus	Sapwood (<i>Pinus radiata</i>)	22 °C; 35 days	Can degrade lignin actively and improve glucose yield	Ray et al. (2010)
<i>Chaetomium globosum</i> (ATCC 6205)	Soft rot fungus	Sapwood (<i>Pinus radiata</i>)	22 °C; 35 days	Can degrade lignin actively and improve glucose yield	Ray et al. (2010)
<i>Trichoderma viride</i>	Mold	Sapwood (<i>Pinus radiata</i>)	22 °C; 35 days	Can grow on softwood but cannot actively degrade lignin	Ray et al. (2010)
<i>Auricularia auricula-judae</i>	White rot fungus	Sweet chestnut leaves and hay	37 °C; 4–5 weeks	15% increase in biogas production	Mackulak et al. (2012)
<i>Ceriporiopsis subvermispora</i> ATCC 90467	White rot fungus	Japanese cedar wood chips	8 weeks	Good methane yield, four-fold enhanced yield than untreated control	Amirta et al. (2006)

(continued)

Table 3.2 (continued)

Microorganism	Group	Feedstock	Process conditions	Major effects on biomass	References
<i>Pringsheimia smilacis</i>	Endophytic fungus (ascomycetes)	<i>Eucalyptus globulus</i> wood	23 °C; 28 days	33.1% lignin degradation	Martín-Sampedro et al. (2015)
<i>Ceriporiopsis subvermispora</i>	White rot fungus	<i>Miscanthus</i>	28 °C; 21 days	30% lignin degradation	Vasco-Correa et al. (2016)
<i>Ceriporiopsis subvermispora</i>	White rot fungus	Sugarcane bagasse	60 days	48% lignin degradation	da Silva Machado and Ferraz (2017)
<i>Cupriavidus basiliensis</i> B-8	Bacterium	Acid-pretreated rice straw	30 °C; 3 days	Downstream saccharification enhanced by 35–70% than the acid-pretreated biomass	Yan et al. (2017)
				Downstream saccharification enhanced by 173–244% than that of control	
<i>Trichoderma reesei</i>	Soft rot fungi	Rice straw	75% moisture; 20 days	Lignin loss was 23.6%	Mustafa et al. (2016)
				78.3% higher methane yield	
<i>Pleurotus ostreatus</i>	White rot fungus	Rice straw	75% moisture; 20 days	33.4% lignin removal	Mustafa et al. (2016)
				Lignin/cellulose removal ratio of 4.2	
				120% higher methane yield	

Although several bacterial and fungal species have been investigated for biomass pretreatment, white rot fungi are appeared to be more prevalent among all other microorganisms. White rot fungi have shown their potential in lignin decomposition and selective lignin degradation with low cellulose loss (Wan and Li 2012). Moreover, this group of fungi can degrade lignin more rapidly and efficiently than any other known groups of organisms. In addition to delignification, white rot fungal pretreatment also increases enzymatic digestibility of cellulose with an increased fermentable sugar yield. For instance, a previous study with corn stover has reported to obtaining a three- to five-fold improvement in enzymatic cellulose digestibility after pretreatment with *Cyathus stercoreus* (Keller et al. 2003).

The species of white rot fungi are broadly disseminated in the environment and occur in both tropical and temperate environments (Cullen 1997). Conventionally, they have been used in bio-pulping, fodder improvement, and bioremediation of soil and wastewaters (Wan and Li 2012). Major lignin-degrading white rot fungi include *Ceriporiopsis subvermispora*, *Coriolus versicolor*, *Cyathus stercoreus*, *Phanerochaete chrysosporium*, *Phlebia subserialis*, and *Pleurotus ostreatus* (Wan and Li 2012). Among these fungi, *Phanerochaete chrysosporium* has most extensively been investigated for biological delignification (Shi et al. 2009).

Due to having the potential to degrade lignin, fungi-assisted pretreatment has attracted much attention in the past decade (Yan et al. 2017). However, one of the major hindrances in fungal pretreatment is the long incubation time. On the other hand, bacteria can grow and metabolize fast with easy genetic manipulation that has been increasingly studied for biomass pretreatment in recent years (Shi et al. 2017; Yan et al. 2017).

3.5 Application of Ligninolytic Enzymes for Pretreatment of Biomass

The utilization of ligninolytic enzymes for biological delignification of biomass has drawn attention as attempts to reduce pretreatment time and get a more specific delignification of biomass. In nature, lignocellulose degradation occurs by a multi-enzyme system that includes both hydrolytic and oxidative transformations. It has been reported that application of lignin-degrading enzymes in biomass delignification was started with the report of a peroxide-dependent ligninolytic enzyme in the cultures of *P. chrysosporium* (Woolridge 2014).

So far, a good number of extracellular enzymes have been screened out from the microorganisms and investigated to evaluate their efficiency in delignification of biomass. The major ligninolytic enzymes include laccase, lignin peroxidase (LiP), manganese peroxidase (MnP), versatile peroxidase (VP), and dye-decolorizing peroxidase (DyP) (Table 3.3). In addition, several other lignin-degrading enzymes were also investigated, such as aryl-alcohol oxidase (AAO) (EC 1.1.3.7), glyoxal oxidase (GLOX), aryl-alcohol dehydrogenases (AAD), and quinone reductases (QR) (Dashtban et al. 2010). Laccases, the most common ligninolytic enzymes, use molecular oxygen as electron acceptor, while peroxidases use hydrogen peroxide

Table 3.3 Sources and characteristics of major ligninolytic enzymes

Name of enzymes	Source	Major features	Main effects or mechanism of action	References
Laccases (E.C. 1.10.3.2)	Fungi higher plants and bacteria	Contain multi-copper (four) in active site	Catalyzes reduction of O ₂ to H ₂ O and oxidizes aromatic amines	Plácido and Capareda (2015)
		Extracellular and inducible		
		Broad substrate specificity		
Small laccases (E.C. 1.10.3.2)	Actinomycetes (<i>Streptomyces</i> spp.)	Good oxidizing power	Not clearly understood	Majumdar et al. (2014)
		High pH versatility		
		High thermal stability		
Lignin peroxidase, LiP (EC 1.11.1.14)	Mostly white rot fungi	Contain heme (Fe) group in active site	Oxidizes non-phenolic components by circulating one electron and generating cation radicals	Binod et al. (2011) and Datta et al. (2017)
		Extracellular oxidoreductase		
		Good redox potential	Breakdown of non-phenolic lignin portions	
Manganese peroxidase, MnP (EC 1.11.1.13)	White rot fungi	Glycosylated glycoproteins with a Fe (heme) prosthetic group	It oxidizes Mn ²⁺ to Mn ³⁺ in a H ₂ O ₂ -dependent reaction where Mn ³⁺ is chelated to an organic acid	Wan and Li (2012) and Wesenberg et al. (2003)
		Molecular weights ranged from 32 to 62.5 kDa		
Versatile peroxidase, VP (EC 1.11.1.16)	Mostly Basidiomycetes fungi	Can oxidize Mn ²⁺ like MnP and non-phenolic compounds like LiP	Mechanism is almost same to that of MnP	Abdel-Hamid et al. (2013) and Datta et al. (2017)
		Can act on lignin without any external mediators		
		Can oxidize phenolic and non-phenolic lignin portions		

(continued)

Table 3.3 (continued)

Name of enzymes	Source	Major features	Main effects or mechanism of action	References
Dye-decolorizing peroxidase, DyP (EC 1.11.1.19)	Mainly bacteria; a fungal DyP has also been reported	Heme-containing peroxidase	Catalyze some interesting synthetic reactions in the absence of H ₂ O ₂ to degrade lignin components	Datta et al. (2017) and de Gonzalo et al. (2016)
		Mostly works at low pH		
		Can act on a broad range of substrates		

(H₂O₂) as a co-substrate (Mai et al. 2004). The applications of different ligninolytic enzymes in the biological pretreatment of some typical biomasses are summarized in Table 3.4.

Among the ligninolytic enzymes, LiP, MnP, and laccase are the most widely studied enzymes in fungi, which oxidize lignin and various lignin equivalent molecules (Winquist et al. 2008). However, an individual fungal strain does not necessarily secrete all of these ligninolytic enzymes. Lignin-degrading enzymes can be non-specific for different lignin analogous compounds and even catalyze the same degradation reactions. As an instance, it can be pointed out that both LiP and MnP were reported to degrade non-phenolic lignin compounds by one-electron oxidation of the aromatic ring (Srebotnik et al. 1997).

Laccases are copper-bearing biocatalysts, which oxidize phenolic components in the presence of oxygen (Gianfreda et al. 1999). The well-characterized laccases are mostly derived from fungi, while bacterial laccases have also received much attraction nowadays in lignin removal and other similar purposes. The achievements in genome study have resulted in much progress in the identification of bacterial laccases as well as their application in lignin degradation (Chandra and Chowdhary 2015). Recently, laccases were also isolated from actinomycetes, which were named as “small laccases” due to the resemblance in amino acid sequence but smaller in size compared to fungal laccases (Machczynski et al. 2004).

LiPs (also called ligninase) are heme-containing glycoproteins of 38–46 kDa, having a distinctive property of an unusually low pH optimum near pH 3 (Binod et al. 2011). In fact, LiP was the first ligninolytic enzyme isolated from *P. chrysosporium* (Brown and Chang 2014). It can oxidize both phenolic and non-phenolic substrates. However, LiPs oxidize aromatic rings moderately by being activated in response to the electron-donating substitutes, in contrast to the common peroxidases (Plácido and Capareda 2015).

MnPs, also called hydrogen-peroxide oxidoreductases, are glycoproteins and secreted by microbes in several isoforms having one molecule of heme as iron protoporphyrin IX (Asgher et al. 2008). Since the discovery of MnP in *P. chrysosporium* in 1985, many other MnPs were isolated from other basidiomycetes (Dashtban et al. 2010). This enzyme catalyzes peroxide-dependent

Table 3.4 Application of ligninolytic enzymes in biological pretreatment of biomass. (Adapted and modified from Plácido and Capareda 2015)

Enzyme	Source	Mode of use	Biomass	Mediator	Process time	Delignification (%)
Laccase	<i>Aspergillus fumigatus</i>	Enzymatic	Wood pulp	HBT	2 h	14
Laccase	<i>Trametes villosa</i>	Enzymatic	Wood pulp	HBT and HPA	15 h	50 (HBT); 39 (HPA)
Laccase	<i>Trametes versicolor</i>	Enzymatic	Hardwood chips	VA	2 h	54.2
Laccase	<i>Myceliophthora thermophila</i>	Enzymatic	<i>Eucalyptus globulus</i>	MS	12 h	>25
Laccase	<i>Pycnoporus cinnabarinus</i>	Enzymatic	Paper pulp	AC, SA, HBT	4–24 h	21 (AC), 25 (SA), 40 (HBT)
Laccase	<i>Ceriporiopsis subvermispora</i>	Fungal	Corn stover	–	18 days	>25
Laccase	<i>Ceriporiopsis subvermispora</i>	Fungal	Switchgrass	–	18 days	>25
Laccase, LiP, and MnP	<i>Ceriporiopsis subvermispora</i>	Fungal	Sugarcane bagasse	–	30 days	20
Laccase, LiP, and MnP	<i>Ceriporiopsis subvermispora</i>	Fungal	Wheat straw	–	21 days	34
Laccase, LiP, and MnP	<i>Irpex lacteus</i>	Fungal	Wheat straw	–	21 days	39
MnP, Laccase	<i>Ceriporiopsis subvermispora</i>	Fungal	Corn stover	–	42 days	39.2
MnP, LiP, Laccase	<i>Pleurotus ostreatus</i> IBL-02	Enzymatic	Sugarcane bagasse	–	48 h	33.6
MnP	<i>Irpex lacteus</i>	Fungal	Corn stover	–	28 days	25.8
MnP laccase	<i>Pleurotus florida</i>	Fungal	Sugarcane bagasse	–	25 days	7.91

AC acetosyringone, HBT 1-hydroxybenzotriazole, HPA N-hydroxyphthalimide, MS methyl syringate, SA syringaldehyde, VA violuric acid

oxidation and converts Mn^{2+} to Mn^{3+} , which is then released as a complex with oxalate or with other chelators from the enzyme surface. The Mn^{3+} complex works as a reacting compound having low molecular weight and a diffusible redox mediator of phenolic components such as phenols, amines, dyes, phenolic lignin substructures, and dimers (Dashtban et al. 2010).

Versatile peroxidase (VP) isolated from several Basidiomycete fungi (*Pleurotus eryngii*, *Pleurotus ostreatus*, *Pleurotus pulmonarius*, *Bjerkandera adusta*, and *Bjerkandera fumosa*) is considered as the third peroxidase (Dashtban et al. 2010). It is a LiP-MnP hybrid that shows Mn^{2+} independent activity (Wan and Li 2012). VPs have a dual oxidative capability to oxidize both phenolic and non-phenolic molecules (Datta et al. 2017).

It seems that lignin-degrading peroxidases (such as LiP and MnP) are restricted to fungi, while recent investigations reported that bacteria contain another type of heme-containing peroxidase called dye-decolorizing peroxidases (DyP) (van Bloois et al. 2010). The first member of DyP was isolated and characterized from *Bjerkandera adusta* by Kim and Shoda (1999). In recent years, bacterial DyPs have been reported to be able to degrade lignin-derived molecules. However, bacterial DyPs have lower oxidative capability compared to similar fungal enzymes and so have limited oxidation of phenolic compounds (de Gonzalo et al. 2016).

3.6 Factors Affecting Biological Pretreatment of Biomass

Although biological pretreatment can improve overall conversion of biomass, several factors affect the efficiency and outcome of this pretreatment process, particularly when fungi or bacteria are used. To attain good biological pretreatment efficiency, knowledge about the factors affecting microbial growth and metabolism is critical (Wan and Li 2012). The first and foremost factor is the pretreatment time that takes, in general, several days to months. In fact, long incubation period required for effective lignin degradation is considered a major bottleneck in the microbial pretreatment of biomass. It was reported that pretreatment time can be reduced to an extent by utilizing microbial consortia (Sindhu et al. 2016).

Although lignocellulosic biomass is an abundant source of biomass, it varies widely in its physical and chemical properties. The major sources of biomass are agricultural and forestry residues, energy crops, aquatic plants, and municipal solid waste (Zabed et al. 2016d). As stated earlier, lignocellulosic biomass consist of cellulose, hemicelluloses, and lignin together with small amounts of other components.

The effectiveness and output of biological pretreatment significantly depend on the type of microorganisms or enzymes involved. Although a variety of microorganisms have been investigated till date, most of them did not show similar efficiency even when the biomass sources were used. Instead, there were wide variations in the major outputs of a biological pretreatment such as delignification and downstream sugar yields. Pretreatment with fungi may enhance the downstream saccharification rate.

It is vital to ensure the optimum temperature during biological pretreatment. Temperature out of the optimal range may inhibit the growth of microorganisms or even kill the viable cells. The optimum temperature, however, might be different for various types of microorganism used for biological pretreatment. For example, the optimum growth temperature for ascomycetes is around 39 °C. On the other hand, basidiomycetes show good growth and activity between 15 and 35 °C, even though optimum lignin degradation rate is usually found between 25 and 30 °C (Sindhu et al. 2016; Reid 1985). The reasons for variations in the optimum temperatures among the microorganisms used for biological pretreatment are attributed to the microbial physiology, types of strains, and nature of substrates (Millati et al. 2011).

Moisture content in the biomass is another critical factor, and sufficient moisture level is necessary for a healthy microbial growth and ligninolytic activity (Gervais and Molin 2003; Singhanian et al. 2009). However, the optimum moisture can be different based on the type of microorganism, species, strain, and biomass (Mustafa et al. 2016). A lower level of moisture than the optimum may prevent microbial growth and affects delignification process. Overall, high water content is necessary for the optimum growth of microbial cells as well as to carry out the active metabolic functions. However, an excess level of water may decrease interparticle spaces as well as substrate porosity during solid-state fermentation, which consequently reduces oxygen distribution in the system and thereby inhibits the aerobic growth of the microorganisms.

Aeration can influence the efficiency of biological pretreatment by affecting the production and activity of ligninolytic enzymes. Sufficient aeration level is required for some important physiological functions of biological agents, such as oxygenation, removal of CO₂, dissipation of heat, maintenance of proper humidity level and circulation of volatile compounds generated during microbial metabolism (Millati et al. 2011). Since lignin decomposition is an oxidative process, ensuring the availability of oxygen is essential for activating the ligninolytic enzymes. Moreover, proper aeration is also required for ensuring the uniform air distribution when biological pretreatment is done in packed reactors. It has been reported that a high aeration can increase the lignin degradation rate (Sindhu et al. 2016).

3.7 Conclusions

Ligninolytic microorganisms and their enzymes show some biophysical and biochemical potentials that have led them to be involved in the biological delignification of biomass as a mean of pretreatment. Although biological agents have the potential for pretreating biomass, there are some bottlenecks with the application of these agents on large scale. The major challenging factors are the low degree of cellulose modification, nonselective lignin degradation, sugar loss, and long incubation time. To overcome these challenges, some technological improvements have been achieved in recent years that include, for example, selection of white rot fungi for reducing sugar loss by their selective delignification. Long pretreatment time is a

major and common issue in the biological pretreatment, where utilization of microbial consortia and purified enzymes are found to be promising options for reducing incubation time.

Other approaches for solving the long pretreatment time issue would be the use of fungal treatment concurrently with on-farm wet storage and application of combined pretreatment techniques involving a microbial pretreatment and a physical or thermochemical pretreatment. Getting industrially suitable optimum pretreatment conditions is another challenge in the biological pretreatment due to wide variations in the growth and metabolic conditions of various ligninolytic microorganisms, and effective efforts should be made to address this issue. Compared to direct microbial pretreatment, usage of ligninolytic enzymes for biological pretreatment would be more promising for sustainable biofuel production. However, there is a need to focus on the improvements of the process efficiency, cost reduction, and more specialized mediators in future studies to make enzymatic pretreatment implementable in commercial facilities.

Acknowledgments This work was supported by the China Postdoctoral Science Foundation (Grant No.: 2017M621657), NSFC (Grant No.: 31571806), and Six Talent Peaks in Jiangsu Province (SWYY-018).

References

- Abdel-Hamid AM, Solbiati JO, Cann I (2013) Insights into lignin degradation and its potential industrial applications. *Adv Appl Microbiol* 82:1–28
- Achinas S, Euverink GJW (2016) Consolidated briefing of biochemical ethanol production from lignocellulosic biomass. *Electron J Biotechnol* 23:44–53
- Ambye-Jensen M, Johansen KS, Didion T, Kádár Z, Schmidt JE, Meyer AS (2013) Ensiling as biological pretreatment of grass (*Festulolium hykor*): the effect of composition, dry matter, and inocula on cellulose convertibility. *Biomass Bioenergy* 58:303–312
- Amirta R, Tanabe T, Watanabe T, Honda Y, Kuwahara M, Watanabe T (2006) Methane fermentation of Japanese cedar wood pretreated with a white rot fungus, *Ceriporiopsis subvernispora*. *J Biotechnol* 123:71–77
- Asgher M, Bhatti HN, Ashraf M, Legge RL (2008) Recent developments in biodegradation of industrial pollutants by white rot fungi and their enzyme system. *Biodegradation* 19:771–783
- Bell PJ, Attfield PV (2009) Breakthrough in yeast for making bio-ethanol from lignocellulosics. Microbiogen Pty Ltd, Macquarie University Campus, Sydney <https://dokumen.tips/documents/breakthrough-in-yeasts-for-making-bioethanol-from-lignocellulosics.html>
- Binod P, Janu K, Sindhu R, Pandey A (2011) Hydrolysis of lignocellulosic biomass for bioethanol production. In: *Biofuels: alternative feedstocks and conversion processes*, pp. 229–250
- van Bloois E, Pazmiño DET, Winter RT, Fraaije MW (2010) A robust and extracellular heme-containing peroxidase from *Thermobifida fusca* as prototype of a bacterial peroxidase superfamily. *Appl Microbiol Biotechnol* 86:1419–1430
- Brown ME, Chang MC (2014) Exploring bacterial lignin degradation. *Curr Opin Chem Biol* 19:1–7
- Chandra R, Chowdhary P (2015) Properties of bacterial laccases and their application in bioremediation of industrial wastes. *Environ Sci Process Impacts* 17:326–342
- Chen C-Y, Zhao X-Q, Yen H-W, Ho S-H, Cheng C-L, Lee D-J, Bai F-W, Chang J-S (2013) Microalgae-based carbohydrates for biofuel production. *Biochem Eng J* 78:1–10

- Claassen P, Van Lier J, Contreras AL, Van Niel E, Sijtsma L, Stams A, De Vries S, Weusthuis R (1999) Utilisation of biomass for the supply of energy carriers. *Appl Microbiol Biotechnol* 52:741–755
- Crawford DL, Crawford RL (1980) Microbial degradation of lignin. *Enzym Microb Technol* 2:11–22
- Cullen D (1997) Recent advances on the molecular genetics of ligninolytic fungi. *J Biotechnol* 53:273–289
- Dashban M, Schraft H, Syed TA, Qin W (2010) Fungal biodegradation and enzymatic modification of lignin. *Int J Biochem Mol Biol* 1:36–50
- Datta R, Kelkar A, Baraniya D, Molaei A, Moulick A, Meena RS, Formanek P (2017) Enzymatic degradation of lignin in soil: a review. *Sustainability* 9:1163
- Dewar W, McDonald P, Whittenbury R (1963) The hydrolysis of grass hemicelluloses during ensilage. *J Sci Food Agric* 14:411–417
- Gervais P, Molin P (2003) The role of water in solid-state fermentation. *Biochem Eng J* 13:85–101
- Gianfreda L, Xu F, Bollag J-M (1999) Laccases: a useful group of oxidoreductive enzymes. *Bioresour Technol* 70:23–32
- Gírio F, Fonseca C, Carvalheiro F, Duarte L, Marques S, Bogel-Lukasik R (2010) Hemicelluloses for fuel ethanol: a review. *Bioresour Technol* 101:4775–4800
- de Gonzalo G, Colpa DI, Habib MH, Fraaije MW (2016) Bacterial enzymes involved in lignin degradation. *J Biotechnol* 236:110–119
- Gupta A, Verma JP (2015) Sustainable bio-ethanol production from agro-residues: a review. *Renew Sustain Energy Rev* 41:550–567
- Hahn-Hägerdal B, Galbe M, Gorwa-Grauslund M-F, Lidén G, Zacchi G (2006) Bio-ethanol—the fuel of tomorrow from the residues of today. *Trends Biotechnol* 24:549–556
- Kalyani D, Lee K-M, Kim T-S, Li J, Dhiman SS, Kang YC, Lee J-K (2013) Microbial consortia for saccharification of woody biomass and ethanol fermentation. *Fuel* 107:815–822
- Keller FA, Hamilton JE, Nguyen QA (2003) Microbial pretreatment of biomass. *Appl Biochem Biotechnol* 105:27–41
- Kim SJ, Shoda M (1999) Purification and characterization of a novel peroxidase from *Geotrichum candidum* Dec 1 involved in decolorization of dyes. *Appl Environ Microbiol* 65:1029–1035
- Liers C, Arnstadt T, Ullrich R, Hofrichter M (2010) Patterns of lignin degradation and oxidative enzyme secretion by different wood-and litter-colonizing basidiomycetes and ascomycetes grown on beech-wood. *FEMS Microbiol Ecol* 78:91–102
- Lu Y, Cheng Y-F, He X-P, Guo X-N, Zhang B-R (2012) Improvement of robustness and ethanol production of ethanologenic *Saccharomyces cerevisiae* under co-stress of heat and inhibitors. *J Ind Microbiol Biotechnol* 39:73–80
- Machczynski MC, Vijgenboom E, Samyn B, Canters GW (2004) Characterization of SLAC: a small laccase from *Streptomyces coelicolor* with unprecedented activity. *Protein Sci* 13:2388–2397
- Mackulak T, Prousek J, Švorc L, Drtil M (2012) Increase of biogas production from pretreated hay and leaves using wood-rotting fungi. *Chem Pap* 66:649–653
- Mai C, Kües U, Militz H (2004) Biotechnology in the wood industry. *Appl Microbiol Biotechnol* 63:477–494
- Majumdar S, Lukk T, Solbiati JO, Bauer S, Nair SK, Cronan JE, Gerlt JA (2014) Roles of small laccases from *Streptomyces* in lignin degradation. *Biochemistry* 53:4047–4058
- Martín-Sampedro R, Fillat Ú, Ibarra D, Eugenio ME (2015) Use of new endophytic fungi as pretreatment to enhance enzymatic saccharification of *Eucalyptus globulus*. *Bioresour Technol* 196:383–390
- Millati R, Syamsiah S, Niklasson C, Cahyanto MN, Ludquist K, Taherzadeh MJ (2011) Biological pretreatment of lignocelluloses with white-rot fungi and its applications: a review. *Bioresources* 6:5224–5259

- Mustafa AM, Poulsen TG, Sheng K (2016) Fungal pretreatment of rice straw with *Pleurotus ostreatus* and *Trichoderma reesei* to enhance methane production under solid-state anaerobic digestion. *Appl Energy* 180:661–671
- Nanda S, Mohammad J, Reddy SN, Kozinski JA, Dalai AK (2014) Pathways of lignocellulosic biomass conversion to renewable fuels. *Biomass Conv Bioref* 4:157–191
- Pérez J, Munoz-Dorado J, de la Rubia T, Martínez J (2002) Biodegradation and biological treatments of cellulose, hemicellulose and lignin: an overview. *Int Microbiol* 5:53–63
- Plácido J, Capareda S (2015) Ligninolytic enzymes: a biotechnological alternative for bioethanol production. *Bioresour Bioprocess* 2:23
- Poszytek K, Cieczkowska M, Sklodowska A, Drewniak L (2016) Microbial consortium with high cellulolytic activity (MCHCA) for enhanced biogas production. *Front Microbiol* 7:324
- Ray MJ, Leak DJ, Spanu PD, Murphy RJ (2010) Brown rot fungal early stage decay mechanism as a biological pretreatment for softwood biomass in biofuel production. *Biomass Bioenergy* 34:1257–1262
- Reid ID (1985) Biological delignification of aspen wood by solid-state fermentation with the white-rot fungus *Merulius tremellosus*. *Appl Environ Microbiol* 50:133–139
- Rodríguez C, Alaswad A, Benyounis K, Olabi A (2017) Pretreatment techniques used in biogas production from grass. *Renew Sust Energ Rev* 68:1193–1204
- Rouches E, Herpoël-Gimbert I, Steyer J, Carrere H (2016) Improvement of anaerobic degradation by white-rot fungi pretreatment of lignocellulosic biomass: a review. *Renew Sust Energ Rev* 59:179–198
- Saxena R, Adhikari D, Goyal H (2009) Biomass-based energy fuel through biochemical routes: a review. *Renew Sust Energ Rev* 13:167–178
- Shi J, Sharma-Shivappa RR, Chinn M, Howell N (2009) Effect of microbial pretreatment on enzymatic hydrolysis and fermentation of cotton stalks for ethanol production. *Biomass Bioenergy* 33:88–96
- Shi Y, Yan X, Li Q, Wang X, Xie S, Chai L, Yuan J (2017) Directed bioconversion of Kraft lignin to polyhydroxyalkanoate by *Cupriavidus basilensis* B-8 without any pretreatment. *Process Biochem* 52:238–242
- da Silva Machado A, Ferraz A (2017) Biological pretreatment of sugarcane bagasse with basidiomycetes producing varied patterns of biodegradation. *Bioresour Technol* 225:17–22
- Sindhu R, Binod P, Pandey A (2016) Biological pretreatment of lignocellulosic biomass—an overview. *Bioresour Technol* 199:76–82
- Singhania RR, Patel AK, Soccol CR, Pandey A (2009) Recent advances in solid-state fermentation. *Biochem Eng J* 44(1):13–18
- Song L, Yu H, Ma F, Zhang X (2013) Biological pretreatment under non-sterile conditions for enzymatic hydrolysis of corn stover. *Bioresources* 8:3802–3816
- Srebotnik E, Jensen K, Kawai S, Hammel KE (1997) Evidence that *Ceriporiopsis subvermispora* degrades nonphenolic lignin structures by a one-electron-oxidation mechanism. *Appl Environ Microbiol* 63:4435–4440
- Suhara H, Kodama S, Kamei I, Maekawa N, Meguro S (2012) Screening of selective lignin-degrading basidiomycetes and biological pretreatment for enzymatic hydrolysis of bamboo culms. *Int Biodeterior Biodegrad* 75:176–180
- Vasco-Correa J, Ge X, Li Y (2016) Fungal pretreatment of non-sterile miscanthus for enhanced enzymatic hydrolysis. *Bioresour Technol* 203:118–123
- Wan C, Li Y (2012) Fungal pretreatment of lignocellulosic biomass. *Biotechnol Adv* 30:1447–1457
- Wesenberg D, Kyriakides I, Agathos SN (2003) White-rot fungi and their enzymes for the treatment of industrial dye effluents. *Biotechnol Adv* 22:161–187
- Winquist E, Moilanen U, Mettälä A, Leisola M, Hatakka A (2008) Production of lignin modifying enzymes on industrial waste material by solid-state cultivation of fungi. *Biochem Eng J* 42:128–132

- Wongwilaiwalin S, Rattanachomsri U, Laothanachareon T, Eurwilaichitr L, Igarashi Y, Champreda V (2010) Analysis of a thermophilic lignocellulose degrading microbial consortium and multi-species lignocellulolytic enzyme system. *Enzym Microb Technol* 47:283–290
- Woolridge EM (2014) Mixed enzyme systems for delignification of lignocellulosic biomass. *Catalysts* 4:1–35
- Yan X, Wang Z, Zhang K, Si M, Liu M, Chai L, Liu X, Shi Y (2017) Bacteria-enhanced dilute acid pretreatment of lignocellulosic biomass. *Bioresour Technol* 245:419–425
- Zabed H, Faruq G, Sahu JN, Azirun MS, Hashim R, Nasrulhaq Boyce A (2014) Bioethanol production from fermentable sugar juice. *Sci World J*, Article ID 957102
- Zabed H, Boyce A, Faruq G, Sahu J (2016a) A comparative evaluation of agronomic performance and kernel composition of normal and high sugary corn genotypes (*Zea mays* L.) grown for dry-grind ethanol production. *Ind Crop Prod* 94:9–19
- Zabed H, Faruq G, Boyce AN, Sahu JN, Ganesan P (2016b) Evaluation of high sugar containing corn genotypes as viable feedstocks for decreasing enzyme consumption during dry-grind ethanol production. *J Taiwan Inst Chem Eng* 58:467–475
- Zabed H, Faruq G, Sahu J, Boyce A, Ganesan P (2016c) A comparative study on normal and high sugary corn genotypes for evaluating enzyme consumption during dry-grind ethanol production. *Chem Eng J* 287:691–703
- Zabed H, Sahu J, Boyce A, Faruq G (2016d) Fuel ethanol production from lignocellulosic biomass: an overview on feedstocks and technological approaches. *Renew Sust Energy Rev* 66:751–774
- Zabed H, Boyce AN, Sahu J, Faruq G (2017a) Evaluation of the quality of dried distiller's grains with solubles for normal and high sugary corn genotypes during dry-grind ethanol production. *J Clean Prod* 142:4282–4293
- Zabed H, Sahu J, Suely A (2017b) Bioethanol production from lignocellulosic biomass: an overview of pretreatment, hydrolysis, and fermentation. In: Mondal P, Dalai AK (eds) Sustainable utilization of natural resources. Taylor & Francis, Boca Raton, p 145
- Zabed H, Sahu JN, Suely A, Boyce AN, Faruq G (2017c) Bioethanol production from renewable sources: current perspectives and technological progress. *Renew Sust Energy Rev* 71:475–501
- Zhang Q, He J, Tian M, Mao Z, Tang L, Zhang J, Zhang H (2011) Enhancement of methane production from cassava residues by biological pretreatment using a constructed microbial consortium. *Bioresour Technol* 102:8899–8906
- Zheng Y, Zhao J, Xu F, Li Y (2014) Pretreatment of lignocellulosic biomass for enhanced biogas production. *Prog Energy Combust Sci* 42:35–53



Role of Natural Deep Eutectic Solvents (NADES) in the Pretreatment of Lignocellulosic Biomass for an Integrated Biorefinery and Bioprocessing Concept

Shaishav Sharma and Adepu Kiran Kumar

Abstract

Currently, biorefinery process from cellulosic biomass is complex and energy-intensive where biomass fractionation, a key step for production of biomass-derived chemicals, demands conventional organic solvents. Since there is a clear and an unmet need for a robust and affordable biomass conversion technology, researchers are constantly developing novel, cost-effective green solvents that are eco-friendly, benign, renewable, and biodegradable in nature. In this perspective, natural deep eutectic solvents, commonly referred as NADES, have been evolved as the most advanced green solvents entirely made up of natural compounds to combat and deconstruct the recalcitrance of lignocellulosic biomass into the extraction of potential renewable chemicals. Although NADES are characteristically similar to deep eutectic solvents (DESS) and ionic liquids, NADES have shown advantages to combat the challenges associated with ionic liquids and DES by being highly specific and green in nature. Moreover, NADES could be recovered and recycled without losing their efficiency, making these solvents highly economical and sustainable. In this chapter, we have comprehensively described the applicability of NADES in biorefinery and bioprocessing as an effective tool of lignocellulosic biomass pretreatment for bioconversion processes.

Keywords

Natural deep eutectic solvents (NADES) · Pretreatment · Lignocellulosic biomass · Biorefinery · Bioprocessing · Bioconversion

S. Sharma · A. K. Kumar (✉)

Bioconversion Technology Division, Sardar Patel Renewable Energy Research Institute, Vallabh Vidyanagar, Gujarat, India

e-mail: kiranbio@gmail.com

Abbreviations

Ala	Alanine
BA	Butyric acid
BE	Betaine
CA	Citric acid
CC	Choline chloride
DA	Decanoic acid
DEG	Diethylene glycol
DOA	Dodecanoic acid
EG	Ethylene glycol
Fru	Fructose
GA	Glutaric acid
Gal	Galactose
Glu	Glucose
Gly	Glycerol
H ₂ O	Water
HA	Hexanoic acid
LA	Lactic acid
LE	Levulinic acid
MA	Malic acid
MAL	Malonic acid
Mnl	Menthol
NA	Nicotinic acid
OA	Oxalic acid
OCA	Octanoic acid
PD	Propane diol
Pro	Proline
Suc	Sucrose
TA	Tartaric acid
TEG	Triethylene glycol
Ur	Urea
Xtl	Xylitol
Xyl	Xylose

4.1 Introduction

Bioconversion of lignocellulosic agricultural residues to biofuel and value-added products is gaining importance globally. The development of second-generation bioethanol from agro-residues has several advantages in terms of energy and environment. Lignocellulosic biomass is an abundantly available sustainable and

renewable feedstock having the potential to replace fossil fuels and other fossil-based materials and chemicals. Lignocellulose is the basic structural constituent of all the plants (woody and non-woody) and mostly consists of three main fractions, i.e., lignin, cellulose, and hemicellulose. The optimized utilization of these key constituents has a major role in the viability and sustainability of biorefinery and bioprocessing industries. In a biorefinery, along with the production of second- and third-generation liquid biofuels such as bioethanol and biodiesel, the valorization of other by-products generated in the process also plays a major role. The conversion of biomass to liquid fuels (bioethanol) commonly involves five process steps: (i) selection of suitable lignocellulosic biomass, (ii) effective pretreatment, (iii) enzymatic saccharification of cellulose and hemicellulose, (iv) fermentation of monomeric sugars (hexose and pentose), and (v) downstream processing for recovery and reuse of solvents. Lignocellulosic biomass despite being a potential candidate for biofuel and other value-added products suffers from various obstacles that are associated in their effective deconstruction.

The structure of a plant cell wall is highly recalcitrant owing to the structural intricacy of lignocellulosic portions. In addition, the inhibitors and by-products produced during the pretreatment process create a strong hindrance. Some other obstacles that are needed to be taken into consideration are the selection of an appropriate pretreatment method, understanding the physicochemical complexity of feedstock cell walls, and degree of cell wall destruction for production of value-added by-products. Lignocellulosic biomass pretreatment is one of the key processes in biorefinery and bioprocessing. Within the context of production of fuels from biomass, pretreatment is known as the process by which cellulosic biomass is made available to the action of hydrolytic enzymes.

There are several points that need to be considered for selecting a suitable pretreatment method: (i) size reduction of biomass particles should not be required, (ii) deconstruction of hemicellulose fraction should be minimum, (iii) there should be minimum energy demands, (iv) there should be no or minimum inhibitory products formation, (v) catalyst involved should be inexpensive and recyclable, and (vi) there should be a recovery of value-added products such as lignin (Wyman 1999). The selected pretreatment method should defend as well as justify its effect on the cost of subsequent downstream processing steps and the trade-off between capital costs, operating costs, biomass costs, etc. (Lynd et al. 1996). At present, the technologies developed and applied for pretreatment have several drawbacks, such as (i) high cost and harmful impact of chemicals involved in the pretreatment process; (ii) high cost of reactors developed to withstand high temperature, pressure, and corrosive effect of chemicals; (iii) inhibitory effect caused due to the formation of several by-products; (iv) incomplete destruction of lignin-carbohydrate matrix; (v) large volumes of water required for washing, neutralization, etc.; and (vi) an expensive process of recovery of solvents.

In order to overcome the above mentioned disadvantages, a new class of green solvents with low melting temperatures has been developed. Developing these types of new and advanced green solvents for a wide variety of applications has attracted the researchers working in the field of green chemistry worldwide. Recently, such

group of green solvents termed as natural deep eutectic solvents (NADES) is gaining interest rapidly. As the name suggests, these solvents are very similar to the well-established deep eutectic solvents (DES) related to its functions and properties; however, they differ in the chemical components involved in their synthesis. DES involves mixtures of chemically synthesized inorganic and organic chemicals, whereas NADES are solely produced from natural metabolites such as sugars, amino acids, organic acids, sugar alcohols, and amines. This provides NADES an inherent advantage over other conventional solvents. Moreover, NADES are completely eco-friendly, nontoxic, cost-effective, easy to handle, synthesizable and recyclable, biocompatible, and highly biodegradable. In the recent years, NADES generated a great attention in many industrial applications ranging from pharmaceutical, chemical, and food processing to enzyme and biofuel industries due to their mode of action. Observing their prospective application in several industries, NADES are considered as the solvents of the twenty-first century (Paiva et al. 2014; Smith et al. 2014).

The current advances in NADES pretreatment have shown high specificity for lignin solubility and extraction from lignocellulosic biomass (rice and wheat straw) (Kumar et al. 2016) and woody biomass (Alvarez-Vasco et al. 2016). Another important aspect is the mechanism involved in the interaction of NADES and water, which has brought additional focus on them. It is well known that water being the most abundant solvent plays a vital function in biological systems. Apart from water and lipids, NADES in combination with water and biological fluids may possibly play a major role as another type of solvent inside the cells of living organisms (Dai et al. 2015). Supporting this phenomenon, a research study on NADES showed that they involve in the synthesis, transportation, and storage of various inadequately water-soluble compounds (Choi et al. 2011). Through a biological viewpoint, the simultaneous existence of NADES and water in living organisms is very important to understand the effect of water on NADES to further enhance their applicability. The presence of NADES in organisms points toward a vital phenomenon, i.e., the presence of an alternate medium for conducting various metabolic functions that are not able to occur in water and lipids. The presence of NADES can provide answers to the mechanisms of various reactions that could not occur in water and lipids alone such as biosynthesis of hydrophobic metabolites, the adaptive ability of organisms in extreme climatic conditions, etc. (Abbott et al. 2009; Dai et al. 2013a). This chapter deals with different pretreatment methods with emphasis on NADES pretreatment, its synthesis, physicochemical properties, and its role in biorefinery and bioprocessing.

4.2 Lignocellulosic Feedstocks

The world is directly or indirectly dependent on agriculture for food requirements, and this leads to the generation of million metric tons of lignocellulosic biomass and residual wastes annually. This resource has not been fully utilized and in some cases yet untapped and has huge potential for bioconversion into an excellent source of

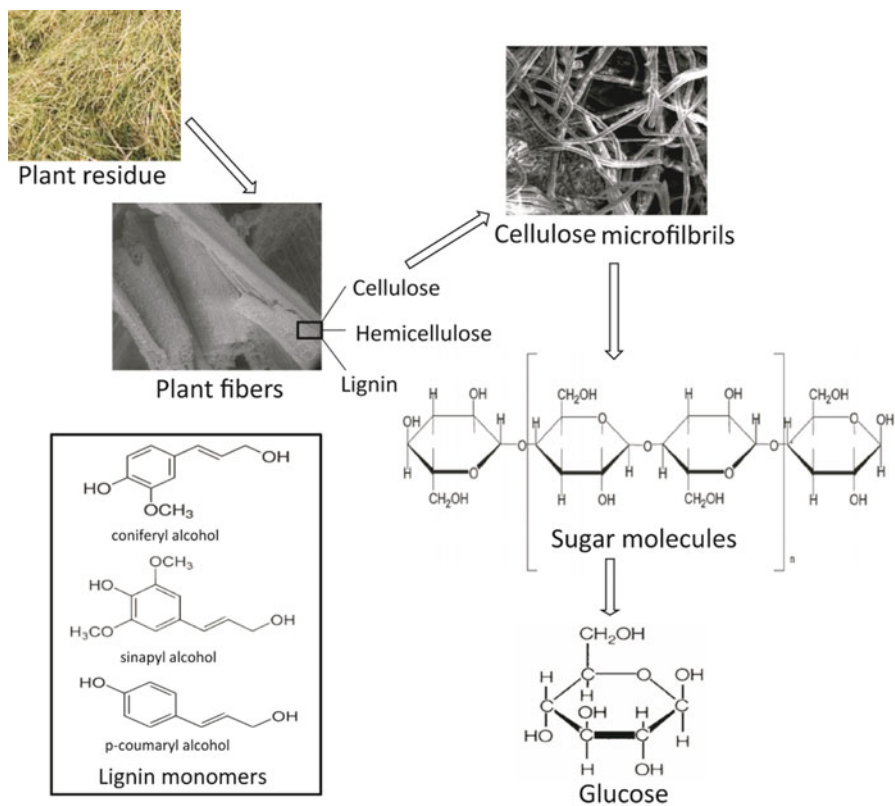


Fig. 4.1 Illustration depicting the lignocellulosic framework

energy generation (Prasad et al. 2007). Lignocellulosic biomass is defined as a biological material available in the form of vegetation, forest waste, by-products of crops, and agro- or food industrial waste. A variety of biomass resources are available and classified on the basis of their physicochemical nature, viz., grasses, woody plants, fruits, vegetables, agricultural crop residues, municipal and industrial waste, etc. (Kumar and Sharma 2017). An illustration depicting the typical lignocellulosic biomass framework and its main constituents is shown in Fig. 4.1.

The organic by-products produced during the processing and harvesting of agricultural crops are called as agricultural residues. Based on the time of yield, the agricultural residues can further be categorized into primary and secondary residues. Agro-residual waste materials obtained at the time of yield in the field are termed as primary residues. Sugarcane tops and rice straw are the examples of the primary residues, while secondary residues are the residues that are obtained during the processing of the crops such as rice husk, sugarcane bagasse, etc. (Murali et al. 2008). The primary residues are mainly used as animal feed, fertilizers, etc. and therefore cannot be used for energy applications. Secondary residues are obtained in

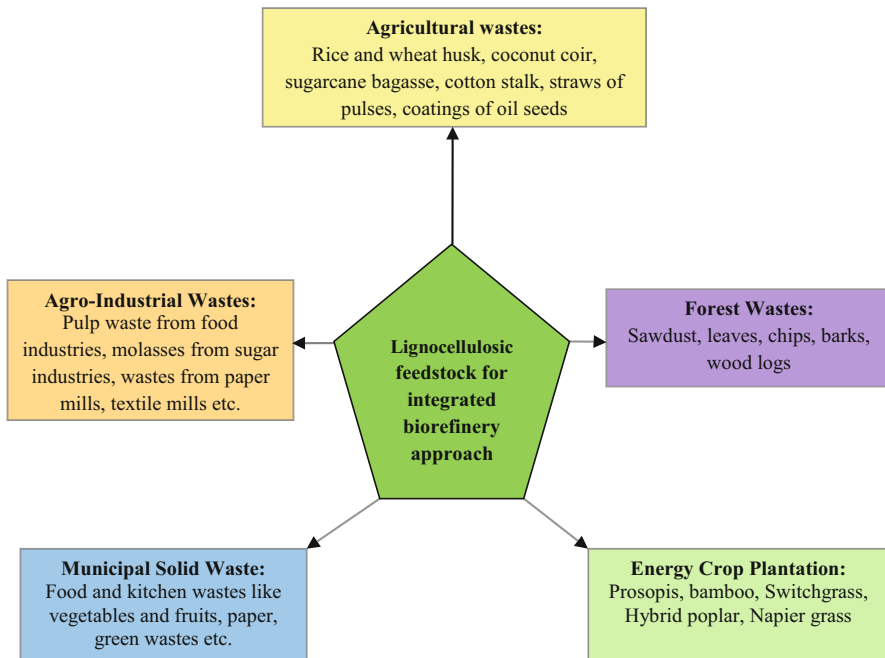


Fig. 4.2 Different types of biomass resources

large quantities and have potential to be developed as a raw material for energy production. A simple classification of biomass resources based on their source is shown in Fig. 4.2 (Kumar et al. 2015a).

Wood is primarily composed of hemicellulose, cellulose, and lignin. Based on the varying proportions of these substances, woods are classified into softwoods and hardwoods. Softwood hemicellulose has a higher fraction of glucose and mannose than hardwood hemicellulose, which has a higher fraction of xylose. Moreover, hemicellulose has been found to be more acetylated in hardwoods as compared to softwoods. Lignin is divided into two categories: syringyl lignins and guaiacyl lignins. The difference between the two lies in the substituents of phenyl-propanoid skeleton. Syringyl lignin has methoxy group in three-carbon position, while guaiacyl lignin has a methoxy group in three-carbon position. Hardwoods contain guaiacyl-syringyl lignin, while softwoods majorly contain guaiacyl lignin (Palmqvist and Hagerdal 2000). Hardwoods have been found to contain a lesser quantity of lignin than softwoods (Saka 1991). The examples of hardwoods are maple, beech, teak, oak, and walnut, while Douglas fir, cedar, pine, redwood, juniper, and spruce are examples of softwoods. Other lignocellulosic residues include garden waste, dried leaves, forest waste, etc. In all these lignocellulosic biomass residues, the main constituents are cellulose, hemicellulose, and lignin, and their compositional variation in a few biomasses is shown in Table 4.1.

Table 4.1 Cellulose, hemicellulose, and lignin content in common lignocellulosic feedstocks

Lignocellulosic materials	Lignin fraction (wt %)	Cellulose fraction (wt %)	Hemicellulose fraction (wt %)	Ash content (wt %)	References
Agro-residues	25–50	5–15	37–50	–	Kumar and Sharma (2017)
Banana peels	14	13.2	14.8	–	Kumar and Sharma (2017)
Corn cobs	15	45	35	12–16	Kumar and Sharma (2017) and Saini et al. (2015)
Corn stover	19	38	26	3.6	Kumar and Sharma (2017) and Saini et al. (2015)
Cotton seed hairs	0	80–95	5–20	–	Kumar and Sharma (2017)
Grasses	10–30	25–40	25–50	–	Kumar and Sharma (2017)
Hardwood	18–25	40–55	24–40	0.6	Kumar and Sharma (2017) and Saini et al. (2015)
Hardwood barks	25–40	20–25	45–47	0.8	Kumar and Sharma (2017) and Saini et al. (2015)
Leaves	0	15–20	80–85	–	Kumar and Sharma (2017)
Newspaper high grade	18–30	40–55	25–40	–	Kumar and Sharma (2017)
Newspaper low grade	25–40	12	40–55	–	Kumar and Sharma (2017)
Nutshells	30–40	25–30	25–30	–	Kumar and Sharma (2017)
Rice straw	18	32	24	14–20	Kumar and Sharma (2017) and Saini et al. (2015)
Softwood	25–35	45–50	25–35	0.5	Kumar and Sharma (2017) and Saini et al. (2015)
Softwood barks	25–29	30–60	40–45	0.8	Kumar and Sharma (2017) and Saini et al. (2015)
Sorted refuse	20	60	20	–	Kumar and Sharma (2017)
Sugarcane bagasse	20	42	25	1.5–5	Kumar and Sharma (2017) and Saini et al. (2015)
Sweet sorghum	21	45	27	–	Kumar and Sharma 2017

(continued)

Table 4.1 (continued)

Lignocellulosic materials	Lignin fraction (wt %)	Cellulose fraction (wt %)	Hemicellulose fraction (wt %)	Ash content (wt %)	References
Switchgrass	12	45	31.4	–	Kumar and Sharma (2017)
Waste paper pulps	12–20	6–10	50–70	–	Kumar and Sharma (2017)
Wheat straw	16–21	29–35	26–32	6–8	Kumar and Sharma (2017)
White paper	0–15	85–99	0	–	Kumar and Sharma (2017)

4.3 Biomass Pretreatment Processes

Lignocellulosic feedstock represents an extremely large quantity of renewable bioresource available in excess on earth and is an appropriate raw matter for a variety of applications for human sustainability. However, effective utilization of lignocellulosic biomass is a hard nut to crack due to several obstacles associated with it. Some of the major factors are the recalcitrance of the plant cell wall due to the integral structural complexity of lignocellulosic fractions and strong obstruction from the by-products and inhibitors formed during pretreatment. Moreover, other challenges such as understanding the physicochemical structure of their cell walls, appropriate pretreatment method, and extent of cell wall decomposition for production of value-added by-products.

Lignocellulosic biomass pretreatment is an indispensable step required for modifying the strongly bound lignocellulosic structure, which exposes the constituents for effortless accessibility to an enzyme for hydrolysis, which in turn increases the pace and amount of reducing sugars (Alvira et al. 2010). Based on the type of agent involved, pretreatment methods are classified into two categories: biological and non-biological. Non-biological pretreatment methods which do not involve any microbial agent are broadly classified into physical, chemical, and physicochemical methods. A list of promising and most commonly used pretreatment methods is shown in Fig. 4.3.

4.4 Biological Pretreatment

Biological pretreatment methods are more efficient, environmentally safe, and low energy consuming as compared to conventional chemical pretreatment methods. Nature supplies an extensive array of hemicellulolytic and cellulolytic microorganisms, which can be exclusively applied for efficient biomass pretreatment (Vats et al. 2013). Among these microorganisms, white rot, soft rot, and brown rot

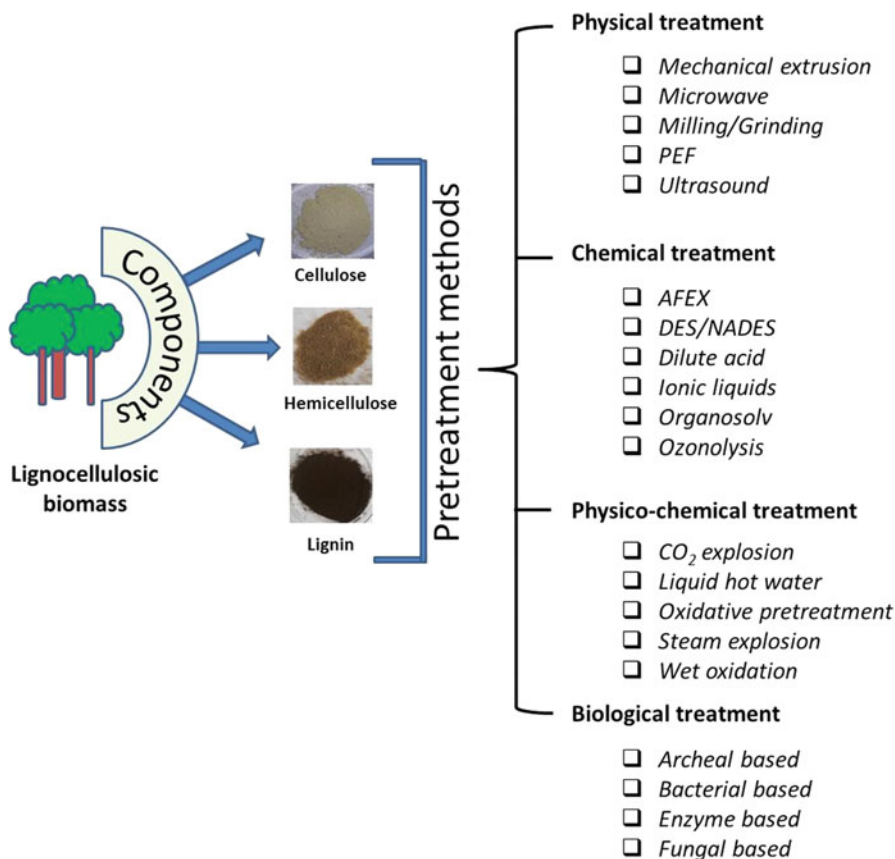


Fig. 4.3 Overview of different pretreatment processes

fungi possess the capacity to denature hemicellulose and lignin (Sanchez 2009). White rot fungi have the ability to degrade lignin due to the presence of laccases (lignin-degrading enzymes) and peroxidases (Kumar et al. 2009). Normally employed white rot fungi species are *Pleurotus ostreatus*, *Phanerochaete chrysosporium*, *Cyathus stercoreus*, *Pycnoporus cinnabarinus*, *Ceriporiopsis subvermisporea*, and *Ceriporia lacerata*. The microorganisms that are reported to have shown high delignification efficiency are *Fomes fomentarius*, *Bjerkandera adusta*, *Irpex lacteus*, *Ganoderma resinaceum*, *Lepista nuda*, *Trametes versicolor*, and *Phanerochaete chrysosporium* (Kumar et al. 2009; Shi et al. 2008). Different classes of microbes used for pretreatment along with their effects on different lignocellulosic biomasses are summarized in Table 4.2. Although biological pretreatment is captivating, hydrolysis rate has been found to be slow which obstructs the application of biological agents for pretreatment at commercial scale. Other robust fungal species having the capability to delignify the lignocellulosic biomass need to be tested for further applications.

Table 4.2 Different biological pretreatment strategies involved for pretreatment of lignocellulosic biomass and its advantages

Agro-residues	Biological agent	Significant alterations after pretreatment	References
Bamboo culms	<i>Punctularia sp.</i>	>50% removal of lignin	Suhara et al. (2012)
Cornstalks	<i>Irpex lacteus</i>	82% reducing sugar yield	Du et al. (2011)
Corn stover	Fungal consortium	>44% lignin removed, hydrolysis efficiency improved by sevenfold	Song et al. (2013)
Corn stover	<i>Irpex lacteus</i>	>66% saccharification efficiency	Xu et al. (2010)
Corn stover	<i>Ceriporiopsis subvermispora</i>	Reducing sugars enhanced by 2–3 times	Wan and Li (2011)
<i>Eucalyptus grandis</i> sawdust	<i>Pleurotus ostreatus/ Pleurotus pulmonarius</i>	Hydrolysis efficiency increased by 20-fold	Castoldi et al. (2014)
Plant feedstock	Fungal consortium	Toxic chemicals completely removed	Dhiman et al. (2015)
Rice husk	<i>Phanerochaete chrysosporium</i>	–	Potumarthi et al. (2013)
Rice straw	<i>Dichomitus squalens</i>	>55% enzymatic hydrolysis	Bak et al. (2010)
Straw	Fungal consortium	Hydrolysis efficiency increased by 20-fold	Taha et al. (2015)
Wheat straw	<i>Ceriporiopsis subvermispora</i>	Negligible loss of cellulose	Cianchetta et al. (2014)

4.5 Physical Pretreatment

The non-biological pretreatment includes various physical, chemical, and physico-chemical methods. Various pretreatment methods summarised here as the detailed analysis of these methods is beyond the scope of this chapter. The readers are suggested to refer the recent review by Kumar and Sharma (2017) for further details on various pretreatment methods.

The physical pretreatment methods involve the use of different physical forces for altering the tightly bound lignocellulosic structure for exposure to the enzyme. Commonly applied physical pretreatment methods are:

1. **Mechanical extrusion:** It is the oldest and most common method used for the lignocellulosic biomass pretreatment. Under this process, the biomass is subjected to high temperature (>300 °C) along with shear mixing. However, this method is highly energy-intensive thereby increasing the cost and unfeasible for industrial-scale applications (Zhu and Pan 2010).

2. *Milling*: This technique is majorly applied to reduce the crystallinity of cellulose. This process commonly includes grinding, chipping, and milling techniques. Chipping reduces the size of biomass up to 10–30 mm, while grinding and milling reduce it further up to 0.2–0.4 mm. Chipping process decreases the limitations of heat and mass transfer, whereas grinding and milling efficiently decrease the cellulose crystallinity and particle size owing to the shear forces produced during milling (Kumar and Sharma 2017). There are various milling methods, viz., hammer milling, two-roll milling, vibratory milling, and colloid milling, which are used to increase the degradability of the lignocellulosic biomass (Tahezadeh and Karimi 2008).
3. *Microwave*: It is an extensively used method for pretreatment of lignocellulosic agro-residues. This method is useful because of (i) low energy requirement, (ii) simple operating conditions, (iii) minimum inhibitor formation, (iv) high heating capacity in short time duration, and (v) the ability to degrade cellulose structural organization (Kumar and Sharma 2017).
4. *Sonication*: Ultrasound waves produce chemical and physical effects which alter the morphology of the lignocellulosic biomass. This results in the formation of cavitation bubbles, which disrupts the cellulosic and hemicellulosic portions resulting in the increased availability of cellulose-degrading enzymes for efficient breakdown into simpler sugars. However, the duration and power of sonication need to be optimized further for maximum pretreatment efficiency.
5. *Pulsed electric field*: This treatment subjects the biomass to a rapid burst of high voltage in the range of 5–20 kV/cm for small durations (nano- to milliseconds). The pulsed electric field has certain advantages, viz., low energy requirement, ambient conditions required for pretreatment, and simplicity in design due to lack of moving parts (Kumar et al. 2009).

4.6 Physicochemical Pretreatment

These methods involve a blend of chemical effects and mechanical forces for the pretreatment of lignocellulosic biomass. A few of such methods have been described here:

1. *Steam explosion*: This method involves autohydrolysis of acetyl groups of hemicellulose and pressure drop as chemical and mechanical effects, respectively, for the effective pretreatment of biomass. High-pressure (0.7–4.8 MPa) saturated steam at elevated temperatures (between 160 and 260 °C) for few seconds to minutes is applied to biomass, which leads to hydrolysis and release of hemicellulose. Steam penetrates the biomass leading to expansion of fibers thereby increasing the accessibility of enzymes for cellulose. Steam explosion has several disadvantages such as partial digestion of lignin-carbohydrate matrix, creation of fermentation inhibitors at high temperature, and the hydrolysate washing which reduces the yield of sugar by 20% (Agbor et al. 2011).

2. *Liquid hot water*: This method applies high temperature (170–230 °C) pressure (up to 5 MPa) leading to hydrolysis of hemicellulose and lignin removal increasing cellulose accessibility. Low cost of the solvents, low temperature requirement, and minimum formation of inhibitory compounds are advantages of liquid hot water. However, liquid hot water becomes energy-intensive due to the requirement of large amount of water for downstream processing (Agbor et al. 2011).
3. *Wet oxidation*: This method is most suited for lignin-rich biomass residues. This method works on the principle that when water reaches above 170 °C, it starts behaving like an acid and catalyzes hydrolytic reactions. Hemicelluloses are converted to simpler pentose monomers along with oxidation, but the cellulose remains unaltered (Kumar and Sharma 2017).
4. *SPORL pretreatment*: SPORL is the abbreviated form of sulfite pretreatment to overcome recalcitrance of lignocellulose. It is commonly carried out in two steps. In the first step, lignin is removed from lignocellulosic biomass by treating with magnesium or calcium sulfite. In the second step, disk milling is used to reduce the size of the biomass. The advantages of SPORL pretreatment are rapid conversion of cellulose to glucose, less energy consuming, ability to process diverse types of biomass, and easy to scale up the existing mills for commercial production of biofuels, while certain drawbacks of this method are expensive recovery of pretreatment chemicals, degradation of sugars, and large amount of water needed for post-pretreatment washing (Bajpai 2016).
5. *Pretreatment using ammonia*: Various methods that are known to use ammonia for lignocellulosic biomass pretreatment are ammonia fiber explosion (AFEX), ammonia recycle percolation (ARP), and soaking aqueous ammonia (SAA). Under AFEX, the biomass is heated with ammonia in 1:1 ratio in a closed reactor at 60–90 °C and >3 MPa pressure for 30–60 min. After the biomass has undergone desired conditions for 5 min, the valve is opened to release the pressure explosively resulting in evaporation of ammonia and drop in temperature (Alizadeh et al. 2005). The difference between AFEX and steam explosion lies in the use of ammonia instead of water in AFEX (Rabemanolontsoa and Saka 2016). In ARP, 5–15 wt% aqueous ammonia is passed through biomass in a reactor. Optimum temperature for this process is between 140 and 210 °C, while the percolation rate is 5 mL/min with 90 min reaction time. After the pretreatment is completed, the ammonia is recycled and reused (Sun and Cheng 2002; Kim et al. 2008). The high energy requirement in ARP to maintain the process temperature is a major drawback. SAA is a modification of AFEX in which the biomass undergoes treatment with aqueous ammonia in a reactor at 30–60 °C. The advantage of this method is the reduction of liquid throughput in pretreatment (Kim and Lee 2005).
6. *CO₂ explosion*: Supercritical CO₂ is used in this method, which implies that the gas behaves like a solvent. Biomass is subjected to supercritical CO₂ in a high-pressure vessel (Kim and Hong 2001). Biomass under the effect of CO₂ at high pressure forms carbonic acid, which leads to hydrolysis of hemicellulose. The biomass organization is easily disrupted when the pressurized gas is released

(Zheng et al. 1995). The biomass having low or zero moisture content cannot be treated through this method. Advantages of this method are low cost of CO₂, high solid loading, minimum inhibitor generation, and low temperature requirement. However, the expensive reactors capable of withstanding high pressure create hindrance in its scaling up for commercial applications (Agbor et al. 2011).

7. *Oxidative pretreatment*: Various oxidizing agents, viz., hydrogen peroxide, ozone, oxygen, or air, are used for the treatment of lignocellulosic biomass in this method (Nakamura et al. 2004). During this process, several chemical reactions such as side-chain displacement, cleavage of aromatic ether linkages, and electrophilic substitution may occur. This method leads to delignification due to the conversion of lignin to acids, which may act as inhibitors. These acids must be removed for carrying out further steps (Alvira et al. 2010). In addition, hemicellulose is damaged to an extent making it unavailable for fermentation (Lucas et al. 2012).

4.7 Chemical Pretreatment

These methods involve the use of different chemicals and their characteristic reactions for disrupting the complex lignocellulosic structure. A few commonly used chemical pretreatment methods have been briefed here:

1. *Dilute acid*: The low cost of acids makes it the most commonly used pretreatment method. The formation of a high amount of inhibitory products such as phenolic acids, furfurals, aldehydes, and 5-hydroxymethylfurfural is a major disadvantage of this method. In addition, the reaction vessel should be constructed from a suitable material, which has the capacity to handle extreme experimental conditions and corrosive property of acids (Saha et al. 2005).
2. *Mild alkali treatment*: In this method, hydroxyl derivatives of potassium, calcium, ammonium, and sodium salts are used for the lignocellulosic biomass pretreatment. Unlike acid treatment, this method can be carried out at ambient pressure and temperature. The side chains of esters and glycosides are degraded by alkali reagents resulting in modification of lignin, decrystallization and swelling of cellulose, and hemicellulose solvation. However, the high downstream processing cost is a major drawback of this method. In addition, the method requires a large volume of water for removal of salt from the biomass and is an exhaustive process to remove them.
3. *Ozonolysis*: Ozone is mainly applied for decreasing the lignin portion of lignocellulosic biomass residue as it majorly degrades lignin (Kumar et al. 2009). Although ozonolysis is an effective method, the large amount of ozone required makes it a difficult option for commercial applications.
4. *Organosolv*: This method uses various organic and aqueous solvents, viz., glycol, ethanol, methanol, acetone, etc. for the pretreatment of lignocellulose biomass under specific pressure and temperature (Ichwan and Son 2011; Alriols et al. 2009). This method is commonly carried out in the presence of a base, acid, or salt

catalyst (Bajpai 2016). The drawbacks with this process are high acid concentration, long reaction time, and formation of inhibitors.

5. *Ionic liquids (IL)*: These solvents are synthesized from cations and anions. Major characteristics of these solvents are low melting points (<100 °C), high polarity, high thermal stabilities, and negligible vapor pressure (Behera et al. 2014; Zavrel et al. 2009). Ionic liquids disrupt the lignocellulosic network by competing with its components or hydrogen bonding (Moultrop et al. 2005). However, drawbacks such as difficulty in recycling and reuse, high cost, and formation of inhibitors obstruct the commercial application of ionic liquids (Kumar and Sharma 2017).
6. *Deep eutectic solvents (DES)*: These eutectic mixtures are commonly synthesized by mixing two or three components, which have the capability of self-association (usually hydrogen bonds). A major characteristic feature of these solvents is that the melting point of the mixture is lower than that of each individual component (Zhang et al. 2012a, b). DESs are very similar to ionic liquids, but the difference lies in their composition. Unlike ionic liquids, DESs are not composed of ionic species and can be synthesized from nonionic species. In the last few years, a number of natural products, viz., urea, choline, sugars, amino acids, and many other organic acids, have been considered in the DES category (Dai et al. 2013a). These solvents have been categorized separately into a new class of solvents termed as natural deep eutectic solvents (NADES). In contrast to ionic liquids, NADES are easier to synthesize, cost-effective, nontoxic, recyclable, reusable, biocompatible, and highly biodegradable. NADES synthesis, components, characteristic properties, and applications have been described in the next sections.

4.8 Natural Deep Eutectic Solvents (NADES): Synthesis and Mechanism

NADES have proved to be an alternative to ionic liquids. The ionic liquids' green nature has been strongly challenged owing to their poor biocompatibility, sustainability, and biodegradability. DESs are similar to ionic liquids in having an ionic character but comprise a mixture of organic compounds having a melting point remarkably lower than that of individual components (Paiva et al. 2014). A schematic representation of the lowered melting temperature of the so formed NADES is shown in Fig. 4.4. A timeline of various processes and various solvents developed in chronological order is shown in Fig. 4.5.

NADES are synthesized by a complex formation between a hydrogen-bond donor (HBD) and hydrogen-bond acceptor (HBA). Table 4.3 shows various HBA and HBD components that can be combined to form NADES. The decrease in the melting point of the mixture as compared to its constituents is mainly due to the delocalization of charge. Another advantage of NADES is the availability of a wide variety of solvents with the possibility of a large number of combinations, which give rise to tailored solvents with desired properties for various applications. NADES are synthesized in two ways. It can either be prepared from the aqueous solutions consisting of each compound in which a component is in the molten state

Fig. 4.4 Schematic design showing the lowering of the melting point of the mixture than individual components

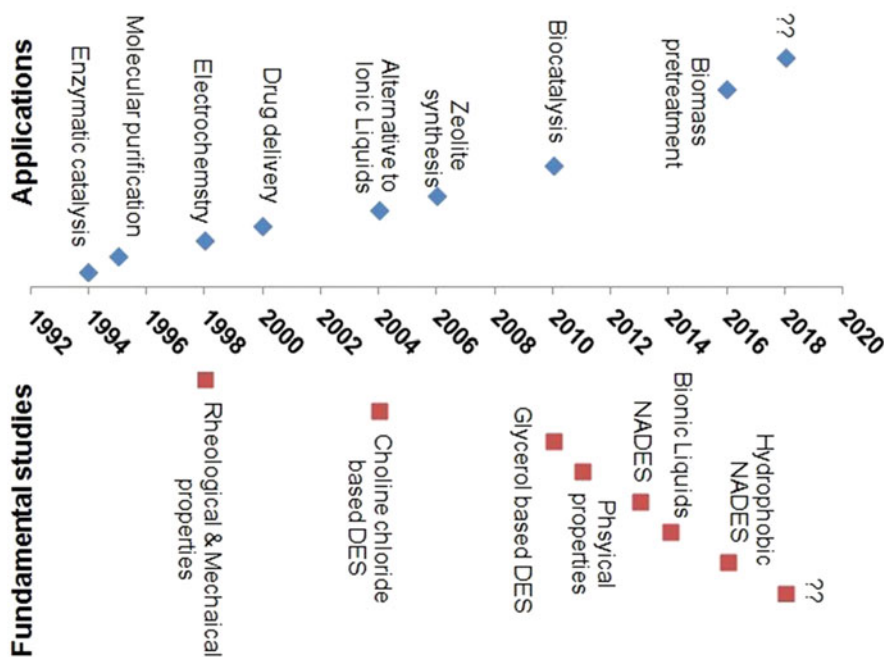
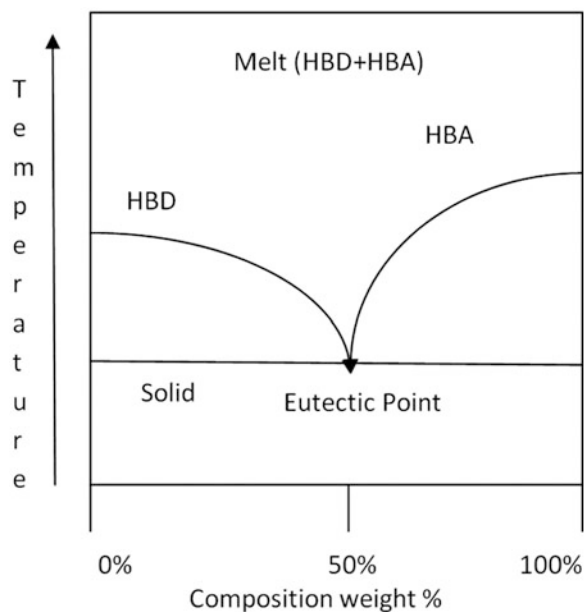


Fig. 4.5 A road map of reported developments, both on applications and fundamental studies on deep eutectic solvents

Table 4.3 Commonly used HBA and HBD for synthesis of NADES

Hydrogen-bond donors (HBD)	Hydrogen-bond acceptors (HBA)
Oxalic acid	Ethylammonium chloride
Malonic acid	Nicotinic acid
Xylitol	Trimethylammonium chloride
Urea	Betaine
Benzoic acid	Choline nitrate
Citric acid	Tetraethylammonium chloride
Imidazole	Choline chloride
Cinnamic acid	Histidine
Ethylene glycol	Alanine
D-sorbitol	Acetylcholine chloride
Lactic acid	Glycine
Levulinic acid	Choline fluoride
Glycerol	Proline
Succinic acid	Lidocaine
Hexanoic acid	Methyltriphenylphosphonium chloride
Stearic acid	Tetrabutylammonium chloride
Oleic acid	
Linoleic acid	
Adipic acid	
Suberic acid	

and the other component is dissolved or by mixing the two solid components heated to a predetermined value (Francisco et al. 2013; Paiva et al. 2014).

NADES are most commonly synthesized from carboxylic acids, choline chloride, and hydrogen-bond donors such as succinic acid, glycerol, urea, citric acid, etc. NADES despite being similar to ionic liquids have an upper hand over ionic liquids due to their low cost, less toxic, and biodegradable nature. In the recent past, a large variety of stable NADES have been developed from natural compounds such as organic acids, amino acids, and sugars (Dai et al. 2013a; Choi et al. 2011).

The composition of a eutectic mixture is commonly determined through differential scanning calorimeter (Morisson et al. 2009; Kareem et al. 2010). This process determines the freezing point of the eutectic mixture. The eutectic point refers to the lower melting point of the mixture, which is significantly lower than the individual components, thereby allowing the mixture to be used at room temperature (Durand et al. 2013). A possible reason behind the depression in freezing point of the mixture is that HBD acts as an agent for complex formation with the anionic species leading to an increase in its effective size, thereby decreasing the interaction with a cation (Abbott et al. 2006; D'Agostino et al. 2011). Choline chloride (CC) is the most widely used cationic constituent for NADES. The major reasons behind the popularity of CC are its nontoxic biodegradable nature and low cost (Hayyan et al. 2012). In addition, its combination with other HBD components such as glycerol, urea, etc. provides a sustainable mixture. Moreover, Dai et al. (2015) have extensively studied

the supermolecular structure of synthesized NADES, i.e., malic acid and proline (MA-Pro) mixture at a molar ratio of 1:1 using Fourier-transform infrared spectroscopy (FTIR), and have observed that an extensive network of hydrogen bonds exists between the components of the NADES, making these green solvents as supermolecule with coherent hydrogen bonding network system.

4.9 Types of NADES Reagents

4.9.1 Hydrophilic

The most commonly synthesized NADES have shown high miscibility in water and are regarded as hydrophilic NADES reagents. Since these form monophasic solvents, they could perform similar functions as aqueous solvents and have significant applications in broad areas of research. Bosiljkov et al. (2017) studies revealed that extraction of wine lees anthocyanins was enhanced using hydrophilic NADES mixture containing choline chloride and malic acid when coupled with ultrasonic waves. Unlike conventional phenolic extraction technique, green solvent approach opened a new branch of study for aromatic compound extraction. Similarly, studies performed by Kumar et al. (2016) showed that hydrophilic NADES could replace other harsh chemical agents such as hydrochloric acid and sodium hydroxide for pretreatment of lignocellulosic agro-residues. Moreover, based on the pH, they have grouped hydrophilic NADES into acidic or neutral NADES reagents (Kumar et al. 2016). The high stability of Cellic CTec2, a commercial cellulose-degrading enzyme cocktail, was also recorded in neutral NADES reagent. Hydrophilic NADES synthesized along with their components and molar ratios are described in Table 4.4. Besides, the applicability of hydrophilic NADES has also been found in the improvement of chondroitinase ABCI (cABCI) stability from *Proteus vulgaris* (Daneshjou et al. 2017), CO₂ capture (Mulia et al. 2017), microalgal lipid extraction (Lu et al. 2016), and bioavailability of nutraceutical products (Faggian et al. 2016).

4.9.2 Hydrophobic

Synthesis of hydrophobic DES is relatively a new concept, and studies are recently initiated exploring novel environmentally friendly green solvents that could replace conventional organic solvents. Since the majority of complex organic compounds are either sparingly or completely insoluble in aqueous solvents, the dependency is entirely on the common organic reagents such as hexane, dimethyl sulfoxide, acetone, phenols, and chloroform for extraction processes. Multiple cost-intensive downstream processing is needed to recover these chemicals. Recently, for the first time, Van Osch et al. (2015) synthesized hydrophobic DES using a mixture of decanoic acid and quaternary ammonium salts. The hydrophobicity was maintained from the long alkyl chain of fatty acids and a two-phase system was generated. The efficiency of recovery of volatile fatty acids from diluted aqueous solutions was

Table 4.4 Hydrophilic NADES tested in different studies

NADES reagent ^a	Molar ratio	References
CC-MA	1:1	Kumar et al. (2016) and Zhang et al. (2016)
CC-MAL	1:1, 1:2	Kumar et al. (2016) and Rengstl et al. (2014)
CC-Gly	1:1, 1:2	Kumar et al. (2016), Alvarez-Vasco et al. (2016), Xia et al. (2014), and Zhang et al. (2016)
CC-Ur	1:1, 1:2	Kumar et al. (2016), Jablonsky et al. (2015), and Xia et al. (2014)
CC-TA	1:1	Kumar et al. (2016)
CC-OA	1:1	Kumar et al. (2016), Jablonsky et al. (2015), and Zhang et al. (2016)
CC-EG	1:1, 1:2	Kumar et al. (2016) and Zhang et al. (2016)
CC-LA	1:5, 1:9, 1:10	Kumar et al. (2016), Alvarez-Vasco et al. (2016), and Jablonsky et al. (2015)
CC-GA	1:1	Zhang et al. (2016)
BE-LA	1:1, 1:2	Kumar et al. (2015b)
Suc-MA	1:1	Yiin et al. (2015)

^aNADES reagents used in different studies: *CC-MA* choline chloride-malic acid, *CC-MAL* choline chloride-malonic acid, *CC-Gly* choline chloride-glycerol, *CC-Ur* choline chloride-urea, *CC-TA* choline chloride-tartaric acid, *CC-OA* choline chloride-oxalic acid, *CC-EG* choline chloride-ethylene glycol, *CC-LA* choline chloride-lactic acid, *CC-GA* choline chloride-glutaric acid, *BE-LA* betaine-lactic acid, *Suc-MA* sucrose-malic acid

Table 4.5 Hydrophobic DES tested in different studies

Component 1 ^a	Component 2 ^b	Molar ratio	References
Mnl	AA	1:1	Ribeiro et al. (2015)
Mnl	BA	1:1	Florindo et al. (2017)
Mnl	DA	1:1	Florindo et al. (2017)
Mnl	DOA	2:1	Florindo et al. (2017)
Mnl	HA	1:1	Florindo et al. (2017)
Mnl	LA	1:2	Ribeiro et al. (2015)
Mnl	OCA	1:1	Florindo et al. (2017)
Mnl	PA	1:2	Ribeiro et al. (2015)
MTAC	Bnl	1:4	Cao et al. (2017)

^aComponent 1: *Mnl* menthol, *MTAC* methyltrioctyl ammonium chloride

^bComponent 2: *AA* acetic acid, *BA* butyric acid, *Bnl* butanol, *DA* decanoic acid, *DOA* dodecanoic acid, *HA* hexanoic acid, *LA* lactic acid, *OCA* octanoic acid, *PA* pyruvic acid

studied by altering the alkyl chain length of HBD. Similarly, Florindo et al. (2017) also studied the applicability of hydrophobic DES in the extraction of pesticides, a major micro-pollutant in wastewater treatment plants (Table 4.5).

4.10 Physicochemical Properties of NADES

4.10.1 Structure

Various spectroscopy techniques, viz., nuclear magnetic resonance (NMR) spectroscopy and Fourier-transform infrared (FTIR) spectroscopy, have been applied by the researchers to study the structure of NADES. NMR studies found the presence of hydrogen bond in the NADES. Abbott and coworkers performed heteronuclear Overhauser effect spectroscopy (HOESY) and found a cross-correlation between protons from urea and fluoride from choline fluoride (Abbott et al. 2003). Mele et al. (2003) also observed a clear intramolecular as well as intermolecular bonding between 1-*n*-butyl-3-methylimidazolium tetrafluoroborate molecules through ^1H - ^1H -nuclear Overhauser effect spectroscopy (NOESY). Dai et al. (2013b) conducted HOESY spectrum studies on 1,2-propanediol, choline chloride-water (PD-CC-H) and proline-malic acid-water (Pro-MA-H). A signal was revealed corresponding to a proton present on the methyl group of 1,2-propanediol which was found to have interactions with both methylene carbon and methyl carbon and of CC.

The spectrum revealed that there was strong interaction between protons on hydroxyl groups from 1,2-propanediol, choline chloride, and water thereby confirming the presence of hydrogen bond between hydroxyl groups. Similar observations were observed in Pro-MA-H. Also, the stability of NADES is affected by the varying ratio of different components. For example, glucose/CC is stable at 2:5, but solid precipitation takes place at 2:1, 1:1, and 1:4 molar ratios. This confirms that a chloride ion of CC forms two hydrogen bonds with two hydroxyl groups from sugars. Similar results were also observed in a mixture of CC and carboxylic acid (Abbott et al. 2004). An equal proportion of the two components (1:1) have been found suitable for most other combinations. Sugars, organic acids, amino acids, and sugar alcohols belong to both HBA and HBD which is considered to be a possible reason for the formation of a complex by the components forming liquids with supramolecular structure. This brings to the conclusion that NADES can be considered as liquid crystals where the arrangement of molecules takes place through hydrogen bonding along with other intermolecular binding forces. Dai et al. (2013a) also observed the effect of the structure on the formation and stability of NADES and found that a number of groups of HBA and HBD, the position of the bonds, and the spatial structure of those groups influenced the formation and stability of NADES. It has been observed that organic acids, malic acids, citric acid, and tartaric acids form a mixture in a liquid state with choline salts, while such phenomenon is not observed in succinic acid. Based on the structure of these acids, it can be assumed that the presence of an extra hydroxyl or carboxyl group leads to the formation of more hydrogen bonds, which in turn increases the stability of liquids.

Similarly, the mixture of organic acids and sugars having more number of carboxylic groups (citric acid) forms a stable mixture with more number of sugars than those with less number of carboxylic groups (malic acid). The hydrogen bond formation and its stability also depend on the spatial structure of NADES. It has been observed that NADES formed by CC and galactose is not stable and precipitates,

while the combination of glucose and CC forms a stable liquid mixture. Other sugars and sugar alcohols, viz., sorbitol and mannitol, have also shown similar results. Disaccharides such as trehalose have been found to form liquid mixtures with choline salts, while cellobiose, which has different glycosidic bond than trehalose, does not form a liquid mixture (Dai et al. 2013a). Aissaoui et al. (2016) used TmoleX for studying the molecular structure and charge density of NADES synthesized from triethylene glycol and CC, diethylene glycol and CC, ethylene glycol and CC, and glycerol and CC.

4.10.2 Viscosity

The high viscosity of NADES is a major obstacle in their wide-scale application. The viscosity of NADES lies in the range of 200–500 mm²/s at 40 °C which leads to slow mass transfer in extractions/dissolutions leading to time-consuming solvent transfer operations (Dai et al. 2013b, 2015). Researchers have found that diluting the solvents with a small amount of water led to a major drop in viscosity and modulates the function of the solvents (Kohno and Ohno 2012). This property is useful in designing appropriate NADES for specific applications. There is an interesting aspect regarding the mechanism of interaction between NADES and water. Water plays a very vital role in the biological systems. Besides water and lipids, NADES can have an important role as a solvent in biological systems. NADES can provide an alternate medium for carrying out various metabolic activities that could not occur in water and lipids. Their presence can explain metabolic activities such as biosynthesis of hydrophobic metabolites, an adaption of organisms in extreme climatic conditions (Abbott et al. 2009). Figure 4.6 shows the changing behavior of NADES viscosity with increasing water content.

Dai et al. (2013b) added 25% water to glucose-choline and 1,2-propanediol-choline chloride (PD-CC) which reduced the viscosity of mixtures from 397 to 7.2 mm²/s and 33 to 6.1 mm²/s, respectively. Dai et al. (2015) explained the mechanism of effect of the addition of water to NADES with the help of ¹H NMR and FTIR. It was observed that the strong hydrogen bonds between the NADES constituents weakened gradually with the addition of water and ended completely upon addition of 50% (v/v) water.

A small amount of water addition decreases the viscosity of NADES and brings it down to the range of water, while the conductivity of some NADES increases by up to 100 times. Therefore, dilution of NADES with water not only reduces NADES viscosity but also alters the structure of NADES facilitating their application for specific purposes.

4.10.3 Density

Density is an important criterion for the purpose of process designing. The effect of pressure and temperature on density is needed for the optimization of

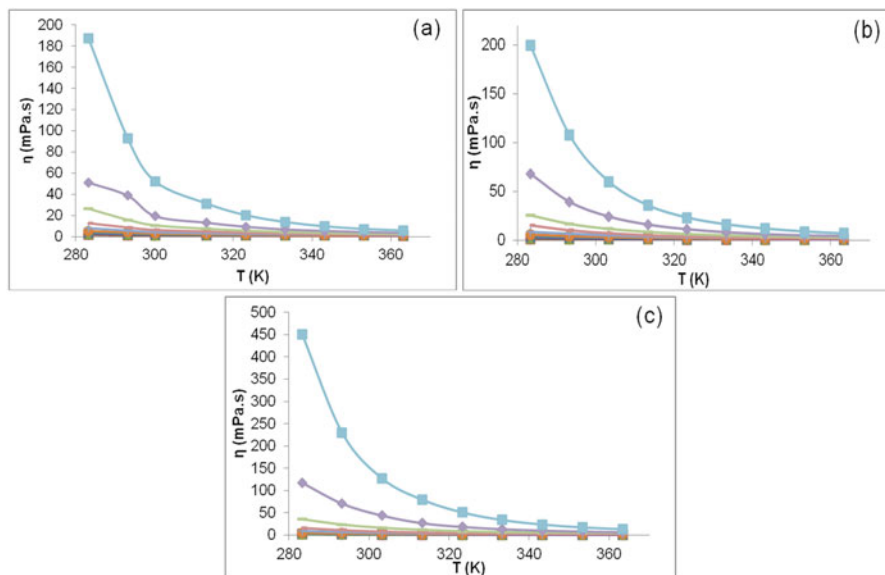


Fig. 4.6 Change in viscosity with temperature for aqueous NADES reagents. (a) LA-CC (9:1), (b) LA-CC (5:1), and (c) LA-CC (2:1). (◆) 5%, blue; (■) 10%, red; (▲) 20%, green; (x) 30%, purple; (*) 40%, magenta; (●) 50%, orange; (+) 60%, light blue; (−) 70%, pink; (−) 80%, green; (◆) 90%, purple; and (■) 100%, light blue

thermodynamic equations necessary for the development of industrial processes (Valderrama 2003). The majority of NADES that has been synthesized and tested has been found to have densities in the range of 1.0–1.35 g/cm³ at 298.15 K. Density of NADES is largely affected by the molar ratio of the constituents of NADES and molecular characteristics of HBD (Garcia et al. 2015).

The group reported higher density for 1:3 NADES synthesized from ethanolamine and 2,2,2-trifluoroacetamide. In addition, the density of NADES increases with the number of hydroxyl (OH[−]) groups present in HBD, e.g., higher density was obtained for glycerol than ethylene glycol. The group also reported that the density of NADES decreased with the introduction of aromatic group in the HBD, e.g., phenol was found to have the lowest density among the group of NADES evaluated. In addition, it was observed that in diacid NADES, density decreases with the increase in chain length. The order of density in such condition would be oxalic acid followed by malonic and glutaric acid. Hence, it has been proven that the density of NADES is determined by the steric effects and ionic strength of HBD. The type of salt present in the NADES is also a major factor behind the density of NADES. It has been observed that for a specific HBD, i.e., ethylene glycol, NADES based on ammonium have less density in comparison to phosphonium-based NADES. The density of NADES has been found to decrease with the increase in the length of cation alkyl chains. Increase in the length of the alkyl chain in NADES enhances the compressibility, which leads to increase in the free volume.

Similarly, the anion has an effect on the density, as in the case of halogen; the bromide salts have a higher density than chloride ones. This is because the NADES containing bromide are more compressible as compared to the chloride ones which are probably due to larger free volumes of NADES that contain bulkier anions and weaker anion-HBD and anion-cation interactions for larger anions (Garcia et al. 2015).

4.10.4 Conductivity

Temperature-dependent specific conductivity (k) of NADES reagents was measured in a custom-designed apparatus between 25 and 85 °C (Rengstl et al. 2014) and dielectric relaxation spectroscopy (Craveiro et al. 2016). Conductivity data can clarify the mechanism of charge transport of the NADES. The conductivity of tested NADES was nearly similar to common ionic liquids but higher than imidazolium ionic liquids. With respect to hydrogenbond donor (HBD), dicarboxylic acid-based NADES showed higher conductivity than urea-based NADES and varies with variation in temperature. Furthermore, the calculated activation energy (E_A) using simulation studies through Vogel-Fulcher-Tammann (VFT) model predicted that the smaller the size of the HBD, the lower the activation energy. One such example is E_A of choline chloride with the succinic acid mixture is 54.3 kJ/mol whereas with oxalic and malic acid is 34.6 kJ/mol and 29.0 kJ/mol, respectively. The VFT equation typically explains the dependence of temperature on the relaxation time linked with the dynamic glass transition. Another study by Kumar et al. (2016) investigated the electrical conductivity of choline chloride-based acidic and neutral NADES reagents. Diols as HBD showed marginally higher conductivity than dicarboxylic acids. Similarly, Craveiro et al. (2016) studied conductivity of NADES synthesized from organic acids, choline chloride, amino acids, sugars, and amino acids and had demonstrated that high polar organic acid-based NADES have higher conductivities as compared to NADES based on sugars and amino acids.

4.10.5 Thermal Properties

Thermal properties are commonly studied by differential scanning calorimetry (DSC) and thermogravimetric analysis (TGA). Dai et al. (2013a) reported that heating a variety of NADES up to 100 °C for 1 h did not show any sign of decomposition. They also observed that NADES formed from sugars have a low decomposition temperature (~135 °C), while other NADES have significantly higher decomposition temperature (>200 °C). The glass transition temperature (T_g) corresponds to the temperature at which the structure of the material transforms from a glassy state to rubbery state (Craveiro et al. 2016). The glass transition temperatures (T_g) of different NADES evaluated were found to be below -50 °C, but their melting point was not present which concludes that NADES are stable supramolecular liquid complexes over a large range of temperature. In addition, the

liquid state of NADES supports the theory that NADES play a critical role in plants for providing resistance against cold. Moreover, it also implies that NADES can be used as solvents in the range of 0–100 °C (Dai et al. 2013b). Different thermal properties of various NADES have been presented in Table 4.6 (Craveiro et al. 2016).

Craveiro et al. (2016) applied DSC for evaluating the thermal stability of NADES up to 250 °C. The NADES samples evaluated were found to have only one degradation peak signifying decomposition temperature above 120 °C. T_g helps in classifying all the NADES studied as glass formers and found it true for all the pure components except CC. The reason behind the decrease of T_g upon hydration is the plasticizing effect of water (Carvalho et al. 2012). The plasticizing effect of water on NADES was confirmed by adding water to CC-Xyl (2:1) and was inferred that upon addition of 5% water, T_g decreased by 4 °C.

4.10.6 Polarity

The polarity of NADES is an important property as it affects their solubilizing capacity. NADES consisting of organic acids are found to be most polar (~45 kcal/mol) followed by NADES synthesized from sugars and amino acids (polarity equivalent to water = ~48 kcal/mol). NADES consisting of sugars and polyalcohols have the least polarity almost equivalent to that of methanol (~52 kcal/mol). Addition of water to NADES also affects their polarity largely. The polarity of Pro-CC-H (1,2-propanediol-CC-water) and LA-Glu-H (lactic acid-glucose-water) was affected by adding 50% (v/v) water signifying a major change in the structure of Pro-CC-H and LA-Glu-H. This structural modification possibly occurs owing to the breakdown of hydrogen bonds between the components. Similar results were observed with urea-CC and glycerol-CC (Dai et al. 2013b). The physical characteristics of NADES are summarized in Table 4.7 as reported by Dai et al. (2013a).

4.11 Functional Properties of NADES

4.11.1 Specificity

Although vast studies were performed on DES specificity, there were very limited studies on NADES which are confined mainly toward solubilization of individual components of lignocellulosic biomass. Kroon et al. (2014) have synthesized a group of NADES reagents and tested for solubility of commercial products, viz., lignin, starch, and cellulose in a mixture. In their study, a specific solubility of lignin was observed in NADES mixtures of lactic acid-proline (2:1), lactic acid-betaine (2:1), and lactic acid-choline chloride (3:1, 2:2, and 5:1), respectively. Among these lactic acid-betaine (2:1) showed a maximum solubility of 12.03 wt% with no solubility of starch and cellulose. Similarly, a specific solubility of starch was

Table 4.6 Thermal properties of different NADES, viz., degradation temperature (T_d), melt and cold crystallization temperatures (T_{melt} and T_{ccold}), melting temperature (T_m), and glass transition temperature (T_g)

NADES [#]		Molar ratio	T_d (°C)	T_g (°C)	T_{cmelt} (°C)	T_{ccold} (°C)	T_m (°C)	References
Component 1	Component 2							
CA	Glu	1:1	130.1	9.8/48.7	-	-	-	Craveiro et al. (2016)
CA	Suc	1:1	121.2	-14.0	-	-	-	Craveiro et al. (2016)
CC	CA	1:1	154.49	-	-	-	-	Haz et al. (2016)
CC	CA	1:1	171.3	-21.4	-9.7	-	76.0	Craveiro et al. (2016)
CC	EG	1:2	84	-	-	-	-	Dietz et al. (2017)
CC	Glu	1:1	129.8	-28.4	-	-	-	Craveiro et al. (2016)
CC	LA	1:1	212	-	-	-	-	Skulcova et al. (2017)
CC	LA	1:1	196.83	-	-	-	-	Haz et al. (2016)
CC	MAL	1:1	126	-	-	-	-	Skulcova et al. (2017)
CC	OA	1:1	134.81	-	-	-	-	Haz et al. (2016)
CC	Suc	4:1	141.7	-42.0	-33.9	51.8	79.2	Craveiro et al. (2016)
CC	Suc	1:1	126.8	-15.8	-	-	-	Craveiro et al. (2016)
CC	TA	1:1	197.84	-	-	-	-	Haz et al. (2016)
CC	TA	1:1	194	-	-	-	-	Skulcova et al. (2017)
CC	TA	2:1	130.8	-41.6	-	-	-	Craveiro et al. (2016)
CC	Xyl	3:1	165.2	-46.4	20.1	59.9	78.5	Craveiro et al. (2016)
CC	Xyl	2:1	172.7	-51.2	-	56.9	78.3	Craveiro et al. (2016)
CC	UR	1:2	186	-	-	-	-	Dietz et al. (2017)
Glu	TA	1:1	117.5	-18.3	-	-	-	Craveiro et al. (2016)
LE	BE	2:1	166	-	-	-	-	Dietz et al. (2017)

[#]NADES solvents tested: CA-Glu citric acid-glucose, CA-Suc citric acid-sucrose, CC-CA choline chloride-citric acid, CC-EG choline chloride-ethylene glycol, CC-Glu choline chloride-glucose, CC-LA choline chloride-lactic acid, CC-MAL choline chloride-malonic acid, CC-OA choline chloride-oxalic acid, CC-Suc choline chloride-sucrose, CC-TA choline chloride-tartaric acid, CC-Xyl choline chloride-xylose, Glu-TA glucose-tartaric acid, LE-BE levulinic acid-betaine

Table 4.7 Physical properties of NADES using water and methanol as references

NADES reagent ^a	Molar ratio	Water (wt %)	Water activity (40 °C)	Density (40 °C) g/cm ³	Viscosity (40 °C) mm ² /s	T _{decom} (°C)	T _g (°C)	E _{NR} (kcal/mol)	Reference
MA-CC-H ₂ O	(1:1:2)	11.62	0.195	1.230	445.9	201	-71.32	44.81	Dai et al. (2013a, b)
Gly-CC-H ₂ O	(2:1:1)	5.26	0.126	1.174	51.3	187	-101.59	49.55	Dai et al. (2013a, b)
LA-CC	(9:1)	-	-	1.1785	31.27	-	-	-	This study
LA-CC	(5:1)	-	-	1.1729	35.62	-	-	-	This study
LA-CC	(2:1)	-	-	1.1546	79.44	-	-	-	This study
LA-CC	(1:1)	-	-	1.1453	157.55	-	-	-	This study
LA-CC-H ₂ O	(9:1:3.3)	30	-	1.1292	1.83	-	-	-	This study
LA-CC-H ₂ O	(5:1:3.3)	30	-	1.1257	5.31	-	-	-	This study
LA-CC-H ₂ O	(2:1:3.3)	30	-	1.1207	6.10	-	-	-	This study
LA-CC-H ₂ O	(1:1:3.3)	30	-	1.0417	9.43	-	-	-	This study
MA-Ala-H ₂ O	(1:1:3)	19.48	0.573	1.352	174.6	164	-70.88	48.05	Dai et al. (2013a, b)
Pro-MA-H ₂ O	(1:1:3)	17.81	0.591	1.318	251.0	156	-61.29	48.30	Dai et al. (2013a, b)
Fru-CC-H ₂ O	(2:5:5)	7.84	0.151	1.209	280.8	160	-84.58	49.81	Dai et al. (2013a, b)
Xyl-CC-H ₂ O	(1:2:2)	7.74	0.141	1.209	308.3	178	-81.80	49.81	Dai et al. (2013a, b)

(continued)

Table 4.7 (continued)

NADES reagent ^a	Molar ratio	Water (wt %)	Water activity (40 °C)	Density (40 °C) g/cm ³	Viscosity (40 °C) mm ² /s	T _{decom} (°C)	T _g (°C)	E _{NR} (kcal/mol)	Reference
Suc-CC-H ₂ O	(1:4:4)	7.40	0.182	1.227	581.0	>200	-82.96	49.72	Dai et al. (2013a, b)
Fru-Glu-Suc- H ₂ O	(1:1:1:1)	22.0	0.662	1.366	720.0	138	-50.77	48.21	Dai et al. (2013a, b)
Glu-CC-H ₂ O	(2:5:5)	7.84	0.162	1.207	397.4	170	-83.86	49.72	Dai et al. (2013a, b)
LA-Glu-H ₂ O	(5:1:3)	7.89	0.496	1.250	37.0	135	-77.06	44.81	Dai et al. (2013a, b)
Xyl-CC-H ₂ O	(1:2:3)	11.17	0.116	1.178	86.1	>200	-93.33	59.72	Dai et al. (2013a, b)
H ₂ O	Water	100	1	0.992	1	-	-	58.21	Dai et al. (2013a, b)
MeOH	Methanol	-	-	0.791	-	-	-	51.89	Dai et al. (2013a, b)

^aNADES solvents tested: MA-CC-H₂O malic acid-choline chloride-water, Gly-CC-H₂O glycerol-choline chloride-water, LA-CC lactic acid-choline chloride, LA-CC-H₂O lactic acid-choline chloride-water, MA-Ala-H₂O malic acid-alanine-water, Pro-MA-H₂O proline-malic acid-water, Fru-CC-H₂O fructose-choline chloride-water, Xyl-CC-H₂O xylose-choline chloride-water, Suc-CC-H₂O sucrose-choline chloride-water, Fru-Glu-Suc-H₂O fructose-glucose-sucrose-water, LA-Glu-H₂O lactic acid-glucose-water, Xyl-CC-H₂O xylose-choline chloride-water, MeOH-H₂O methanol-water

observed in NADES mixtures of malic acid-betaine (1:1) and oxalic acid-nicotinic acid (9:1). When oxalic acid was mixed with histidine at a molar ratio of 9:1, the specificity of NADES was shifted toward cellulose solubility. In some comparable studies by Kumar et al. (2015b, 2016), the specificity of NADES remained similar when lignocellulosic biomass residues were pretreated with selected NADES reagents. They have found that NADES mixtures of lactic acid-CC (5:1 and 9:1) effectively removed lignin fraction from rice straw without any effect on cellulose and hemicelluloses. The primary reason behind the non-dissolution of cellulose in choline chloride mixtures was that the hydroxyl groups of choline are linked to cellulose by strong hydrogen-bond interactions and hence stabilizes the cellulose system protecting from solubilization (Rengstl et al. 2014).

Besides solubility, recently, Martinez et al. (2016) studied enantioselective L-proline-catalyzed intermolecular aldol reaction in biorenewable NADES formed by glucose and malic acid. The products generated from aldol reaction are specifically diastereomers. Moreover, NADES had proven to be a clean media to carry out volatile organic compound-free selective process.

4.11.2 Toxicity and Biodegradability

An advantage of NADES is the fact that these solvents are synthesized by natural components thereby having significantly lower toxicity than ionic liquids. Hayyan et al. (2013) evaluated the toxicity of phosphonium-based NADES on brine shrimp and gram-positive and gram-negative bacteria. This study observed that NADES toxicity depends on viscosity, composition, and concentration of NADES. The researchers also concluded that the eutectic mixture of the two components is more toxic as compared to the aqueous solutions of the individual components. The delocalization of the charges in NADES led to the disruption of cell walls of the bacteria. This property might help in using NADES as antibacterial agents.

Another study evaluated the effect of NADES on acetyl cholinesterase (AChE) which is an enzyme found in the nervous system of higher organisms. Choline chloride- and amino acid (CC-AA)-based NADES have been found to have lower toxicity than imidazolium-based ionic liquids. However, the toxic effect varies based on amino acid present in NADES. In addition, the CC-AA NADES showed less toxicity toward the bacteria. The biodegradability of CC-AA with different amino acids was tested, and all the combinations were found readily biodegradable. The extra amide or carboxyl group on amino acid side chain makes NADES more vulnerable to microbial breakdown. Most of the combinations of CC-AA NADES synthesized and tested were found to have low toxicity and high biodegradability (Hou et al. 2013). This makes NADES a promising candidate for application as green solvents in several industries. Paiva et al. (2014) studied the impact of more than ten NADES on model cell line (L929 fibroblast-like cells) and observed that NADES containing tartaric acid has negative impact on cellular metabolic activity. However, choline-based NADES were found to be non-cytotoxic.

4.11.3 Recyclability

Sustainability of chemical processing depends on recycling the process inputs for maximizing the benefits. Recycling of conventional chemical solvents demands high-energy input and capital expenditure. Hence, simple recovery mechanisms are preferred for recycling. Unlike multiple downstream recovery processing of organic solvents, NADES recovery is a comparatively easy process. Synthesis of NADES involves weak intermolecular hydrogen bonding between the HBA and HBD molecules, and the mixture formed does not form a complex. Hydrogen bond could easily be broken and involve any chemical reaction. NADES are nonvolatile in nature due to their high boiling points, and hence no major losses are observed.

4.11.4 Biocatalysis

Despite NADES being synthesized from denaturing agents, viz., citric acid, urea, etc., several enzymes have been found to show high activity and stability in NADES. Durand et al. (2013) observed *Candida antarctica* lipase B (CALB) showing very high activity and stability in choline chloride-based NADES. Gorke et al. (2010) performed the transesterification of ethyl valerate with butanol by hydrolase enzymes. The enzymatic stability of CALB showed an improvement of 20–35-folds when choline chloride-urea was used as cosolvent as compared to the aqueous solution. Choline chloride-based NADES have been used as cosolvents for hydrolysis of methylstyrene oxide by epoxide hydrolases (Lindberg et al. 2010). Reetz et al. (2003) had proposed a two-phase separation system using ionic liquids and supercritical fluids (supercritical carbon dioxide). However, the drawback of this technique is the high cost of ionic liquids and poor biodegradability. With the advent of NADES, which are cheaper and greener and have excellent biodegradability, this opens new possibilities for biocatalysis in biphasic systems. Gunny et al. (2015) studied the applicability of NADES on cellulose-degrading enzymes. Their study has shown that >90% of the cellulase activity was retained in the presence of 10% (v/v) for glycerol-based DES (GLY) and ethylene glycol-based DES (EG).

4.11.5 Biorefinery and Bioprocessing

A biorefinery is an integrated facility that includes biomass fractionation and bio-conversion processes for production of various separated products. These products are of high importance in generation of transport fuels, power, and other value-added chemicals. For production of transport fuels, pretreatment is considered as one of the key steps of bioprocessing. An efficient pretreatment process improves overall downstream processing steps in a biorefinery. For example, in bioethanol production, the conversion efficiency of biomass residues into its constituent reducing sugars and monomers from a pretreated biomass is significantly higher than the

untreated biomass. This further improves the overall cellulosic ethanol production yields during fermentation.

4.11.6 Production of Reducing Sugars

The sole purpose of pretreatment is to expose the cellulose for enzymatic saccharification leading to the formation of reducing sugars. The production of reducing sugars from cellulose by enzymes is a key connecting step between lignocellulosic biomass and ethanol production from biorefinery point of view. Researchers have reported that application of NADES for the pretreatment process does not have an inhibitory effect on the enzyme, which in turn increases the overall sugar yield. Kumar et al. (2015b) tested several different concentrations of lactic acid-betaine (LA-BE) (2:1 and 5:1) and lactic acid-choline chloride (LA-CC) (2:1, 5:1, and 9:1). Among these reagents, lactic acid-choline chloride (LA-CC) (5:1)-treated biomass produced maximum reducing sugars (333 mg/g) with 36% saccharification efficiency in 24 h at a solid loading of 10%. Kumar et al. (2016) studied the effect of CC-glycerol NADES on cellulase enzyme Cellic CTec2 and obtained maximum reducing sugars of 226.7 g/L with saccharification efficiency of 87.1% at 20% solids loading and 12 filter paper units (FPU) Cellic CTec2. Zhang et al. (2016) studied three kinds of choline chloride-based NADES reagents mixed with monocarboxylic acid, dicarboxylic acid, and polyalcohols for saccharification of corncobs. Among these, maximum glucose yields of 96.4% were observed with CC-glycerol (CC-Gly) (2:1) reagent, followed by monocarboxylic acid mixtures. However, dicarboxylic acid-based NADES reagents produced a lower amount of reducing sugars. This was possibly due to the high acidic strength of dicarboxylic NADES solvents, which had limited the lignin extractability hindering enzyme interaction with the cellulosic fraction. Gunny et al. (2015) studied saccharification of NADES-pretreated rice husk using polyalcohol-based NADES reagents.

4.11.7 Bioethanol Production

Studies on bioethanol production using NADES-pretreated biomass are very limited. Since applicability of NADES is still in nascent stage, research needs to be explored further in cellulosic ethanol production from a large variety of lignocellulosic biomasses and agro-residual waste materials. Following saccharification, the formed reducing sugars are fermented by yeast to produce bioethanol. Cellulosic ethanol production from NADES-pretreated rice straw was evaluated by Kumar et al. (2016). Studies showed that choline chloride-glycerol (CC-Gly)-treated rice straw produced maximum ethanol of 36.7 g/L with a conversion efficiency of 90.1%. Besides, in this study, the tolerance level of *Clavispora* NRRL Y-50464, a β -glucosidase-producing ethanol-fermenting yeast, was evaluated in acidic and neutral NADES reagents. Fermentation of glucose in the presence of CC-glycerol and CC-propane diol (CC-PD) at 10% (v/v) has not shown any effect on the rate of

yeast growth, sugar consumption, and ethanol production from *Clavispora* NRRL Y-50464, while 10% (v/v) CC-ethylene glycol repressed and delayed the cell growth of the microbe.

4.11.8 Carbon Dioxide Sequestration

Ionic liquids were found to have a high solubility for CO₂, but the high price and low biodegradability are major obstacles in the commercial application of ionic liquids. NADES can prove to be a viable substitute for ionic liquids as they have very low vapor pressure like that of ionic liquids and are biodegradable, biocompatible, and inexpensive (Wu et al. 2012). Chen et al. (2014) measured CO₂ solubility in NADES synthesized from CC and dihydric alcohols, viz., 1,4-butanediol, 2,3-butanediol, and 1,2-propanediol in a molar ratio of 1:3 and 1:4 at a temperature difference of 10 K ranging from 293.15 to 323.15 K at 6 bar pressure with the help of isochoric saturation method. The solubility of CO₂ in the mixtures increased linearly with the decrease in temperature or increase in pressure. Paiva et al. (2014) suggested the application of amine-based NADES for the sequestration of CO₂ in order to provide a cheaper and cleaner alternative to the conventional processes applied today.

4.11.9 Chemical Extraction

The dissolution property is mainly responsible for the efficiency of an extraction agent. As mentioned earlier, NADES possess the capacity to donate and accept protons and electrons which makes them suitable to form hydrogen bonds which in turn increases their dissolution capacity (Zhang et al. 2012b). Dai et al. (2013b) used NADES (lactic acid-glucose, CC-glucose, and fructose-glucose-sucrose) for the removal of phenolic compounds from safflower. This study established the hypothesis of the formation of hydrogen bond between the NADES and phenolic compounds by showing a high ability of NADES for the removal of phenolic compounds. Authors have also reported higher phenolic compound extraction as compared to conventional solvents like water and ethanol.

Molecules having poor solubility in water, viz., griseofulvin, benzoic acid, itraconazole, and danazol, were reported to have higher solubility in CC-urea and CC-malic acid (Morrison et al. 2009). NADES have also been found to successfully dissolve transition metal oxides from minerals (Abbott et al. 2004). NADES being green and safe solvents are employed in extracting natural products in several industries such as pharmaceutical and food industries. Since NADES have been found to dissolve both polar and nonpolar metabolites (Biswas et al. 2006), specific NADES can be synthesized and applied for the extraction of desired natural components. Paiva et al. (2014) used CC-xylose (3:1), CC-tartaric acid (1:1), and CC-citric acid (1:1) for extracting phenolic compounds from coffee beans. The amounts of phenolic compounds were found to be greater than the conventional solvents such as acetone and citric acid.

4.12 Technical Assessment of NADES

Comprehensive techno-economical evaluation using NADES was not reported till date. Since study on NADES is relevantly a new topic of research, a majority of the studies are still in nascent stage and are exploring the potentiality and applicability of NADES in diverse applications. In continuation to our earlier studies on the applicability of NADES in lignocellulosic biomass pretreatment, we have further studied the technical assessment of NADES in an integrated process for biorefinery applications. All the details with respect to the mass balance of the integrated technology given in Fig. 4.7 are based on an experimental evaluation performed in our laboratory. In brief, the integrated process includes cellulosic production from NADES pretreated rice straw (Kumar et al. 2016), and recovery, recycle NADES reagent, recovery of high purity lignin and xylan as the value-added products under four different conditions (Kumar et al. 2018). The conditions maintained were (I) biomass pretreatment at 5% solids loading and enzymatic saccharification at 10% solids loading, (II) biomass pretreatment at 5% solids loading and enzymatic saccharification at 25% solids loading, (III) biomass pretreatment at 10% solids loading and enzymatic saccharification at 10% solids loading biomass, and

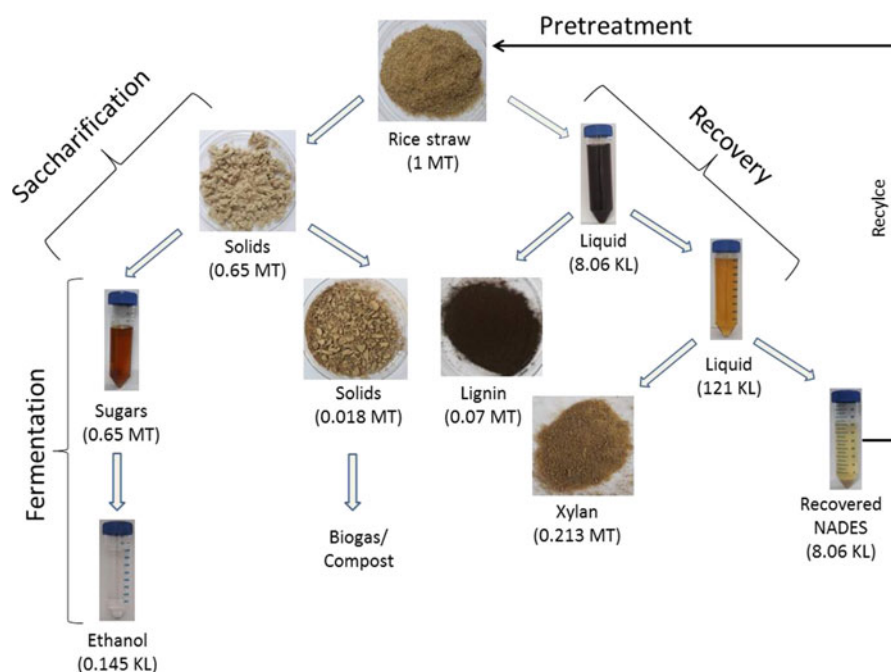


Fig. 4.7 Process flow steps of an integrated biorefinery approach for lignocellulosic feedstock pretreatment, cellulosic ethanol production and recovery and reuse of solvents, and recovery of value-added products

(IV) biomass pretreatment at 10% solids loading and enzymatic saccharification at 25% solids loading pretreatment.

A detailed flow diagram of the process is given in Fig. 4.7. Based on the mass balance analysis, it is evident from the conditions I and II, pretreatment at 5% solids loading demands a 20-fold higher NADES solvent, which increases the overall cost of the chemical reagents and makes the entire process cost-intensive. Besides, the requirement of acetonitrile and water was also twofold high as compared to the process conditions III and IV. Although no significant losses were observed during recovery of acetonitrile and water, high capacity distillation units are required for process conditions I and II, thus increasing the capital and operational expenditures. Besides, irrespective of pretreatment conditions, hydrolysis of pretreatment biomass also plays an important role in reducing the cost of cellulosic ethanol production. Enzymatic saccharification at 10% solids loading (conditions I and III) yielded the low concentration of reducing sugars (3–4%); thus an additional pre-concentration process was required in order to obtain 10% glucose, which was found to be optimum for *Clavispora* NRRL Y-50464 to produce ethanol yields up to 3.7% ethanol. Whereas, hydrolysis at 25% solids loading (conditions II and IV), yielded high concentrations of glucose (9–11%) and the pre-concentration process could be avoided, thus making the entire process more cost-effective and commercially feasible for production of cellulosic ethanol. Overall, condition IV was found to be optimum for an integrated process for the production of cellulosic ethanol and value-added products and recovery and reuse of solvents.

4.13 Future Perspective

Research on NADES toward unravelling the bottleneck applications in biorefinery and bioprocessing is still in nascent stage. Applicability of NADES is needed primarily to replace the harsh synthetic chemical solvents with eco-friendly natural solvents. Moreover, being benign, recovery of NADES seems to be significantly higher, and without losing the efficiency, these are preferred for industrial applications. There are several examples of future direction of NADES and its uses. Recently, it was reported that NADES extracts high-purity unique low-molecular-weight lignin. The new sources of lignin extract may provide a breakthrough toward truly realizing the high value potential of lignin (Kumar et al. 2016). In another study, pretreatment of microalga enhances the lipid recovery for biodiesel production (Lu et al. 2016). In addition, it is reported that some of the NADES could capture carbon dioxide efficiently (Mulia et al. 2017). The hydrophilic and hydrophobic NADES reagents have already shown their great potential in specific solubilization of macromolecules that seemed to be limited earlier. The rapidly increasing reports clearly suggest that NADES are being explored for the discovery of new areas of applications. Above all, preparation of NADES involves only physical mixing of natural compounds, numerous designer NADES reagents could be synthesized with specific usage. Thus, NADES are regarded as the next-generation green solvents.

4.14 Conclusions

The historical developments on NADES and its versatile applications in biorefinery and bioprocessing have shown clear advantages over ionic liquids or other chemical solvents. Having much lower cost and greenness, applications of NADES in the fields of biocatalysis, extraction, electrochemistry, etc. are expected to be boosted with the in-depth understanding of the mechanism of NADES action. NADES show a great possibility as the next generation of solvents, and though many efforts are needed to be executed, these novel solvents will certainly make a massive impact for the clean, green, and sustainable industrial development.

References

- Abbott AP, Capper G, Davies DL, Rasheed RK, Tambyrajah V (2003) Novel solvent properties of choline chloride/urea mixtures. *Chem Commun* 7:70–71
- Abbott AP, Boothby D, Capper G, Davies DL, Rasheed RK (2004) Deep eutectic solvents formed between choline chloride and carboxylic acids: versatile alternatives to ionic liquids. *J Am Chem Soc* 126:9142–9147
- Abbott AP, Capper G, Gray S (2006) Design of improved deep eutectic solvents using hole theory. *ChemPhysChem* 7:803–806
- Abbott AP, Collins J, Dalrymple I, Harris RC, Mistry R, Qiu F, Scheirer J, Wise WR (2009) Processing of electric arc furnace dust using deep eutectic solvents. *Aust J Chem* 62:341–347
- Agbor VB, Cicek N, Sparling R, Berlin A, Levin DB (2011) Biomass pretreatment: fundamentals toward application. *Biotechnol Adv* 29:675–685
- Aissauoui T, AlNashef IM, Benguerba Y (2016) Dehydration of natural gas using choline chloride based deep eutectic solvents: COSMO-RS prediction. *J Nat Gas Sci Eng* 30:571–577
- Alizadeh H, Teymouri F, Gilbert TI, Dale BE (2005) Pretreatment of switchgrass by ammonia fibre explosion (AFEX). *Appl Biochem Biotechnol* 121:1133–1141
- Alriols MG, Tejado A, Blanco M, Mondragon I, Labidi J (2009) Agricultural palm oil tree residues as raw material for cellulose, lignin and hemicelluloses production by ethylene glycol pulping process. *Chem Eng J* 148:106–114
- Alvarez-Vasco C, Ma R, Quintero M, Guo M, Geleynse S, Ramasamy KK, Wolcott M, Zhang X (2016) Unique low-molecular-weight lignin with high purity extracted from wood by deep eutectic solvents (DES): a source of lignin for valorization. *Green Chem* 18:5133–5141
- Alvira P, Tomas-Pejo E, Ballesteros M, Negro MJ (2010) Pretreatment technologies for an efficient bioethanol production process based on enzymatic hydrolysis: a review. *Bioresour Technol* 10:4851–4861
- Bajpai P (2016) Pretreatment of lignocellulosic biomass for biofuel production. Springer, Singapore
- Bak JS, Kim MD, Choi IG, Kim KH (2010) Biological pretreatment of rice straw by fermenting with *Dichomitus squalens*. *New Biotechnol* 27:424–434
- Behera S, Arora R, Nandhagopal N, Kumar S (2014) Importance of chemical pretreatment for bioconversion of lignocellulosic biomass. *Renew Sust Energ Rev* 36:91–106
- Biswas A, Shogren RL, Stevenson DG, Willett JL, Bhowmik PK (2006) Ionic liquids as solvents for biopolymers: acylation of starch and zein protein. *Carbohydr Polym* 66:546–550
- Bosiljkov T, Dujmić F, Bubalo MC, Hribar J, Vidrih R, Brnčić M, Zlatic E, Redovniković IR, Jokić S (2017) Natural deep eutectic solvents and ultrasound-assisted extraction: green approaches for extraction of wine lees anthocyanins. *Food Bioprod Process* 102:195–203
- Cao J, Yang M, Cao F, Wang J, Su E (2017) Well-designed hydrophobic deep eutectic solvents as green and efficient media for the extraction of artemisinin from *Artemisia annua* leaves. *ACS Sustain Chem Eng* 5:3270–3278

- Carvalho T, Augusto V, Brás AR, Lourenço NMT, Afonso CAM, Barreiros S, Correia NT, Vidinha P, Cabrita EJ, Dias CJ, Dionísio M, Roling B (2012) Understanding the ion jelly conductivity mechanism. *J Phys Chem B* 116:2664–2676
- Castoldi R, Bracht A, de Moraes GR, Baesso ML, Correa RCG, Peralta RA, Moreira RFP, Polizeli MT, de Souza CGM, Peralta RM (2014) Biological pretreatment of *Eucalyptus grandis* sawdust with white-rot fungi: study of degradation patterns and saccharification kinetics. *Chem Eng J* 258:240–246
- Chen Y, Ai N, Li G, Shan H, Cui Y, Deng D (2014) Solubilities of carbon dioxide in eutectic mixtures of choline chloride and dihydric alcohols. *J Chem Eng Data* 59(4):1247–1253
- Choi YH, van Spronsen J, Dai YT, Verberne M, Hollmann F, Arends IWCE, Witkamp GJ, Verpoorte R (2011) Are natural deep eutectic solvents the missing link in understanding cellular metabolism and physiology? *Plant Physiol* 156:1701–1705
- Cianchetta S, Maggio BD, Burzi PL, Galletti S (2014) Evaluation of selected white-rot fungal isolates for improving the sugar yield from wheat straw. *Appl Biochem Biotechnol* 173:609–623
- Craveiro R, Aroso I, Flammia V, Carvalho T, Viciosa MT, Dionísio M, Barreiros S, Reis RL, Duarte ARC, Paiva A (2016) Properties and thermal behavior of natural deep eutectic solvents. *J Mol Liq* 215:534–540
- D'Agostino C, Harris RC, Abbott AP, Gladden LF, Mantle MD (2011) Molecular motion and ion diffusion in choline chloride based deep eutectic solvents studied by 1H pulsed field gradient NMR spectroscopy. *Phys Chem Chem Phys* 13:21383–21391
- Dai Y, van Spronsen J, Witkamp G-J, Verpoorte R, Choi YH (2013a) Natural deep eutectic solvents as new potential media for green technology. *Anal Chim Acta* 766:61–68
- Dai YT, Witkamp GJ, Verpoorte R, Choi YH (2013b) Natural deep eutectic solvents as a new extraction media for phenolic metabolites in *Carthamus tinctorius* L. *Anal Chem* 85:6272–6278
- Dai Y, Witkamp GJ, Verpoorte R, Choi YH (2015) Tailoring properties of natural deep eutectic solvents with water to facilitate their applications. *Food Chem* 187:14–19
- Daneshjou S, Bahareh D, Fereshteh R, Khosro K (2017) Porous silicon nanoparticle as a stabilizing support for chondroitinase. *Int J Biol Macromol* 94:852–858
- Dhiman SS, Haw J, Kalyani D, Kalia VC, Kang YC, Lee J (2015) Simultaneous pretreatment and saccharification: green technology for enhanced sugar yields from biomass using a fungal consortium. *Bioresour Technol* 179:50–57
- Dietz CHJT, Kroon MC, van Sint Annaland M, Gallucci F (2017) Thermophysical properties and solubility of different sugar-derived molecules in deep eutectic solvents. *J Chem Eng Data* 62:3633–3641
- Du W, Yu H, Song L, Zhang J, Weng C, Ma F, Zhang X (2011) The promising effects of by products from *Irpex lacteus* on subsequent enzymatic hydrolysis of bio-pretreated corn stalks. *Biotechnol Biofuels* 4:37
- Durand E, Lecomte J, Villeneuve P (2013) Deep eutectic solvents: synthesis, application, and focus on lipase-catalyzed reactions. *Eur J Lipid Sci Technol* 115:379–385
- Faggian M, Sut S, Perissutti B, Baldan V, Grabnar I, Dall'Acqua S (2016) Natural Deep Eutectic Solvents (NADES) as a tool for bioavailability improvement: pharmacokinetics of rutin dissolved in proline/glycine after oral administration in rats: possible application in nutraceuticals. *Molecules* 21(11):1531
- Florindo C, Branco LC, Marrucho IM (2017) Development of hydrophobic deep eutectic solvents for extraction of pesticides from aqueous environments. *Fluid Phase Equilib* 448(25):135–142
- Francisco M, van den Bruinhorst A, Kroon MC (2013) Low transition- temperature mixtures (LTTMs): a new generation of designer solvents. *Angew Chem Int* 52:3074–3085
- García G, Aparicio S, Ullah R, Atilhan M (2015) Deep eutectic solvents: physicochemical properties and gas separation applications. *Energy Fuel* 29:2616–2644
- Gorke JT, Srienc F, Kazlauskas RJ (2010) Deep eutectic solvents for *Candida antarctica* lipase B-catalyzed reactions. In: Malhotra SV (ed), *Ionic liquid applications: pharmaceuticals, therapeutics, and biotechnology*. ACS Symposium Series 1038: Chapter 14, pp 169–180

- Gunny AAN, Arbain D, Nashef EM, Jamal P (2015) Applicability evaluation of deep eutectic solvents-cellulase system for lignocellulosic hydrolysis. *Bioresour Technol* 181:297–302
- Hayyan M, Hashim MA, Hayyan A, Al-Saadi MA, Al Nashef IM, Mirghani ME, Saheed OK (2012) Are deep eutectic solvents benign or toxic? *Chemosphere* 90:2193–2195
- Hayyan M, Hashim MA, Al-Saadi MA, Hayyan A, Al Nashef IM, Mirghani MES (2013) Assessment of cytotoxicity and toxicity for phosphonium-based deep eutectic solvents. *Chemosphere* 93:455–459
- Haz A, Strzincova P, Majova V, Skulcova A, Jablonsky M (2016) Thermal stability of selected deep eutectic solvents. *Int J Recent Sci Res* 7:14441–14444
- Hou XD, Liu QP, Smith TJ, Li N, Zong MH (2013) Evaluation of toxicity and biodegradability of cholinium amino acids ionic liquids. *PLoS One* 8:e59145
- Ichwan M, Son TW (2011) Study on organosolv pulping methods of oil palm biomass. In: *International seminar on chemistry*. p 364–370
- Jablonsky M, Skulcova A, Kamenska L, Vrska M, Sima J (2015) Deep eutectic solvents: fractionation of wheat straw. *Bioresources* 10(4):8039–8047
- Kareem MA, Mjalli FS, Hashim MA, Al Nashef IM (2010) Phosphonium-based ionic liquids analogues and their physical properties. *J Chem Eng Data* 55:4632–4637
- Kim HK, Hong J (2001) Supercritical CO₂ pretreatment of lignocellulose enhances enzymatic cellulose hydrolysis. *Bioresour Technol* 77:139–144
- Kim TH, Lee YY (2005) Pretreatment and fractionation of corn stover by soaking in aqueous ammonia. *Appl Biochem Biotechnol* 121:1119–1131
- Kim JS, Kim H, Lee JS, Lee JP, Park SC (2008) Pretreatment characteristics of waste oak wood by ammonia percolation. *Appl Biochem Biotechnol* 148:15–22
- Kohno Y, Ohno H (2012) Ionic liquid/water mixtures: from hostility to conciliation. *Chem Commun* 48:7119–7130
- Kroon MC, Casal MF, Vanden BA (2014) Pretreatment of lignocellulosic biomass and recovery of substituents using natural deep eutectic solvents/compound mixtures with low transition temperatures. *International Patent*. Publication Number: WO 2013/153203 A1
- Kumar AK, Sharma S (2017) Recent updates on different methods of pretreatment of lignocellulosic feedstocks: a review. *Bioresour Bioproc* 4:7
- Kumar P, Barrett DM, Delwiche MJ, Stroeve P (2009) Methods for pretreatment of lignocellulosic biomass for efficient hydrolysis and biofuel production. *Ind Eng Chem Res* 48:3713–3729
- Kumar A, Kumar N, Baredar P, Shukla A (2015a) A review on biomass energy resources, potential, conversion and policy in India. *Renew Sustain Energy Rev* 45:530–539
- Kumar K, Parikh BS, Pravakar M (2015b) Natural deep eutectic solvent mediated pretreatment of rice straw: bioanalytical characterization of lignin extract and enzymatic hydrolysis of pretreated biomass residue. *Environ Sci Pollut Res* 23(10):9265–9275
- Kumar AK, Parikh BS, Pravakar M (2016) Natural deep eutectic solvent mediated pretreatment of rice straw: bioanalytical characterization of lignin extract and enzymatic hydrolysis of pretreated biomass residue. *Environ Sci Pollut Res Int* 23:9265–9275
- Kumar AK, Sharma S, Shah E, Patel A (2018) Technical assessment of natural deep eutectic solvent (NADES) mediated biorefinery process: a case study. *J Mol Liq*. <https://doi.org/10.1016/j.molliq.2018.03.107>
- Lindberg D, Revenga MD, Widersten M (2010) Deep eutectic solvents (DESs) are viable cosolvents for enzyme-catalyzed epoxide hydrolysis. *J Biotechnol* 147:169–171
- Lu W, Alam MA, Pan Y, Wu J, Wang Z, Yuan Z (2016) A new approach of microalgal biomass pretreatment using deep eutectic solvents for enhanced lipid recovery for biodiesel production. *Bioresour Technol* 218:123–128
- Lucas M, Hanson SK, Wagner GL, Kimball DB, Rector KD (2012) Evidence for room temperature delignification of wood using hydrogen peroxide and manganese acetate as a catalyst. *Bioresour Technol* 119:174–180
- Lynd LR, Elander RT, Wyman CE (1996) Likely features and costs of mature biomass ethanol technology. *Appl Biochem Biotechnol* 57:741–761

- Martínez R, Berbegal L, Guillena G, Ramón DJ (2016) Bio-renewable enantioselective aldol reaction in natural deep eutectic solvents. *Green Chem* 18(6):1724–1730
- Mele A, Tran CD, De Paoli Lacerda SH (2003) The structure of a room-temperature ionic liquid with and without trace amounts of water: the role of C H...O and C H...F interactions in 1-n-Butyl-3-Methylimidazolium Tetrafluoroborate. *Angew Chem Int* 42:4364–4366
- Morrison HG, Sun CC, Neervannan S (2009) Characterization of thermal behavior of deep eutectic solvents and their potential as drug solubilization vehicles. *Int J Pharm* 378:136–139
- Moultrop JS, Swatloski RP, Moyna G, Rogers RD (2005) High resolution 13-C NMR studies of cellulose and cellulose oligomers in ionic liquid solutions. *Chem Commun* 2005:1557–1559
- Mulia K, Putri S, Krisanti E, Nasruddin (2017) Natural deep eutectic solvents (NADES) as green solvents for carbon dioxide capture. *AIP Conf Proc* 1823:020022
- Murali S, Shrivastava R, Saxena M (2008) Quantification of agricultural residues for energy generation – a casestudy. *J Inst Public Health Eng* 3:27
- Nakamura Y, Daidai M, Kobayashi F (2004) Ozonolysis mechanism of lignin model compounds and microbial treatment of organic acids produced. *Water Sci Technol* 50:167–172
- Paiva A, Craveir R, Aroso I, Martins M, Reis RL, Duarte ARC (2014) Natural deep eutectic solvents – solvents for the 21st century. *ACS Sustain Chem Eng* 2:1063–1071
- Palmqvist E, Hahn-Hagerdal B (2000) Fermentation of lignocellulosic hydrolysates II: inhibitors and mechanisms of inhibition. *Bioresour Technol* 74:25–33
- Potumarthi R, Baadhe RR, Nayak P, Jetty A (2013) Simultaneous pretreatment and saccharification of rice husk by *Phanerochaete chrysosporium* for improved production of reducing sugars. *Bioresour Technol* 128:113–117
- Prasad S, Singh A, Joshi HC (2007) Ethanol as an alternative fuel from agricultural, industrial and urban residues. *Resour Conserv Recycl* 50:1–39
- Rabemanolntsoa H, Saka S (2016) Various pretreatments of lignocellulosics. *Bioresour Technol* 199:83–91
- Reetz MT, Wiesenhofer W, Francio G, Leitner W (2003) Continuous flow enzymatic kinetic resolution and enantiomer separation using ionic liquid/supercritical carbon dioxide media. *Adv Synth Catal* 345:1221–1228
- Rengstl D, Fischer V, Kunz W (2014) Low –melting mixtures based on choline ionic liquids. *Phys Chem Chem Phys* 16:22815–22822
- Ribeiro BD, Florindo C, Iff LC, Coelho MAZ, Marrucho IM (2015) Menthol-based eutectic mixtures: hydrophobic low viscosity solvents. *ACS Sustain Chem Eng* 3:2469–2477
- Saha BC, Iten BL, Cotta M, Wu YV (2005) Dilute acid pretreatment, enzymatic saccharification, and fermentation of rice hulls to ethanol. *Biotechnol Prog* 21:3816–3822
- Saini JK, Saini R, Tewari L (2015) Lignocellulosic agriculture wastes as biomass feedstocks for second-generation bioethanol production: concepts and recent developments. 3. *Biotechnology* 5:337–353
- Saka S (1991) Chemical composition and distribution. Dekker, New York, pp 3–58
- Sanchez C (2009) Lignocellulosic residues: biodegradation and bioconversion by fungi. *Biotechnol Adv* 27:185–194
- Shi J, Chinn MS, Sharma-Shivappa RR (2008) Microbial pretreatment of cotton stalks by solid state cultivation of *Phanerochaete chrysosporium*. *Bioresour Technol* 99:6556–6564
- Skulcova A, Majova V, Haz A, Kreps F, Russ A, Jablonsky M (2017) Long-term isothermal stability of deep eutectic solvents based on choline chloride with malonic or lactic or tartaric acid. *Int J Sci Eng Res* 8:2249–2252
- Smith EL, Abbott AP, Ryder KS (2014) Deep eutectic solvents (DESs) and their applications. *J Chem Eng Data* 61(12):4215–4221
- Song L, Yu H, Ma F, Zhang X (2013) Biological pretreatment under non-sterile conditions for enzymatic hydrolysis of corn stover. *Bioresources* 8:3802–3816
- Suhara H, Kodama S, Kamei I, Maekawa N, Meguro S (2012) Screening of selective lignin degrading basidiomycetes and biological pretreatment for enzymatic hydrolysis of bamboo culms. *Int Biodeter Biodegr* 75:176–180

- Sun Y, Cheng J (2002) Hydrolysis of lignocellulosic materials for ethanol production: a review. *Bioresour Technol* 83:1–11
- Taha M, Shahsavari E, Al-Hothaly K, Mouradov A, Smith AT, Ball AS, Adetutu EM (2015) Enhanced biological straw saccharification through co-culturing of lignocellulose degrading microorganisms. *Appl Biochem Biotechnol* 175:3709–3728
- Taherzadeh MJ, Karimi K (2008) Pretreatment of lignocellulosic wastes to improve ethanol and biogas production: a review. *Int J Mol Sci* 9:1621–1651
- Valderrama J (2003) The state of the cubic equations of state. *Ind Eng Chem Res* 42:1603–1618
- Van Osch DJGP, Zubeir LF, van den Bruinhorst A, Rochaa MAA, Kroon MC (2015) Hydrophobic deep eutectic solvents as water-immiscible extractants. *Green Chem* 17:4518–4521
- Vats S, Maurya DP, Shaimoon M, Negi S (2013) Development of a microbial consortium for the production of blend enzymes for the hydrolysis of agricultural waste into sugars. *J Sci Ind Res* 72:585–590
- Wan C, Li Y (2011) Effectiveness of microbial pretreatment by *Ceriporiopsis subvermispora* on different biomass feed stocks. *Bioresour Technol* 102:7507–7512
- Wu SH, Caparanga AR, Leron RB, Li MH (2012) Vapor pressure of aqueous choline chloride-based deep eutectic solvents (ethaline, glyceline, maline and reline) at 30–70 °C. *Thermochim Acta* 544:1–5
- Wyman CE (1999) Biomass ethanol: technical progress, opportunities, and commercial challenges. *Ann Rev Energy Environ* 24:189–226
- Xia S, Baker GA, Li H, Ravula S, Zhao H (2014) Aqueous ionic liquids and deep eutectic solvents for cellulosic biomass pretreatment and saccharification. *RSC Adv* 4:10586–10596
- Xu C, Ma F, Zhang X, Chen S (2010) Biological pretreatment of corn stover by *Irpex lacteus* for enzymatic hydrolysis. *J Agric Food Chem* 58:10893–10898
- Yiin CL, Quitain AT, Yusup S, Sasaki M, Uemura Y, Kida T (2015) Characterization of natural low transition temperature mixtures (LTTMs): green solvents for biomass delignification. *Bioresour Technol* 199:258–264
- Zavrel M, Bross D, Funke M, Buchs J, Spiess AC (2009) High-throughput screening for ionic liquids dissolving (ligno-)cellulose. *Bioresour Technol* 100:2580–2587
- Zhang SH, Xu YX, Hanna MA (2012a) Pretreatment of corn stover with twin screw extrusion followed by enzymatic saccharification. *Appl Biochem Biotechnol* 166:458–469
- Zhang Q, De Vigier KO, Royer S, Jérôme F (2012b) Deep eutectic solvents: syntheses, properties and applications. *Chem Soc Rev* 41:7108–7146
- Zhang CW, Xia SQ, Ma PS (2016) Facile pretreatment of lignocellulosic biomass using deep eutectic solvents. *Bioresour Technol* 219:1–5
- Zheng YZ, Lin HM, Tsao GT (1995) Supercritical carbon-dioxide explosion as a pretreatment for cellulose hydrolysis. *Biotechnol Lett* 17:845–850
- Zhu JY, Pan XJ (2010) Woody biomass pretreatment for cellulosic ethanol production technology and energy consumption evaluation. *Bioresour Technol* 101:4992–5002



Recent Developments and Challenges of Acetone-Butanol-Ethanol Fermentation

5

Prakash K. Sarangi and Sonil Nanda

Abstract

The major concern for sustainable industrial development is the transition from fossil-based fuels to renewable resources for fuel, chemicals and materials production. The exploiting usage of fossil fuels is not only environmentally unsafe but also prone to price inflation and concerns related to ozone layer depletion and global warming. Therefore, lignocellulosic materials are seen as potential renewable resources to supply the future green energy and materials. Butanol is considered a superior biofuel due to greater energy density, better fuel properties, engine compatibility and less hygroscopic nature than ethanol. Also, it has created popularity among biofuels in higher blending ratios with gasoline. However, the major limitation of butanol production is the cost of acetone-butanol-ethanol (ABE) fermentation process that subsequently affects the yield and productivity in bioprocessing. For conversion of renewable resources into valuable base chemicals and liquid fuels, ABE fermentation has been receiving renewed interest in utilizing lignocellulosic biomass that is abundant and incompetent with food sources. In this chapter, some recent developments in ABE process are discussed along with certain major challenges and future prospects.

Keywords

Acetone-butanol-ethanol fermentation · *Clostridium* · Butanol · Butanol toxicity · Genetic engineering

P. K. Sarangi (✉)

Directorate of Research, Central Agricultural University, Imphal, Manipur, India

e-mail: sarangi77@yahoo.co.in

S. Nanda

Department of Chemical and Biochemical Engineering, University of Western Ontario, London, Ontario, Canada

© Springer Nature Singapore Pte Ltd. 2018

P. K. Sarangi et al. (eds.), *Recent Advancements in Biofuels and Bioenergy Utilization*, https://doi.org/10.1007/978-981-13-1307-3_5

111

5.1 Introduction

Recently, the concerns about global warming, the increase in the fossil price and legislative restrictions for the use of non-renewable energy sources are leading to increased interests towards the exploration in the biotechnology route for biofuels production. The global consumption of petroleum and other fossil-based liquid fuels was 86 million barrels per day in 2008, which is predicted for an increase to 98 million barrels per day in 2020 and 112 million barrels per day in 2035 (USEIA 2011). The main objective worldwide is to deploy the renewable resources to produce fuels, power, heat and value-added chemicals. Lignocellulosic biomasses are renewable and non-edible plant materials that can produce biofuels thus mitigating the dependency on fossil fuels. In general, there are various options to produce alternative transportation fuels from biomass.

The expanding energy industries are facing many concerns although the global biofuel production has been increasing rapidly over the last decade. Moreover, the first-generation biofuels (bioethanol from corn) have created many challenges over food vs fuel debate, thereby exposing better grounds for the waste-to-energy scenario. Hence, second-generation biofuel technologies have become efficient in terms of net lifecycle greenhouse gas (GHG) emission reductions that are socially and environmentally acceptable.

Lignocellulosic feedstocks (including agricultural and forestry residues), municipal solid wastes and sewage sludge have the incredible potential to supplement the production of biofuels, thereby achieving energy security and reducing GHG emissions (Nanda et al. 2014b, 2015). Being an inexpensive resource and abundantly available in nature on a global scale, lignocellulosic biomass can support the production of alternative liquid biofuels. About 40 million tons of lignocellulosic biomass is generated globally (Sanderson 2011). Another advantage of lignocellulosic biomass is their non-edible nature; hence their biorefining possesses the least threat to the domestic and international food security unlike food-based feedstocks (Nanda et al. 2015).

Biobutanol is regarded as a better competitor than bioethanol due to many advanced fuel properties (Dürre 2007; Ni and Sun 2009; Patakova et al. 2013; Tiginova et al. 2013; Karimi and Pandey 2014; Li et al. 2014). Compared to ethanol, butanol has 30% higher energy content and is less corrosive, less volatile, less flammable, less hazardous and less hygroscopic (Nanda et al. 2014a). Having low vapour pressure, butanol can be used as a biofuel in gasoline supply pipelines and is mixed well in flexible proportions (Qureshi and Ezeji 2008). Butanol can be blended with gasoline in any ratio or can also be used as a drop-in fuel in current vehicle engines.

Having bestowed with various chemical and physical properties, butanol has been focused towards the production of second-generation biofuels. Butanol has 4 carbon atoms that are 6 times less evaporative than ethanol and 13.5 times less evaporative than gasoline, thereby facilitating its use in existing transport systems relying predominantly on gasoline (Lee et al. 2008). Butanol can be used as a total replacement for gasoline without any modifications to car engines. The important

Table 5.1 Comparison of properties of common biofuels with butanol

Characteristic	Gasoline	Butanol	Ethanol	Methanol
Formula	H, C ₄ -C ₁₂	C ₄ H ₉ OH	CH ₃ CH ₂ OH	CH ₃ OH
Boiling point (°C)	32–210	118	78	65
Auto-ignition temperature (°C)	280	343	365	435
Energy density (MJ/kg)	44.5	33.1	26.9	19.6
Air-fuel ratio	14.6	11.2	9.0	6.5
Research octane number	91–99	96	129	136
Viscosity at 25 °C (mPa.s)	0.6	2.573	1.074	0.544
Motor octane number	81–89	78	102	104
Density at 20 °C (g/m ³)	0.7	0.81	0.789	0.797
Lower heating value (MJ/kg)	43.4	34.3	26.9	22.7
Higher heating value (MJ/kg)	46.5	37.3	29.8	37.18
Heat of vaporization (MJ/kg)	0.36	0.43	0.92	1.20

References: Chan et al. (2010), Cheng (2010), Dürre (2007), Lee et al. (2008), Surisetty et al. (2011), MacLean and Lave (2003) and Szulczyk (2010)

fuel properties of biobutanol are summarized in Table 5.1 with a comparison to other biofuels (fuel alcohols).

The biological production of butanol is achieved through acetone-butanol-ethanol (ABE) fermentation process. Due to the high demand for acetone in the production of cordite as explosive during the First World War, this process was commercialized in the Union of Soviet Socialist Republics, United Kingdom, Canada and the USA. ABE fermentation was developed in 1912 at Manchester University by the Russian chemist C. Weizmann. Several reports have been found regarding the establishment of ABE fermentation as industrial units in Japan, Australia, China and South Africa (Linden et al. 1986; García et al. 2011; Köpke and Dürre 2011; Dong et al. 2012). Although ABE fermentation was mainly used for the production of acetone as a solvent for military applications, there is an increasing interest in butanol as a liquid renewable fuel recently (Dürre 2007). Elevated substrate cost, low yield and a high cost of product recovery are the major limitations in the economical production of butanol through ABE fermentation. In this regard, global research has been devoted in last two decades for exploration of a wide range of alternate cheap renewable feedstock for ABE fermentation such as bagasse, wheat straw, wheat bran, corn fibre and other agriculture residues.

Several *Clostridium* spp., especially *Clostridium acetobutylicum* and *Clostridium beijerinckii*, have been utilized for production of biobutanol through ABE fermentation process. Attempts have been made to obtain butanol from many starch-based and cellulosic substrates. Various fermentation technologies like batch, fed-batch and continuous fermentation utilizing with wild-type and modified strains are applied in ABE fermentation process (Setlhaku et al. 2012; Survase et al. 2012; Xue et al. 2012; Chen et al. 2013, 2014). The list of *Clostridium* spp. along with feedstocks used in ABE fermentation process is summarized in Table 5.2.

Table 5.2 List of biomasses and *Clostridium* spp. used in ABE fermentation

Bacteria	Feedstock	Total ABE concentration (g/L)	References
<i>C. acetobutylicum</i> P262	Aspen wood	20.1–24.6	Parekh et al. (1988)
<i>C. acetobutylicum</i> 824A	Lactose	1.43	Napoli et al. (2010)
<i>C. acetobutylicum</i> DSM 1731	Potato	33	Grobben et al. (1993)
<i>C. acetobutylicum</i> IFP 921	Wheat straw	17.7	Marchal et al. (1985)
<i>C. saccharoperbutylacetonicum</i> ATCC 27022	Bagasse	18.1	Soni et al. (1982)
<i>C. beijerinckii</i> P260	Barley straw	26.6	Qureshi et al. (2010a)
<i>C. beijerinckii</i> BA101	Corn fibre	9.3	Qureshi et al. (2008b)
<i>C. acetobutylicum</i> P262	Corn stover	25.8	Parekh et al. (1988)
<i>C. acetobutylicum</i> P262	Pinewood	17.6	Parekh et al. (1988)
<i>C. beijerinckii</i> B-592	Pinewood	18.5	Nanda et al. (2014a)
<i>C. saccharoperbutylacetonicum</i> ATCC 27022	Rice straw	13.0	Soni et al. (1982)
<i>C. beijerinckii</i> B-592	Wheat straw	17.9	Nanda et al. (2014a)
<i>C. beijerinckii</i> P260	Wheat straw	21.4	Qureshi et al. (2008a)
<i>C. beijerinckii</i> P260	Switchgrass	14.6	Qureshi et al. (2010b)
<i>C. saccharobutylicum</i> DSM 13864	Sago	9.1	Liew et al. (2005)
<i>C. saccharoperbutylacetonicum</i> ATCC 27022	Rice straw	13.0	Soni et al. (1982)
<i>C. beijerinckii</i> B-592	Timothy grass	17.4	Nanda et al. (2014a)

5.2 Acetone-Butanol-Ethanol (ABE) Fermentation Process

Clostridium bacterium is heterogeneous gram-positive, spore-forming, obligatory anaerobic, rod-shaped in nature that can grow on a wide range of substrates producing many enzymes thereby breaking complex polymeric carbohydrates into monomers. Various types of enzymes such as α -amylase, α -glucosidase, glucoamylase, pullulanase and amylopullulanase (Ezeji et al. 2007) draw the catalytic effect. Availability of various suitable biocatalytic systems in *Clostridium* can

enhance the production of butanol over broad ranges of carbon sources (e.g. arabinose, cellobiose, galactose, glucose, mannose and xylose) to acetone, butanol and ethanol (Ezeji et al. 2007b). In particular, butanol production by ABE fermentation is mostly carried out using *Clostridium* spp. like *C. acetobutylicum* and *C. beijerinckii*. Other species including *C. acetobutylicum*, *C. beijerinckii*, *C. aurantibutyricum*, *C. butylicum*, *C. saccharobutylicum*, *C. saccharoperbutylacetonicum*, etc. can also be used in ABE fermentation with a broad range of organic substrates.

Some traditional starch-based feedstocks for butanol production include corn, millet, molasses, potatoes, rice, wheat, whey permeate and tapioca that restrict the requirement of biomass pretreatment and hydrolysis (Qureshi and Blascheck 2005) due to the intense amylolytic activity of *Clostridium*. Various lignocellulosic biomasses including crop residues and agro-wastes such as barley straw, corn cobs, corn fibre, corn stover, hemp waste, pinewood, rice straw, sunflower shells, switchgrass, timothy grass and wheat straw are used for biobutanol production through ABE fermentation (Zverlov et al. 2006; Qureshi and Ezeji 2008).

Having complex intracellular pathway, ABE fermentation principally produces three types of important products such as (i) solvents, i.e. acetone, butanol and ethanol; (ii) organic acids, i.e. lactic acid, acetic acid and butyric acid; and (iii) gases, i.e. carbon dioxide and hydrogen (Zheng et al. 2009; Xue et al. 2013). The entire ABE fermentation is a biphasic process which consists of both the acidogenic phase and the solventogenic phase. The ABE fermentation in a typical batch system is initiated with carbohydrate substrates (usually glucose or equivalent sugars). The fermentation medium is created by an anaerobic environment inside the reactor using N_2 or CO_2 followed by suitable butanol-producing *Clostridium* culture incubating at 35 °C. The typical incubation period of ABE fermentation lasts for 36–72 h producing total ABE up to 20–25 g/L (Qureshi and Ezeji 2008).

A biphasic stage, ABE fermentation starts with acidogenic phase within the exponential growth phase of bacterial growth in which each mole of glucose produces either 2 moles of acetic acid or 1 mole of butyric acid. The production of the acids not only causes a decrease in the pH but also appears unsuitable for bacterial growth. There is a metabolic and morphological shift by *Clostridium* sp. during the acidogenic phase such as (i) completion of the exponential growth phase, (ii) endospore formation and cessation of growth and (iii) conversion of the acids to solvents. Acetone-butanol-ethanol is formed in a typical molar ratio of 3:6:1.

The pathway for ABE fermentation performed by *Clostridium* is shown in Fig. 5.1. During the acidogenesis, the inhibition of the metabolic pathway can also occur even after no proper pH control, which is regarded as acidic stress. However, the causes of acidic stress are the rapid production of these acids compared to their consumption or degradation (Kumar and Gayen 2011; Xue et al. 2013). The exponential growth stage of *Clostridium* favours the acidogenic phase as the formation of acid is complemented by the synthesis of adenosine triphosphate (ATP) required for the cell growth. Being an obligate anaerobe, the acidogenic phase plays a vital role in energy metabolism of *Clostridium*. Due to the reduction in pH, the bacterium slows down acid production and utilizes the excreted acetic acid and

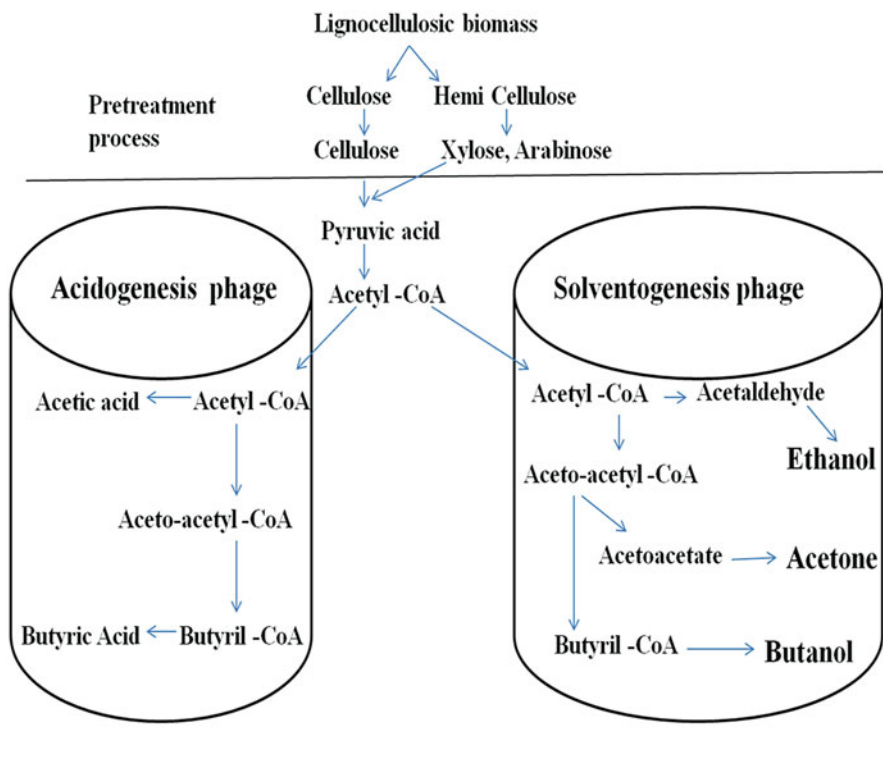


Fig. 5.1 Simplified pathways for ABE fermentation by *Clostridium* sp.

butyric acid, thereby converting them to acetone and butanol, respectively. During the acidogenic phase, the production of butyric acid is more than acetic acid because of a better balance of the redox equilibrium of the former (Zheng et al. 2009). The formation of butyric acid requires NADH from glycolysis rather than acetate formation, thereby producing more butanol from butyric acid than ethanol. Hence, more conversion of butyrate than acetate occurs during the solventogenetic phase in ABE fermentation almost twice as much butyrate produced compared to acetate (Dürre 2007). Thus, butanol is the most important product of ABE fermentation as the typical proportions of acetone, butanol and ethanol are 3:6:1 (Jones and Woods 1986).

Clostridium metabolism involves the phase shift from acidogenesis to solventogenesis, thereby products of the former are then transferred to the latter followed by 70–80% conversion of viable cells into spores thereby cessation of growth (García et al. 2011). At around pH 5.5, the concentrations of acids remain nearly constant or slightly lower, thereby facilitating the production of the solvent (acetone, butanol and ethanol). The causative parameters of phase shift may be due to the non-dissociated butyric acid (García et al. 2011). Although low pH is preferable for solvent production, a pH below 4.5 results in enough acid formation,

thus lowering the duration and effectiveness of the solventogenic phase. However, the enhancement of bacterial growth can occur by increasing the buffering capacity of the fermentation medium so that carbohydrate utilization and butanol production can also be increased (Bryant and Blaschek 1988).

Butyric acid and acetic acid also induce the respective enzymes such as butyrate kinase and acetate kinase needed for the butanol biosynthesis (Ballongue et al. 1986). Moreover, the roles of butyryl-CoA and butyryl phosphate are also there for shifting from acidogenesis to solventogenesis phase (Harris et al. 2000). Acetic acid can be converted to ethanol or acetone, while butyric acid is converted to butanol. The cessation of fermentation process happens at high concentration of the solvents inhibiting the process so that cell membranes are solubilized leading to cell death. However, the maximum solvent concentration about 2 wt% is the limitation of this ABE fermentation process (Dürre 1998).

The anaerobic ABE fermentation, lasting for 36–72 h, produces total ABE up to 20–25 g/L (Qureshi and Ezeji 2008). However, butanol is very toxic to the cells showing the inhibition at a concentration range of 5–10 g/L because *Clostridia* can rarely withstand more than 2% butanol (Qureshi and Ezeji 2008; Liu and Qureshi 2009). There are various research cases available on the solvent stress due to the sensitiveness of *Clostridia* to the medium composition and fermentation conditions (Linden et al. 1986; Xue et al. 2013). Even small amounts of oxygen can completely inhibit the activity of the cells, and some quantities of chemicals can also affect the product distribution (Choi et al. 2012; Han et al. 2013). A case study of the small amount of zinc, i.e. 0.001 g/L ($\text{ZnSO}_4 \cdot 7\text{H}_2\text{O}$), can result in premature phase shift to solventogenesis (Wu et al. 2013).

The best-studied bacterium is *C. acetobutylicum* that basically grows on the starch-based substrates. Some other phylogenetically interconnected strains are *C. beijerinckii*, *C. saccharobutylicum* and *C. saccharoperbutylacetonicum* having saccharolytic activities. Studies indicate the production of solvent at concentrations up to 14–18 g/L with solvent yields of 25–30% (Shaheen et al. 2000) by some of the strains of *C. acetobutylicum*. Production of solvents over a wide range of pH occurs by the saccharolytic industrial strains belong to *C. beijerinckii* species utilizing a wider variety of carbohydrates as the substrate due to its genetic potential. *C. beijerinckii* is also less susceptible to acid crash and therefore more suitable for longer (continuous) fermentations than *C. acetobutylicum* (Qureshi and Blaschek 2000). The less studied clostridia are *C. saccharobutylicum* and *C. saccharoperbutylacetonicum* producing an average solvent concentration of 19.6 g/L with a yield of 30% (Shaheen et al. 2000).

The role of electron flow in the glycolytic pathway is very crucial for the production butanol from ABE fermentation process. The presence of ferredoxin oxidoreductase in clostridia helps in the oxidation of NADH and FADH produced during the solventogenic phase. Any alteration in the direction of electron flow around reduced ferredoxin can alter the type and quantity of fermentation products. The enhancing effect on the production of butanol and ethanol is detected at the expense of acetone synthesis in the presence of these electron carriers (Zverlov et al. 2006; Gapes 2000). The mainly four principal groups of solventogenic *Clostridia*

bacteria such as *C. acetobutylicum*, *C. beijerinckii*, *C. saccharobutylicum* and *C. saccharoperbutylacetonicum* can be utilized for ABE fermentation process.

The attention towards the developments in genetic engineering utilizing hyper butanol-producing strains such as *C. beijerinckii* P260 and *C. beijerinckii* BA101 are being focussed on (Ezeji et al. 2007). In addition, the novel separation technologies can prevent the product inhibition process due to the removal of accumulated butanol from the fermentation medium. As compared to the final solvent accumulation of 12–20 g/L in batch fermentation, the fed-batch fermentation has the more product recovery but has problems with butanol toxicity, which can be reduced by the supplementation of in situ recovery processes such as gas stripping (Ezeji et al. 2004).

5.3 Challenges and Possible Outcomes in the ABE Fermentation

With many advantages over ethanol, the commercial production of butanol through ABE fermentation has also some challenges at various stages of the process. Although lignocellulosic biomass can be used as a cheap source of substrates for ABE fermentation, the main challenge of using lignocellulosic biomass as feedstock is the additional costs of sugar production compared to molasses or starches. Another limitation that builds up is the selection of biomass along with pretreatment process. Whatever the pretreatment process may be, detoxification is very crucial for removal of inhibitors generated during this processes (Ezeji et al. 2007). Apart from other technical challenging issues associated with ABE fermentation common to all feedstocks, butanol toxicity and low recovery can hinder its commercial production, which significantly increases the cost of recovery and separation (Ezeji et al. 2007). Hence, the production cost of biobutanol becomes more expensive, and selling price per litre could be higher than that of gasoline, making it competitive in the transportation fuels. Although the sustainable production of butanol from renewable biomass is gaining momentum in the biofuel sector (Jung et al. 2013; Gao et al. 2014), the cost of the substrate only accounts for 60% of the overall production cost. Hence, low cost and year-round availability are the key issues for the success of the biofuel production through the biotechnological route.

Different pretreatment methods such as physical, chemical and biological techniques have been well investigated for biofuel production from lignocellulosic biomass (Kumar et al. 2009; Mussatto and Teixeira 2010) aiming to increase the accessibility of cellulose and hemicelluloses for obtaining fermentable monomeric sugars (Galbe and Zacchi 2007). Lignocellulosic biomass is regarded as the suitable substrate for conversion into biobutanol through ABE fermentation, but due to its recalcitrant nature, intense pretreatment requirement and requirement of expensive hydrolytic enzymes, the price of butanol could increase manyfold, thereby limiting

its commercial production (Shafiei et al. 2011, 2013, 2014; Boonsombuti et al. 2015). The pretreatment of lignocellulosic biomasses also produces certain inhibitors in the hydrolysates, e.g. hydroxymethylfurfural, furfural and lignin derivatives, which pose toxic threats to clostridia (Kudahettige-Nilsson et al. 2015). The inhibitors slow the growth of *Clostridium* species, and the yield of butanol is drastically reduced (Cai et al. 2013). An ideal pretreatment process should efficiently improve the enzymatic hydrolysis, consume lower amounts of chemicals and produce fewer by-products/inhibitors (Karimi et al. 2013). The use of dilute acid pretreatment produces a high concentration of inhibitors and requires a detoxification process to neutralize the fermenting solution. This detoxification step not only adds cost to the process but also leads to some sugar loss. Liquid hot water, ammonia, ionic liquid and organosolv treatments are among the most applied methods (Amiri et al. 2014), but all these methods have their own drawbacks (Taherzadeh and Karimi 2008).

The major limitation of the industrial production of ABE is the butanol toxicity. Fermentation by *Clostridium* spp. has to face such hurdles as the said microbes rarely tolerate more than 2% butanol as mentioned earlier. Butanol toxicity is a limiting factor for the final butanol yield in ABE fermentation, which is more severe than acetone and ethanol. The maximum limit tolerated by wild-type *Clostridium* strains (Garcia et al. 2011) is reported to be butanol 12–13 g/L by the conventional ABE fermentation. Butanol concentration of 19.6 g/L is reportedly produced from genetically modified *C. beijerinckii* BA101 (Qureshi and Blaschek 1999). Another issue that hinders the butanol production level is the bacteriophage infection during ABE fermentation. Some report states the *Siphoviridae* and *Podoviridae* infect *Clostridium madisonii* and *C. beijerinckii* P260, respectively, thereby lowering the growth of bacterium, thus showing reduced solvent production (Jones et al. 2000).

Although butanol has the partial miscibility nature of water, this feature leads to several technical issues during its recovery from the fermentation broth. In addition to distillation, which is a traditional solvent recovery method, various techniques such as perstraction (Qureshi et al. 1992), pervaporation (Xue et al. 2014) and supercritical methods (Reddy et al. 2014) have been undertaken for maximum butanol recovery. The recent development towards the genetic and metabolic engineering is also applied for the butanol-producing microorganisms to overcome several limitations such as low butanol titre, yield and productivity.

Construction of mutant strains of *Clostridium* and other microorganisms are vital factors for improvement of industrial-scale butanol refinery (Ezeji et al. 2007). Another new novel technology for enhancing the microbial efficiency for butanol production is antisense RNA technology implemented in producing mutants for improved ABE fermentation (Tummala et al. 2003). Hence, synthetic biology approach can be implemented to develop better microbial strains tolerant to high butanol concentration and other solvent stress. This can potentially mitigate the future fuel crisis due to decline and the adverse effect of fossil fuel uses.

5.4 Conclusions

Biobutanol is a promising substitute for other biofuels and petroleum-based products. The major merits of butanol are its high-energy content, less corrosiveness than ethanol, compatibility with existing vehicle engines in either blended or pure form. ABE fermentation process has been utilized for production of acetone, butanol and ethanol in the ratio of 3:6:1 utilizing *Clostridium* species. ABE fermentation is biphasic that generated acids (acetic acid, butyric acid, CO₂ and H₂) and solvents (acetone, ethanol and butanol). During ABE fermentation, *Clostridium* is prone to butanol toxicity, spore formation, opportunistic bacteriophage infection and incomplete sugar conversion, which are commonly encountered issues. Other challenges of ABE fermentation include low concentration and difficulty in separation of products, higher feedstock consumption rate (i.e. lower production yield) and sensitivity to substrate composition and inhibitors and to the presence of oxygen.

Genetic engineering of butanol-producing microorganisms can induce oxygen and butanol tolerance, high cell density, prolonged viability, asporogenesis and high butanol selectivity. Thus, the development of genetically modified and metabolically engineered strains can produce a higher quantity of butanol lowering the side chain products. Due to the unique physiology of *Clostridium* and lack of understanding of its induced genomic regulation, recombinant DNA technology still struggles to develop a hyper-butanol-producing strain. Improvement in biotechnological processes, bioprocess technology and consolidated bioprocessing system involving ABE fermentation may solve some of the challenges and difficulties for higher butanol production that could make a sustainable fuel replacement for gasoline in the future.

References

- Amiri H, Karimi K, Zilouei H (2014) Organosolvent pretreatment of rice straw for efficient acetone, butanol, and ethanol production. *Bioresour Technol* 152:450–456
- Ballongue J, Amine J, Masion E, Petitdemange H, Gay D (1986) Regulation of acetate kinase and butyrate kinase by acids in *Clostridium acetobutylicum*. *FEMS Microbiol Lett* 35:295–301
- Boonsombuti A, Luengnaruemitchai A, Wongkasemjit S (2015) Effect of phosphoric acid pretreatment of corncobs on the fermentability of *Clostridium beijerinckii* TISTR 1461 for biobutanol production. *Prep Biochem Biotechnol* 45:173–191
- Bryant DL, Blaschek HP (1988) Buffering as a means for increasing growth and butanol production by *Clostridium acetobutylicum*. *J Ind Microbiol* 3:49–55
- Cai D, Zhang T, Zheng J, Chang Z, Wang Z, Qin PY, Tan TW (2013) Biobutanol from sweet sorghum bagasse hydrolysate by a hybrid pervaporation process. *Bioresour Technol* 145:97–102
- Chan CC, Horng JL, Chi MS, Yen CH (2010) Autoignition temperature data for methanol, ethanol, propanol, 2-butanol, 1-butanol, and 2-methyl-2,4-pentanediol. *J Chem Eng Data* 55:5059–5064
- Chen C, Xiao Z, Tang X, Cui H, Zhang J, Li W, Ying C (2013) Acetone-butanol-ethanol fermentation in a continuous and closed-circulating fermentation system with PDMS membrane bioreactor. *Bioresour Technol* 128:246–251
- Chen C, Wang L, Xiao G, Liu Y, Xiao Z, Deng Q, Yao P (2014) Continuous acetone-butanol-ethanol (ABE) fermentation and gas production under slight pressure in a membrane bioreactor. *Bioresour Technol* 163:6–11

- Cheng (2010) Biomass to renewable energy processes. CRC Press, Boca Raton
- Choi SJ, Lee J, Jang YS, Park JH, Lee SY, Kim IH (2012) Effects of nutritional enrichment on the production of acetone-butanol-ethanol (ABE) by *Clostridium acetobutylicum*. J Microbiol 50:063–1066
- Dong H, Tao W, Dai Z, Yang L, Gong F, Zhang Y, Li Y (2012) Biobutanol. Adv Biochem Eng Biotechnol 128:85–100
- Dürre P (1998) New insights and novel developments in clostridial acetone/butanol/isopropanol fermentation. Appl Microbiol Biotechnol 49:639–648
- Dürre P (2007) Biobutanol: an attractive biofuel. Biotechnol J 2:1525–1534
- Ezeji TC, Qureshi N, Blaschek HP (2004) Acetone butanol ethanol (ABE) production from concentrated substrate: reduction in substrate inhibition by fed-batch technique and product inhibition by gas stripping. Appl Microbiol Biotechnol 63:653–658
- Ezeji TC, Qureshi N, Blaschek HP (2007) Bioproduction of butanol from biomass: from genes to bioreactors. Curr Opin Biotechnol 18:220–227
- Ezeji TC, Qureshi N, Blaschek H (2007b) Butanol production from agricultural residues: impact of degradation products on *Clostridium beijerinckii* growth and butanol fermentation. Biotechnol Bioeng 97:1460–1469
- Galbe M, Zacchi G (2007) Pretreatment of lignocellulosic materials for efficient bioethanol production. Adv Biochem Eng Biotechnol 108:41–65
- Gao K, Rehmann L, Boiano S, Marzocchella A (2014) Cellulosic butanol production from alkali-pretreated switchgrass (*Panicum virgatum*) and phragmites (*Phragmites australis*). Bioresour Technol 174:176–181
- Gapes J (2000) The economics of acetone-butanol fermentation: theoretical and market considerations. J Mol Microbiol Biotechnol 2:27–32
- García V, Pääkkilä J, Ojamo H, Muurinen E, Keiski RL (2011) Challenges in biobutanol production: how to improve the efficiency? Renew Sust Energy Rev 15:964–980
- Grobben NG, Eggink G, Cuperus FP, Huizing HJ (1993) Production of acetone, butanol and ethanol (ABE) from potato wastes: fermentation with integrated membrane extraction. Appl Microbiol Biotechnol 39:494–498
- Han B, Ujor V, Lai LB, Gopalan V, Ezeji TC (2013) Use of proteomic analysis to elucidate the role of calcium in acetone-butanol-ethanol fermentation by *Clostridium beijerinckii* NCIMB 8052. Appl Environ Microbiol 79:282–293
- Harris LM, Desai RP, Welker NE, Papoutsakis ET (2000) Characterization of recombinant strains of the *Clostridium acetobutylicum* butyrate kinase inactivation mutant: need for new phenomenological models for solventogenesis and butanol inhibition? Biotechnol Bioeng 67:1–11
- Jones DT, Woods DR (1986) Acetone-butanol fermentation revisited. Microbiol Rev 50:484–524
- Jones DT, Shirley M, Wu X, Keis S (2000) Bacteriophage infections in the industrial acetone butanol (AB) fermentation process. J Mol Microbiol Biotechnol 2:21–26
- Jung YH, Kim IJ, Kim HK, Kim KH (2013) Dilute acid pretreatment of lignocellulose for whole slurry ethanol fermentation. Bioresour Technol 132:109–114
- Karimi K, Pandey A (2014) Current and future ABE processes. Biofuel Res J 3:77
- Karimi K, Shafiei M, Kumar R (2013) Progress in physical and chemical pretreatment of lignocellulosic biomass. In: Gupta VK, Tuohy MG (eds) Biofuel technologies. Springer, Berlin, pp 53–96
- Köpke M, Dürre P (2011) Biochemical production of biobutanol. In: Luque R, Campelo J, Clark J (eds) Handbook of biofuels production. Woodhead Publishing, Cambridge, UK, pp 221–257
- Kudahettige-Nilsson RL, Helmerius J, Nilsson RT, Sjöblom M, Hodge DB, Rova U (2015) Biobutanol production by *Clostridium acetobutylicum* using xylose recovered from birch Kraft black liquor. Bioresour Technol 176:71–79
- Kumar M, Gayen K (2011) Developments in biobutanol production: new insights. Appl Energy 88:1999–2012
- Kumar P, Barrett DM, Delwiche MJ, Stroeve P (2009) Methods for pretreatment of lignocellulosic biomass for efficient hydrolysis and biofuel production. Ind Eng Chem Res 48:3713–3729

- Lee SY, Park JH, Jang SH, Nielsen LK, Kim J, Jung KS (2008) Fermentative butanol production by *Clostridia*. *Biotechnol Bioeng* 101:209–228
- Li J, Baral NR, Jha AK (2014) Acetone-butanol-ethanol fermentation of corn stover by *Clostridium* species: present status and future perspectives. *World J Microbiol Biotechnol* 30:1145–1157
- Liew ST, Arbakariya A, Rosfarizan M, Raha AR (2005) Production of solvent (acetone–butanol–ethanol) in continuous fermentation by *Clostridium saccharobutylicum* DSM 13864 using gelatinised sago starch as a carbon source. *Malays J Microbiol* 2:42–45
- Linden JC, Moreira AR, Lenz TG (1986) Acetone and butanol. In: Moo Young M (ed) *Comprehensive biotechnology*. Pergamon Press, Oxford, pp 915–931
- Liu S, Qureshi N (2009) How microbes tolerate ethanol and butanol? *New Biotechnol* 26:117–121
- MacLean HL, Lave LB (2003) Evaluating automobile fuel/propulsion system technologies. *Prog Energy Combust Sci* 29:1–69
- Marchal R, Blanchet D, Vandecasteele JP (1985) Industrial optimization of acetone-butanol fermentation: a study of the utilization of Jerusalem artichokes. *Appl Microbiol Biotechnol* 23:92–98
- Mussatto SI, Teixeira JA (2010) Lignocellulose as raw material in fermentation processes. *Appl Microbiol* 2:897–907
- Nanda S, Dalai AK, Kozinski JA (2014a) Butanol and ethanol production from lignocellulosic feedstock: biomass pretreatment and bioconversion. *Energy Sci Eng* 2:138–148
- Nanda S, Mohammad J, Reddy SN, Kozinski JA, Dalai AK (2014b) Pathways of lignocel-lulosic biomass conversion to renewable fuels. *Biomass Convers Bioref* 4:157–191
- Nanda S, Azargohar R, Dalai AK, Kozinski JA (2015) An assessment on the sustainability of lignocellulosic biomass for biorefining. *Renew Sust Energy Rev* 50:925–941
- Napoli F, Olivieri G, Russo ME, Marzocchella A, Salatino P (2010) Production of butanol in a continuous packed bed reactor of *Clostridium acetobutylicum*. *J Ind Microbiol Biotechnol* 37:603–608
- Ni Y, Sun Z (2009) Recent progress on industrial fermentative production of acetone-butanol-ethanol by *Clostridium acetobutylicum* in China. *Appl Microbiol Biotechnol* 83:415–423
- Parekh SR, Parekh RS, Wayman M (1988) Ethanol and butanol production by fermentation of enzymatically saccharified SO₂-prehydrolysed lignocellulosics. *Enzym Microbiol Technol* 10:660–668
- Patakova P, Linhova M, Rychtera M, Paulova L, Melzoch K (2013) Novel and neglected issues of acetone-butanol-ethanol (ABE) fermentation by clostridia: *Clostridium* metabolic diversity, tools for process mapping and continuous fermentation systems. *Biotechnol Adv* 31:58–67
- Qureshi N, Blascheck HP (2005) Butanol production from agricultural biomass. In: Pometto A, Shetty K, Paliyath G, Levin RE (eds) *Food biotechnology*. CRC Press, Boca Raton, pp 525–549
- Qureshi N, Blascheck HP (1999) Production of acetone butanol ethanol (ABE) by a hyper-producing mutant strain of *Clostridium beijerinckii* BA101 and recovery by pervaporation. *Biotechnol Prog* 15:594–602
- Qureshi N, Blascheck H (2000) Butanol production using *Clostridium beijerinckii* BA101 and recovery by pervaporation. *Appl Biochem Biotechnol* 84:225–230
- Qureshi N, Ezeji TC (2008) Butanol, ‘a superior biofuel’ production from agricultural residues (renewable biomass): recent progress in technology. *Biofuels Bioprod Biorefin* 2:319–230
- Qureshi N, Maddox IS, Friedl A (1992) Application of continuous substrate feeding to the ABE fermentation: relief of product inhibition using extraction, perstraction, stripping and pervaporation. *Biotechnol Prog* 8:382–390
- Qureshi N, Saha BC, Hector RE, Hughes SR, Cotta MA (2008a) Butanol production from wheat straw by simultaneous saccharification and fermentation using *Clostridium beijerinckii*: part I—batch fermentation. *Biomass Bioenergy* 32:168–175
- Qureshi N, Ezeji TC, Ebener J, Dien BS, Cotta MA, Blascheck HP (2008b) Butanol production by *Clostridium beijerinckii*. Part I: use of acid and enzyme hydrolyzed corn fiber. *Bioresour Technol* 99:5915–5922

- Qureshi N, Saha BC, Dien B, Hector RE, Cotta MA (2010a) Production of butanol (a biofuel) from agricultural residues: part I—use of barley straw hydrolysate. *Biomass Bioenergy* 34:559–565
- Qureshi N, Saha BC, Hector RE, Dien B, Hughes S, Liu S, Iten L, Bowman MJ, Sarath G, Cotta MA (2010b) Production of butanol (a biofuel) from agricultural residues: part II – use of corn stover and switchgrass hydrolysates. *Biomass Bioenergy* 34:566–571
- Reddy SN, Nanda S, Dalai AK, Kozinski JA (2014) Supercritical water gasification of biomass for hydrogen production. *Int J Hydrog Energy* 39:6912–6926
- Sanderson K (2011) Lignocellulose: a chewy problem. *Nature* 474:S12–S14
- Setlhaku M, Brunberg S, Villa Edel A, Wichmann R (2012) Improvement in the bioreactor specific productivity by coupling continuous reactor with repeated fed-batch reactor for acetone-butanol-ethanol production. *J Biotechnol* 161:147–152
- Shafiei M, Karimi K, Taherzadeh MJ (2011) Techno-economical study of ethanol and biogas from spruce wood by NMMO-pretreatment and rapid fermentation and digestion. *Bioresour Technol* 102:7879–7886
- Shafiei M, Kabir MM, Zilouei H, Sarvari HI, Karimi K (2013) Techno-economical study of biogas production improved by steam explosion pretreatment. *Bioresour Technol* 148:53–60
- Shafiei M, Karimi K, Zilouei H, Taherzadeh MJ (2014) Economic impact of NMMO pretreatment on ethanol and biogas production from pinewood. *Biomed Res Int* 2014:320254
- Shaheen R, Shirley M, Jones D (2000) Comparative fermentation studies of industrial strains belonging to four species of solvent-producing clostridia. *J Mol Microbiol Biotechnol* 2:115–124
- Soni BK, Das K, Ghose TK (1982) Bioconversion of agro-wastes into acetone butanol. *Biotechnol Lett* 4:19–22
- Surisetty VR, Dalai AK, Kozinski J (2011) Alcohols as alternative fuels: an overview. *Appl Catal A Gen* 404:1–11
- Survase SA, Van Heiningen A, Granstrom T (2012) Continuous bio-catalytic conversion of sugar mixture to acetone-butanol-ethanol by immobilized *Clostridium acetobutylicum* DSM 792. *Appl Microbiol Biotechnol* 93:2309–2316
- Szulczyk KR (2010) Which is a better transportation fuel – butanol or ethanol? *Int J Energy Environ* 1:501–512
- Taherzadeh M, Karimi K (2008) Pretreatment of lignocellulosic wastes to improve ethanol and biogas production: a review. *Int J Mol Sci* 9:1621–1651
- Tigunova EA, Shul'ga SM, Blium Ia B (2013) Alternative type of fuel – biobutanol. *Tsitol Genet* 47:51–71
- Tummala SB, Welker NE, Papoutsakis ET (2003) Design of antisense RNA constructs for downregulation of the acetone formation pathway of *Clostridium acetobutylicum*. *J Bacteriol* 185:1923–1934
- United States Energy Information Administration (USEIA) (2011) International energy outlook 2011. [http://www.eia.gov/forecasts/ieo/pdf/0484\(2011\).pdf](http://www.eia.gov/forecasts/ieo/pdf/0484(2011).pdf). Accessed 3 Jan 2012
- Wu YD, Xue C, Chen LJ, Bai FW (2013) Effect of zinc supplementation on acetone -butanol-ethanol fermentation by *Clostridium acetobutylicum*. *J Biotechnol* 165:18–21
- Xue C, Zhao J, Lu C, Yang ST, Bai F, Tang IC (2012) High-titer n-butanol production by *Clostridium acetobutylicum* JB200 in fed-batch fermentation with intermittent gas stripping. *Biotechnol Bioeng* 109:2746–2756
- Xue C, Zhao XQ, Liu CG, Chen LJ, Bai FW (2013) Prospective and development of butanol as an advanced biofuel. *Biotechnol Adv* 31:1575–1584
- Xue C, Zhao JB, Chen LJ, Bai FW, Yang ST, Sun JX (2014) Integrated butanol recovery for an advanced biofuel: current state and prospects. *Appl Microbiol Biotechnol* 98:3463–3474
- Zheng YN, Li LZ, Xian M, Ma YJ, Yang JM, Xu X, He DZ (2009) Problems with the microbial production of butanol. *J Ind Microbiol Biotechnol* 36:1127–1138
- Zverlov VV, Berezina O, Velikodvorskaya GA, Schwartz WH (2006) Bacterial acetone and butanol production by industrial fermentation in the Soviet Union: use of hydrolyzed agricultural waste for biorefinery. *Appl Microbiol Biotechnol* 71:587–597



Current Advancements, Prospects and Challenges in Biomethanation

6

Soumya Nair, Anushree Suresh, and Jayanthi Abraham

Abstract

The underdeveloped state of waste management in developing country like India is a motivation for the study of eco-friendly processes like biomethanation and bioremediation. The current article focuses on bioremediation via methanotrophy by using methanotrophs. The biomethanation process is a multistep process leading to the production of biogas. Anaerobic digestion is a traditional practice used in urban parts of India. Improper management of waste leads to propagation of innumerable ailments. The current status of waste management in India has improved at a much higher rate. The installation of biogas plants across various research institutes in India, like Sardar Patel Renewable Energy Research Institute (SPRERI) in Gujrat, Biogas Plant at Trombay, Appropriate Rural Technology Institute (ARTI) in Pune and Bhabha Atomic Research Centre (BARC) in Mumbai, practice biomethanation in a full-fledged process and yield high rate of biogas fuel from waste materials. The biogas produced is clean, economical and used for commercial purposes.

Keywords

Methanotrophs · *Proteobacteria* · Anaerobic digester · Biomass pretreatment · Biogas

6.1 Introduction

Methane (CH₄) is a well-known and the most copious hydrocarbon present in the atmosphere. It plays an important role in balancing the Earth's radioactivity. The formation of CH₄ gas is natural as well as anthropogenic. It can be removed from the

S. Nair · A. Suresh · J. Abraham (✉)

Microbial Biotechnology Laboratory, School of Biosciences and Technology, VIT University, Vellore, Tamil Nadu, India

e-mail: jayanthi.abraham@gmail.com

aquatic system following its emission to the atmosphere by methane oxidation aided by a certain group of microorganisms. The microorganisms responsible for the methane oxidation are none other than the methanotrophs, which act as a natural bio-sink for atmospheric CH_4 . The microbial methane oxidation is one of the important processes to control the global warming by preventing the escape of the CH_4 gas from the sediments to the atmosphere. Apart from methane-oxidizing bacteria, CH_4 can also be oxidized in the atmosphere photochemically or in the terrestrial and aquatic system by means of biological processes. Microbial oxidation of CH_4 that takes place on the surface of the Earth may exceed the methane oxidation by the free $-\text{OH}$ radicals present in the troposphere (Knittel et al. 2005). Besides, there are reports of methane oxidation occurring in aerobic and microhabitats of wetlands and other aquatic systems, which is close to the site for CH_4 reduction (Knittel and Boetius 2009). The factors controlling microbial methane oxidation have been exemplified in wetlands and rice paddy soils.

Majority of the CH_4 produced from wetland ecosystems is oxidized completely or partially before reaching the atmosphere. CH_4 production would be higher in case it was not consumed by microorganism-mediated oxidation in the oxic layer and around the plant roots. Aerobic methane oxidation is often at its maximum where CH_4 and O_2 coexist (Beal et al. 2009; Semrau et al. 2010). CH_4 oxidation mainly occurs in the areas near to the water table as there is no O_2 supply and CH_4 is limited. Likewise, methane consumption occurs in the oxygenated zone as mentioned earlier. The microorganisms can, therefore, limit the quantity of methane that is released into the atmosphere.

6.2 Methanotrophs

Methanotrophs or methane-oxidizing bacteria are a phylogenetically varied group, which belong to the subset of a physiological group named methylotrophs. These organisms have the capability to take up methane as their sole carbon source for their growth and development. They are Gram-negative prokaryotes in nature. Methanotrophs help in the methane flux regulation from the biosphere to the atmosphere. They play a significant role in the global cycling of carbon (C), nitrogen (N_2) and oxygen (O_2). They also help in the degradation and decomposition of perilous organic matter (Lontoh et al. 2000).

Currently, global warming is a growing concern for the ecosystem and environment. CH_4 is one of the major greenhouse gases responsible for global warming, being the fact that it is a 24 times more effective greenhouse gas when compared to CO_2 (Shukla et al. 2009). Methanotrophs are omnipresent, playing a primary role in maintaining the CH_4 balance in the atmosphere via the carbon and nitrogen cycle. Methanotrophs are a very good model for bioremediation by detoxifying environmental contaminants like hydrocarbons, which are chlorinated. Methane-oxidizing bacteria help in reducing the release of methane gas into the atmosphere from places such as agricultural land, landfills, swamps and marshes as in these places the gas is produced in more volume (Tsubota et al. 2005).

Methanotrophic population in the soil can vary due to the variation in the environmental parameters like temperature, salinity, pH, oxygen content, tides, nitrogen sources and presence of organic matter (Durisch et al. 2005; Dubey 2005; Barcena et al. 2010). These organisms can be both aerobic and anaerobic in nature. They could be rods, cocci or vibrio (Lindner et al. 2007). Despite the differences in their basic requirement and being physiologically and phylogenetically diversified, methanotrophs are associated with the bacterial phylum of α -Proteobacteria and γ -Proteobacteria as well as the Archaea phylum of Euryarchaeota. Their habitat is mostly in environments where methane production is observed such as ocean, mud, marshes, etc.; because of their significant role in universal methane budget, researchers take a special interest in exploring them.

Initially, it was believed that only aerobic methanotrophs could oxidize CH_4 , but reports suggest that CH_4 can also be oxidized anaerobically by the coupled reaction of methanotrophs and other microorganisms like sulphate-reducing bacteria (Ettwig et al. 2010). They deploy the process of manganese, sulphur iron or nitrite reduction, to name a few (Boetius et al. 2000; Michaelis et al. 2002).

Not all methane-oxidizing bacteria can be referred to as methanotrophs as there are organisms that can oxidize methane but do not rely on it as their sole source of energy. This is the basis of the separation of the methane oxidizers into groups, which are as follows:

1. Methane-assimilating bacteria
2. Methanotrophs
3. Autotrophic ammonia-oxidizing bacteria

The methane-oxidizing bacteria are divided into Type I and Type II, bacteria which differ in features like mode of carbon assimilation and the intracellular membrane arrangement. The Type I subgroup is more diverse when compared to Type II, which is found in nature or can be isolated using molecular techniques that are culture cultivation independent. Methane monooxygenase is the enzyme which catalyses the methane oxidation reaction—the conversion of methane to methanol via the production of the intermediate compounds (Hanson and Hanson 1996).

Methane monooxygenase has two forms, namely, particulate methane monooxygenase (pMMO) and soluble methane monooxygenase (sMMO) (Theisen et al. 2010; Op den Camp et al. 2009). Methanotrophs containing pMMO have higher growth abilities and affinity for methane. Under aerobic conditions, the enzyme catalyses the reaction between oxygen and methane to produce formaldehyde, which is later introduced into organic compounds following any one of the two pathways, such as RuMP (ribulose monophosphate) or serine pathway (Trotsenko and Murrell 2008).

Methanotrophs are grouped based on characters, namely, morphology, physiology, intracytoplasmic membrane and the type of resting stage. In spite of the fact that in 1906, the first methanotrophic bacteria was isolated, it was not until Whittenburry and his colleagues had isolated and characterized 100 new methane oxidizers, the basis of the foundation of the current classification of methanotrophs. They proposed

five new genera of methanotrophs based on the nature of the resting stages formed, morphological differences, intracytoplasmic membrane structure and other physiological characteristics. They are *Methylomonas*, *Methylosinus*, *Methylobacter*, *Methyl cystis* and *Methylococcus*. There has been an addition to the list of genera named *Methylomicrobium*. These organisms are classified into two assemblies, especially Type I and Type II methanotrophs. Type I includes the genera *Methylobacter* and *Methylomonas*. Type II methanotrophs include *Methyl cystis* and *Methylosinus* (Dedysh et al. 2000, 2002, 2004, 2005). Recently, group Type X is added to the list, which shares similarity to *Methylococcus capsulatus* that utilizes RuMP as the primary pathway for formaldehyde assimilation. Type X is different from Type I as they have low levels of ribulose biphosphate carboxylase of the serine pathway.

6.3 Bioremediation via Methanotrophy

There are many reports based on the research conducted by scientists on methanotrophs (Trotsenko and Khmelenina 2002; Dalton 2005; Lieberman and Rosenzweig 2005; Dumont and Murrell 2005; Hakemian and Rosenzweig 2007; McDonald et al. 2007; Trotsenko and Murrell 2008; Chowdhury and Dick 2013). From these reports, one can infer the various aspects of methanotrophs such as their ecology, taxonomy, metabolic pathways, their role in methane oxidation in a wetland system, genetic regulations, metabolic activities, biochemistry and kinetics behind oxidation. Surprisingly, there are very few reports focussing on exploiting methanotrophs for their bioremediation potential. Advanced and improved knowledge on the subject could help us to make use of their different applications for an eco-friendly and a sustainable ecosystem. The possible ways to exploit the methanotrophs for degrading the different types of pollutants are mentioned below.

Methanotrophs can be exploited for bioremediation as proposed by Overland et al. (2010) and Jiang et al. (2010). Furthermore, there are reports which suggest that methanotrophs can influence various factors such as the availability of different metals, speciation, reduction in heavy metal toxicity, etc. (Choi et al. 2006). Chromium [Cr (VI)] is a toxic and a soluble metal when compared to its counterpart Cr (III) which is less toxic and insoluble in nature. It is released as a waste product from many industrial processes such as pigment production, tannery, leather industry, etc. (Cheng et al. 1998). Several factors such as mutagenicity, carcinogenicity, teratogenicity and toxicity make Cr (VI) contamination a matter of concern (Chen and Dixon 1998; Shumilla et al. 1999). Cr (III) tends to form a precipitate when subjected to high pH and is poorly absorbed by the body. It is present in nature in trace amounts and mainly in the form of ions in human beings. The process of reduction leads to the conversion of the toxic form of chromium to its less toxic form. Methanotrophs have the potential to perform this transformation reaction. Reports suggest that certain class of methanotrophs such as *Methylococcus capsulatus* (Bath) were able to reduce Cr (VI) to Cr (III) over a broad range of heavy metal concentration. The genomic sequence of the said methanotroph reveals the presence of five genes responsible for chromium ion reductase activity.

Reduction in toxicity of the heavy metal or its transformation to its non-toxic analogue is an important and a crucial aspect which is directly associated with the copper (Cu) atom-carrying molecule (methanobactin) present in the methanotrophs, which is attributed to their noteworthy habitat. It helps in cellular protection from copper toxicity. Oxides of the metals undergo redox cycling in these geochemical areas. Examples of such metal oxides, which precipitate actively due to this type of reaction, are manganese and ferrous oxides (Kim et al. 2004). In order to perform methane oxidation and due to its high reactivity, the methanotrophs require a strong copper defence mechanism. Reports suggest that methanobactin-mediated copper release catalyses the gene expression of pMMO in methanotrophs followed by changing the metal availability in the environment. Hence, it can be inferred that the above mentioned factor could be the reason behind the ecological success and evolution of methanotrophs in heavy metal-polluted areas. This scenario is peculiar when these microorganisms have carrier molecules such as methanobactin, which only allows the selective procurement of the copper metal from the environment while safe guarding the methanotrophs themselves against other potentially toxic heavy metals.

Bioremediation of heavy metals generated as a waste product from many industries such as plating, tannery, paper, etc. is mediated by methanotrophs (Zayed and Terry 2003). De Marco et al. (2004) first studied heavy metal tolerance in these microorganisms. Amongst the 31 strains isolated from the soil, 4 of the strains were able to withstand higher concentrations of an array of heavy metal pollutants. Therefore, these strains were called as superbugs (Cervantes et al. 2001).

6.4 Factors Affecting Methanotrophy

6.4.1 Temperature

Temperature is a significant factor that plays a vital role in biomethanation. Optimum temperature enhances the activity of the microbial system to a greater level. It has been reported that the growth rate of methanotrophs often increases with the rise in temperature, while there is a drastic decrease in the bacterial growth as the environmental temperature approaches the upper limit of the methanotrophs survival. Therefore, it is inferred that the methanotrophs found in the biogas digester tanks may not be able to tolerate a wide range of temperature. Besides influencing the growth rates, temperature also influences other factors such as surface tension and the viscosity of the surrounding medium. The role of temperature in biomethanation is so important that even a slight variation can cause the decrease in its efficiency, making the adaptation tough for the organisms. Different class of methanotrophs adapted to a wide range of environments can help in biomethanation under an array of temperatures, i.e. from 2 to 100°C and above. In a certain report, it was found that at 4% solid content, the amount of methane present was found to be 58% at 20°C, 65% at 35°C and 62% at 55°C. It is also reported that at 8% solid content, the amount of methane present was found to be

57% at 35°C and 59% at 55°C (Bouallagui et al. 2004). A similar experiment was performed, and the reports show that the amount of methane produced was 65.6% at 40°C, 66.2% at 45°C, 67.4% at 50°C and 58.9% at 55°C (Kim et al. 2006). In another set of experiment, it was reported that the co-digestion of the activated sludge along with the food waste had the highest methane gas production at 55°C, which was 1.6 times higher than that produced at 35°C and 1.3 times higher than that produced at 45°C (Gou et al. 2014)

There are two optimal temperature ranges for methanogenesis to take place. They are 30–37 °C (mesophilic range) (Arsova 2010) and 50–67 °C (thermophilic range) (Van Haandel and Lettinga 1994). Biomethanation in the thermophilic range offers a great number of advantages, which have been reported earlier. Some of the notable advantages are listed below:

1. The accelerated metabolic activity of the methanotrophs in the thermophilic range helps in the reduction of the retention time, followed by the increase of the loading rates. This in turn leads to the reduced digester volume.
2. The methane gas production in this range is 1.5 times faster than the mesophilic digestion.
3. Thermophilic digestion has enhanced removal of the pathogenic strains compared to the mesophilic digestion (Buhr and Andrews 1977).
4. Digestion at the thermophilic range also shows higher rate and hydrolysis efficiency.

The weak stability of methanotrophs was usually associated with the thermophilic range of temperature. However, reports show a positive effect of the temperature on the rate of digestion. Biomethanation is also possible in a lower temperature range, such as below 25°C. However, at low temperatures, the metabolic activity is also lowered. Under the psychrophilic conditions, the anaerobic methanotrophs can easily get adapted, and their metabolic rates can be increased by either retaining them in the biomethanation process or by immobilizing them. Reports show that when the mesophilic methanotrophs are subjected to the psychrophilic conditions, the microbial populations are still able to adapt themselves to the temperature without any alteration in the compositions, indicating that the methanotrophs are psychrotolerant rather than being true psychrophilic organisms.

6.4.2 pH

The pH is another principal factor responsible for biomethanation and in the anaerobic digestion. The sensitivity of the anaerobic digester to the varying pH level is mainly due to the presence of the pH-sensitive methanogenic population. However, there are reports of the presence of the acid-tolerant methanogens in peat environment. Few reports suggest that the optimum pH required for the process of biomethanation to take place is between 6.8 and 7.2. This pH range was found to be optimum for utilizing the hydrogen ions by *Methanobacterium ruminantium*

(present in the cattle rumen and the digesters). Lee et al. (2009) suggested that the optimum pH for methanogenesis using the food waste leachate was between 6.4 and 8.2, while there are reports that the optimal pH range is between 5.5 and 8.5. Besides, a very narrow pH range is required for the optimal growth of methanotrophs.

The most common problem seen during the anaerobic digestion is souring. During souring, the volatile fatty acids and CO₂ are produced by the fermentation accumulate. This complex halts CH₄ production since the methanogens have a low tolerance level for the pH variation. Souring usually takes place at a lower pH (less than 5.5). Other reasons for pH variations are the presence of volatile fatty acids, the concentration of bicarbonates and the overall alkalinity of the digester. Maintaining a desirable pH range is possible by the addition of simple buffers or by feeding organic substrate to the anaerobic digester at an optimum environmental condition. Excess loading of the digester or accumulation of the toxic end products can also cause lowering of the pH value along with other issues. Researchers have reported that CH₄ production was affected drastically when the pH of the slurry in the digester was lowered below 5. Along with the pH, the cellulolytic, proteolytic and amylolytic organisms was also reduced. A pH of 7.2 was used to maintain the two-stage laboratory digester, although a different group of researchers preferred a pH of 7.8 (Cohen et al. 1979).

6.4.3 Organic Loading Rate

Organic loading rate is one of the important factors on which the biomethanation process depends. Each digester of a particular dimension has its own optimum rate at which the substrates should be added. Beyond this rate, if the load or the speed is increased, it may affect the biogas production. Continuous stirring of the digester tank content plays a vital role in the biofuel production. This is to ensure maximum substrate-microorganism contact, thereby increasing the substrate's surface area and biogas production. Reports suggest that pretreating the substrate could reduce the organic load without decreasing the methane gas yield. The digester volume (internal volume) is related to the feed rate, hydraulic loading and retention time (Nagao et al. 2012; Agyeman and Tao 2014; Carlsson et al. 2012; Hagen et al. 2014). The thermophilic digester shows the maximum load bearing capacity than the mesophilic digester, whereas the mesophilic system showed higher stability at relatively low loading.

6.4.4 Anaerobiosis

Methanogenesis is a strictly anaerobic process. The presence of a little amount of oxygen becomes toxic to the microorganism, leading to their inhibition followed by death. Even though different classes of methanotrophs carry out the process, there are reports on the presence of facultative and aerobic methanotrophs taking part in methanogenesis. The number of facultative anaerobic bacteria in the waste

digester systems was found to be the same as that of the anaerobic methanotrophs. Studies suggest that these organisms do not have any direct role in the digester system but they may play the role of oxygen radical scavengers, making the digester suitable for the growth of other methanotrophic bacteria. Therefore, it can be concluded that anaerobiosis can play a vital role in minimizing or rather eliminating the diffused air from the digester content.

6.4.5 C:N Ratio

An optimal carbon-to-nitrogen (C:N) ratio in the digester system is another important factor that affects the efficiency of biomethanation (Lee et al. 2009). Usually, the C:N ratio is maintained at around 25–31:1 (Zeshan et al. 2012). This is mainly because the methanotrophs utilize carbon more than that of nitrogen for their metabolic activities. Presence of high amount of nitrogen can also be toxic or rather inhibit the biomethanation process. The ratio should be maintained for enhancing the biogas production. If the C:N ratio is higher than the usual range, the biogas production can be enhanced by the addition of the nitrogen gas (Zhong et al. 2013; Park and Li 2012; Yen and Brune 2007). Similarly, if the C:N ratio is low, the gas production can be easily enhanced following the addition of carbon gas. The C:N ratio can also be maintained by proper mixing of the digester system content. Traditionally, a digester system involves single substrate digestion. However, the recent biomethanation process involves the digestion of more than one substrate to improve the rate of efficiency. Co-digestion of these substrate yields better and improved biogas followed by the prevention of ammonia gas build-up (Wu 2007; Chen et al. 2008). Ammonia gas is produced due to the degradation of nitrogenous compound (e.g. proteins). Co-digestion can be performed with dairy manure as suggested by Ramasamy (1998). Nitrogen is essential for the cellular activity and it acts as a buffer to the digester system by releasing the ammonia gas.

6.4.6 Substrate Composition

Substrate composition also affects biomethanation process. A number of substrates can be used as carbon sources such as lipid, cellulose, protein, etc. The rate of biomethanation depends on the concentration and the nature of the substrate. Biogas production from different organic matter was 0.886 m³/kg for carbohydrates with CH₄ content of 50%, 1.535 m³/kg for fat with CH₄ content of 70% and 0.587 m³/kg for proteins with CH₄ content of 84% (Attila and Valéria 2012).

6.4.7 Sulphate Concentration

Presence of sulphate ion in the anaerobic digester system in high concentration can cause inhibition. This is due to the formation of hydrogen sulphide. Reports

suggest that the presence of hydrogen sulphide in the concentration of 90–300 mg/L leads to severe inhibition of biomethanation process.

6.4.8 Long-Chain Fatty Acids and Volatile Fatty Acids

The presence of long-chain fatty acids (oleate and stearate) in the anaerobic digester has been reported to be toxic to the anaerobiosis process for biomethanation. Methanotrophs do not show any adaptations towards the fatty acid toxicity. However, it is seen that the presence of any particulate matter in the system tends to elevate the resistance towards the long-chain fatty acids as these fatty acids tend to get absorbed on the particulate material. This is not the case as seen in formaldehyde, chloroform or phenols. Reverse toxicity was observed in this system.

Similar mode of action has been observed in the anaerobic process in presence of volatile fatty acids (such as acetic acid). It has been reported that the acetic acid concentration on such systems should not exceed above 3000 mg/L (Taiganides 1980). Studies have been conducted to evaluate the toxicity of volatile fatty acids such as n-valerate, n-butyrate, etc. on *Methanobacterium formicum*, *Methanobacterium bryantii* and *Methanosarcina barkeri*. It was observed that the said volatile acids are more toxic than their isoforms (Hajarnis and Ranade 1994). Similarly, the toxicity of caproic acid and propionate was assessed on *Methanobacterium* sp. and *Methanosarcina* sp. It was observed that a concentration as low as 20 mM of caproic acid and 8 mM of propionate was toxic to inhibit the activity of the abovementioned methanotrophic strains, thereby affecting the rate of biomethanation.

6.4.9 Metals

Methanotrophs utilize carbon and nitrogen for their cellular activities and for the proper cellular functioning. In addition, these strains require micronutrients in lower concentration such as calcium, magnesium, chlorine and potassium, to name a few, for biomethanation. Researchers have evaluated the effect of these micronutrients on the biogas production (Zayed and Winter 2000; Yu et al. 2001; Raposo et al. 2011; Facchin et al. 2013). In one study, the researchers observed that with the addition of metals such as calcium, cobalt, iron, nickel, molybdenum and magnesium in concentration of 5 mM, 50 µg/g total solids, 50 mM, 10 µg/g total solids, 10–20 mM and 7.5 mM, respectively, the biomethanation process was enhanced, when applied individually or in combination of two or more metals (Seenayya et al. 1992). This concludes that with the addition of the metals, the methanotrophic activity increases in the digester system (Seenayya et al. 1992). A similar experiment was conducted to evaluate the effect of nickel on biomethanation. It was observed that at a concentration of 2.5 ppm, the biogas production was enhanced drastically. It was later found that the enzyme involved in anaerobic digestion was nickel dependant (Geetha et al. 1990). In one such report, it was observed that with the addition of cadmium and

nickel (600 $\mu\text{g/g}$ and 400 $\mu\text{g/g}$) to the dry matter, the biogas production increased in the digester system. However, no such effect was observed when manganese or iron was added to the system at a concentration of 1100 $\mu\text{g/g}$ (Jain et al. 1992). In this case, addition of iron in the form of ferrous sulphate at a concentration of 50 mM improved and enhanced bioconversion of poultry waste and dung waste. It was further seen that with the addition of 20 mM of iron, the methanotroph population and rate of biomethanation increased (Preeti and Seenayya 1994). The addition of cobalt also influenced the biomethanation process at a concentration of 0.2 mg/L (Jarvis et al. 1997).

6.5 Biomethanation Process

6.5.1 Substrate Pretreatment

Anaerobic digestion is one of the oldest known methods or technologies for stabilizing the organic waste. Of all the new technologies studied, anaerobic digestion has limited effect on the environment and has a high potential for energy recovery. Anaerobic digester uses microorganisms in the absence of oxygen to convert complex substrates by following four main steps such as hydrolysis, acidogenesis, acetogenesis and methanogenesis. Depending on the characteristics of various substrates, the pretreatment methods also differ. The three commonly used pretreatment methods are mechanical pretreatment, thermal pretreatment and chemical pretreatment.

6.5.1.1 Mechanical Pretreatment

Mechanical pretreatment involves the disintegration and/or grinding of solid particles of the substrate, thereby releasing internal cell compounds and hence increasing the surface area. A better contact between the substrate and anaerobic bacteria, which is due to increase in the surface area, enhances the anaerobic digester process (Carrere et al. 2010). Some of the mechanical pretreatments used are high-pressure homogenizer, maceration, sonication, lysis-centrifuge, liquid shear, collision and liquefaction. All the abovementioned methods are used to reduce the substrate particle size.

For disrupting the cell structure and flux matrix, a vibrating probe is used for sonication process (Elliott and Mahmood 2007). Sound waves of high frequency supplement the formation of radicals such as OH^+ , HO_2^+ and H^+ resulting in oxidation of solid waste substances (Bougrier et al. 2006). A high-pressure homogenizer uses the mechanism of building up the pressure to several hundred bars and then homogenizing the substrates under strong depressurization condition (Mata-Alvarez et al. 2000). These pretreatment methods are used with substrates such as manure, lignocellulosic materials and wastewater treatment plant sludge. Bead mill, electroporation and liquefaction pretreatments have been studied for size reduction process at lab scale, whereas rotary drum, screw press, disc screen shredder and

Table 6.1 Different pretreatment methods to supplement anaerobic digestion using various substrates

Substrates	Pretreatment methods	Inference	References
Organic fraction of municipal solid waste	All pretreatment methods	Physical pretreatments are widely applied for organic fraction of municipal solid waste	Cesaro and Belgiorno (2014)
Lignocellulosic substrates	Thermal, thermochemical, and chemical	Pretreatments improve the digestibility of lignocellulosic substrates	Modenbach and Nokes (2012)
Pulp and paper sludge	Thermal, thermochemical, and chemical	Pretreatments result in low hydraulic retention time, high production of methane and low sludge size	Hendriks and Zeeman (2009)
Wastewater treatment plant sludge	Ultrasound, chemical, thermal, and microwave	Pretreatments result in intensified production of biogas (30–50%)	Elliott and Mahmood (2007)
Wastewater treatment plant sludge	Thermal and thermochemical	Sludge dewaterability can be improved using thermal pretreatment at increased temperature of (>175 °C) as well as thermochemical methods	Carrere et al. (2010)

piston press treatment are successfully applied at a full-scale process. The mechanical pretreatment has advantages such as low odour generation, easy implementation and moderate energy consumption. The disadvantage is that mechanical pretreatment does not completely remove pathogens present in the effluent (Toreci et al. 2009). Different pretreatment methods to supplement anaerobic digestion using various substrates are listed in Table 6.1.

6.5.1.2 Thermal Pretreatment

Thermal pretreatment method is one of the most studied industrial-scale methods (Carrere et al. 2010). The mode of action of pretreatment using thermal is the disintegration of cell membranes, which leads to solubilization of organic compounds (Ferrer et al. 2008). The disadvantage of this process is lack of volatile organic compound and production of potential biomethane from substrates. Hence, it is important to use this method according to the type of substrate and different range of temperature.

1. Pretreatment using thermal process at temperatures below 110°C

Studies have confirmed thermal pretreatment at temperatures below 100°C is unable to degrade complex molecules. However, it induces the deflocculation of macromolecules (Protot et al. 2011). Another study done by Neyens and Baeyens (2003) concluded the pretreatment using thermal methods results in the protein solubilization and removal of particulate carbohydrates.

2. *Pretreatment using thermal process at temperatures higher than 110°C*

In a study conducted by Ma et al. (2011), there was a 24% increase in the production of biomethane at 120°C. Liu et al. (2012) showed that at 175°C, there was a decline from 7.9% to 11.7% in biomethane production due to the formation of melanoidins from the organic substrates. It was observed that with a temperature higher than 120°C, organic wastes are formed into recalcitrant and dark compounds, which eventually resulted in a low yield of biogas production. The colour change of the compound is due to the occurrence of Maillard reaction at high temperatures (Rafique et al. 2010).

6.5.1.3 Chemical Pretreatment

Pretreatment using chemical methods involves organic compound destruction adding alkalis, strong acids or oxidants. Depending on the substrates used and the methods applied, chemical agents vary. Acidic pretreatments and oxidative methods such as ozonation yield an increased production of biogas. Substrates containing high amount of carbohydrates, which are easily biodegradable, cannot be chemically pretreated due to their accelerated degradation of the particulates (Wang et al. 2011).

1. *Alkali pretreatment*

Solvation and saponification are the first reactions that occur during alkali pretreatment which induce the swelling of solids (Carlsson et al. 2012). As a result, there is an increase in the specific surface area and microbes easily degrade the substrates in the absence of oxygen (Hendriks and Zeeman 2009).

2. *Acid pretreatment*

Hydrolysis plays an important role during acid pretreatment as it converts hemicellulose compound to monosaccharides leading to the condensation and precipitation of lignin (Mata-Alvarez 2005). Hence, pretreatment using strong acid is not used. Instead, pretreatment using dilute acids is used in combination with thermal methods.

3. *Ozonation*

Ozonation is another chemical pretreatment method (Carrere et al. 2010), and with no increase in the concentration of salt, fewer residues of chemical remain in comparison with other pretreatment methods using chemicals. This procedure helps in disinfecting the infectious microorganisms (Weemaes et al. 2000) and hence, ozonation is best used for sludge pretreatment. Ozone is known to have maximum oxidizing potential, thereby degrading the substrates into radicals reacting with substrates of organic nature either indirectly or directly. The direct reaction process involves the reactant structure, while the reaction undergoing indirect process depends on the radicals containing the hydroxyl groups.

6.5.2 Digestion: Use of Anaerobic Digester

Biogas is produced depending on the chemical composition and the physical characteristics. It is a combined mixture of (CH_4) and inert carbonic gas (CO_2). However, biogas has a large variety of gases, which are the byproducts of various specific treatment processes of industrial, animal or domestic origin wastes. The presence of H_2S , CO_2 and water makes biogas very corrosive and hence the use of adapted materials is required. Volatile organic compounds are commonly used in industries like flex printing, pulp and paper industry, dairy industry, etc. The byproducts of the effluents from these industries contain volatile organic compounds. One of the generally used treatment methods is loading the volatile organic compounds in an aqueous liquid stream by wet scrubbing and subjecting it to an anaerobic biomethanation process. This provides a methane-rich and combustible gaseous output and a purified liquid stream suitable for recycling.

The biodegradation process using anaerobic materials is composed of organic compounds with the help of anaerobic organisms. Biomethanation process simultaneously takes place when compounds containing organic matter are maintained at $5\text{--}70^\circ\text{C}$. There are primarily four steps in digestion process such as hydrolysis, acidogenesis, acetogenesis and methanogenesis.

The microorganisms produce enzymes hydrolysing the polymeric compounds to simpler monomeric compounds such as glucose, glycerol, amino acids, etc. Simpler compounds formed using the first step are converted into higher molecular weight compounds using acetogenic bacteria. Lastly, methanogenic bacteria convert H_2 , CO_2 and acetate to CH_4 . An outline of the anaerobic digestion process is shown below in Fig. 6.1.

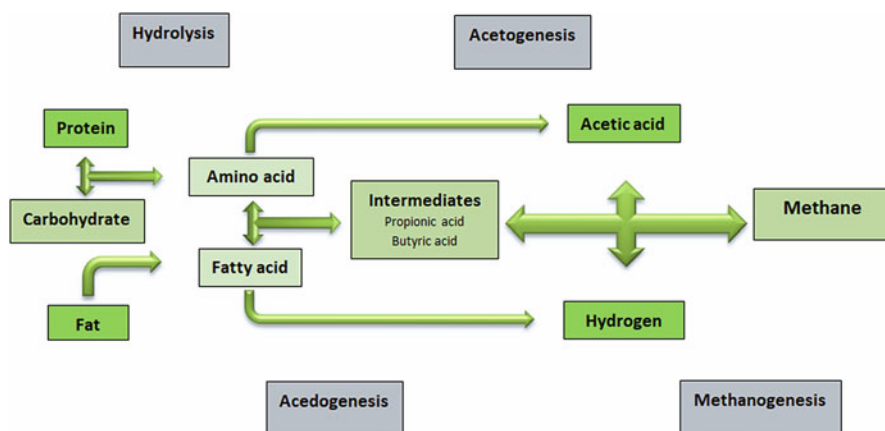


Fig. 6.1 Degradation steps of anaerobic digestion process

6.5.2.1 Hydrolysis

Bacteria growing in anoxic conditions degrade complex molecules into soluble monomer molecules. These complex molecules are catalysed by extracellular enzymes such as cellulase, lipases and proteases.

6.5.2.2 Acidogenesis

Acidogenesis process uses anaerobic microorganisms to decompose organic compounds into simpler low-molecular organic acids. Some of the compounds produced by acidogens from glucose are acetate, lactate, succinate, ethanol, butanol and acetone. Certain polysaccharides are decomposed to monosaccharide sugars, proteins to amino acids and fats to fatty acids and glycerol. Under high hydrogen partial pressure, acetate formation is reduced, and the substrate is converted to propionic acid, butyric acid and ethanol rather than methane. Acidogenic bacteria transform the products of the hydrolysis step into compounds containing short-chain alcohols, volatile acids, hydrogen, carbon dioxide and ketones. The end product of acidogenesis is formic acid (HCOOH), acetic acid (CH_3COOH), propionic acid ($\text{CH}_3\text{CH}_2\text{COOH}$), methanol (CH_3OH), lactic acid ($\text{C}_3\text{H}_6\text{O}_3$), ethanol ($\text{C}_2\text{H}_5\text{OH}$) and butyric acid ($\text{CH}_3\text{CH}_2\text{CH}_2\text{COOH}$). A schematic diagram of anaerobic methane generation from complex organic substances is depicted in Fig. 6.2.

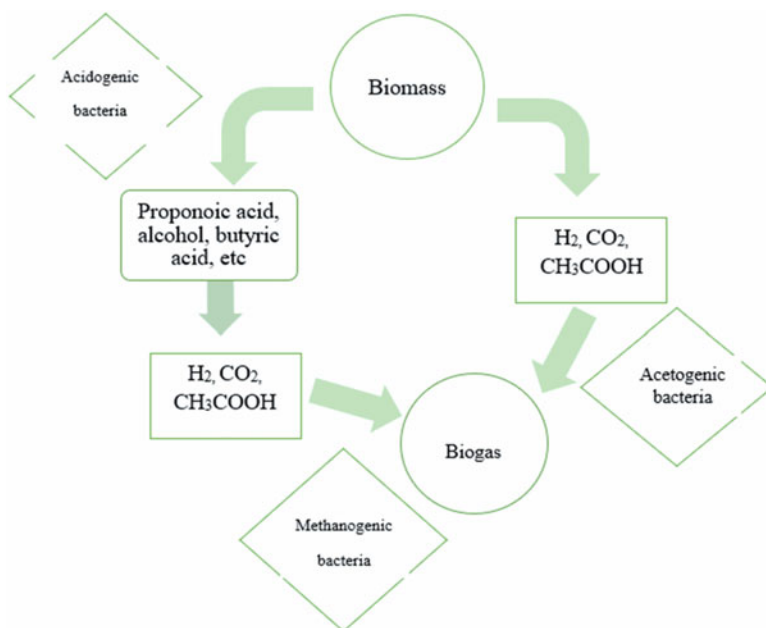


Fig. 6.2 Schematic diagram of anaerobic methane generation from complex organic substances

6.5.2.3 Acetogenesis

In acetogenesis process, the end products like propionic acid, butyric acid and alcohols are converted into simpler compounds such as hydrogen, carbon dioxide and acetic acid by acetogenic bacteria. Hydrogen has a vital role in acetogenesis process.

6.5.2.4 Methanogenesis

Some of the methanogens like *Methanobacter* sp. and *Methanosaeta* sp. are used for methanogenesis process. Methanogens can use hydrogen, formate, acetate, 2-propanol, 2-butanol, methylamine, methanol and methyl mercaptan to produce methane.

6.6 Advantages of Anaerobic Digestion

Anaerobic digestion helps in the reduction of organic load and in the pollution load of the digested sludge. An anaerobic digestion, which is maintained properly, leads to high purification rate. It also has other advantages as summarized below.

6.6.1 Economic Advantages

1. Increase in the demand and alternative use of crop residues and other organic wastes.
2. Revitalizes the rural economy and increases employment opportunities.

6.6.2 Environmental Advantages

1. Biogas production anaerobic digestion process plays a major source of renewable energy and hence can replace fossil fuels.
2. Reduction in pollution levels due to nitrogen stripping.
3. Sustainable management of organic waste.

6.7 Municipal Solid Waste Management: A Scenario in the Indian Subcontinent

India is rapidly growing in population every year and shifting from being an agriculture-driven country to industrialization. About 31.2% population are from urban areas. Population along with metropolitan cities and other urban areas have increased to 100,000 million or even more (Census 2011). India is a divergent geographic and climatic country with four different seasons; hence, the pattern of

food consumption and generation of waste is diverse. Municipal solid waste management plays a critical role in the sustainability of metropolitan and urban cities.

Municipal solid waste in India is approximately 40–60% compostable, 30–50% inert waste and 10–30% recyclable. In India, MSWR [municipal solid waste (handling and treating) rules, 2000] governs the MSWM (municipal solid waste management). Some of the practices followed in India are as follows:

1. Segregation
2. Collection
3. Reuse/recycle
4. Transportation
5. Disposal
 - (a) Open dumping
 - (b) Landfilling
 - (c) Biological treatment of organic waste
 - Aerobic composting
 - Vermicomposting
 - Anaerobic digestion
 - (d) Thermal treatment

6.8 Some Notable Demonstration Scale Biomethanation Plants in India

6.8.1 Biogas Plant in Trombay, Maharashtra

The biogas plant situated at Trombay uses thermophilic microorganisms that flourish in extreme environment in the production of biogas from kitchen waste. It consists of following components such as mixer/pulper (5 HP motor) for grinding the solid waste, predigester tank, premix tanks, main digestion tank (35 m³), a solar heater for water heating and gas lamps for utilizing the biogas generated in the plant.

6.8.2 Bhabha Atomic Research Centre (BARC) in Mumbai, Maharashtra

NISARGRUNA is a biomethanation plant developed by the Nuclear Agriculture and Biotechnology Division of BARC, Mumbai. The main aim of this plant is to process the biodegradable wastes into superior-quality manure. The residual sludge after biomethanation contains increased level of nitrogen content that is used as bio-fertilizer and soil conditioner. This biomethanation plant has higher potential of solving the current waste management issues in the rural areas.

6.8.3 Appropriate Rural Technology Institute (ARTI) in Pune, Maharashtra

The biogas plant in ARTI, Pune, uses simple technology and is eco-friendly. The raw material used for the conversion into biogas is food waste like spoiled grains, leftover grain flour, nonedible seeds, etc. Using waste food as substrate, microorganisms yield a large amount of methane. For example, about 2 kg substrate can produce 500 g of methane in 24 h. Since the process is faster, it can yield higher amount of biogas for commercial purpose. Instalment of ARTI compact biogas is much easier compared to the conventional biogas plants, which occupies about 4 m³.

6.8.4 Sardar Patel Renewable Energy Research Institute (SPRERI) Plant in Anand, Gujarat

Sardar Patel Renewable Energy Research Institute (SPRERI) is located in Gujarat. It is one of the leading organizations for research and development of renewable energy technologies, focusing majorly on sustainable biomass conversion and solar-based solutions, which are eco-friendly, economical and efficient and meet the basic needs of the society. They develop technologies for utilization of bioconversion of wastes. The SPRERI plant was built to process dairy products. The dairy wastes are manually differentiated according to their size and type and later fed into acid reactors. Waste materials containing organic compounds are dissolved in the acid reactors and flushed out into a separate tank. The effluents thus obtained are rich in organic content and pumped into an enclosed anaerobic chamber filter for further decomposition of waste materials. Biogas produced are stored in the top tank of the plant and pressurized into gas holder. This stored biogas can be used for commercial or domestic purpose.

6.9 Conclusions

Population explosion is a major reason behind the increase of the municipal solid waste, which calls for immediate and effective waste management technologies. Anaerobic digester systems are being used globally in order to generate biogas as an alternative source of energy from the municipal solid wastes. It proves to be profitable and cheaper than the existing technologies. Like other energy-generating systems, the use of conventional biogas is not always eco-friendly. Recognizing and troubleshooting the problems associated with biomethanation will definitely help in new improved strategies for biogas production, thereby enhancing the credibility of the technology on a wider scale. The advantages of biomethanation technology are well understood. Solid fuel produces smoke and certain particulates in the atmosphere, leading to various severe respiratory diseases, whereas biogas fuel is a clean and eco-friendly fuel.

Recent studies discuss the production of biogas from the available biomass. Biogas production plays a vital role in energy utilization in the urban and rural parts of India and other developing countries. Optimization of all the factors such as pH, temperature, hydraulic retention time and microbial inoculum helps in increasing the yield of biogas production per unit of biomass. Use of biomethane for cooking and other domestic purposes would decrease the natural resource depletion drastically. The slurry obtained from the anaerobic digesters can also be used as manure to enhance the soil fertility. This would help in increasing the agricultural yield and crop productivity. In other words, these organic manures can replace the chemical fertilizers and lead towards a sustainable agricultural system. However, for a proper functioning of biomethanation technology, there must be proper upgradation of the operations involved in both upstream and downstream processing.

References

- Agyeman FO, Tao W (2014) Anaerobic co-digestion of food waste and dairy manure: effects of food waste particle size and organic loading rate. *J Environ Manag* 133:268–274
- Arsova L (2010) Anaerobic digestion of food waste: current status, problems and an alternative product. M.S. thesis, Columbia University, Berlin, Germany
- Barcena TG, Yde JC, Finster KW (2010) Methane flux and high affinity methanotrophic diversity along the chronosequence of a receding glacier in Greenland. *Ann Glaciol* 51:23–31
- Beal EJ, House CH, Orphan VJ (2009) Manganese- and iron-dependent marine methane oxidation. *Science* 325:184–187
- Boetius A, Ravensschlag K, Schubert C, Rickert D, Widdel F, Gieseke A, Amann R, Jørgensen BB, Witte U, Pfannkuche O (2000) A marine microbial consortium apparently mediating anaerobic oxidation of methane. *Nature* 407:6236–6626
- Bouallagui H, Haouari O, Touhami Y, Ben Cheikh R, Marouani L, Hamdi M (2004) Effect of temperature on the performance of an anaerobic tubular reactor treating fruit and vegetable waste. *Process Biochem* 39:2143–2148
- Bougrier C, Albasi C, Delgenes JP, Carrere H (2006) Effect of ultrasonic, thermal and ozone pretreatments on waste activated sludge solubilization and anaerobic biodegradability. *Chem Eng Process* 45:711–718
- Buhr HO, Andrews JF (1977) The thermophilic anaerobic digestion process. *Water Res* 11:129–143
- Carlsson M, Lagerkvist A, Morgan-Sagastume F (2012) The effects of substrate pre-treatment on anaerobic digestion: a review. *Waste Manag* 32:1634–1650
- Carrere H, Dumas C, Battimelli A, Batsone DJ, Delgenes JP, Steyer JP et al (2010) Pre-treatment methods to improve sludge anaerobic degradability: a review. *J Hazard Mater* 183:1–15
- Census (2011) Provisional population totals, India. Retrieved from <http://censusindia.gov.in/2011provesults/datafiles/india/povpoputotalpresentation2011.pdf>
- Cervantes C, Campos-García J, Devars S, Gutierrez-Corona F, LozaTavera H, Torres-Guzman JC, Moreno-Sanchez R (2001) Interactions of chromium with microorganisms and plants. *FEMS Microbiol Lett* 25:335–347
- Cesaro A, Belgiorno V (2014) Pre-treatment methods to improve anaerobic biodegradability of organic municipal solid waste fractions. *Chem Eng J* 240:24–37
- Chen L, Dixon K (1998) Analysis of repair and mutagenesis of chromium induced DNA damage in yeast mammalian cells and transgenic mice. *Environ Health Perspect* 106:1027–1032

- Chen Y, Cheng JJ, Creamer KS (2008) Inhibition of anaerobic digestion process: a review. *Bioresour Technol* 99:4044–4064
- Cheng YS, Halsey JL, Anderson PD, Remsen CC, Collins MLP (1998) Use of PCR to detect particulate methane monooxygenase in groundwater. In: Abstracts of the 98th general meeting of the American Society for Microbiology. American Society for Microbiology, Washington, DC, p 377
- Choi DW, Do YS, Zea CJ, McEllistrem MT, Lee SW, Semrau JD, Pohl NL, Kisting CJ, Scardino LL, Hartsel SC, Boyd ES, Geesey GG, Riedel TP, Shafe PH, Kranski KA, Tritsch JR, Antholine WE, DiSpirito AA (2006) Spectral and thermodynamic properties of Ag(I), Au(III), Cd(II), Co(II), Fe(III), Hg(II), Mn(II), Ni(II), Pb(II), U(IV), and Zn(II) binding by methanobactin from *Methylosinus trichosporium* OB3b. *J Inorg Biochem* 100:2150–2161
- Chowdhury TR, Dick RP (2013) Ecology of aerobic methanotrophs in controlling methane fluxes from wetlands. *Appl Soil Ecol* 65:8–22
- Cohen A, Zoetemeyer RJ, van Deursen A, van Andel JG (1979) Anaerobic digestion of glucose with separated acid production and methane formation. *Water Res* 13:571–580
- Dalton H (2005) The Leeuwenhoek lecture 2000. The natural and unnatural history of methane-oxidizing bacteria. *Philos Trans R Soc Lond Ser B Biol Sci* 360:1207–1222
- De Marco P, Pacheco CC, Figueiredo AR, Moradas-Ferreira P (2004) Novel pollutant-resistant methylophilic bacteria for use in bioremediation. *FEMS Microbiol Lett* 234:75–80
- Dedysh SN, Liesack W, Khmelenina VN, Suzina NE, Trotsenko YA, Semrau JD, Bares AM (2000) *Methylocella palustris* gen. nov., sp. nov., a new methane-oxidizing acidophilic bacterium from peat bogs, representing a novel subtype of serine-pathway methanotrophs. *Int J Syst Evol Microbiol* 50:955–969
- Dedysh SN, Khmelenina VN, Suzina NE, Trotsenko YA, Semrau JD, Liesack W, Tiedje JM (2002) *Methylocapsa acidiphila* gen. nov., sp. nov., a novel methane-oxidizing and dinitrogen-fixing acidophilic bacterium from Sphagnum bog. *Int J Syst Evol Microbiol* 52:251–261
- Dedysh SN, Berestovskaya YY, Vasylieva LV, Belova SE, Khmelenina VN, Suzina NE, Trotsenko YA, Liesack W, Zavarzin GA (2004) *Methylocella tundrae* sp. nov., a novel methanotrophic bacterium from acidic tundra peatlands. *Int J Syst Evol Microbiol* 54:151–156
- Dedysh SN, Miguez CB, Murrell JC (2005) Regulation of methane oxidation in the facultative methanotroph *Methylocella silvestris* BL2. *Mol Microbiol* 58:682–692
- Dubey SK (2005) Microbial ecology of methane emission in rice agroecosystem: a review. *Appl Ecol Environ Res* 2:1–27
- Dumont MG, Murrell JC (2005) Community-level analysis: key genes of aerobic methane oxidation. In: Leadbetter J (ed) *Methods in enzymology*. SPI, St Louis, pp 413–427
- Durisch-Kaiser E, Klauser L, Wehrli B, Schubert C (2005) Evidence of intense archaeal and bacterial methanotrophic activity in the Black Sea water column. *Appl Environ Microbiol* 71:8099–8106
- Elliott A, Mahmood T (2007) Pretreatment technologies for advancing anaerobic digestion of pulp and paper biotreatment residues. *Water Res* 41:4273–4286
- Ettwig KF, Butler MK, Le Paslier D, Pelletier E, Mangenot S, Kuypers MMM et al (2010) Nitrite-driven anaerobic methane oxidation by oxygenic bacteria. *Nature* 464:543–548
- Facchin V, Cavinato C, Fatone F, Pavan P, Cecchi F, Bolzonella D (2013) Effect of trace element supplementation on the mesophilic anaerobic digestion of foodwaste in batch trials: the influence of inoculum origin. *Biochem Eng J* 70:71–77
- Ferrer I, Ponsa S, Vasquez F, Font X (2008) Increasing biogas production by thermal sludge pretreatment prior to thermophilic anaerobic digestion. *Biochem Eng J* 42:186–192
- Geetha GS, Jagadeesh KS, Reddy TKR (1990) Nickel as an accelerator of biogas production in water hyacinth (*Eichornia crassipes* solms.). *Biomass* 21:157–161
- Gou C, Yang Z, Huang J, Wang H, Xu H, Wang LB (2014) Effects of temperature and organic loading rate on the performance and microbial community of anaerobic co-digestion of waste activated sludge and food waste. *Chemosphere* 105:146–151

- Hagen LH, Vivekanand V, Linjordet R, Pope PB, Eijsink VGH, Horn SJ (2014) Microbial community structure and dynamics during co-digestion of whey permeate and cow manure in continuous stirred tank reactor systems. *Bioresour Technol* 171:350–359
- Hajamis SR, Ranade DR (1994) Inhibition of methanogens by n- and iso-volatile fatty acids. *World J Microbiol Biotechnol* 10:350–351
- Hakemian AS, Rosenzweig AC (2007) The biochemistry of methane oxidation. *Annu Rev Biochem* 76:18.11–18.19
- Hanson RS, Hanson TE (1996) Methanotrophic bacteria. *Microbiol Rev* 60:439–471
- Hendriks ATWM, Zeeman G (2009) Pretreatments to enhance the digestibility of lignocellulosic biomass: a review. *Bioresour Technol* 100:10–18
- Jain SK, Gujral GS, Jha NK, Vasudevan P (1992) Production of biogas from *Azolla pinnata* R Br and *Lemna minor* L.: effects of heavy metal contamination. *Bioresour Technol* 41:273–277
- Jarvis A, Nordberg A, Jarlsvik T, Mathisen B, Svensson BH (1997) Improvement of a grass-clover silage-fed biogas process by the addition of cobalt. *Biomass Bioenergy* 12:453–460
- Jiang H, Chen Y, Jiang P, Zhang C, Smith TJ, Murrell JC, Xing X-H (2010) Methanotrophs: multifunctional bacteria with promising applications in environmental bioengineering. *Biochem Eng J* 49:277–288
- Kim HJ, Graham DW, DiSpirito AA, Alterman MA, Galeva N, Larive CK, Asunskis D, Sherwood PMA (2004) Methanobactin, a copper-acquisition compound from methane-oxidizing bacteria. *Science* 305:1612–1615
- Kim JK, Oh BR, Chun YN, Kim SW (2006) Effects of temperature and hydraulic retention time on anaerobic digestion of food waste. *J Biosci Bioeng* 102:328–332
- Knittel K, Boetius A (2009) Anaerobic oxidation of methane: progress with an unknown process. *Annu Rev Microbiol* 63:311–334
- Knittel K, Lösekann T, Boetius A, Kort R, Amann R (2005) Diversity and distribution of methanotrophic archaea at cold seeps. *Appl Environ Microbiol* 71:467–479
- Lee DH, Behera SK, Kim JW, Park HS (2009) Methane production potential of leachate generated from Korean food waste recycling facilities: a lab-scale study. *Waste Manag* 29:876–882
- Lieberman RL, Rosenzweig AC (2005) Crystal structure of a membrane-bound metalloenzyme that catalyses the biological oxidation of methane. *Nature* 434:177–182
- Lindner AS, Pacheco A, Aldrich HC, Staniec AC, Uz I, Hodson DJ (2007) *Methylocystis hirsuta* sp. nov., a novel methanotroph isolated from a groundwater aquifer. *Int J Syst Evol Microbiol* 57:1891–1900
- Liu X, Wang W, Gao X, Zhou Y, Shen R (2012) Effect of thermal pretreatment on the physical and chemical properties of municipal biomass waste. *Waste Manag* 32:249–255
- Lontoh S, Zahn JA, DiSpirito AA, Semrau JD (2000) Identification of intermediates of in vivo trichloroethylene oxidation by the membrane-associated methane monooxygenase. *FEMS Microbiol Lett* 186:109–113
- Ma J, Duong TH, Smits M, Vestraete W, Carballa M (2011) Enhanced biomethanation of kitchen waste by different pre-treatments. *Bioresour Technol* 102:592–599
- Mata-Alvarez J (2005) Biomethanation of the organic fraction of municipal solid wastes. IWA Publishing, London
- Mata-Alvarez J, Mace S, Llabres P (2000) Anaerobic digestion of organic solid waste. An overview of research achievements and perspectives. *Bioresour Technol* 74:3–16
- McDonald IR, Bodrossy L, Chen Y, Murrell JC (2007) Molecular techniques for the study of aerobic methanotrophs. *Appl Environ Microbiol* 74:1305–1315
- Michaelis W, Seifert R, Nauhaus K, Treude T, Thiel V, Blumenberg M et al (2002) Microbial reefs in the black sea fueled by anaerobic oxidation of methane. *Science* 297:1013–1015
- Modenbach AA, Nokes SE (2012) The use of high-solids loading in biomass pretreatment – a review. *Biotechnol Bioeng* 109:1430–1442
- Nagao N, Tajima N, Kawai M, Niwa C, Kurosawa N, Matsuyama T, Yusoff FM, Toda T (2012) Maximum organic loading rate for the single-stage wet anaerobic digestion of food waste. *Bioresour Technol* 118:210–218

- Neyens E, Baeyens J (2003) A review of thermal sludge pre-treatment processes to improve dewaterability. *Hazard Mater* 98:51–67
- Op den Camp HJM, Islam T, Stott MB, Harhangi HR, Hynes A, Schouten S, Jetten MSM, Birkeland NK, Pol A, Dunfield PF (2009) Environmental, genomic and taxonomic perspectives on methanotrophic *Verrucomicrobia*. *Environ Microbiol Rep* 5:293–306
- Overland M, Tauson AH, Shearer K, Skrede A (2010) Evaluation of methane-utilizing bacteria products as feed ingredients for monogastric animals. *Arch Anim Nutr* 64:171–189
- Park S, Li Y (2012) Evaluation of methane production and macronutrient degradation in the anaerobic co-digestion of algae biomass residue and lipid waste. *Bioresour Technol* 111:42–48
- Preeti, Seenayya G (1994) Improvement of methanogenesis from cow dung and poultry litter waste digesters by addition of iron. *World J Microbiol Biotechnol* 10:211–214
- Protot A, Julien L, Christophe D, Partick L (2011) Sludge disintegration during heat treatment at low temperature: a better understanding of involved mechanisms with a multi-parametric approach. *Biochem Eng J* 54:178–184
- Rafique R, Poulse TG, Nizami A-S, Asam ZZ, Murphy JD, Kiely G (2010) Effect of thermal, chemical and thermo-chemical pretreatments to enhance methane production. *Energy* 35:4556–4561
- Ramasamy K (1998) In: Gupta CL (ed) *Renewable energy – basics and technology*. Auroville Foundation and Solar Agni International, Pondicherry, pp 239–271
- Raposo F, Fernandez-Cegr V, de la Rubia MA et al (2011) Biochemical methane potential (BMP) of solid organic substrates: evaluation of anaerobic biodegradability using data from an international interlaboratory study. *J Chem Technol Biotechnol* 86:1088–1098
- Seenayya G, Rao CV, Shivaraj D, Preeti Rao S, Venkatswamy M (1992) *Biogas production technology: an Indian perspective*. Final report submitted to Department of Non-Conventional Energy Sources, Government of India, New Delhi, p 85
- Semrau JD, DiSpirito AA, Yoon S (2010) Methanotrophs and copper. *FEMS Microbiol Rev* 34:496–531
- Shukla AK, Vishwakarma P, Upadhyay SN, Tripathi AK, Prasana HC, Dubey SK (2009) Biodegradation of trichloroethylene (TCE) by methanotrophic community. *Bioresour Technol* 100:2469–2474
- Shumilla AJ, Broderick JR, Wang Y, Barchowsky A (1999) Chromium Cr(VI) inhibits the transcriptional activity of nuclear factor – B by decreasing the interaction of p65 with c AMP – responsive element – binding protein. *J Biol Chem* 274:36207–36212
- Taiganides EP (1980) Biomass-energy recovery from animal waste part I. *World Anim Rev* 35:2–12
- Theisen AR, Ali MH, Radajewski S, Dumont MG, Dunfield PF, McDonald IR, Hasin AAL, Gurman SJ, Murphy LM, Perry A, Simth TJ, Gardiner PHE (2010) Remediation of chromium (VI) by a methane-oxidizing bacterium. *Environ Sci Technol* 44:400–405
- Toreci I, Kennedy KJ, Droste RL (2009) Evaluation of continuous mesophilic anaerobic sludge digestion after high temperature microwave pretreatment. *Water Res* 43:1273–1284
- Trotsenko YA, Khmelenina VN (2002) Biology of extremophilic and extremotolerant methanotrophs. *Arch Microbiol* 177:123–131
- Trotsenko YA, Murrell JC (2008) Metabolic aspects of aerobic obligate methanotrophy. *Adv Appl Microbiol* 63:183–229
- Tsubota J, Eshinimaev BT, Khmelenina VN, Yuri A, Trotsenko YA (2005) *Methylothermus thermalis* gen. nov., sp. nov., a novel moderately thermophilic obligate methanotroph from a hot spring in Japan. *Int J Syst Evol Microbiol* 55:1877–1884
- Van Haandel AC, Lettinga G (1994) *Anaerobic sewage treatment—a practical guide for regions with a hot climate*. Wiley, New York
- Wang L, Mattsson M, Rundstedt J, Karlsson N (2011) Different pretreatments to enhance biogas production. Master of Science thesis, Halmstad University
- Weemaes M, Grootaerd H, Simens F, Verstaete W (2000) Anaerobic digestion of ozonized biosolids. *Water Res* 34:2330–2336

- Wu W (2007) Anaerobic co-digestion of biomass for methane production: recent research achievements. Iowa State University. Retrieved 20 April 2011 from: home.eng.iastate.edu/~tge/ce421-521/wei.pdf
- Yen HW, Brune DE (2007) Anaerobic co-digestion of algal sludge and waste paper to produce methane. *Bioresour Technol* 98:130–134
- Yu HQ, Tay JH, Fang HHP (2001) The roles of calcium in sludge granulation during UASB reactor start-up. *Water Res* 35:1052–1060
- Zayed AM, Terry N (2003) Chromium in the environment: factors affecting biological remediation. *Plant Soil* 249:139–156
- Zayed G, Winter J (2000) Inhibition of methane production from whey by heavy metals—protective effect of sulphide. *Appl Microbiol Biotechnol* 53:726–731
- Zeshan O, Karthikeyan P, Visvanathan C (2012) Effect of C/N ratio and ammonia-N accumulation in a pilot-scale thermophilic dry anaerobic digester. *Bioresour Technol* 113:294–302
- Zhong W, Chi L, Luo Y, Zhang Z, Wu WM (2013) Enhanced methane production from Taihu Lake blue algae by anaerobic co-digestion with corn straw in continuous feed digesters. *Bioresour Technol* 134:264–270



An Overview of Biomass Gasification

7

Maharshi Thakkar, Pravakar Mohanty, Mitesh Shah,
and Vishal Singh

Abstract

The emission of greenhouse gases in the environment in order to satisfy the demand for electricity and fuel has raised severe climate change issues in various parts of the world. Thus, switching from conventional to renewable power sources has become necessary. Biomass a renewable energy source has the potential of becoming an alternative to the conventional energy sources. Gasification is a thermochemical process that converts waste biomass into a gaseous product known as a syngas and provides environment-friendly waste disposal. Synthesis gas produced through biomass gasification process can be further utilized for power generation or various thermal applications. This chapter discusses various conventional gasification systems existing for biomass gasification along with new technological development. It also delivers an assessment of the impacts of fundamental and interrelating process parameters such as reactor temperature, equivalence ratio, biomass particle size, bed material, etc. on gasification process. Further, a section on various producer gas cleaning technologies to make syngas suitable for power generation applications is also included in this chapter.

Keywords

Gasification · Syngas · Gasifier · Tar · Equivalence ratio · Catalyst

M. Thakkar · M. Shah · V. Singh

Department of Mechanical Engineering, A.D. Patel Institute of Technology, Anand, Gujarat, India

P. Mohanty (✉)

Science and Engineering Research Board, Department of Science and Technology, Government of India, New Delhi, India

e-mail: pravakar.mohanty@gmail.com

© Springer Nature Singapore Pte Ltd. 2018

P. K. Sarangi et al. (eds.), *Recent Advancements in Biofuels and Bioenergy Utilization*, https://doi.org/10.1007/978-981-13-1307-3_7

147

Abbreviations

BFBG	Bubbling fluidized bed gasifier
CFBG	Circulating fluidized bed gasifier
CGE	Cold gas efficiency
CV	Calorific value
ER	Equivalence ratio
FBG	Fluidized bed gasifier
HHV	Higher heating value
LHV	Lower heating vale
S/B	Steam to biomass

7.1 Introduction

Nonconventional energy sources are becoming increasingly important to address the environmental concerns raised due to excessive usages of fossil fuels. In this context, biomass, both plants and waste (agricultural/municipal), represent an abundant and renewable energy resource (Bridgewater 2003). Moreover, biomass, a global energy resource, has been considered to produce a CO₂ neutral effect on the environment, contributing significantly to the objectives of the Kyoto Protocol (Shen et al. 2007). As a result, biomass is accounted as a nonconventional source of energy, which has the calibre of satisfying the energy demands of modern and developing economies all over the globe (Foscolo et al. 2007). Currently, it is estimated that biomass contributes to nearly 14% of the world energy supply (Cui and Grace 2007).

In addition, biomass is characterized by low-energy density, so that many practical applications require that it should be first transformed into a usable form of fuels. Biomass can be converted into gaseous, liquid and solid fuels through thermochemical, biological and physical processes. In particular, there are three main thermochemical processes that can convert biomass into a more useful form of energy: combustion, pyrolysis and gasification. Out of which, biomass gasification process has achieved greatest interest due to the following reasons (Bridgewater 2003):

1. Greater efficiency compared to direct burning and pyrolysis.
2. Hydrogen-rich gas generated through biomass gasification is suitable for thermal as well as power generation applications.
3. In addition, biomass gasification processes can be easily reduced to scale and allow good product distribution control.

However, the impurities in fuel gas present in noncatalytic biomass gasification technology currently make it unsuitable for power generation applications before

cleaning. The condensable heavy tar in the product gas must be reduced before utilizing it for any application in order to make biomass gasification an economically viable option (Sutton et al. 2001).

7.2 Biomass and Its Conversion Technologies

One of the most important biomass fuels is wood, but wood is often too precious to be used for energy production, and the timber industry is able to use trees better by transforming them into building materials. Therefore, residues such as bark, sawdust and odd parts are often used as fuel. In fact, many agricultural wastes can be used as feedstocks. They include wheat straw, rice skins, cornstarch or cotton sticks, sugarcane and manure. In addition to these, dedicated energy crops, such as switchgrass, are used as fuel sources. Biomass gasification will provide environment-friendly disposal of such waste biomass. Biomass also includes a wide range of materials, from plastic to agricultural waste.

Biomass suitable for extracting different forms of fuels can be classified as follows:

- Wastes (food waste, nonfood residues, cattle manure)
- Crop or agricultural residues
- Woody biomass
- Alcoholic fuels (distillers' grains, sugarcane, corn, etc.)

The processes for conversion of biomass into more valuable forms are described in Fig. 7.1.

Combustion is the most common technique of biomass conversion. It involves the direct burning of biomass in order to convert its chemical energy into heat or electrical energy. Combustion processes are still widely used in developing countries for heat or cogeneration production; however, it has low thermal efficiency and higher emission of pollutants in the environment. Pyrolysis and gasification are the most studied conversion processes for advanced applications which give biomass to fuel conversion efficiency of around 75–85%.

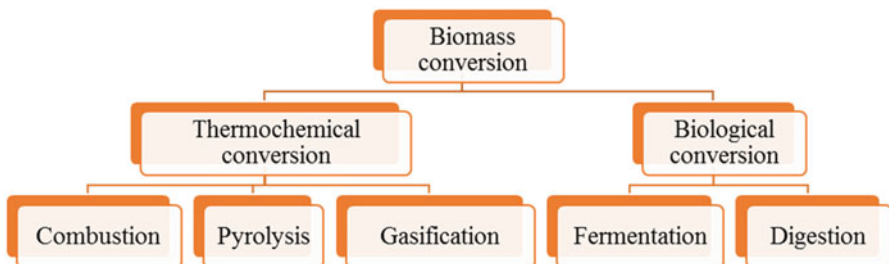


Fig. 7.1 The basic biomass conversion processes

7.3 Biomass Gasification

Gasification is a relatively old technology. Coal gasification was invented in 1792 and was extensively used to produce town gas in the nineteenth century. Gasification refers to a group of processes that converts solid or liquid fuels into a combustible gas with or without contact with a gasification medium (Basu 2006).

Gasification is a thermochemical process. The word (thermochemical) means:

1. The chemical reactions are required for the desirable conversion.
2. The reactions are possible in specific thermal environment.

Gasification of carbonaceous materials (coal and materials of similar characteristics including biomass) is possible through such reactions providing required thermal environment. The gasification reactions produced are useful convenient gaseous fuel (producer gas) or chemical feedstock that can be burned to release energy or used for production of value-added chemicals.

Gasification and combustion are closely related thermochemical processes. But there are important differences between them. Gasification reactions take place in oxygen-deficient environment, and therefore, complete oxidation of feedstock does not take place. Subsequently, energy is embedded into chemical bonds in resultant gas (known as producer gas). On the other hand, in combustion process, the constituents of feedstock are completely oxidized as full supply of oxygen is ensured; as a result, chemical bonds are broken down to release energy during the process itself. The basic processes in gasification are summarized and explained in the following subsections.

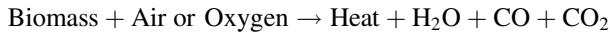
7.3.1 Drying and Pyrolysis

In drying process (<150 °C), the biomass entering the reactor is dried and heated. The moisture in biomass is evaporated during its processing. Pyrolysis is also known as a devolatilization process during which the release of the volatile matter and char would take place. Pyrolysis takes place in the absence of oxygen at temperature around 200–400 °C. Pyrolysis process results in the formation of solids such as char and ash, liquids like tar which is a mixture of heavy hydrocarbons and gases like H₂, CO, CO₂, CH₄ and N₂. A typical pyrolysis reaction is shown by the following equation:



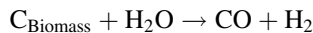
7.3.2 Combustion

Oxidation involves the exothermic reactions during which the release of the heat would take place which is useful for the subsequent endothermic reactions. In the oxidation process, the volatile matters and char released during the pyrolysis process react with the oxygen present in the gasification agent and produce CO_2 and CO . The H_2 that is present in the fuel reacts with the oxygen and produces steam. The reactions which take place during the oxidation are given below. The oxidation reactions can be represented by the following equation:



7.3.3 Gasification

Gasification/reduction reactions occur in oxygen-deficient environment. These reactions are endothermic in nature so it would require heat. The heat released during the oxidation reactions are utilized, which lead towards the reduction in the temperature. The major reactions that will take place during the reduction process are given below:



Water-gas shift reaction: $\text{CO} + \text{H}_2\text{O} \rightarrow \text{CO}_2 + \text{H}_2$

Steam reforming reaction: $\text{CH}_4 + \text{H}_2\text{O} \rightarrow \text{CO} + 3\text{H}_2$

Boudouard reaction: $\text{C}_{\text{Biomass}} + \text{CO}_2 \rightarrow 2\text{CO}$

Methanation reaction: $\text{C}_{\text{Biomass}} + 2\text{H}_2 \rightarrow \text{CH}_4$

7.4 Types of Gasifier

Classification of the gasifier based on the type of bed and gasification medium is given in Fig. 7.2.

The recent development involves plasma gasifiers and entrained bed gasifiers. From the above-mentioned gasification systems, the downdraft and fluidized bed gasifiers or FBGs (i.e. bubbling fluidized bed gasifiers (BFBGs) and circulating fluidized bed gasifiers (CFBGs)) are the most commonly used gasifiers. Approximately 70% of the gasifiers utilized at commercial level are downdraft type, 20–25% is FBGs, 2–3% is updraft type, and 2% is of the remaining types (Warnecke 2000).

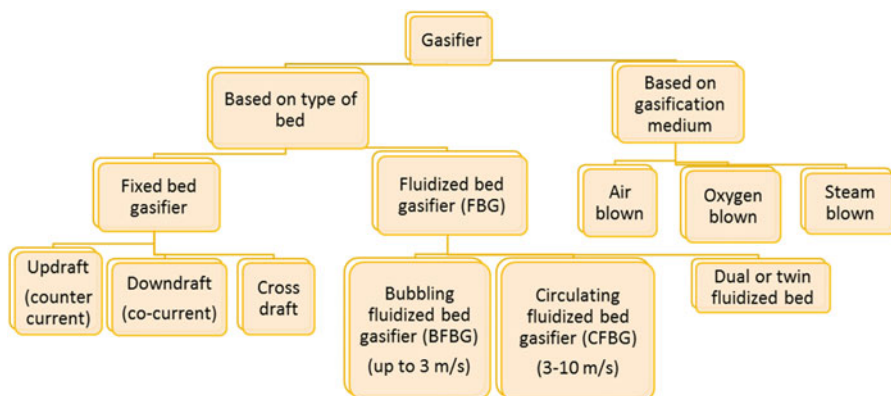


Fig. 7.2 Different types of gasifiers

7.4.1 Updraft Gasifier

It is the oldest and simplest type of gasifier shown in Fig. 7.3. In updraft gasifier, the biomass is supplied from the top of the gasifier where it undergoes drying, pyrolysis, reduction and oxidation. The resultant gas is collected from the top of the gasifier. Updraft gasifier provides higher efficiency as the gas passes through a hot bed of fuel and leaves the gasifier at a lower temperature.

The major drawback of this system is the tar content of the producer gas that leaves the gasifier will be quite high around $10\text{--}150\text{ g/m}^3$. The advantages of this system include high fuel adaptability (sawdust, wood, etc.), higher fuel burning rate, simplicity in construction and lower gas exit temperature. This system is suitable for thermal applications up to 10 MW due to their higher thermal efficiency and ability to handle fuel having higher moisture content (around 50%).

7.4.2 Downdraft Gasifier

Downdraft gasifiers are the upgradation of updraft gasifiers in which the problem of gas leaving with higher tar content is eliminated. In downdraft gasifier biomass and producer gas, both flow in the same direction (Fig. 7.4); therefore it is also known as co-current gasifiers. Air is supplied through the nozzles in the oxidation zone. Downdraft gasifiers are generally operated at around $1000\text{--}1200\text{ }^\circ\text{C}$. Time period required to bring the downdraft gasifier to the working condition is quite less around 10–15 min. Downdraft gasifiers are suitable for thermal as well as for small- to medium-scale power generation applications (up to 1 MW). The problem with the downdraft gasification system is their reservations in fuel adaptability, fuel preprocessing requirements and non-uniform temperature inside the reactor.

Fig. 7.3 Typical schematics of an updraft gasifier

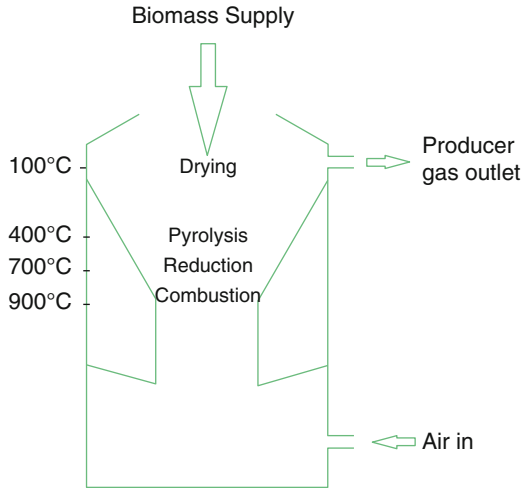
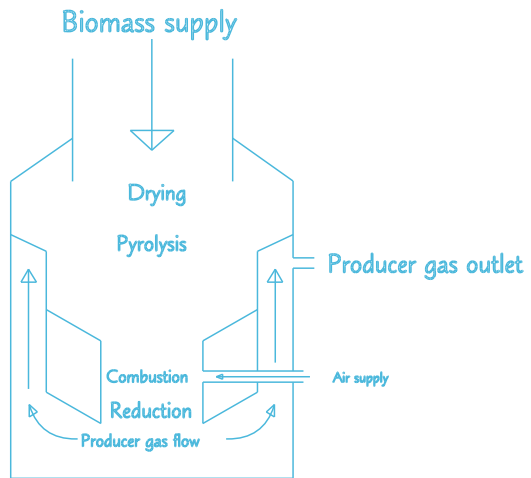


Fig. 7.4 Typical schematics of a downdraft gasifier



7.4.3 Cross-Draft Gasifier

In this system, air is supplied from one side of the gasifier, and producer gas leaves from the other side. The advantage of this system is that it can be built for very small capacity of 10–15 kW shaft power economically. The reason is that the updraft gasifier requires very simple cleaning system comprising only bag filters and cyclone separators along with a small capacity engine. The disadvantages of the system are requirement of good-quality charcoal to produce fuel gas with lower tar content.

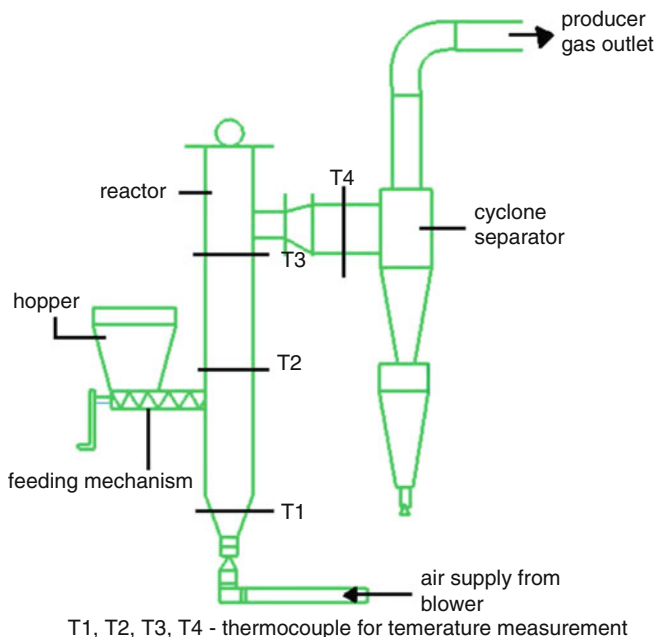


Fig. 7.5 Typical schematics of a bubbling fluidized bed gasifier

7.4.4 Bubbling Fluidized Bed Gasifier

A bubbling fluidized bed gasifier consists of a bed of inert material such as sand. This bed will be fluidized with the help of gasification agent (air, steam, etc.) and kept in the bubbling state as shown in Fig. 7.5. Since the BFBGs are operated just above the minimum fluidization velocities (around 1–3 m/s) of the material, the char and unburned particles carried away by the gas would be less. The advantages of the BFBG are its simplicity in construction, better rate of heat transfer between the fuel and inert materials that improves the carbon conversion efficiency and reduced tar yields during the process and uniform temperature inside the reactor (Couto et al. 2013).

7.4.5 Circulating Fluidized Bed Gasifier

Figure 7.6 shows circulating fluidized bed gasifier. Circulating fluidized bed gasifiers are operated at higher velocities (3–10 m/s); therefore the char and other unburned particles carried away by the gas will be higher. Therefore, in

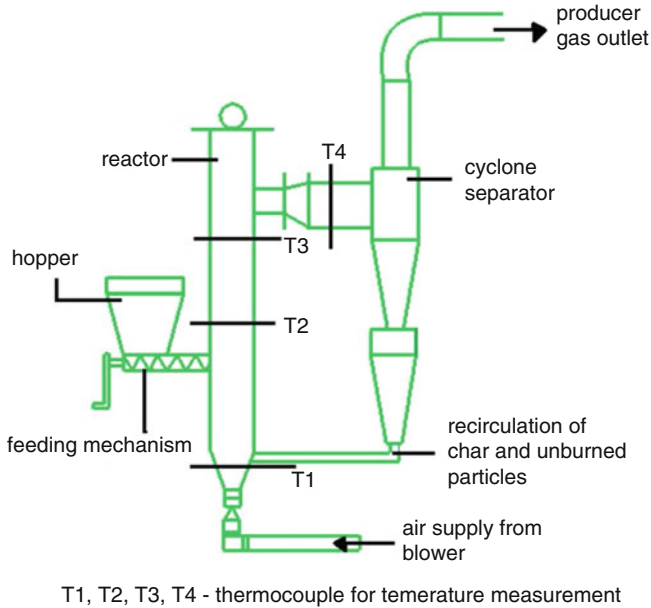


Fig. 7.6 Typical schematics of a circulating fluidized bed gasifier

order to improve the efficiency of the system, the particles are circulated again through the reactor after they were separated by the cyclone.

7.5 Comparison of Basic Characteristics of Different Types of Gasifier

The fuel sensitivity is very good for fluidized bed on a condition that their size is less than 6 mm, whereas in a fixed bed, the size limitation is 25–90 mm. A higher ash content fuel can also be easily used for fluidized bed gasifier, while for fixed-bed ash, the content of fuel should be low (Foscolo et al. 2007). The reaction temperature is slightly lower in the fluidized bed, and fuel mixing is excellent in fluidized bed. Tar and dust content is higher in BFBGs than in fixed-bed gasifiers. However, this is not true in the case of CFBG. The scale-up potentials refer to the ability to increase the output of the gasifier. The higher efficiency in fluidized beds makes them more suitable for scaling up. The starting up of fluidized bed is much easier than fixed bed as the flow of gasifying medium and fuel can be controlled independently. As a result, it also gives a good control facility in fluidized bed gasifiers.

7.6 Effect of Various Operating Parameters on the Gasification Process

The quality and quantity of the resultant gas produced during the gasification process depend upon the operating parameters such as reactor temperature, equivalence ratio (ER), biomass particle size, bed material, bed height, etc. The process parameters' influence on the gas quality and on the performance of gasifier has been discussed in this section which involves the trends of variation in the producer gas quality and gasifier performance with the variation in the operating parameters.

7.6.1 Effect of Reactor Temperature

Reactor temperature plays a significant role during the gasification process as it would affect the gas composition, gas heating value, carbon conversion and tar content in the producer gas. Influence of reactor temperature on the reactions that occurs in the gasifier depends upon the nature of the reaction. Temperature rise increases endothermic reactions rate. Similar to steam reforming, water-gas shift and Boudouard reactions are endothermic, so temperature rise would increase their rate. This also results in an increase in the H₂ content of the producer gas (Lv et al. 2007). The quality of the gas and gasifier performance at low (650 °C) and high (900 °C) reactor temperature is shown in Fig. 7.7. At low temperature, the low heating value (LHV) of the producer gas will be higher because of the higher hydrocarbon content. LHV of the gas reduces with a rise in temperature due to the cracking of hydrocarbons at higher temperatures. Lower reactor temperature will also result in less gas yield and char conversion because of the lower conversion rate of unburned particles into gaseous products at low temperatures.

Karmakar et al. (2013) have investigated the effect of variation in temperature from 650 to 725 °C on a pilot-scale FBG with the rice husk as the feedstock and air as a fluidizing and gasifying media at equivalence ratio (ER) of 0.25. They observed that with the rise in temperature, H₂ content increased from 17.22% to 18.49%, CO content increased from 24.89% to 26.59%, CO₂ content decreased from 14.92% to 12.61% and CH₄ content decreased from 2.62% to 1.96%. Regarding gasifier performance, a rise in reactor temperature improved the carbon conversion

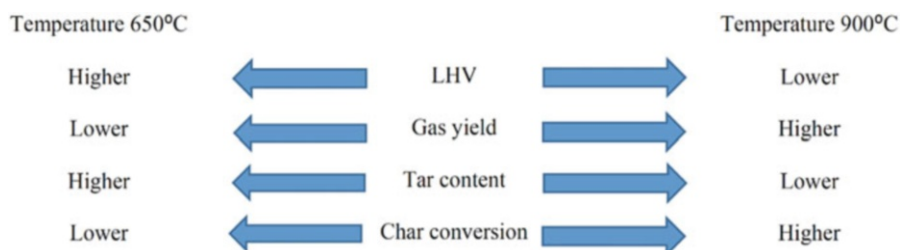


Fig. 7.7 Summary of the effect of reactor temperature on gasification process

efficiency from 71.51% to 75.82% and cold gas efficiency from 48.28% to 54.82%. The improvement in the gasifier performance is because of the increase in the conversion rate of unburned particles and tars into gaseous products at high temperatures.

Subbaiah et al. (2014) have studied the effect of variation in reactor temperature from low (650 °C) to high (850 °C) range on gasifier performance. During the rise in temperature from 650 to 850 °C, the CO₂ and CH₄ content were reduced from 17.3% to 15.6% and 4.92% to 4%, respectively. As the temperature rose, gas yield improved from 2.03 to 2.52 m³/kg of biomass, carbon conversion improved from 79.24% to 82.70%, and cold gas efficiency improved from 60.25% to 65.27%, while LHV of the producer gas decreased from 5.9 to 5.7 MJ/m³. The reduction in LHV at higher reactor temperature is because of the cracking of hydrocarbons like CH₄, tars, etc. Therefore, it is necessary to consider that too high reactor temperature could produce gas with less heating value.

Rapagnaa et al. (2000) have investigated the effect of variation in the temperature from 690 to 810 °C in a catalytic gasification. Olivine was used as a catalyst for tar reduction. They reported that tar content reduced from 2.4 to 0.7 Ng/m³ with the rise in temperature. In case of steam gasification in the trend of variation of CO and CO₂, content of the producer gas was reversed with the increase in reactor temperature compared to air gasification (Lv et al. 2004; Franco et al. 2003). It is due to increase in water-gas shift reaction rate in the presence of steam. Lv et al. (2004) have investigated the effect of variation in temperature in the range of 700–900 °C on gas composition, gas yield, steam decomposition and LHV of the fuel gas for steam gasification. They have observed that with the rise in temperature, H₂ content increased from 20% to 40%, while the CO content decreased from 42% to 32%. Gas yield increased from 1.43 to 2.53 Nm³/kg of biomass as the rise in temperature increased the rate of endothermic reactions. It was also observed that steam decomposition increased from 16.85% to 33.09% due to increase in steam reformation reaction rate with rise in temperature.

Franco et al. (2003) have observed the influence of variation in temperature from 700 to 900 °C in the BFB with the steam as a gasification agent and soft wood as a feedstock. They have observed that with the increase in the temperature, the H₂ content increased from 26% to 33%, while the CO content decreased from 41% to 38%. They found that it was the presence of steam that has increased the rate of water-gas shift reaction which resulted in an increase in H₂ content and decrease in CO content. CO₂ concentration increased with the increase in temperature, and it found maximum at 830 °C (20%). After 830 °C, a slow decrease in the CO₂ content was observed which indicated that at higher temperature, water-gas shift reaction became less active.

Lahijani et al. (2011) have observed the influence of high-temperature gasification (up to 1050 °C). They reported that at higher temperatures (above 800 °C), the bed agglomeration tendency started to increase which caused the operational difficulties. Therefore, it is necessary to consider that too high reactor temperature would reduce the heating value of the producer gas due to cracking of the CH₄ and

other hydrocarbons like tar. It would also cause difficulty during the operation of gasifier due to the formation of bed agglomerates and clinkers.

7.6.2 Effect of Equivalence Ratio

It is another vital parameter during the gasification of the biomass in the FBG as it would control the heat that would be released during the oxidation reactions. ER controls the temperature in the reactor; with the increase in ER, the amount of air delivered in the reactor increases which increases the rate of oxidation reactions due to which the heat release in the gasifier increases which results in a rise of temperature. The minimum value of ER depends upon the minimum temperature of the bed required to be maintained so that the heat released during the oxidation process would be sufficient for the endothermic reactions of gasification and also overcome the heat losses by char and ash. It is observed that at higher values of ER, content of H_2 and CO has reduced, while CO_2 content has increased because of the increase in the rate of oxidation reactions (Kim et al. 2013; Lim and Alimuddin 2008; Mansaray et al. 1999). At higher values of ER, the quality of the producer gas degrades because of the dilution of gas by N_2 which reduces the heating value of the producer gas. Increase in ER results in higher reactor temperature which leads towards the cracking of CH_4 , tar and other hydrocarbons. Summary of the effect of low (0.18) and high (0.45) value of ER on gas quality and gasifier performance is shown in Fig. 7.8. It is necessary to consider that conducting experiments at too high ER would provide the producer gas with low heating value and high N_2 content, and at the same time, too small ER would provide the producer gas with high tar content. Therefore, the results obtained by different researchers for the different ranges of ER are provided in this section to give an idea regarding the suitable range of ER for conducting the experiments.

Karmakar et al. (2013) have led the trial to research the impact of variation in ER with rice husk as a fuel, air as a gasifying medium and reactor temperature of $700\text{ }^\circ\text{C}$. They considered three estimations of ER 0.25, 0.35 and 0.45. They observed that the

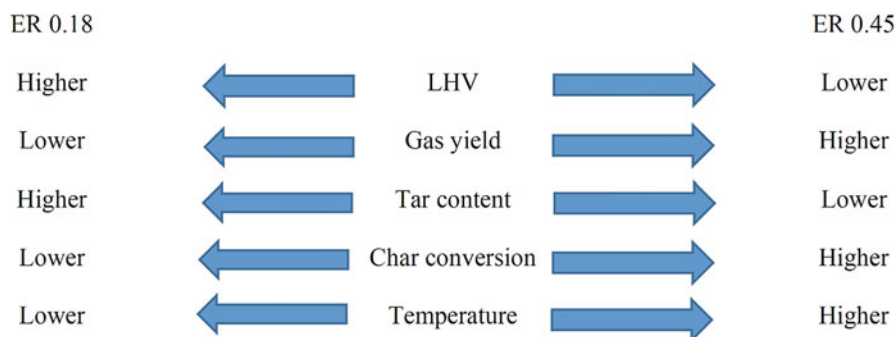


Fig. 7.8 Summary of the effect of ER on gasification process

most noteworthy estimation of H_2 18.12% was obtained when the ER was kept up to 0.25 after which it begins to diminish. The CO content diminished from 25.31% to 15.13% because of increment in air amount. The CO_2 content increased from 13.56% to 21.42% because of the increase in the rate of oxidation reactions with increment in ER. The N_2 content increased from 40.63% to 52.09%, while LHV of the fuel gas diminished at higher ER which was because of the increase in the rate of oxidation reactions and weakening of the fuel gas with N_2 . Carbon conversion efficiency enhanced from 74.07% to 84.17%, and gas yield enhanced from 1.16 to 1.44 m^3/kg of biomass with an increase in ER from 0.25 to 0.35.

Xiao et al. (2007) have examined the impact of increment in ER on bed temperature. They observed that with the rise in ER from 0.2 to 0.45, the bed temperature increased from 703 to 915 °C. Lv et al. (2007) have considered the impact of variation in the ER on the producer gas composition and tar content. They considered two estimations of ER of 0.25 and 0.3. They observed that with the variation in ER, the CO content diminished from 26.06% to 24.89%, while the CO_2 content rose from 26.20% to 27.62%. Likewise, they have explored that with the increase in ER, the tar yield diminished from 19.05 to 13.85 g/kg of biomass.

In another set of investigations, Lv et al. (2004) examined the impact of variation in the ER (0.19–0.27) on gas yield, carbon conversion efficiency and LHV of the fuel gas. They observed that when ER varied from 0.19 to 0.23, the gas yield, LHV and carbon conversion enhanced; however when the ER varied from 0.23 to 0.27, the LHV, gas yield and carbon conversion have demonstrated a diminishing pattern. They detailed the ER equivalent to 0.23 as the ideal esteem. They additionally revealed that H_2 content differed little with the variation of ER, while the CO content diminished, and CO_2 content raised with the increase in ER in light of the fact that with the increment in ER, reactions shifted towards combustion instead of the fractional oxidation of the carbon particles.

Mansaray et al. (1999) have performed tests at the ER of 0.25, 0.30 and 0.35 in rice husk gasification. They have observed that with the increase in ER, the H_2 content diminished from 4% to 3.39%, CO content diminished from 19% to 12.75% and CO_2 content increased from 14.45% to 17.14%. It was observed that the N_2 content was greatest (63.59%) at the most noteworthy ER of 0.35. They have also observed that the CH_4 and C_nH_m content tend to diminish with an increase in ER. They have also reported that the LHV of the producer gas diminished from 5.03 to 3.28 MJ/m^3 with an increase in ER because of the splitting of hydrocarbons.

7.6.3 Effect of Bed Material

Bed material is one of the most important parameters that influence the gasification process especially in case of fluidized bed gasification. Bed material plays a critical role in enhancing H_2 content in the producer gas by promoting tar and steam reforming reactions. In general, sand is utilized as a bed material due to its high heat retention property, inertness, high melting point and high resistance to wear. However, it doesn't contribute towards the decrease in the tar and other impurity

content in the producer gas. In order to enhance the quality of producer gas, catalysts like olivine, dolomite, alumina, etc. are utilized as added substance in the bed or as a bed material. The residence time of the fuel gas inside the reactor is very less; therefore, it becomes difficult to establish chemical equilibrium. This issue can be resolved by using catalysts as a bed material which will improve the rate of reactions.

As per the Sutton et al. (2001), the catalysts having the following properties are suitable as a bed material in the FBG:

1. It should improve rate of steam and tar reforming reactions.
2. It should have higher resistance to wear.
3. Its regeneration should be easy.
4. It should be easily available and cost-effective.

Dolomite ($\text{CaMg}(\text{CO}_3)_2$) is normally used in FBG as a bed material due to its ability to reform tar, cost-effectiveness and availability. A drawback in the utilization of dolomite as a bed material is its poor resistance against attrition at temperatures around 800–850 °C. At this temperature, dolomite becomes fragile, and its particles break down. Rapagna et al. (2000) have reported that this would result in carryover of large bed particles in the fuel gas.

Gil et al. (1999) have examined the impact of utilization of calcined dolomite as a bed material. They have reported that with the utilization of calcined dolomite as a bed material, H_2 substance and CO content were raised from 6 to 12 vol.% and 9–16 vol.%, respectively. The tar content reduced to 1 g/m^3 at ER 0.3. The LHV of the producer gas increased by 1.5 MJ/m^3 because of an increment in H_2 content. Similar trends were reported by Berrueco et al. (2014), in which they have observed that with the utilization of dolomite as bed material, tar decay enhanced which brought about higher gas yield and higher H_2 and CO content in the producer gas.

Lahijani et al. (2011) have explored the impact of the addition of dolomite in the sand. Results have shown that addition of dolomite improved H_2 content in the producer gas from 12% to 17%. They have also examined that at temperature above 850 °C, the bed particles carried away by the producer gas increased. But dolomite has shown better resistance to the bed agglomeration tendency compared with the silica sand as the size of the agglomerates produced was quite small compared with the sand. Olivine, a natural mineral that contains magnesium, iron oxides and silica, is another commonly used catalyst in the FBG. Olivine has a decent mechanical quality and also great protection from the wearing down.

Rapagna et al. (2000) have utilized olivine ($(\text{Mg}^{2+}\text{Fe}^{2+})_2 \text{SiO}_4$) inside FBG as a catalyst. They have reported with the olivine as a bed material and at the steam-to-biomass proportion (S/B proportion) of 1, H_2 and CO_2 content raised from 43% to 52% and from 11% to 16%, respectively, compared to the sand bed. CH_4 content stayed almost the same, which demonstrated that olivine isn't contributed towards methane reforming.

Corella et al. (2004) have compared the performance of two catalysts, namely, olivine and dolomite. They have maintained the ER in the range of 0.36–0.48, and the temperature of the bed was maintained around 820–880 °C. They have reported

that in case of dolomite as a bed material, tar content in the producer gas was around 1.5 g/m^3 , and it was around 2.1 g/m^3 when olivine was used as a bed material. They have reported that the higher content of iron oxides (7-8 wt%) in the olivine compared with the dolomite (0.12 wt%) contributed towards the reduction in the NH_3 content in the producer by more cracking of NH_3 into N_2 and H_2 in case of the olivine compared with the dolomite. They have also investigated the effectiveness of the Ni-olivine catalyst (14.5 wt% Ni-olivine and 85.5 wt% sand). They reported that with the Ni-olivine catalyst, the tar content was around 5 g/m^3 which was quite high compared with the raw olivine and dolomite. This was due to deactivation of it due to deposition of the coke and carbon particles on its active side produced due to the cracking of tar.

Nickel is effective in tar reduction in the producer gas. However, the real problem with Ni and other metal-based catalysts is their deactivation due to the formation of a layer of the carbon particles produced due to the splitting of tars and different hydrocarbons. So as to prevent deactivation of nickel, Rapagnà et al. (2010) impregnated it with magnesium, potassium and calcium oxides.

Miccio et al. (2009) utilized Ni-alumina as a catalyst and compared its performance with the sand bed. They have reported that Ni-alumina bed provided gas with 50% less tar content compared with the sand bed. They have reported that the Ni-alumina catalyst remained stable during the entire experiment lasting about 120 min and it did not show any sign of deactivation due to the deposition of the carbon particles.

Detournay et al. (2011) investigated the effectiveness of bed materials like sand, alumina and Ni-alumina during steam gasification in BFBG. They have observed that when sand is utilized as a bed material, H_2 content was 35%; when alumina is utilized as a bed material, H_2 content was 54%; and when Ni-alumina is utilized as a bed material, H_2 content was 58%. It was observed that with the utilization of the alumina and Ni-alumina as a bed material, the CO content diminished, while CO_2 content marginally increased in the syngas which showed that chemically dynamic bed material improved the water-gas shift reaction rate.

Ergudenler and Ghaly (1993) have researched the agglomeration inclination of alumina. They have observed that at temperatures over 920°C , the agglomeration of alumina bed was very high. The temperature at which alumina demonstrated the tendency of agglomeration (920°C) in the gasifier was very high than the temperature (i.e. 800°C) at which silica sand bed demonstrated the tendency of agglomeration.

Hurley et al. (2012) have formed the bed of limonite iron ore inside FBG. They have compared its performance with olivine at the ER of 0.3–0.4. They have reported that limonite iron ore showed poor resistance to the attrition compared with olivine. At higher temperature, this can be a major obstacle for utilizing it for the high-temperature applications (above 800°C). Sun et al. (2013) have explored the gasification process inside FBG utilizing sand and porous media as a bed material. It was explored that porous media comprising silica gel, zeolite and alumina gave better quality gas in contrast with sand as bed material as they provided a larger surface area which increased overall heat transfer inside the reactor compared with sand bed. In

case of the sand bed, maximum H₂ content was 20% by volume, and in case of porous media as a bed material, it was 36% by volume at 900 °C and S/B 1.56.

The effect of different bed materials on the producer gas composition and tar content is summarized in Table 7.1.

7.6.4 Effect of Gasification Agent

Necessary environment required for the gasification process is maintained by providing the optimal amount of gasifying agent. Gasifying medium also serves the purpose of keeping the bed in the fluidized state in case of fluidized bed gasifiers. Most commonly used gasifying agents are listed below (Alauddin et al. 2010):

1. Air (Calvo et al. 2012; Gil et al. 1999; Karmakar et al. 2013)
2. Steam (Loha et al. 2011a, b)
3. Air + steam (Lv et al. 2007; Subbaiah et al. 2014)
4. Oxygen + steam (Aydar et al. 2014; Gil et al. 1997)
5. O₂-enriched air (Campoy et al. 2008)
6. Gases containing oxygen such as CO₂ (Karatas et al. 2012)

In general most of the fixed-bed gasifiers utilize air as a gasifying medium. Air is most economical and popularly used in many industrial gasifiers. However, utilization of air as a gasifying agent limits the LHV of gas due to dilution of it by N₂. Producer gas generated through air gasification has LHV in the range of 4–7 MJ/m³ (Weerachanchai et al. 2009; Calvo et al. 2012; Couto et al. 2013) and H₂ content around 3–17 vol.% (Parthasarathy and Narayanan 2014). Kim et al. (2013) and Mansaray et al. (1999) have conducted a study on air gasification of woody biomass. They have reported that the producer gas was having H₂ content around 12–15%, CO content around 10–13% and N₂ content around 52–55% and heating value around 4.7–5.7 MJ/m³.

After air, it is the steam gasification process which is becoming popular nowadays due to its ability to generate hydrogen-rich syngas. Dominance of steam reforming and water-gas shift reaction during steam gasification process provides hydrogen-rich syngas. On the other hand, the endothermic nature of these reactions makes steam gasification an energy-intensive process as a continuous supply of external heat is required to maintain the bed temperature. Through steam gasification producer, gas having H₂ content around 45–55% and LHV around 10–12 MJ/m³ can be produced (Karmakar and Datta 2011).

Combination of air and steam as a gasification agent makes gasification process less energy-intensive compared to steam gasification. Air is supplied to the gasifier because of which the oxidation reactions are started after that the steam is introduced inside the reactor. Heat released during the oxidation process is utilized by the subsequent steam reforming and other endothermic reactions. Lv et al. (2004) have used such sort of

Table 7.1 Experimental results for different bed materials

Bed material	Gasification agent	Gas composition (vol.%)					Tar, g/m ³	References
		H ₂	CO	CO ₂	CH ₄			
Sand	Air	7.3–12	11.5–19	16–17.4	2–3.5	–	Lahijani et al. (2011)	
Sand	Steam	43.6	33.2	11.7	11.5	43	Rapagna et al. (2000)	
Dolomite	Air	12–17	16–22	12–15	4–5.2	1	Gil et al. (1999)	
Dolomite	Air	7–8	15–17	17–19	3–4	4	Thakkar et al. (2016)	
Dolomite	Steam	55.5	24	14.1	6.4	0.6	Rapagna et al. (2000)	
Dolomite	Air + steam	22.8	11.7	17.7	4.1	2.5	Miccioa et al. (2009)	
Olivine	Steam	52.2	23	16.9	7.9	2.4	Rapagna et al. (2000)	
Olivine	Air + steam	20.3	13.8	16.9	4.4	2.7	Miccioa et al. (2009)	
Alumina	Steam	54	16	22	6	–	Detournay et al. (2011)	
Ni + alumina	Steam	58	21	17	3	–	Detournay et al. (2011)	
Silica + zeolite + alumina	Air + steam	36.06	28.37	22.15	10.18	–	Sun et al. (2013)	
Fe/olivine	Air + steam	29.6	26.2	29.6	10.2	3.7	Virginie et al. (2012)	
Calcedined limestone	Steam	63.5	4.8	24.7	5.75	1.16	Weerachanchai et al. (2009)	

combination of air and steam as a gasification medium. They have supplied preheated air first and then steam at a temperature of around 160 °C.

Enrichment of air by enhancing its O₂ content and then utilizing it as a gasification agent improves the quality of the fuel gas. O₂-enriched air provides producer gas with the LHV around 8–10 MJ/m³. Campoy et al. (2008) have utilized air having O₂ content around 40 vol.%. It resulted in the reduction in N₂ content in the producer gas which improved the LHV of producer gas from 5 to 9.3 MJ/m³. Sun et al. (2013) have utilized air having O₂ content around 50 vol.%. They have detailed that with the enrichment of air, the H₂ content increased from 12.36% to 20.21%. Another option as a gasification medium is the mixture of steam and oxygen. Gil et al. (1997) have reported that supply of oxygen along with steam provided the heat required for the exothermic reactions which brought down the temperature at which the steam is required to supply. They reported that producer gas had a heating value of around 11–15 MJ/m³. The H₂ content in the producer gas was around 13–29 vol.%.

Karatas et al. (2012) have performed experiments for three different combinations of gasification agent: air + CO₂, air + steam and steam. They have reported that H₂ contents of 48% (maximum), 30% and 22% were found in case of steam, air + CO₂ and air + steam gasification, respectively. In another set of experiments, Gil et al. (1999) have utilized air, steam and mixture of steam+ O₂ as a gasification medium. They have reported that H₂ content was around 8–10%, 53–55% and 25–30% in case of air, steam and steam + O₂ gasification, respectively. The effect of different gasification agents on the producer gas composition is summarized in Table 7.2.

7.6.5 Effect of Steam-to-Biomass Ratio

Steam-to-biomass (S/B) proportion is another vital parameter when steam is utilized in the gasification process. Steam would affect the producer gas composition and heating value based on its supply rate. Steam-to-biomass ratio is defined as a steam supply rate to biomass feed rate. Increase in S/B ratio would raise the H₂ and CO₂ content of the producer gas. On the other side, CO and CH₄ content of the producer gas would be reduced (Loha et al. 2011a; Shen et al. 2008). This is based on the fact that with the increase in S/B ratio, the rate of steam reforming and water-gas shift reactions increases. Despite the fact that the H₂ content increased with the increase in the S/B proportion, in the meantime, the CO₂ content of the producer gas also rose. Keeping in mind the end goal to generate gas having lower CO₂ content, sorbents like calcium oxide (CaO) are included in the bed which will absorb the CO₂ during steam gasification (Udomsirichakorn et al. 2013). It has been observed that rise in S/B ratio would lower the bed temperature due to endothermic nature of steam reforming reactions which results raise in tar content of the producer gas (Pfeifer et al. 2011). Therefore, an optimum range of S/B ratio should be determined (Karmakar and Datta 2011). As too high S/B proportion will increase the organic vapour content of producer gas (Umeki et al. 2010), too low S/B ratio will not provide gas with sufficient H₂ content (Andrés et al. 2011).

Table 7.2 Experimental results for different gasification agents

Biomass	GA	ER or S/B	Gas composition (vol. %)						CV (MJ/m ³)	CGE (%)	References
			H ₂	CO	CO ₂	CH ₄	N ₂				
Wood pallet	Air	0.19–0.27	16.5	16	16.4	5.3	–	5.7	–	Kim et al. (2013)	
Rice straw	Air	0.5	10	18	19	4	46	5.14	52	Calvo et al. (2012)	
Rice husk	Air	0.25–0.45	17–18.5	24–27	12–15	2–3	40	6.5	54	Couto et al. (2013)	
Rice husk	Air	0.25–0.35	3–4	12–20	14–18	2–3	56–64	5	–	Mansaray et al. (1999)	
Rice husk	Steam	1.32	47–53	11–17	24–32	5–10	0	11.09	66	Karmakar and Datta (2011)	
Rice husk	Steam	1.32	50–53	14–18	22–27	4–9	0	13.5	–	Loha et al. (2011b)	
Rice husk	Steam	0.75–2	50–54	14–24	19–27	5–8	0	–	–	Loha et al. (2011a)	
Groundnut shell	Steam + air	0.18	20–21	16–19	15–17	3–5	–	6.1	65.82	Subbarah et al. (2014)	
Pine sawdust	Steam + air	0.22	20–35	35–42	17–20	2–5	–	8.5	–	Lv et al. (2004)	
Pine sawdust	Steam + air	0.25	46–52	11–15	30–33	3–5	–	–	–	Lv et al. (2007)	
Coal	Steam + O ₂	0.21	34.4–36	16–17.5	39–41	8–9	0.4–0.7	8.8–9.2	62	Aydar et al. (2014)	
Waste tire	Air + CO ₂	0.21	30.7	5.4	12.7	15.5	–	9.5	–	Karatas et al. (2012)	
Wood pellets	Air+ O ₂ + steam	–	21–25	28–36	16–18	6–7	–	6–8	64	Yanga et al. (2005)	

GA gasification agent, ER equivalence ratio, S/B steam-to-biomass ratio, CV calorific value, CGE cold gas efficiency

Subbaiah et al. (2014) have explored the impact of variation in S/B proportion from 0 to 1. They have reported that the maximum H₂ content (24.2 vol.%) was obtained at S/B proportion of 0.6. A minimum concentration of CO (17 vol.%) was acquired at S/B proportion of 0.6. The CO₂ content increased from 20% to 23.5% with increment in S/B proportion from 0 to 1. They have considered S/B proportion of 0.6 ideal as it had given highest H₂/CO proportion (1.35). In another study Campoy et al. (2008) has investigated the effect of increase in S/B ratio on bed temperature. It was observed that with the increase in S/B ratio from 0 to 0.45, the bed temperature lowered from 780 to 720 °C. This is due to the increase in the rate of steam reforming reactions with increase in S/B ratio.

7.6.6 Effect of Biomass Particle Size

Biomass particle size is another parameter that would influence the gasification process. As smaller particles of biomass would provide a larger surface area, the heat transfer rates and char burning rate will be higher for the biomass having smaller particle size compared to biomass having a larger particle size (Yanga et al. 2005). It is the biomass particle size that determines the region in which gasification would take place, i.e. in the bed or in the free board area. This is due to the fact that the gasification reactions begin towards the end of the devolatilization procedure. In general, most of the char gasification reactions in case of biomass having larger particle size would take place in the free board region due to lower heat transfer surface area provided by the larger particles of biomass in the bed (Hernández et al. 2010). Lv et al. (2004) have investigated the impacts of variation in particle size of pine sawdust on gas yield, LHV and the carbon conversion in FBG. It was observed that with the increase in biomass, particle size from 0.3 to 0.8 mm LHV of the producer gas decreased from 8.7 to 6.9 MJ/m³, carbon conversion efficiency decrease from 95% to 77% and gas yield diminished from 2.57 to 1.53 m³/kg of biomass.

In order to obtain the producer gas quality of the desired level, it is necessary to provide sufficient residence time. An increase in the residence time allows various reactions such as devolatilization reactions, reforming reactions and cracking reactions to reach towards their completion stage. The residence time of the producer gas inside the gasifier is affected by the velocity or mass flow rate of gasification agent, size of the reactor and length of the free board region. It was investigated that with the increase in the residence time of the producer gas, the product gas with the higher H₂ content and low tar content could be obtained (Detournay et al. 2011; Subramanian et al. 2011).

Hernández et al. (2010) have investigated the effect of the increase in residence time on the quality of producer gas in the gasifier, and they have observed that increase in residence time enhanced the quality of the producer gas by increasing H₂,

CO and CH₄ content and by decreasing the CO₂ content in the producer gas. The cold gas efficiency of the producer gas also increased due to increase in the LHV and the carbon conversion with the increase in residence time. Arena et al. (2009) have investigated the effect of an increase in the gas residence time on tar content, and they observed that with the increase in the gas residence time, the tar residual amount reduced from 12.1 to 6.2 kg/h.

Murakami et al. (2007) have investigated that increasing gas residence time inside the reactor would increase the cold gas efficiency and carbon conversion efficiency as well as H₂ yield. They also made an observation that too longer gas residence time would not provide much improvement in the quality of the producer gas. Chen et al. (2003) have also investigated the effect of increase in the residence time from 1.3 to 10 s on the gas yield by considering the rice straw and sawdust as feed material, and they observed that with the increase in the residence time, the gas yield increased from 35% to 41% for rice straw and 42% to 47% for sawdust, respectively.

7.6.7 Effect of Bed Height

Fuel/inert bed material has the highest temperature zone in any gasification system. The height of the bed would determine the residence time of the reactants and products in the high-temperature dense bed. With the increase in the bed height, the residence time of the products such as gas, tars and char is increased. Increase in the residence time in the high-temperature region could also improve the reforming reactions as well as secondary cracking reactions of tars and other heavy hydrocarbons which would result in less tar and char yields and improve the carbon conversion and gas yields. At the same time, a high bed height could have adverse effects on the producer gas as a higher bed height provides less contact between the gas and solid.

Xiao et al. (2007) have investigated the effect of variation in bed height from 100 to 300 mm, and they reported that with the increase in the bed height from 100 to 300 mm, both the CO and CO₂ contents increased, and they became maximum (20% and 12%, respectively) when the height of bed was around 200 mm. The content of different hydrocarbons which included methane and tar of different classes decreased as the height of bed increased; at the same time, H₂ content slightly increased because of the cracking of the hydrocarbons. By increasing the static bed height, the gas's higher heating value (HHV) decreased steadily from 8.312 to 7.612 MJ/Nm³ due to a decrease in the hydrocarbons content. Additionally, it was investigated that the increase in the bed height reduce the tar content in the producer gas as it would increase the residence time of the gas in the high-temperature bed which enhanced the cracking reactions.

7.7 Cleaning Technologies for Producer Gas

Biomass gasification is a quite efficient and environment-friendly technology, but still the application of the producer gas derived from different gasification systems is limited because of the following impurities in the producer gas, which prevent the successful application of the producer gas in the downstream equipment such as internal combustion engine, gas turbine, fuel cells, etc. (Aravind and Jong 2012):

1. Tar
2. Suspended particles of char, bed material, etc.
3. Sulphur-based acids and gas such as sulfuric acid, e.g. SO_x
4. Ammonia; HCN; nitrogen-based compounds, e.g. NO_x ; etc.
5. Acids like HCl

These impurities would cause the operational difficulties for downstream equipment. For example, the dew point of tar is 500°C , so when the temperature falls below this, it starts condensing which might clog the filters and valves and also cause the corrosion of the metallic parts (Hasler et al. 1998). The particulate matter such as ash, char and bed material can cause the erosion of metallic components, blockage of filters and environmental pollution. Therefore, it is necessary to remove such impurities from the producer gas. The level of impurities in the fuel gas produced by different gasification systems is given in Table 7.3.

Producer gas should have $<100\text{ mg/m}^3$ tar and $<5\text{ mg/m}^3$ of particulate matter content to utilize it for power generation application in an internal combustion engine (Asadullah 2014). For the utilization in gas turbine, the permissible limit of impurities is even lesser, i.e. $<50\text{ mg/m}^3$ of tar. There are basically two methods for the removal of impurities from the producer gas, namely, primary or necessary method and secondary or auxiliary method (Asadullah 2014; Hasler et al. 1998). The primary method involves the removal of the impurities within the gasifier by the application of the catalytically active bed material, using catalytic candle filter in the free board region, or by operating the gasifier at a higher temperature (above 900°C). However, the results have shown that application of only primary method does not provide the gas with desired quality. Therefore, it is necessary to use a secondary method which involves the use of the downstream equipment such as cyclones, water scrubbers, spray tower, filters of different types, catalytic reactor,

Table 7.3 Tar and particulate content in the producer gas generated through different gasification processes (Couto et al. 2013; Asadullah 2014; Hasler et al. 1998)

Gasification system	Tar (mg/m^3)	Particulate matter (mg/m^3)
Downdraft	10–6000	100–8000
Updraft	10,000–1,50,000	100–3000
Bubbling fluidized bed	1500–9000	12,000–16,000
Circulating fluidized bed	2000–30,000	8000–1,20,000

etc. (Aravind and Jong 2012). The syngas filtration system, based on cleaning temperature, is classified as hot gas filtration system and cold gas filtration system.

7.7.1 Hot Gas Filtration Systems

A hot gas filtration system is also referred as a dry gas filtration system which involves removal of impurities from the gas at the higher temperature generally above 200 °C (Aravind and Jong 2012). Hot gas filtration systems are advantageous over the cold gas filtration system as it does not involve the cooling and reheating of the producer gas, which could improve the thermal efficiency. Additionally, the generation of wastewater can be completely eliminated by the application of hot gas filtration systems. In the hot gas filtration system, the tar reduction can be accomplished by two methods that are catalytic cracking and thermal cracking. The particulate removal can be obtained by two types of filters, especially ceramic filter and metallic filter, because of their ability to withstand the high temperatures (Seville et al. 2003).

7.7.1.1 Tar Removal by Catalytic Cracking

Catalytic cracking is the most effective method for tar reduction which can provide tar reduction up to 95% (Asadullah 2014). There are three ways to reduce the tar concentration in the producer gas with the help of catalytic cracking (Asadullah 2014; Hasler et al. 1998):

1. In-bed use of the catalysts such as dolomite, olivine, Ni-based catalysts, etc.
2. Use of the catalytic reactor in the downstream side
3. Use of the catalytic candle filter in the free board region of gasifier

Catalytic cracking by the in-bed use of catalysts has been discussed in the previous section. Catalytic cracking of producer gas with the help of catalytic reactor involves the use of hot gas filter for the particulate removal and secondary reactor which consists the bed of catalysts. The producer gas that leaves the gasifier first passes through the particulate removal filter, which is maintained at a temperature above 400 °C in order to prevent the condensation of the tar. Further, it passes through the catalytic guard bed of natural catalyst such as dolomite to improve the life of metal-based catalyst used in the catalytic reactor. Finally, it passes through the catalytic reactor, which acts as a steam reformer, and water-gas shift reactor, whose performance could be improved by providing the supply of steam.

Such kind of an arrangement for the producer gas cleaning has been employed by Zhang et al. (2004) where the producer gas leaving the gasifier was passed through the particulate removal filter maintained at 450 °C. The gas then passed through a catalytic guard bed consisting of dolomite to remove the fine particles as well as reform the heavy tars. The lifetime of the metal-based catalyst used in the catalytic

reactor could be improved. The gas then passed through the catalytic reactor which consists of Ni-based catalysts with additives like potassium, calcium and magnesium oxides to prevent deposition of coke on the active side of Ni-catalyst. The results have shown that the tar reduction up to 99% can be obtained, and the H₂ content in the producer gas can be increased by 6–12% with such kind of arrangements.

Huang et al. (2012) have used 7Ni-2Cu/Al₂O₃ catalyst in the catalytic reactor, and they have reported that not only the H₂ yield increased but the air contaminants such as 1,3-cyclopentadiene, benzene, toluene, etc. which are produced during the process of gasification were also decreased when the producer gas passed through this secondary reactor, which provided the conversion rates ranging from 23% to 99%.

Another way to reduce the tar in producer gas is by using catalytic candle filter in the free board region of the gasifier. This method helps to perform both the operation of particulate removal and tar reduction in a single step which simplifies the process and reduces the cost. Catalytic candle filter can be produced by integrating a catalyst in the ceramic filter candle. Heidenreich et al. (2008) have employed silicon carbide as a ceramic filter material and TiO₂-V₂O₅-WO₃ as a catalyst which was integrated into the inner structure of the support body of the filter element and provided fine-filtering membrane on the outer side of the filter element which prevented the deactivation of the catalyst.

They reported that the filter not only reduced the particulate matter and tar, but also the poisonous gases like SO_x and NO_x were reduced efficiently. Rapagna et al. (2010) have also used catalytic candle filter in the free board of fluidized bed gasifier. They employed Ni-based catalyst which was impregnated with MgO. Results have shown that the filter worked satisfactorily for 22 h. Increase in the H₂ yield by 30% and increase in the gas yield by 60% with the corresponding decrease in the methane and tar content of 20% and 79% were obtained, respectively.

7.7.1.2 Tar Removal by Thermal Cracking

Thermal cracking is the process in which the large heavy organic compounds reduced to light noncondensable gases such as H₂, CO, etc. at higher temperatures. Amount of tar reduction and the residence time of the gas at higher temperature depend upon the value of temperature employed. The higher temperature could provide more tar reduction and require less residence time of gas compared to lower temperature. Qin et al. (2007) have tried to reduce tar by increasing the temperature from 700 to 900 °C inside the gasifier, and they observed that maximum amount of heavy tar cracked at 900 °C. Phuphuakrat et al. (2010) have performed thermal cracking of the tar at 800 °C in a reactor which was employed in the downstream side in which air and steam were supplied to perform the reforming reactions. It was observed that 78% reduction in the tar was obtained at 800 °C. Brandt (2000) developed a reactor of pure Al₂O₃ in which the producer gas from updraft gasifier heated at 1200, 1250 and 1290 °C with the residence time of 0.5 s at these temperatures. It was observed that tar content as low as 15 mg/m³ was obtained at 1290 °C.

7.7.2 Cold Gas Filtration System

A cold gas filtration system is a well-established method that can remove the impurities from the producer gas up to desired levels. This method involves two processes, i.e. cooling and cleaning. Since in most of the applications of the producer gas it is required to supply at the ambient temperature, the cooling of the producer becomes necessary. Cooling of the gas might take place before the cleaning, or both the cooling and cleaning might take place simultaneously.

The equipment involved in this method includes cyclone separator, wet scrubbers, spray tower, tar condensers, electrostatic precipitator and filters of different types such as sand bed filter, fabric filter, charcoal filter, bag filter, etc. In the cold gas filtration system, the producer gas that leaves the gasifier passes through the cyclone separator, which can remove up to 90% of the particulate matter larger than an approximately 5 μm diameter (Aravind and Jong 2012). Then the producer gas can pass through the cooling system which consists of a wet scrubber, spray tower and tar condensers. As the producer gas passes through the wet scrubber or tar condensers, the simultaneous process of cooling and removal of the particulates, tars and other impurities such as NH_3 , HCl , etc. takes place which are soluble in water. The effectiveness of the wet scrubber depends upon the residence time of the producer gas in the wet scrubber. Furthermore, the producer gas passes through the different types of filters in order to reduce the impurities up to the desired level.

Such kind of cold gas filtration system for producer gas cleaning was used by Pathak et al. (2007). They have employed spray tower for the cooling of producer gas and sand-based filter for cleaning of the producer gas. It was observed that tar and particulate reduction efficiency in the range of 83–97% was obtained. In another set of experiment, Bhave et al. (2008) employed a wet packed bed scrubber-based producer gas cooling and cleaning system. The hot gas is supplied from the bottom and water supplied from the top of the wet packed bed scrubber, where the wet packed bed scrubber behaved as counterflow direct contact heat exchanger. It was observed that tar and water vapour in the producer gas were condensed in the wet scrubber and some portion of tar and particulates removed and washed away with the water. It was reported that tar and dust content were reduced up to 150 mg/m^3 . Han and Kim (2008) have reported tar reduction up to 90% by using venturi scrubbers and particulate reduction up to 99% by using electrostatic precipitator.

In another study, Henriksen et al. (2006) passed the producer that came out from the gasifier first through the cyclone and then through the heat exchanger for reducing the temperature of the gas in which the gas cooled down just above the water dew point, and then it supplied in the bag filter after which it passed through the cartridge filter which acted as a polish filter. Then the gas further cooled down to 50 $^\circ\text{C}$ and condensate removed from the gas, last to ensure that the droplets produced during the condensation were removed from the gas passed through another cartridge filter which behaved as a demister. The entire flow of the gas through the cooling and cleaning system was driven by a roots blower. They operated the gas engine using those gases, and it worked satisfactorily, and no deposits were seen in the engine.

7.8 Recent Developments in the Field of Biomass Gasification

Recent developments in the field of biomass gasification include entrained bed reactors and plasma reactors for the gasification process.

7.8.1 Entrained Flow Reactor

Entrained flow reactors are suitable for the gasification of fine fuel particles (0.1–1 mm particles). The gasifier operates at high temperature around 1000–1500 °C and pressures around 20–30 bar (Molino et al. 2015). Usually pretreatment of biomass is required to reduce the bulk density and moisture content, when biomass fine particles are used as feedstock. Using biomass powder as fuel during entrained flow gasification may give an extra cost due to its low bulk density, which might be reduced by an initial torrefaction process. The advantages and disadvantages of the entrained flow reactors are given below (Molino et al. 2015):

Advantages:

1. Higher fuel adaptability
2. Uniform reactor temperature
3. No problem of scale deposition
4. Low tar content in producer gas
5. Higher carbon conversion

Disadvantages:

1. Requires higher flow rate of gasification medium.
2. Heat recovery is required to improve efficiency.
3. Lower cold gas efficiency.
4. Fuel pretreatment is required.
5. Higher maintenance cost.

7.8.2 Plasma Reactor

The plasma gasification process involves an atomic degradation of the biomass in the presence of a gasification agent. Plasma an ionized gas stream at high temperature obtained through an electric discharge provides the rise in temperature necessary for the reactions that make up the gasification process, while in the absence of a gasification agent, the plasma process is similar to the pyrolysis at higher temperature. The advantages and disadvantages of the plasma reactors are given below (Molino et al. 2015):

Advantages:

1. Lower flow rate of syngas inside reactor provides greater residence time.
2. Low content of CO₂, SO₂ and other polluting compounds in syngas.

3. Extremely short reaction times.
4. No problem of scale deposition.

Disadvantages:

1. It is an intermediate process.
2. Requires an auxiliary fuel to maintain uniform temperature.
3. Safety-related issues.
4. Short life of refractories.
5. Higher capital and operation cost.

7.9 Conclusions

Biomass is one of the largest sources of energy in the world that has a great potential in solving the current problem that the world is facing, such as pollution-free energy generation. Biomass gasification is a highly efficient process to extract the energy from biomass. In this chapter, different types of gasification systems, effect of different operating parameters on producer gas quality and gasifier performance along with different arrangements for producer gas cooling and cleaning have been discussed. The following important conclusions were drawn:

- Downdraft gasifiers are the most widely used gasification system for thermal and power generation applications. However, the drawbacks of these systems are their limitation in adaptability of wide variety of fuels and requirement of preprocessing of fuels. Fluidized bed gasifiers are suitable for fuels with higher ash content, i.e. agricultural wastes, because of their lower operating temperature requirement.
- The major roadblock in utilization of biomass gasification systems at commercial level for power generation application is the high level of impurities present in the producer gas. Therefore, the use of different cooling and cleaning systems is necessary. This makes the gasification plant more complex and increases the capital investment. Cold gas and hot gas filtration systems are the most commonly used producer gas cleaning systems. At present, these cleaning systems have certain issues which required to be addressed. The cold gas filtration system is well established and can provide the producer gas with desirable quality but generates a lot of wastewater, which further requires to be treated before disposal. On the other side, the hot gas filtration systems do not require any water supply, but their operation and built-up cost is relatively higher.
- Recent developments in the field of biomass gasification systems like plasma gasifiers, entrained flow gasifiers, etc. which produce syngas with a very low tar content indicate that days are not far before this technology will play a dominant role in the power generation at a commercial level.

References

- Alauddin ZABZ, Lahijani P, Mohammadi M, Mohamed AR (2010) Gasification of lignocellulosic biomass in fluidized beds for renewable energy development: a review. *Renew Sust Energy Rev* 14:2852–2862
- Andrés JM, Narros A, Rodríguez ME (2011) Behaviour of dolomite, olivine and alumina as primary catalysts in air-steam gasification of sewage sludge. *Fuel* 90:521–527
- Aravind PV, Jong W (2012) Evaluation of high temperature gas cleaning options for biomass gasification product gas for solid oxide fuel cells. *Prog Energy Combust Sci* 38:737–764
- Arena U, Zaccariello L, Mastellone ML (2009) Tar removal during the fluidized bed gasification of plastic waste. *Waste Manag* 29:783–791
- Asadullah M (2014) Biomass gasification gas cleaning for downstream applications: a comparative critical review. *Renew Sust Energy Rev* 40:118–132
- Aydar E, Gul S, Unlu N, Akgun F, Livatyali H (2014) Effect of the type of gasifying agent on gas composition in a bubbling fluidized bed reactor. *J Energy Inst* 87:35–42
- Basu P (2006) *Combustion and gasification in fluidized bed*. Taylor & Francis Group LLC, Boca Raton
- Berruoco C, Montané D, Güell BM, Alamo G (2014) Effect of temperature and dolomite on tar formation during gasification of torrefied biomass in a pressurized fluidized bed. *Energy* 66:849–859
- Bhave AG, Vyas DK, Patel JB (2008) A wet packed bed scrubber-based producer gas cooling–cleaning system. *Renew Energy* 33:1716–1720
- Brandt P (2000) High tar reduction in a two-stage gasifier. *Energy Fuel* 14:816–819
- Bridgewater AV (2003) Renewable fuels and chemicals by thermal processing of biomass. *Chem Eng* 91:87–102
- Calvo LF, Gil MV, Otero M, Morán A, García AI (2012) Gasification of rice straw in a fluidized-bed gasifier for syngas application in close-coupled boiler-gasifier systems. *Bioresour Technol* 109:206–214
- Campoy M, Gómez-Barea A, Villanueva AL, Ollero P (2008) Air-steam gasification of biomass in a fluidized bed under simulated autothermal and adiabatic conditions. *Ind Eng Chem Res* 47:5957–5965
- Chen G, Andries J, Luo Z, Spliethoff H (2003) Biomass pyrolysis/gasification for product gas production: the overall investigation of parametric effects. *Energy Convers Manag* 44:1875–1884
- Corella J, Toledo JM, Padilla R (2004) Olivine or dolomite as in-bed additive in biomass gasification with air in a fluidized bed: which is better? *Energy Fuel* 18:713–720
- Couto N, Rouboaa A, Silvaa V, Monteiro E, Bouziane K (2013) Influence of the biomass gasification processes on the final composition of syngas. *Energy Procedia* 36:596–606
- Cui H, Grace JR (2007) Fluidization of biomass particles: a review of experimental multiphase flow aspects. *Chem Eng Sci* 67:45–55
- Detournay M, Hemati M, Andreux R (2011) Biomass steam gasification in fluidized bed of inert or catalytic particles: comparison between experimental results and thermodynamic equilibrium predictions. *Powder Technol* 208:558–567
- Ergudenler A, Ghaly AE (1993) Agglomeration of alumina sand in a fluidized bed straw gasifier at elevated temperatures. *Bioresour Technol* 43:259–268
- Foscolo P, Germana A, Jand N, Rapagnà S (2007) Design and cold model testing of a biomass gasifier consisting of two interconnected fluidized beds. *Powder Technol* 173:179–188
- Franco C, Pinto F, Gulyurtlu I, Cabrita I (2003) The study of reactions influencing the biomass steam gasification process. *Fuel* 82:835–842
- Gil J, Aznar MP, Caballero MA, Frances E, Corella J (1997) Biomass gasification in fluidized bed at pilot scale with steam-oxygen mixtures. Product distribution for very different operating conditions. *Energy Fuel* 11:1109–1118

- Gil J, Corella J, Aznara MP, Caballero MA (1999) Biomass gasification in atmospheric and bubbling fluidized bed: effect of the type of gasifying agent on the product distribution. *Biomass Bioenergy* 17:389–403
- Han J, Kim H (2008) The reduction and control technology of tar during biomass gasification/pyrolysis: an overview. *Renew Sust Energ Rev* 12:397–416
- Hasler P, Buehler R., Nussbaumer T (1998) Evaluation of gas cleaning technologies for biomass gasification. Biomass for energy and industry, 10th European conference and technology exhibition, June 8–11 Wurzburg, Germany
- Heidenreich S, Nacken M, Hackel M, Schaub G (2008) Catalytic filter elements for combined particle separation and nitrogen oxides removal from gas streams. *Powder Technol* 180:86–90
- Henriksen U, Ahrenfeldt J, Jensen TK, Gøbel B, Bentzen JD, Hindsgaul C, Sørensen LH (2006) The design, construction and operation of a 75 Kw two-stage gasifier. *Energy* 31:1542–1553
- Hernández JJ, Aranda-Almansa G, Bula A (2010) Gasification of biomass wastes in an entrained flow gasifier: effect of the particle size and the residence time. *Fuel Process Technol* 91:681–692
- Huang B, Chen H, Kuo J, Chang C, Wey M (2012) Catalytic upgrading of syngas from fluidized bed air gasification of sawdust. *Bioresour Technol* 110:670–675
- Hurley S, Xu CC, Preto F, Shao Y, Li H, Wang J, Tourigny G (2012) Catalytic gasification of woody biomass in an air-blown fluidized-bed reactor using Canadian limonite iron ore as the bed material. *Fuel* 91:170–176
- Karatas H, Olgun H, Akgun F (2012) Experimental results of gasification of waste tire with air & CO₂, air & steam and steam in a bubbling fluidized bed gasifier. *Fuel Process Technol* 102:166–174
- Karmakar MK, Datta AB (2011) Generation of hydrogen rich gas through fluidized bed gasification of biomass. *Bioresour Technol* 102:1907–1913
- Karmakar MK, Mandal J, Haldar S, Chatterjee PK (2013) Investigation of fuel gas generation in a pilot scale fluidized bed auto-thermal gasifier using rice husk. *Fuel* 111:584–591
- Kim YD, Yang CW, Kim BJ, Kim KS, Lee JW, Moon JH, Yang W, Yu TU, Lee UD (2013) Air-blown gasification of woody biomass in a bubbling fluidized bed gasifier. *Appl Energy* 112:414–420
- Lahijani P, Najafpour GD, Zainal ZA, Mohammadi M (2011) Air gasification of palm empty fruit bunch in a fluidized bed gasifier using various bed materials. *World Renewable Energy Congress*, Linköping
- Lim MT, Alimuddin Z (2008) Bubbling fluidized bed biomass gasification – performance, process findings and energy analysis. *Renew Energy* 33:2339–2343
- Loha C, Chatterjee PK, Chattopadhyay H (2011a) Performance of fluidized bed steam gasification of biomass – modeling and experiment. *Energy Convers Manag* 52:1583–1588
- Loha C, Chattopadhyay H, Chatterjee PK (2011b) Thermodynamic analysis of hydrogen rich synthetic gas generation from fluidized bed gasification of rice husk. *Energy* 36:4063–4071
- LV PM, Xiong ZH, Chang J, Wu CZ, Chen Y, Zhu JX (2004) An experimental study on biomass air–steam gasification in a fluidized bed. *Bioresour Technol* 95:95–101
- LV P, Yuan Z, Wu C, Ma L, Chen Y, Tsubaki N (2007) Bio-syngas production from biomass catalytic gasification. *Energy Convers Manag* 48:1132–1139
- Mansaray KG, Ghalya AE, Al-Taweela AM, Hamdullahpur F, Ugursal VI (1999) Air gasification of rice husk in a dual distributor type fluidized bed gasifier. *Biomass Bioenergy* 17:315–332
- Miccio F, Pirioua B, Ruoppoloa G, Chirone R (2009) Biomass gasification in a catalytic fluidized reactor with beds of different materials. *Chem Eng J* 154:369–374
- Molino A, Chianese, S, Musmarra D (2015) Biomass gasification technology: the state of the art overview. *J Energy Chem* 16–52
- Murakami T, Xu G, Suda T, Matsuzawa Y, Tani H, Fujimori T (2007) Some process fundamentals of biomass gasification in dual fluidized bed. *Fuel* 86:244–255
- Parthasarathy P, Narayanan KS (2014) Hydrogen production from steam gasification of biomass: influence of process parameters on hydrogen yield: a review. *Renew Energy* 66:570–579

- Pathak BS, Patel DV, Bhoi PR, Sharma AM, Vyas DK (2007) Design and development of sand bed filter for upgrading producer gas to IC engine quality fuel. *Int Energ J* 8:15–20
- Pfeifer C, Koppatz S, Hofbauer H (2011) Steam gasification of various feedstocks at a dual fluidised bed gasifier: impacts of operation conditions and bed materials. *Biomass Convers Bioref* 1:39–53
- Phuphuakrat T, Namioka T, Yoshikawa K (2010) Tar removal from biomass pyrolysis gas in two-step function of decomposition and adsorption. *Appl Energy* 87:2203–2211
- Qin Y, Huang HF, Wu ZB, Feng J, Li W, Xie KC (2007) Characterization of tar from sawdust gasified in the pressurized fluidized bed. *Biomass Bioenergy* 31:243–249
- Rapagna S, Janda N, Kiennemann A, Foscoloa PU (2000) Steam-gasification of biomass in a fluidised-bed of olivine particles. *Biomass Bioenergy* 19:187–197
- Rapagnà S, Gallucci K, Di Marcello M, Matt M, Nacken M, Heidenreich S, Foscolo PU (2010) Gas cleaning, gas conditioning and tar abatement by means of a catalytic filter candle in a biomass fluidized-bed gasifier. *Bioresour Technol* 101:7123–7130
- Seville J, Chuah TG, Sibanda V, Knight P (2003) Gas cleaning at high temperatures using rigid ceramic filters. *Adv Powder Technol* 14:657–672
- Shen L, Xiao J, Niklasson F, Johnsson F (2007) Biomass mixing in a fluidized bed biomass gasifier for hydrogen production. *Chem Eng Sci* 62:636–643
- Shen L, Gao Y, Xiao J (2008) Simulation of hydrogen production from biomass gasification in interconnected fluidized beds. *Biomass Bioenergy* 32:120–127
- Subbaiah BS, Murugan DK, Deenadayalan DB, Dhamodharan MI (2014) Gasification of biomass using fluidized bed. *Int J Innov Res Sci Eng Technol* 3:2319–8753
- Subramanian P, Sampathrajan A, Venkatachalam P (2011) Fluidized bed gasification of select granular biomaterials. *Bioresour Technol* 102:1914–1920
- Sun Y, Li R, Yang T, Kai X, He Y (2013) Gasification of biomass to hydrogen-rich gas in fluidized beds using porous medium as bed material. *Int J Hydrogen Energy* 38:14208–14213
- Sutton D, Kelleher B, Ross JRH (2001) Review of literature on catalysts for biomass gasification. *Fuel Process Technol* 73:155–173
- Thakkar M, Makwana JP, Mohanty P, Shah M, Singh V (2016) In bed catalytic tar reduction in the autothermal fluidized bed gasification of rice husk: extraction of silica, energy and cost analysis. *Ind Crop Prod* 87:324–332
- Udomsirichakorn J, Basu P, Salam PA, Acharya B (2013) Effect of CaO on tar reforming to hydrogen enriched gas with in-process CO₂ capture in a bubbling fluidized bed biomass steam gasifier. *Int J Hydrogen Energy* 38:14495–14504
- Umeki K, Yamamoto K, Namioka T, Yoshikawa K (2010) High temperature steam-only gasification of woody biomass. *Appl Energy* 87:791–798
- Virginie M, Adánez J, Courson C, de Diego LF, Labiano GF, Niznansky D, Kiennemann A, Gayán P, Abad A (2012) Effect of Fe-olivine on the tar content during biomass gasification in a dual fluidized bed. *Appl Catal B Environ* 121:214–222
- Warnecke R (2000) Gasification of biomass: comparison of fixed bed and fluidized bed gasifier. *Biomass Bioenergy* 18:489–497
- Weerachanchai P, Horio M, Tangsathitkulchai C (2009) Effects of gasifying conditions and bed materials on fluidized bed steam gasification of wood biomass. *Bioresour Technol* 100:1419–1427
- Xiao R, Jin B, Zhou H, Zhong Z, Zhang M (2007) Air gasification of polypropylene plastic waste in fluidized bed gasifier. *Energy Convers Manag* 48:778–786
- Yanga YB, Ryua C, Khora A, Yates NE, Sharifia VN, Swithenbank J (2005) Effect of fuel properties on biomass combustion. Part II. Modelling approach-identification of the controlling factors. *Fuel* 84:2116–2130
- Zhang R, Brown RC, Suby A, Cummer K (2004) Catalytic destruction of tar in biomass derived producer gas. *Energy Convers Manag* 45:995–1014



Hydrogen-Rich Syngas Production via Ethanol Dry Reforming over Rare-Earth Metal-Promoted Co-based Catalysts

Fahim Fayaz, Mahadi B. Bahari, Thong L. M. Pham, Chinh Nguyen-Huy, Herma Dina Setiabudi, Bawadi Abdullah, and Dai-Viet N. Vo

Abstract

This chapter is the synopsis of the recent investigation on hydrogen-rich syngas generation using ethanol dry reforming approach over rare-earth metal-supported cobalt catalysts. Ce- and La-promoted and unpromoted 10%Co/Al₂O₃ catalysts were synthesized by co-impregnation technique and were characterized using a wide range of methods, namely, Brunauer-Emmett-Teller (BET) surface area, X-ray diffraction (XRD) measurement, temperature-programmed oxidation (TPO), H₂ temperature-programmed reduction (H₂-TPR), NH₃ temperature-programmed desorption (NH₃-TPD) and Raman spectroscopy measurements. The influence of operating conditions including varying CO₂:C₂H₅OH ratios from 2.5:1 to 1:2.5 and reaction temperature range of 923–973 K was also investigated in this chapter. The addition of both CeO₂ and La₂O₃ promoters facilitated the H₂ reduction, enhanced the basic property of catalysts and improved active metal dispersion. Regardless of reaction temperature and reactant composition, La-promoted catalyst exhibited the highest C₂H₅OH and CO₂

F. Fayaz · M. B. Bahari · H. D. Setiabudi · D.-V. N. Vo (✉)

Faculty of Chemical & Natural Resources Engineering, Universiti Malaysia Pahang, Kuantan, Pahang, Malaysia

e-mail: vietvo@ump.edu.my

T. L. M. Pham

Institute of Research and Development, Duy Tan University, Quang Trung, Danang, Vietnam

C. Nguyen-Huy

School of Energy & Chemical Engineering, Ulsan National Institute of Science and Technology, Ulsan, South Korea

B. Abdullah

Chemical Engineering Department, Universiti Teknologi Petronas, Seri Iskandar, Perak, Malaysia

conversions followed by Ce-promoted and unpromoted catalysts. The increment of CO₂ partial pressure from 20 to 50 kPa enhanced C₂H₅OH and CO₂ conversions by up to 20.0% and 27.4%, respectively. However, reactant conversions significantly declined with growing C₂H₅OH partial pressure from 20 to 50 kPa. La and Ce addition hindered carbon deposition on catalyst surface during ethanol dry reforming reaction, and the amount of carbon deposition declined from 51.49% to 30.06% with the addition of La.

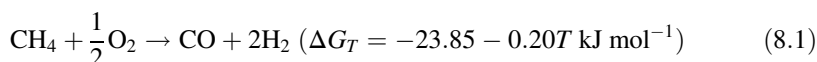
Keywords

Ethanol dry reforming · Co-based catalysts · Syngas · Hydrogen · Rare-earth promoter

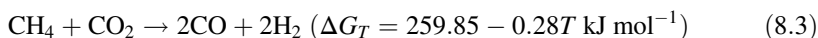
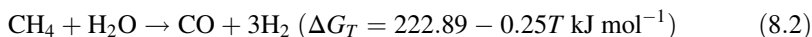
8.1 Introduction

The continuous growth in the current consumption of fossil fuels has resulted in urgent global concerns about rising CO₂ greenhouse gas emissions in the atmosphere and the depletion of non-renewable petroleum-based energy in the next decades. Therefore, the exploration of alternative and renewable energy sources mitigating greenhouse gas emissions and lessening the severe reliance on conventional fuels has received significant interests from both industry and academics. As an alternative to fossil fuels, syngas (a mixture of CO and H₂) has been considered as a potential energy source for the production of environmentally friendly synthetic fuels via downstream Fischer-Tropsch synthesis, FTS (Abdullah et al. 2017; Venvik and Yang 2017).

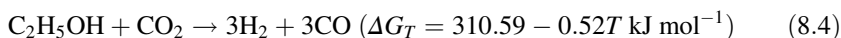
The conventional methods for syngas production are methane partial oxidation, MPO (Eq. 8.1); steam reforming of methane, SRM (Eq. 8.2); or methane dry reforming, MDR (Eq. 8.3) using heterogeneous transition metal catalysts (Usman et al. 2015). However, the utilization of methane as a feedstock for generating the secondary energy source is unsustainable since methane, a main component of natural gas, is also a non-renewable fossil fuel and most likely depleting in the next century. Thus, there is a growing interest in the employment of biomass-derived feedstocks, namely, glycerol (Shahirah et al. 2017), bio-oils (Bimbela et al. 2017) and ethanol (Nanda et al. 2017), in reforming processes for syngas generation.



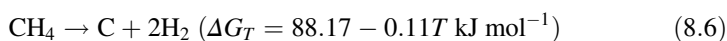
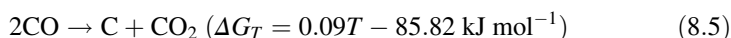
where, ΔG_T and T are Gibbs free energy (kJ mol⁻¹) and reaction temperature (K), respectively.



Ethanol dry reforming, EDR (cf. Eq. 8.4), has been recently recognized as an alluring and promising approach for producing sustainable and green syngas since this synthesis route not only utilizes a renewable $\text{C}_2\text{H}_5\text{OH}$ reactant but also consumes undesirable CO_2 greenhouse gas (Kumar et al. 2016; Zhao et al. 2017). In fact, ethanol is a hydrogen-rich compound, which is highly available, safely stored and easily produced via the fermentation of biomasses such as lignocellulose, sugar cane or starch-rich materials (Ni et al. 2007; Vicente et al. 2014). Additionally, H_2/CO molar ratio obtained from EDR reaction is quite close to unity, and hence it is preferable as feedstock for FTS to produce high molecular weight hydrocarbons (Yang et al. 2014; Vo and Adesina 2012).



EDR reaction is conventionally conducted over Ni-based catalysts due to their relatively low cost compared with noble metals, high availability and strong capability of cleaving C-C and C-O bonds in ethanol (Hu and Lu 2009; Bellido et al. 2009). However, Ni-based catalysts have a propensity for catalytic deactivation, which normally occurs due to thermal Ni sintering and carbon deposition (Bartholomew 2001). Indeed, Ni metal has a relatively low Tammann temperature of about 964 K and hence being susceptible to metal sintering and accumulation (Sharma et al. 2007). In EDR reaction, carbonaceous species could be unavoidably formed through the Boudouard (Eq. 8.5), methane cracking (Eq. 8.6) and ethylene polymerization reactions (Eq. 8.7) (Zawadzki et al. 2014; Bellido et al. 2009).



In order to improve carbon resilience during EDR reaction, lanthanide metal oxides such as La_2O_3 and CeO_2 have been recently used as promoters or supports for Ni-based catalysts due to their intrinsically basic properties, strong CO_2 adsorption capacity and great oxygen storage capacity (Srisiriwat et al. 2009; Mazumder and de Lasa 2014). Zawadzki et al. (2014) studied the effect of different types of supports, namely, CeO_2 , Al_2O_3 , ZrO_2 and MgO , on Ni-based catalysts for EDR reaction and found that CeO_2 -supported Ni catalyst exhibited the highest ethanol conversion, and H_2 reduction process for this catalyst was alleviated in terms of reaction temperature. Bahari et al. (2017) also found that 3%La-10%Ni/ Al_2O_3 catalyst appeared to be stable with time-on-stream during EDR reaction due to the redox characteristic of La_2O_3 promoter inhibiting carbon deposition.

Apart from Ni-based catalysts, cobalt has also attracted considerable interests as an active catalyst for reforming reactions due to its high availability, low cost and relatively comparable activity to precious metal catalysts (Budiman et al. 2012). Maia et al. (2014) evaluated the catalytic performance of Co catalysts supported on γ -Al₂O₃, CeO₂ and mixed CeO₂/ γ -Al₂O₃ supports for steam reforming of ethanol at reaction temperature range of 673–873 K and ethanol/water molar ratio of 1:3. These Co-based catalysts reportedly exhibited high ethanol conversion of about 90%. To the best of our knowledge, although great efforts have been carried out on steam reforming of ethanol over Co-based catalysts (Batista et al. 2003; Maia et al. 2014), there are no or negligible previous studies about the promotional effect on Co-based catalysts for EDR reaction. Therefore, the aim of this chapter is to investigate the influence of La₂O₃ and CeO₂ dopants on the physicochemical properties of Co/Al₂O₃ catalyst and its catalytic performance for EDR reaction.

8.2 Experimental

8.2.1 Catalyst Preparation

In this investigation, 3%M-10%Co/Al₂O₃ (with M: La or Ce) catalysts were synthesized by wet co-impregnation method, whilst the wet impregnation approach was implemented for the preparation of unpromoted 10%Co/Al₂O₃ catalyst. All metal precursors, namely, Co(NO₃)₂.6H₂O, La(NO₃)₃.6H₂O and Ce(NO₃)₃.6H₂O, were purchased from Sigma-Aldrich Chemicals. Prior to catalyst preparation, an accurate amount of γ -Al₂O₃ support procured from Sasol (Puralox SCCa-150/200) was air-calcined in a Carbolite furnace at a temperature of 1023 K for 5 h with a ramping rate of 5 K min⁻¹ in order to guarantee the thermal phase stability. The pretreated γ -Al₂O₃ support was then mixed with the precisely calculated quantity of the aqueous solution of aforementioned metal precursors and magnetically stirred constantly for 3 h at the ambient temperature. The resulting mixture was subsequently dried in an oven for 24 h at 383 K followed by calcination in flowing air at the temperature of 773 K for 5 h with a heating rate of 5 K min⁻¹. After calcination, the solid particles were further crushed and sieved to the desired particle size of 125–160 μ m for loading into the fixed-bed reactor.

8.2.2 Catalyst Characterization

The textural properties including multipoint Brunauer-Emmett-Teller (BET) surface area, total pore volume and average pore diameter of γ -Al₂O₃ support, promoted and unpromoted 10%Co/Al₂O₃ catalysts were determined in a Micromeritics ASAP-2020 unit employing N₂ adsorption-desorption isotherms at 77 K. Before each N₂ adsorption measurement, specimen was degassed at 573 K for 1 h to guarantee the complete removal of moisture and associated volatile compounds. The crystalline structure of fresh and spent catalysts was identified in a Rigaku Miniflex II X-ray diffraction

(XRD) system using Cu target as radiation source with wavelength, λ , of 1.5418 Å operating at 30 kV and 15 mA. The Bragg angle (2θ) was scanned from 3° to 80° with slow scan speed and step size of 1° min⁻¹ and 0.02°, respectively.

The acidic properties of support and catalysts were measured by NH₃ temperature-programmed desorption (NH₃-TPD) on a Micromeritics AutoChem II-2920 chemisorption system. About 0.1 g of the sample placed in a quartz U-tube was pretreated for 1 h at 773 K under He flow of 50 ml min⁻¹ to eliminate trace moisture and physisorbed compounds prior to each measurement. The sample was then reduced in situ in 50 ml min⁻¹ of 10% H₂/Ar for 30 min at the same temperature before cooling down to 423 K in inert gas for adsorption step. 5% NH₃ in He balance (50 ml min⁻¹) employed as an adsorption media flowed through the H₂-reduced sample at 423 K for 1 h. Thereafter, the system was purged with He gas at the same temperature for 30 min to remove NH₃ molecules in gas phase followed by heating up to 1073 K at 10 K min⁻¹. The amount of desorbed NH₃ gas from the outlet of U-tube was measured online using a thermal conductivity detector (TCD).

H₂-TPR measurements were also performed on a Micromeritics AutoChem II-2920 apparatus for support, promoted and unpromoted catalysts. Typically, about 0.1 g of specimen was loaded in a quartz U-tube and mounted by quartz wool. All samples were previously treated at 373 K for 30 min in He flow of 50 ml min⁻¹ for removal of volatile materials. Specimens were then heated from 373 to 1173 K with a ramping rate of 10 K min⁻¹ in flowing 10% H₂/Ar mixture (50 ml min⁻¹) followed by an isothermal treatment for 30 min in the same reducing gaseous mixture. The amount of carbon accumulating on the surface of spent catalysts was quantified by temperature-programmed oxidation (TPO) using a TGA Q500 unit from TA Instruments. Each sample was previously heated in 100 ml min⁻¹ flow of N₂ at 373 K for 30 min to remove moisture and volatile compounds on catalyst surfaces. The temperature was subsequently increased to 1023 K in 100 ml min⁻¹ flow of 20% O₂/N₂ mixture with a heating rate of 10 K min⁻¹. The programming temperature was further kept constant at 1023 K in similar gas mixture for 30 min before cooling down to room temperature in N₂ flow.

Raman spectroscopy analyses of spent catalysts were carried out on a DXR Raman Microscope (Thermo Fisher Scientific) employing a laser beam emitting at 532 nm. Scanning electron microscopy (SEM) images of selected spent catalysts after EDR reaction were obtained from a Carl Zeiss AG – EVO® 50 Series instrument operated by SmartSEM software. The sample was coated on platinum plate in BAL-TEC SCD 005 sputter coater for 70 s before SEM measurement in order to ensure the sharpness of SEM images. Additionally, SEM coupled with energy-dispersive X-ray analysis (EDX) was conducted for selected spent catalysts on a Hitachi Tabletop Microscope TM3030Plus unit.

8.2.3 Catalytic Activity Tests

The catalytic evaluation of EDR reaction was performed in a quartz tubular fixed-bed reactor (with length, $L = 17$ in., and outer diameter, $O.D. = 3/8$ in., as seen in

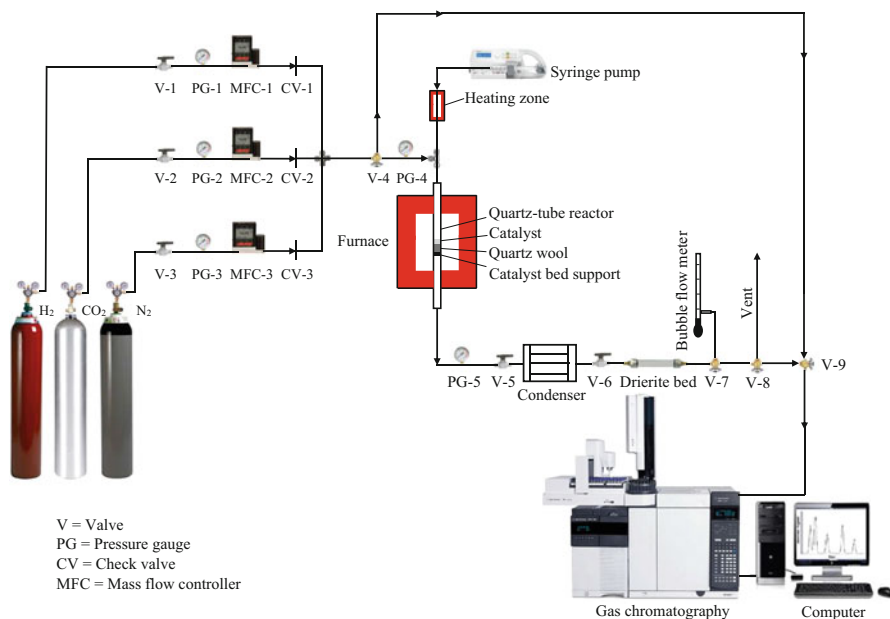


Fig. 8.1 Schematic diagram of experimental set-up for EDR reaction

Fig. 8.1) at reaction temperature range of 923–973 K with varying feed ratios of $\text{CO}_2:\text{C}_2\text{H}_5\text{OH}$ from 1:2.5 to 2.5:1 under atmospheric pressure. Approximately, 0.1 g of catalyst was mounted by quartz wool in the middle of quartz tube reactor placed vertically in a split tubular furnace. Prior to EDR runs, H_2 reduction was carried out in situ from room temperature to 923 K with a heating rate of 10 K min^{-1} in a flowing 50% H_2/N_2 mixture (60 ml min^{-1}). Specimen was kept isothermally at the final temperature for 2 h before heating up to the desired EDR reaction temperature in 60 ml min^{-1} of N_2 flow. High gas hourly space velocity, $\text{GHSV} = 42 \text{ L g}_{\text{cat}}^{-1} \text{ h}^{-1}$ and small particle size of catalyst within 125–160 μm were applied for each EDR run to ensure the negligibility of internal and external transport intrusions. Ethanol was accurately fed into the top of fixed-bed reactor using a syringe pump (KellyMed KL-602). The flow rates of gaseous CO_2 reactant and inert N_2 diluent were also precisely regulated by electronic Alicat mass flow controllers. The gaseous products from the outlet of reactor were analysed in an Agilent 6890 GC Gas Chromatograph Series equipped with thermal conductivity detector (TCD) and flame ionization detector (FID).

The catalytic performance of EDR reaction was assessed in terms of reactant conversions, X_i (i : $\text{C}_2\text{H}_5\text{OH}$ or CO_2), gaseous product yields, Y_j (j : H_2 , CO or CH_4) and product ratios (H_2/CO and CH_4/CO) as given in Eqs. 8.8, 8.9, 8.10, 8.11, 8.12, and 8.13.

$$X_i(\%) = \frac{F_i^{\text{In}} - F_i^{\text{Out}}}{F_i^{\text{In}}} \times 100\% \quad (8.8)$$

$$Y_{\text{H}_2}(\%) = \frac{2F_{\text{H}_2}^{\text{Out}}}{6F_{\text{C}_2\text{H}_5\text{OH}}^{\text{In}}} \times 100\% \quad (8.9)$$

$$Y_{\text{CO}}(\%) = \frac{F_{\text{CO}}^{\text{Out}}}{F_{\text{CO}_2}^{\text{In}} + 2F_{\text{C}_2\text{H}_5\text{OH}}^{\text{In}}} \times 100\% \quad (8.10)$$

$$Y_{\text{CH}_4}(\%) = \frac{F_{\text{CH}_4}^{\text{Out}}}{F_{\text{CO}_2}^{\text{In}} + 2F_{\text{C}_2\text{H}_5\text{OH}}^{\text{In}}} \times 100\% \quad (8.11)$$

$$\text{H}_2/\text{CO ratio} = \frac{F_{\text{H}_2}^{\text{Out}}}{F_{\text{CO}}^{\text{Out}}} \quad (8.12)$$

and

$$\text{CH}_4/\text{CO ratio} = \frac{F_{\text{CH}_4}^{\text{Out}}}{F_{\text{CO}}^{\text{Out}}} \quad (8.13)$$

where F^{in} and F^{out} refer to the inlet and outlet molar flow rates (mol s^{-1}), respectively.

8.3 Results and Discussion

8.3.1 Textural Properties of Catalysts

The multipoint BET surface area, total pore volume and average pore diameter of $\gamma\text{-Al}_2\text{O}_3$ support, promoted and unpromoted catalysts are summarized in Table 8.1. The unpromoted catalyst had BET surface area and total pore volume of $143.1 \text{ m}^2 \text{ g}^{-1}$ and $0.36 \text{ cm}^3 \text{ g}^{-1}$, respectively, lower than those of $\gamma\text{-Al}_2\text{O}_3$ support. This observation was possibly due to the successful introduction of Co oxides on the support surface resulting in an inevitable drop in BET surface area and total pore volume.

However, as seen in Table 8.1, the addition of Ce and La promoters did not induce a significant decline in BET surface area, total pore volume and average pore diameter in comparison with unpromoted $10\%\text{Co}/\text{Al}_2\text{O}_3$ catalyst. This could suggest that both Ce and La promoters were well dispersed on the catalyst surface and did not cause an adverse effect on the textural properties of catalysts.

Table 8.1 Physical properties of calcined γ -Al₂O₃ support, as well as promoted and unpromoted 10%Co/Al₂O₃ catalysts

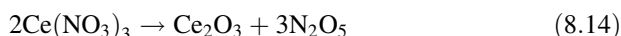
Sample	BET surface area (m ² g ⁻¹)	Total pore volume (cm ³ g ⁻¹)	Average pore diameter (nm)	Co ₃ O ₄ average crystallite size, $d(\text{Co}_3\text{O}_4)$ (nm) ^a
γ -Al ₂ O ₃	175.2	0.46	10.7	–
10%Co/Al ₂ O ₃	143.1	0.36	10.6	14.1
3%Ce-10%Co/Al ₂ O ₃	142.2	0.35	10.5	10.1
3%La-10%Co/Al ₂ O ₃	136.0	0.34	10.4	7.7

^aCo₃O₄ average crystallite size was computed from Scherrer equation at 2θ line of 31.45° (Patterson 1939)

8.3.2 X-Ray Diffraction Analysis

Figure 8.2 shows the XRD patterns of La-promoted, Ce-promoted and unpromoted 10%Co/Al₂O₃ catalysts. The X-ray diffractogram of calcined Al₂O₃ support is also given as a reference for comparison and easing the interpretation of XRD patterns. The Joint Committee on Powder Diffraction Standards (JCPDS) database was used to determine the crystalline phases of all catalysts (JCPDS powder diffraction file 2000). As seen in Fig. 8.2, γ -Al₂O₃ phase possessing typical peaks at 2θ of 18.92°, 32.88°, 37.10°, 45.61° and 67.17° was detected on all catalysts (JCPDS card No. 04–0858). For both promoted and unpromoted catalysts, the Co₃O₄ phase was observed at $2\theta = 31.45^\circ, 37.10^\circ, 44.79^\circ$ and 55.66° (JCPDS card No. 74-2120). In addition, as seen in Fig. 8.2b–d), the spinel CoAl₂O₄ phase, formed by the strong interaction between Al₂O₃ support and cobalt oxide, was identified at $2\theta = 59.51^\circ$ and 65.38° on the surface of all catalysts (JCPDS card No. 82-2246).

For the calcined 3%Ce-10%Co/Al₂O₃ catalyst (cf. Fig. 8.2c), the characteristic peak located at 2θ of 28.57° corresponded to CeO₂ phase (JCPDS card No. 34-0394) in agreement with findings from Manfro et al. (2011) and Moraes et al. (2015). The CeO₂ phase could be formed from the decomposition of Ce(NO₃)₃ promoter precursor to Ce₂O₃ phase which was subsequently oxidized to the final CeO₂ phase during air-calcination as seen in Eqs. 8.14 and 8.15 (Foo et al. 2011; Bahari et al. 2016).



and



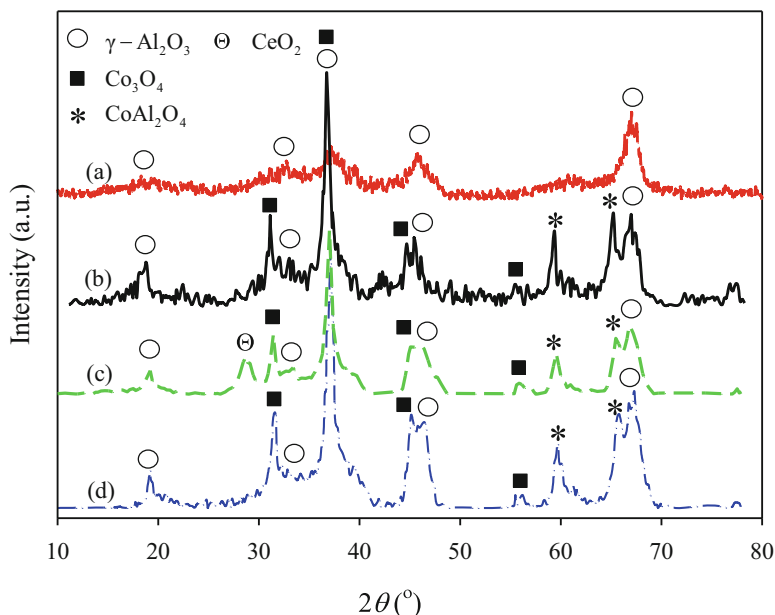


Fig. 8.2 XRD patterns of (a) calcined $\gamma\text{-Al}_2\text{O}_3$ support, (b) 10%Co/Al₂O₃, (c) 3%Ce-10%Co/Al₂O₃ and (d) 3%La-10%Co/Al₂O₃ catalysts

However, as seen in Fig. 8.2d, La_2O_3 phase with typical diffraction peaks at 2θ of 29.87° and 53.42° (JCPDS card No. 83-1355) was not detected on the surface of 3% La-10%Co/Al₂O₃ catalyst. It could be due to high metal dispersion and hence forming La_2O_3 nanoparticles with small crystallite size lower than the XRD detection limit.

The average crystallite size, $d(\text{Co}_3\text{O}_4)$, of Co_3O_4 phase was also computed using Scherrer equation as given in Eq. 8.16 (Patterson 1939; Bartholomew and Farrauto 2005).

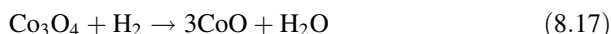
$$d(\text{Co}_3\text{O}_4)(\text{nm}) = \frac{0.94\lambda}{B \times \cos \theta} \quad (8.16)$$

where, λ is the X-ray wavelength, B is the line broadening at half the maximum intensity in radian (FWHM) and θ is the Bragg angle. As summarized in Table 8.1, the average crystallite size of Co_3O_4 phase was reduced considerably from 14.1 (unpromoted catalyst) to 7.7 nm (La-promoted catalyst) with the addition of promoter. The drop in the crystallite size of Co_3O_4 form with Ce and La promoters could be assigned to the dilution effect of CeO_2 and La_2O_3 particles, which act as spacers, isolate Co_3O_4 grains and prevent them from excessive growth at high calcination temperature during catalyst preparation (Yang et al. 2010; Bahari et al. 2016).

8.3.3 H₂ Temperature-Programmed Reduction

The reducibility of promoted and unpromoted catalysts during H₂ activation was examined by H₂-TPR measurements. As seen in Fig. 8.3a, there were no observable peaks for the H₂-TPR profile of γ -Al₂O₃ support indicating that γ -Al₂O₃ support was stable and resistant to H₂ reduction. Therefore, three discrete peaks (P1, P2 and P3) detected for 10%Co/Al₂O₃, 3%Ce-10%Co/Al₂O₃ and 3%La-10%Co/Al₂O₃ catalysts (see Fig. 8.3b–d) could belong to the reduction of Co-containing compounds.

The low-temperature peak (P1) ranging from 458 to 720 K for all catalysts was ascribed to the reduction of Co₃O₄ to intermediate CoO phase (cf. Eq. 8.17), whilst the second peak (P2 centred at about 743–765 K) was assigned to CoO reduction to final metallic Co⁰ form as given in Eq. 8.18 (Jabbour et al. 2014; Ogo et al. 2015).



The small shoulder (P3) located at the high reduction temperature of 766–1014 K for promoted and unpromoted catalysts was most likely due to the reduction of spinel CoAl₂O₄ species (see Eq. 8.19) possessing strong metal-support interaction (Hull and Trawczynski 2014; Cooper et al. 2008). Papageridis et al. (2016) also reported that Co²⁺ ions could migrate into the lattice of Al₂O₃ support and reside in

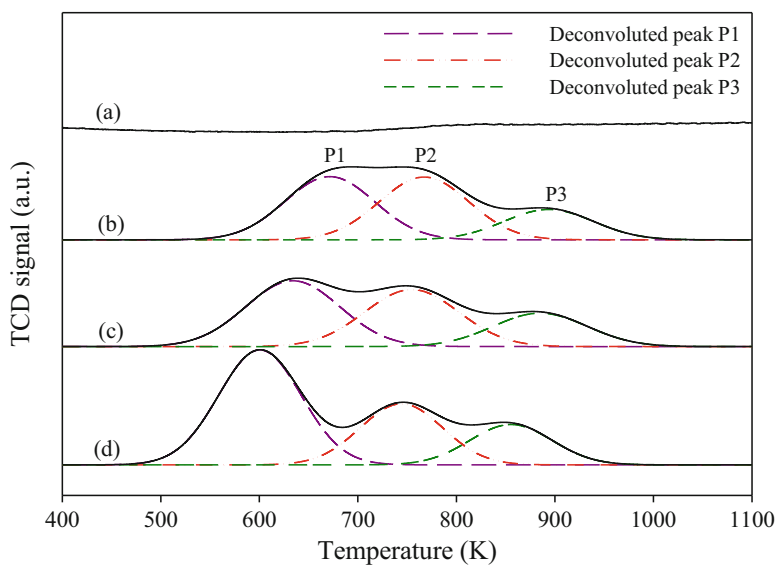
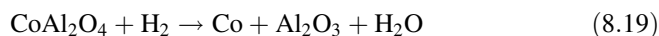


Fig. 8.3 H₂-TPR profiles of (a) calcined γ -Al₂O₃ support, (b) 10%Co/Al₂O₃, (c) 3%Ce-10%Co/Al₂O₃ and (d) 3%La-10%Co/Al₂O₃ catalysts at a ramping rate of 10 K min⁻¹

the tetrahedral positions of spinel CoAl_2O_4 form due to high calcination temperature. Thus, the strong interaction between CoO and Al_2O_3 in CoAl_2O_4 species could induce great resistance to H_2 reduction.



As seen in Table 8.2, the reduction temperature for three peaks (P1, P2 and P3) was slightly shifted to lower reaction temperature region with promoter addition in the order $10\%\text{Co}/\text{Al}_2\text{O}_3 > 3\%\text{Ce}-10\%\text{Co}/\text{Al}_2\text{O}_3 > 3\%\text{La}-10\%\text{Co}/\text{Al}_2\text{O}_3$ catalysts. The easing of H_2 reduction could be due to the high density of electrons donated by CeO_2 or La_2O_3 promoter to Co-containing compounds (Zhi et al. 2011; Fayaz et al. 2016). In addition, the total H_2 uptake during H_2 -TPR increased from 1.45 to 1.66 $\text{mmol H}_2 \text{ g}_{\text{cat}}^{-1}$ in the opposite trend, i.e. $10\%\text{Co}/\text{Al}_2\text{O}_3 < 3\%\text{Ce}-10\%\text{Co}/\text{Al}_2\text{O}_3 < 3\%\text{La}-10\%\text{Co}/\text{Al}_2\text{O}_3$ catalysts (see Table 8.2), further confirming the facilitation of H_2 reduction and the enhancing degree of reduction with promoter addition.

8.3.4 NH_3 Temperature-Programmed Desorption

The NH_3 -TPD measurements were conducted over $\gamma\text{-Al}_2\text{O}_3$ support, promoted and unpromoted $10\%\text{Co}/\text{Al}_2\text{O}_3$ catalysts to quantify acid site concentration (NH_3 uptake) on the catalyst surface. The NH_3 -TPD envelopes for support and catalysts are shown in Fig. 8.4. Three discrete peaks (P1, P2 and P3) observed at different desorption temperature regions of 423–570 K, 571–710 K and 721–1026 K could be categorized as weak, medium and strong acid sites, respectively, for Al_2O_3 support and catalysts (Firoozi et al. 2009; e Santos et al. 2014). Since the strong acid sites have greater NH_3 desorption temperature than 713 K, it could correspond to Brønsted acid site (Zhang et al. 1999), whilst the weak and medium acid sites possessing lower NH_3 desorption temperature could be due to the presence of Lewis and/or Brønsted acid sites (Firoozi et al. 2009).

As seen in Fig. 8.4, Al_2O_3 support also possessed three different types of acid centres with the total NH_3 uptake of 4.77 $\text{mmol NH}_3 \text{ g}_{\text{cat}}^{-1}$. The addition of Co metal on Al_2O_3 support increased significantly the amount of NH_3 uptake from 4.77 to 6.89 $\text{mmol NH}_3 \text{ g}_{\text{cat}}^{-1}$ (about 44.44%) as seen in Table 8.3. This observation could suggest the formation of an extra acid site on the interface between Co metal and Al_2O_3 support in agreement with other studies (Cheng et al. 2010). Interestingly, a

Table 8.2 Summary of H_2 consumption during H_2 -TPR measurements for $10\%\text{Co}/\text{Al}_2\text{O}_3$, $3\%\text{Ce}-10\%\text{Co}/\text{Al}_2\text{O}_3$ and $3\%\text{La}-10\%\text{Co}/\text{Al}_2\text{O}_3$ catalysts

Catalyst	Reduction temperature (K)			Total H_2 consumed ($\text{mmol H}_2 \text{ g}_{\text{cat}}^{-1}$)
	P1	P2	P3	
$10\%\text{Co}/\text{Al}_2\text{O}_3$	667.6	764.6	891.3	1.45
$3\%\text{Ce}-10\%\text{Co}/\text{Al}_2\text{O}_3$	632.5	752.7	883.3	1.55
$3\%\text{La}-10\%\text{Co}/\text{Al}_2\text{O}_3$	598.1	743.4	850.9	1.66

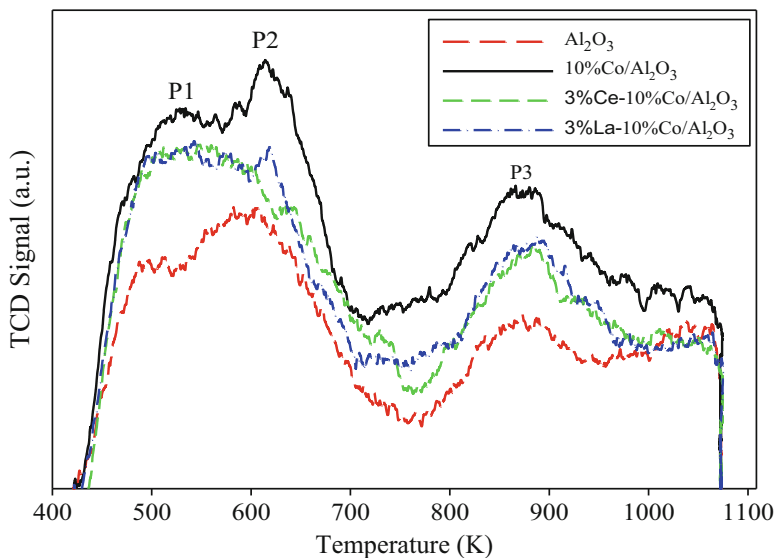


Fig. 8.4 NH_3 -TPD profiles of Al_2O_3 support, Ce-promoted, La-promoted and unpromoted 10% $\text{Co}/\text{Al}_2\text{O}_3$ catalysts

Table 8.3 Summary of NH_3 desorption over Al_2O_3 support, promoted and unpromoted 10% $\text{Co}/\text{Al}_2\text{O}_3$ catalysts

Sample	Total NH_3 uptake ($\text{mmol NH}_3 \text{ g}_{\text{cat}}^{-1}$)
$\gamma\text{-Al}_2\text{O}_3$ support	4.77
10% $\text{Co}/\text{Al}_2\text{O}_3$	6.89
3%Ce-10% $\text{Co}/\text{Al}_2\text{O}_3$	6.16
3%La-10% $\text{Co}/\text{Al}_2\text{O}_3$	6.12

substantial reduction in total NH_3 uptake for 10% $\text{Co}/\text{Al}_2\text{O}_3$ catalyst with Ce and La promoter addition from 6.89 to 6.12 $\text{mmol NH}_3 \text{ g}_{\text{cat}}^{-1}$ (see Table 8.3) was observed in the order of 10% $\text{Co}/\text{Al}_2\text{O}_3 > 3\% \text{Ce-}10\% \text{Co}/\text{Al}_2\text{O}_3 > 3\% \text{La-}10\% \text{Co}/\text{Al}_2\text{O}_3$ catalysts. In the study of glycerol steam reforming over La- and Ce-promoted $\text{Pt}/\text{Al}_2\text{O}_3$ catalysts, Montini et al. (2010) also observed a similar trend for acid site concentration with the addition of La and Ce promoters. The decline in NH_3 uptake for Ce- and La-promoted catalysts was reasonably due to the electron-rich character and alkaline property of the CeO_2 and La_2O_3 promoters (Yang et al. 2010). The higher electron density donated by these dopants to active metal could reduce the concentration of acid sites and hence hindering NH_3 chemisorption. In fact, the acid site was widely reported as a favourable centre for ethanol dehydration (a side reaction of EDR) to ethylene, which could be further prone to filamentous carbon via ethylene polymerization (Hou et al. 2015). Thus, the drop in acid site concentration with the promotion of Ce and La rare-earth oxides could inhibit the dehydration of ethanol to an undesirable intermediate ethylene compound and hence reducing the formation rate of deposited carbon during EDR reaction (Zawadzki et al. 2014; Drif et al. 2015).

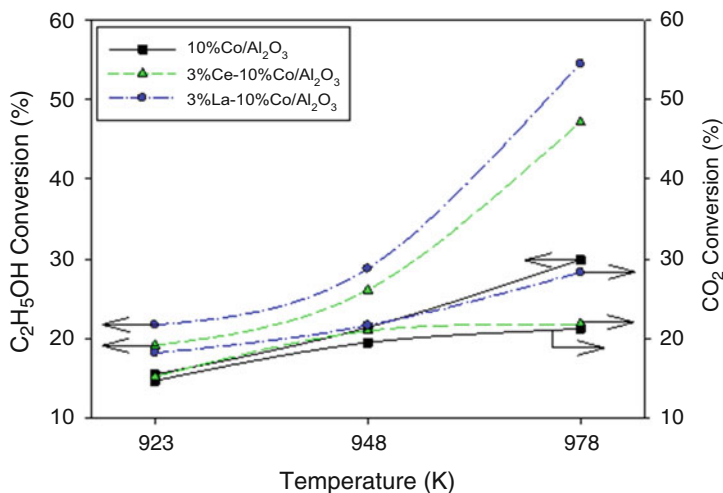


Fig. 8.5 Effect of reaction temperature on C₂H₅OH and CO₂ conversions at $P_{\text{CO}_2} = P_{\text{C}_2\text{H}_5\text{OH}} = 20$ kPa

8.3.5 Ethanol Dry Reforming Evaluation

8.3.5.1 Effect of Reaction Temperature

The EDR runs for promoted and unpromoted catalysts were conducted at varying reaction temperature of 923–973 K and stoichiometric feed ratio (with reactant partial pressure, P_i , of $P_{\text{CO}_2} = P_{\text{C}_2\text{H}_5\text{OH}} = 20$ kPa) in order to examine the effect of reaction temperature on the catalytic performance of EDR. As seen in Fig. 8.5, both C₂H₅OH and CO₂ conversions increased significantly up to 150.6% and 55.5%, respectively, as reaction temperature increased from 923 to 973 K reasonably due to the endothermic nature of EDR reaction (Wang and Wang 2009). Regardless of reaction temperature, promoted 10%Co/Al₂O₃ catalysts exhibited greater conversions of C₂H₅OH and CO₂ than those of unpromoted catalyst in the order; 3%La-10%Co/Al₂O₃ > 3%Ce-10%Co/Al₂O₃ > 10%Co/Al₂O₃ catalysts parallel to the trend of H₂ consumption during H₂-TPR measurement (see Table 8.2). This relationship could suggest that the promotion of La₂O₃- and CeO₂-enhanced reduction degree and hence increasing the number of Co active sites for greater EDR activity. In fact, Bahari et al. (2016) also found that Ce-doped Ni/Al₂O₃ catalyst performed a higher EDR activity than unpromoted Ni/Al₂O₃ catalyst due to easing H₂ reduction. Additionally, the improvement of metal dispersion with promoter addition resulting in smaller Co₃O₄ crystallite size (cf. Table 8.1) could contribute to an increase in catalytic activity. Moreover, as seen in Table 8.3, the total NH₃ uptake of catalysts followed an opposite trend (i.e. 10%Co/Al₂O₃ > 3%Ce-10%Co/Al₂O₃ > 3%La-10%Co/Al₂O₃ catalysts) to the sequence of EDR activity. This behaviour could suggest that the

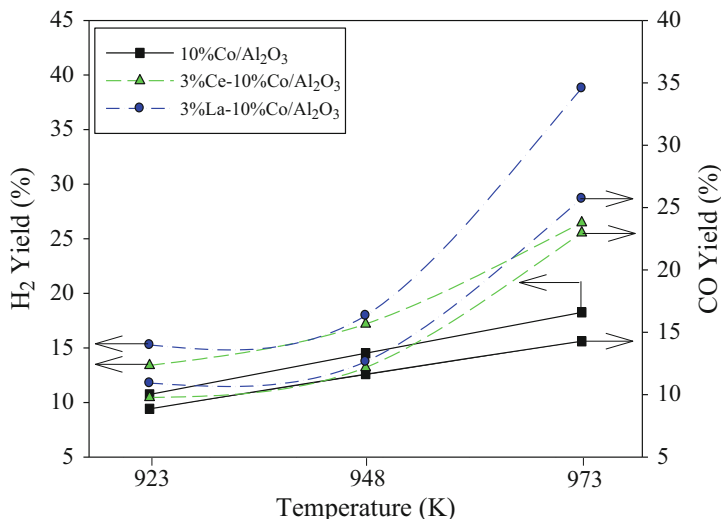
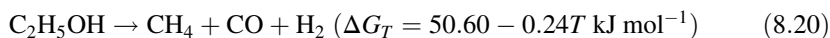


Fig. 8.6 Effect of reaction temperature on H₂ and CO yields at $P_{\text{CO}_2} = P_{\text{C}_2\text{H}_5\text{OH}} = 20$ kPa

concentration of basic site on catalyst surface was improved with basic CeO₂ and La₂O₃ addition, and the basic site was the active and favourable site for EDR reaction. Osorio-Vargas et al. (2016) and Yang et al. (2010) also reported that the basic property of CeO₂ and La₂O₃ dopants could attract CO₂ chemisorption on the catalyst surface and hence improve the catalytic activity as well as accelerate the CO₂ gasification of surface carbon for maintaining catalytic stability.

The influence of reaction temperature on H₂ and CO yields of both promoted and unpromoted catalysts is shown in Fig. 8.6, whilst the relationship between CH₄ yield and reaction temperature is illustrated in Fig. 8.7. As seen in Fig. 8.6, irrespective of reaction temperature, promoted catalysts exhibited greater H₂ and CO yields than those of unpromoted catalyst in the order of 3%La-10%Co/Al₂O₃ > 3%Ce-10%Co/Al₂O₃ > 10%Co/Al₂O₃ catalysts. The considerable enhancement of both H₂ and CO yields was observed with rising reaction temperature from 923 to 973 K for all catalysts (see Fig. 8.6). Jankhah et al. (2008) also experienced a similar behaviour for EDR reaction over carbon steel catalyst and deduced that the enhancing secondary endothermic methane dry reforming reaction was responsible for the increment of H₂ and CO yields. In fact, Bahari et al. (2017) previously proposed an overall reaction pathway over Al₂O₃-supported Ni catalysts for EDR reaction in which C₂H₅OH was initially decomposed to CH₄ intermediate product (cf. Eq. 8.20) followed by methane dry reforming reaction (cf. Eq. 8.21) to yield the final H₂ and CO product.



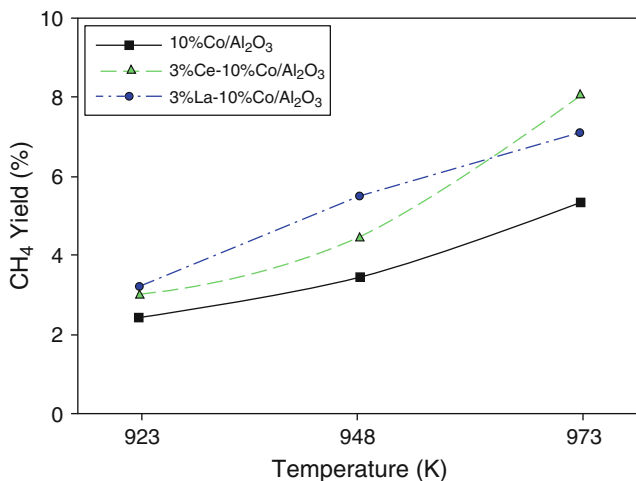
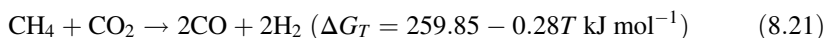


Fig. 8.7 Effect of reaction temperature on CH₄ yield at $P_{\text{CO}_2} = P_{\text{C}_2\text{H}_5\text{OH}} = 20$ kPa

and



However, as seen in Fig. 8.7, the CH₄ formation was always detected regardless of employed catalysts and reaction temperature indicating that CH₄ intermediate by-product was not fully converted to syngas via MDR reaction. Additionally, the yield of CH₄ for all catalysts experienced a nonlinear increase from about 2%–8% with growing reaction temperature from 923 to 973 K. This could indicate that the rising rate of C₂H₅OH decomposition to CH₄ with reaction temperature was superior to the rate of subsequent MDR reaction to CO and H₂. In fact, C₂H₅OH decomposition also has a lower endothermic character than that of MDR reaction based on Gibbs free energies, ΔG_T (cf. Eqs. 8.20 and 8.21).

Figure 8.8 shows the effect of reaction temperature on H₂/CO and CH₄/CO ratios for promoted and unpromoted 10%Co/Al₂O₃ catalysts. Both H₂/CO and CH₄/CO ratios improved with rising reaction temperature from 923 to 973 K for all catalysts. The ratio of H₂ to CO was evidently greater than the stoichiometric or theoretical ratio (H₂/CO = 1:1) for EDR reaction. The higher H₂/CO ratio than unity and its enhancement with growing reaction temperature was probably due to the presence of simultaneous endothermic ethanol dehydrogenation reaction during EDR reaction (Zawadzki et al. 2014). Additionally, the values of H₂/CO ratio obtained from EDR reaction were favoured as raw materials in downstream FTS for generating oxygenated chemicals and long-chain hydrocarbons (Vo and Adesina 2012). The increment of CH₄/CO ratio with rising reaction temperature for all catalysts could further confirm that secondary MDR rate was lower than that of ethanol decomposition (see Fig. 8.8).

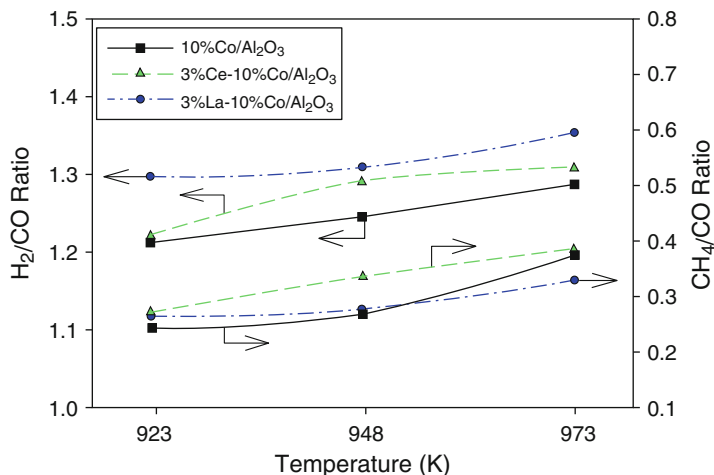


Fig. 8.8 Effect of reaction temperature on H_2/CO and CH_4/CO ratios at $P_{CO_2} = P_{C_2H_5OH} = 20$ kPa

8.3.5.2 Effect of CO_2 Partial Pressure

The partial pressure of CO_2 was also adjusted from 20 to 50 kPa during EDR reaction at 973 K, whereas the partial pressure of ethanol, $P_{C_2H_5OH}$, was kept constant at 20 kPa in order to investigate the effect of P_{CO_2} on EDR performance. The reactant conversions as a function of CO_2 partial pressure obtained for promoted and unpromoted catalysts are presented in Fig. 8.9. The conversions of C_2H_5OH and CO_2 for unpromoted, Ce-promoted and La-promoted catalysts grew with increasing P_{CO_2} from 20 to 50 kPa by up to 20.0% and 27.4%, respectively. Hu and Lu (2009) also observed similar results for EDR reaction over Ni/Al_2O_3 catalyst with CO_2 -rich feedstock and reported that the improvement of MDR side reaction in the CO_2 -excess environment could convert the CH_4 intermediate product to final syngas and in turn increased reactant conversions. Based on the thermodynamic results, Jankhah et al. (2008) found that the high ratio of CO_2 to C_2H_5OH was thermodynamically preferred for enhancing EDR conversion. Additionally, the enhancement of reverse Boudouard reaction (see Eq. 8.5) with rising CO_2 partial pressure could contribute to the elimination of deposited carbon from C_2H_5OH decomposition and hence improve the catalytic activity. As seen in Fig. 8.9, La-promoted catalyst always performed the highest activity followed by Ce-promoted and unpromoted catalysts for all CO_2 feed compositions.

As seen in Fig. 8.10, a linear increment of H_2 and CO yields with rising P_{CO_2} from 20 to 50 kPa for all catalysts could further confirm the enhancement of EDR and MDR side reactions in the CO_2 -rich environment. Regardless of P_{CO_2} , the greatest H_2 and CO yields were always observed over La-doped catalyst, whilst unpromoted catalyst possessed the lowest product yields. These results could be assigned to the enhancement of metal dispersion, reduction degree and basic property with the doping of La_2O_3 and CeO_2 promoters.

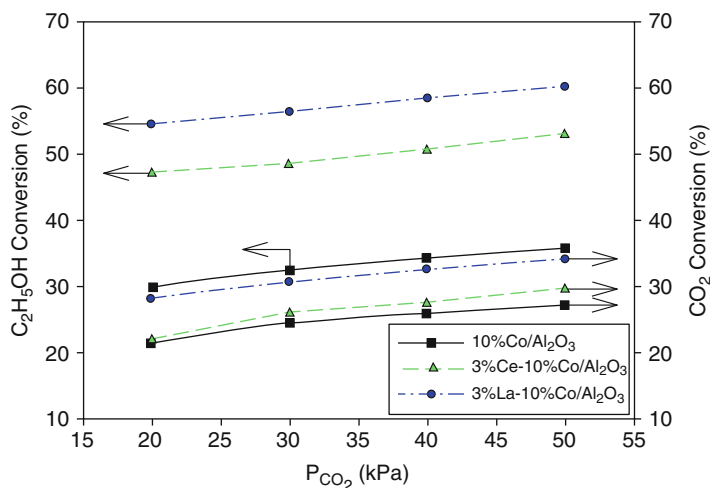


Fig. 8.9 Effect of P_{CO_2} on C_2H_5OH and CO_2 conversions at $P_{C_2H_5OH} = 20$ kPa and $T = 973$ K

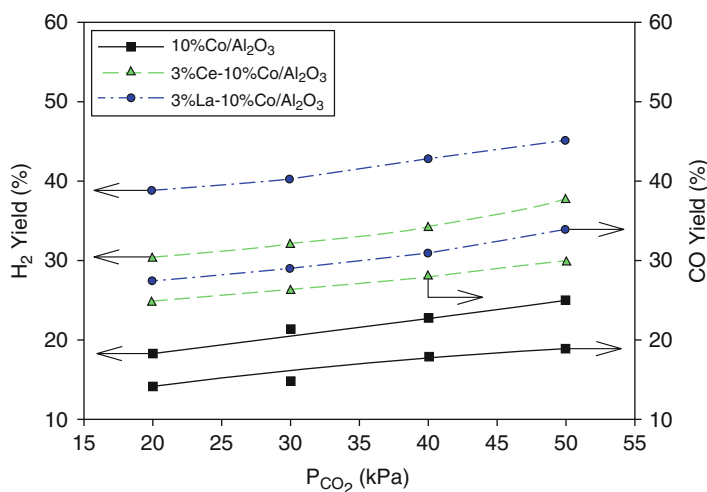


Fig. 8.10 Effect of P_{CO_2} on the yields of H_2 and CO at $P_{C_2H_5OH} = 20$ kPa and $T = 973$ K

Figure 8.11 depicts the relationship between product ratios (i.e. H_2/CO and CH_4/CO ratios) and CO_2 partial pressure at 973 K and $P_{C_2H_5OH} = 20$ kPa. For all catalysts, CH_4/CO ratio experienced a significant decline with rising P_{CO_2} further confirming the growth of secondary MDR reaction. In fact, Foo et al. (2011) previously proposed the general MDR reaction mechanism in which

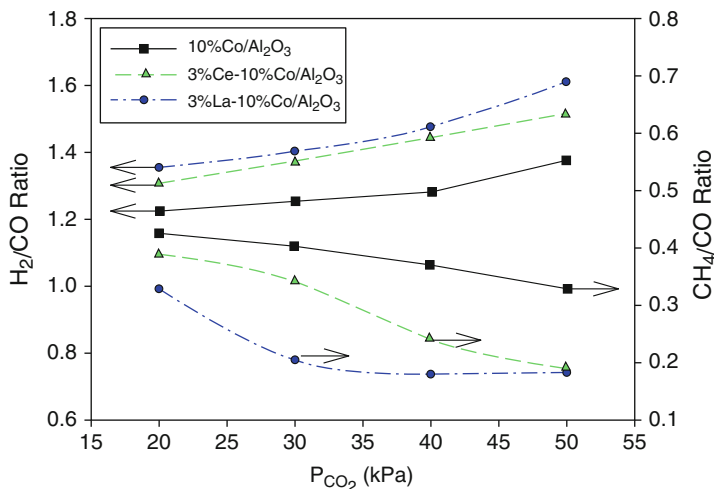


Fig. 8.11 Effect of P_{CO_2} on product ratio at $P_{C_2H_5OH} = 20$ kPa and $T = 973$ K

carbonaceous species (C_xH_{1-x} with $x \leq 1$) initially formed from CH_4 decomposition was gasified to CO and H_2 by CO_2 reactant. Thus, the utilization of CO_2 -excess feedstock could induce the rising rate of MDR reaction, which in turn reduces CH_4/CO ratio. Irrespective of P_{CO_2} , H_2/CO ratio varied from about 1.2 to 1.6 and declined in the order of 3%La-10%Co/Al₂O₃ > 3%Ce-10%Co/Al₂O₃ > 10%Co/Al₂O₃ catalysts.

8.3.5.3 Effect of Ethanol Partial Pressure

The influence of C_2H_5OH partial pressure on EDR performance was also studied at fixed P_{CO_2} of 20 kPa and varying $P_{C_2H_5OH}$ of 20–50 kPa and $T = 973$ K as seen in Fig. 8.12. Although both C_2H_5OH and CO_2 conversions for 3%La-10%Co/Al₂O₃ and 3%Ce-10%Co/Al₂O₃ catalysts were greater than those of 10%Co/Al₂O₃ catalyst regardless of $P_{C_2H_5OH}$, the decreasing reactant conversions with growing $P_{C_2H_5OH}$ was most likely due to the competing reactant adsorption effect in which the presence of excessive ethanol could hinder the access of CO_2 to catalyst surface and hence suppressing CO_2 adsorption. In addition, the same behaviour was evidenced for the yield of H_2 and CO for all catalysts further confirming the drop in EDR activity related to the hindrance of CO_2 adsorption in ethanol-rich feedstocks (Fig. 8.13).

8.3.6 Post-reaction Characterization

8.3.6.1 X-Ray Diffraction Measurements of Spent Catalysts

The crystalline structure of spent promoted and unpromoted catalysts after EDR reaction at $P_{CO_2} = P_{C_2H_5OH} = 20$ kPa and $T = 973$ K was also analysed by XRD measurements as seen in Fig. 8.14. Both promoted and unpromoted catalysts

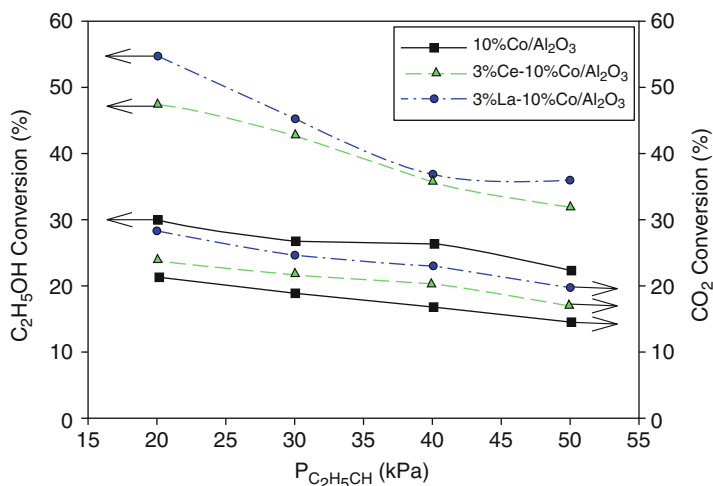


Fig. 8.12 Influence of $P_{C_2H_5OH}$ on C_2H_5OH and CO_2 conversions at $P_{CO_2} = 20$ kPa and $T = 973$ K

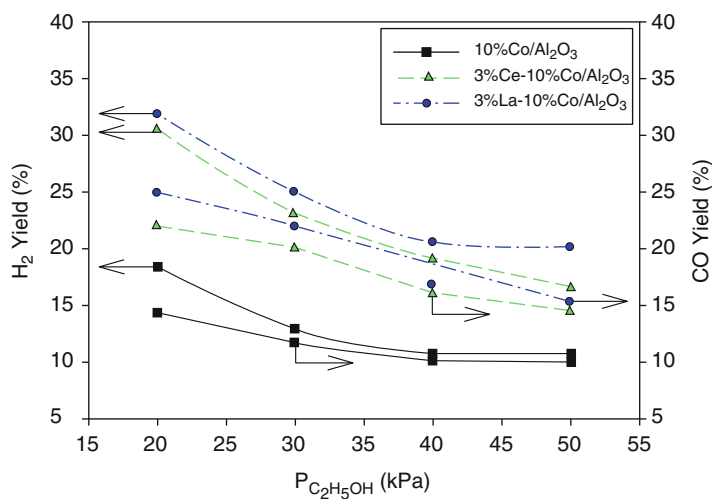


Fig. 8.13 Influence of $P_{C_2H_5OH}$ on H_2 and CO yields at $P_{CO_2} = 20$ kPa and $T = 973$ K

possessed a high-intensity peak centred at 2θ of 26.38° corresponding to graphitic carbon (JCPDS card No. 75-0444). The inevitable formation of graphite on catalyst surface was due to ethanol decomposition at the high reaction temperature. In comparison with XRD patterns of fresh catalysts (see Fig. 8.2), a new peak with low intensity was detected at $2\theta = 51.50^\circ$ for all spent catalysts. This characteristic peak could belong to metallic Co phase (JCPDS card No. 15-0806) generated during H_2 reduction (Homsí et al. 2014; Wu et al. 2014). However, the Co_3O_4 phase was

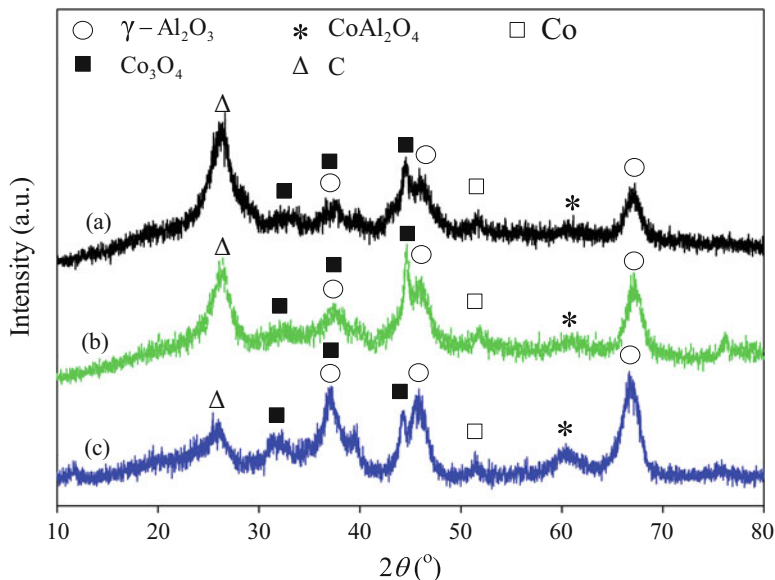


Fig. 8.14 XRD patterns of spent (a) 10%Co/Al₂O₃, (b) 3%Ce-10%Co/Al₂O₃ and (c) 3%La-10%Co/Al₂O₃ catalysts after EDR reaction at $P_{\text{CO}_2} = P_{\text{C}_2\text{H}_5\text{OH}} = 20$ kPa and $T = 973$ K

also detected for spent promoted and unpromoted catalysts probably due to the reoxidation of active metallic Co⁰ phase in the presence of CO₂ oxidizing agent during EDR reaction. The reoxidation of cobalt metallic form was also evidenced in MDR reaction over Co-based catalysts in other studies (Chen et al. 2010). Additionally, the typical peak for CeO₂ phase at 2θ of 28.57° was not detected on the spent Ce-promoted catalyst (cf. Fig. 8.14b) most likely owing to the overlapping of the broad graphitic peak.

8.3.6.2 Raman Spectroscopy Measurements

The Raman spectra of spent 10%Co/Al₂O₃, 3%Ce-10%Co/Al₂O₃ and 3%La-10%Co/Al₂O₃ catalysts obtained from EDR reaction at $P_{\text{CO}_2} = P_{\text{C}_2\text{H}_5\text{OH}} = 20$ kPa and $T = 973$ K are shown in Fig. 8.15. Two characteristic peaks belonging to D-band and G-band were detected at Raman shift of 1232.5–1430.5 cm⁻¹ and 1511.9–1679.7 cm⁻¹, respectively, for all spent promoted and unpromoted catalysts. Indeed, the D-band was related to the vibrations of sp³-bonded carbon (C–C) atoms of amorphous or filamentous carbons, whereas the G-band was attributed to sp² carbon bonding (C=C) of an ordered carbon structure (viz. graphite previously detected in XRD measurements as seen in Fig. 8.14) (Ferrari and Robertson 2000; Omeregbe et al. 2017). The presence of both D- and G-bands in Raman spectra of spent catalysts was indicative of heterogeneous nature of deposited carbon on the spent catalyst surface.

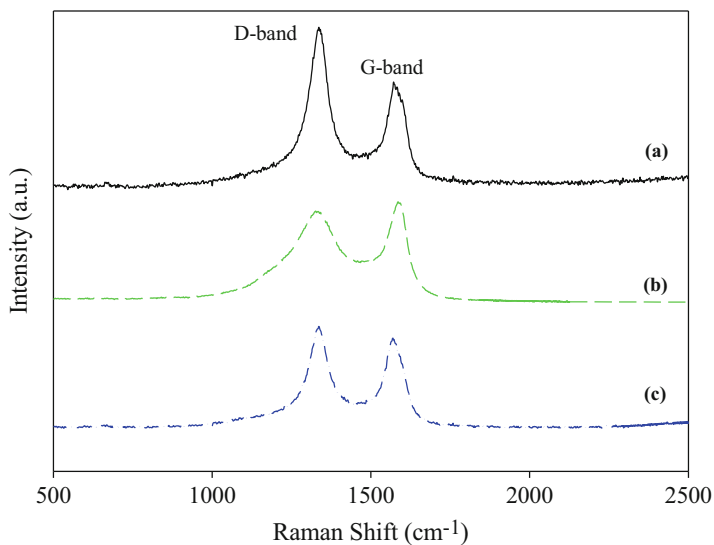


Fig. 8.15 The Raman spectra of spent (a) 10%Co/Al₂O₃, (b) 3%Ce-10%Co/Al₂O₃ and (c) 3%La-10%Co/Al₂O₃ catalysts after EDR reaction at $P_{\text{CO}_2} = P_{\text{C}_2\text{H}_5\text{OH}} = 20$ kPa and $T = 973$ K

8.3.6.3 Temperature-Programmed Oxidation Measurements

Although the type of deposited carbon (i.e. graphitic and amorphous carbons) on spent catalysts could be determined via Raman analysis, quantifying the amount of carbonaceous species by TPO measurements is essential for the justification of catalytic performance. Figure 8.16 shows the derivative weight profiles of spent promoted and unpromoted catalysts during TPO measurements. For all catalysts, the first oxidation peak, P1 located at low temperature region of 700–750 K, was due to the gasification of more reactive carbon, i.e. amorphous carbon, whilst the high-temperature peak (P2) observed at 750–850 K could belong to the elimination of less reactive graphitic carbon (Bartholomew 2001) in agreement with results from Raman analyses (see Fig. 8.15). Da Silva et al. (2011) also observed the heterogeneity of deposited carbon on spent EDR catalyst. Indeed, the amorphous or filamentous carbons were reportedly formed from the polymerization of intermediate ethylene generated from ethanol dehydration, whilst ethanol and methane decomposition could induce the formation of graphite or crystalline carbon (Zawadzki et al. 2014).

As seen in Fig. 8.16, spent 3%La-10%Co/Al₂O₃ catalyst possessed the lowest carbon content of 30.06% followed by Ce-promoted (31.16%) and unpromoted (51.49%) catalysts in line with estimated carbon from EDX measurements (cf. Table 8.4). The resistance to carbonaceous deposition of promoted catalysts was reasonably due to their smaller crystallite sizes (see Table 8.1). In fact, da Silva et al. (2014) also reported that the nucleation of coke and carbon sheets on catalyst surface preferred larger crystal sizes than 10 nm. La-promoted catalyst exhibiting the

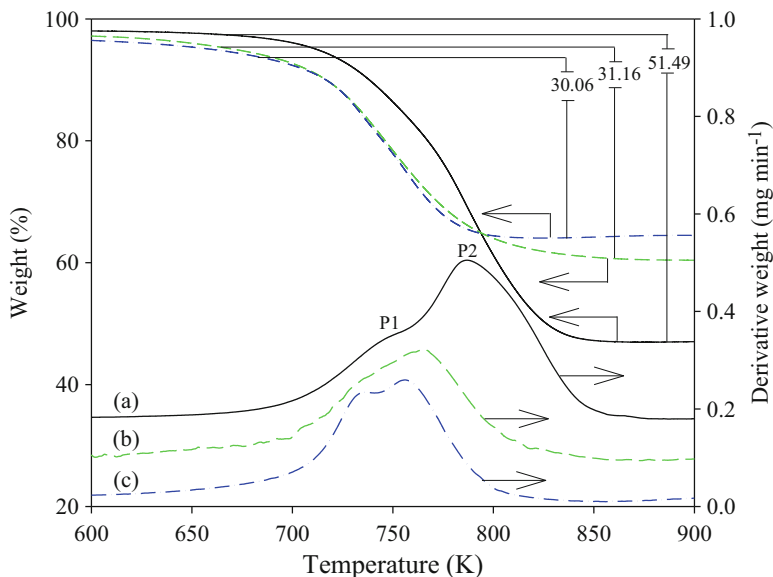
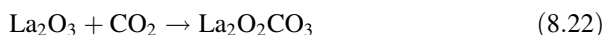


Fig. 8.16 Weight percentage and derivative weight profiles of spent (a) 10%Co/Al₂O₃, (b) 3%Ce-10%Co/Al₂O₃ and (c) 3%La-10%Co/Al₂O₃ catalysts after EDR reaction at $P_{\text{CO}_2} = P_{\text{C}_3\text{H}_5\text{OH}} = 20$ kPa and $T = 973$ K

Table 8.4 EDX measurements of spent Ce-, La-promoted and unpromoted 10%Co/Al₂O₃ catalysts

Element	Weight (%)		
	10%Co/Al ₂ O ₃	3%Ce-10%Co/Al ₂ O ₃	3%La-10%Co/Al ₂ O ₃
Carbon (C)	51.89	31.28	30.60
Oxygen (O)	23.09	24.15	20.71
Aluminium (Al)	15.36	31.84	36.17
Cobalt (Co)	9.66	10.15	9.90
Cerium (Ce)	–	2.58	–
Lanthanum (La)	–	–	2.62

highest carbon resistance was also due to the formation of intermediate lanthanum dioxycarbonate, La₂O₂CO₃. It is a stable compound that could in situ react with surface carbon to form CO and hence extend catalyst lifetime as seen in Eqs. 8.22 and 8.23 (Chen et al. 2010).



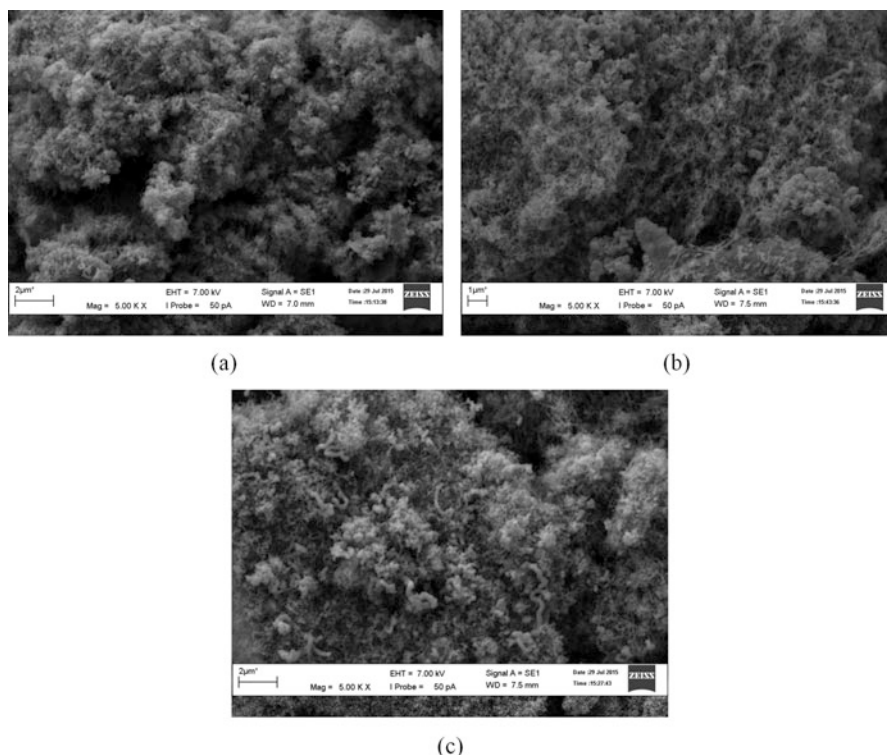
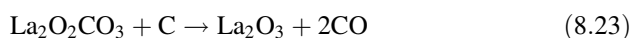


Fig. 8.17 SEM images of spent (a) 10%Co/Al₂O₃, (b) 3%Ce-10%Co/Al₂O₃ and (c) 3%La-10%Co/Al₂O₃ catalysts after EDR reaction at $P_{\text{CO}_2} = P_{\text{C}_2\text{H}_5\text{OH}} = 20$ kPa and $T = 973$ K

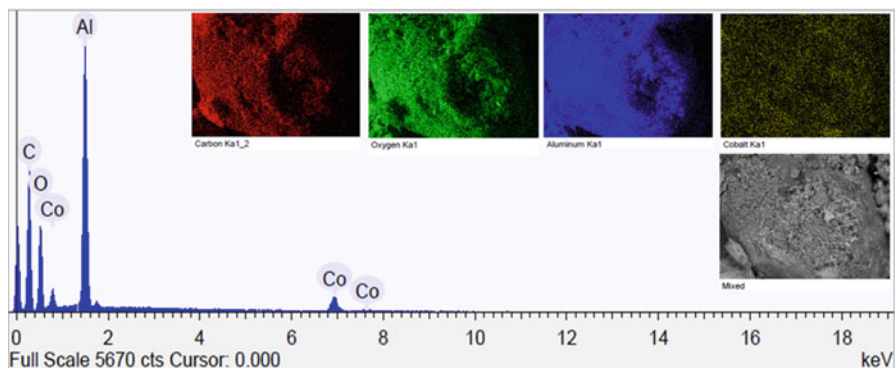
and



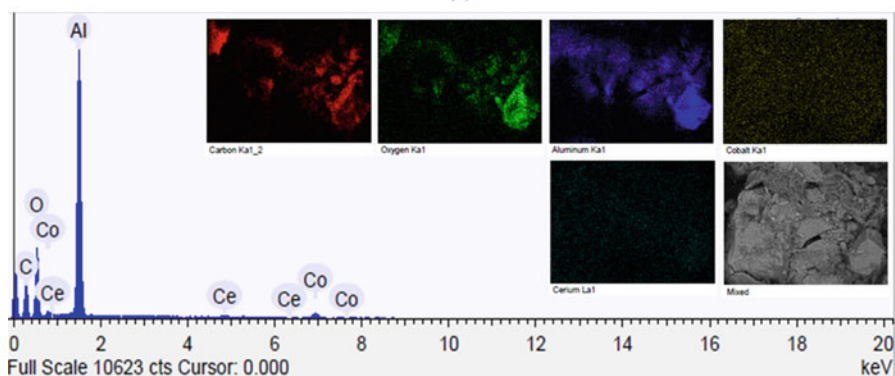
Additionally, the superior carbon resistance of Ce-doped catalyst to that of unpromoted catalyst could be assigned to the redox property of CeO₂ promoter. The high oxygen mobility of CeO₂ promoter could simultaneously eliminate deposited carbon formed from ethanol and methane decomposition reactions (Hou et al. 2015).

8.3.6.4 SEM-EDX Measurements

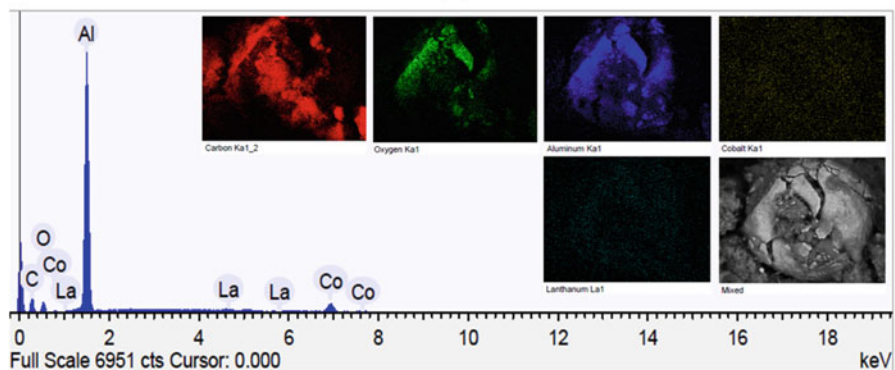
The morphology and elemental composition of spent catalysts were examined using SEM and EDX measurements, respectively. As seen in Fig. 8.17, SEM images of spent Ce- and La-promoted and unpromoted 10%Co/Al₂O₃ catalysts show the presence of carbon nanofilament (CNF) covering catalyst surface in agreement with results obtained from Raman and TPO measurements (see Figs. 8.15 and 8.16). The images of SEM-EDX metal mapping for the spent promoted and unpromoted catalysts are shown in Fig. 8.18. The dispersion of Co particles was



(a)



(b)



(c)

Fig. 8.18 SEM-EDX images of spent (a) 10%Co/Al₂O₃, (b) 3%Ce-10%Co/Al₂O₃ and (c) 3%La-10%Co/Al₂O₃ catalysts after EDR reaction at $P_{\text{CO}_2} = P_{\text{C}_2\text{H}_5\text{OH}} = 20$ kPa and $T = 973$ K

evidently better with the addition of CeO_2 and La_2O_3 promoters. As seen in Table 8.4, the elemental composition of Co, Ce and La metals estimated from EDX measurements was relatively close to the theoretically calculated catalyst composition prior to catalyst synthesis.

8.4 Conclusions

EDR evaluation was conducted in a quartz fixed-bed reactor using rare-earth metal-promoted $10\%\text{Co}/\text{Al}_2\text{O}_3$ catalysts at different $\text{CO}_2:\text{C}_2\text{H}_5\text{OH}$ ratios of 2.5:1–1:2.5 and varying reaction temperature from 923 to 973 K under atmospheric pressure. Increasing reaction temperature from 923 to 973 K enhanced the conversion of both $\text{C}_2\text{H}_5\text{OH}$ and CO_2 up to 150.6% and 55.5%, respectively, owing to the endothermic character of EDR reaction. Although both $\text{C}_2\text{H}_5\text{OH}$ and CO_2 conversions increased with rising CO_2 partial pressure from 20 to 50 kPa for all catalysts, the decline in reactant conversions was observed with growing partial pressure of $\text{C}_2\text{H}_5\text{OH}$ due to the competing reactant adsorption on catalyst surface in the presence of excessive ethanol. In EDR runs, H_2/CO ratio was always higher than unity due to the concomitant presence of ethanol dehydrogenation side reaction. Regardless of reaction conditions, La-promoted catalyst appeared to be the optimal catalyst in terms of $\text{C}_2\text{H}_5\text{OH}$ and CO_2 conversions. Reactant conversions of catalysts increased in the order $10\%\text{Co}/\text{Al}_2\text{O}_3 < 3\%\text{Ce}-10\%\text{Co}/\text{Al}_2\text{O}_3 < 3\%\text{La}-10\%\text{Co}/\text{Al}_2\text{O}_3$ catalysts for all operating conditions. This observation could be due to the increasing basic property, H_2 reduction degree and metal dispersion with the addition of rare-earth promoters. Although both amorphous and graphitic carbons were inevitably formed on spent catalyst surface due to high reaction temperature employed, the addition of La and Ce promoters reduced the formation of deposited carbon from 51.49% to 30.06%.

Acknowledgements The authors are grateful for the financial support from UMP Research Grant Scheme (RDU160323) for conducting this research. Fahim Fayaz is also thankful for the Graduate Research Scheme Award (GRS) from Universiti Malaysia Pahang (UMP).

References

- Abdullah B, Ghani NAA, Vo D-VN (2017) Recent advances in dry reforming of methane over Ni-based catalysts. *J Clean Prod* 162:170–185. <https://doi.org/10.1016/j.jclepro.2017.05.176>
- Bahari MB, Phuc NHH, Abdullah B, Alenazey F, Vo D-VN (2016) Ethanol dry reforming for syngas production over Ce-promoted $\text{Ni}/\text{Al}_2\text{O}_3$ catalyst. *J Environ Chem Eng* 4:4830–4838. <https://doi.org/10.1016/j.jece.2016.01.038>
- Bahari MB, Phuc NHH, Alenazey F, Vu KB, Ainirazali N, Vo D-VN (2017) Catalytic performance of La-Ni/ Al_2O_3 catalyst for CO_2 reforming of ethanol. *Catal Today* 291:67–75. <https://doi.org/10.1016/j.cattod.2017.02.019>
- Bartholomew CH (2001) Mechanisms of catalyst deactivation. *Appl Catal A Gen* 212:17–60. [https://doi.org/10.1016/S0926-860X\(00\)00843-7](https://doi.org/10.1016/S0926-860X(00)00843-7)

- Bartholomew CH, Farrauto RJ (2005) Fundamentals of industrial catalytic processes, 2nd edn. Wiley, New York, pp 151–152
- Batista MS, Santos RKS, Assaf EM, Assaf JM, Ticianelli EA (2003) Characterization of the activity and stability of supported cobalt catalysts for the steam reforming of ethanol. *J Power Sources* 124:99–103. [https://doi.org/10.1016/S0378-7753\(03\)00599-8](https://doi.org/10.1016/S0378-7753(03)00599-8)
- Bellido JDA, Tanabe EY, Assaf EM (2009) Carbon dioxide reforming of ethanol over Ni/Y₂O₃–ZrO₂ catalysts. *Appl Catal B Environ* 90:485–488. <https://doi.org/10.1016/j.apcatb.2009.04.009>
- Bimbela F, Ábrego J, Puerta R, García L, Arauzo J (2017) Catalytic steam reforming of the aqueous fraction of bio-oil using Ni-Ce/Mg-Al catalysts. *Appl Catal B Environ* 209:346–357. <https://doi.org/10.1016/j.apcatb.2017.03.009>
- Budiman AW, Song SH, Chang TS, Shin CH, Choi MJ (2012) Dry reforming of methane over cobalt catalysts: a literature review of catalyst development. *Catal Surv Jpn* 16:183–197. <https://doi.org/10.1007/s10563-012-9143-2>
- Chen L, Zhu Q, Hao Z, Zhang T, Xie Z (2010) Development of a Co–Ni bimetallic aerogel catalyst for hydrogen production via methane oxidative CO₂ reforming in a magnetic assisted fluidized bed. *Int J Hydrogen Energy* 35:8494–8502. <https://doi.org/10.1016/j.ijhydene.2010.06.003>
- Cheng CK, Foo SY, Adesina AA (2010) H₂-rich synthesis gas production over Co/Al₂O₃ catalyst via glycerol steam reforming. *Catal Commun* 12:292–298. <https://doi.org/10.1016/j.catcom.2010.09.018>
- Cooper CG, Nguyen TH, Lee YJ, Hardiman KM, Safinski T, Lucien FP, Adesina AA (2008) Alumina-supported cobalt-molybdenum catalyst for slurry phase Fischer-Tropsch synthesis. *Catal Today* 131:255–261. <https://doi.org/10.1016/j.cattod.2007.10.056>
- da Silva AM, de Souza KR, Jacobs G, Graham UM, Davis BH, Mattos LV, Noronha FB (2011) Steam and CO₂ reforming of ethanol over Rh/CeO₂ catalyst. *Appl Catal B Environ* 102:94–109. <https://doi.org/10.1016/j.apcatb.2010.11.030>
- da Silva ALM, den Breejen JP, Mattos LV, Bitter JH, de Jong KP, Noronha FB (2014) Cobalt particle size effects on catalytic performance for ethanol steam reforming – smaller is better. *J Catal* 318:67–74. <https://doi.org/10.1016/j.jcat.2014.07.020>
- Drif A, Bion N, Brahmi R, Ojala S, Pirault-Roy L, Turpeinen E, Seelam PK, Keiski RL, Epron F (2015) Study of the dry reforming of methane and ethanol using Rh catalysts supported on doped alumina. *Appl Catal A Gen* 504:576–584. <https://doi.org/10.1016/j.apcata.2015.02.019>
- e Santos MAF, Lôbo IP, da Cruz RS (2014) Synthesis and characterization of Novel ZrO₂–SiO₂ mixed oxides. *Mater Res* 17:700–707. <https://doi.org/10.1590/S1516-14392014005000046>
- Fayaz F, Danh HT, Nguyen-Huy C, Vu KB, Abdullah B, Vo D-VN (2016) Promotional effect of Ce-dopant on Al₂O₃-supported Co catalysts for syngas production via CO₂ reforming of ethanol. *Procedia Eng* 148:646–653. <https://doi.org/10.1016/j.proeng.2016.06.530>
- Ferrari A, Robertson J (2000) Interpretation of Raman spectra of disordered and amorphous carbon. *Phys Rev B Condens Matter* 61:14095–14107. <https://doi.org/10.1103/PhysRevB.61.14095>
- Firoozi M, Baghalha M, Asadi M (2009) The effect of micro and nano particle sizes of H-ZSM-5 on the selectivity of MTP reaction. *Catal Commun* 10:1582–1585. <https://doi.org/10.1016/j.catcom.2009.04.021>
- Foo SY, Cheng CK, Nguyen TH, Adesina AA (2011) Evaluation of lanthanide-group promoters on Co-Ni/Al₂O₃ catalysts for CH₄ dry reforming. *J Mol Catal A Chem* 344:28–36. <https://doi.org/10.1016/j.molcata.2011.04.018>
- Homsí D, Aouad S, Gennequin C, Aboukaïs A, Abi-Aad E (2014) A highly reactive and stable Ru/Co_{6-x}Mg_xAl₂ catalyst for hydrogen production via methane steam reforming. *Int J Hydrogen Energy* 39:10101–10107. <https://doi.org/10.1016/j.ijhydene.2014.04.151>
- Hou T, Zhang S, Chen Y, Wang D, Cai W (2015) Hydrogen production from ethanol reforming: catalysts and reaction mechanism. *Renew Sust Energ Rev* 44:132–148. <https://doi.org/10.1016/j.rser.2014.12.023>
- Hu X, Lu H (2009) Syngas production by CO₂ reforming of ethanol over Ni/Al₂O₃ catalyst. *Catal Commun* 10:1633–1637. <https://doi.org/10.1016/j.catcom.2009.04.030>

- Hull S, Trawczynski J (2014) Steam reforming of ethanol on zinc containing catalysts with spinel structure. *Int J Hydrogen Energy* 39:4259–4265. <https://doi.org/10.1016/j.ijhydene.2013.12.184>
- Jabbour K, Hassan NE, Casale S, Estephane J, Zakhem HE (2014) Promotional effect of Ru on the activity and stability of Co/SBA-15 catalysts in dry reforming of methane. *Int J Hydrogen Energy* 39:7780–7787. <https://doi.org/10.1016/j.ijhydene.2014.03.040>
- Jankhah S, Abatzoglou N, Gitzhofer F (2008) Thermal and catalytic dry reforming and cracking of ethanol for hydrogen and carbon nanofilaments' production. *Int J Hydrogen Energy* 33:4769–4779. <https://doi.org/10.1016/j.ijhydene.2008.06.058>
- JCPDS Powder Diffraction File, International Centre for Diffraction Data (2000) Swarthmore
- Kumar A, Bhosale RR, Malik SS, Abusrafa AE, Saleh MAH, Ghosh UK, Al-Marri MJ, Almomani FA, Khader MM, Abu-Reesh IM (2016) Thermodynamic investigation of hydrogen enrichment and carbon suppression using chemical additives in ethanol dry reforming. *Int J Hydrogen Energy* 41:15149–15157. <https://doi.org/10.1016/j.ijhydene.2016.06.157>
- Maia TA, Assaf JM, Assaf EM (2014) Study of Co/CeO₂- γ -Al₂O₃ catalysts for steam and oxidative reforming of ethanol for hydrogen production. *Fuel Process Technol* 128:134–145. <https://doi.org/10.1016/j.fuproc.2014.07.009>
- Manfro RL, Da Costa AF, Ribeiro NFP, Souza MMVM (2011) Hydrogen production by aqueous-phase reforming of glycerol over nickel catalysts supported on CeO₂. *Fuel Process Technol* 92:330–335. <https://doi.org/10.1016/j.fuproc.2010.09.024>
- Mazumder J, de Lasa H (2014) Fluidizable Ni/La₂O₃- γ -Al₂O₃ catalyst for steam gasification of a cellulosic biomass surrogate. *Appl Catal B Environ* 160–161:67–79. <https://doi.org/10.1016/j.apcatb.2014.04.042>
- Montini T, Singh R, Das P, Lorenzut B, Bertero N, Riello P, Benedetti A, Giambastiani G, Bianchini C, Zinoviev S, Miertus S, Fornasiero P (2010) Renewable H₂ from glycerol steam reforming: effect of La₂O₃ and CeO₂ addition to Pt/Al₂O₃ catalysts. *ChemSusChem* 3:619–628. <https://doi.org/10.1002/cssc.200900243>
- Moraes TS, Neto RCR, Ribeiro MC, Mattos LV, Kourtelesis M, Verykios X, Noronha FB (2015) Effects of ceria morphology on catalytic performance of Ni/CeO₂ catalysts for low temperature steam reforming of ethanol. *Top Catal* 58:281–294. <https://doi.org/10.1007/s11244-015-0369-x>
- Nanda S, Rana R, Zheng Y, Kozinski JA, Dalai AK (2017) Insights on pathways for hydrogen generation from ethanol. *Sustain Energy Fuels* 1:1232–1245. <https://doi.org/10.1039/C7SE00212B>
- Ni M, Leung DYC, Leung MKH (2007) A review on reforming bio-ethanol for hydrogen production. *Int J Hydrogen Energy* 32:3238–3247. <https://doi.org/10.1016/j.ijhydene.2007.04.038>
- Ogo S, Shimizu T, Nakazawa Y, Mukawa K, Mukai D, Sekine Y (2015) Steam reforming of ethanol over K promoted Co catalyst. *Appl Catal A Gen* 495:30–38. <https://doi.org/10.1016/j.apcata.2015.01.018>
- Omorgbe O, Danh HT, Nguyen-Huy C, Setiabudi HD, Abidin SZ, Truong QD, Vo D-VN (2017) Syngas production from methane dry reforming over Ni/SBA-15 catalyst: effect of operating parameters. *Int J Hydrogen Energy* 42:11283–11294. <https://doi.org/10.1016/j.ijhydene.2017.03.146>
- Osorio-Vargas P, Flores-González NA, Navarro RM, Fierro JLG, Campos CH, Reyes P (2016) Improved stability of Ni/Al₂O₃ catalysts by effect of promoters (La₂O₃, CeO₂) for ethanol steam-reforming reaction. *Catal Today* 259:27–38. <https://doi.org/10.1016/j.cattod.2015.04.037>
- Papageridis KN, Siakavelas G, Charisiou ND, Avraam DG, Tzounis L, Kousi K, Goula MA (2016) Comparative study of Ni, Co, Cu supported on γ -alumina catalysts for hydrogen production via the glycerol steam reforming reaction. *Fuel Process Technol* 152:156–175. <https://doi.org/10.1016/j.fuproc.2016.06.024>
- Patterson AL (1939) The Scherrer formula for I-Ray particle size determination. *Phys Rev* 56:978–982. <https://doi.org/10.1103/PhysRev.56.978>

- Shahirah MNN, Gim bun J, Ideris A, Khan MR, Cheng CK (2017) Catalytic pyrolysis of glycerol into syngas over ceria-promoted Ni/ α -Al₂O₃ catalyst. *Renew Energy* 107:223–234. <https://doi.org/10.1016/j.renene.2017.02.002>
- Sharma A, Saito I, Nakagawa H, Miura K (2007) Effect of carbonization temperature on the nickel crystallite size of a Ni/C catalyst for catalytic hydrothermal gasification of organic compounds. *Fuel* 86:915–920. <https://doi.org/10.1016/j.fuel.2006.11.001>
- Sirisriwat N, Therdthianwong S, Therdthianwong A (2009) Oxidative steam reforming of ethanol over Ni/Al₂O₃ catalysts promoted by CeO₂, ZrO₂ and CeO₂-ZrO₂. *Int J Hydrogen Energy* 34:2224–2234. <https://doi.org/10.1016/j.ijhydene.2008.12.058>
- Usman M, Wan Daud WMA, Abbas HF (2015) Dry reforming of methane: influence of process parameters – a review. *Renew Sust Energ* 45:710–744. <https://doi.org/10.1016/j.rser.2015.02.026>
- Ven vik HJ, Yang J (2017) Catalysis in microstructured reactors: short review on small-scale syngas production and further conversion into methanol, DME and Fischer-Tropsch products. *Catal Today* 285:135–146. <https://doi.org/10.1016/j.cattod.2017.02.014>
- Vicente J, Montero C, Ereña J, Azkoiti MJ, Bilbao J, Gayubo AG (2014) Coke deactivation of Ni and Co catalysts in ethanol steam reforming at mild temperatures in a fluidized bed reactor. *Int J Hydrogen Energy* 39:12586–12596. <https://doi.org/10.1016/j.ijhydene.2014.06.093>
- Vo D-VN, Adesina AA (2012) A potassium-promoted Mo carbide catalyst system for hydrocarbon synthesis. *Cat Sci Technol* 2:2066. <https://doi.org/10.1039/c2cy20385e>
- Wang W, Wang Y (2009) Dry reforming of ethanol for hydrogen production: thermodynamic investigation. *Int J Hydrogen Energy* 34:5382–5389. <https://doi.org/10.1016/j.ijhydene.2009.04.054>
- Wu Z-Y, Chen P, Wu Q-S, Yang L-F, Pan Z, Wang Q (2014) Co/Co₃O₄/C-N a novel nanostructure and excellent catalytic system for the oxygen reduction reaction. *Nano Energy* 8:118–125. <https://doi.org/10.1016/j.nanoen.2014.05.019>
- Yang R, Xing C, Lv C, Shi L, Tsubaki N (2010) Promotional effect of La₂O₃ and CeO₂ on Ni/ γ -Al₂O₃ catalysts for CO₂ reforming of CH₄. *Appl Catal A Gen* 385:92–100. <https://doi.org/10.1016/j.apcata.2010.06.050>
- Yang J, Ma W, Chen D, Holmen A, Davis BH (2014) Fischer–Tropsch synthesis: a review of the effect of CO conversion on methane selectivity. *Appl Catal A Gen* 470:250–260. <https://doi.org/10.1016/j.apcata.2013.10.061>
- Zawadzki A, Bellido JDA, Lucrédio AF, Assaf EM (2014) Dry reforming of ethanol over supported Ni catalysts prepared by impregnation with methanolic solution. *Fuel Process Technol* 128:432–440. <https://doi.org/10.1016/j.fuproc.2014.08.006>
- Zhang W, Burckle EC, Smirniotis PG (1999) Characterization of the acidity of ultrastable Y, mordenite, and ZSM-12 via NH₃-stepwise temperature programmed desorption and Fourier transform infrared spectroscopy. *Microporous Mesoporous Mater* 33:173–185. [https://doi.org/10.1016/S1387-1811\(99\)00136-5](https://doi.org/10.1016/S1387-1811(99)00136-5)
- Zhao S, Cai W, Li Y, Yu H, Zhang S, Cui L (2017) Syngas production from ethanol dry reforming over Rh/CeO₂ catalyst. *J Saudi Chem Soc*. <https://doi.org/10.1016/j.jscs.2017.07.003>
- Zhi G, Guo X, Wang Y, Jin G, Guo X (2011) Effect of La₂O₃ modification on the catalytic performance of Ni/SiC for methanation of carbon dioxide. *Catal Commun* 16:56–59. <https://doi.org/10.1016/j.catcom.2011.08.037>



High-Temperature Conversion of Fats: Cracking, Gasification, Esterification, and Transesterification

Federico Galli, Nicolas A. Patience, and Daria C. Boffito

Abstract

Burning fossil fuels increases the concentration of carbon dioxide in the atmosphere. Alternative sources of energy are necessary to control global warming. Diverse synthetic methods transform vegetable oils, animal fats and inexpensive carbon sources to biofuels. This chapter reviews the main chemical and thermal processes that transform triglycerides into fuels. We collected the most cited and recent scientific publications about high-temperature transesterification, thermal and catalytic cracking, and gasification reactions and their respective technologies.

Keywords

Vegetable oil · Animal fat · Biofuel · Thermal conversion · Cracking · Transesterification · Esterification · Gasification · Catalysis · Reactor design

9.1 Introduction

Fossil fuel depletion, global warming, and marketing push companies and researchers to develop renewable energies (Demirbas 2007a). Biofuels can be derived from animal and vegetable sources. Vegetables consume CO₂ to grow; thus their adoption as a source of biofuel has ideally a hypothetical null contribution to greenhouse gas emissions. Shonnard et al. (2015) reviewed the most recent studies

F. Galli · N. A. Patience · D. C. Boffito (✉)

Department of Chemical Engineering, Polytechnique Montréal, Montréal, Québec, Canada

e-mail: daria-camilla.boffito@polymtl.ca

© Springer Nature Singapore Pte Ltd. 2018

P. K. Sarangi et al. (eds.), *Recent Advancements in Biofuels and Bioenergy Utilization*, https://doi.org/10.1007/978-981-13-1307-3_9

205

about life cycle assessment of biofuel production. Even though there is the need to develop common frameworks to assess biofuel impact (because depending on the lifecycle analysis (LCA) model different conclusions are obtained), in general, all models predict from 35% to 50% less greenhouse gas emissions.

Biofuels are classified into three categories: first-, second-, and third-generation. Those derived from vegetable oils (soybean, canola, sunflower, etc.) and animal fats are first-generation biofuels. The technology to treat these feedstocks is known and present at the commercial level. Energy derived from nonedible feedstock is classified as second generation (Naik et al. 2010). These biofuels are less socioeconomically concerning since there is no competition with the food supply chain and are gradually replacing first-generation biomass (Azad et al. 2016). The European Biodiesel Board estimates that by 2050, second-generation crops will sustain 50% of biodiesel production (Pilzecker 2011). The third-generation biofuels are mostly algae-based. Despite their advantages, such as a low water footprint and low land use (Havlík et al. 2011), the cost of production makes commercial scale-up unfeasible (Quereshi et al. 2017).

The main processes for raw biomass transformation rely on thermolysis or chemical treatments. Pyrolysis and cracking are the main processes to treat oil or fat and yield short- and long-chain hydrocarbons, as well as oxygenated compounds like alcohol or esters. Esterification and transesterification are the main chemical routes adopted and yield fatty acid alkyl esters of different natures, depending on the alcohol used.

In the topic field of Web of Science Core Collection, between 1985 and 2017, we selected the keyword “vegetable oil” or “animal fat” and “pyrolysis” or “esterification” or “transesterification” or “cracking.” Nearly 44% of the 4179 documents were published between 2013 and 2017. Publications increased steadily and stabilized to 390 per year (Fig. 9.1).

The USA, India, and Brazil contributed 34% of the papers. The USA and Brazil were the leading fatty acid methyl ester producers in 2016 (Statista.com 2017), while India is one of the most promising developing countries.

This chapter reviews the technology used to transform first- and second-generation sources into fuels. We focused on certain high-temperature reactions.

9.2 Chemical Modification: Esterification and Transesterification

Oils and fats are triglycerides, i.e. glycerol esterified with various linear long-chain acids (fatty acid, from 12 to 24 carbon atoms in the main chain). Ma and Hanna reported the fatty acid composition of 12 main sources of oil and fats (Ma and Hanna 1999).

Triglycerides cannot be injected into engines because they are too viscous and nonvolatile. Fort and Blumberg (1982) have demonstrated that after 200 h of

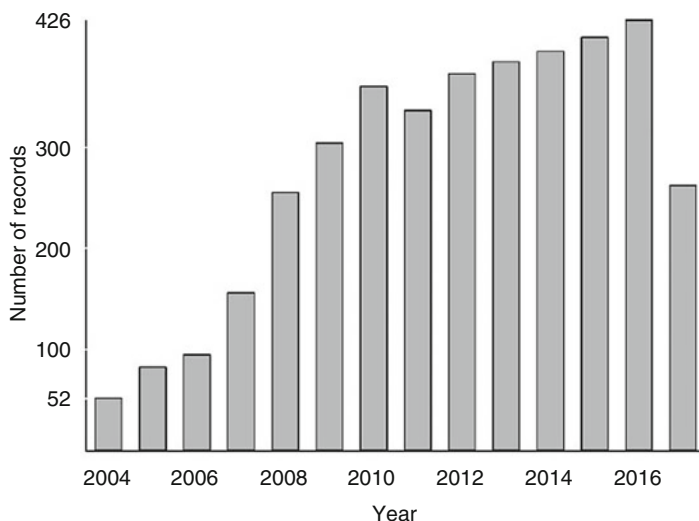


Fig. 9.1 Scientific publications on biofuels prepared by high-temperature conversion of fats and oils

operation, an engine powered by various blends of diesel and cottonseed oil formed carbon and gum substances in the combustion chamber lowering performance. Prior to transesterification, a pretreatment removes free fatty acids (FFA) from oil.

Several deacidification treatments exist. Bhosle and Subramanian (2005) reviewed chemical and physical deacidification methods (Table 9.1).

After deacidification, oil is transesterified with a short-chain alcohol to give biodiesel (fatty acid methyl esters, FAME). Asakuma et al. (2009) demonstrated, by quantum computational chemical models, that the influence of the acidic composition does not affect the triglyceride reactivity. They identified a mechanism by which a pentagonal ring intermediate forms between triglyceride and alcohol. Moreover, activation energy analysis demonstrated that the first bond to be esterified is the central one. Diasakou et al. (1998) studied the non-catalyzed transesterification of soybean oil at different oil/alcohol molar ratios. The reaction followed a first-order kinetic for each component, and monoglycerides did not react. In 1 h, with temperatures between 220 and 235 °C at 55 and 62 bar, triglycerides converted to monoglycerides.

A catalyst is necessary to reduce the operative temperature and pressure and to make the process economical. Catalysts are either homogeneous or heterogeneous.

Alcohol transesterifies triglycerides in the presence of basic or acid catalysts (Fig. 9.2). Acids are three orders of magnitude less efficient than basic catalysts in the transesterification reaction, but free fatty acids (FFAs) contained in oil do not affect their performances, while in a process that uses a basic catalyst, a proper deacidification eliminates them.

Table 9.1 Oil deacidification technologies

Deacidification	Technology	Advantages and disadvantages
Chemical	Alkali solution removes FFA by forming soap, which is then mechanically separated	Most oil is transesterified and soap is hard to remove. However, it is the most applied since this method permits to reach a FFA content lower than 0.5% (Shahidi 2005)
Physical	Vacuum steam stripping of FFA	Low investment costs (Cvengros 1995) and more efficient than chemical deacidification, but high vacuum and temperature favor side reaction such as trans isomerization and polymerization (Sengupta and Bhattacharyya 1992)
Miscella	Hexane dilutes crude vegetable oil and then alkali react with FFA	Low alkali concentration gives satisfactory result. Water washing is eliminated
Biological	Cell or enzymes metabolizes FFA	Linoleic acid and short-chain FFA are inhibitors
Pre-esterification	Catalytic esterification of FFA	Higher biodiesel yield, heterogeneous catalysts can be separated easily. It requires over 2 h (Pirola et al. 2014a, b)

Bhosle and Subramanian (2005), Copyright (2004), with permission from Elsevier

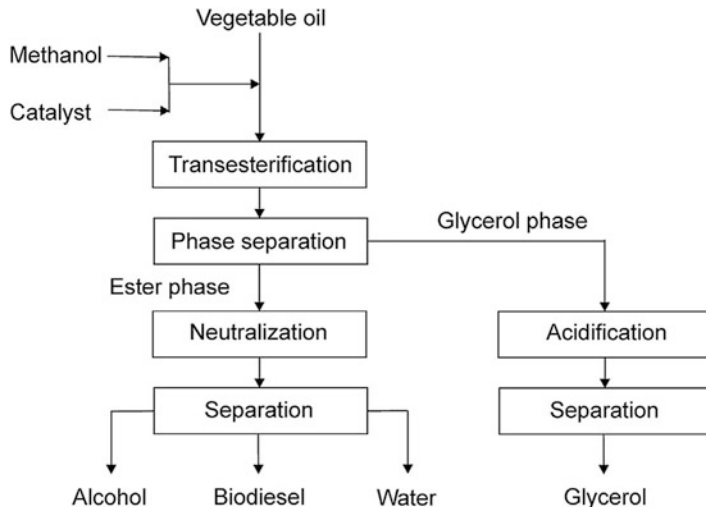


Fig. 9.2 General scheme of vegetable oil or fat transesterification. Catalyst is either a strong base or an acid. (Reprinted with permission from Elsevier. Stojković et al. 2014)

Table 9.2 Kinetic parameters of oil transesterification

Oil	Best conditions	Kinetic parameters (Arrhenius model)	References
Waste cooking oil	Methanol/oil volume ratio of 3:7. Sodium hydroxide as catalyst (1% by weight)	$k = 0.008 \text{ min}^{-1}$ $E_a = 88.8 \text{ kJ mol}^{-1}$	Jain et al. (2011)
<i>Jatropha</i> oil	Methanol/oil volume ratio of 3:7. Sodium hydroxide as catalyst (1% by weight)	$k = 0.008 \text{ min}^{-1}$ $E_a = 87.8 \text{ kJ mol}^{-1}$	Jain and Sharma (2010)
<i>Spirulina platensis</i> algae oil	1:4 algae biomass to methanol ratio (w/v). Sulfuric acid as catalyst (60% by weight)	$k = 0.001 \text{ min}^{-1}$ $E_a = 14.5 \text{ kJ mol}^{-1}$	Nautiyal et al. (2014)
Waste cooking oil	9:1 methanol/oil molar ratio. KOH as catalyst (0.7% by weight)	$k = 0.054\text{--}0.099 \text{ min}^{-1}$ $E_a = 21.9 \text{ kJ mol}^{-1}$	Encinar et al. (2016)

The transesterification is carried out in batch or continuous reactor (Go et al. 2016; Navarro-Pineda et al. 2016; Dash and Lingfa 2017). The commercial plants use sodium and potassium methanolate (Markolwitz 2004). In North America, Vertellus Specialities and InChem Corp are the main producers of these basic homogeneous catalysts.

A single triglyceride \rightarrow FAME mechanism simplifies the kinetic analysis of transesterification. Verma and Sharma collected the kinetic parameters for the transesterification of diverse oils (Verma and Sharma 2016) (Table 9.2).

Nowadays, research on transesterification focuses on heterogeneous catalysts and recycling waste oils. The latter, even if they need severe pretreatment, are inexpensive and do not pose any ethical problems with the food chain competition. On the other hand, heterogeneous catalysts are easily recoverable and less corrosive than homogeneous catalysts (Helwani et al. 2009). Mardihah et al. (2017) reviewed state-of-the-art biodiesel production processes. Strong Brønsted acid catalysts like sulfated zirconia (Mardhiah et al. 2017), sulfated titania, or strong cation exchange resins (Pirola et al. 2014a, b) catalyze the esterification reaction (Alaba et al. 2016). An alternative to this type of Brønsted acid catalyst is titanate (Siling and Laricheva 1996). Titanates converted more than 95% of FFA into FAME.

Basic solids are moist and have an affinity for water but could reach high triglyceride conversion and FAME yield. CaO is one of the most used catalysts for heterogeneous transesterification. It converted 93% of *Jatropha* oil at 70 °C in 2.5 h with a methanol/oil molar ratio of nine (Zhu et al. 2006). Methanol solubility in oil (6–8% by weight) (Boffito et al. 2014a, b) makes the mass transfer limitation a problem, due to the low concentration of methanol in triglycerides that is thermodynamically set at a certain temperature.

Galli et al. (2015) overcame the problem of methanol and oil immiscibility using a cosolvent. They tested various solvents, namely, acetone, tetrahydrofuran, ethyl acetate, chloroform, dichloromethane, and n-heptane. The methanol/oil molar ratio was 12 and the mass fraction of the catalyst was 2.5%. Tetrahydrofuran and ethyl acetate combined with CaO yielded full oil conversion in 2 h at 60 °C. Moreover, glycerol is not soluble in tetrahydrofuran: it formed a second liquid phase that was easy to recover.

Singh et al. (2017) reacted waste vegetable oil with methanol and calcium aluminum oxide ($\text{Ca}_2\text{Al}_2\text{O}_5$). Acetone was the cosolvent. After 25 min at reflux (55 °C), the FAME yield was 98%. Furthermore, catalyst activity decreased linearly due to initial oil acidity but converted more than 75% of the oil after eight runs.

Non-catalytic transesterification is possible at high pressure and temperature (>250 °C and >78.5 bar), i.e., over methanol's critical point. At these conditions, the solubility of methanol in oil increases, and reaction rates increase since they depend exponentially on temperature. Garcia-Martinez et al. (2017) transesterified tobacco oil in 90 min at 300 °C. However, the reaction was difficult to control: temperatures of 325 °C decomposed the oil. Glycerol degraded and reacted with FAME to give oxygenated compounds. Even though no catalyst is necessary and any kind of oil reacts within 1–2 h, a simulation study done by Marchetti and Errazu (2008) demonstrated that supercritical transesterification is economically unfeasible.

Glycerol is the main coproduct of biodiesel synthesis. For each kg of FAME, about 0.1 kg of glycerol is formed. Its cost reduced drastically due to overproduction. Glycerol is an additive in the cosmetic industry, but it has also been used as a carbon source for the microbiology industry (da Silva et al. 2009). Moreover, depending on its technical grade, glycerol can become a building block for diverse molecules or it can be used to feed animals (Yang et al. 2012) (Table 9.3).

The technologies for its purification and use as chemical or building block are out of the scope of this chapter, but Ardi et al. (2015) and Tan et al. (2013) have reviewed and cataloged the technologies regarding the reuse of glycerol.

9.3 Thermal Modification: Cracking and Pyrolysis

Cracking consists of breaking the molecule(s) with a radical or a catalytic reaction. Thermal cracking leads to a radical reaction network, while the catalytic process proceeds with the formation of carbocation species. The first thermal cracking unit was invented in 1912 and used to convert oil to increase gasoline yield (Alfke et al. 2007). When thermal cracking is carried out in an inert atmosphere, i.e., without oxygen and halogens, the process is named pyrolysis. Cracking produces three fractions of products: gases, liquids, and chars. The liquid fraction is maximized by adjusting the operative parameters. Chars and gases are usually burned to recover energy.

Table 9.3 Application (or possible application) of glycerol derived by transesterification reaction

Field of application	New applications of glycerol	Remarks
Chemical industry	Textile industry, plastic industry, explosives industry, polymer industry	Lubricant, sizer, and softener of yarn and fabric. Production of nitroglycerine comonomer for polyester production (coatings or spray) (Pagliaro et al. 2007; Yang et al. 2012)
Commodity chemicals	Natural organic building blocks	Synthesis of acrolein, methacrylic acid, 1,3-propanediol, and antifogging additives (Wang et al. 2003; Edake et al. 2017)
Pharmaceutical and oral care	Additive in drugs, heart disease drugs, love potion, health supplements, cosmetics, tanning agent	Additive in toothpaste and health-care products. Carrier for antibiotics
Food	Safe sweeteners, preservation, thickening agent	Margarine thickener and sweetener in low-fat foods
Livestock feed	Cow and other animals feed, pigs diet, poultry feed	Cows, pigs, and chickens (DeFrain et al. 2004)
Energy as fossil fuel substitution and biogas	Liquid fuel, conversion into ethanol or hydrogen, burning as fuel pellets, combustion in incinerators, combustion as boiler fuel	Steam reforming (Takeshi Ito et al. 2005), anaerobic conversion, fuel (Johnson and Taconi 2007)
Biotechnology	Organic acid, omega-3, succinic acid by fermentation, EPA by fungus	Fermentation routes to citric acid (Papanikolaou and Aggelis 2002) and acetic, butyric, lactic, and succinic acid (Lee et al. 2001)
Miscellaneous	Basic materials, hydraulic and fire-resistant fluid, de-icing aircraft, thermochemical products	Formulant in powders, adhesives, lubricants, solvents, and antifreeze liquids

Reprinted from with permission from Elsevier. Ayoub and Abdullah (2012)

Generally, thermal cracking units operate at more than 350 °C and moderate pressures. Thermal cracking is more compatible with infrastructure, produces a liquid more similar to diesel, and has lower processing costs (Stumborg et al. 1996). Melting vessels, furnaces, and tubular or fixed bed reactors have been employed for pyrolysis of biomass (Scheirs and Kaminsky 2006).

Egloff was one of the first to study the thermal cracking of cottonseed oil and Alaskan fur seal oil in 1932 and 1933, respectively. Cottonseed oil cracked at 445–485 °C at a pressure of 930.8 kPa. The yield of unrefined gasoline was 58.7%. Methane accounted for 35% of the gas products (Egloff and Morrell 1932). Seal fat cracked at 481 °C and 1.4 MPa. The yield of gasoline was 59.9% with a water content of 5.1% (Egloff and Nelson 1933). Several vegetable oils have been used as feedstock for thermal cracking (Table 9.4):

Table 9.4 Thermal cracking of various oils at ambient pressure

Triglyceride	T (°C)	Results	References
Tung oil	300–350	70% of liquid fraction in 120 min of operation	Chang and Wan (1947)
		Gasoline content of 25%	
Canola oil	300–500	Aromatics and gas yield is proportional to temperature, while coke formation is independent	Idem et al. (1996)
		The maximum amount of liquids was obtained at 370 °C	
Soybean oil	350–400	Carboxylic acid quantity was acceptable according to Brazilian standards	Lima et al. (2004)
		No aromatics detected	
Macauba fruit oil	700–800	Aldehydes and carboxylic acid formed mainly	Fortes and Baugh (2004)
		CO ₂ generated from decarboxylation reaction	
		The longer the time, the lower the alkane yield	
Babassu, pequi, and palm oils	300–500	Triglycerides constituted mainly by oleic acid produced cycloparaffins and cycloolefins in small amount	Alencar et al. (1983)
		Liquid yield of 60–80 v/v	

Understanding the mechanism of cracking is essential to maximize the liquid hydrocarbon yield. According to Chang and Wan (1947), Alencar et al. (1983), and Idem et al. (1996), the determining step is the elimination of oxygenate molecules such as carboxylic acids, ketones, aldehydes, and esters.

Lappi and Alèn (2009) have evaluated the pyrolysis of fatty acid sodium salts. They pyrolyzed at 500–750 °C in a quartz tube and analyzed the evolution of products. Sodium stearate formed alkanes, alkenes, and long-chain alkyl ketones by decarboxylation (Raven et al. 1997). Stearic acid pyrolysis yields less aromatics (Joshi and Pegg 2007). Sodium oleate pyrolysis leads to the formation of various alkenes and aromatics. Hartgers reached the same conclusion (Hartgers et al. 1995). With both the substrates, increasing the temperature resulted in a higher fraction of C3–C7 hydrocarbons. Aromatics increased when cracking sodium linoleate. The optimal pyrolysis conditions to maximize the diesel-like product fraction were 700–750 °C and 20 s.

Crossley cracked two reference triglycerides, namely, tricaprins and 2-oleodipalmitin. Oil was stable below 300 °C. Above that temperature, cracking occurred. Due to glycerol decomposition, acrolein was one of the major products. Zhang et al. (2015) employed computational molecular dynamics to study the pyrolysis of oleic-type triglycerides. The first reaction is the fission of the carbonyl to give an oleic acid radical (Fig. 9.3). Unsaturation degree affects the product distribution since more radicals form. In an unsaturated triglyceride (like animal fat), radical formation occurs before decarboxylation (Idem et al. 1996). A power law model describes the overall pyrolysis reaction (Fuentes et al. 2007). A detailed kinetic description of all pyrolytic reactions is possible by looping the components. Meier et al. (2015) regressed the kinetic constants for the thermal cracking of waste cooking oil pyrolysis.

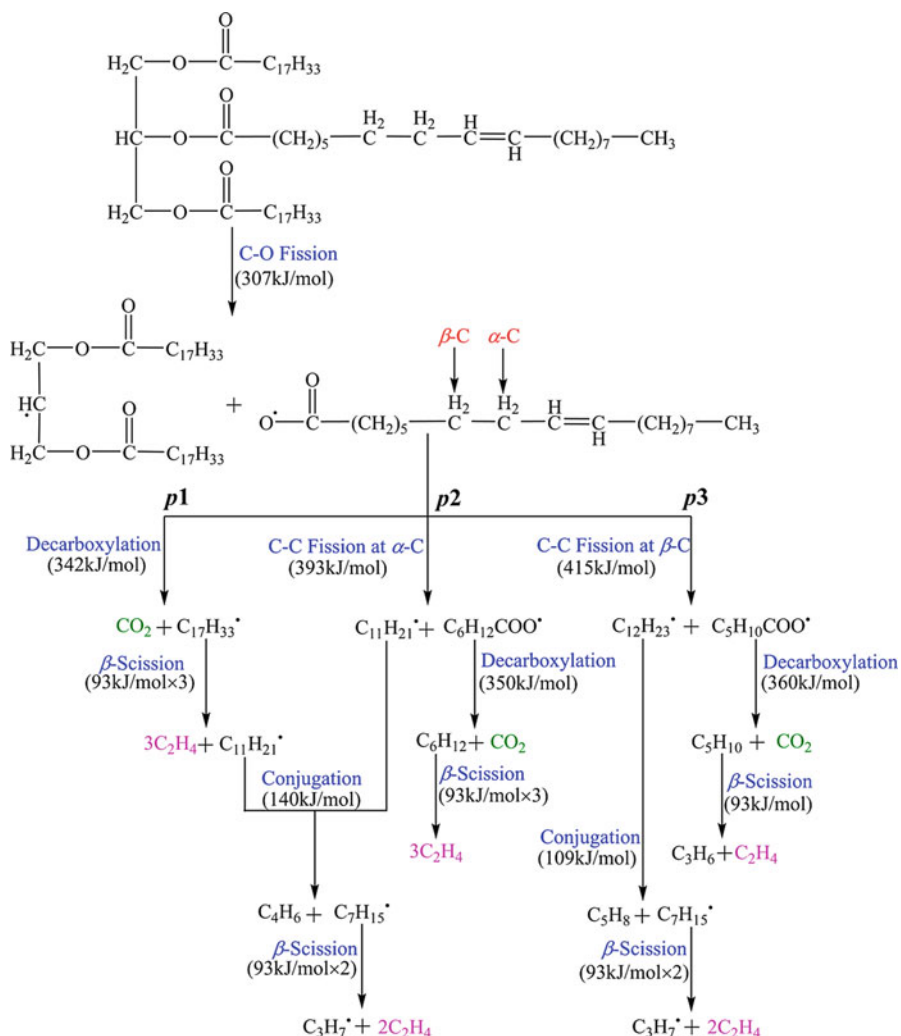


Fig. 9.3 Main decomposition reactions occurring in oleic triglyceride pyrolysis with enthalpies calculated with density functional theory. (Reprinted with permission from American Chemical Society. Zhang et al. 2015)

Hassen-Trabelsi et al. (2014) pyrolyzed waste animal fat in a fixed bed reactor under a nitrogen atmosphere. They obtained bio-oil yields between 60 and 75 wt.%. Demirbas (2007b) reported 77.1 wt.% of bio-oil for the pyrolysis of beef tallow at 500 °C, while Wiggers et al. (2009) and Wisniewski et al. (2010) got similar results (72% and 73% of bio-oil, respectively) from waste fish fat pyrolysis at 525 °C. 500 °C is found to be the optimal temperature for producing bio-oil.

Ito et al. (2012) compared the bio-oil derived from pyrolysis of animal fat with the biodiesel obtained from transesterification. Pyrolysis formed hydrocarbons at 420 °C after free fatty acid decarboxylation. Pyrolysis improved the pseudo-cold filter plugging point of the final fuel by 5 °C. Adebajo et al. (2005) pyrolyzed chicken lard in a fixed bed at 600 °C. They also applied ultrasound and solvent extraction pretreatment to increase the bio-oil yield. This raised the yield by 5% in the liquid. Generalizing pyrolysis reactors is difficult because of the variety of operative parameters as well as the diversity of oil fed. Mohan et al. (2006) concluded the same after reviewing all wood biomass pyrolysis processes.

9.4 Catalytic Cracking

Rao (1978) reviewed most of the studies on catalytic pyrolysis of vegetable oils before 1978. Three varieties of catalysts have been used: transition metals, with high hydrogen partial pressures, also called hydrocracking, molecular sieve catalysts such as zeolites, and other oxides like γ -alumina or magnesium oxide (Maher and Bressler 2007). Alumina pyrolyzes triolein, canola oil, trilaurin, and coconut oil at 450 °C yielding 65–79% of liquid products, mainly linear hydrocarbons (Konar et al. 1994). MgO is less active and partially converts soya oil to hydrocarbons and carboxylic acids at 300–350 °C (Dos Anjos et al. 1983).

Zeolites have a narrow particle size distribution (PSD) and are size-selective because only molecules smaller than the pore diameter can pass through the catalyst. Prasad et al. (1986) cracked refined soybean oil with HZSM-5 zeolite between 340 and 400 °C. The aromatic fraction maximized at 370–375 °C. The yield in aromatics depends on the effective hydrogen/carbon (H/C) ratio of the triglyceride used. Low H/C results in higher aromatic content (Haag et al. 1980). The higher the temperature, the higher is the fraction of gases. It consisted of C1–C4 hydrocarbons. The catalyst was regenerated after 12 h at 500 °C.

Changing the Si/Al ratio of zeolite results in different pore dimensions. The higher the amount of Al, the higher is the acidity. In the catalytic pyrolysis of palm oil, gasoline fraction maximizes at Al/Si = 5, while the optimal ratio for the highest diesel fraction is 20–50 (Twaiq et al. 2003a, b). HZSM-5 is one of the most promising catalysts, but it produces a high amount of gas. Mesoporous MCM-41 is more selective toward olefins (Twaiq et al. 2003a, b). Emori et al. (2017) studied the catalytic cracking of soybean oil in a micro fixed bed reactor. Under a reductive atmosphere (101 kPa of hydrogen partial pressure), unrefined oil yielded a higher amount of diesel, since it deactivated the catalyst faster, which was also demonstrated by the presence of oxygenated compounds. Under an inert atmosphere (nitrogen), hydrogen yield increased. Melero et al. (2010) reported the catalytic cracking of a mixture of fossil and vegetable oils with an FCC catalyst. They found that co-processing decreased the liquid fraction production but increased its aromatic content (mainly mono- and di-aromatic).

Buzetzki et al. (2011) studied the influence of triglyceride structure on cracking product distribution using NaY zeolite as a catalyst at 350–440 °C. They did not

observe a significant difference in liquid product distribution, even with waste cooking oil. Al-Sabawi et al. (2012) reviewed the literature on catalytic cracking in fluidized bed reactors in 2012. A fluidized bed configuration requires less investment for a high capacity plant (Warnecke 2000). Moreover, heat and mass transfer are favored by the fluidizing gas.

9.5 Concurrent Cracking and Transesterification

Boffito et al. (2014a, b, 2015, 2017) simultaneously cracked and transesterified canola oil in a fluidized bed reactor for the first time. They co-fed oil and methanol in a micro-fluidized bed reactor with a diameter of 7 mm at 416–425 °C in an inert atmosphere (Ar). A nozzle sprayed oil and alcohol directly into the catalytic bed. Two traps blocked all the reaction products. The first one was in an ice bath and the second contained toluene, to solubilize all the polar products (Fig. 9.4).

Although the catalyst was 10% CaO/alumina and the contact time was less than 1 s, it converted all the injected triglycerides. Maximum methyl ester yield was 44%. Cracking reactions formed C_6 – C_{24} hydrocarbons, including diolefins. Olefin polymerization formed coke. To regenerate the catalyst, oxidation cycles alternated the reaction cycles.

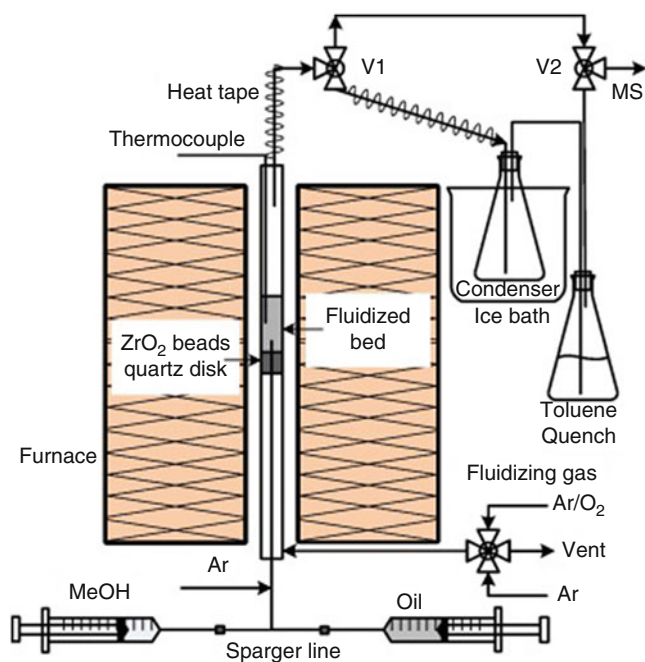


Fig. 9.4 Scheme of the fluidized ben bench reactor for the simultaneous transesterification and cracking of vegetable oils. (Reprinted with permission from Elsevier. Boffito et al. 2015)

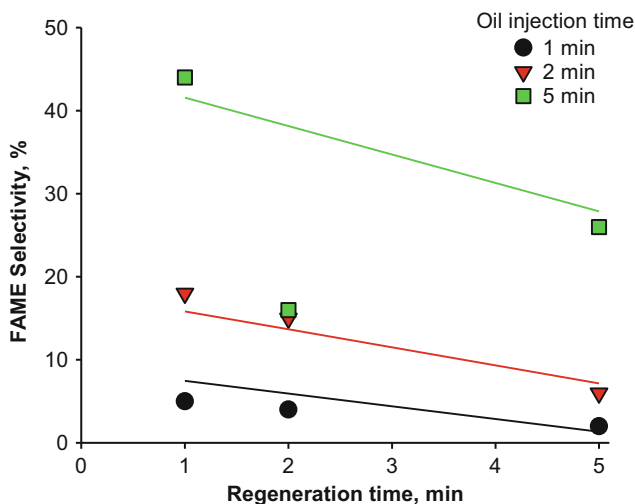


Fig. 9.5 FAME yield decreases linearly with regeneration time in a micro-fluidized bed reactor. Coke increases FAME selectivity. (Reprinted with permission from Elsevier. Boffito et al. 2015)

Boffito et al. (2015) introduced oxygen (33% in Ar) into the reactor to burn the coke. This way, the reactor works continuously. Interestingly, authors noted that a longer reaction time favored methyl ester formation and reduced to a negligible amount, the hydrocarbons. FAME selectivity increased from 5% to 16% and to 26% for reaction time to regeneration time of 1 s:1 s, 2 s:2 s, and 5 s:5 s, respectively (Fig. 9.5). Increasing the amount of coke on the catalyst increases FAME yield. They modeled selectivity of FAME depending on time of reaction (t_{react}) and time of regeneration (t_{regen}) with a good fitting ($R^2 = 0.98$):

$$S_{\text{FAME}} = 9 * t_{\text{react}} * \left(1 - 0.17 * \frac{t_{\text{regen}}}{t_{\text{react}}^{0.5}} \right) \quad (9.1)$$

The selectivity toward coke varied between 1% and 18%. According to the signals of CO and CO₂, recorded by a mass spectrometer, methanol and oil reduce CaO. In addition, O₂ re-oxidizes CaO.

Boffito et al. (2015) tested MgO/Al₂O₃ and Mg–Al hydrotalcite, but the biodiesel yield was lower compared to CaO catalyst. Hydrotalcites were too active toward coke formation. To avoid excess coking on the catalyst, they fed oxygen every 3 min. The isopropyl esters and hydrocarbons yield ranged from 2% to 31% and 0% to 42%, respectively. Increasing the alcohol dosing resulted in higher FAME production.

Boffito et al. (2017) have improved the cold flow properties of cracked/transesterified fuel by reacting oil with isopropanol (iPrOH) at diverse molar ratios

with 10% CaO/Al₂O₃ as a catalyst. Branched esters, such as isopropyl, compared with FAME, have a cloud and pour point 10/15 °C lower (Joshi and Pegg 2007). Furthermore, isopropanol solubilizes oil better than methanol, and a better fluidization occurs. The reaction condition remained the same except for the temperature (450 °C) and the reactant molar ratio in the feed that varied between 28 and 51 mol iPrOH/mol oil.

Compared to the experiment with methanol, coke and ester yields decreased because of the steric hindrance of isopropanol (Likozar and Levec 2014). The maximum isopropyl ester yield was 31%, with the highest molar ratio of alcohol. Authors speculated about the deactivation of cracking sites by coke, a result that was also stressed in a paper by Dalil et al. (2015) that studied glycerol dehydration over WO₃/TiO₂. Cold trap collected hydrocarbons in the range of C8–C19 (the heaviest products), while the trap with toluene blocked C5–C8 hydrocarbons. Here, 5 mL of toluene flushed the connection pipes at the end of the tests. That fraction was also analyzed. The products contained cyclic and branched molecules, which means that reactions such as isomerization and cyclization also take place besides cracking at 450 °C (Table 9.5). Regeneration cycles with air (21% of oxygen) permitted a continuous operation.

The main advantage of this technology is that the high operating temperatures allow the injection of waste oils, which are more viscous and acidic (Boffito et al. 2013). Besides short reaction times, the economic incentive includes low-cost feedstock and little catalyst loading (10 t of the catalyst may yield 80 kt biodiesel per year). Moreover, existing fluidized catalytic cracking units in refineries are already available to integrate this technology into established infrastructures.

9.6 Oil and Fat Gasification

Gasification converts coal, char, or biomass into a mixture of carbon monoxide, carbon dioxide, and hydrogen. Carbon monoxide and hydrogen react to give sulfur-free fuels in the Fischer-Tropsch process (Comazzi et al. 2016; Dry 2002) or other chemicals such as methanol or dimethyl ether. As opposed to cracking units, gasification aims at maximizing the gas products and minimizing the char (tar) formation. The reaction medium is either gas (air) or water. In the latter case, the process is called steam gasification. The molecules crack and decarboxylate in an oxidizing atmosphere (Ni et al. 2006).

In a typical gasification process, the oil is first dried and then gasified at temperatures between 800 and 1300 °C. Gasification, globally, is an endothermic process. The reaction is not lacking energy thanks to some of the carbon being burnt. Oxidation reactions are the fastest, while the rate of water gas shift is two to five times faster than Boudouard equilibrium (Di Blasi 2009). In a gasifier, gas and solid gasification reactions occur as summarized in Table 9.6.

A catalyst reduces tar and methane content in the gasification product and maximizes CO and H₂ concentration. It reforms the tar with steam or CO₂ (dry reforming). Typical gasification catalysts are alkali metals, carbonates, and Ni-based

Table 9.5 Hydrocarbons detected during the concurrent cracking and transesterification of canola oil with isopropanol at 450 °C in argon

Hydrocarbon	Lines	Ice trap	Toluene trap
C ₅ hydrocarbons			✓
i-Pentane			✓
n-Pentane			✓
C ₆ hydrocarbons			✓
2-Methylpentane			✓
3-Methylpentane			✓
n-Hexane			✓
C ₆ hydrocarbons			✓
2,2-Dimethylpentane			✓
2,4-Dimethylpentane			✓
Trans-1,2-dimethylcyclopentane			✓
n-Heptane			✓
C ₈ hydrocarbons	✓	✓	✓
2,5-Dimethylhexane	✓	✓	✓
1-Methylheptane	✓	✓	✓
n-Octane	✓	✓	✓
2,4-Dimethylheptane	✓	✓	
C ₉ hydrocarbons	✓	✓	
C ₁₀ hydrocarbons	✓	✓	
C ₁₁ hydrocarbons	✓	✓	
C ₁₂ hydrocarbons	✓	✓	
C ₁₃ hydrocarbons	✓	✓	
C ₁₄ hydrocarbons	✓	✓	
C ₁₅ hydrocarbons	✓	✓	
C ₁₆ hydrocarbons	✓	✓	
C ₁₇ hydrocarbons	✓	✓	
C ₁₈ hydrocarbons	✓	✓	
C ₁₉ hydrocarbons	✓	✓	

Reprinted with permission from Elsevier Boffito et al. (2017)

catalysts. Sutton et al. (2001) reviewed and discussed the main catalysts adopted for biomass gasification.

Hydrogen and paraffin yield goes from 20% to 50% increasing the amount of sodium carbonate from 10% to 45% at 850 °C (Demirbaş 2002). Markevich et al. (2001) reported steam reforming of sunflower oil, rapeseed oil, soybean oil, and corn oil with three different Ni-based commercial catalysts in a fixed-bed micro-reactor operating at 1500 kPa and 570–580 °C. All substrates gave the same hydrogen yields, i.e., about 70%. The higher the Ni content, the higher the hydrogen yield.

The reactors employed for biomass gasification differ depending on the feedstock flowrate and the type of liquid and solid fed.

In the *moving bed reactor* configuration, air, oxygen, or steam is fed from the bottom and biomass from the top. The temperature inside the reactor varies

Table 9.6 Different gasification reactions

Name	Type	Reaction	Enthalpy (kJ/mol)
Boudouard	Carbon reaction	$C + CO_2 \leftrightarrow 2CO$	+172
Carbon steam		$C + H_2O \leftrightarrow CO + H_2$	+131
Hydrogasification		$C + 2H_2 \leftrightarrow CH_4$	-74.8
Carbon partial	Oxidation	$C + 0.5O_2 \rightarrow CO$	-111
Carbon monoxide		$CO + 0.5O_2 \rightarrow CO_2$	-394
Carbon		$C + O_2 \rightarrow CO_2$	-284
Methane		$CH_4 + 2O_2 \rightarrow CO_2 + 2H_2O$	-803
Methane partial		$CH_4 + 0.5O_2 \rightarrow CO + 2H_2$	-36
Hydrogen		$H_2 + 0.5O_2 \rightarrow H_2O$	-242
Water-gas shift		Reduction	$CO + H_2O \leftrightarrow CO_2 + H_2$
Methanation	$2CO + 2H_2 \rightarrow CH_4 + CO_2$		-247
	$CO + 3H_2 \rightarrow CH_4 + H_2O$		-206
	$CO_2 + 4H_2 \rightarrow CH_4 + 2H_2O$		-165
Steam reforming		$CH_4 + H_2O \leftrightarrow CO + 3H_2$	+206

Reprinted with permission from Basu (2013)

depending on the position. At the bottom, where the oxygen concentration is highest, combustion reactions occur (700 °C). Then, temperature rises to 1000–1100 °C and gasification prevails. The peak of the reactor is dedicated to pyrolysis and gas drying.

A *fluidized bed gasifier* contains nonreactive solids that act as heat carriers. The gasifying gas is fed to the bottom of the reactor and fluidizes the solid. Maximum temperatures are lower than a moving bed reactor to avoid ash sintering and consequent reactor plugging.

Finally, in *entrained flow reactors*, biomass and the gas stream are co-fed at the bottom of the reactor. It operates at temperatures of about 1400 °C and pressures between 1000 and 4000 kPa (Basu 2013).

Even though the know-how and the technology for biomass gasification are at the industrial stage, few works were published in this field. Biomass feedstock like wood, lignin, or agricultural residues is preferred (Carvalho et al. 2017; Hejazi et al. 2017; Pala et al. 2017). We speculate that the reason lies in the high cost of fats and oils that makes the whole process expensive (gasification and Fischer-Tropsch process to have fuel) compared to the others presented in this chapter.

9.7 Conclusions

We reviewed the state of the art on high-temperature conversion of triglycerides into biofuels and biochemicals. The technology to crack triglycerides into hydrocarbons is mature, being this either thermal or catalytic. In the latter, coking remains an issue. Operating the reactor as a fluidized catalytic cracker, rather than in a batch reactor, overcomes this drawback. The conversion of triglycerides into biodiesel (fatty acid methyl esters) at high temperature accepts a wide range of feedstocks, including used

cooking oils. Transesterification occurs over basic catalysts starting from 40 °C and acid catalysts starting from 120 °C. Above these temperatures, a solid acid catalyst activates concurrently esterification and transesterification. However, transesterification at high temperature remains a challenge because cracking inevitably occurs thermally at temperatures beyond 300 °C. Together with cracking, coking occurs deactivating the transesterification catalyst. The solution is once again to operate the transesterification reactor as a fluidized catalytic cracker and regenerate the catalyst periodically. The concurrent transesterification and cracking offer a series of advantages, such as a drop-in fuel with improved flow properties as a product, as well as less gaseous by-products compared to traditional cracking and pyrolysis. Designing a catalytic system for gas-phase transesterification and conceiving an ad hoc reactor for reaction-regeneration cycles are interesting avenues to pursue.

Acknowledgments The authors gratefully acknowledge the support of the Natural Sciences and Engineering Research Council of Canada (NSERC). This research was undertaken, in part, thanks to the funding from the Canada Research Chair program.

References

- Adebanjo AO, Dalai AK, Bakhshi NN (2005) Production of diesel-like fuel and other value-added chemicals from pyrolysis of animal fat. *Energy Fuel* 19:1735–1741. <https://doi.org/10.1021/ef040091b>
- Alaba PA, Sani YM, Daud WMAW (2016) Efficient biodiesel production via solid superacid catalysis: a critical review on recent breakthrough. *RSC Adv* 6:78351–78368. <https://doi.org/10.1039/C6RA08399D>
- Alencar JW, Alves PB, Craveiro AA (1983) Pyrolysis of tropical vegetable oils. *J Agric Food Chem* 31:1268–1270. <https://doi.org/10.1021/jf00120a031>
- Alfke G, Irion WW, Neuwirth OS (2007) Oil refining. In: Ullmann's encyclopedia of industrial chemistry. Wiley-VCH Verlag GmbH & Co. KGaA, Weinheim. https://doi.org/10.1002/14356007.a18_051.pub2
- Al-Sabawi M, Chen J, Ng S (2012) Fluid catalytic cracking of biomass-derived oils and their blends with petroleum feedstocks: a review. *Energy Fuel* 26:5355–5372. <https://doi.org/10.1021/ef3006417>
- Anjos JSD, Gonzalez WDA, Lam YL, Frety R (1983) Catalytic decomposition of vegetable oil. *Appl Catal* 5:299–308. [https://doi.org/10.1016/0166-9834\(83\)80158-4](https://doi.org/10.1016/0166-9834(83)80158-4)
- Ardi MS, Aroua MK, Hashim NA (2015) Progress, prospect and challenges in glycerol purification process: a review. *Renew Sust Energ Rev* 42:1164–1173. <https://doi.org/10.1016/j.rser.2014.10.091>
- Asakuma Y, Maeda K, Kuramochi H, Fukui K (2009) Theoretical study of the transesterification of triglycerides to biodiesel fuel. *Fuel* 88:786–791. <https://doi.org/10.1016/j.fuel.2008.10.045>
- Azad AK, Rasul MG, Khan MMK, Sharma SC, Bhuiya MMK, Mofijur M (2016) A review on socio-economic aspects of sustainable biofuels. *Int J Global Warm* 10:32–54. <https://doi.org/10.1504/IJGW.2016.077903>
- Ayoub M, Abdullah AZ (2012) Critical review on the current scenario and significance of crude glycerol resulting from biodiesel industry towards more sustainable renewable energy industry. *Renew Sust Energy Rev* 16:2671–2686. <https://doi.org/10.1016/j.rser.2012.01.054>
- Basu P (2013) Biomass gasification, pyrolysis and torrefaction: practical design and theory. Elsevier. <https://doi.org/10.1016/C2011-0-07564-6>

- Bhosle BM, Subramanian R (2005) New approaches in deacidification of edible oils—a review. *J Food Eng* 69:481–494. <https://doi.org/10.1016/j.jfoodeng.2004.09.003>
- Blasi CD (2009) Combustion and gasification rates of lignocellulosic chars. *Prog Energy Combust Sci* 35:121–140. <https://doi.org/10.1016/j.peccs.2008.08.001>
- Boffito DC, Pirola C, Galli F, Michele AD, Bianchi CL (2013) Free fatty acids esterification of waste cooking oil and its mixtures with rapeseed oil and diesel. *Fuel* 108:612–619. <https://doi.org/10.1016/j.fuel.2012.10.069>
- Boffito DC, Galli F, Pirola C, Bianchi CL, Patience GS (2014a) Ultrasonic free fatty acids esterification in tobacco and canola oil. *Ultrason Sonochem* 21:1969–1975. <https://doi.org/10.1016/j.ultsonch.2014.01.026>
- Boffito DC, Neagoe C, Edake M, Pastor-Ramirez B, Patience GS (2014b) Biofuel synthesis in a capillary fluidized bed. *Catal Today* 237:13–17. <https://doi.org/10.1016/j.cattod.2014.01.018>
- Boffito DC, Manrique GB, Patience GS (2015) One step cracking/transesterification of vegetable oil: reaction–regeneration cycles in a capillary fluidized bed. *Energy Convers Manag* 103:958–964. <https://doi.org/10.1016/j.enconman.2015.07.025>
- Boffito DC, Galli F, Pirola C, Patience GS (2017) CaO and isopropanol transesterify and crack triglycerides to isopropyl esters and green diesel. *Energy Convers Manag* 139:71–78. <https://doi.org/10.1016/j.enconman.2017.02.008>
- Buzetzkı E, Sidorova K, Cvengrošova Z, Cvengroš J (2011) Effects of oil type on products obtained by cracking of oils and fats. *Fuel Process Technol* 92:2041–2047. <https://doi.org/10.1016/j.fuproc.2011.06.005>
- Carvalho L, Furusjo E, Kirtania K, Wetterlund E, Lundgren J, Anheden M, Wolf J (2017) Techno-economic assessment of catalytic gasification of biomass powders for methanol production. *Bioresour Technol* 237:167–177. <https://doi.org/10.1016/j.biortech.2017.02.019>
- Chang CC, Wan SU (1947) China’s motor fuels from Tung oil. *Ind Eng Chem* 39:1543–1548. <https://doi.org/10.1021/ie50456a011>
- Comazzi A, Pirola C, Bianchi CL, Galli F, Longhi M, Manenti M (2016) High-loaded Fe-supported catalyst for the thermochemical BTL-FT process: experimental results and modelling. *Can J Chem Eng* 94:696–702. <https://doi.org/10.1002/cjce.22357>
- Cvengros J (1995) Physical refining of edible oils. *J Am Oil Chem Soc* 72:1193–1196. <https://doi.org/10.1007/BF02540987>
- da Silva GP, Mack M, Contiero J (2009) Glycerol: a promising and abundant carbon source for industrial microbiology. *Biotechnol Adv* 27:30–39. <https://doi.org/10.1016/j.biotechadv.2008.07.006>
- Dalil M, Carnevali D, Dubois JL, Patience GS (2015) Transient acrolein selectivity and carbon deposition study of glycerol dehydration over WO₃/TiO₂ catalyst. *Chem Eng J* 270:557–563. <https://doi.org/10.1016/j.cej.2015.02.058>
- Dash SK, Lingfa P (2017) A review on production of biodiesel using catalyzed transesterification. In: AIP conference proceedings, 20100. <https://doi.org/10.1063/1.4990253>
- DeFrain JM, Hippen AR, Kalscheur KF, Jardon PW (2004) Feeding glycerol to transition dairy cows: effects on blood metabolites and lactation performance. *J Dairy Sci* 87:4195–4206. [https://doi.org/10.3168/jds.S0022-0302\(04\)73564-X](https://doi.org/10.3168/jds.S0022-0302(04)73564-X)
- Demirbař A (2002) Gaseous products from biomass by pyrolysis and gasification: effects of catalyst on hydrogen yield. *Energy Convers Manag* 43:897–909. [https://doi.org/10.1016/S0196-8904\(01\)00080-2](https://doi.org/10.1016/S0196-8904(01)00080-2)
- Demirbas A (2007a) Progress and recent trends in biofuels. *Prog Energy Combust Sci* 33:1–18. <https://doi.org/10.1016/j.peccs.2006.06.001>
- Demirbas A (2007b) The influence of temperature on the yields of compounds existing in bio-oils obtained from biomass samples via pyrolysis. *Fuel Process Technol* 88:591–597. <https://doi.org/10.1016/j.fuproc.2007.01.010>
- Diasakou M, Louloudi A, Papayannakos N (1998) Kinetics of the non-catalytic transesterification of soybean oil. *Fuel* 77:1297–1302. [https://doi.org/10.1016/S0016-2361\(98\)00025-8](https://doi.org/10.1016/S0016-2361(98)00025-8)

- Dry ME (2002) High quality diesel via the Fischer-Tropsch process – a review. *J Chem Technol Biotechnol* 77:43–50. <https://doi.org/10.1002/jctb.527>
- Edake M, Dalil M, Mahboub MJD, Dubois JL, Patience GS (2017) Catalytic glycerol hydrogenolysis to 1,3-propanediol in a gas–solid fluidized bed. *RSC Adv* 7:3853–3860. <https://doi.org/10.1039/C6RA27248G>
- Egloff G, Morrell JC (1932) The cracking of cottonseed oil. *Ind Eng Chem* 24:1426–1427. <https://doi.org/10.1021/ie50276a020>
- Egloff G, Nelson EF (1933) Cracking Alaskan fur-seal oil. *Ind Eng Chem* 25:386–387. <https://doi.org/10.1021/ie50280a009>
- Emori EY, Hirashima FH, Zandonai CH, Ortiz-Bravo CA, Fernandes-Machado NRC, Olsen-Scalante MHN (2017) Catalytic cracking of soybean oil using ZSM5 zeolite. *Catal Today* 279:168–176. <https://doi.org/10.1016/j.cattod.2016.05.052>
- Encinar JM, Pardal A, Sánchez N (2016) An improvement to the transesterification process by the use of co-solvents to produce biodiesel. *Fuel* 166:51–58. <https://doi.org/10.1016/j.fuel.2015.10.110>
- Fort EF, Blumberg PN (1982) Performance and durability of a turbocharged diesel fueled with cottonseed oil blends. In: ASAE Publ
- Fortes ICP, Baugh PJ (2004) Pyrolysis–GC/MS studies of vegetable oils from Macauba fruit. *J Anal Appl Pyrol* 72:103–111. <https://doi.org/10.1016/j.jaap.2004.03.005>
- Fuentes MJ, Font R, Gómez-Rico MF, Martín-Gullón I (2007) Pyrolysis and combustion of waste lubricant oil from diesel cars: decomposition and pollutants. *J Anal Appl Pyrol* 79:215–226. <https://doi.org/10.1016/j.jaap.2006.12.004>
- Galli F, Bonfanti L, Capelli S, Manenti F, Bianchi CL, Patience GS, Pirola C (2015) Heterogeneous oil transesterification in a single-phase liquid mixture using a co-solvent for improved biofuels production. *Energy Technol* 3:1170–1173. <https://doi.org/10.1002/ente.201500186>
- García-Martínez N, Andreo-Martínez P, Quesada-Medina J, de los Ríos AP, Chica A, Beneito-Ruiz R, Carratalá-Abril J (2017) Optimization of non-catalytic transesterification of tobacco (*Nicotiana tabacum*) seed oil using supercritical methanol to biodiesel production. *Energy Convers Manag* 131:99–108. <https://doi.org/10.1016/j.enconman.2016.10.078>
- Go AW, Sutanto S, Ong LK, Tran-Nguyen PL, Ismadji S, Ju YH (2016) Developments in in-situ (trans) esterification for biodiesel production: a critical review. *Renew Sust Energy Rev* 60:284–305. <https://doi.org/10.1016/j.rser.2016.01.070>
- Haag WO, Rodewald PG, Weisz PB (1980) Catalytic production of aromatics and olefins from plant materials. *ACS Symp Ser*
- Hartgers WA, Damsté JSS, de Leeuw JW (1995) Curie-point pyrolysis of sodium salts of functionalized fatty acids. *J Anal Appl Pyrol* 34:191–217. [https://doi.org/10.1016/0165-2370\(94\)00881-Z](https://doi.org/10.1016/0165-2370(94)00881-Z)
- Hassen-Trabelsi AB, Kraiem T, Naoui S, Belayouni H (2014) Pyrolysis of waste animal fats in a fixed-bed reactor: production and characterization of bio-oil and bio-char. *Waste Manag* 34:210–218. <https://doi.org/10.1016/j.wasman.2013.09.019>
- Havlík P, Schneider UA, Schmid E, Böttcher H, Fritz S, Skalský R, Aoki K et al (2011) Global land-use implications of first and second generation biofuel targets. *Energy Policy* 39:5690–5702. <https://doi.org/10.1016/j.enpol.2010.03.030>
- Hejazi B, Grace JR, Bi X, Mahecha-Botero A (2017) Kinetic model of steam gasification of biomass in a bubbling fluidized bed reactor. *Energy Fuel* 31:1702–1711. <https://doi.org/10.1021/acs.energyfuels.6b03161>
- Helwani Z, Othman MR, Aziz N, Kim J, Fernando WJN (2009) Solid heterogeneous catalysts for transesterification of triglycerides with methanol: a review. *Appl Catal A Gen* 363:1–10. <https://doi.org/10.1016/j.apcata.2009.05.021>
- Idem RO, Katikaneni SPR, Bakshhi NN (1996) Thermal cracking of canola oil: reaction products in the presence and absence of steam. *Energy Fuel* 10:1150–1162. <https://doi.org/10.1021/ef960029h>

- Ito T, Nakashimada Y, Senba K, Matsui T, Nishio N (2005) Hydrogen and ethanol production from glycerol-containing wastes discharged after biodiesel manufacturing process. *J Biosci Bioeng* 100:260–265. <https://doi.org/10.1263/jbb.100.260>
- Ito T, Sakurai Y, Kakuta Y, Sugano M, Hirano K (2012) Biodiesel production from waste animal fats using pyrolysis method. *Fuel Process Technol* 94:47–52. <https://doi.org/10.1016/j.fuproc.2011.10.004>
- Jain S, Sharma MP (2010) Kinetics of acid base catalyzed transesterification of *Jatropha curcas* oil. *Bioresour Technol* 101:7701–7706. <https://doi.org/10.1016/j.biortech.2010.05.034>
- Jain S, Sharma MP, Rajvanshi S (2011) Acid base catalyzed transesterification kinetics of waste cooking oil. *Fuel Process Technol* 92:32–38. <https://doi.org/10.1016/j.fuproc.2010.08.017>
- Johnson DT, Taconi KA (2007) The glycerin glut: options for the value-added conversion of crude glycerol resulting from biodiesel production. *Environ Prog* 26:338–348. <https://doi.org/10.1002/ep.10225>
- Joshi RM, Pegg MJ (2007) Flow properties of biodiesel fuel blends at low temperatures. *Fuel* 86:143–151. <https://doi.org/10.1016/j.fuel.2006.06.005>
- Konar SK, Boocock DGB, Mao V, Liu J (1994) Fuels and chemicals from sewage sludge: 3. Hydrocarbon liquids from the catalytic pyrolysis of sewage sludge lipids over activated alumina. *Fuel* 73:642–646. [https://doi.org/10.1016/0016-2361\(94\)90002-7](https://doi.org/10.1016/0016-2361(94)90002-7)
- Lappi H, Alén R (2009) Production of vegetable oil-based biofuels—thermochemical behavior of fatty acid sodium salts during pyrolysis. *J Anal Appl Pyrol* 86:274–280. <https://doi.org/10.1016/j.jaap.2009.07.005>
- Lee PC, Lee WG, Lee SY, Chang HN (2001) Succinic acid production with reduced by-product formation in the fermentation of *Anaerobiospirillum succiniciproducens* using glycerol as a carbon source. *Biotechnol Bioeng* 72:41–48. [https://doi.org/10.1002/1097-0290\(20010105\)72:1<41::AID-BIT6>3.0.CO;2-N](https://doi.org/10.1002/1097-0290(20010105)72:1<41::AID-BIT6>3.0.CO;2-N)
- Likozar B, Levec J (2014) Transesterification of canola, palm, peanut, soybean and sunflower oil with methanol, ethanol, isopropanol, butanol and tert-butanol to biodiesel: modelling of chemical equilibrium, reaction kinetics and mass transfer based on fatty acid composition. *Appl Energy* 123:108–120. <https://doi.org/10.1016/j.apenergy.2014.02.046>
- Lima DG, Soares VCD, Ribeiro EB, Carvalho DA, Cardoso ECV, Rassi FC, Mundim KC, Rubim JC, Suarez PAZ (2004) Diesel-like fuel obtained by pyrolysis of vegetable oils. *J Anal Appl Pyrol* 71:987–996. <https://doi.org/10.1016/j.jaap.2003.12.008>
- Ma F, Hanna MA (1999) Biodiesel production: a review. *Bioresour Technol* 70:1–15. [https://doi.org/10.1016/S0960-8524\(99\)00025-5](https://doi.org/10.1016/S0960-8524(99)00025-5)
- Maher KD, Bressler DC (2007) Pyrolysis of triglyceride materials for the production of renewable fuels and chemicals. *Bioresour Technol* 98:2351–2368. <https://doi.org/10.1016/j.biortech.2006.10.025>
- Marchetti JM, Errazu AF (2008) Technoeconomic study of supercritical biodiesel production plant. *Energy Convers Manag* 49:2160–2164. <https://doi.org/10.1016/j.enconman.2008.02.002>
- Mardhiah HH, Ong HC, Masjuki HH, Lim S, Lee HV (2017) A review on latest developments and future prospects of heterogeneous catalyst in biodiesel production from non-edible oils. *Renew Sust Energy Rev* 67:1225–1236. <https://doi.org/10.1016/j.rser.2016.09.036>
- Markolwitz M (2004) Consider Europe's most popular Catalyst. <http://www.biodieselmagazine.com/articles/462/consider-europes-most-popular-catalyst>
- Marquevich M, Farriol X, Medina F, Montané D (2001) Hydrogen production by steam reforming of vegetable oils using nickel-based catalysts. *Ind Eng Chem Res* 40:4757–4766. <https://doi.org/10.1021/ie010135t>
- Meier HF, Wiggers VR, Zonta GR, Scharf DR, Simionatto EL, Ender L (2015) A kinetic model for thermal cracking of waste cooking oil based on chemical lumps. *Fuel* 144:50–59. <https://doi.org/10.1016/j.fuel.2014.12.020>
- Melero JA, Clavero MM, Calleja G, García A, Miravalles R, Galindo T (2010) Production of biofuels via the catalytic cracking of mixtures of crude vegetable oils and nonedible animal fats with vacuum gas oil. *Energy Fuel* 24:707–717. <https://doi.org/10.1021/ef900914e>

- Mohan D, Pittman CU, Steele PH (2006) Pyrolysis of wood/biomass for bio-oil: a critical review. *Energy Fuel* 20:848–889. <https://doi.org/10.1021/ef0502397>
- Naik SN, Goud VV, Rout PK, Dalai AK (2010) Production of first and second generation biofuels: a comprehensive review. *Renew Sust Energ Rev* 14:578–597. <https://doi.org/10.1016/j.rser.2009.10.003>
- Nautiyal P, Subramanian KA, Dastidar MG (2014) Kinetic and thermodynamic studies on biodiesel production from *Spirulina platensis* algae biomass using single stage extraction–transesterification process. *Fuel* 135:228–234. <https://doi.org/10.1016/j.fuel.2014.06.063>
- Navarro-Pineda FS, Baz-Rodríguez SA, Handler R, Sacramento-Rivero JC (2016) Advances on the processing of *Jatropha curcas* towards a whole-crop biorefinery. *Renew Sust Energ Rev* 54:247–269. <https://doi.org/10.1016/j.rser.2015.10.009>
- Ni M, Leung DYC, Leung MKH, Sumathy K (2006) An overview of hydrogen production from biomass. *Fuel Process Technol* 87:461–472. <https://doi.org/10.1016/j.fuproc.2005.11.003>
- Pagliaro M, Ciriminna R, Kimura H, Rossi M, Pina CD (2007) From glycerol to value-added products. *Angew Chem Int Ed*. <https://doi.org/10.1002/anie.200604694>
- Pala LPR, Wang Q, Kolb G, Hessel V (2017) Steam gasification of biomass with subsequent syngas adjustment using shift reaction for syngas production: an aspen plus model. *Renew Energy* 101:484–492. <https://doi.org/10.1016/j.renene.2016.08.069>
- Papanikolaou S, Aggelis G (2002) Lipid production by *Yarrowia lipolytica* growing on industrial glycerol in a single-stage continuous culture. *Bioresour Technol* 82:43–49. [https://doi.org/10.1016/S0960-8524\(01\)00149-3](https://doi.org/10.1016/S0960-8524(01)00149-3)
- Pilzecker A (2011) An agricultural policy perspective. European Biodiesel Board General Assembly. http://www.ebb-eu.org/EBBpressreleases/Future_of_biofuels-Agricultural_policy_perspective_Pilzecker.pdf
- Pirola C, Galli F, Bianchi CL, Boffito DC, Comazzi A, Manenti F (2014a) Vegetable oil deacidification by methanol heterogeneously catalyzed esterification in (monophasic liquid)/solid batch and continuous reactors. *Energy Fuel* 28:5236–5240. <https://doi.org/10.1021/ef501397h>
- Pirola C, Manenti F, Galli F, Bianchi CL, Boffito DC, Corbetta M (2014b) Heterogeneously catalyzed free fatty acids esterification in (monophasic liquid)/solid packed bed reactors (PBR). *Chem Eng Trans* 37:553–558. <https://doi.org/10.3303/CET1437093>
- Prasad YS, Bakhshi NN, Mathews JF, Eager RL (1986) Catalytic conversion of canola oil to fuels and chemical feedstocks part I. Effect of process conditions on the performance of HZSM-5 catalyst. *Can J Chem Eng* 64:278–284. <https://doi.org/10.1002/cjce.5450640218>
- Quereshi S, Ahmad E, Pant KK, Dutta S (2017) Algal biofuels. In: Gupta SK, Malik A, Faizal B (eds) *Algal biofuels: recent advances and future prospects*. Springer Nature, Cham. <https://doi.org/10.1007/978-3-319-51010-1>
- Rao KVC (1978) Production of hydrocarbons by thermolysis of vegetable oils. US Patent 4,102,938. <http://www.google.com/patents/US4102938>
- Raven AM, van Bergen PF, Stott AW, Dudd SN, Evershed RP (1997) Formation of long-chain ketones in archaeological pottery vessels by pyrolysis of acyl lipids. *J Anal Appl Pyrol* 40–41:267–285. [https://doi.org/10.1016/S0165-2370\(97\)00036-3](https://doi.org/10.1016/S0165-2370(97)00036-3)
- Scheirs J, Kaminsky W (2006) Feedstock recycling and pyrolysis of waste plastics: converting waste plastics into diesel and other fuels. *Wiley Ser Polym Sci*. <https://doi.org/10.1002/0470021543>
- Sengupta R, Bhattacharyya DK (1992) A comparative study between biorefining combined with other processes and physical refining of high-acid mohua oil. *J Am Oil Chem Soc* 69:1146–1149. <https://doi.org/10.1007/BF02541052>
- Shahidi F (ed) (2005) *Bailey's industrial oil and fat products*. Wiley, Hoboken. <https://doi.org/10.1002/047167849X>.
- Shonnard DR, Klemetsrud B, Sacramento-Rivero J, Navarro-Pineda F, Hilbert J, Handler R, Suppen N, Donovan RP (2015) A review of environmental life cycle assessments of liquid transportation biofuels in the Pan American region. *Environ Manag* 56:1356–1376. <https://doi.org/10.1007/s00267-015-0543-8>

- Siling MI, Laricheva TN (1996) Titanium compounds as catalysts for esterification and transesterification. *Russ Chem Rev* 65:279–286. <https://doi.org/10.1070/RC1996v065n03ABEH000210>
- Singh V, Yadav M, Sharma YC (2017) Effect of co-solvent on biodiesel production using calcium aluminium oxide as a reusable catalyst and waste vegetable oil. *Fuel* 203:360–369. <https://doi.org/10.1016/j.fuel.2017.04.111>
- Statista.com (2017) Leading biodiesel producers worldwide in 2016
- Stojković IJ, Stamenković OS, Povrenović DS, Veljković VB (2014) Purification technologies for crude biodiesel obtained by alkali-catalyzed transesterification. *Renew Sust Energ Rev* 32:1–15. <https://doi.org/10.1016/j.rser.2014.01.005>
- Stumborg M, Wong A, Hogan E (1996) Hydroprocessed vegetable oils for diesel fuel improvement. *Bioresour Technol* 56:13–18. [https://doi.org/10.1016/0960-8524\(95\)00181-6](https://doi.org/10.1016/0960-8524(95)00181-6)
- Sutton D, Kelleher B, Ross JRH (2001) Review of literature on catalysts for biomass gasification. *Fuel Process Technol* 73:155–173. [https://doi.org/10.1016/S0378-3820\(01\)00208-9](https://doi.org/10.1016/S0378-3820(01)00208-9)
- Tan HW, Aziz ARA, Aroua MK (2013) Glycerol production and its applications as a raw material: a review. *Renew Sust Energ Rev* 27:118–127. <https://doi.org/10.1016/j.rser.2013.06.035>
- Twaiq FA, Mohamed AR, Bhatia S (2003a) Liquid hydrocarbon fuels from palm oil by catalytic cracking over aluminosilicate mesoporous catalysts with various Si/Al ratios. *Microporous Mesoporous Mater* 64:95–107. <https://doi.org/10.1016/j.micromeso.2003.06.001>
- Twaiq FA, Zabidi NAM, Mohamed AR, Bhatia S (2003b) Catalytic conversion of palm oil over mesoporous aluminosilicate MCM-41 for the production of liquid hydrocarbon fuels. *Fuel Process Technol* 84:105–120. [https://doi.org/10.1016/S0378-3820\(03\)00048-1](https://doi.org/10.1016/S0378-3820(03)00048-1)
- Verma P, Sharma MP (2016) Review of process parameters for biodiesel production from different feedstocks. *Renew Sust Energ Rev* 62:1063–1071. <https://doi.org/10.1016/j.rser.2016.04.054>
- Wang K, Hawley MC, DeAthos SJ (2003) Conversion of glycerol to 1,3-propanediol via selective dehydroxylation. *Ind Eng Chem Res* 42:2913–2923. <https://doi.org/10.1021/ie020754h>
- Warnecke R (2000) Gasification of biomass: comparison of fixed bed and fluidized bed gasifier. *Biomass Bioenergy* 18:489–497. [https://doi.org/10.1016/S0961-9534\(00\)00009-X](https://doi.org/10.1016/S0961-9534(00)00009-X)
- Wiggers VR, Wisniewski A, Madureira LAS, Barros AAC, Meier HF (2009) Biofuels from waste fish oil pyrolysis: continuous production in a pilot plant. *Fuel* 88:2135–2141. <https://doi.org/10.1016/j.fuel.2009.02.006>
- Wisniewski A, Wiggers VR, Simionatto EL, Meier HF, Barros AAC, Madureira LAS (2010) Biofuels from waste fish oil pyrolysis: chemical composition. *Fuel* 89:563–568. <https://doi.org/10.1016/j.fuel.2009.07.017>
- Yang F, Hanna MA, Sun R (2012) Value-added uses for crude glycerol—a byproduct of biodiesel production. *Biotechnol Biofuels* 5:13. <https://doi.org/10.1186/1754-6834-5-13>
- Zhang Y, Wang X, Li Q, Yang R, Li C (2015) A Reaxff molecular dynamics study of the pyrolysis mechanism of oleic-type triglycerides. *Energy Fuel* 29:5056–5068. <https://doi.org/10.1021/acs.energyfuels.5b00720>
- Zhu H, Wu Z, Chen Y, Zhang P, Duan S, Liu X, Mao Z (2006) Preparation of biodiesel catalyzed by solid super base of calcium oxide and its refining process. *Chin J Catal* 27:391–396. [https://doi.org/10.1016/S1872-2067\(06\)60024-7](https://doi.org/10.1016/S1872-2067(06)60024-7)



A Review on Pyrolysis of Biomass and the Impacts of Operating Conditions on Product Yield, Quality, and Upgradation

10

Anil Kumar Varma, Ravi Shankar, and Prasenjit Mondal

Abstract

Pyrolysis is a thermochemical conversion process where biomass is converted into liquid (bio-oil), solid (bio-char), and gaseous products (pyro-gas) under oxygen-depleted condition due to the application of heat. The composition and yield of pyrolysis products depend upon the operating parameters of the pyrolysis process and types of biomass. In pyrolysis process, it is essential to explore the effect of operating parameters on product yield and instinct about their optimization. The present study reviews the influence of operating parameters on product yield from existing literature on the pyrolysis biomass as well as product characterization and upgrading. The major operating parameters include pyrolysis temperature, heating rate, sweeping gas flow rate, and particle size of biomass. The study concludes that most biomass residues are suitable for pyrolysis and all the operating parameters play an important role in the yield of products and their characterization.

Keywords

Biomass · Pyrolysis · Bio-oil · Bio-char · Pyrolysis conditions

A. K. Varma · P. Mondal (✉)

Department of Chemical Engineering, Indian Institute of Technology Roorkee, Roorkee, Uttarakhand, India

e-mail: pmondfch@iitr.ac.in

R. Shankar

Department of Chemical Engineering, Madan Mohan Malaviya University of Technology, Gorakhpur, Uttar Pradesh, India

10.1 Introduction

Energy plays a crucial role in economic and industrial development of a country. Nowadays, global demand for energy is increasing rapidly due to the industrialization and growth of world population (Mohanty et al. 2014). Currently, the annual world energy demand is approximately 0.55 quadrillion MJ, and it is expected to rise over 50% by 2030 (Dalai and Bassi 2010). At present, around 90% of world energy demand is fulfilled by fossil fuels (coal, petroleum, and natural gas) (Maity et al. 2014). The continuous use of fossil fuels is a serious threat to their limited world reserve as well as responsible for energy insecurity and environmental concern over global warming due to the release of greenhouse gases during their combustion (Razzak et al. 2013). Hence, it is realized that energy should be renewable, cost-effective, convenient, safe, and sustainable. To overcome the demand for energy as well as the environmental threats, other available alternative energy sources must be utilized efficiently. Nowadays, several nations all over the world have started to replace the fossil fuel-based energy sources with renewable, sustainable, alternative, and carbon-neutral energy sources. Renewable energy sources such as biomass and waste, solar, wind, hydropower, and geothermal play a vital role in world energy balance. Among these, biomass and waste hold a share of around 12% (Balat and Kirtay 2010). However, in the near future, it may appear as the most promising alternative to fossil fuels (Panwar et al. 2011). Biomass is nontoxic, carbon neutral, biodegradable, and abundantly available with a yearly production of 10^{11} – 10^{12} tons on the land area all around the world (Demiral and Şensöz 2006). Moreover, biomass contains very less quantity of sulfur, nitrogen, and ash, so it releases low amounts of SO_x , NO_x , and soot in comparison to the fossil fuels (Demiral and Şensöz 2006). Biomass is the only energy resource which produces fuels in the form of liquid, solid, and gases.

Pyrolysis is a thermochemical conversion process converting biomass/organic materials into solid (bio-char), liquid (bio-oil), and gaseous products (pyro-gas) by heating in the absence of oxygen. Based on temperature, heating rate, and vapor residence time, pyrolysis is categorized into three types such as slow (conventional), intermediate, and fast pyrolysis. Slow pyrolysis occurs at a low temperature range (200–400 °C) with lower heating rate (5–10 °C/min) and high solid residence time (min to days). Typical product yield of slow pyrolysis is 30% liquid, 35% solid, and 35% gaseous products (Mohan et al. 2006). Unlike slow pyrolysis, intermediate pyrolysis corresponds mainly to liquid production. It occurs at a moderate temperature of 500 °C, with moderate hot vapor residence time of 10–20 s. The product yield of intermediate pyrolysis is 50% liquid, 20% solid, and 30% gaseous products. Fast pyrolysis occurs at a very high heating rate (~10 to 600 °C/s) at a moderate temperature of around 500 °C with short vapor residence times (0.5–10 s, typically ~2 s) and maximizes the liquid product yield.

Previously, many researchers have reviewed the biomass pyrolysis process such as Meier and Faix (1999) who briefed the updates for the pyrolysis of lignocellulosic

biomass. Bridgwater and Peacocke (2000) summarized the features of fast pyrolysis and provided the history of major processes developed since 1970. Bridgwater (2003) described the design consideration to optimize the operation of pyrolysis reactors. Mohan et al. (2006) critically reviewed the pyrolysis of different biomass in various reactors for bio-oil production. Babu (2008) described the chronological improvements in the theoretical study on kinetic modeling, heat and momentum transfer for plasma, and conventional pyrolysis. Isahak et al. (2012) described the characteristics of biomass, the design of reactors, product formation, and its upgradation for pyrolysis of biomass. Sharma et al. (2015) provided a critical review on the mathematical modeling studies of biomass pyrolysis, process parameters, and catalytic studies. Murugan and Gu (2015) reviewed the research and development activities in India toward the growth of pyrolysis technology since three decades. Dhyani and Bhaskar (2017) addressed the pyrolysis of lignocellulosic biomass, mainly describing the characteristics of feedstocks, technology development, and silencing features of different reactors used in pyrolysis as well as various properties of the pyrolysis products. These reviews covered mainly the state of the art for the developments of pyrolysis reactors, optimization procedures, and developments and industrialization of biomass pyrolysis in different countries. However, a review on pyrolysis of biomass describe the impact of operating parameters on the products is missing from the literature, since properties of pyrolysis products (bio-char, bio-oil, and fuel gas) depend upon the operating parameters.

In this chapter, a brief description has been provided on the importance of biomass for use as a source of renewable energy and its conversion routes and the mechanisms of the pyrolysis process. Moreover, the effect of operating parameters on product yield and their quality have been described with more stress being laid on bio-oil and its upgradation.

10.2 Biomass as a Source of Renewable Energy and Its Conversion Routes

Biomass is regarded as one of the oldest and abundantly available sources of energy. In the present time, it is the third largest source of energy. Biomass as direct energy source shares up to 40–50% of energy usage in domestic and industrial energy system in many developing countries, which have large forest and agriculture land (Vamvuka et al. 2003).

Biomass can be renewed into the various forms of energy and other value-added products through two main conversion processes such as thermochemical and biological conversion. The physical conversion process is the other conversion process to convert biomass into energy. The choice of the conversion process is mainly dependent upon the quantity and type of biomass as well as the form of energy required for a specific application. The main routes for biomass to energy conversion are shown in Fig. 10.1.

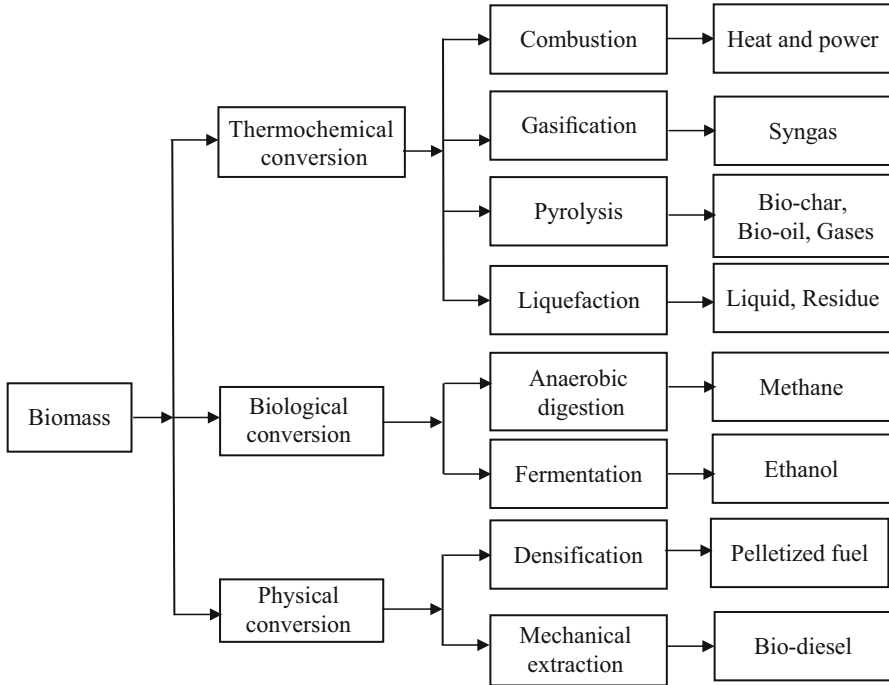


Fig. 10.1 Main processes for biomass to energy conversion (Farid 2006)

Thermochemical conversion processes are most commonly employed for converting biomass into higher heating value fuels. In the biological conversion process, biomass is converted into methane, biomethanol, bioethanol, or biobutanol with the help of enzymes or microorganisms (Demirbas 2008). In comparison with biological and physical conversion processes, thermochemical conversion of biomass to energy is the most favorable. Thermochemical conversion of biomass is categorized into four processes such as:

1. Combustion
2. Gasification
3. Pyrolysis
4. Hydrothermal liquefaction

The advantages and disadvantages of combustion, gasification, pyrolysis, and hydrothermal liquefaction are summarized in Table 10.1. It shows that among different thermochemical processes, pyrolysis is one of the most promising and a feasible process as it produces fuel in the form of liquid, solid, and gaseous products with various utilization options.

Table 10.1 Advantages and disadvantages of combustion, gasification, pyrolysis, and hydrothermal liquefaction

	Advantages	Disadvantages
Combustion	Produced process heat can be used directly for power generation	Emissions problems
	Industrially mature and commercial technology	Heat cannot be stored and it must be used immediately Larger gas cleaning equipment is required because of large volume of gaseous products
Gasification	Lower emissions	High capital cost
	Lower process operating temperature than combustion so better control of process	Complex operation as oxygen separation units is required
	Less gas cleaning equipment is required because of comparatively smaller volume of gaseous products	Costs associated with steam and oxygen
	Char produced from the low temperature gasification which can be consumed as activated carbon or soil amendment	High ash content feedstocks can result in agglomeration
Pyrolysis	No emissions	Relatively less industrial experience of technology
	Lower operating temperature than gasification and combustion	High heating value (HHV) of bio-oil is lower than heavy oil
	Variety of products in the form of solid (bio-char), liquid (bio-oil), gas (pyro-gas)	Separate upgradation step for bio-oil is required
	Bio-oil can be stored and more easily transported than solid biomass and syngas	Bio-oil is immiscible with hydrocarbons
	Bio-oil can be used as a fuel for power, as a biofuels and chemicals production	Long-term storage of bio-oil is difficult because of its corrosive nature
	Energy density of bio-oil is higher than syngas	
	Bio-char can be used as solid fuels, activated carbon, or soil amendment	
Potential integration in biorefinery		
Hydrothermal liquefaction	Lower oxygen content in bio-oil as compared to the pyrolysis bio-oil	More expensive and complex process than pyrolysis
	Less processing of biomass is required	Requires high pressure and long residence time

Reference: Patel (2013)

10.3 Pyrolysis and Its Reaction Mechanisms

Pyrolysis is a thermochemical conversion process, which converts biomass into bio-oil, bio-char, and pyro-gas in the absence of oxygen. The word pyrolysis is derived from the Greek words “pyro” means fire and “lysis” means breaking or decomposition. In pyrolysis, thermal decomposition of biomass involves the complex interaction of heat and mass transfer which constitute several chemical reactions resulting into the condensable vapors (bio-oil), gaseous products (pyro-gas), and solid charcoal (bio-char). The main chemical reactions which occur during the pyrolysis of biomass are decarboxylation and decomposition of hemicellulose, cellulose, and lignin. Decarboxylation starts at 250 °C, where CO₂ is released and left aliphatic or aromatic char. Hemicellulose decomposed first within the temperature range of 220–315 °C followed by the cellulose between 315 and 400 °C and finally lignin in between 100 and 900 °C (Dhyani and Bhaskar 2017). Decomposition of these compounds produces their monomer units, which are further decomposed into volatile products such as CO, CO₂, condensable vapors (liquids), and tars.

During biomass pyrolysis, many chemical reactions which occur in series and parallel include dehydration, depolymerization, decarboxylation, isomerization, aromatization, and charring. In general, biomass pyrolysis occurs in three steps: (i) evaporation of free moisture, (ii) primary decomposition (char formation, depolymerization, and fragmentation), and (iii) secondary reactions (vapor cracking and repolymerization) (Collard and Blin 2014).

10.3.1 Evaporation of Free Moisture

Removal of free moisture (water vapor) from biomass occurs in the form of dehydration. It starts at 100 °C leaving behind the amorphous carbon in the char.

10.3.2 Primary Decomposition

At the start of pyrolysis, different chemical bonds present in biomass are broken, which results in the release of volatiles and rearrangement reactions. These are the primary reactions which consist of char formation, depolymerization, and fragmentation.

10.3.2.1 Char Formation

This includes the conversion of biomass into solid residue, which results due to the formation and rearrangement of benzene rings into stable polycyclic structures. The release of non-condensable gases occurs during these rearrangement reactions.

10.3.2.2 Depolymerization

Depolymerization involved in the breakage of polymers units into the individual monomers, which results in the decrease of the degree of polymerization in the chains and produces volatiles. These volatiles are frequently recovered into liquid fraction. Depolymerization reactions occur between the temperature range of 250 and 500 °C.

10.3.2.3 Fragmentation

It refers to the destruction of bonds within the monomer units of polymers which convert into non-condensable gas and linear compounds. Such type of breakage of ring/bonds generally occurs above 600 °C temperature.

10.3.3 Secondary Reactions

Volatile compounds generated during depolymerization or fragmentation step are not stable under the reactor temperature, and they may be further involved in secondary reactions. These reactions occur in the vapor phase and/or between the vapor and solid phase. These are particular to cracking and recombination (repolymerization) reactions. In cracking reactions, volatiles undergo breaking of chemical bonds to form the lighter molecular weight components. In recombination reactions, the volatiles recombine to form higher molecular weight components such as polycyclic hydrocarbons. Furthermore, additional solids such as secondary char are promoted to form when the recombination of volatiles occurs inside the pores of the solid residue. Figure 10.2 shows the reaction pathways for pyrolysis of biomass.

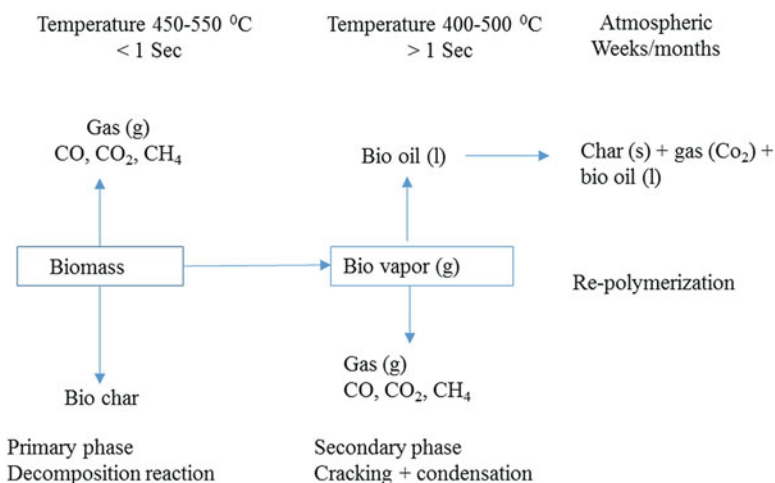


Fig. 10.2 Reaction pathways for pyrolysis of biomass (Jahirul et al. 2012)

10.4 Effect of Operating Parameters on Product Yield of Pyrolysis Process

Many factors affect the pyrolysis rate with product distribution and their quality. These factors can be summarized as the types of biomass, operating parameters (temperature, heating rate, biomass particle size, sweeping gas flow rate), and physicochemical properties of biomass. Here, we have discussed the effects of operating parameters on pyrolysis product distribution. The optimization of reaction conditions can enhance the yield of any of the three pyrolysis products (Beis et al. 2002). The effects of operating parameters on the product yield are summarized below.

10.4.1 Temperature

Temperature is the most important and significant parameter in the pyrolysis. It is known from the available literature that pyrolysis temperature plays a key role in the product yield (Yorgun et al. 2001; Putun et al. 2002). Temperature provides the required heat for decomposition of biomass. It is known that when the temperature of a molecule exceeds its boiling point, it forms vapor. Therefore, with an increase in the reactor temperature, possibilities for the conversion of different molecules of biomass into vapor phase increase. In pyrolysis process, the temperature difference between the reactor inside and the fresh feedstock provides the driving force for heat transfer for the decomposition and fragmentation of biomass. With an increase in reactor temperature, this temperature difference increases and consequently the rate of decomposition of biomass increases (Valliyappan et al. 2008). It is observed from the literature that bio-oil yield increases with an increase in pyrolysis temperature, attains a maximum value at around 500–550 °C, and decreases thereafter. The yield of bio-char is found maximum at the lower temperature of around 350 °C; furthermore, it decreases with an increase in temperature. Gaseous product yield increases continuously with an increase in temperature and maximum yield found at a higher temperature (Varma and Mondal 2017).

The characteristic properties of the bio-oil, bio-char, and gaseous product yield with an increase in operating temperature are because of the following reason. During pyrolysis, different types of reactions (primary and secondary) and devolatilization of biomass take place, and the produced vapor further undergoes different secondary reactions. When condensed, the condensable compounds produce bio-oil. Non-condensed molecules produce gaseous products. Secondary reactions help to increase gaseous product yield by producing non-condensable molecules. At lower temperature, the primary reactions predominate, and with the increase in reaction temperature, vapor formation increases. Consequently, the condensation of the vapors increases, which results in higher bio-oil yield. However, with an increase in temperature, the incidence of secondary reactions also increases.

Thus, after a certain temperature range, the bio-oil production decreases when secondary reactions predominate. A temperature exists at which the condensation of produced vapor to the liquid product becomes optimum, resulting in maximum bio-oil yield.

With an increase in temperature, more volatiles are formed as discussed above. Consequently, residual biomass (bio-char) reduced. The yield of bio-char always decreases as temperature and heating rate increases, which is due to the significant loss of volatile matter or secondary decomposition of char at a higher temperature (Chutia et al. 2014). Secondary decomposition of the char at a higher temperature produces non-condensable gases, which contribute to the increase in gaseous product yield.

The yield of gaseous products increases with an increase in temperature since at higher temperature secondary cracking reactions of pyrolysis vapors and secondary decompositions of char occur, which results in an overall increase in gaseous products' yield.

The composition of bio-oil varies remarkably with temperature. It is well known that bio-oils are a mixture of several chemical compounds. These chemical compounds are mainly alkanes, alkenes, carboxylic acids, aromatic, aliphatic and aromatic nitriles, and polycyclic aromatic hydrocarbons (PAHs) (Akhtar and Amin 2012). Table 10.2 shows the major chemical compounds present in bio-oils and their dependence on temperature.

10.4.2 Heating Rate

The heating rate is an important parameter in pyrolysis process. Rapid heating and cooling of primary vapors are required to minimize the possibilities of secondary reactions which reduce the liquid yield and have a negative impact on its quality, whereas slow heating favors the higher char yield (Kersten et al. 2005). Biomass pyrolysis with high heating rate decreases the limitations of heat and mass transfer as well as controls the secondary reactions (Yorgun et al. 2001). High heating rate produces more volatiles by fast endothermic decomposition of biomass, which reduces

Table 10.2 Major chemical compounds present in bio-oil and their dependence on temperature

Biomass type	Pyrolysis temperature (°C)	Bio-oil composition	References
Wood	300	Levoglucosan, levoglucosenone, acetic acid, guaiacyl acetone, hydroxyacetaldehyde, furan-(5H)-2-one, 2-furaldehyde, hydroxyacetone	Fu et al. (2008)
Yellow pine	552	Methanol, acetone, acetaldehyde, acetic acid, hydroxyacetaldehyde, propanal, 2-butanone, furan, methyl acetate, guaiacol, 4-methyl-guaiacol, 1-hydroxy-2 propanone, 1-hydroxy-2-butanone, furfural, furfurylic alcohol	Demirbas (2002)

the time required for secondary reactions (tars cracking or repolymerization). This results in the faster removal of high molecular char and volatiles from the decomposing biomass and left fewer amounts of char.

10.4.3 Biomass Particle Size

It is obvious that biomass is a poor conductor of heat; thus in some pyrolyzer, sand is used as a media for quick heat transfer. In batch pyrolyzer, where no sand is used for heat transfer media, heat is transferred from the surface of the pyrolyzer wall to the biomass through its surface. Thus, the higher surface area of biomass particles increases the heat transfer. Smaller particles possess more surface area than the bigger particles, and hence heat transfer is higher when the smaller particle-sized biomass is used in pyrolyzer. Due to this reason, more vapors are formed during pyrolysis, which result in less char and more gaseous products when particle size is smaller. With an increase in particle size, the heat transfer reduces, as a result, the rate of vaporization decreases, which gives more char formation and less gas formation. Furthermore, larger particle-sized biomass results in high-temperature gradients inside the particles; thus all the mass of the particle does not attain similar temperature when compared to smaller particle-sized biomass. Large particle-sized biomass also requires a high activation energy (Haykiri-Acma 2006). Due to these reasons, more char formation takes place and the vaporized products become relatively more condensable as compared to that of lower particle size feedstock. This is the probable reason for which bio-oil yield does not vary significantly due to the variation in particle size (Encinar et al. 2000).

10.4.4 Sweeping Gas (N₂) Flow Rate

The reactive environment of pyrolysis process can affect the nature and composition of the pyrolysis products. The interaction between the pyrolysis vapors with surrounding solid responsible for secondary exothermic reactions which lead to the formation of char. Pyrolysis conditions that support quick mass transfer are useful to minimize these reactions such as vacuum pyrolysis, fast purging of pyrolysis vapors, and rapid quenching of hot vapors (Demiral and Sensoz 2006). Inert gases such as N₂, Ar, and water vapor are used for the rapid purging of hot pyrolysis vapors. In most of the studies, N₂ gas is generally used due to its low cost.

In pyrolysis, the biomass first forms volatile vapors, which are carried out from the reactor by an inert gas like N₂ and condensed to produce bio-oil. The uncondensed vapors along with the carrier gas result in gaseous products. At lower N₂ flow rate, the residence time of the volatiles in the hot reactor zone is higher, as a result, the formation of more vapors from the biomass is affected, which yields more char formation. However, at a higher N₂ flow rate, the residence time of the vapor in the reactor hot zone decreases; consequently, more vapor formation takes place, which result in lower char yield and higher gas yield.

At a higher residence time, vapors in the reactor hot zone are converted to either smaller molecules by cracking or partial oxidation and generate more gaseous product as well as bigger molecules through repolymerization, recondensation, etc. The relative contribution of these secondary reactions depends on the vapor residence time. The decrease in residence time reduces the contribution of repolymerization reactions. Further, if the residence time is too less, the repolymerization reactions may not be considerable, which results in the lower production of bio-oil. Thus, with an increase in N_2 flow rate, initially the yield of bio-oil increases because of the formation of more vapors and their condensation as well as polymerization. However, after certain N_2 flow rate, the yield of bio-oil decreases as the contribution of repolymerization reactions reduces (Saikia et al. 2015).

Different types of biomass such as corncob, wheat straw, rice straw, coconut shell, hornbeam shell, etc. have also been exploited to produce bio-oil, bio-char, and pyro-gas through pyrolysis using different reactors and operating conditions as summarized in Table 10.3. This shows the range of operating parameters for the pyrolysis of different biomass and their optimum conditions for maximum bio-oil.

10.5 Pyrolysis Product Characteristics

The important products of biomass pyrolysis are bio-char, pyro-gas, and bio-oil. Characteristics and utilization potential of these products are described below:

10.5.1 Bio-char

Bio-char is the solid residue left after pyrolysis of carbonaceous biomass. The properties of bio-char mainly depend on the process and the biomass used. It is usually characterized for bulk density, proximate and ultimate composition, heating values, and surface properties. Thermal decomposition removes the moisture and volatile matter contents from biomass, and the remaining solid char has different properties than the parent biomass. Significant differences are mostly observed in the surface area, porosity, pore structures, and physicochemical properties such as proximate and ultimate composition (Haykiri-Acma et al. 2006).

It has high carbon content with calorific value in the range of 17–36 MJ/kg, as a result of which it can be utilized as a potential source of energy and may internally provide heat for pyrolysis process (Garcia-Perez et al. 2002). In addition, it can also be used as a precursor for activated carbon production and in the purification of wastewater through adsorption (Yargicoglu et al. 2015). In recent years, bio-char has gained enormous attention as it can be utilized as a fertilizer and also improves the quality of soil by increasing the retention time and availability of water and nutrients in the soil (Lehmann 2007; Chirakkara and Reddy 2015). In many cases, it also increases the crop growth (Chan and Xu 2009).

Table 10.3 Summary of pyrolysis of different biomass

Biomass	Reactor	Range of operating parameters				Optimum conditions	Optimum product yield (wt.%)	References
		Temperature (°C)	Heating rate (°C/min)	Biomass particle size (mm)	N ₂ flow rate (mL/min)			
Corn cob	Fixed bed	300–450	20	0.5–2	50	Temperature: 450 °C	Bio-oil: 47.3	Biswas et al. (2017)
							Bio-char: 24.0	
							Pyro-gas: 28.7	
Wheat straw						Temperature: 400 °C	Bio-oil: 36.7	Biswas et al. (2017)
							Bio-char: 34.4	
							Pyro-gas: 28.9	
Rice straw						Temperature: 400 °C	Bio-oil: 28.4	Biswas et al. (2017)
							Bio-char: 33.5	
							Pyro-gas: 38.1	
Rice husk						Temperature: 450 °C	Bio-oil: 38.1	Biswas et al. (2017)
							Bio-char: 35.0	
							Pyro-gas: 26.9	
Soursop seed cake	Batch	400	15	–	–	Temperature: 400 °C	Bio-oil: 18.6	Schroeder et al. (2017)
							Bio-char: 32.2	
							Pyro-gas: 17.7	
							Aqueous: 31.5	
Cashew nut shell	Batch	300–700	22.5	0.25	100	Temperature: 400 °C	Bio-oil: 40	Moreira et al. (2017)
							Bio-char: 30	
							Pyro-gas: 30	
<i>Anchusa azurea</i>	Fixed bed	350–550	100	0.6	100	Temperature: 450 °C	Bio-oil: 31.31	Aysu et al. (2016)
							Bio-char: 37.46	
							Pyro-gas: 31.23	
Mahogany wood	Batch	350–460	20	–	–	Temperature: 450 °C	Bio-oil: 60	Chukwunke et al. (2016)

<i>Xanthium strumarium</i>	Fixed bed	350–550	50	0.150–0.224	100	Temperature: 450 °C	Bio-oil: 22.75	Durak (2016)
							Bio-char: 32.23	
Babool seeds	Fixed bed	400–700	25	0.4–1	100–400	Temperature: 450 °C	Bio-oil: 38.3	Garg et al. (2016)
						Heating rate: 25 °C/min		
						Particle size: < 0.4 mm		
						N ₂ flow rate: 100 mL/min		
Energy cane	Batch	500–700	–	0.5–1	1000	Temperature: 550 °C	Bio-oil: 48.9	Henkel et al. (2016)
Chinese tallow wood		500–700	–	0.5–1	1000	Temperature: 600 °C	Bio-oil: 38.1	Henkel et al. (2016)
Tegument	Fixed bed	450–600	100	<1	1000	Temperature: 650 °C	Bio-oil: 38.8	Lazzari et al. (2016)
Almond						Temperature: 450 °C	Bio-oil: 28.1	Lazzari et al. (2016)
Mahua seed	Semi-batch	450–600	20	0.55–1	30	Temperature: 525 °C	Bio-oil: 49	Pradhan et al. (2016)
Coconut shell	Semi-batch	450–600	20	<1 (average)	–	Temperature: 575 °C	Bio-oil: 49.5	Rout et al. (2016)
<i>Calophyllum inophyllum</i> shell	Fixed bed	350–550	10–40	0.7–4.75	–	Temperature: 425 °C	Bio-oil: 41	Alagu et al. (2015)
						Heating rate: 40 °C/min		
						Particle size: 0.7–1.8 mm		

(continued)

Table 10.3 (continued)

Biomass	Reactor	Range of operating parameters				Optimum conditions	Optimum product yield (wt.%)	References
		Temperature (°C)	Heating rate (°C/min)	Biomass particle size (mm)	N ₂ flow rate (mL/min)			
Cornelian cherry stone	Fixed bed	300–700	7	<0.5	30	Temperature: 500 °C	Bio-oil: 47.5	Alper et al. (2015)
Grape seeds				<0.45		Temperature: 700 °C	Bio-oil: 41.04	Alper et al. (2015)
Liquorice stalks	Fixed bed	350–550	40	0.150–0.224	100	Temperature: 450 °C	Bio-oil: 30	Aysu and Durak (2015)
<i>Eremurus spectabilis</i>	Fixed bed	350–550	10, 30, and 50	0.224–0.850	100–250	Temperature: 500 °C Heating rate: 50 °C/min Particle size: 0.15–0.224 mm N ₂ flow rate: 100 mL/min	Bio-oil: 34.62	Aysu (2015)
<i>Mesua ferrea</i> seed cover	Fixed bed	350–650	40	0.2	100	Temperature: 500 °C	Bio-oil: 29.6	Bordoloi et al. (2015)
<i>Pongamia glabra</i> seed cover						Temperature: 500 °C	Bio-oil: 28.5	Bordoloi et al. (2015)
Cotton stalk	Fixed bed	500–600	20	–	20–50	Temperature: 600 °C N ₂ flow rate: 20 °C	Bio-oil: 17.14 Bio-char: 38 Pyro-gas: 44.86	Chouhan (2015)

<i>Jatropha curcas</i> cake	Fixed bed	350–600	5	0.5–0.8	100	Temperature: 550 °C	Bio-oil: 45	Majhi et al. (2015)
Hornbeam shell	Fixed bed	400–600	7–50	0.5–1	50–150	Temperature: 500 °C Heating rate: 50 °C/min N ₂ flow rate: 100 mL/min	Bio-oil: 24.67	Morali and Senoz (2015)
Napier grass stem	Fixed bed	450–650	30	0.2–2	20–60	Temperature: 500 °C N ₂ flow rate: 100 mL/min	Bio-oil: 32.26	Mohammad et al. (2015)
Perennial grass	Fixed bed	350–650	10 and 40	0.5–1.5	50–250	Temperature: 500 °C Heating rate: 40 °C/min N ₂ flow rate: 150 mL/min	Bio-oil: 26	Saikia et al. (2015)
Cotton seed	Batch	350–600	20	<1	5	Temperature: 550 °C	Bio-oil: 58.6	Seal et al. (2015)
Paulownia wood	Fixed bed	350–550	10 and 50	0.224–1.8	100–300	Temperature: 500 °C Heating rate: 50 °C/min Particle size: 0.425–1 mm N ₂ flow rate: 100 mL/min	Bio-oil: 54.0	Yorgun and Yildiz (2015)

(continued)

Table 10.3 (continued)

Biomass	Reactor	Range of operating parameters				Optimum conditions	Optimum product yield (wt.%)	References
		Temperature (°C)	Heating rate (°C/min)	Biomass particle size (mm)	N ₂ flow rate (mL/min)			
Eastern giant fennel stalks	Fixed bed	350–600	15, 30, and 50	0.15–0.85	–	Temperature: 500 °C	Bio-oil: 45.22	Aysu and Kucuk (2014)
						Heating rate: 50 °C/min	Bio-char: 24.32	
						Particle size: 0.15–0.224 mm N ₂ flow rate: 100 mL/min	Pyro-gas: 30.46	
Jute dust	Fixed bed	400–700	10 and 40	0.5–1.5	50–250	Temperature: 500 °C	Bio-oil: 31.11	Choudhury et al. (2014)
						Heating rate: 40 °C/min	Bio-char: 31.42	
						N ₂ flow rate: 150 mL/min	Pyro-gas: 20.34 Aqueous: 17.13	
<i>Pongamia glabra</i> de-oiled cake	Fixed bed	350–600	10, 20, and 40	0.2–0.4	–	Temperature: 500 °C	Bio-oil: 30.6	Chutia et al. (2014)
						Heating rate: 40 °C/min		
						Temperature: 500 °C		
Apricot kernel shell	Fixed bed	400–550	10 and 50	0.425–0.6	50–200	Temperature: 500 °C	Bio-oil: 30.6	Demiral and Kul (2014)
						Heating rate: 50 °C/min		
						N ₂ flow rate: 150 mL/min		

Castor seeds	Semi-batch	400–600	20	–	–	Temperature: 550 °C	Bio-oil: 62.45	Mohammed et al. (2014)
Rice straw	Fixed bed	300–700	10	–	1500	Temperature: 550 °C	Bio-oil: 43.3	Park et al. (2014)
Sal seed	Semi-batch	400–625	20	–	35	Temperature: 600 °C	Bio-oil: 52.8	Singh et al. (2014)
Giant miscanthus	Fixed bed	300–700	10	–	–	Temperature: 550 °C	Bio-oil: 50.75	Lee et al. (2013)
							Bio-char: 26.21 Pyro-gas: 23.23	
Neem seed	Semi-batch	400–500	20	–	–	Temperature: 475 °C	Bio-oil: 38	Nayan et al. (2013)
Mahua seed	Semi-batch	400–600	20	0.4–0.7	–	Temperature: 525 °C	Bio-oil: 59.95	Pradhan and Singh (2013)
Linseed seeds	Semi-batch	350–575	20	–	–	Temperature: 550 °C	Bio-oil: 68	Sinha et al. (2013)
<i>Imperata cylindrica</i>	Fixed bed	450–600	22	0.25–1	100	Temperature: 500 °C	Bio-oil: 20.88	Azduwin et al. (2012)
						Particle size: 0.5–1 mm		
Switchgrass	Fixed bed	400–600	–	<2	–	Temperature: 600 °C	Bio-oil: 37	Imam and Capareda (2012)
						Pyro-gas: 35		
						Bio-char: 26		
Karanja seeds	Semi-batch	450–550	20	–	–	Temperature: 500 °C	Bio-oil: 57	Nayan et al. (2012)
						Bio-char: 27		
						Pyro-gas: 16		

(continued)

Table 10.3 (continued)

Biomass	Reactor	Range of operating parameters				Optimum conditions	Optimum product yield (wt.%)	References
		Temperature (°C)	Heating rate (°C/min)	Biomass particle size (mm)	N ₂ flow rate (mL/min)			
Sesame de-oiled cake	Semi-batch					Temperature: 550 °C	Bio-oil: 58.5 Bio-char: 29.0 Pyro-gas: 12.4	Volli and Singh (2012)
Mustard de-oiled cake		350–700	25	–	–	Temperature: 550 °C	Bio-oil: 53.2 Bio-char: 29.9 Pyro-gas: 16.7	
Neem de-oiled cake						Temperature: 400 °C	Bio-oil: 40.2 Bio-char: 51.1 Pyro-gas: 8.5	
Groundnut de-oiled cake	Semi-batch	200–500	20	–	–	Temperature: 450 °C	Bio-oil: 50 Bio-char: 30 Pyro-gas: 20	Agrawalla et al. (2012)
Grape bagasse	Fixed bed	350–600	10 and 50	–	50–200	Temperature: 550 °C Heating rate: 50 °C/min	Bio-oil: 27.6 Bio-char: 28.24 Pyro-gas: 30.17	Demiral and Ayan (2011)
Castor seeds	Semi-batch	450–600	20	–	–	Temperature: 550 °C	Bio-oil: 64.4	Singh and Shadangi (2011)
Napier grass	Fixed bed	500	50–200	1–2	–	Temperature: 500 °C Heating rate: 150 °C/min Particle size (avg): 0.224 mm	Bio-oil: 36 Bio-char: 30	Lee et al. (2010)

Oil palm empty fruit bunches	Fluidized fixed bed	300–700	10–100	0.09–0.25	1500 (Ar)	Temperature: 500 °C	Bio-oil: 42.28	Mohamad et al. (2009)
						Heating rate: 100 °C/min		
						Particle size: 0.09–0.106 mm		
Coconut shell	Fixed bed	400–600	20, 40, and 60	<0.15–1.8	–	Temperature: 550 °C	Bio-oil: 45	Sundaram and Natarajan (2009)
						Heating rate: 60 °C/min	Bio-char: 24	
						Particle size: 1.18–1.80 mm	Pyro-gas: 32	
Pomegranate seeds	Fixed bed	400–800	30	3.2 (average)	5	Temperature: 600 °C	Bio-oil: 54.20	Ucar and karagoz (2009)
							Bio-char: 29.28	
							Pyro-gas: 16.52	
Safflower seed press cake	Fixed bed	400–600	10, 30, and 50	1.8 (average)	50–200	Temperature: 500 °C	Bio-oil: 36.1	Senoz and Angin (2008)
						Heating rate: 50 °C/min		
						N ₂ flow rate: 100 mm		
Rapeseed oil cake	Fixed bed	400–900	30	2 (average)	5	Temperature: 600 °C	Bio-oil: 58.58	Ucar and Ozkan (2008)
							Bio-char: 33.23	
							Pyro-gas: 8.18	
Pistachio shell	Fixed bed	300–700	7	1.82 (average)	–	Temperature: 550 °C	Bio-oil: 20.5	Apaydin-Varol et al. (2007)
							Bio-char: 25.8	
							Pyro-gas: 27.4	

(continued)

Table 10.3 (continued)

Biomass	Reactor	Range of operating parameters				Optimum conditions	Optimum product yield (wt.%)	References
		Temperature (°C)	Heating rate (°C/min)	Biomass particle size (mm)	N ₂ flow rate (mL/min)			
Safflower seed	Fixed bed	400–700	100, 300, and 800	0.85–1.25	50–400	Temperature: 600 °C Heating rate: 300 °C/min N ₂ flow rate: 100 mL/min	Bio-oil: 54.0	Onay (2007)
Rice husk	Fixed bed	400–800	100–500	0.125–0.5	500–1500	Temperature: 500 °C Heating rate: 200 °C/min Particle size: 0.125–0.177 mm	Bio-oil: 40.0	Tsai et al. (2007)
Hazelnut bagasse	Fixed bed	350–550	10 and 50	0.224–1.8	50–200	Temperature: 500 °C Heating rate: 10 °C/min Particle size: 0.425–0.6 mm N ₂ flow rate: 150 mL/min	Bio-oil: 34.4	Demiral and Senoz (2006)
Rapeseed	Free fall	400–700		0.224–1.8	50–400	Temperature: 600 °C Particle size: 0.224 to 0.6 mm N ₂ flow rate: 100 mL/min	Bio-oil: 75	Onay and Kocakar (2006)

Soybean oil cake	Fixed bed	350–550	10 and 50	0.425–1.8	–	Temperature: 400 °C	Bio-oil: 25.81	Senoz and Kaynar (2006)
						Heating rate: 50 °C/min	Bio-char: 23.56	
						Particle size: 0.425–0.6 mm		
Olive bagasse	Fixed bed	350–550	10 and 50	0.224–1.8	50–200	Temperature: 500 °C	Bio-oil: 37.7	Senoz et al. (2006)
						Heating rate: 10 °C/min		
						Particle size: 0.425–0.6 mm		
						N ₂ flow rate: 150 mL/min		
Soybean cake	Fixed bed	400–700	5, 100, 300, and 700	0.224–1.8	50–400	Temperature: 550 °C	Bio-oil: 42.83	Uzun et al. (2006)
						Heating rate: 700 °C/min		
						Particle size: 0.425–0.85 mm		
						N ₂ flow rate: 200 mL/min		
Olive residue	Fixed bed	400–700	7	1.29 (avg)	50–200	Temperature: 500 °C	Bio-oil: 39	Putun et al. (2005)
						N ₂ flow rate: 200 mL/min		

(continued)

Table 10.3 (continued)

Biomass	Reactor	Range of operating parameters				Optimum conditions	Optimum product yield (wt.%)	References
		Temperature (°C)	Heating rate (°C/min)	Biomass particle size (mm)	N ₂ flow rate (mL/min)			
Sesame stalk	Fixed bed	400–700	100–700	0.224–1.8	50–800	Temperature: 550 °C	Bio-oil: 37.2	Ates et al. (2004)
						Heating rate: 500 °C/min		
						Particle size: 0.425–0.85 mm		
						N ₂ flow rate: 200 mL/min		
Rapeseed	Fixed bed	400–700	30	0.425–1.8	50–400	Temperature: 550 °C	Bio-oil: 51.7	Onay and Kocakar (2004)
						Particle size: 0.6–1.8 mm		
						N ₂ flow rate: 100 mL/min		
<i>Miscanthus giganteus</i>	Fixed bed	350–650	10, 50, and 75	0.112–1.8	–	Temperature: 550 °C	Bio-oil: 23.92	Yorgun (2003)
						Heating rate: 50 °C/min		
						Particle size: 0.425–0.6 mm		

Safflower seed	Fixed bed	400–700	5, 40, and 80	0.425–1.8	50–200	Temperature: 500 °C	Bio-oil: 44.0	Beis et al. (2002)
						Heating rate: 5 °C/min		
						Particle size: 0.425–1.25 mm		
						N ₂ flow rate: 100 mL/min		
Sunflower oil cake	Fixed bed	400–700	300	0.425–0.85	25–400	Temperature: 500 °C	Bio-oil: 48.69	Gerzel (2002)
						N ₂ flow rate: 100 mL/min		
						Temperature: 550 °C		
Soybean cake	Fixed bed	400–700	5	0.224–1.8	50–400	Particle size: 0.850–1.25 mm	Bio-oil: 33.78	Putun et al. (2002)
						N ₂ flow rate: 200 mL/min		
						Temperature: 550 °C		

10.5.2 Gaseous Products/Pyro-gas

It mainly consists of CO, CH₄, CO₂, and H₂ with the heating value of 6.4–9.8 MJ/kg and internally utilized as process heat for pyrolysis. It can also be used as synthesis gas with extensive reforming (Islam et al. 2010).

10.5.3 Bio-oil

Bio-oil is a dark brown color, free-flowing organic liquid, which contains oxygenated compounds and is immiscible with other petrochemical liquid fuels. It is highly viscous, acidic, relatively unstable, corrosive, and chemically complex in nature (Shadangi and Mohanty 2014). It has a distinctive smoky odor. The heating value of bio-oil is lower than the conventional petroleum fuels due to the high water and oxygen content (Mohan et al. 2006). Bio-oil contains various chemical compounds such as water, water-insoluble lignin fragments, alcohols, aldehydes, carboxylic acids, ketones, carbohydrates, furfurals, and phenols. Table 10.4 represents the typical chemical compositions of bio-oil. Typical properties of bio-oil are shown in Table 10.5.

Bio-oil finds its utility in numerous places such as in power and chemical sectors. These include usage as a fuel in furnaces and boilers to powering diesel engines. Although the utilization of bio-oil as the transportation fuel is feasible in the form of methanol and Fischer-Tropsch fuels, more research is required in this field. Furthermore, another benefit of bio-oil is that it can be used in the extraction of a number of chemical products. A general overview of the applications of bio-oil is shown in Fig. 10.3.

10.6 Upgradation of Bio-oil

Considering the above discussion on the properties of bio-oil, it is clear that the fuel quality of bio-oil is lower than the petroleum fuels. Recently, there are several studies that have been done on the upgradation of bio-oil. Table 10.6 shows the current technology used for the upgradation of bio-oil. The characteristics as well as advantages and disadvantages of each technique are also described below.

10.6.1 Hydrotreating

Hydrotreating (HDT) is a nondestructive/simple hydrogenation process used to improve the quality of bio-oils by alteration of their boiling range. In this process, bio-oil reacts with hydrogen at moderate temperature up to 500 °C and low pressure in the presence of the catalyst to remove the oxygen present in bio-oil (Augustínová et al. 2013). The commonly used catalysts for this process are sulfided CoMo or NiMo supported on alumina or aluminosilicates. The main problems that arise due to

Table 10.4 Typical chemical compositions of bio-oil

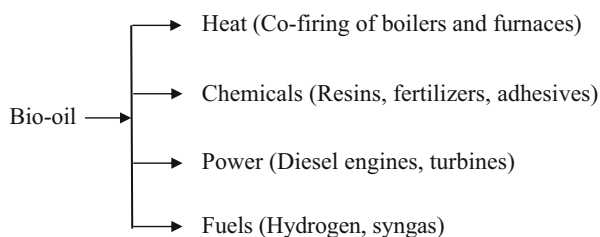
Major components	Quantity (wt.%)
Water	20–30
Lignin fragments	15–30
Aldehydes	10–20
Carboxylic acids	5–10
Carbohydrates	2–5
Alcohols	2–5
Ketones	1–5
Phenols	1–4
Furfurals	2–5

Reference: Bridgwater et al. (2002)

Table 10.5 Typical properties of bio-oil

Properties	Value
C (%)	44–63.5
H (%)	5.2–7.2
N (%)	0.07–0.39
O (%)	32–46
Moisture content (wt. %)	10.2–35
Ash (wt. %)	0–0.2
pH	2–3.5
Density (kg/m^3)	1210–1240
Viscosity (at 50 °C), cP	40–100
Flash point (°C)	40–110
Pour point (°C)	–9 to –36
High heating value (MJ/kg)	15–24.3
Solids (wt.%)	0.17–1.14
Distillation residue (wt.%)	30–50

References: Dhyani and Bhaskar (2017) and Mohan et al. (2006)

Fig. 10.3 Applications of bio-oil (Jahirul et al. 2012)

the use of these catalysts are the instability of alumina and aluminosilicates in the high water content environment of the bio-oil and sulfur stripping from the catalysts. Other suitable catalysts such as Ru/C (Bridgwater 2012), Pd/C (Zheng and Wie 2011), Pt/SiO₂/Al₂O₃ (Sheu et al. 1998), vanadium nitride (Ramanathan and Oyama 1995), and Ru (Centeno et al. 1999) have also been used for hydrotreating.

Table 10.6 Upgradation techniques of bio-oil with their advantages and disadvantages (Xiu and Shahbazi 2012)

Upgrading techniques	Process conditions	Advantages	Disadvantages
Hydrotreating	Temperature: ~500 °C	Commercialized	High coking (8–25%)
	Pressure: Low		Poor quality of fuels obtained
	Chemical: H ₂ /CO		
	Catalyst: HZSM-5 CoMo, NiMo		
Hydrocracking	Temperature: >350 °C	Makes larger quantities of light products	Need complicated equipment
	Pressure: 100–2000 psi		Reactor clogging
	Chemical: H ₂ /CO		Catalyst deactivation
	Catalyst: Ni/Al ₂ O ₃ -TiO ₂		
Steam reforming	Temperature: 800–900 °C	Produces H ₂ as a fuel	Complicated
	Catalyst: Ni		Require steady, dependable, and fully developed reactors
Supercritical fluids	Chemical: Alcohol, acetone, ethyl acetate, glycerol	High oil yield	Solvent is expensive
		Good fuel quality (lower oxygen content, lower viscosity)	
Esterification	Chemical: Alcohol	Simple	Solvents required
	Catalyst: Solid acid/base	Low cost of solvents Reduces bio-oil viscosity	Mechanisms involved in adding solvent are not quite understood yet
Emulsification	Chemical: Surfactant	Simple	Requires high energy for production
		Less corrosive	

This process operates at mild conditions, but the yield of bio-oil is relatively low. Moreover, this process generates a large amount of coke, char, and tar, which are responsible for deactivation of catalysts and reactor clogging.

10.6.2 Hydrocracking

Hydrocracking is a thermal process (>350 °C) in which hydrogenation accompanies cracking which occurs at relatively high pressure (100–2000 psi) (Xiu and Shahbazi 2012). Hydrocracking of bio-oil produces a wide range of products due to the combination of catalytic cracking reactions with hydrogenation and the multiplicity of reactions. This process is performed by dual-function catalysts in which silica-alumina or zeolite (HZSM-5, HY) catalysts provide the cracking function. In

addition, platinum and tungsten oxide catalyze the reactions, and nickel provides the hydrogenation function. Alumina is mostly used as a support for catalyst. This process is more effective for production of a large amount of light product. However, it requires more severe conditions of temperature and pressure to deal with acids, which is not economical and energy efficient.

10.6.3 Steam Reforming

This process converts the petroleum fractions to more volatile products with higher octane number and represents the combined effect of various reactions such as cracking, isomerization, and dehydrogenation. In this process, hydrocarbons are converted into syngas ($\text{CO} + \text{H}_2$), by reaction with steam at high temperature. Commercial nickel catalysts show good activity in the processing of bio-oil. Hydrogen production from steam reforming of bio-oils has been extensively studied by the National Renewable Energy Laboratory (NREL) in fixed-bed and fluidized-bed reactor along with the reaction mechanisms (Wang et al. 1998). Hydrogen is a clean energy resource and crucial in the chemical industry. The increasing focus on reforming the water fraction of bio-oil looks promising.

10.6.4 Supercritical Fluids

Supercritical fluids have the ability to dissolve materials which are not usually soluble in either gaseous or liquid phase of the solvent and hence to promote the liquefaction/gasification reactions (Xu and Etcheverry 2008). Supercritical fluids have the ability to improve the yield and quality of bio-oil and have demonstrated a great potential for producing bio-oil with much higher caloric value and lower viscosity. Water is the cheapest and most commonly used supercritical fluid in hydrothermal processing, but utilizing water as the solvent for liquefaction of biomass has the following drawbacks: (1) lower yield of the water-insoluble oil product and (2) yields bio-oil that is very viscous and has high oxygen content. To improve the quality and yield of bio-oil, utilization of organic solvents such as ethanol, butanol, acetone, and methanol has been adopted. All these solvents have the ability to significantly affect the quality and yield of bio-oil, although the process of upgrading bio-oil using supercritical fluids is environment friendly and required relatively lower temperature. However, this process is not economically feasible on a broad scale due to the high cost of the organic solvents.

10.6.5 Esterification

Esterification of bio-oils with low molecular weight alcohols is an effective approach to improve their qualities. In the last few years, a lot of work has been done to upgrade the bio-oils by esterification (Cui et al. 2010; Zhang 2006). Zhang (2006)

demonstrated the solid acid/base catalyst to esterify the bio-oil under atmosphere pressure and found that the acidity, density, heating value, and storage stability of the bio-oil improved remarkably.

10.6.6 Emulsification

Emulsification is a simplest technique, where the bio-oil is emulsified with diesel using a surfactant. However, it is considered as a short-term approach, because this process is not economical, and corrosion issues are associated with this technique (Zhang et al. 2007). Heating value and cetane number were also unsatisfactory. Recently, this process has been investigated by many researchers (Jiang and Ellis 2009; Chiaramonti et al. 2003; Ikura et al. 2003).

10.7 Conclusions

Pyrolysis process follows indirect thermal decomposition mechanism by which biomass under oxygen-depleted condition can be converted into three major products such as bio-oil, bio-char, and pyro-gas. The yield of these pyrolysis products depends upon the operating parameters such as temperature, heating rate, biomass particle size, and sweeping gas flow rate. Temperature is the most important operating parameter in the pyrolysis process, and intermediate temperature between 500 and 550 °C maximizes the bio-oil yield in the products. Low- and high-temperature ranges favor the formation of char and gases, respectively. Overall, moderate pyrolysis temperature, high heating rate, and short vapor residence time maximize the yield of bio-oil in the product. Sweeping gas flow rates do not much influence the yield of bio-oil. However, it reduces the volatile residence times, which helps to minimize the secondary cracking and repolymerization of vapors. Moreover, a rapid quenching of hot pyrolysis vapors is crucial for high bio-oil yield. The optimum pyrolysis product yield which varied for different biomass depends upon the reactor types and operating parameters. Studies have also been carried out for properties and application of pyrolysis products as well as the upgradation of bio-oil.

References

- Agrawalla A, Kumar S, Singh RK (2012) Pyrolysis of groundnut de-oiled cake and characterization of the liquid product. *Bioresour Technol* 102:10711–10716
- Akhtar J, Amin NS (2012) A review on operating parameters for optimum liquid oil yield in biomass pyrolysis. *Renew Sust Energ Rev* 16:5101–5109
- Alagu RM, Sundaram EG, Natarajan E (2015) Thermal and catalytic slow pyrolysis of Calophyllum inophyllum fruit shell. *Bioresour Technol* 193:463–468
- Alper K, Tekin K, Karagöz S (2015) Pyrolysis of agricultural residues for bio-oil production. *Clean Technol Environ Policy* 17:211–223

- Apaydin-Varol E, Pütün E, Pütün AE (2007) Slow pyrolysis of pistachio shell. *Fuel* 86:1892–1899
- Ateş F, Pütün E, Pütün AE (2004) Fast pyrolysis of sesame stalk: yields and structural analysis of bio-oil. *J Anal Appl Pyrolysis* 71:779–790
- Augustínová J, Cvengrošová Z, Mikulec J, Vasilková B, Cvengroš J (2013) Upgrading of biooil from fast pyrolysis. In: 46th international conference on petroleum processing. 7 June
- Aysu T (2015) Catalytic pyrolysis of *Eremurus spectabilis* for bio-oil production in a fixed-bed reactor: effects of pyrolysis parameters on product yields and character. *Fuel Process Technol* 129:24–38
- Aysu T, Durak H (2015) Catalytic pyrolysis of liquorice (*Glycyrrhiza glabra* L.) in a fixed-bed reactor: effects of pyrolysis parameters on product yields and character. *J Anal Appl Pyrolysis* 111:156–172
- Aysu T, Küçük MM (2014) Biomass pyrolysis in a fixed-bed reactor: effects of pyrolysis parameters on product yields and characterization of products. *Energy* 64:1002–1025
- Aysu T, Durak H, Güner S, Bengü AŞ, Esim N (2016) Bio-oil production via catalytic pyrolysis of *Anchusa azurea*: effects of operating conditions on product yields and chromatographic characterization. *Bioresour Technol* 205:7–14
- Azduwin K, Ridzuan MJ, Hafis SM, Amran T (2012) Slow pyrolysis of *Imperata cylindrica* in a fixed bed reactor. *Int J Biol Ecol Environ Sci* 1:176–180
- Babu BV (2008) Biomass pyrolysis: a state-of-the-art review. *Biofuels Bioprod Biorefin* 2:393–414
- Balat H, Kırtay E (2010) Hydrogen from biomass—present scenario and future prospects. *Int J Hydrog Energy* 35:7416–7426
- Beis SH, Onay Ö, Koçkar ÖM (2002) Fixed-bed pyrolysis of safflower seed: influence of pyrolysis parameters on product yields and compositions. *Renew Energy* 26:21–32
- Biswas B, Pandey N, Bisht Y, Singh R, Kumar J, Bhaskar T (2017) Pyrolysis of agricultural biomass residues: comparative study of corn cob, wheat straw, rice straw and rice husk. *Bioresour Technol* 237:57–63
- Bordoloi N, Narzari R, Chutia RS, Bhaskar T, Katak R (2015) Pyrolysis of *Mesua ferrea* and *Pongamia glabra* seed cover: characterization of bio-oil and its sub-fractions. *Bioresour Technol* 178:83–89
- Bridgwater AV (2003) Renewable fuels and chemicals by thermal processing of biomass. *Chem Eng J* 91:87–102
- Bridgwater AV (2012) Review of fast pyrolysis of biomass and product upgrading. *Biomass Bioenergy* 38:68–94
- Bridgwater AV, Peacocke GV (2000) Fast pyrolysis processes for biomass. *Renew Sust Energy Rev* 4:1–73
- Bridgwater AV, Toft AJ, Brammer JG (2002) A techno-economic comparison of power production by biomass fast pyrolysis with gasification and combustion. *Renew Sust Energy Rev* 6:181–246
- Centeno A, Maggi R, Delmon B (1999) Use of noble metals in hydrodeoxygenation reactions. *Stud Surf Sci Catal* 127:77–84
- Chan KY, Xu Z (2009) Biochar: nutrient properties and their enhancement. *Biochar Environ Manag Sci Technol* 1:67–84
- Chiaromonti D, Bonini M, Fratini E, Tondi G, Gartner K, Bridgwater AV, Grimm HP, Soldaini I, Webster A, Baglioni P (2003) Development of emulsions from biomass pyrolysis liquid and diesel and their use in engines-part 1: emulsion production. *Biomass Bioenergy* 25:85–99
- Chirakkara RA, Reddy KR (2015) Biomass and chemical amendments for enhanced phytoremediation of mixed contaminated soils. *Ecol Eng* 85:265–274
- Choudhury ND, Chutia RS, Bhaskar T, Katak R (2014) Pyrolysis of jute dust: effect of reaction parameters and analysis of products. *J Mater Cycles Waste Manag* 16:449–459
- Chouhan APS (2015) A slow pyrolysis of cotton stalk (*Gossypium arboretum*) waste for bio-oil production. *J Pharma Chem Biol Sci* 3:143–149
- Chukwunke JL, Sinebe JE, Ugwuegbu DC, Agulonu CC (2016) Production by pyrolysis and analysis of bio-oil from mahogany wood (*Swietenia macrophylla*). *Brit J Appl Sci Technol* 17:1–9

- Chutia RS, Katakı R, Bhaskar T (2014) Characterization of liquid and solid product from pyrolysis of *Pongamia glabra* deoiled cake. *Bioresour Technol* 165:336–342
- Collard FX, Blin J (2014) A review on pyrolysis of biomass constituents: mechanisms and composition of the products obtained from the conversion of cellulose, hemicelluloses and lignin. *Renew Sust Energ Rev* 38:594–608
- Cui HY, Wang JH, Zhuo SP, Li ZH, Wang LH, Yi WM (2010) Upgrading bio-oil by esterification under supercritical CO₂ conditions. *J Fuel Chem Technol* 38:673–678
- Dalai AK, Bassi A (2010) Bioenergy and green engineering. *Energy Fuel* 24:4627
- Demiral İ, Ayan EA (2011) Pyrolysis of grape bagasse: effect of pyrolysis conditions on the product yields and characterization of the liquid product. *Bioresour Technol* 102:3946–3951
- Demiral İ, Kul ŞÇ (2014) Pyrolysis of apricot kernel shell in a fixed-bed reactor: characterization of bio-oil and char. *J Anal Appl Pyrolysis* 107:17–24
- Demiral İ, Şensöz S (2006) Fixed-bed pyrolysis of hazelnut (*Corylus avellana* L.) bagasse: influence of pyrolysis parameters on product yields. *Energy Sources Part A* 28:1149–1158
- Demirbaş A (2002) Analysis of liquid products from biomass via flash pyrolysis. *Energy Sour* 24:337–345
- Demirbaş A (2008) Biofuels sources, biofuel policy, biofuel economy and global biofuel projections. *Energy Convers Manag* 49:2106–2116
- Dhyani V, Bhaskar T (2017) A comprehensive review on the pyrolysis of lignocellulosic biomass. *Renew Energy*. <https://doi.org/10.1016/j.renene.2017.04.035>
- Durak H (2016) Pyrolysis of *Xanthium strumarium* in a fixed bed reactor: effects of boron catalysts and pyrolysis parameters on product yields and character. *Energy Sources Part A* 38:1400–1409
- Encinar JM, Gonzalez JF, Gonzalez J (2000) Fixed-bed pyrolysis of *Cynara cardunculus* L. product yields and compositions. *Fuel Process Technol* 68:209–222
- Farid NA (2006) Fast pyrolysis of bioresources into energy and other applications. In: *Proceedings of the seminar on energy from biomass 2006. Conversion of bioresources into energy and other applications*, Forest Research Institute Malaysia (FRIM), Kepong, pp 27–37.
- Fu Q, Argyropoulos DS, Tilotta DC, Lucia LA (2008) Understanding the pyrolysis of CCA-treated wood: Part II. Effect of phosphoric acid. *J Anal Appl Pyrolysis* 82:140–144
- Garcia-Perez M, Chaala A, Roy C (2002) Co-pyrolysis of sugarcane bagasse with petroleum residue. Part II. Product yields and properties. *Fuel* 81:893–907
- Garg R, Anand N, Kumar D (2016) Pyrolysis of babool seeds (*Acacia nilotica*) in a fixed bed reactor and bio-oil characterization. *Renew Energy* 96:167–171
- Gercel HF (2002) The production and evaluation of bio-oils from the pyrolysis of sunflower-oil cake. *Biomass Bioenergy* 23:307–314
- Haykiri-Acma H (2006) The role of particle size in the non-isothermal pyrolysis of hazelnut shell. *J Anal Appl Pyrolysis* 75:211–216
- Haykiri-Acma H, Yaman S, Kucukbayrak S (2006) Gasification of biomass chars in steam–nitrogen mixture. *Energy Convers Manag* 47:1004–1013
- Henkel C, Muley PD, Abdollahi KK, Marculescu C, Boldor D (2016) Pyrolysis of energy cane bagasse and invasive Chinese tallow tree (*Triadica sebifera* L.) biomass in an inductively heated reactor. *Energy Convers Manag* 109:175–183
- Ikura M, Stanculescu M, Hogan E (2003) Emulsification of pyrolysis derived bio-oil in diesel fuel. *Biomass Bioenergy* 24:221–232
- Imam T, Capareda S (2012) Characterization of bio-oil, syn-gas and bio-char from switchgrass pyrolysis at various temperatures. *J Anal Appl Pyrolysis* 93:170–177
- Isahak WN, Hisham MW, Yarmo MA, Hin TY (2012) A review on bio-oil production from biomass by using pyrolysis method. *Renew Sust Energ Rev* 16:5910–5923
- Islam MR, Haniu H, Islam MN, Uddin MS (2010) Thermochemical conversion of sugarcane bagasse into bio-crude oils by fluidized-bed pyrolysis technology. *J Therm Sci Technol* 5:11–23
- Jahirul MI, Rasul MG, Chowdhury AA, Ashwath N (2012) Biofuels production through biomass pyrolysis—a technological review. *Energies* 5:4952–5001

- Jiang X, Ellis N (2009) Upgrading bio-oil through emulsification with biodiesel: mixture production. *Energy Fuel* 24:1358–1364
- Kersten SR, Wang X, Prins W, van Swaaij WP (2005) Biomass pyrolysis in a fluidized bed reactor. Part 1: literature review and model simulations. *Ind Eng Chem Res* 44:8773–8785
- Lazzari E, Schena T, Primaz CT, da Silva Maciel GP, Machado ME, Cardoso CA, Jacques RA, Caramão EB (2016) Production and chromatographic characterization of bio-oil from the pyrolysis of mango seed waste. *Ind Crop Prod* 83:529–536
- Lee MK, Tsai WT, Tsai YL, Lin SH (2010) Pyrolysis of Napier grass in an induction-heating reactor. *J Anal Appl Pyrolysis* 88:110–116
- Lee Y, Ryu C, Park YK, Jung JH, Hyun S (2013) Characteristics of biochar produced from slow pyrolysis of *Geodae-Uksae* 1. *Bioresour Technol* 130:345–350
- Lehmann J (2007) Bio-energy in the black. *Front Ecol Environ* 5:381–387
- Maity JP, Bundschuh J, Chen CY, Bhattacharya P (2014) Microalgae for third generation biofuel production, mitigation of greenhouse gas emissions and wastewater treatment: present and future perspectives—a mini review. *Energy* 78:104–113
- Majhi A, Sharma YK, Naik DV, Chauhan R (2015) The production and evaluation of bio-oil obtained from the *Jatropha curcas* cake. *Energy Sources Part A* 37:1782–1789
- Meier D, Faix O (1999) State of the art of applied fast pyrolysis of lignocellulosic materials—a review. *Bioresour Technol* 68:71–77
- Mohamad AS, Chow M, Nor K (2009) Bio-oils from pyrolysis of oil palm empty fruit bunches. *Am J Appl Sci* 6:869–875
- Mohammad I, Abakar Y, Kabir F, Yusuf S, Alshareef I, Chin S (2015) Pyrolysis of Napier grass in a fixed bed reactor: effect of operating conditions on product yields and characteristics. *Bioresources* 10:6457–6478
- Mohammed T, Lakhmiri R, Azmani A (2014) Bio-oil from pyrolysis of castor seeds. *Int J Basic Appl Sci* 14:217–226
- Mohan D, Pittman CU, Steele PH (2006) Pyrolysis of wood/biomass for bio-oil: a critical review. *Energy Fuel* 20:848–889
- Mohanty P, Pant KK, Naik SN, Parikh J, Hornung A, Sahu JN (2014) Synthesis of green fuels from biogenic waste through thermochemical route—the role of heterogeneous catalyst: a review. *Renew Sust Energ Rev* 38:131–153
- Moralı U, Şensöz S (2015) Pyrolysis of hornbeam shell (*Carpinus betulus L.*) in a fixed bed reactor: characterization of bio-oil and bio-char. *Fuel* 150:672–678
- Moreira R, dos Reis Orsini R, Vaz JM, Penteado JC, Spinacé EV (2017) Production of biochar, bio-oil and synthesis gas from cashew nut shell by slow Pyrolysis. *Waste Biomass Valor* 8:217–224
- Murugan S, Gu S (2015) Research and development activities in pyrolysis—contributions from Indian scientific community—a review. *Renew Sust Energ Rev* 46:282–295
- Nayan NK, Kumar S, Singh RK (2012) Characterization of the liquid product obtained by pyrolysis of karanja seed. *Bioresour Technol* 124:186–189
- Nayan NK, Kumar S, Singh RK (2013) Production of the liquid fuel by thermal pyrolysis of neem seed. *Fuel* 103:437–443
- Onay O (2007) Influence of pyrolysis temperature and heating rate on the production of bio-oil and char from safflower seed by pyrolysis, using a well-swept fixed-bed reactor. *Fuel Process Technol* 88:523–531
- Onay O, Koçkar OM (2004) Fixed-bed pyrolysis of rapeseed (*Brassica napus L.*). *Biomass Bioenergy* 26:289–299
- Onay O, Koçkar OM (2006) Pyrolysis of rapeseed in a free fall reactor for production of bio-oil. *Fuel* 85:1921–1928
- Panwar NL, Kaushik SC, Kothari S (2011) Role of renewable energy sources in environmental protection: a review. *Renew Sust Energ Rev* 15:1513–1524
- Park J, Lee Y, Ryu C, Park YK (2014) Slow pyrolysis of rice straw: analysis of products properties, carbon and energy yields. *Bioresour Technol* 155:63–70

- Patel M (2013) Pyrolysis and gasification of biomass and acid hydrolysis residues. Doctoral dissertation, Aston University.
- Pradhan D, Singh RK (2013) Bio-oil from biomass: thermal pyrolysis of mahua seed. In: Energy efficient technologies for Sustainability (ICEETS), 2013 International Conference on 2013 April 10, pp 487–490.
- Pradhan D, Singh RK, Bendu H, Mund R (2016) Pyrolysis of Mahua seed (*Madhuca indica*)-production of biofuel and its characterization. *Energy Convers Manag* 108:529–538
- Pütün AE, Apaydin E, Pütün E (2002) Bio-oil production from pyrolysis and steam pyrolysis of soybean-cake: product yields and composition. *Energy* 27:703–713
- Pütün AE, Uzun BB, Apaydin E, Pütün E (2005) Bio-oil from olive oil industry wastes: pyrolysis of olive residue under different conditions. *Fuel Process Technol* 87:25–32
- Ramanathan S, Oyama ST (1995) New catalysts for hydroprocessing: transition metal carbides and nitrides. *J Phys Chem* 99:16365–16372
- Razzak SA, Hossain MM, Lucky RA, Bassi AS, de Lasa H (2013) Integrated CO₂ capture, wastewater treatment and biofuel production by microalgae culturing—a review. *Renew Sust Energ Rev* 27:622–653
- Rout T, Pradhan D, Singh RK, Kumari N (2016) Exhaustive study of products obtained from coconut shell pyrolysis. *J Environ Chem Eng* 4:3696–3705
- Saikia R, Chutia RS, Katak R, Pant KK (2015) Perennial grass (*Arundo donax* L.) as a feedstock for thermo-chemical conversion to energy and materials. *Bioresour Technol* 188:265–272
- Schroeder P, do Nascimento BP, Romeiro-ga, Figueiredo MK, da Cunha Veloso MC (2017) Chemical and physical analysis of the liquid fractions from soursop seed cake obtained using slow pyrolysis conditions. *J Anal Appl Pyrolysis* 124:161–174
- Seal S, Panda AK, Kumar S, Singh RK (2015) Production and characterization of bio oil from cotton seed. *Environ Prog Sustain Energy* 34:542–547
- Şensöz S, Angın D (2008) Pyrolysis of safflower (*Charthamus tinctorius* L.) seed press cake: part 1. The effects of pyrolysis parameters on the product yields. *Bioresour Technol* 99:5492–5497
- Şensöz S, Kaynar İ (2006) Bio-oil production from soybean (*Glycine max* L.); fuel properties of bio-oil. *Ind Crop Prod* 23:99–105
- Şensöz S, Demiral İ, Gerçel HF (2006) Olive bagasse (*Olea europaea* L.) pyrolysis. *Bioresour Technol* 97:429–436
- Shadangi KP, Mohanty K (2014) Production and characterization of pyrolytic oil by catalytic pyrolysis of Niger seed. *Fuel* 126:109–115
- Sharma A, Pareek V, Zhang D (2015) Biomass pyrolysis—a review of modelling, process parameters and catalytic studies. *Renew Sust Energ Rev* 50:1081–1096
- Sheu YH, Anthony RG, Soltes EJ (1998) Kinetic studies of upgrading pine pyrolytic oil by hydrotreatment. *Fuel Process Technol* 19:31–50
- Singh RK, Shadangi KP (2011) Liquid fuel from castor seeds by pyrolysis. *Fuel* 90:2538–2544
- Singh VK, Soni AB, Kumar S, Singh RK (2014) Pyrolysis of sal seed to liquid product. *Bioresour Technol* 151:432–435
- Sinha R, Kumar S, Singh RK (2013) Production of biofuel and biochar by thermal pyrolysis of linseed seed. *Biomass Conv Biorefr* 3:327–335
- Sundaram EG, Natarajan E (2009) Pyrolysis of coconut shell: an experimental investigation. *J Eng Res* 6:33–39
- Tsai WT, Lee MK, Chang YM (2007) Fast pyrolysis of rice husk: product yields and compositions. *Bioresour Technol* 98:22–28
- Uçar S, Karagöz S (2009) The slow pyrolysis of pomegranate seeds: the effect of temperature on the product yields and bio-oil properties. *J Anal Appl Pyrol* 84:151–156
- Ucar S, Ozkan AR (2008) Characterization of products from the pyrolysis of rapeseed oil cake. *Bioresour Technol* 99:8771–8776
- Uzun BB, Pütün AE, Pütün E (2006) Fast pyrolysis of soybean cake: product yields and compositions. *Bioresour Technol* 97:569–576

- Valliyappan T, Bakhshi NN, Dalai AK (2008) Pyrolysis of glycerol for the production of hydrogen or syn gas. *Bioresour Technol* 99:4476–4483
- Vamvuka D, Kakaras E, Kastanaki E, Grammelis P (2003) Pyrolysis characteristics and kinetics of biomass residuals mixtures with lignite. *Fuel* 82:1949–1960
- Varma AK, Mondal P (2017) Pyrolysis of sugarcane bagasse in semi batch reactor: effects of process parameters on product yields and characterization of products. *Ind Crop Prod* 95:704–717
- Volli V, Singh RK (2012) Production of bio-oil from de-oiled cakes by thermal pyrolysis. *Fuel* 96:579–585
- Wang D, Czernik S, Chornet E (1998) Production of hydrogen from biomass by catalytic steam reforming of fast pyrolysis oils. *Energy Fuel* 12:19–24
- Xiu S, Shahbazi A (2012) Bio-oil production and upgrading research: a review. *Renew Sust Energ Rev* 16:4406–4414
- Xu C, Etcheverry T (2008) Hydro-liquefaction of woody biomass in sub-and super-critical ethanol with iron-based catalysts. *Fuel* 87:335–345
- Yargicoglu EN, Sadasivam BY, Reddy KR, Spokas K (2015) Physical and chemical characterization of waste wood derived biochars. *Waste Manag* 36:256–268
- Yorgun S (2003) Fixed-bed pyrolysis of *Miscanthus x giganteus*: product yields and bio-oil characterization. *Energy Sour* 25:779–790
- Yorgun S, Yıldız D (2015) Slow pyrolysis of paulownia wood: effects of pyrolysis parameters on product yields and bio-oil characterization. *J Anal Appl Pyrolysis* 114:68–78
- Yorgun S, Şensöz S, Koçkar ÖM (2001) Characterization of the pyrolysis oil produced in the slow pyrolysis of sunflower-extracted bagasse. *Biomass Bioenergy* 20:141–148
- Zhang Q (2006) Upgrading bio-oil over solid acid and base by catalytic esterification. PhD thesis, University of Science and Technology of China
- Zhang Q, Chang J, Wang T, Xu Y (2007) Review of biomass pyrolysis oil properties and upgrading research. *Energy Convers Manag* 48:87–92
- Zheng JL, Wei Q (2011) Improving the quality of fast pyrolysis bio-oil by reduced pressure distillation. *Biomass Bioenergy* 35:1804–1810



Applications of Supercritical Fluids for Biodiesel Production

11

Sivamohan N. Reddy, Sonil Nanda, and Prakash K. Sarangi

Abstract

The direction to opt for renewable fuels has become essential due to the overconsumption of fossil fuels and their emissions challenging the safe and clean environment. Biodiesel, preliminarily the fatty acid alkyl esters, is resultant of transesterification of oils and fats with alcohols. Owing to the problems associated with the conventional biodiesel production in the presence of basic catalysts, non-catalytic supercritical processes eliminates mass transfer resistances, enhancing reaction rates approaching near complete conversion. Supercritical transesterification processes require temperature greater than critical temperature and pressure to attain the desirable biodiesel yields. High alcohol-to-oil ratio with temperatures higher than 300 °C and residence times within minutes are used to maximize the biodiesel yields with methanol/ethanol for different oil feedstocks. Green technologies by implementing enzymatic catalysts such as lipases in supercritical carbon dioxide (SCCO₂) have received attention due to enhanced interactions between the reactant molecules. The key findings of enzymatic transesterification in SCCO₂ and their combination with ionic liquids are presented in this chapter along with the operating parameters at maximum biodiesel yields. To improve the biodiesel economy, products superior to glycerol can be synthesized by replacing conventional alcohols with other solvents. Solvents such as methyl acetate (MeOAc) and dimethyl carbonate (DMC) are applied to

S. N. Reddy (✉)

Department of Chemical Engineering, Indian Institute of Technology Roorkee, Roorkee, Uttarakhand, India
e-mail: nsiva.fch@iitr.ac.in

S. Nanda

Department of Chemical and Biochemical Engineering, University of Western Ontario, London, Ontario, Canada

P. K. Sarangi

Directorate of Research, Central Agricultural University, Imphal, Manipur, India

get the triacetin and glycerol carbonate, which have more economic value. The challenges involved in enzymatic and non-catalytic supercritical processes both in terms of operation and economics are discussed.

Keywords

Transesterification · Supercritical fluid · Biodiesel · Carbon dioxide · Enzymatic catalysts · Methyl acetate · Dimethyl carbonate

11.1 Introduction

The uncertainty in crude oil economy with their contribution to greenhouse gas emissions directs to look for clean, affordable, and renewable energy to meet the global energy demand. The key features of energy resources that gain the attention are abundant availability, low-carbon emissions, and economic viability in the current energy sector. Biomass has been found to be an alternative crude energy resource to the petroleum-based fuels. Biofuels produced from different bio-feedstock are carbon neutral with no additional emissions in the carbon cycle. Biodiesel derived from biomass has lower sulfur content with high aromaticity and high flash point, and biodegradability can be blended with diesel as transportation fuel without modification in engine design and operation (Wen et al. 2009). Thermochemical technologies offer a relatively faster and inexpensive route to produce biodiesel over the biochemical methods.

Biodiesel can be produced from a variety of feedstocks both from edible and nonedible sources. A large number of research works have been performed on the conversion of edible oils to biodiesel (Aransiola et al. 2014; Lee et al. 2014). However, the concerns of the shortage of food due to the fuel production direct to look out for possible alternate renewable sources. Nonedible oils, waste cooking oils, and effluents of oil mills are found to be potential feedstocks with the similar requirements to produce biodiesel (Kiss 2009). The unproductive lands are cultivated to produce secondary fuel resources to convert them into biodiesel. This ensures to bring down the cost of feedstocks in the biodiesel production. Nonedible oil plantations such as *Jatropha curcas*, *Pongamia pinnata* (karanja), linseed, *Calophyllum inophyllum*, and *Cerbera odallam* are performed to extract the oils, whereas the de-oiled residues are used to produce fertilizers and drugs (Coniglio et al. 2014; Lee et al. 2014). In addition, tobacco, mahua, rubber, castor, and cotton have gained attention due to their potential in biodiesel production (Banković-Ilić et al. 2012; Bora and Baruah 2012; Atabani et al. 2013). Besides, some plants such as *Balanites aegyptiaca*, *Azadirachta indica*, *Pistacia chinensis* Bunge, and *Amygdalus pedunculata* grow without intentional plantation and are suitable candidates for biodiesel production (Karmakar et al. 2012; Tang et al. 2012). The extracted oils are subjected to transesterification to produce fatty acid alkyl esters. However, the free fatty acid's presence along with water limits them to use in conventional alkali-catalyzed transesterification. As a result, transesterification and esterification with alcohols at supercritical conditions could be feasible to convert both triglycerides and fatty acids in a single-step to biodiesel components.

Biodiesel is known to be fatty acid alkyl esters produced from transesterification reaction with short-chain alcohols. Transesterification reactions are reversible reactions where triglycerides combine with methanol/ethanol to form fatty acid alkyl esters (FAAE) and glycerol. Each mole of triglycerides present in oil reacts with three moles of methanol to form fatty acid methyl esters (biodiesel). Alcohol molecules interact with triglycerides to form fatty acid alkyl ester and diglyceride. The diglyceride obtained in the first step further reacts with more of alcohols resulting in monoglyceride and FAAE. Further, the monoglyceride formed combines with alcohol molecules to produce glycerol and another FAAE. High alcohol-to-oil ratio is required to shift the equilibrium toward the product side to improve the biodiesel yields. The hydrogen bond-induced polar alcohols limits their solubility with nonpolar organic contents of oil (triglycerides and free fatty acids) resulting in low reaction rates. The solubility of a component in a fluid is an important parameter in extraction, reaction, and separation processes. To promote the reaction rates, the interactions between the oil molecules and alcohols could be enhanced by altering the operating conditions, mixing phenomena, and application of homogeneous and heterogeneous catalysts.

Homogeneous and heterogeneous catalysts can enhance the yield of products to improve the overall economy of the biodiesel production. Homogeneous catalysts comprise of alkalis and acids. However, their recovery and preference of undesired saponification reactions are challenging in terms of the process economy (Sivasamy et al. 2009; Tan and Lee 2011). The commercialized route for the synthesis of biodiesel with high yield applies to sodium and potassium hydroxides. The feedstock containing free fatty acids and water constrains the transesterification reaction in the presence of alkalis leading to the formation of soap, thus lowering the biodiesel yield. In addition, they end up in the by-products which need to be disposed or purified to put the economic value of the glycerol. As a result, they are not recommended for feedstocks with high free fatty acids and water. This can be overcome by adding suitable acids during pretreatment to convert them into esters followed by transesterification.

Heterogeneous catalysts have also been implemented for biodiesel production to alleviate the economic and purification problems encountered with homogeneous catalysts (e.g., recovery and separation of end products with desired quality). The impurities in the feed, especially free fatty acids, do not have any impact on the functioning of catalysts during the biodiesel production. The flexibility to tune the heterogeneous catalyst with desired properties to catalyze the transesterification reactions enables to opt for biodiesel production suppressing some side reactions. A high purity of esters was observed with heterogeneous catalysts approaching complete yields along with glycerol purity of 98% (Helwani et al. 2009). The solid catalysts impose three-phase system retarding the speed of reaction and are prone to leaching with water content lowering its activity (Marchetti et al. 2007). Owing to the problems linked with catalytic transesterification in terms of purity, slow reaction rates have driven the researchers to perform the experiments at supercritical conditions with short reaction times with near-complete conversions.

11.2 Enzymatic Catalysis

To avoid the severity of operating conditions of non-catalytic transesterification of oils with supercritical alcohols, enzymatic catalysis at lower operating conditions has been implemented for biodiesel production. Lipases are hydrolytic enzymes acting on ester bonds of triglycerides during the transesterification of oils with low energy and lesser number of steps involved in biodiesel production (Marchetti et al. 2007). Mittlebach (1990) first attempted lipase-catalyzed transesterification of sunflower oil to produce biodiesel with different alcohols at very mild operating conditions of 25–65 °C. The lipases do not have any constraints on the feed quality and act on a variety of oils to produce high-quality biodiesel with less number of downstream process (Fukuda et al. 2001).

Typically, the enzymatic catalysts are denatured at high temperatures. Hence, temperature below 50 °C would be identical for biodiesel production (Sim et al. 2010; Taher et al. 2014b). Methanol-to-oil ratio of 3:1–4:1 was found to be suitable beyond which lipase activity decreased for biodiesel production (Kumari et al. 2009). The hydrophilic nature of methanol strips off the water molecules surrounding the lipase resulting in the loss of activity and configuration (Fjerbaek et al. 2009). High enzyme loadings are preferable due to access to more number of active sites for the reaction to proceed. However, due to the high cost of enzymes, the optimum concentrations essentially not more than 20–35% of oil are used (Varma and Madras 2007; Rathore and Madras 2007; Taher et al. 2011). The by-product of biodiesel also acts as an inhibition agent, which forms a hydrophilic layer around lipase hindering the interaction between the oil and alcohols and prevents the substrates to reach the active sites to proceed for reaction (Xu et al. 2011).

A solvent is generally preferred for dissolution and acceleration of interactions between the reactant substrates during the lipase catalytic biodiesel production. An organic solvent has the priority, which can dissolve the reactants and enhance the diffusion of components to the active sites of an enzyme (Klibanov 2001). Hydrophobic solvents were found to increase the biodiesel yields due to their lower ability to strip off the water molecules leading to the stable confirmation of the active enzyme (Adamczak and Krishna 2004; Doukyu and Oginio 2010). Hexane and tertiary butanol are widely used for lipase-catalytic transesterification processes. However, the latter has high solubility with methanol and glycerol resulting in higher biodiesel yields (Al-Zuhair et al. 2007; Xie and Wang 2012; Lai et al. 2012). The high volatility of these organic solvents and toxicity along with the additional cost of downstream process for product purification opt to search for alternate green solvents. The high molar ratio of alcohol-to-oil (>40:1) in the production of biodiesel through non-catalytic supercritical alcoholysis directs to opt for the addition of new green solvents to reduce the alcohol consumption. Cosolvents such as CO₂ and hydrocarbons are added to the conventional supercritical alcohols to improve the biodiesel yields (Tan et al. 2010b; Muppaneni et al. 2012). Alternatively, CO₂ is suggested to replace these organic solvents, which can dissolve reactants resulting in high biodiesel yields and low-cost separation of products.

Lipases are abundant and easier to produce using bacteria, yeast, and fungi for industrial applications (Borrelli and Trono 2015). Lipases can be categorized as intra- and extracellular. Intracellular lipases reside inside the cell or in the cell wall, while the extracellular lipases are extracted from the fermentation broth and purified for their applications. The vital microorganisms which are capable of producing lipases are *Mucor miehei*, *Rhizopus oryzae*, *Candida antarctica*, and *Pseudomonas cepacia*. Lipases that are soluble are inexpensive and simple to produce. However, they are prone to deactivation once used. Their stability and reusability at optimum temperature without any loss in activity leading to high conversion rates with short reaction times can be addressed with immobilization of enzymes (Al-Zuhair et al. 2003). The enzymes that received wide attention and are commercialized over the past few years are Novozyme 435, Lipozyme TL IM, Lipozyme RM IM, and Lipase PS-C.

The different routes through which the enzymes are immobilized are adsorption, cross-linking, entrapment, encapsulation, and covalent bonding (Jegannathan et al. 2008). The isolation and purification of extracellular lipases are costly due to which the production cost of biodiesel increases and hence are limited. However, intracellular lipases as whole cell act as a biocatalyst for biodiesel production at a relatively cheaper cost. *Rhizopus* and *Aspergillus* belonging to the class of filamentous fungi can serve as a promising cell biocatalyst for the synthesis of biodiesel (Fukuda et al. 2008). Lipases are selective with their specificity depending on the substrate structure of acyl chains, double-bond positions, branched positions, and chain length. At the optimum conditions, *Rhizopus oryzae* acts on C₁₈ fatty acids in combination with C₂–C₄ alcohols present in the oils (Ghamgui et al. 2004). The typical molecular weight of microbial lipases lies in the range of 30–50 kDa and is effective at a pH range of 7.5–9 (Kakugawa et al. 2002). Lipases are also classified based on their selectivity, regioselectivity, and enantioselectivity. Most of the lipases fall under regioselectivity. Lipases can also be nonselective and act arbitrarily with ester bonds of triacylglycerols. Both regioselective and nonselective lipases can catalyze both fatty acid esterification and triacylglyceride transesterification (Sandoval et al. 2017).

Two routes activate the lipases. In the first route, they are activated in the presence of an oil–water interface, while in the other one, they are transformed into an active state by the interaction with oil–water interface (Malcata et al. 1992). Overall, acidic or basic reactions happen on the active site of the enzyme, which is associated with acidic hydroxyl and basic amine groups. The carboxylate ions act as proton acceptors, while conjugate acids of amines play as proton donors initiating the acid–base reaction at the active sites (Al-Zuhair et al. 2007). Three routes have been proposed for lipase-catalyzed biodiesel production by several authors (Canet et al. 2016; Zarejoushghani et al. 2016; Norjannah et al. 2016). The first one is the direct alcoholysis of oil triglycerides. The second route involves initial hydrolysis where the glycerides are converted to free fatty acids followed by their esterification with the alcohol. The third mechanism proposed is the combination of the abovementioned routes, i.e., simultaneous alcoholysis and hydrolysis succeeded by esterification process.

The transesterification of oils with alcohols and lipases was explained by the “ping-pong mechanism” (Amini et al. 2017). The nucleophilic addition leads to the substrate–enzyme interaction resulting in the formation of the enzyme–substrate complex. Proton donation by the conjugate acid of the amine can be attached to the oxygen atom of an alkyl group of the substrate leading to the formation of glycerol moiety. The initial substrate triacylglycerides is converted to diacylglycerides, which subsequently changes to monoacylglycerol. The carbon atom of (CO) acyl–enzyme intermediate and the oxygen atom of the alcohol combine to form an acylated complex of enzyme and alcohol. The oxygen atom of the complex is eliminated with the transfer of a proton from the conjugate acid of the amine for the final product, i.e. fatty acid methyl ester (FAME).

11.3 Supercritical Fluids

Any fluid above its critical temperature and pressure is known as a supercritical fluid (SCF). SCFs have gained importance over the last few decades because of their liquid-like densities, gas-like diffusivities, and negligible surface tension. The density of vapor becomes similar to that of liquid at the critical point of a component. SCFs are highly compressible and have transport properties like that of a gas. Table 11.1 compares the physical properties of SCFs with liquids and gases. The unique properties of SCFs make them attractive for many chemical processes. Both liquids and SCFs have similar densities, but SCFs have higher diffusivity and thermal conductivity, lower viscosity, and negligible surface tension. These characteristics of SCFs make them superior to the liquids, and hence, the liquids are replaced by SCFs in many chemical processes. The critical parameters of some fluids are presented in Table 11.2.

Beyond the critical point of a fluid, the hydrogen bonds associated in alcohol molecules break up leading to a decrease in the dielectric constant providing an access for the complete solubility of triglycerides resulting in homogeneous phase reactions (Hiejima et al. 2001). Furthermore, it has been observed with the rise in temperature that the triglyceride solubilities increase indicating the enhancement of both esterification and transesterification reactions (Ma et al. 1998; Anitescu and Bruno 2012). The general constraints of free fatty acids and moisture can be overruled with the supercritical transesterification of different feedstocks going to completion in minutes (Pinnarat and Savage 2008; Sawangkeaw et al. 2010; Lee and Saka 2010). The transesterification reactions are usually performed at operating conditions greater than the critical conditions of alcohols for biodiesel yields. Methanol and ethanol were widely used for biodiesel production through the transesterification process. However, ethanol has an edge due to its bioavailability and synthesis from renewable agricultural sources (Aransiola et al. 2014). Methanol has gained attention due to its low cost and physical and chemical characteristics with high conversions at same operating conditions over the other alcohols (Lee et al. 2014).

Table 11.1 Physical properties of supercritical fluids compared against liquids and gases

Attribute	Liquids	Supercritical fluids	Gases
Density (g cm^{-3})	1.0	0.1–0.5	10^{-3}
Viscosity (Pa s)	10^{-3}	10^{-4} – 10^{-5}	10^{-5}
Diffusivity ($\text{cm}^2 \text{s}^{-1}$)	10^{-5}	10^{-3}	10^{-1}

Table 11.2 Critical properties of some fluids

Substance	T_c (K)	P_c (MPa)
Acetic acid	590	5.80
Ammonia	405.5	11.3
Argon	150.6	4.8
Carbon dioxide	304.2	7.38
Dimethyl carbonate	548	4.63
Ethane	305	4.9
Ethanol	514	6.3
Ethene	282	5.0
Fluoroform	299	4.9
Methane	190.5	4.6
Methanol	512	8.1
Methyl acetate	507	4.69
Nitrous oxide	310	7.2
Propane	370	4.3
Propene	364.9	4.6
Water	647.2	22.1

T_c critical temperature, P_c critical pressure

Transesterification reactions are initiated through aliphatic alcohols, which are monohydric primary or secondary with carbon atoms in the range of 1–8 (Demirbas 2005). Depending on the type of alcohol (methanol or ethanol) implemented during the transesterification, methyl esters or ethyl esters of fatty acids are generated as biodiesel components. During the transesterification reaction, the acetyl group of fatty acid is replaced with another acetyl group of alcohol in successive steps with monoglycerides and diglycerides as intermediates leading to the formation of fatty acid alkyl esters and glycerol (Agarwal 2007; Tan and Lee 2011).

The biodiesel production process involves triglycerides and fatty acids of oils as reactants in the presence of supercritical alcohols (Gonzalez et al. 2013; Bensaid et al. 2013; Kiss et al. 2014). The choice of the alcohols depends on its reactivity, and methanol has been found to be highly reactive compared to other alcohols (Warabi et al. 2004; Demirbas 2009). It is essential to understand the phase equilibrium between the reactants of the transesterification process (e.g., alcohols, triglycerides, monoglycerides, diglycerides, and glycerol) at supercritical conditions to estimate the optimal conditions (Sawangkeaw et al. 2011; Anikeev et al. 2012; Sakdasri et al. 2016). Supercritical alcohol-assisted transesterification process involves the feeding of high alcohol-to-oil ratio of feed (methanol/ethanol) in the reactor and heating to a

temperature and pressure greater than the critical point of alcohol (methanol: $T_c = 239\text{ }^\circ\text{C}$, $P_c = 8.1\text{ MPa}$; ethanol: $T_c = 241\text{ }^\circ\text{C}$, $P_c = 6.3\text{ MPa}$) for a predefined residence time to obtain diesel. Saka and Kusdiana (2001) initially attempted biodiesel production using rapeseed oil with supercritical methanol at 350–400 °C in the range of 45–65 MPa with a high methanol-to-oil ratio and achieved nearly 95% conversion.

The methanol-to-oil ratio is one of the significant operating parameters along with reaction temperature and pressure of supercritical alcohol transesterification of oils (Demirbas 2016). Majorly, non-catalytic transesterification process with different sources of oil was performed to determine the optimum conditions for biodiesel production. Supercritical methanol was applied to convert oil derived from crude tobacco to biodiesel at an optimum operating condition of 300 °C in a residence time of 90 min with 43:1 methanol-to-oil ratio to yield 92.8% of FAME (Garcia-Martinez et al. 2017). To reduce the harsh operating conditions, cosolvents such as CO₂ and propane were applied to accelerate the reaction rates in a homogeneous phase, which can be easily separated from the reactants and products to enhance the biodiesel (Cao et al. 2005; Han et al. 2005; Ghoreishi and Moein 2013). A maximum biodiesel yield of 95.27% was reported using the methanol–CO₂ system for waste vegetable oil at optimal conditions such as a methanol-to-oil ratio of 33.8:1, the temperature of 271 °C, the pressure of 23.1 MPa, and the residence time of 20.4 min (Ghoreishi and Moein 2013).

Rubber seed oil was transesterified using supercritical methanol to produce a maximum oil yield of 86.9% at 260 °C and 16 MPa in 5 min with 1:40 oil-to-methanol ratio (Sawiwat and Kajorncheappunngam 2015). A comparative study of transesterification of camelina oil using different alcohols at similar operating conditions (1:40 oil-to-alcohol ratio, 290 °C and 60 min) was conducted, and the performance was evaluated based on ester yields (Sun et al. 2014). Lower ester yields were obtained with 1-butanol due to the high inductive effect of the alkyl group of large alcohols followed by ethanol and methanol. The highest yield of 97.9% biodiesel was reported with in situ extraction and transesterification at 280 °C and 12 MPa in 30 min with methanol-to-oil ratio of 40:1 (Ishak et al. 2017). Free fatty acids undergo esterification to generate fatty acid alkyl esters overcoming the limitation of the composition of different feeds. Waste cooking oil was subjected to transesterification process to produce yield at 91% at optimum conditions of 253 °C, 19.85 MPa in 15 min, and 37:1 methanol-to-oil ratio (Aboelazayem et al. 2017). A yield of 96.5% was observed with non-catalytic transesterification of crude castor oil with 43:1 methanol-to-oil ratio at 300 °C and 21 MPa in 90 min (Román-Figueroa et al. 2016).

Continuous production of biodiesel was attempted at 20 MPa with an oil-to-1-propanol ratio of 1:40 over the temperature range of 200–400 °C and residence time of 5–30 min (Farobie et al. 2016). Biodiesel yield of nearly 94% was observed at an optimum temperature of 350 °C in 30 min. Canola oil was used for biodiesel production with supercritical butanol in a continuous reactor to attain a yield of 95% at 400 °C and 20 MPa in 14 min with 1:40 oil-to-alcohol ratio (Farobie et al. 2017). Furthermore, it was inferred that the reactivity of alcohol decreases with its

chain length. Biodiesel production using canola oil with different solvents such as methanol, ethanol, and methyl tert-butyl ether (MTBE) was performed by Farobie and Matsumura (2015). It has been reported that the complete conversion was achieved in 10 min for methanol while 30 min for the remaining two solvents at 350 °C and 20 MPa with 1:40 oil-to-methanol ratio.

11.4 Supercritical Carbon Dioxide (SCCO₂)

CO₂ is cheaply available, non-flammable, and nontoxic and has ambient critical temperature and moderate critical pressure. It is the most widely used SCF because of its characteristics. Its phase diagram is shown in Fig. 11.1. The curves “AB,” “BD,” and “BC” represent the solid–vapor equilibrium, solid–liquid equilibrium, and liquid–vapor equilibrium, respectively. The three curves that intersect at a point (represented by the symbol ○ and known as the triple point) have a characteristic temperature and pressure of 216.6 K and 0.5185 MPa, respectively. The BC curve terminates at critical point “C” where the distinction between the liquid and vapor phase disappears. The critical temperature and pressure of CO₂ are 304.2 K and 7.38 MPa, respectively. Beyond its critical points, CO₂ attains a supercritical fluid state termed as supercritical carbon dioxide (SCCO₂). The shaded region in Fig. 11.1 represents the supercritical region of the fluid.

The thermophysical property that should be known prior to the design of a supercritical process is the solubility of the solute in SCCO₂. The solubility of a component in SCCO₂ depends on its density. The effect of temperature and pressure on the density of SCCO₂ is shown in Fig. 11.2. The density of SCCO₂ can be calculated from 27-parameter equation of state, which was developed by Span and Wagner (1996). The density of SCCO₂ increases with pressure for each isotherm. At the critical point, the density of both gas and liquid becomes identical, and a sharp increase in the density of SCCO₂ near critical point is observed. The density of

Fig. 11.1 Phase diagram of carbon dioxide. (Data extracted from Mukhopadhyay 2000)

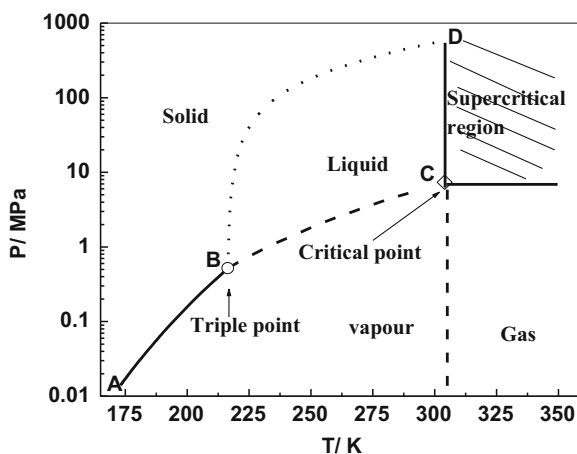
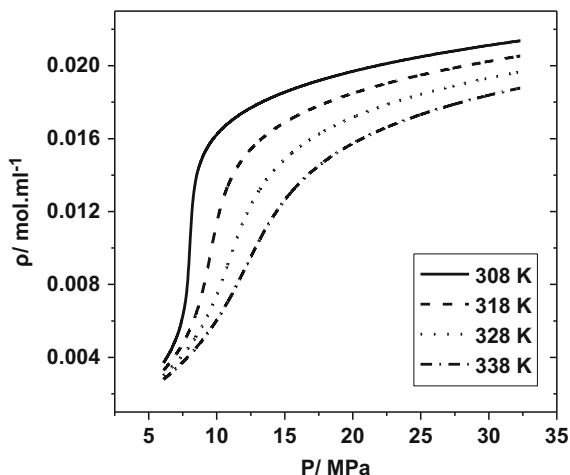


Fig. 11.2 Variation of the density of CO₂ with pressure and temperature (the calculated densities using 27-parameter Span and Wagner equation of state were plotted against pressure at different temperatures). (Data extracted from Span and Wagner 1996)



SCCO₂ decreases with isobaric rise in temperature and increases significantly near the critical point of CO₂. The density increases monotonically with pressure beyond the critical point of CO₂, thus resulting in the increase in solvent capacity of the SCF. CO₂ does not have a net dipole moment; hence, its nonpolar nature can be used to extract or separate natural molecules, which are nonpolar in nature. The quadruple nature of CO₂ is useful to dissolve slightly polar compounds (Saharay and Balasubramanian 2004; Raveendran et al. 2005). The phase behavior of the reactant mixture becomes essential when the fat is used for the biodiesel production. The solubilities of different components of oils (e.g., triglycerides and fatty acids), reaction intermediates (e.g., mono- and di-), and FAME have been experimentally determined and established correlations in SCCO₂ (Yu et al. 1994; Güçlü-Üstündağ and Tamelli 2000).

The solubility of a component depends on temperature and pressure (Mukhopadhyay 2000). The solubility isotherms intersect with each other at a point which is known as crossover pressure (Foster et al. 1994). The solubility decreases with the temperature below the crossover pressure, while it increases above the crossover pressure with temperature. This phenomenon is termed as retrograde phase behavior of a component and generally occurs in the highly compressible region of an SCF (Mukhopadhyay 2000). The retrograde solubility behavior is attributed to the density and vapor pressure effects. The addition of small amount of a solvent/solid to SCCO₂ increases the solubility of the solute. These substances are known as entrainers or cosolvents. When a cosolvent or solid is added to SCF, the polarity changes considerably, which increases the solubility of the solute in SCF (Reddy and Madras 2011, 2012). The cosolvent + SCF mixture forms a homogeneous phase above its critical parameters. Therefore, the mixture is usually maintained above its critical temperature and pressure for the reactions to proceed in a single phase.

The increase or decrease in the solubility of a ternary triglyceride over the solubility of its pure component is due to the strong attractive or repulsive interactions between the molecules. The inter- and intramolecular hydrogen bonds result in solute–solute and solute–solvent interactions enhancing the solubility of the reactant and product species during transesterification processes. Though SCCO_2 demands high pressure, the catalytic activity is found to be stable at pressures below 20 MPa (Novak et al. 2003). On the other hand, at high pressure, the lipase attains its favorable configuration to have access to substrates with enhanced activity and complete dissolution, thus eliminating any mass transfer resistances (Celia et al. 2005). SCCO_2 has good tuning with lipases for both esterification and transesterification (Lozano et al. 2004). Fatty acid esterification using SCCO_2 has proved to be efficient with near-complete conversion using lipases (Lee et al. 2014).

11.5 Transesterification with Combination of SCCO_2 and Enzymes

Isoamyl acetate and oleic oleate synthesis using SCCO_2 in the presence of lipozymes were reported with conversions approaching 100% without the loss of enzymatic activity for more than a month (Romero et al. 2005; Laudani et al. 2007). Palmitic and oleic acid esterification were esterified using ethanol and methanol, respectively, using Novozyme 435 with yields attaining >95% (Kumar et al. 2004; Jackson et al. 2006). Only a few studies have been reported on the transesterification process for biodiesel production (Lee et al. 2014; Aransiola et al. 2014). Both palm kernel and *Jatropha* oils are subjected to transesterification process using Novozyme 435 to achieve biodiesel yields of 63% (Oliveira and Oliveira 2001; Rathore and Madras 2007; Varma and Madras 2007). Lamb meat fat and microalgae were transesterified at 50 °C and 20 MPa with 4:1 methanol-to-oil ratio using 30 wt% Novozyme 435 and reported yields of 45% and 80%, respectively, for 24 h (Taher et al. 2014a, b).

Lipases comprise of α/β hydrolase-fold with a nucleophile, an acidic residue, histidine, and oxyanion hole with the capability to stabilize intermediate formed during the reactions of biodiesel production (Casas-Godoy et al. 2012). Lipases are characterized by a lid-like structure associated with α -helixes shadowing the active site to enable the transesterification process (Reis et al. 2009). The conformational changes are associated with the lid with the presence of different substrates. The lipases are activated with the opening of the lid allowing the substrates to form complexes by interacting with the hydrophilic source at lipid–water interface. The confirmation attains the closed lid structure in the absence of the hydrophilic source, thus disabling the activity of the enzymes. The activity of the enzyme is related to the opening of the lid and shutting down of the lid. The lipid–water interface aids the opening of lid enabling to be in its active form, while in the absence of interface, it impairs the active site. This phenomenon is termed as interfacial activation of the enzyme.

The enzymatic synthesis of biodiesel depends on lipase activity, water content, reaction temperature, pH, and reaction time. The catalytic activity of lipases depends on the water content of the feedstock (Sankaran et al. 2016). The water content enhances the interfacial interaction between the organic (oil) and aqueous environment providing the substrates to occupy the active sites of the enzyme (Christopher et al. 2014). High quantities of water are also not recommended for the transesterification due activation of hydrolysis of triglycerides. Furthermore, the hydrophobic substrates denied the access to the enzyme because of the excess water that occupies the hydrophilic pores at high concentrations, thus lowering the biodiesel yields (Guldhe et al. 2015; Sankaran et al. 2016). A few reports infer that water concentration ranging from trace level up to 20 wt% is recommended depending on the type of lipase and immobilization support with or without the solvent (Narwal and Gupta 2013; Guldhe et al. 2015; Yang et al. 2015; Sankaran et al. 2016).

The added advantage of enzyme-catalyzed biodiesel production is to perform the reactions at relatively low temperatures. Temperature has been found to have a positive impact on the enzyme activity, and thereby biodiesel yields to a certain extent. However, at elevated temperatures, the enzyme is denatured lowering the reaction rate and biodiesel yields. An optimal temperature range of 20–70 °C is recommended for biodiesel production depending on the source (Guldhe et al. 2015). However, the enzyme activity and stability can be enhanced by employing the immobilization procedure (Al-Zuhair 2007). The transesterification of oils proceeds faster in the presence of solvents rather than being solvent-free, which is limited due to the mass transfer and the inhibition of excess alcohol. The choice of solvent for ester yields depends on the reaction type. Hydrophobic solvents are preferred for esterification while transesterification chooses hydrophilic solvents for the continuous production of biodiesel (Sandoval et al. 2001; Rivera et al. 2009). High concentrations of the acyl acceptors (alcohols) retard the activity of enzyme lowering the number of cycles for biodiesel production, which need to be replaced frequently making its production expensive (Lotti et al. 2015). In general, stepwise addition of alcohol is chosen to protect biocatalyst activity against the alcohol inhibition.

Ester yields above 90% have been observed with the application of various lipases from different sources for various acylating agents capable of catalyzing both free fatty acids and triglycerides (Fjerbaek et al. 2009; Fernandez-Lafuente 2010; Liu et al. 2010). Fatty acid ethyl esters synthesis were attempted with different compressible fluids (CO₂, propane, and butane), and the experiment results confirmed the superiority of propane using immobilized Novozyme 435 at 70 °C and 6 MPa at short reaction times (Dalla Rosa et al. 2009). Different oils such as sesame oil and mustard oil were subjected to the transesterification process to synthesize FAME using immobilized *Candida antarctica* in SCCO₂ using a batch reactor with the attainment of 70% yields (Varma et al. 2010). Maximum experimental biodiesel yield of 93% with a predicted yield of 99% was obtained from corn oil with Novozyme 435 as biocatalyst at an optimum temperature of 63 °C, a pressure of 19.4 MPa, a methanol-to-oil ratio of 7.03, and a SCCO₂ flow rate of 0.72 L/min

(Ciftci and Temelli 2011). Virgin sunflower oil was subjected to transesterification to achieve high biodiesel production yields >98% at 40 °C and 20 MPa with methanol-to-oil ratio of 24:1 in 20 s with Lipozyme TL IM, whereas waste cooking oil yielded >99% by the combination of Novozyme 435 and Lipozyme TL IM (Rodrigues et al. 2011). A similar enzyme was applied for transesterification of waste cooking oil with ethanol to determine the economic viability of biodiesel production at a price of 1.64 €/L (Lisboa et al. 2014).

FAMES were obtained from *Nannochloropsis oculata* with SCCO₂ in the presence of cosolvents with a motive to combine extraction and transesterification (McKennedy et al. 2016). Biodiesel yield of 80% from microalgae lipids was obtained using a batch reactor in 4 h with 35% enzyme loading at 50 °C and 20 MPa with the upscaling in continuous production (Taher et al. 2014a). Methanol and CO₂ mixtures were tested for the biodiesel production at supercritical conditions (280–350 °C and 1–28 MPa) with palm oil, sunflower oil, and borage oil in a batch reactor with CO₂ to methanol molar ratio of 0.05–0.2 (García-Jarana et al. 2016). The results indicated that the addition of CO₂ does not improve the biodiesel yields; however, it could be advantageous if transesterification is combined with extraction. Extraction and reaction were integrated for continuous biodiesel production from chicken feather meal where more than 90% of the oil was extracted with biodiesel yield reaching 96.7% using Lipozyme RM IM at 40 °C and 25 MPa (Gameiro et al. 2015).

The most commonly implemented reactor configurations for biodiesel production either in batch or continuous modes are stirred tank reactors, packed bed reactors, fluidized bed reactors, and membrane bioreactors (Sandoval et al. 2017). Stirred tank reactors are simple and easy to operate with optimal reaction times, but due to constant stirring, the immobilized particles are broken and the enzyme activity is lost. On the other hand, packed bed reactors are found to be a suitable alternative for continuous biodiesel production at a lower substrate-to-enzyme ratio (Lotti et al. 2015). However, the yield is limited due to the channeling of substrates due to the multiphase mixture. Enhanced mass transfer rates were observed with the fluidization of biocatalyst at flow rates greater than minimum fluidization velocities. However, the scaling up for the continuous production of biodiesel is complex over the conventional batch and packed bed reactors (Poppe et al. 2015). The membrane reactors are expensive due to the membranes and catalyst employed, which can perform biocatalysis with recovery and reuse of the applied biocatalyst for a longer period (Badenes et al. 2011).

11.6 Transesterification with Combination of SCCO₂ and Ionic Liquids

The implementation of solvents during the biodiesel production is to enhance the substrate solubility and sustain the catalytic activity of the lipases, and hydrophobic ionic liquids are found to be suitable. The immiscibility of SCCO₂ and ionic liquids is the key criterion making their combination applicable for biodiesel production to

generate biodiesel of high purity (Lozano 2010). The substrates are miscible with the hydrophobic ionic liquids, and glycerol is immiscible with ionic liquids leading to its separation from the reaction mixture. The high cost of ionic liquids opts for their recycling where biodiesel is highly soluble. As a result, the equilibrium might shift back decelerating the reaction rate. Furthermore, the enzyme deactivates due to the interaction of amine groups and pH variation with SCCO_2 (Antonia et al. 2007). A combination of SCCO_2 with ionic liquids can address the stability, separation, and miscibility with a motive to enhance the biodiesel yield (Taher and Al-Zuhair 2017). Recovery of biodiesel using SCCO_2 and ionic liquids creates a biphasic system where esters produced are completely miscible with SCCO_2 . Initially, the oils extracted from the solid matrices using SCCO_2 are directly fed to transesterification to enzyme + ionic liquid reactor system. The substrates diffuse efficiently through the interface of SCCO_2 -ionic liquid approaches the active sites of the enzyme where the reaction proceeds to produce esters (Blanchard et al. 1999). The generated biodiesel components are transported back to SCCO_2 phase resulting in high-purity product (Blanchard and Brennecke 2001). Triolein transesterification was conducted with methanol in the presence of Novozyme 435 at 60–80 °C and attained a biodiesel yield of 98% with the reaction time of 6 h (Lozano et al. 2011).

11.7 Other Supercritical Solvents

Due to the expensive purification process during biodiesel production, the conventional alcohols are replaced with other solvents to produce more valuable products to enhance the economics (Ang et al. 2014). Various acyl acceptors such as esters (methyl acetate and ethyl acetate) and dimethyl carbonate were tested for biodiesel yields for enzymatic transesterification (Norjannah et al. 2016). Figure 11.3 represents the biodiesel synthesis reactions with various organic solvents including conventional alcohols. Glycerol-free non-catalytic supercritical transesterification of oils has gained attention to improve the economics of biodiesel production (Saka and

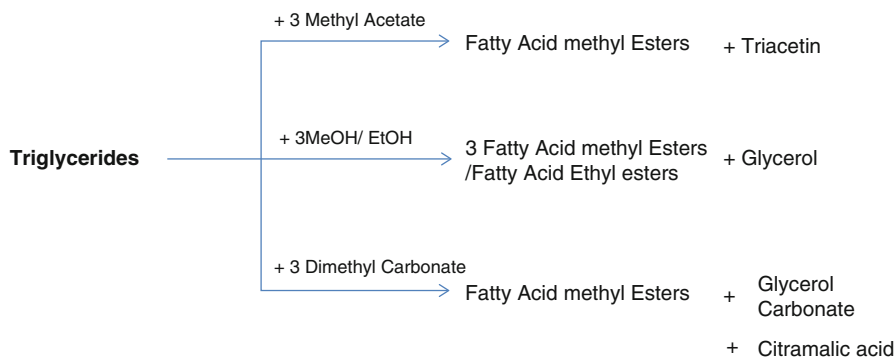


Fig. 11.3 Reactions involved with application of various supercritical solvents

Isayama 2009; Ilham and Saka 2009). Methyl acetate is the choice of solvent applied for biodiesel production in the place of alcohol to generate more value-added product triacetin than glycerol (Campanelli et al. 2010; Tan et al. 2010a).

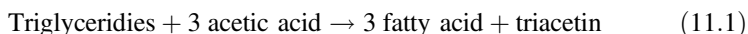
The oils and the solvents were mixed and subjected to transesterification process by heating them above the critical points of methyl acetate ($T_c = 233.7\text{ }^\circ\text{C}$ and $P_c = 4.69\text{ MPa}$) and dimethyl carbonate ($T_c = 274.9\text{ }^\circ\text{C}$ and $P_c = 4.63\text{ MPa}$). The transesterification process happens in reversible consecutive steps to generate FAME and triacetin. Triglyceride reacts with a molecule of methyl acetate reacting to form monoacetylglyceride and FAME. The generated monoacetylglyceride further combines with another molecule methyl acetate to form FAME and diacetylglyceride. At the end, these diacetylglycerides interact with more methyl acetate to have FAME and glycerol. Triacetin finds its application as a fuel additive to improve the viscosity and cloud point of diesel fuels. With the application of supercritical methyl acetate in biodiesel production along with fatty acid methyl esters, triacetin can be constituted as biodiesel. It was found that a mass ratio of 1:4 of triacetin-to-FAME is attained in the synthesis of biodiesel. As a result, the biodiesel yields can go beyond 100% with the accounting of triacetin as a biodiesel component (Tan and Lee 2011). Nonedible oil was transesterified through non-catalytic supercritical solvents such as methanol, methyl acetate, methyl tert-butyl ether (MTBE), and dimethyl carbonate (DMC) over temperature range of 250–400 °C at 30 MPa with oil-to-solvent mole ratio of 40:1 for reaction times varying from 3 min to 3 h (Lamba et al. 2017). Reactions conveyed high biodiesel yield with methanol (>80%) followed by DMC, MTBE (70%) and methyl acetate (60%).

In addition to methyl acetate, another solvent which has proven to be an alternative to alcohol is dimethyl carbonate (Ilham and Saka 2009, 2010). Supercritical dimethyl carbonate converts triglycerides and free fatty acids to FAME and glycerol carbonate, which are much more valuable than the conventional glycerol (Ilham and Saka 2011). Glycerol carbonate is used in polymers and membranes with the high economic value of crude glycerol. The optimum conditions for supercritical DMC transesterification of rapeseed oil was attained at 300°C and 20 MPa in 20 min with DMC to oil ratio of 42: 1 which resulted in maximum yield of 97%. DMC interacts with triglycerides resulting in methyl carbonate diglycerides, which further reacts to one more molecule of DMC to form dimethyl carbonate monoglyceride (DMCMG). Finally, DMCMG associates with a molecule of DMC to produce FAME, glycerol carbonate, and citramalic acid. Instead of two-step conventional glycerol carbonate synthesis where the yields are low, this single-step supercritical DMC synthesis of biodiesel production results in the higher process expenditure. Tan et al. (2010a) subjected palm oil for transesterification with DMC and tuned the maximum biodiesel yield of 91% at optimum conditions of 380 °C 25 MPa in 30 min and 39:1 mole ratio of DMC-to-oil.

Compared to conventional single-step supercritical transesterification to produce biodiesel, two-step biodiesel production with initial step operated at subcritical conditions followed by supercritical conditions to generate biodiesel. The triglycerides in oil were initially converted to fatty acids and triacetin at subcritical conditions in the presence of acetic acid. These fatty acids obtained in subcritical

acetic acid were reacted with supercritical methanol to produce biodiesel. Acetic acid leads to hydrolysis of triglycerides in three steps with the production of triacetin and fatty acids. Triglyceride undergoes acid hydrolysis with acetic acid under the subcritical state to form monoacetyl diglyceride and fatty acid. In the second step, the resultant monoacetyl diglyceride further undergoes hydrolysis to generate diacetyl monoglyceride and fatty acid. Finally, diacetyl monoglyceride reacts with additional acetic acid to generate triacetin and fatty acid. These fatty acids are subjected to esterification to yield fatty acid methyl esters with supercritical methanol.

Saka et al. (2010) conducted two-step acid hydrolysis and methanolysis (esterification) consecutively at subcritical and supercritical operating conditions to produce biodiesel. The mixture of acetic acid and rapeseed oil underwent hydrolysis upon heating and pressuring the system to the desired subcritical conditions and yielded nearly 85% triacetin and 91% of fatty acid at 300 °C and 20 MPa in 30 min (Eq. 11.1). The second step of biodiesel production, i.e., fatty acid esterification at 270 °C and 17 MPa, produced a biodiesel yield of 97% in 15 min. In another investigation on a two-step hydrolysis accompanied with esterification, water and DMC were used as reactants to produce fatty acids in the first step followed by FAME and glycerol carbonate and glyoxal as final end products, as shown in Eq. (11.2) (Ilham and Saka 2010). The initial step of subcritical hydrolysis was performed at 27 MPa and 270 °C to convert triglycerides into fatty acids and glycerol. The extracted fatty acids underwent transesterification with DMC in the subsequent step at 300 °C and 9 MPa to produce biodiesel with 97% yield in 15 min. The by-products obtained using methyl acetate and dimethyl carbonate in the transesterification process generated triacetin and glycerol carbonate.



11.8 Challenges and Perspectives

The performance of different biodiesel production processes is summarized in Table 11.3. Biodiesel produced through conventional homogeneous catalytic transesterification routes are commercialized due to their simple setup and well-established design methods. The biodiesel production involves the cost of raw material, production process, and purification process (West et al. 2008). With the application of supercritical technology, the constraint of handling various feeds can be overcome with the potential to convert them into biodiesel (Lim and Lee 2014). The major equipment involved during production and separation process involves high operating and installation cost. The conventional catalytic processes require low reaction temperatures (<150 °C) and normal pressures, whereas supercritical

Table 11.3 Performance of different biodiesel production process

Parameters	Supercritical process	Enzymatic process	Conventional catalytic process
Feed concentration	Flexible with fatty acids and water content	Flexible with fatty acids and water content	Soap formation, oil hydrolysis
Reaction time	2–4 min	12 h	1–8 h
Catalyst	Usually not required	Lipases (reusable but costly)	Cheap but difficult to recover
Biodiesel yields	Very high (~99%)	High (>90%)	Higher than 95%
Energy requirement	High temperature (>300 °C) and high pressure (>10 MPa)	Low temperature (30–70 °C) and ambient pressure	Moderate temperature (>100 °C)
Product purification	Methanol	Methanol and enzyme	Methanol, catalyst, and soap

processes require temperatures higher than 250 °C and pressure greater than 10 MPa. An enormous amount of energy is required for the reactions to initiate with supercritical solvents at these high temperatures and pressures.

Economic analysis of transesterification of rapeseed oil with supercritical methanol was performed and compared with alkali-catalyzed process (Lim et al. 2009). A high alcohol-to-oil ratio with the aim to shift the equilibrium toward the right resulted in most of the alcohol to remain unreacted in the glycerol phases, which required recovery. Distillation columns known for their expensive operating and installation costs are employed to separate methanol from glycerol for its reuse for the biodiesel production. The supercritical methanol process involves settlers to separate the immiscible phases of glycerol and oil followed by the purification of glycerol to recover methanol in a distillation column. The use of glycerol-free supercritical process to produce high market value products rules out the settling process since the products are miscible with FAME and requires only thermal energy to recover the unreacted components.

In supercritical methyl acetate process, triacetin, a fuel additive (20%), combined with biodiesel has enhanced combustion characteristics. Hence, the overall energy required to purify the product needs less thermal energy compared to supercritical alcohol process. In supercritical DMC process, the unreacted DMC can be retrieved by evaporation and the mixture of FAME, and glycerol carbonate can be separated with settlers due to their immiscibility. The non-glycerol supercritical process involves lesser equipment and requires low energy compared to supercritical methanol process.

The analysis of supercritical processes indicates that the production cost goes majorly high due to the involvement of high-pressure pumps, high-efficiency heaters and heat exchangers, as well as distillation towers for product purification compared

to the alkali process. Biodiesel production through supercritical synthesis of methanol was performed with *Jatropha curcas* oil, and comparative economic analysis was done with alkali-catalyzed process (Yusuf and Kamarudin 2013). They reported that supercritical process involves low product cost due to high product selectivity and suppression of competent side reactions. From the life cycle analysis of biodiesel production process through supercritical and catalytic processes, it was reported that supercritical methanol process demands an initial energy of 250 and 160 MJ/Kg of diesel for supercritical and basic catalytic process, respectively (Rosmeika et al. 2014). With the consideration of by-product value and recycling of the energy, the energy requirement is on par with that of basic catalytic biodiesel production process. By the integration of extraction with reactions and purification, the energy constraints of the supercritical processes can be overcome.

11.9 Conclusions

Supercritical synthesis of biodiesel using conventional and other solvents was reviewed. The operating parameters for different oil feedstocks such as temperature, residence time, pressure, and alcohol-to-oil ratio on the biodiesel yield was discussed. Although the conversion reaches near-completion, the high alcohol-to-oil ratio (40:1) for supercritical processes demands high energy with the high cost of product purification. Lipases are active for transesterification reactions with a flexible composition of triglycerides, and fatty acids for different feedstocks to generate biodiesel are a possible option to rule out the high-energy demand. However, to improve the interactions between the molecules and enhance the product yields, SCCO_2 can be considered as a potential media to replace the toxic organic solvents. The scaling up of these enzymatic supercritical processes is limited due to the high cost of enzymes with high pumping costs. To enhance the biodiesel economy, supercritical solvents other than alcohols were implemented. However, the high-energy input to reach the supercritical conditions can be balanced with the production of value-added industrial products. Triacetin and glycerol carbonate with high market value directs to opt for methyl acetate and dimethyl carbonate that can boost the biodiesel economy.

References

- Abuelazayem O, Gadalla M, Saha B (2017) Biodiesel production from waste cooking oil via supercritical methanol: optimisation and reactor simulation. *Renew Energy*. <https://doi.org/10.1016/j.renene.2017.06.076>
- Adamczak M, Krishna SH (2004) Strategies for improving enzymes for efficient biocatalysis. *Food Technol Biotechnol* 42:251–264
- Agarwal AK (2007) Biofuels (alcohols and biodiesel) applications as fuels for internal combustion engines. *Prog Energy Combust Sci* 33:233–271
- Al-Zuhair S (2007) Production of biodiesel: possibilities and challenges. *Biofuels Bioprod Bioref* 1:57–66

- Al-Zuhair S, Hasan M, Ramachandran KB (2003) Kinetics of the enzymatic hydrolysis of palm oil by lipase. *Process Biochem* 38:1155–1163
- Al-Zuhair S, Ling FW, Jun LS (2007) Proposed kinetic mechanism of the production of biodiesel from palm oil using lipase. *Process Biochem* 42:951–960
- Amini Z, Ilham Z, Ong HC, Mazaheri H, Chen WH (2017) State of the art and prospective of lipase-catalyzed transesterification reaction for biodiesel production. *Energy Convers Manag* 141:339–353
- Ang GT, Tan KT, Lee KT (2014) Recent development and economic analysis of glycerol-free processes via supercritical fluid transesterification for biodiesel production. *Renew Sust Energ Rev* 31:61–70
- Anikeev V, Stepanov D, Yermakova A (2012) Thermodynamics of phase and chemical equilibrium in the processes of biodiesel fuel synthesis in subcritical and supercritical methanol. *Ind Eng Chem Res* 51:4783–4796
- Anitescu G, Bruno TJ (2012) Fluid properties needed in supercritical transesterification of triglyceride feedstocks to biodiesel fuels for efficient and clean combustion—a review. *J Supercrit Fluids* 63:133–149
- Antonia P, Hernández-Fernández FJ, Gómez D, Rubio M, Tomás-Alonso F, Vllora G (2007) Understanding the chemical reaction and mass-transfer phenomena in a recirculating enzymatic membrane reactor for green ester synthesis in ionic liquid/supercritical carbon dioxide biphasic systems. *J Supercrit Fluids* 43:303–309
- Aransiola EF, Ojumu TV, Oyekola OO, Madzimbamuto TF, Ikhu-Omoregbe DIO (2014) A review of current technology for biodiesel production: state of the art. *Biomass Bioenergy* 61:276–297
- Atabani AE, Silitonga AS, Ong HC, Mahlia TMI, Masjuki HH, Badruddin IA, Fayaz H (2013) Non-edible vegetable oils: a critical evaluation of oil extraction, fatty acid compositions, biodiesel production, characteristics, engine performance and emissions production. *Renew Sust Energ Rev* 18:211–245
- Badenes SM, Lemos F, Cabral J (2011) Performance of a cutinase membrane reactor for the production of biodiesel in organic media. *Biotechnol Bioeng* 108:1279–1289
- Banković-Ilić IB, Stamenković OS, Veljković VB (2012) Biodiesel production from non-edible plant oils. *Renew Sust Energ Rev* 16:3621–3647
- Bensaid S, Hoang D, Bellantoni P, Saracco G (2013) Supercritical fluid technology in biodiesel production: pilot plant design and operation. *Green Process Synth* 2:397–406
- Blanchard LA, Brennecke JF (2001) Recovery of organic products from ionic liquids using supercritical carbon dioxide. *Ind Eng Chem Res* 40:287–292
- Blanchard LA, Hancu D, Beckman EJ, Brennecke JF (1999) Green processing using ionic liquids and CO₂. *Nature* 399:28
- Bora DK, Baruah DC (2012) Assessment of tree seed oil biodiesel: a comparative review based on biodiesel of a locally available tree seed. *Renew Sust Energ Rev* 16:1616–1629
- Borrelli GM, Trono D (2015) Recombinant lipases and phospholipases and their use as biocatalysts for industrial applications. *Int J Mol Sci* 16:20774–20840
- Campanelli P, Banchemo M, Manna L (2010) Synthesis of biodiesel from edible, non-edible and waste cooking oils via supercritical methyl acetate transesterification. *Fuel* 89:3675–3682
- Canet A, Bonet-Ragel K, Benaiges MD, Valero F (2016) Lipase-catalysed transesterification: viewpoint of the mechanism and influence of free fatty acids. *Biomass Bioenergy* 85:94–99
- Cao W, Han H, Zhang J (2005) Preparation of biodiesel from soybean oil using supercritical methanol and co-solvent. *Fuel* 84:347–351
- Casas-Godoy L, Duquesne S, Bordes F, Sandoval G, Marty A (2012) Lipases: an overview. In: Sandoval G (ed) *Lipases and phospholipases: methods and protocols*. Humana Press, New York, pp 3–30
- Celia E, Cernia E, Palocci C, Soro S, Turchet T (2005) Tuning *Pseudomonas cepacea* lipase (PCL) activity in supercritical fluids. *J Supercrit Fluid* 33:193–199
- Christopher LP, Kumar H, Zambare VP (2014) Enzymatic biodiesel: challenges and opportunities. *Appl Energy* 119:497–520

- Ciftci ON, Temelli F (2011) Continuous production of fatty acid methyl esters from corn oil in a supercritical carbon dioxide bioreactor. *J Supercrit Fluids* 58:79–87
- Coniglio L, Coutinho JA, Clavier JY, Jolibert F, Jose J et al (2014) Biodiesel via supercritical ethanolysis within a global analysis “feedstocks-conversion-engine” for a sustainable fuel alternative. *Prog Energy Combust Sci* 43:1–35
- Dalla Rosa C, Morandim MB, Ninow JL, Oliveira D, Treichel H, Oliveira JV (2009) Continuous lipase-catalyzed production of fatty acid ethyl esters from soybean oil in compressed fluids. *Bioresour Technol* 100:5818–5826
- Demirbas A (2005) Biodiesel production from vegetable oils via catalytic and non-catalytic supercritical methanol transesterification methods. *Prog Energy Combust Sci* 31:466–487
- Demirbas A (2009) Production of biodiesel fuels from linseed oil using methanol and ethanol in non-catalytic SCF conditions. *Biomass Bioenergy* 33:113–118
- Demirbas A (2016) Biodiesel from corn germ oil catalytic and non-catalytic supercritical methanol transesterification. *Energy Sour A* 38P:1890–1897
- Doukyu N, Ogino H (2010) Organic solvent-tolerant enzymes. *Biochem Eng J* 48:270–282
- Farobie O, Matsumura Y (2015) A comparative study of biodiesel production using methanol, ethanol, and tert-butyl methyl ether (MTBE) under supercritical conditions. *Bioresour Technol* 191:306–311
- Farobie O, Leow ZYM, Samanmulya T, Matsumura Y (2016) New insights in biodiesel production using supercritical 1-propanol. *Energy Convers Manag* 124:212–218
- Farobie O, Leow ZYM, Samanmulya T, Matsumura Y (2017) In-depth study of continuous production of biodiesel using supercritical 1-butanol. *Energy Convers Manag* 132:410–417
- Fernandez-Lafuente R (2010) Lipase from *Thermomyces lanuginosus*: uses and prospects as an industrial biocatalyst. *J Mol Catal B Enzym* 62:197–212
- Fjerbaek L, Christensen KV, Norrdahl B (2009) A review of the current state of biodiesel production using enzymatic transesterification. *Biotechnol Bioeng* 102:1298–1315
- Foster NR, Gurdial GS, Yun JSL, Liang KK, Tilly KD, Ting SST, Singh H, Lee JH (1994) Significance of the crossover pressure in solid-supercritical fluid phase equilibria. *Ind Eng Chem Res* 30:1955–1964
- Fukuda H, Kondo A, Noda H (2001) Biodiesel fuel production by transesterification of oils. *J Biosci Bioeng* 92:405–416
- Fukuda H, Hama S, Tamalampudi S, Noda H (2008) Whole-cell biocatalysts for biodiesel fuel production. *Trends Biotechnol* 26:668–673
- Gameiro M, Lisboa P, Paiva A, Barreiros S, Simões P (2015) Supercritical carbon dioxide-based integrated continuous extraction of oil from chicken feather meal, and its conversion to biodiesel in a packed-bed enzymatic reactor, at pilot scale. *Fuel* 153:135–142
- García-Jarana MB, Sánchez-Oneto J, Portela JR, Casas L, Mantell C, de la Ossa EM (2016) Use of supercritical methanol/carbon dioxide mixtures for biodiesel production. *Korean J Chem Eng* 33:2342–2349
- García-Martínez N, Andreo-Martínez P, Quesada-Medina J, de los Ríos AP, Chica A, Beneito-Ruiz R, Carratalá-Abril J (2017) Optimization of non-catalytic transesterification of tobacco (*Nicotiana tabacum*) seed oil using supercritical methanol to biodiesel production. *Energy Convers Manag* 131:99–108
- Ghangui H, Karra-Chaâbouni M, Gargouri Y (2004) 1-butyl oleate synthesis by immobilized lipase from *Rhizopus oryzae*: a comparative study between n-hexane and solvent-free system. *Enzym Microb Technol* 35:355–363
- Ghoreishi SM, Moein P (2013) Biodiesel synthesis from waste vegetable oil via transesterification reaction in supercritical methanol. *J Supercrit Fluids* 76:24–31
- Gonzalez SL, Sychoski MM, Navarro-Díaz HJ, Callejas N, Saibene M, Vieitez I et al (2013) Continuous catalyst-free production of biodiesel through transesterification of soybean fried oil in supercritical methanol and ethanol. *Energy Fuel* 27:5253–5259

- Güçlü-Üstündağ Ö, Temelli F (2000) Correlating the solubility behavior of fatty acids, mono-, di-, and triglycerides, and fatty acid esters in supercritical carbon dioxide. *Ind Eng Chem Res* 39:4756–4766
- Guldhe A, Singh B, Mutanda T, Permaul K, Bux F (2015) Advances in synthesis of biodiesel via enzyme catalysis: novel and sustainable approaches. *Renew Sust Energ Rev* 41:1447–1464
- Han H, Cao W, Zhang J (2005) Preparation of biodiesel from soybean oil using supercritical methanol and CO₂ as co-solvent. *Process Biochem* 40:3148–3151
- Helwani Z, Othman MR, Aziz N, Fernando WJN, Kim J (2009) Technologies for production of biodiesel focusing on green catalytic techniques: a review. *Fuel Process Technol* 90:1502–1514
- Hiejima Y, Kajihara Y, Kohno H, Yao M (2001) Dielectric relaxation measurements on methanol up to the supercritical region. *J Phys Condens Matter* 13:10307
- Ilham Z, Saka S (2009) Dimethyl carbonate as potential reactant in non-catalytic biodiesel production by supercritical method. *Bioresour Technol* 100:1793–1796
- Ilham Z, Saka S (2010) Two-step supercritical dimethyl carbonate method for biodiesel production from *Jatropha curcas* oil. *Bioresour Technol* 101:2735–2740
- Ilham Z, Saka S (2011) Production of biodiesel with glycerol carbonate by non-catalytic supercritical dimethyl carbonate. *Lipid Technol* 23:10–13
- Ishak MAM, Ismail K, Nawawi WI, Jawad AH, Ani AY, Zakaria Z (2017) In-situ transesterification of *jatropha curcas* l. seeds for biodiesel production using supercritical methanol. In: MATEC web of conferences, vol 97. EDP Sciences, p 1082
- Jackson MA, Mbaraka IK, Shanks BH (2006) Esterification of oleic acid in supercritical carbon dioxide catalyzed by functionalized mesoporous silica and an immobilized lipase. *Appl Catal A Gen* 310:48–53
- Jegannathan KR, Abang S, Poncelet D, Chan ES, Ravindra P (2008) Production of biodiesel using immobilized lipase—a critical review. *Crit Rev Biotechnol* 28:253–264
- Kakugawa K, Shobayashi M, Suzuki O, Miyakawa T (2002) Purification and characterization of a lipase from the glycolipid-producing yeast *Kurtzmanomyces* sp. I-11. *Biosci Biotechnol Biochem* 66:978–985
- Karmakar A, Karmakar S, Mukherjee S (2012) Biodiesel production from neem towards feedstock diversification: Indian perspective. *Renew Sust Energ Rev* 16:1050–1060
- Kiss AA (2009) Novel process for biodiesel by reactive absorption. *Sep Purif Technol* 69:280–287
- Kiss FE, Micic RD, Tomić MD, Nikolić-Djorić EB, Simikić MĐ (2014) Supercritical transesterification: impact of different types of alcohol on biodiesel yield and LCA results. *J Supercrit Fluids* 86:23–32
- Klibanov AM (2001) Improving enzymes by using them in organic solvents. *Nature* 409:241
- Kumar R, Madras G, Modak J (2004) Enzymatic synthesis of ethyl palmitate in supercritical carbon dioxide. *Ind Eng Chem Res* 43:1568–1573
- Kumari A, Mahapatra P, Garlapati VK, Banerjee R (2009) Enzymatic transesterification of *Jatropha* oil. *Biotechnol Biofuels* 2(1)
- Lai J-Q, Hu Z-L, Wang P-W, Yang Z (2012) Enzymatic production of microalgal biodiesel in ionic liquid [BMIm][PF₆]. *Fuel* 95:329–333
- Lamba N, Gupta K, Modak JM, Madras G (2017) Biodiesel synthesis from *Calophyllum inophyllum* oil with different supercritical fluids. *Bioresour Technol* 241:767–774
- Laudani CG, Habulin M, Knez Ž, Della Porta G, Reverchon E (2007) Lipase-catalyzed long chain fatty ester synthesis in dense carbon dioxide: kinetics and thermodynamics. *J Supercrit Fluids* 41:92–101
- Lee JS, Saka S (2010) Biodiesel production by heterogeneous catalysts and supercritical technologies. *Bioresour Technol* 101:7191–7200
- Lee KT, Lim S, Pang YL, Ong HC, Chong WT (2014) Integration of reactive extraction with supercritical fluids for process intensification of biodiesel production: prospects and recent advances. *Prog Energy Combust Sci* 45:54–78

- Lim S, Lee KT (2014) Investigation of impurity tolerance and thermal stability for biodiesel production from *Jatropha curcas* L. seeds using supercritical reactive extraction. *Energy* 68:71–79
- Lim Y, Lee HS, Lee YW, Han C (2009) Design and economic analysis of the process for biodiesel fuel production from transesterificated rapeseed oil using supercritical methanol. *Ind Eng Chem Res* 48:5370–5378
- Lisboa P, Rodrigues AR, Martín JL, Simões P, Barreiros S, Paiva A (2014) Economic analysis of a plant for biodiesel production from waste cooking oil via enzymatic transesterification using supercritical carbon dioxide. *J Supercrit Fluids* 85:31–40
- Liu Y, Yan Y, Hu F, Yao AN, Wang Z, Wei F (2010) Transesterification for biodiesel production catalyzed by combined lipases: optimization and kinetics. *AIChE J* 56:1659–1665
- Lotti M, Pleiss J, Valero F, Ferrer P (2015) Effects of methanol on lipases: molecular, kinetic and process issues in the production of biodiesel. *Biotechnol J* 10:22–30
- Lozano P (2010) Enzymes in neoteric solvents: from one-phase to multiphase systems. *Green Chem* 12:555–569
- Lozano P, Villora G, Gómez D, Gayo AB, Sánchez-Conesa JA, Rubio M et al (2004) Membrane reactor with immobilized *Candida antarctica* lipase B for ester synthesis in supercritical carbon dioxide. *J Supercrit Fluid* 29(1–2):121–128
- Lozano P, Bernal JM, Vaultier M (2011) Towards continuous sustainable processes for enzymatic synthesis of biodiesel in hydrophobic ionic liquids/supercritical carbon dioxide biphasic systems. *Fuel* 90:3461–3467
- Ma F, Clements LD, Hanna MA (1998) Biodiesel fuel from animal fat. Ancillary studies on transesterification of beef tallow. *Ind Eng Chem Res* 37:3768–3771
- Malcata FX, Reyes HR, Garcia HS, Hill CG, Amundson CH (1992) Kinetics and mechanisms of reactions catalysed by immobilized lipases. *Enzym Microb Technol* 14:426–446
- Marchetti JM, Miguel VU, Errazu AF (2007) Possible methods for biodiesel production. *Renew Sust Energ Rev* 11:1300–1311
- McKennedy J, Önenç S, Pala M, Maguire J (2016) Supercritical carbon dioxide treatment of the microalgae *Nannochloropsis oculata* for the production of fatty acid methyl esters. *J Supercrit Fluids* 116:264–270
- Mittelbach M (1990) Lipase catalyzed alcoholysis of sunflower oil. *J Am Oil Chem Soc* 67:168–170
- Mukhopadhyay M (2000) Natural extracts using supercritical carbon dioxide. CRC Press, Boca Raton, pp 1–93
- Muppaneni T, Reddy HK, Patil PD, Dailey P, Aday C, Deng S (2012) Ethanolysis of Camelina oil under supercritical condition with hexane as a co-solvent. *Appl Energy* 94:84–88
- Narwal SK, Gupta R (2013) Biodiesel production by transesterification using immobilized lipase. *Biotechnol Lett* 35:479–490
- Norjannah B, Ong HC, Masjuki HH, Juan JC, Chong WT (2016) Enzymatic transesterification for biodiesel production: a comprehensive review. *RSC Adv* 6:60034–60055
- Novak Z, Habulin M, Krmelj V, Åe K (2003) Silica aerogels as supports for lipase catalyzed esterifications at sub- and supercritical conditions. *J Supercrit Fluid* 27:169–178
- Oliveira D, Oliveira JV (2001) Enzymatic alcoholysis of palm kernel oil in n-hexane and SCCO₂. *J Supercrit Fluids* 19:141–148
- Pinnarat T, Savage PE (2008) Assessment of noncatalytic biodiesel synthesis using supercritical reaction conditions. *Ind Eng Chem Res* 47:6801–6808
- Poppe JK, Fernandez-Lafuente R, Rodrigues RC, Ayub MAZ (2015) Enzymatic reactors for biodiesel synthesis: present status and future prospects. *Biotechnol Adv* 33:511–525
- Rathore V, Madras G (2007) Synthesis of biodiesel from edible and non-edible oils in supercritical alcohols and enzymatic synthesis in supercritical carbon dioxide. *Fuel* 86:2650–2659
- Raveendran P, Ikushima Y, Wallen SL (2005) Polar attributes of supercritical carbon dioxide. *Acc Chem Res* 38:478–485

- Reddy SN, Madras G (2011) A new semi-empirical model for correlating the solubilities of solids in supercritical carbon dioxide with cosolvents. *Fluid Phase Equilib* 310:207–212
- Reddy SN, Madras G (2012) Mixture solubilities of nitrobenzoic acid isomers in supercritical carbon dioxide. *J Supercrit Fluids* 70:66–74
- Reis P, Holmberg K, Watzke H, Leser ME, Miller R (2009) Lipases at interfaces: a review. *Adv Colloid Interf Sci* 147:237–250
- Rivera I, Villanueva G, Sandoval G (2009) Biodiesel production from animal grease wastes by enzymatic catalysis. *Grasas Aceites* 60:470–476
- Rodrigues AR, Paiva A, da Silva MG, Simões P, Barreiros S (2011) Continuous enzymatic production of biodiesel from virgin and waste sunflower oil in supercritical carbon dioxide. *J Supercrit Fluids* 56:259–264
- Román-Figueroa C, Olivares-Carrillo P, Paneque M, Palacios-Nereo FJ, Quesada-Medina J (2016) High-yield production of biodiesel by non-catalytic supercritical methanol transesterification of crude castor oil (*Ricinus communis*). *Energy* 107:165–171
- Romero MD, Calvo L, Alba C, Habulin M, Primožič M, Knez Ž (2005) Enzymatic synthesis of isoamyl acetate with immobilized *Candida antarctica* lipase in supercritical carbon dioxide. *J Supercrit Fluids* 33:77–84
- Rosmeika, Yuwono AS, Tambunan AH (2014) Comparison of biodiesel production by conventional and superheated methanol vapor technologies using life cycle assessment method. *Environ Eng Sci* 31:107–116
- Saharay M, Balasubramanian S (2004) Ab initio molecular dynamics study of supercritical carbon dioxide. *J Chem Phys* 120:9694–9702
- Saka S, Isayama Y (2009) A new process for catalyst-free production of biodiesel using supercritical methyl acetate. *Fuel* 88:1307–1313
- Saka S, Kusdiana D (2001) Biodiesel fuel from rapeseed oil as prepared in supercritical methanol. *Fuel* 80:225–231
- Saka S, Isayama Y, Ilham Z, Jiayu X (2010) New process for catalyst-free biodiesel production using subcritical acetic acid and supercritical methanol. *Fuel* 89:1442–1446
- Sakdasri W, Sawangkeaw R, Medina-Gonzalez Y, Camy S, Condoret JS, Ngamprasertsith S (2016) Experimental study and modeling of phase equilibrium of the methanol–tripalmitin system: application to palm oil transesterification with supercritical methanol. *Ind Eng Chem Res* 55:5190–5199
- Sandoval GC, Marty A, Condoret JS (2001) Thermodynamic activity-based enzyme kinetics: efficient tool for nonaqueous enzymology. *AIChE J* 47:718–726
- Sandoval G, Casas-Godoy L, Bonet-Ragel K, Rodrigues J, Ferreira-Dias S, Valero F (2017) Enzyme-catalyzed production of biodiesel as alternative to chemical-catalyzed processes: advantages and constraints. *Curr Biochem Eng* 4:109–141
- Sankaran R, Show PL, Chang JS (2016) Biodiesel production using immobilized lipase: feasibility and challenges. *Biofuels Bioprod Biorefin* 10:896–916
- Sawangkeaw R, Bunyakiat K, Ngamprasertsith S (2010) A review of laboratory-scale research on lipid conversion to biodiesel with supercritical methanol (2001–2009). *J Supercrit Fluids* 55:1–13
- Sawangkeaw R, Satayanon W, Bunyakiat K, Camy S, Condoret JS, Ngamprasertsith S (2011) Continuous production of biodiesel with supercritical methanol: a simple compressible flow model for tubular reactors. *Int J Chem React Eng* 9:A96
- Sawiwat T, Kajorncheappunngam S (2015) Biodiesel production from crude rubber seed oil using supercritical methanol transesterification. In: *Applied mechanics and materials*, vol 781. Trans Tech Publications, pp 655–658
- Sim JH, Kamaruddin AH, Bhatia S (2010) Biodiesel (FAME) productivity, catalytic efficiency and thermal stability of lipozyme TL IM for crude palm oil transesterification with methanol. *J Am Oil Chem Soc* 87:1027–1034
- Sivasamy A, Cheah KY, Fornasiero P, Kemausuor F, Zinoviev S, Miertus S (2009) Catalytic applications in the production of biodiesel from vegetable oils. *ChemSusChem* 2:278–300

- Span R, Wagner W (1996) A new equation of state for carbon dioxide covering the fluid region from the triple point temperature to 1100 K at pressures up to 800 MPa. *J Phys Chem Ref Data* 25:1509–1596
- Sun Y, Reddy HK, Muppaneni T, Ponnusamy S, Patil PD, Li C et al (2014) A comparative study of direct transesterification of camelina oil under supercritical methanol, ethanol and 1-butanol conditions. *Fuel* 135:530–536
- Taher H, Al-Zuhair S (2017) The use of alternative solvents in enzymatic biodiesel production: a review. *Biofuels Bioprod Biorefin* 11:168–194
- Taher H, Al-Zuhair S, Al-Marzouqi A, Hashim I (2011) Extracted fat from lamb meat by supercritical CO₂ as feedstock for biodiesel production. *Biochem Eng J* 55:23–31
- Taher H, Al-Zuhair S, Al-Marzouqi AH, Haik Y, Farid M (2014a) Enzymatic biodiesel production of microalgae lipids under supercritical carbon dioxide: process optimization and integration. *Biochem Eng J* 90:103–113
- Taher H, Al-Zuhair S, Al-Marzouqi AH, Haik Y, Farid M, Tariq S (2014b) Supercritical carbon dioxide extraction of microalgae lipid: process optimization and laboratory scale-up. *J Supercrit Fluids* 86:57–66
- Tan KT, Lee KT (2011) A review on supercritical fluids (SCF) technology in sustainable biodiesel production: potential and challenges. *Renew Sust Energ Rev* 15:2452–2456
- Tan KT, Lee KT, Mohamed AR (2010a) A glycerol-free process to produce biodiesel by supercritical methyl acetate technology: an optimization study via response surface methodology. *Bioresour Technol* 101:965–969
- Tan KT, Lee KT, Mohamed AR (2010b) Effects of free fatty acids, water content and co-solvent on biodiesel production by supercritical methanol reaction. *J Supercrit Fluids* 53:88–91
- Tang M, Zhang P, Zhang L, Li M, Wu L (2012) A potential bioenergy tree: *Pistacia chinensis* Bunge. *Energy Proc* 16:737–746
- Varma MN, Madras G (2007) Synthesis of biodiesel from castor oil and linseed oil in supercritical fluids. *Ind Eng Chem Res* 46:1–6
- Varma MN, Deshpande PA, Madras G (2010) Synthesis of biodiesel in supercritical alcohols and supercritical carbon dioxide. *Fuel* 89:1641–1646
- Warabi Y, Kusdiana D, Saka S (2004) Reactivity of triglycerides and fatty acids of rapeseed oil in supercritical alcohols. *Bioresour Technol* 91:283–287
- Wen D, Jiang H, Zhang K (2009) Supercritical fluids technology for clean biofuel production. *Prog Nat Sci* 19:273–284
- West AH, Posarac D, Ellis N (2008) Assessment of four biodiesel production processes using HYSYS. *Plant Bioresour Technol* 99:6587–6601
- Xie W, Wang J (2012) Immobilized lipase on magnetic chitosan microspheres for transesterification of soybean oil. *Biomass Bioenergy* 36:373–380
- Xu Y, Nordblad M, Nielsen PM, Brask J, Woodley JM (2011) In situ visualization and effect of glycerol in lipase-catalyzed ethanolysis of rapeseed oil. *J Mol Catal B Enzym* 72:213–219
- Yang X, Jin G, Gong Z, Shen H, Bai F, Zhao ZK (2015) Recycling microbial lipid production wastes to cultivate oleaginous yeasts. *Bioresour Technol* 175:91–96
- Yu ZR, Singh B, Rizvi SS, Zollweg JA (1994) Solubilities of fatty acids, fatty acid esters, triglycerides, and fats and oils in supercritical carbon dioxide. *J Supercrit Fluids* 7:51–59
- Yusuf NNAN, Kamarudin SK (2013) Techno-economic analysis of biodiesel production from *Jatropha curcas* via a supercritical methanol process. *Energy Convers Manag* 75:710–717
- Zarejousheghani F, Kariminia HR, Khorasheh F (2016) Kinetic modelling of enzymatic biodiesel production from castor oil: temperature dependence of the Ping Pong parameters. *Can J Chem Eng* 94:512–517



Application of Microalgae for CO₂ Sequestration and Wastewater Treatment

12

Nilotpala Pradhan and Biswaranjan Das

Abstract

Microalgae are unicellular to multicellular simple autotrophic organisms with simple growth requirements like light, carbon dioxide, nitrogen, phosphorous, and potassium present dissolved in their aqueous ecosystem. During the course of their growth, they intake these elements present in a different compound form in the water system. This makes them beneficial for removal of such moieties from wastewater where these are present in high amount as pollutants and may cause havoc to the natural ecosystem if released untreated. In this chapter, we have discussed algae with respect to their properties related to uptake of carbon dioxide from flue gas as well as nitrogen and heavy metal from the wastewater. We have also discussed few systems where different algae are used in conjunction with or without bacteria for increasing the efficiency of waste treatment. Few pilot-scale studies used for wastewater remediation are also discussed.

Keywords

Microalgae · CO₂ sequestration · Wastewater treatment · Heavy metals · Bioremediation

12.1 Introduction

We all are aware of the adversity caused by the extensive use of fossil fuel during the last few decades for rapid and rampant industrialization. The fossil fuel combustion produces CO₂, which causes the greenhouse effect and global warming. The

N. Pradhan (✉) · B. Das

Environment & Sustainability Department, CSIR-Institute of Minerals and Materials Technology, Bhubaneswar, Odisha, India

e-mail: npradhan@immt.res.in

© Springer Nature Singapore Pte Ltd. 2018

P. K. Sarangi et al. (eds.), *Recent Advancements in Biofuels and Bioenergy Utilization*, https://doi.org/10.1007/978-981-13-1307-3_12

285

aftermath is that now the non-renewable fossil fuels are depleted and we are facing the deleterious effect due to global warming. The effect is more visible as the extent of pollution around us. Mitigation of all these adverse effects requires the substitution of non-renewable fossil fuels with renewable sources of energy like solar energy, wind energy, bioenergy, etc. as well as efforts to sequester CO₂ so that it does not escape to the atmosphere.

Bioenergy includes biodiesel, bioethanol, biohydrogen, etc. Among all these, biodiesel has received significant importance in the recent years. Out of many sources for biodiesel, microalgal biodiesel has received great attention due to the higher rate of productivity of algae and possibility of its mass cultivation multiple times a year. Microalgae may be unicellular or multicellular photosynthetic organisms with great biodiversity (Madigan et al. 1997; Wang and Chen 2009; Mutanda et al. 2011). They are ubiquitous in occurrence and flourish in a variety of environmental condition (Vonshak 1990; Hu et al. 2008). They are highly biodiverse and occur in large numbers mainly in the marine ecosystem. They are able to adapt themselves to widespread environmental conditions in such a way that they thrive efficiently and extensively in different ecosystems. Large surface-to-volume body ratio provided by microscopic structure (generally in millimetre size range) helps them in efficient nutrient uptake and proliferation (Brennan and Owende 2010). They are considered more efficient than higher plants with respect to photosynthesis ability, but the mechanism of photosynthesis is reported to be similar (Walter et al. 2005; Spolaore et al. 2006; Khan et al. 2009; Kirroliia et al. 2013).

They generally have high CO₂ fixing efficiency with high growth rate and may accumulate macromolecules such as lipids (triglycerides), proteins, and carbohydrates in large amounts. Microalgae are used for the wide range of biotechnological applications, but due to their lipid accumulation property, they are primarily considered for the sustainable production of carbon-neutral biodiesel as an alternative to non-renewable petro-diesel. Other high-value products including polyunsaturated fatty acids (PUFA), pigments like carotenoids and phycobiliproteins, and bioactive molecules are useful for nutraceuticals, pharmaceuticals, or other industrial applications as shown in Fig. 12.1 (Aishvarya et al. 2015).

The microalgae mostly grow autotrophically with inorganic forms of macronutrients and micronutrients to fulfil their modest growth requirements and need the presence of sunlight or artificial light source. As a result, they are easy to grow in economical way. In this review, we have discussed how this mode of nutrition may be utilized to get rid of the pollution and some wastes generated by anthropogenic means. Some of these covered in the review are carbon dioxide emission from industries as carbon source and nitrates in waste streams as the nitrogen source during the growth of algae. Algae may also be used for uptake of toxic metal ions from the waste streams. Some hybrid systems utilizing both microalgae and bacteria for wastewater remediation are also discussed. Here, we intend to link algal biomass production with some of the pollution control measures

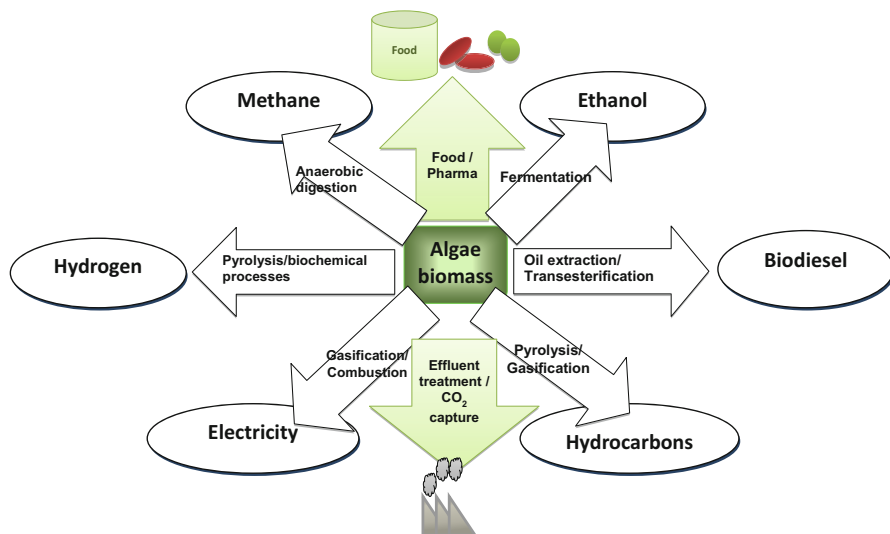


Fig. 12.1 Current industrial uses of algae. (Reproduced with permission from Springer. Aishvarya et al. 2015)

so that biofuel production may have some added advantage to make it more lucrative.

12.2 Microalgal Nutritional Requirement

Naturally occurring algae may have different and specific growth requirement based on the ecosystem they are isolated from (Lavens and Sorgeloos 1996). In the laboratory, they may be grown with those specific requirements, but when grown for commercial or any other large-scale cultivation, these specific requirements may not be fully satisfied. While growing algae under the sun in open raceway pond for different applications like biofuel production, CO₂ sequestration and wastewater treatment may affect the strains or consortia drastically. Therefore, strains developed in the laboratory may not work in open systems, and monoculture system seldom works. Pure strains are not even required for the functions like wastewater treatment or CO₂ sequestration or heavy metal uptake. In addition, population dynamics in such system may change from time to time depending upon the concentration and content variation in the input wastewater. Mixed consortia for such system are more robust and may overcome the changing input efficiently. However, biofuel production may be suitable for the high lipid-producing strains and affected adversely by contamination.

Some basic nutrients are required for cultivation of any algae, and their deficiency may be rate limiting for the growth of algae and for the overall process. These are quality and quantity of carbon, nitrogen, potassium, and phosphorus sources along with the light. Variation in seasonal temperature may affect the population dynamics and hence the process kinetics. Similarly, the variation of pH and salinity along with the input may also affect the process on daily basis. The input carbon source may be inorganic or organic and thus may support the growth of autotrophic or heterotrophic strains, respectively, and even mixotrophic growth may be possible. All these parameters are known to influence photosynthesis, the growth of cell, and overall productivity of biomass by affecting the pattern of cellular metabolism thereby varying the cell composition (Richmond and Hu 2013).

The carbon, nitrogen, and phosphorus present in wastewater may fulfil the major nutrient requirement for microalgal growth. Different wastewaters reported for microalgal growth are domestic (Posadas et al. 2013; Yang et al. 2011), industrial (Tarlán et al. 2002), agriculture (Hernández et al. 2013; Lefebvre et al. 1996), refinery (Chojnacka et al. 2004), leachate (Lin et al. 2007; Mustafa et al. 2012), etc. These reports indicate that microalgae may be effectively used for the removal of nitrogen and phosphorus and are suitable for wastewater treatment strategy. The use of wastewater as a raw material for algal growth has added the advantage of cost reduction as well as environmental concerns (Gonçalves et al. 2017).

12.3 Microalgae for Sequestration of CO₂

Algae have an autotrophic mode of nutrition and mostly dependent on the inorganic source of carbon like bicarbonate, carbonate, or CO₂ dissolved in water for their growth through photosynthesis. This property may be utilized for sequestration of CO₂ escaping through industrial flue gas thereby helping in mitigation of this greenhouse gas and simultaneously generating algal biomass, a renewable energy source (Campbell et al. 2011). As reported by Chisti (2007), 1.83 kg of CO₂ is fixed in the generation of 1 kg of microalgal biomass. Industrial flue gas generally contains 12–20% of CO₂ in the exhaust and after removal of other impurities harmful to algae may act as the potential source of CO₂ for microalgal growth (Mata et al. 2010). The CO₂ gas when passed through the algal growth medium is taken up and is dissolved in an aqueous medium as CO₂, CO₃²⁻, HCO₃⁻, and H₂CO₃ based on medium pH and later utilized by microalgae during photosynthesis (Van Den Hendé et al. 2012). For this, the growth medium is incorporated with an additional intermediate CO₂ sequestering agent, which keeps the CO₂ in the dissolved condition in the aqueous media. This is required as CO₂ is sparingly soluble in water (Aishvarya et al. 2012; Gehl et al. 1990; Smith and Bidwell 1989). The intermediate reagent may be a chemical moiety harmless for algal growth. One of the examples is NaOH, which when dissolved in aqueous medium dissociates into OH⁻ ions and Na⁺ ion. The OH⁻ ion is capable of reacting with gaseous CO₂ and retaining it in the medium as

bicarbonate and carbonate ions. Algae in the presence of light utilize CO₂ present as bicarbonate and carbonate ions during photosynthesis, thus releasing the OH⁻ ions back into the medium, which is available again to take up CO₂ infused into the system (Aishvarya et al. 2012).

It is envisaged that, if not all, a part of flue gas emitted from industrial units using fossil fuel may provide a potential carbon source for microalgal growth and diminish CO₂ emissions as one of the mitigation strategies (Danielo 2005; Chelf et al. 1993; Wojciech 2012). Microalgae that have been well studied for this aspect include *Scenedesmus* (Morais and Costa 2007; Dahai et al. 2011; Kaewkannetra et al. 2012; Tukaj and Aksmann 2007; Ho et al. 2012), *Chlorella* (Ramanan et al. 2010; Borkenstein et al. 2011; Aishvarya et al. 2012; Yeh et al. 2010; Gilles et al. 2008), *Nannochloropsis* (Hsueh et al. 2009; Sheng et al. 2009; Sforza et al. 2012), *Botryococcus braunii* (Ge et al. 2011; RangaRao et al. 2007), *Chlorogleopsis* (Douskova et al. 2009), *Thermosynechococcus* (Hsueh et al. 2009), *Spirulina* (Ramanan et al. 2010), *Chlorococcum*, *Synechococcus*, etc.

The cost economics of microalgal cultivation for biofuel is very much dependent on the growth rate of algae among all other factors. The fast growth rate has many requisite optimum parameters, one of them being the availability of dissolved CO₂ in the growth medium during photosynthesis. External supplement of CO₂ along with intermediate chemical sequestering agent has been proved to enhance the growth many folds decreasing the doubling time (Aishvarya et al. 2012). Thus, clubbing CO₂ sequestration with microalgae cultivation may help in achieving greenhouse gas mitigation with higher biomass and better biofuel productivity (Table 12.1). The CSIR-Institute of Minerals and Materials Technology (CSIR-IMMT) in Bhubaneswar, Odisha, India, has eight numbers of raceway ponds or high rate algal ponds. Each raceway pond is made up of concrete with a capacity of 40,000 L. Each pond has a working capacity of 30,000 L for growing algae in a

Table 12.1 Algae with different CO₂ fixation rate during biomass generation

Algae	CO ₂ fixation rate (mg/L/day)	References
<i>Botryococcus braunii</i>	496.98	Sydney et al. (2010)
<i>Botryococcus braunii</i>	1100	Murukami and Ikenouchi (1997)
<i>Chlorella</i> sp. UK001	31.8	Hirata et al. (1996)
<i>Chlorella vulgaris</i>	251.64	Sydney et al. (2010)
<i>Chlorella vulgaris</i>	865	Hirata et al. (1996)
<i>Chlorella vulgaris</i>	624	Yun et al. (1997)
<i>Dunaliella tertiolecta</i>	272.4	Sydney et al. (2010)
<i>Dunaliella tertiolecta</i>	313	Michimasa et al. (1994)
<i>Spirulina platensis</i>	318.61	Sydney et al. (2010)
<i>Spirulina platensis</i>	413	Morais and Costa (2007)
<i>Synechocystis aquatilis</i>	1500	Murukami and Ikenouchi (1997)

Reproduced from Elsevier. Singh and Singh (2014)

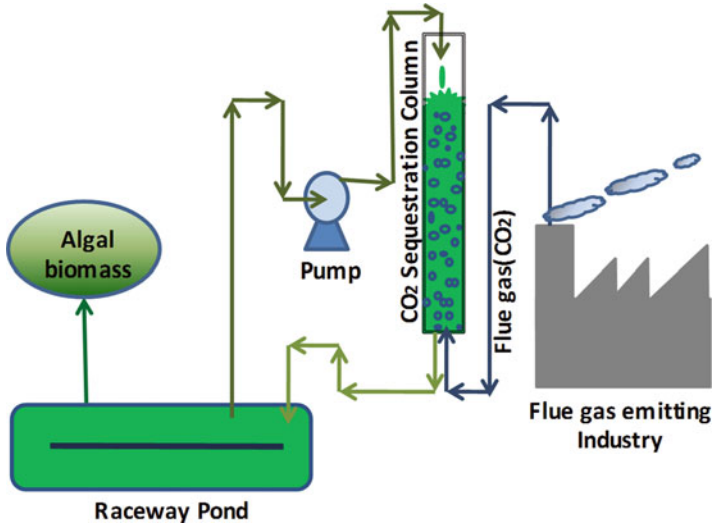


Fig. 12.2 Schematic diagram showing CO₂ bubble column for sequestration of CO₂ from flue gas



Fig. 12.3 Large-scale microalgae cultivation facility at CSIR-IMMT, Bhubaneswar, Odisha, India. Eight raceway ponds fitted with paddle wheels and CO₂ supply system

closed circular loop. Each raceway pond consists of agitation system (paddle wheels), the CO₂ sparging system (CO₂ diffuser), and flow rate controlled system (baffles). Some raceway ponds are fitted with bubble column for better dissolution of CO₂ in growth medium (Fig. 12.2). A few raceway ponds have smooth surfaces for better biomass recovery (Fig. 12.3).

12.4 Microalgae for Removal of Nitrogen from Wastewater

Various inorganic and organic nitrogen sources may be used by microalgae for their growth including nitrates, nitrites, ammonium, urea, etc. (Becker 1994; Lin and Lin 2011). Before being incorporated into amino acids, all the nitrogen sources are first converted to ammonia through different metabolic pathways (Cai et al. 2013). As ammonium is already in the reduced form, it requires less energy to be spent by cells for its assimilation into amino acids. Hence, it is preferred by most of the algae for growth. *Ellipsoidion* sp. is reported to utilize ammonium better than urea and nitrate (Xu et al. 2001). Some of the microalgae like *Botryococcus braunii* and *Dunaliella tertiolecta* are reported to grow better with nitrate (Chen et al. 2011; Ruangsomboon 2015), while *Chlorella* sp. and *Neochloris oleoabundans* prefer urea and nitrate (Liu et al. 2008; Hsieh and Wu 2009; Pruvost et al. 2009).

Source of nitrogen used for growth has a significant role in the biochemical composition of the microalgal cells. *Dunaliella salina* showed a twofold increase in cellular protein concentration when grown with ammonia compared to nitrate as nitrogen source (Norici et al. 2002). Lipid content of *Chlorella sorokiniana* cells increased twofold with ammonium compared to the presence of nitrate or urea as nitrogen source (Wan et al. 2012). Thus, the source of nitrogen may need to be changed depending upon the strains selected and the purpose or application for which they are being grown. However, wastewater may contain a mixture of varied nitrogen compounds at a different ratio depending upon the type of wastewater. Thus, the prevailing nitrogen condition may become selective in the development of efficient adaptive consortia.

12.5 Microalgae for Removal of Toxic Metals from Wastewater

Industrial wastewater effluent arising from mineral processing units, electroplating, and plastic and ceramic industries even after being treated with effluent treatment plants may be high in heavy metals. When discharged into water bodies like lake, rivers, and sea, it enters and accumulates into the flora and fauna through the food chain. The consequences of heavy metals in the ecosystem, especially on the microorganisms vary greatly with their effective concentration and type of the metal. These metals get toxic to microbes by replacing the essential metals required for the normal functioning of the cells at molecular levels (Wong et al. 1978; Nies 1999; Bruins et al. 2000). They disrupt the normal cellular function, and the effect is concentration dependent (Konopka 1999). At higher concentration, they are known to have adverse effects on the enzyme activity and specificity. Additionally, they may bring about structural changes in proteins and nucleic acids (Bruins et al. 2000; Bong et al. 2010). These effects may either kill the microalgae or severely affect their growth.

The algae have overcome these adverse consequences by evolving different defence machinery at cellular levels, which enable them to survive under such

antagonistic conditions. Different functional groups associated with microalgal cells enable them to bind metal ions on the surface and further uptake into the cells. These functional groups may be hydroxyl, thiol, amino, carboxyl, phosphate, exopolysaccharides, etc. (Sag and Kutsal 2001; Jena et al. 2015).

Uptake of heavy metal by microalgae results in the retention of heavy metal present in soluble form, to be bound to biomass, which may be separated. This helps in the removal of metals from the liquid, and later the biomass may be used to recover metal values. Biosorption may prove to be eco-friendly, efficient, and cost-effective. It may act as an efficient option for the treatment of industrial effluents rich in heavy metals or effluent coming out of contaminated mines in a low-energy-intensive way. Microalgae being autotrophic and photosynthetic have low nutritional necessity and do not produce any harmful metabolic intermediates or end products.

Microalgae show remarkable potential in metal remediation because of high growth rate and modest nutritional requirement. Lead removal from contaminated wastewater was studied using live *Spirulina*. An adsorption rate of 74% was observed at the initial stage (0–12 min), and maximum adsorption of 0.62 mg lead per 10^5 alga cells was observed (Chen and Pan 2005). Removal of heavy metals such as Pb, Cd, Cu, Co, Cr, Ni, Zn, Fe, and Mn has also been carried out by *Cladophora glomerata* and *Oedogonium rivulare*. While Ni, Cr, Fe, and Mn were observed to be continuously removed, other metals like Cu, Pb, Cd, and Co were removed more rapidly at an initial stage. It was observed that the presence of humic acids had a negative impact on metal removal (Vymazal 1984). Significant accumulation of Pb and Cr was observed in algae belonging to *Oscillatoria* genus and thus has been reported to be of wide significance in metal removal strategy (Brahmbhatt et al. 2012). *Chlorella* and *Scenedesmus* algae have been reported to possess efficient bioremediation capacity for different heavy metals (Pinto et al. 2003; Tukaj et al. 2007). Microalgae *Spirogyra hyaline* has also been studied for bioremediation of heavy metals like Cd, Hg, Pb, As, and Co (Kumar and Cini 2012).

Biological mitigation of this problem may be attained by treating such water with microalgae after effluent treatment plants. Microalgae are reported to uptake heavy metals through biosorption and bioaccumulation (Chojnacka 2010). Heavy metal biosorption has been studied for heavy metal ions such as Cr^{3+} , Cd^{2+} , Cu^{2+} , etc. (Chojnacka et al. 2005; Jena et al. 2014).

12.6 Hybrid Systems

Microalgae-based wastewater treatment has numerous advantages over conventional wastewater treatment like lower capital, operation, and maintenance cost and lowers energy intensity, which is a greenhouse benefit. Figure 12.4 shows the application of algae in conventional and hybrid wastewater treatment system. Utilization of wastewater for microalgal growth may reduce the input of fertilizers and freshwater required for the large-scale cultivation (Pittman et al. 2011; DeAlva et al. 2013; Prajapati et al. 2013; Craggs et al. 2011).

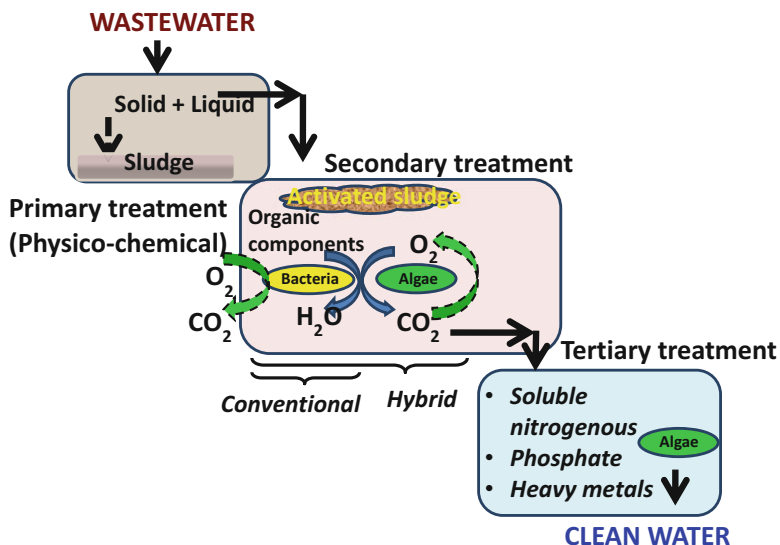


Fig. 12.4 Schematic diagram showing application of algae in conventional and hybrid waste water treatment system

Some recently developed hybrid technologies for wastewater treatment using microalgae are discussed below:

12.6.1 Microalgae: Bacteria Consortia System

Microalgae act as an aerator in natural aquatic systems, which produces oxygen for other bacteria and serves as carbon dioxide sinks that fix CO₂. Other than the exchange of oxygen-carbon dioxide, the interaction between microalgae and bacteria also includes other potential features of the consortia on wastewater treatment (Jia and Yuan 2016).

Microalgae-bacteria consortia can be classified into two systems, the microalgae-assistant systems and microalgae-dominant systems, which are based on the effect of microalgae (Jia and Yuan 2016). In the microalgae-assistant system, microalgae act as oxygen producer for other organisms present in the system. Its main function in the system is to grow and supply dissolved oxygen for bacteria, which ultimately removes nutrients by active uptake. A rapid growth rate of microalgae is desirable for producing sufficient oxygen to keep the system healthy. Karya et al. (2013) have reported cultivation of a bio-flocculent alga-activated sludge, which could remove up to 100% of NH₄⁺ (50 g/L) in a semi-continuous reactor. On the other hand, in a microalgae-dominant system, the key role of microalgae is nutrient removal, and it must produce ample amount of biomass for sufficient uptake. According to Mouget et al. (1995), the growth of green microalgae *Chlorella* sp. and *Scenedesmus*

Table 12.2 List of application of solo microalgae and consortia with some real wastewater

Waste stream	System	Algae species	References
Artificial wastewater	Microalgae-bacteria consortia (microalgae assistant)	<i>Scenedesmus quadricauda</i> (nitrifier- enriched activated sludge)	Karya et al. (2013)
Wastewater	Microalgae-bacteria consortia (microalgae dominant)	<i>Chlorella vulgaris</i> and <i>Bacillus licheniformis</i>	Liang et al. (2013)
Municipal wastewater	Floating offshore photobioreactor	Mixed algal culture dominated by <i>Scenedesmus dimorphus</i>	Novoveska et al. (2016)
Centrate wastewater	Outdoor marine microalgae-based tubular photobioreactor	<i>Nannochloropsis gaditana</i>	Villegas et al. (2017)
Urban wastewater	Mixotrophic cultivation of algae in enclosed photobioreactor	<i>Galdieria sulphuraria</i>	Henkanatte et al. (2015)
Secondary effluent	Duckweed-microalgae constructed wetland (DM-CW)	<i>Chlorella</i> sp., <i>Scenedesmus</i> sp., and <i>Euglena</i> sp.	Bouali et al. (2012)
Sewage	Algal biofilm airlift photobioreactor (ABA-PBR)	<i>Chlorella vulgaris</i>	Tao et al. (2017)
Domestic wastewater	Parallel plate microalgae biofilm reactor	<i>Scenedesmus obliquus</i>	Zamalloa et al. (2013)
Dairy manure wastewater	Rocker algal biofilm system	<i>Chlorella</i> sp.	Johnson and Wen (2010)

bicellularis is promoted by the microbial strains such as *Pseudomonas diminuta* and *Pseudomonas vesicularis* without releasing any growth-promoting substances.

Few studies have evaluated different parameters to increase the efficiency of solo microalgae and consortia systems for nitrogen removal. Table 12.2 lists the experiments carried with solo microalgae and consortia with some real wastewater systems.

12.6.2 Microalgae-Based Wastewater Treatment Systems

12.6.2.1 Floating Offshore Photobioreactors

Algae Systems, LLC, USA, designed a unique approach for wastewater treatment where microalgae are cultivated in modular, floating offshore photobioreactor (Novoveská et al. 2016). Retention of high CO₂, elimination of evaporative loss, minimal land usage, thermoregulation, and mixing provided by the surrounding water body are some of the key features of this process. The initial microalgae grown in the offshore photobioreactors was *Scenedesmus dimorphus*, which was gradually replaced by a mixed culture dominated by genus *Chlorella*, *Cryptomonas*, and *Scenedesmus*. Using this system, up to 50,000 gals/day raw wastewater was treated. Feeding and harvest volume of wastewater, air/CO₂ volume, and ratio were

calculated every day as per experimental design. During continuous operation, the biomass production rate ranged from 3.5 to 22.7 g/m²/day. This system achieved 75% nitrogen removal, 93% phosphorous removal, and 92% biological oxygen demand (BOD) removal.

Offshore bioreactors are highly effective for wastewater treatment due to three key factors, such as:

1. No process aeration is required due to oxygen produced by photosynthesis.
2. Mixing can be supplied by wave energy and pumping during feed and harvesting of photobioreactors.
3. Algae growth improves energy production by increasing biomass available for hydrothermal liquefaction or other conversion technologies.

In this system, Novoveska et al. (2016) demonstrated that coupling algae biofuel production and wastewater treatment is a promising strategy towards a large-scale development of algal biofuel.

12.6.2.2 Centrate from Urban Wastewater Plant As the Nutrient Source

Villagas et al. (2017) demonstrated that the centrate from urban wastewater plant could be used as a nutrient source for outdoor production of marine microalgae *Nannochloropsis gaditana* in a tubular photobioreactor. The working volume of tubular photobioreactors was 340 L each. The reactors were operated in semi-continuous chemostat mode by adding fresh medium to the reactor for 4 h every day in the middle of the solar cycle and, simultaneously, harvesting an equal amount of culture. The temperature during the day was kept under 30 °C by circulating seawater through a heat exchanger. By a diesel oil boiler, flue gas was produced, stored, and injected into the culture.

The percentage of centrate influences the amount of nutrients supplied every day to the reactors, while the imposed dilution rate also influences the microalgae biomass harvesting thereby maintaining the final biomass concentration inside the culture at steady state. This study proved that marine microalgae can be produced under outdoor conditions using centrate as the nutrient source and recovers the nutrient contained in the centrate. The ideal conditions for producing biomass were using 20% centrate and dilution rate of 0.3/day; the biomass productivity was 15.62 g biomass/m²/day. A maximum nutrient removal capacity of up to 36.9 mg N/L/day and 5.38 mg P/L/day was noticed.

12.6.2.3 Duckweed-Microalgae Constructed Wetland (DM-CW) for Wastewater Treatment

Bouali et al. (2012) demonstrated a continuous flow pilot wetland called duckweed-microalgae constructed wetland (DM-CW) for treating wastewater located in Mahdia City, Tunisia. In this pilot plant, duckweed plant, namely, *Lemna minor*, and three microalgae species, namely, *Chlorella* sp., *Scenedesmus* sp., and *Euglena* sp., were used to treat wastewater. After primary treatment (clarification) and secondary treatment (activated sludge process), the wastewater was sent to the

DM-CW, which acts as a tertiary treatment plant. For fixing microalgae, pebbles are used as mineral support. The microalgae immobilized with pebbles were sent to DM-CW. The naturally grown duckweeds were collected from water pond near the Mahdia sanitation company. The duckweeds were harvested in every 15 days by collecting between 50% and 70% of the surface of the basin.

After activated sludge treatment, secondary effluents were sent to a feeding tank of 1000 L capacity. The main part of the treatment system consisted of two back-to-back ponds with a continuous flow setup. The operating depth of each pond was 0.4 m, and the total surface area was 8.5 m². The DM-CW result showed that for all conditions, significant organic matters, nutrients, and microbial removal were achieved. The treated wastewater from the DM-CW can be reused for agricultural purposes. The study demonstrated that the DM-CW was efficient in removing organic matter, ammonia nitrogen, and phosphorous from wastewater.

12.6.2.4 Algal Biofilm Airlift Photobioreactor for Sewage Treatment

Tao et al. (2017) demonstrated a unique algal biofilm airlift photobioreactor (ABA-PBR) for microalgae cultivation and removal of nutrients from sewage. The microalgae *Chlorella vulgaris* was chosen for attached growth using sewage as the culture medium, and suspended solid carriers were used for algal biofilm cultivation with artificial light source. The suspended solid carriers were spread all over the reactor due to fluid flow during aeration of ABA-PBR. The potential of the system was assessed with regard to the production of algal biomass and lipid in addition to nutrient removal from sewage and also by comparing the ABA-PBR with a conventional photobioreactor (C-PBR).

The working volume of each reactor was 20.3 L. The reactors were operated under continuous mode by feeding nonstop filtered sewage water to the reactors and simultaneously withdrawing the same amount of algal culture from the reactor. The reactors were run continuously for 37 days. The nutrient reductions of nitrogen and phosphorous in ABA-PBR were 61.6% and 71.3%, respectively. The ABA-PBR in comparison to conventional photobioreactor (C-PBR) produces more biomass, lipid and removes more nutrients like N and P due to suspended solid carriers in the reactor.

12.6.2.5 Microalgae-Based Waste CO₂ Gas Treatment

Aslam et al. (2017) demonstrated that mixed culture of microalgae can be selected and habituated to grow with 100% flue gas from an unfiltered coal-fired power plant, which contains 11% CO₂. Two numbers of 4 MW coal-fired boilers located at Australian Country Choice (ACC) site in Cannon Hill, Queensland, Australia, were selected as the source of flue gas. The flue gas was collected directly through a pipe from the stack of the 4 MW coal-fired boilers by using an air pump and stored in a storage tank of 41.3 L volume and 10 kg/cm² pressure. From the storage tank, the flue gas was supplied to the photobioreactors. The system consists of 12 numbers of 30 L capacity photobioreactors made up of transparent polyethylene bags. Each photobioreactor contains 15 L culture and 15 L gas space. Bold basal medium

(BBM) was used with municipal water. In this outdoor experiment, sunlight was used for photosynthesis of microalgae.

Due to the presence of SO_x and NO_x in the flue gas, the adaptation of microalgae took a long time. Therefore, the supply of flue gas was gradually increased from 10% to 100%, and also buffering of phosphate was done at high concentration. *Desmodesmus* spp. was found as the dominant microalgae in the mixed culture. The above study demonstrates a proof of concept that mixed algal culture can gradually adapt to grow in 100% unfiltered flue gas. The desired CO₂ uptake can be obtained from flue gas by scaling up this system in various open ponds and photobioreactors.

12.7 Conclusions

The microalgae are photosynthetic organisms that grow autotrophically with inorganic forms of macronutrients and micronutrients to fulfil their modest growth requirements. They have high CO₂ fixing efficiency with high growth rate and accumulate macromolecules such as lipids (triglycerides), proteins, and carbohydrates in large amounts along with many high-value products including polyunsaturated fatty acids (PUFA), pigments like carotenoids and phycobiliproteins, and bioactive molecules in the biomass. All these components are useful either as nutraceuticals and pharmaceuticals or many other biotechnological applications like biofuel, biorefinery, etc. Microalgae may be effectively used for removal of nitrogen and phosphorus, hence considered suitable for wastewater treatment strategy. Algae have shown the potential with respect to uptake of carbon dioxide from flue gas, nitrogen, and heavy metal from wastewater, making them important in the future development with respect to wastewater treatment.

Acknowledgement The authors extend their thanks to Council of Scientific & Industrial Research (CSIR) and the Department of Science and Technology (DST), Government of India, for the financial support and the Director of the Institute of Minerals and Materials Technology (CSIR-IMMT) for providing the adequate laboratory facilities.

References

- Aishvarya V, Pradhan N, Nayak RR, Sukla LB, Mishra BK (2012) Enhanced inorganic carbon uptake by *Chlorella* sp. IMMTCC-2 under autotrophic conditions for lipid production and CO₂ sequestration. *J Appl Phycol* 24:1455–1463
- Aishvarya V, Jena J, Pradhan N, Panda PK, Sukla LB (2015) Microalgae: cultivation and application. In: Sukla L, Pradhan N, Panda S, Mishra B (eds) *Environmental microbial biotechnology*, Soil Biology, vol 45. Springer, pp 289–311
- Aslam A, Thomas-Hall SR, Aziz Mughal T, Schenk PM (2017) Selection and adaptation of microalgae to growth in 100% unfiltered coal-fired flue gas. *Bioresour Technol* 233:271–283
- Becker EW (1994) *Microalgae biotechnology and microbiology*. Cambridge University Press, New York 18 pp

- Bong CW, Malfatti F, Azam F, Obayashi Y, Suzuk S (2010) The effect of zinc exposure on the bacteria abundance and proteolytic activity in seawater. In: Hamamura N, Suzuki S, Mendo S, Barroso CM, Iwata H, Tanabe S (eds) Interdisciplinary studies on environmental chemistry—biological responses to contaminants. Terrapub, Tokyo, pp 57–63
- Borkenstein CG, Knoblochner J, Frühwirth H, Schagerl M (2011) Cultivation of *Chlorella emersonii* with flue gas derived from a cement plant. *J Appl Phycol* 23:131–135
- Bouali M, Zrafi L, Mouna F, Bakhrouf A (2012) Pilot study of constructed wetlands for tertiary wastewater treatment using duckweed and immobilized microalgae. *Afr J Microbiol Res* 6:6066–6074
- Brahmbhatt N, Patel R, Jasrai RT (2012) Bioremediation potential of *Spirogyra* sps and *Oscillatoria* sps for cadmium. *Adv Appl Sci Res* 2:102–107
- Brennan L, Owende P (2010) Biofuels from microalgae—a review of technologies for production, processing, and extractions of biofuels and co-products. *Renew Sust Energ Rev* 14:557–577
- Bruins MR, Kapil S, Oehme FW (2000) Microbial resistance to metals in the environment. *Ecotoxicol Environ Saf* 45:198–207
- Cai T, Park SY, Li Y (2013) Nutrient recovery from waste-water streams by microalgae: status and prospects. *Renew Sust Energ Rev* 19:360–369
- Campbell PK, Beer T, Batten D (2011) Life cycle assessment of biodiesel production from microalgae in ponds. *Bioresour Technol* 102:50–56
- Chelf P, Brown LM, Wyman CE (1993) Aquatic biomass resources and carbon dioxide trapping. *Biomass Bioenergy* 4:175–183
- Chen H, Pan S (2005) Bioremediation potential of *Spirulina*: toxicity and biosorption studies of lead. *J Zhejiang Univ Sci B* 6:171–174
- Chen M, Tang H, Ma H, Holland TC, Ng KY, Salley SO (2011) Effect of nutrients on growth and lipid accumulation in the green algae *Dunaliella tertiolecta*. *Bioresour Technol* 102:1649–1655
- Chisti Y (2007) Biodiesel from microalgae. *Biotechnol Adv* 25:294–306
- Chojnacka K (2010) Biosorption and bioaccumulation—the prospects for practical applications. *Environ Int* 36:299–307
- Chojnacka K, Chojnacki A, Górecka H (2004) Trace element removal by *Spirulina* sp. from copper smelter and refinery effluents. *Hydrometallurgy* 73:147–153
- Chojnacka K, Chojnacki A, Górecka H (2005) Biosorption of Cr^{3+} , Cd^{2+} and Cu^{2+} ions by blue-green algae *Spirulina* sp.: kinetics, equilibrium and the mechanism of the process. *Chemosphere* 59:75–84
- Craggs RJ, Heubeck S, Lundquist TJ, Benemann JR (2011) Algal biofuels from waste water treatment high rate algal ponds. *Water Sci Technol* 63:660–665
- Dahai TWH, Li PN, Miao X, Zhon J (2011) CO_2 biofixation and fatty acid composition of *Scenedesmus obliquus* and *Chlorella pyrenoidosa* in response to different CO_2 levels. *Bioresour Technol* 102:3071–3076
- Danielo O (2005) An algae-based fuel. *Biofuture* 255
- DeAlva MS, Luna-Pabello VM, Cadena E, Ortíz E (2013) Green microalga *Scenedesmus acutus* grown on municipal waste water to couple nutrient removal with lipid accumulation for biodiesel production. *Bioresour Technol* 146:744–748
- Douskova I, Doucha J, Livansky K, Machat J, Novak P, Umysova D, Zachleder V, Vitova M (2009) Simultaneous flue gas bioremediation and reduction of microalgal biomass production costs. *Appl Microbiol Biotechnol* 82:179–185
- Ge Y, Liu J, Tian G (2011) Growth characteristics of *Botryococcus braunii* 765 under high CO_2 concentration in photobioreactor. *Bioresour Technol* 102:130–134
- Gehl KA, Colman B, Sposato LM (1990) Mechanism of inorganic carbon uptake in *Chlorella saccharophila*: the lack of involvement of carbonic anhydrase. *J Exp Bot* 41:1385–1391
- Gilles S, Gerard L, Daniel C, Ngansoumana B, Carla IL, Jacob N, Allassane O, Ousséni O, Xavier L (2008) Mutualism between euryhaline tilapia, *Sarotherodon melanotheron heudelotii* and *Chlorella* sp.- implications for nano-algal production in warmwater phytoplankton-based recirculating systems. *Aquac Eng* 39:113–121

- Gonçalves AL, Pires JCM, Simões M (2017) A review on the use of microalgal consortia for wastewater treatment. *Algal Res* 24:403–415
- Henkanatte GSM, Selvaratnam T, Caskan N, Nirmalakhandan N, Voorhies Van W, Lammers JP (2015) Algal-based, single-step treatment of urban wastewaters. *Bioresour Technol* 189:273–278
- Hernández D, Riaño B, Coca M, García-González M (2013) Treatment of agro-industrial wastewater using microalgae-bacteria consortium combined with anaerobic digestion of the produced biomass. *Bioresour Technol* 135:598–603
- Hirata S, Hayashitani M, Taya M, Tone S (1996) Carbon dioxide fixation in batch culture of *Chlorella* sp. using a photobioreactor with a sunlight-collection device. *J Ferment Bioeng* 81:470–472
- Ho SH, Chen CY, Shu CJ (2012) Effect of light intensity and nitrogen starvation on CO₂ fixation and lipid/carbohydrate production of an indigenous microalga *Scenedesmus obliquus* CNW-N. *Bioresour Technol* 113:244–252
- Hsieh CH, Wu WT (2009) Cultivation of microalgae for oil production with a cultivation strategy for urea limitation. *Bioresour Technol* 100:3921–3926
- Hsueh HT, Li WJ, Chen HH, Chu H (2009) Carbon bio-fixation by photosynthesis of *Thermosynechococcus* sp. CL-1 and *Nannochloropsis oculata*. *J Photochem Photobiol* 95:33–39
- Hu Q, Sommerfeld M, Jarvis E, Ghirardi M, Posewitz M, Seibert M, Darzins A (2008) Microalgal triacylglycerols as feedstocks for biofuel production: perspectives and advances. *Plant J* 54:621–639
- Jena J, Pradhan N, Dash BP, Panda PK, Mishra BK (2014) Pigment mediated biogenic synthesis of silver nanoparticles using diatom *Amphora* sp. and its antimicrobial activity. *J Saudi Chem Soc* 19:661–666
- Jena J, Pradhan N, Aishvarya V, Nayak RR, Dash BP, Sukla LB, Panda PK, Mishra BK (2015) Biological sequestration of cadmium by microalgae *Scenedesmus* as CdS nanoparticles. *J Appl Phycol* 27:2251–2260
- Jia H, Yuan Q (2016) Removal of nitrogen from wastewater using microalgae and microalgae-bacteria consortia. *Cogent Environ Sci* 2:1275089
- Johnson MB, Wen Z (2010) Development of an attached microalgal growth system for biofuel production. *Appl Microbiol Biotechnol* 85:525–534
- Kaewkannetra P, Prayoon E, TzeYen C (2012) The effect of CO₂ and salinity on the cultivation of *Scenedesmus obliquus* for biodiesel production. *Biotechnol Bioprocess Eng* 17:591–597
- Karya N, van der Steen NP, Lens PNL (2013) Photooxygenation to support nitrification in an algal-bacterial consortium treating artificial wastewater. *Bioresour Technol* 134:244–250
- Khan SA, Rashmi Hussain MZ, Prasad S, Banerjee UC (2009) Prospects of biodiesel production from microalgae in India. *Renew Sust Energ Rev* 13:2361–2372
- Kirrolia A, Bishnoi NR, Singh R (2013) Microalgae as a boon for sustainable energy production and its future research & development aspects. *Renew Sust Energ Rev* 20:642–656
- Konopka A (1999) Microbial biomass and activity in lead-contaminated soil. *Appl Environ Microbiol* 65:2256–2259
- Kumar N, Cini O (2012) Removal of heavy metals by biosorption using fresh water alga *Spirogyra hyaline*. *J Environ Biol* 33:27–31
- Lavens P, Sorgeloos P (1996) Manual on the production and use of live food for aquaculture. FAO Tech Pap 361:295
- Lefebvre S, Hussenot J, Brossard N (1996) Water treatment of land-based fish farm effluents by outdoor culture of marine diatoms. *J Appl Phycol* 8:193–200
- Liang Z, Liu Y, Ge F, Xu Y, Tao N, Peng F, Wong M (2013) Efficiency assessment and pH effect in removing nitrogen and phosphorus by algae – bacteria combined system of *Chlorella vulgaris* and *Bacillus licheniformis*. *Chemosphere* 92:1383–1389
- Lin Q, Lin J (2011) Effects of nitrogen source and concentration on biomass and oil production of a *Scenedesmus rubescens* like microalga. *Bioresour Technol* 102:1615–1621

- Lin L, Chan G, Jiang B, Lan C (2007) Use of ammoniacal nitrogen tolerant microalgae in landfill leachate treatment. *Waste Manag* 27:1376–1382
- Liu ZY, Wang GC, Zhou BC (2008) Effect of iron on growth and lipid accumulation in *Chlorella vulgaris*. *Bioresour Technol* 99:4717–4722
- Madigan MT, Martinko JM, Parker J (1997) Brock biology of microorganisms, 8th edn. Prentice Hall, Upper Saddle River
- Mata TM, Martins AA, Caetano NS (2010) Microalgae for biodiesel production and other applications: a review. *Renew Sust Energy Rev* 14:217–232
- Michimasa K, Okakura T, Nagashima H, Minowa T, Yokoyama SY, Yamaberi K (1994) CO₂ fixation and oil production using microalgae. *J Ferment Bioeng* 78:479–482
- Morais MG, Costa JAV (2007) Carbon dioxide fixation by *Chlorella kessleri*, *C. vulgaris*, *Scenedesmus obliquus* and *Spirulina* sp. cultivated in flasks and vertical tubular photobioreactors. *Biotechnol Lett* 29:1349–1352
- Mouget JL, Dakhama A, Lavoie MC, Noüe J (1995) Algal growth enhancement by bacteria: is consumption of photosynthetic oxygen involved? *FEMS Microbiol Ecol* 18:35–43
- Murakami M, Ikenouchi M (1997) The biological CO₂ fixation and utilization project by RITE (2): screening and breeding of microalgae with high capability in fixing CO₂. *Energy Convers Manag* 38:493–497
- Mustafa EM, Phang SM, Chu WL (2012) Use of an algal consortium of five algae in the treatment of landfill leachate using the high-rate algal pond system. *J Appl Phycol* 24:953–963
- Mutanda T, Ramesh D, Karthikeyan S, Kumari S, Anandraj A, Bux F (2011) Bioprospecting for hyper-lipid producing microalgal strains for sustainable biofuel production. *Bioresour Technol* 102:57–70
- Nies DH (1999) Microbial heavy metal resistance. *Appl Microbiol Biotechnol* 51:730–750
- Norici A, Dalsass A, Giordano M (2002) Role of phospho-enolpyruvate carboxylase in anaplerosis in the green microalga *Dunaliella salina* cultured under different nitrogen regimes. *Physiol Plant* 116:186–191
- Novoveská L, Zapata AKM, Zabolotney JB, Atwood MC, Sundstrom ER (2016) Optimizing microalgae cultivation and wastewater treatment in large-scale offshore photobioreactors. *Algal Res* 18:86–94
- Pinto E, Sigaud-Kutner TCS, Leitao MAS, Okamoto OK, Morse D (2003) Heavy metal-induced oxidative stress in algae. *J Phycol* 39:1008–1018
- Pittman JK, Dean AP, Osundeko O (2011) The potential of sustainable algal biofuel production using wastewater resources. *Bioresour Technol* 102:17–25
- Posadas E, García-Encina PA, Soltau A, Domínguez A, Díaz I, Muñoz R (2013) Carbon and nutrient removal from centrates and domestic wastewater using algal–bacterial biofilm bioreactors. *Bioresour Technol* 139:50–58
- Prajapati SK, Kaushik P, Malik A, Vijay VK (2013) Phycoremediation coupled production of algal biomass, harvesting and anaerobic digestion: possibilities and challenges. *Biotechnol Adv* 31:1408–1425
- Pruvost J, Van Vooren G, Cogne G, Legrand J (2009) Investigation of biomass and lipids production with *Neochloris oleoabundans* in photobioreactor. *Bioresour Technol* 100:5988–5995
- Ramanan R, Kannan K, Deshkar A, Yadav R, Chakrabarti T (2010) Enhanced algal CO₂ sequestration through calcite deposition by *Chlorella* sp. and *Spirulina platensis* in a mini-raceway pond. *Bioresour Technol* 101:2616–2622
- RangaRao A, Sarada R, Ravishankar GA (2007) Influence of CO₂ on growth and hydrocarbon production in *Botryococcus braunii*. *J Microbiol Biotechnol* 17:414–419
- Richmond A, Hu Q (2013) Handbook of microalgal culture, applied phycology and biotechnology, 2nd edn. Wiley, Oxford
- Ruangsomboon S (2015) Effects of different media and nitrogen sources and levels on growth and lipid of green microalga *Botryococcus braunii* KMITL and its biodiesel properties based on fatty acid composition. *Bioresour Technol* 191:377–384

- Sag Y, Kutsal T (2001) Recent trends in the biosorption of heavy metals: a review. *Biotechnol Bioprocess Eng* 6:376–385
- Sforza E, Cipriani R, Morosinotto T, Bertucco A, Giacometti GM (2012) Excess CO₂ supply inhibits mixotrophic growth of *Chlorella protothecoides* and *Nannochloropsis salina*. *Bioresour Technol* 104:523–529
- Sheng YC, Kao CY, Tsai MT, Ong SC, Chen CH, Lin CS (2009) Lipid accumulation and CO₂ utilization of *Nannochloropsis oculata* in response to CO₂ aeration. *Bioresour Technol* 100:833–838
- Singh SP, Singh P (2014) Effect of CO₂ concentration on algal growth: a review. *Renew Sust Energ Rev* 38:172–179
- Smith RG, Bidwell RGS (1989) Mechanism of photosynthetic carbon dioxide uptake by the red macroalga, *Chondrus crispus*. *Plant Physiol* 89:93–99
- Spolaore P, Joannis-cassan C, Duran E, Isambert A (2006) Commercial applications of microalgae. *J Biosci Bioeng* 101:87–96
- Sydney EB, Sturm W, de Carvalho JC, Soccol VT, Larroche C, Pandey A, Soccol CR (2010) Potential carbon dioxide fixation by industrially important microalgae. *Bioresour Technol* 101:5892–5896
- Tao Q, Gao F, Qian CY, Guo XZ, Zheng Z, Yang ZH (2017) Enhanced biomass/biofuel production and nutrient removal in an algal biofilm airlift photobioreactor. *Algal Res* 21:9–15
- Tarlan E, Dilek FB, Yetis U (2002) Effectiveness of algae in the treatment of a wood based pulp and paper industry wastewater. *Bioresour Technol* 84:1–5
- Tukaj Z, Aksmann A (2007) Toxic effects of anthraquinone and phenanthrenequinone upon *Scenedesmus* strains (green algae) at low and elevated concentration of CO₂. *Chemosphere* 66:480–487
- Tukaj Z, Remisiewicz AB, Tadeusz S, Tuka C (2007) Cadmium effect on the growth, photosynthesis, ultrastructure and phytochelatin content of green microalga *Scenedesmus armatus*: a study at low and elevated CO₂ concentration. *Environ Exp Bot* 60:291–299
- Van Den Hende S, Vervaeren H, Boon N (2012) Flue gas compounds and microalgae: (bio-) chemical interactions leading to biotechnological opportunities. *Biotechnol Adv* 30:1405–1424
- Villegas GIR, Fiamengo M, Fernandez FGA, Grima EM (2017) Outdoor production of microalgae biomass at pilot-scale in seawater using centrate as the nutrient source. *Algal Res* 25:538–548
- Vonshak A (1990) Recent advances in microalgal biotechnology. *Biotechnol Adv* 8:709–727
- Vymazal J (1984) Short-term uptake of heavy metals by periphyton algae. *Hydrobiologia* 119:171–179
- Walter TL, Purton S, Becker DK, Collet C (2005) Microalgae as bioreactor. *Plant Cell Rep* 24:629–641
- Wan MX, Wang RM, Xia JL, Rosenberg JN, Nie ZY, Kobayashi N, Oyler GA, Betenbaugh MJ (2012) Physiological evaluation of a new *Chlorella sorokiniana* isolate for its biomass production and lipid accumulation in photoautotrophic and heterotrophic cultures. *Biotechnol Bioeng* 109:1958–1964
- Wang J, Chen C (2009) Biosorbents for heavy metals removal and their future. *Biotechnol Adv* 27:195–226
- Wojciech MB (2012) Negative carbon intensity of renewable energy technologies involving biomass or carbon dioxide as inputs. *Renew Sust Energ Rev* 16:6507–6521
- Wong PT, Chau YK, Luxon PL (1978) Toxicity of a mixture of metals on freshwater algae. *J Fish Res Board Can* 35:479–481
- Xu N, Zhang X, Fan X, Lijun H, Chengkui Z (2001) Effects of nitrogen source and concentration on growth rate and fatty acid composition of *Ellipsoidion* sp. (Eustigmatophyta). *J Appl Phycol* 13:463–469
- Yang J, Li X, Hu H, Zhang X, Yu Y, Chen Y (2011) Growth and lipid accumulation properties of a fresh water microalga, *Chlorella ellipsoidea* YJ1, in domestic secondary effluents. *Appl Energy* 88:3295–3299

-
- Yeh K, Chang JS, Chen W (2010) Effect of light supply and carbon source on cell growth and cellular composition of a newly isolated microalga *Chlorella vulgaris* ESP-31. *Eng Life Sci* 10:201–208
- Yun YS, Lee SB, Moon PJ, Lee C-II, Won YJ (1997) Carbon dioxide fixation by algal cultivation using wastewater nutrients. *J Chem Technol Biotechnol* 69:451–455
- Zamalloa C, Boon N, Verstraete W (2013) Decentralised two-stage sewage treatment by chemical – biological flocculation combined with microalgae biofilm for nutrient immobilization on a roof installed parallel plate reactor. *Bioresour Technol* 130:152–160



Current Advances and Applications of Fuel Cell Technologies **13**

Kaustav Saikia, Biraj Kumar Kakati, Bibha Boro, and Anil Verma

Abstract

Increasing energy demand and growing environmental concerns have driven the civilization towards cleaner energy-producing devices. Among the various clean energy devices, fuel cells have gained considerable attention due to their attractive features such as high efficiency, low or zero tail-end carbon emission, quiet operation, modular size, etc. The recent technological advances in the different components of the fuel cell are translated into new fuel cell devices and systems. The commercial application of fuel cells has been made feasible due to these technological advances. Research and development in the low-temperature fuel cells, particularly the polymer electrolyte fuel cell (PEFC), have been advanced more in comparison to the medium- and high-temperature fuel cells. The PEFC has been extensively tested in automobiles. The advent of the microbial fuel cell (MFC) and direct glucose fuel cell (DGFC) has added a new dimension to the low-temperature fuel cell technology. The more attractive application of MFC is often seen in the waste treatment and energy generation. Similarly, the fuel cells are also tested for unmanned machines, vehicles and space application. The medium- and high-temperature fuel cells are usually used as a stand-alone system. This chapter provides an overview of the technological advances and applications of the fuel cells.

Keywords

Catalyst · Contamination · Fuel cell · Membrane · Membrane electrode assembly · Oxygen reduction reaction

K. Saikia · B. K. Kakati · B. Boro
Department of Energy, Tezpur University, Tezpur, Assam, India

A. Verma (✉)
Department of Chemical Engineering, Indian Institute of Technology Delhi, New Delhi, India
e-mail: anilverma@iitd.ac.in

13.1 Introduction

In the twenty-first century, scarcity of energy, environmental pollution and rapidly decreasing fossil fuels are causing a major concern on energy demand-supply gap, which in turn threatens the energy security of the world (Yang et al. 2013; Liu et al. 2014). Fuel cell, which was invented back in the nineteenth century by Sir William Grove, is one of the most promising clean and green energy conversion devices. Fuel cells, particularly the polymer electrolyte fuel cells, have drawn much attention in terms of both fundamental research and applications due to its high efficiency, high energy density and low or zero carbon emission. In addition, the fuel cells are lighter, smaller and easier to implement on a larger scale (Carrette et al. 2000, 2001b; Yuan et al. 2015). Therefore, fuel cells may help to cut down our dependence on fossil fuels and produce clean and green energy.

Fuel cells are electrochemical devices that convert chemical energy in a fuel into electricity in presence of oxygen in the air. As this electrochemical process does not involve any combustion, it is more efficient and quieter than the equivalent-power generators. Moreover, it is also a clean technology because the by-products of the electrochemical reaction are only water and heat where pure hydrogen is fed to the cell as a fuel. Hence, the low chemical, thermal and carbon dioxide emissions of the fuel cells make it a very attractive technology for reducing the carbon emission intensity and may be an option for future energy generation (Acres 2001; Daud et al. 2017).

Since its first invention, work on fuel cell technology has been going up steadily. However, in the recent years, with increasing resources and development of technology, different types of fuel cells have been explored and developed. Fuel cells are usually classified depending on the electrolyte used in the cell and their operating temperature, i.e. low, medium and high temperature. Low-temperature fuel cells are microbial fuel cell (MFC), direct glucose fuel cell (DGFC), phosphoric acid fuel cell (PAFC), alkaline fuel cell (AFC), polymer electrolyte fuel cell (PEFC) and direct methanol fuel cell (DMFC). The fuel cells that work in a temperature range of 600–700 °C can be grouped as medium-temperature fuel cells such as molten carbonate fuel cell (MCFC) and direct carbon fuel cell (DCFC). Solid oxide fuel cell (SOFC) is a high-temperature fuel cell that works at temperature approximately 800–1000 °C (Okamoto et al. 2017; Ormerod 2003; Santoro et al. 2017; Li et al. 2010; Bagotsky 2012; Merle et al. 2011; Mehta and Cooper 2003; Hogarth and Hards 1996; Ong et al. 2017; Zhang et al. 2014; Belousov 2017). An overview of several types of fuel cell is given in Table 13.1.

13.2 Low-Temperature Fuel Cell

13.2.1 Microbial Fuel Cell

The concept of bioelectricity dates back to the eighteenth century, but the ideas of utilizing microorganisms to generate electricity were attributed to Potter (1911). Through the ages, numerous experimental and working biological fuel cells were

Table 13.1 Different types of fuel cells with different operating temperatures

Depending on temperature	Fuel cell type	Common electrolyte	Operating temperature (°C)	Application	References
Low temperature	Microbial fuel cell	Liquid electrolyte	15–45	Wastewater treatment, electricity production	Santoro et al. (2017) and Li et al. (2010)
	Direct glucose fuel cell	Glucose as fuel in aqueous electrolyte	25–40	Medical, power generation	Carrette et al. (2001b) and Bagotsky (2012)
	Phosphoric acid fuel cell	Phosphoric acid	150–200	Distributed power supply, cogeneration systems	Bagotsky (2012)
	Alkaline fuel cell	Potassium hydroxide	90–100	Portable power, backup power, space	Merle et al. (2011)
	Polymer electrolyte fuel cell	Solid polymer	50–100	Portable power, backup power, transportation, small distributed generation	Hogarth and Hards (1996) and Belousov (2017)
	Direct methanol fuel cell	Solid polymer	20–100	Portable power, power small appliances	Hogarth and Hards (1996) and Ong et al. (2017)
Medium temperature	Molten carbonate fuel cell	Alkali carbonate	600–800	Distributed supply, electric utility	Zhang et al. (2014) and Belousov (2017)
	Direct carbon fuel cell	Carbon-rich material	650–850	Electricity generation	Zhang et al. (2014)
High temperature	Solid oxide fuel cell	Ceramic/ solid oxides	500–1000	Distributed power supply, cogeneration systems	Okamoto et al. (2017) and Ormerod (2003)

invented. A biological fuel cell integrates the catalytic redox activity of a living organism with the abiotic electrochemical reactions and physics therein. Biological fuel cells can be categorized into two types, viz. enzymatic fuel cell (EFC) and microbial fuel cell (MFC). The EFC uses selective enzymes as a catalyst to perform redox reactions that produce current, while the MFC uses electroactive microbes to

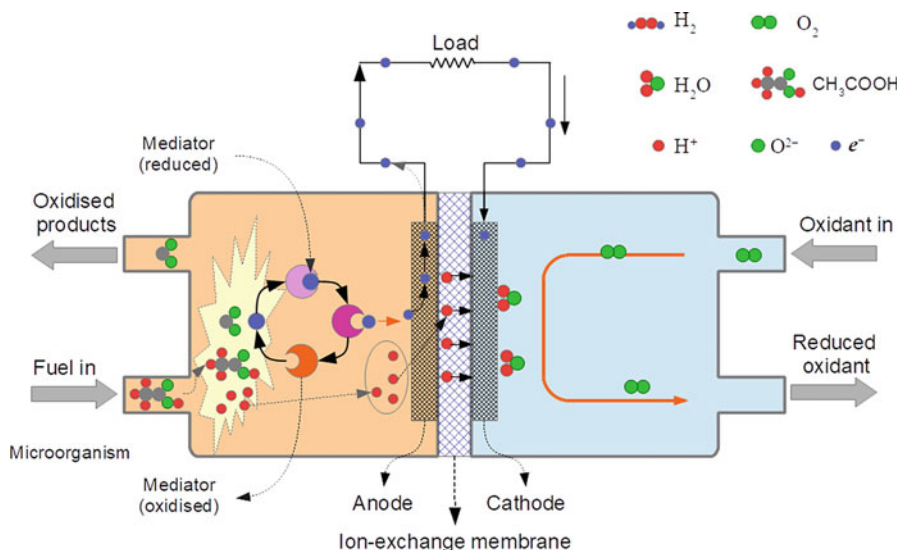


Fig. 13.1 Schematic of a microbial fuel cell and its operating principle

degrade the organic compounds to produce electricity (Santoro et al. 2017). The use of biotic electrocatalyst at the anode, near-ambient operating temperature in the range of 15–45 °C, neutral pH condition, use of complex biomass in the form of effluent as anodic fuel and its moderate environmental impact make the MFC stand apart from conventional low-temperature fuel cells (Borole et al. 2011; Larrosa-Guerrero et al. 2010; Tee et al. 2017; Tremouli et al. 2016; He et al. 2005; Kumar et al. 1998). The operating principle of MFC is shown in Fig. 13.1.

Over the time, many research works were performed to redefine the discovery of bioelectricity. After the initial attempts, some of the notable developments were observed in 1931 from Cohen's 35-unit setup (Cohen 1931). Since then, different catalyst investigations were carried in the 1960s and more in the 1980s and the 1990s (Sisler 1962; Ross et al. 1968; Zeikus 1979; Bennetto et al. 1985; Palmore et al. 1998). The development of the so-called analytical MFC was a result of Allen and Bennetto's research works, and the same design structure is still in use (Allen and Bennetto 1993). Several studies were carried out afterwards to enhance the overall output and the efficiency of electricity generation. Many researchers have tried modifying the structures of the inherent components like the electrodes as well as the solution or the fuel being used. In 2005, one such modification came in the form of enhancing the direct electron transfer mechanism by extracellular conductive connections called conductive pili or bacterial nanowires (Reguera et al. 2005).

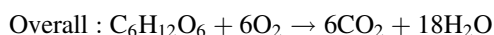
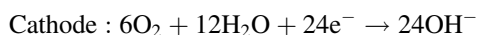
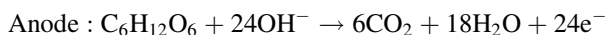
Among all the other bio-electrochemical systems that were being studied, one of the most interesting and well-investigated systems is the microbial electrolysis cell that also came in 2005 (Liu et al. 2005). The recent additions to bio-electrochemical

systems are seen to have co-generative and tri-generative purposes, and among them, the microbial desalination cells have been successfully developed with the objective of treating the wastewater, generating electricity and desalination simultaneously (Cao et al. 2009). The current research has been going on to prove the use of ceramics and clayware compounds as membranes and separators in MFCs (Winfield et al. 2013). Moreover, the current trend speaks of the utilization of air-breathing cathodes in MFCs (Ramachandran et al. 2015; Liu et al. 2011; You et al. 2011). They comprise of the electrode substrate, catalyst layer and an air diffusion layer. For the substrate mainly carbon-based materials are used due to their excellent conductivity and stability. The catalyst layer comprised of oxygen reduction reaction (ORR) catalyst matrix and binder. In case of the cathode, a catalyst is incorporated based on different techniques like spraying, doctor blade, drop casting, pressing and rolling. These types of cells achieve more power density due to their lower internal resistance. Over time, the studies took into consideration the incorporation of multiple chambers for enhancing the overall output and efficiency of the MFCs. In one recent research, the use of carbon nanotubes for replacing the already existing electrodes in MFC showed tremendous potential. They seem to exhibit a nature of being largely porous that allows easy colonization of electroactive bacteria. Additionally, the fibres displayed nano-structuration that promoted excellent growth and adhesion of the electroactive bacteria to the surface of the electrodes. The overall current density achieved by this process was actuated at 7.5 mA/cm^2 (Delord et al. 2017). In another study, a highly diversified community structure of bacteria was developed in a biocathode that can facilitate good cathodic reduction reactions in the MFCs. This study eased the Illumina pyrosequencing method for finding the diversified and novel population structure.

The discovery of graphene opens up a Pandora's box in different research areas. A study was done to propose a three-step method to prepare dual graphene modified bioelectrodes by in situ microbial-induced reduction of graphene oxide and polarity revision of the MFC. The results showed an increase in the coulombic efficiency up to 2.1 times and higher substrate oxidation rates (Chen et al. 2017a). In a similar study for application of bioelectrodes, graphene was used for modifying the electrodes. The results showed a shift of the bacterial community based on the polarity of the graphene-enhanced electrodes. The bioelectrodes tended to decrease the bacterial diversity and enriched the dominant species. The overall power density increased and transfer resistance decreased (Chen et al. 2017b). Zhang et al. (2012) used graphite fibre brushes as cathodes in a dairy manure fed MFC. They claimed to achieve higher open-circuit voltage (OCV) and lower internal resistance using their developed MFC. Attempt to control the cathodic biofilm in MFCs was also carried out by Li et al. (2017) to monitor the stratification structure therein using the freezing microtome method on a single chambered MFC. They use maltodextrin as a cathode substrate and managed to achieve higher bacterial viability. Recently, the MFC has got immense exposure due to its dual functions as energy generation from waste and waste treatment.

13.2.2 Direct Glucose Fuel Cell

The most abundant six-carbon glucose is estimated to be capable of releasing almost 2.87 MJ/mol of energy on complete oxidation to CO₂ via a 24-electron transfer reaction (Rapoport et al. 2012). The corresponding electrochemical reactions and the theoretical cell voltage of a direct glucose fuel cell (GFC) can be given as follows:



$$\Delta G_0 = -2.87 \times 10^6 \text{ J mol}^{-1}; \Delta E_0 = 1.24 \text{ V}$$

However, in practice, the electro-oxidation of glucose does not undergo via transfer of 24 electrons per molecule glucose. Usually, it undergoes a two-electron transfer process and converted to gluconic acid or gluconolactone depending upon the media and the pH used (Rao et al. 1976). The mechanism behind the electro-oxidation of glucose in this field is still a hot area of research.

The rise in the interest for studying GFC is credited to glucose being easily available, cheap, non-toxic and a safe biofuel that is easy to store without any explosion hazard. But there are some problems associated with the development GFC at a rapid pace, such as:

1. High cost and scarcity of noble metal catalysts
2. Incomplete or partial oxidation of the fuel
3. Contamination of the metal catalyst by the products of carbohydrate oxidation

Keeping these problems as well as the future prospects and advantages of using a glucose as a fuel in mind, many developments in the GFC have been observed over the recent years. Basu and Basu (2010) used voltammetry in an alkaline medium to study the electro-oxidation of glucose and fructose on PtRu/C catalyst. They observed that the deactivation of GFC is due to the poor mass transport at higher glucose concentrations, higher rate of conversions of glucose to fructose at higher glucose concentrations and degradation of glucose at a temperature above 40 °C. They also reported that catalyst poisoning during oxidation of glucose is also responsible for the deactivation of GFC. In a later study, they switched to carbon-supported platinum-gold catalyst (Pt-Au/C) to minimize the catalyst poisoning in the GFC (Basu and Basu 2011a). It was reported that the catalyst was capable of electro-oxidation of glucose at a lower potential and thus minimized the poisoning effect. They could achieve a peak power density of 0.72 mW/cm² with 0.2 M of glucose in 1 M KOH solution. The same group carried out similar studies by synthesizing carbon-supported bimetallic platinum-bismuth (Pt-Bi/C) and platinum-palladium (Pt-Pd/C) and trimetallic platinum-palladium-gold (Pt-Pd-Au/C) catalysts (Basu and Basu 2011b, 2012).

In yet another study, a direct GFC was developed using anion exchange membrane and electrodes made of Ag/Ni foam (Chen et al. 2012). The researcher claimed to achieve a peak power density of 2.03 mW/cm at around 80 °C with their direct GFC using the membrane and catalyst. They reported that the high performance of their DGFC was attributed to the enhanced kinetics of both the glucose oxidation and oxygen reduction reaction at higher operating temperature followed by better electrocatalytic activity of Ag/Ni foam. Moreover, the transformation of glucose to enediol also contributed to the enhanced performance of the direct GFC. Later, Li et al. (2013) synthesized MnO₂-carbon supported on a gold catalyst for oxidation of glucose and reported a peak power density of 1.1 mW/cm² at 30 °C in a direct GFC. A development for the performance enhancement of direct GFC can be seen as the structural modification of the electrodes. An attempt was made to design the anion exchange membrane direct GFC anodes by altering the composition of both the microporous layer and catalyst. They reported that electrodes produced by catalyst diffusion medium method exhibited better performance in comparison to catalyst-coated membrane. This may be attributed to better mass transport in the electrodes (Song et al. 2014). The effort to increase the power of a DGFC was also carried out by adding multiple chambers (Yang et al. 2015). A cheap anion exchange membrane was used along with methyl viologen and nickel foam electrocatalyst. Glucose oxidation reaction occurred at the nickel foam anode in an alkaline electrolyte in presence of methyl viologen. They reported a maximum power density of 5.20 W/m² at 15 mM methyl viologen, 3 M KOH and 1 M glucose at 25°. It was also claimed that the performance of the GFC could be further improved by increasing both the operating temperature and concentration of methyl viologen.

In another development, glucose oxidase enzyme supported on multiwalled carbon nanotube was used as a bio-anode (Escalona-Villalpando et al. 2016). Glucose oxidation experiments were performed in presence of glutaraldehyde, and cell performance was evaluated in an exposed-abiotic cathode GFC. They claimed an OCV of 0.72 V and a maximum power density of the 6.10 W/m² with their GFC. Tsang and Leung (2017) expressed concern over the electrocatalyst fabrication method for direct GFC. They claimed that the use of stabilizer like binder may deteriorate the catalytic activity of the electrocatalyst. It was proposed that a binder-free electrocatalytic electrode might be a solution to this problem. The authors used a nickel foam plate to deposit a binder-free bimetallic Pd-Pt-loaded graphene aerogel catalyst and claimed to achieve a maximum power density of 1.25 mW/cm² which is recorded with 0.5 M glucose/3 M KOH as the anodic fuel and Pd₁Pt_{0.98}-loaded graphene aerogel on nickel foam as the catalyst. They also claimed it to be the highest obtained maximum power density of a direct GFC among other types of the electrocatalyst.

13.2.3 Phosphoric Acid Fuel Cell

Phosphoric acid fuel cells (PAFCs) are one of the oldest fuel cell technologies that has been used commercially for several decades since 1967 when commercial PAFC

was developed in the US target plan (Sammes et al. 2004). Elmore and Tanner (1961) first discovered the use of phosphoric acid as an electrolyte in the fuel cell. The PAFC consists of two polytetrafluoroethylene-treated porous carbon electrodes coated with Pt catalyst, between which a phosphoric acid-impregnated SiC matrix is placed. The operating temperature of a PAFC is about 150–210 °C. The performance of the PAFC increases with the increase in operating temperature. However, it accelerates catalyst sintering and dissolution, component corrosion, followed by electrolyte degradation and evaporation. A major fuel cell company UTC Power recommends operating its PAFC at 207 °C to achieve a reasonable performance for a duration of 40,000 h (Okumura 2013). The components of a PAFC and its basic operating principle are shown in Fig. 13.2. The catalyst dissolution, corrosion of components, electrolyte dilution and evaporation are hindering the commercialization of PAFC even though its durability, performance and cost are improved significantly.

The dissolution, dislocation, agglomeration and corrosion of Pt catalyst in phosphoric acid and in a PAFC have been studied by various researchers (Bindra et al. 1979; Honji et al. 1988; Aragane et al. 1988). Bindra et al. (1979) used a gravimetric method to estimate the dissolution rate of a plain Pt electrode immersed in 96% H_3PO_4 at 176 °C and 196 °C in an operating voltage range of 0.8–1.0 V vs RHE (Reversible Hydrogen Electrode). They claimed that agglomeration or formation of large crystallites Pt is more prominent than the loss of Pt at a potential above 0.8 V vs RHE. However, at potentials below 0.75 V vs RHE, where the PAFC cathodes operate, the dissolution of Pt may dominate. The change of Pt particle distribution in the catalyst layer and its agglomeration were studied later by Aragane et al. (1988) and Honji et al. (1988).

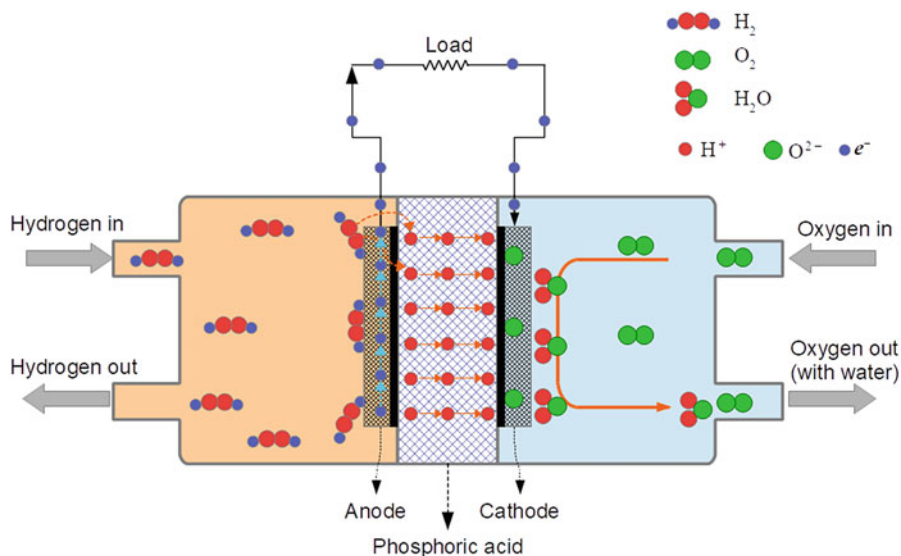


Fig. 13.2 Basic components and operating principle of a PAFC

Aragane et al. (1988) used electron probe microanalyser to study the dissolution of Pt from a working PAFC. They claimed that the dissolution of Pt from the cathode was associated with the migration of Pt to the anode. Their TEM analyses also proved that Pt particle coalescence was also involved in the process. The mechanism behind drying and dilution of PAFC was studied by Paul et al. (2014). Researchers have claimed to enhance the electrocatalytic activity of Pt by alloying it with different transition and non-transition metals. Watanabe et al. (1994) synthesized ordered and disordered Pt-Co alloy catalysts for PAFC system to study their catalytic activity in ORR (oxygen reduction reaction) and a proposed mechanism for corrosion and catalytic activity degradation under cathodic condition. They claimed to achieve 1.35 times catalytic activity with the ordered Pt-Co alloy catalyst in comparison to disordered one. However, the ordered Pt-Co catalyst lost its catalytic activity rapidly due to its higher degradation in PAFC environment as compared to the disordered Pt-Co catalyst. In the long run, they proposed that the disordered Pt-Co catalyst is preferable for better durability and stable long-term electrocatalytic activity.

The success of the phosphoric acid as a fuel cell electrolyte was credited to the designing of a variant for the molecular acid that provides increased temperature range. This was done without any sacrifice of high-temperature conductivity or open-circuit voltage. The result was achieved by the introduction of a hybrid component that is based on silicon coordination of phosphate groups. This prevents decomposition or water loss to 250 °C while enhancing free proton motion. However, careful monitoring of fuel consumption is a must (Ansari et al. 2013).

Attempts to improve the overall efficiency of a PAFC have been made by recovering waste heat (Chen et al. 2015). Chen et al. (2015) proposed and studied the hybridization of a PAFC with thermoelectric generators (TG). The authors reported a PAFC-TG hybrid model system taking into account the effects of irreversibilities due to the activation loss, concentration loss and ohmic loss in the PAFC. They also considered the irreversibilities due to the ohmic heat and thermal leak in the TG coupled with the poor heat transfer between the TG and the reservoir. The operating region in the polarization where the power density of the hybrid system is higher than the power density of a single PAFC was determined, and they proposed that hybridization might improve the maximum power density by 150 W/m². In another similar attempt, Yang et al. (2016a) designed a hybrid system integrating an absorption refrigerator and a PAFC in order to recover the waste heat. They optimized the operating current density for effective cooling and calculated the maximum power density and respective efficiency. Upon hybridization, they reported an increase of 2.6% and 3% in the maximum power density and corresponding efficiency, respectively.

13.2.4 Alkaline Fuel Cell (AFC)

As shown in Fig. 13.3, the structural design of an alkaline fuel cell (AFC) is similar to that of a PAFC. However, instead of H₃PO₄, AFC uses potassium hydroxide

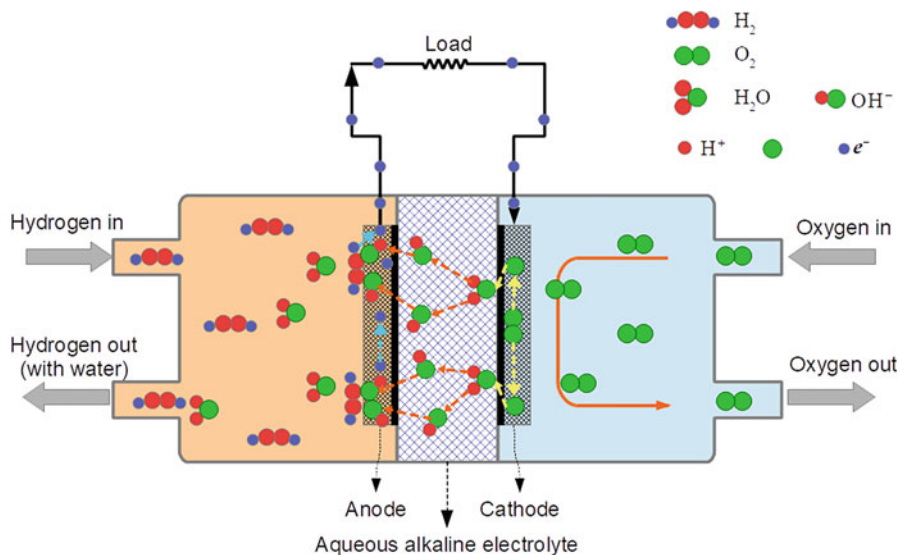


Fig. 13.3 Schematic of an AFC and its components

(KOH) solution as an electrolyte and operates on pure hydrogen and oxygen at an elevated temperature of 150–200 °C. The hydroxyl ions OH⁻ in the KOH migrate from the cathode side to the anode side of an AFC and react with the hydrogen to produce water and release electrons. The electrons generated at the anode power an external circuit and flow back to the cathode. These electrons react with the oxygen in presence of water to produce more OH⁻ ions. The efficiency of an AFC may be as high as 70%, and because they produced potable water, they have been widely used in early space missions. However, AFC requires very pure hydrogen and oxygen, or else an unwanted chemical reaction of KOH with CO_x may form solid carbonate that degrades the performance of the cell. It reduces the number of OH⁻ ions available and therefore reduces the ionic conductivity of the electrolyte solution. Effective electrolyte management can mitigate this solution. Therefore, the AFCs are usually equipped with a ‘scrubber’ to reduce the CO_x content in the fuel and air as much as possible (McBreen et al. 1979; McLean et al. 2002).

Another setback has been the requirement of large amount of Pt catalyst to speed up the sluggish ORR. The amount of Pt required may be minimized by increasing the catalytically active surface area, and hence the catalytic activity, improving the electrode structure, and replacing with a Pt-alloy catalyst instead of pure Pt (Stonehart 1990). A novel idea of providing a three-dimensional electrode for the fuel cell has been into consideration for quite some time (Simonsson 1997). The use of fluidized bed electrode structure, in which a bed of electrode particles mixed with liquid electrolyte, is subjected to reactant gas flowing through the bed. A coarse membrane is used to separate the anode and the cathode reactions, and the electrodes are inserted into the fluidized beds in order to gather the current. Development in the

selection of materials for the electrodes showed significant advancement in the overall performance of AFCs. The baseline performance of Ni as electrodes was initially proposed by Al-Saleh et al. (1994) and Swette and Giner (1988). Later, copper was used to impregnate into the nickel electrode to reduce the contact resistance of the electrode (Al-Saleh et al. 1996). Attempts were also made to impregnate aluminium and tin in Ni electrode and claimed to reduce the hydrogen overpotential (Tanaka et al. 2000).

The fabrication process of the electrodes also influences the performance of the fuel cell. In general, the electrodes are manufactured by wet fabrication method, followed by sintering. In dry fabrication methods, electrodes are fabricated by rolling and pressing different components into the electrode structure. In all the cases, the results have shown that the electrodes consist of the required two layers of hydrophobic and catalysed layer. Other improved electrode manufacturing methods include composite electrode making with carbon fibres pressed into a metal backing (Ahn and Tatarchuk 1997). Also, use of oxygen plasma treatment to increase the surface area of carbon black on a metallic substrate was reported (Li and Horita 2000). A filtration method combining the best features of wet and dry fabrication was used in a study, and the results showed performance of 180 mA/cm^2 current density (Al-Saleh et al. 1997). Similarly, research was also done to look for alternative membrane compositions for application in AFC. It was reported by Kim et al. (2017a) that the water uptake, swelling ratio, anion conductivity and ion-exchange capacity (IEC) of a pyridinium-functionalized poly(arylene ether ketone) membrane increased with increase in pyridinium content. Their composite membrane showed better IEC and anion conductivity in comparison to that of values that were higher than those of a commercial anion exchange membrane. Iravaninia et al. (2017) developed an anion exchange membrane for AFC using functionalized polysulphone. They functionalized polysulphone with trimethylamine and *N,N,N',N'*-tetramethyl-1-6-hexanediamine by chloromethylation, amination and alkalization. The synthesized membranes showed a through-plane ionic conductivity of $2\text{--}42 \text{ mS/cm}$ at $25\text{--}80 \text{ }^\circ\text{C}$, with acceptable water uptake and swelling ratio. A maximum power density of 110 mW/cm^2 at the current density of 195 mA/cm^2 was achieved by an AFC using the synthesized membrane.

A type of the alkaline fuel cell is the alkaline aluminium-air fuel cell. However, the main issue associated with these types of cells is the severe parasitic corrosion of aluminium anode. This significantly restricts the application of aluminium as an electrode material. Addition of inhibitors in the electrolyte is a remedial measure to reduce the corrosion rate of aluminium anode. In a study Na_2SnO_3 and casein was proposed as the hybrid inhibitor in an alkaline aluminium-air fuel cell (Nie et al. 2017). The use of macroalgae in an AFC was also explored by using a saccharified macroalgae. A type of alkaline fuel cell with no precious metal catalyst was developed by Liu et al. (2016a, b) for direct power generation using macroalgae *Enteromorpha prolifera* (Liu et al. 2016b). They claimed to achieve a maximum power density of 3.81 W/m^2 for their optimum condition, which was higher than any other algae-fed fuel cell. Similar studies were performed earlier to develop a

refuelable glucose AFC (Liu et al. 2016c). Activated carbon-nickel foam, immobilized with methyl viologen, was used as the anode. The peak power density was achieved around to 23.6 W/m^2 at room temperature, which is superior to a similar AFC with the non-immobilized anode.

13.2.5 Polymer Electrolyte Fuel Cell (PEFC)

The key components of a PEFC are shown in Fig. 13.4. The use of cation exchange membrane made of the solid polymer electrolyte is the major difference of this cell with that of a PAFC or an AFC. Like all other fuel cells, the catalyst layer is the heart of any PEFC system. The higher ionic conductivity of electrolyte membrane, excellent electrocatalytic activity of Pt in PEFC environment, low operating temperature, high efficiency, rapid start-up and rugged design help PEFC to be a centre of attraction in this field. However, the scarcity and cost of Pt hinder the commercial feasibility of PEFC. Researchers are attempting to reduce the amount of Pt required for catalyst development without compromising the performance of the PEFC (Brankovic et al. 2001; Wilson and Gottesfeld 1992; Qi and Kaufman 2003; Passalacqua et al. 1998; Esmailifar et al. 2010; Ticianelli et al. 1988; Xiong and Manthiram 2005; Cooper et al. 2017).

One of the most important issues that need to be addressed for successful commercialization of PEFCs is the long-term performance of the carbon-supported catalysts. Normally the cathode catalyst layer contains Pt-group metal/alloy nanoparticles supported on high surface area carbon. However, the corrosion of

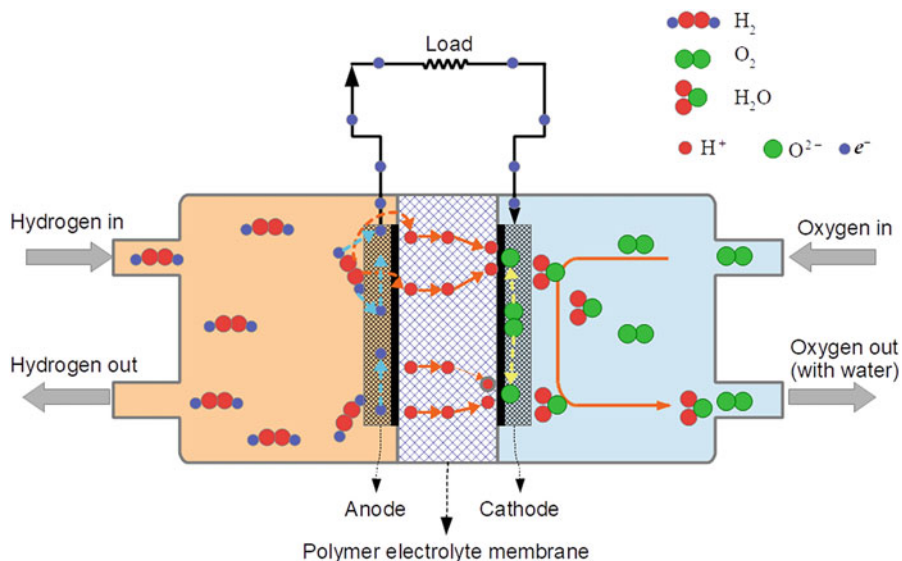


Fig. 13.4 Schematic of a PEFC showing different components along with its operating principle

the carbon supports and dissolution Pt on the harsh cathode environment result in degradation of the performance of the fuel cell. The promising strategies in order to improve the durability of Pt/C catalyst are most likely by building proper surface functional groups or by increasing the basic sites on carbon supports to improve interaction, increasing surface stability of carbon support and finally preparing catalyst with high platinum uniformity and low platinum loading (Yu and Ye 2007a, b). In some studies, ternary or even quaternary catalysts were also synthesized for PEFC application (Götz and Wendt 1998; Seo et al. 2006; Baranton et al. 2015; Sánchez et al. 2016). Sanchez et al. (2016) synthesized quaternary catalysts for ethanol electro-oxidation and for PEFCs. One goal of this study was to check the suitability of iron as a cocatalyst for the electro-oxidation of ethanol. The iron-based alloys that were studied were of compositions: $\text{Ni}_{59}\text{Nb}_{40}\text{Pt}_{0.6}\text{Fe}_{0.4}$ and $\text{Ni}_{59}\text{Nb}_{39}\text{Pt}_1\text{Fe}_1$. The anode electrocatalysts that was based on iron showed better polarization and power values than the rhodium-based ones and the palladium-based ones.

Conventionally the multifunctional bipolar plates or flow field plates of a PEFC are made of either metal or graphite. However, both the metallic and graphitic bipolar plates have their own disadvantages. Due to their high mechanical strength and flexibility, one very likely substitute for the brittle graphite bipolar plate is the carbon fibre, carbon black and graphene-reinforced polymer composites (Oh et al. 2004; Besmann et al. 2000; Kakati et al. 2011). In another study, a randomly oriented non-woven carbon felt and a cyanate ester-modified epoxy were used, and better results were obtained in comparison to traditional cells (Lee and Lim 2017). While it comes to the metallic bipolar plates, one of the popular trends is to adopt cheap metals such as stainless steel and titanium due to its inherent corrosion resistance. However, the naturally occurred corrosion layer in a stainless steel reduces the surface conductivity of the bipolar plate. Different anticorrosion coatings are applied in metallic bipolar plates in order to decrease the contact resistance and to improve its corrosion resistance of metallic bipolar plates (Woodman et al. 1999; Lee et al. 2003; Cho et al. 2005; Yoon et al. 2008; Dundar et al. 2010; Kahraman et al. 2016). Asri et al. (2017) reviewed the coatings of stainless steel and titanium bipolar plates for high-temperature PEFC (HT-PEFC) application. They emphasized that the vapour deposition method is suitable for coating metallic bipolar plates. This method is suitable for producing HT-PEFC-compatible bipolar plate with excellent impact strength and abrasion resistance.

Several modifications are made to the concept for which the results showed reduced catalyst loading, increased power density, improved durability and even usage in prototype PEFC vehicles. Among all other benefits of the PEFC, the HT-PEFC has overwhelming advantages such as improved cathode kinetics, increased current densities, improved tolerance of the catalyst to CO, improved water management and gas transportation, etc. However, the HT-PEFC has some disadvantages as well. At high temperature, the PEFC suffers material degradation, mechanical failures, electrode degradation and lower membrane conductivity (Liu et al. 2006). Several attempts have been made to develop membrane suitable for HT-PEFC

(Lobato et al. 2006, 2007; Li et al. 2008, 2009). Among different high-temperature compatible membranes, polybenzimidazole (PBI) and its composites are found to be a most suitable HT-PEFC application.

Attempts were also made to improve the system level efficiency by improving water management, improving temperature control, increasing fuel tolerance and rejuvenating contaminated fuel cells (Carrette et al. 2001a; Mirza 2011; Im 2015; Strahl et al. 2014; Kakati and Kucernak 2014; Kakati et al. 2016a, b). The water and thermal management issues are studied by various researchers (Fuller and Newman 1993; Yu et al. 2005; Bao et al. 2006; Weber and Newman 2006; Reddy and Jayanti 2012; Asghari et al. 2011; Lu et al. 2011; Reiser and Sawyer 1988). In many cases of water management, the focus is given widely on the configuration of flow channels and hydrophobicity of catalyst layers. Some researchers have also suggested using porous separator plate between two adjacent cells in a stack.

Wang et al. (2017a, b) demonstrate the same technique by introducing a porous hydrophilic water transport plate as a bipolar plate in a PEFC. They claimed that the humidification and drainage of water from the porous plate significantly helped in improving the performance of the PEFC in comparison to a cell with solid bipolar plates (Wang et al. 2017b). Moreover, the humidification and water drainage functions of the porous plate can be altered by decreasing the air stoichiometry without changing the hydrogen stoichiometry.

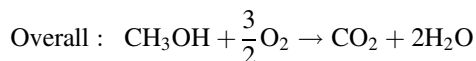
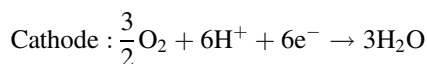
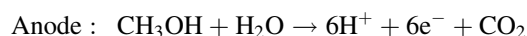
Water percolates down from the cathode side to the anode side and gets evaporated there to perform cooling of the stacks (Reiser and Sawyer 1988). The effects of different contaminants on the performance of PEFC have been studied widely in recent past (Dhar et al. 1986; Ross 1985; Chu et al. 2006; Mohtadi et al. 2003; Halseid et al. 2006; Uribe et al. 2002). However, most of the researchers have studied effects of CO and H₂S as potential contaminants for the anodes of PEFC. Few researchers have also studied the air side contamination of PEFC by air pollutants, such as SO_x, NO_x, NH₃, etc. (Shi et al. 2009; Jing et al. 2007; Li et al. 2011; Liu 2013). However, only a few researchers have worked on the removal of contaminants from fuel cell catalyst layer and rejuvenation of the contaminants (Chabot et al. 1988; Oh and Sinkevitch 1993; Mukerjee et al. 1999; Gottesfeld 1990). Among them, air/O₂ bleeding and potential cycling of the contaminated electrode are two widely tested techniques for removal of contaminants. However, both the techniques are not adequate to get rid of some strong contaminants such as H₂S, NH₃, etc. (Kakati et al. 2016b; Kakati and Kucernak 2014) used in gas phase chemical recovery of H₂S and SO₂ contaminated PEFC by using O₃ gas as a cleaning agent. They successfully rejuvenated a unit cell and a five-cell stack which were contaminated earlier with H₂S and SO₂.

The modelling of PEFC has been studied extensively by different researchers on various aspects. A thermodynamic model of the PEFC system was obtained in an attempt. The system comprised of the PEFC stack along with heat exchanger, water tank, cooling pumps as well as the humidifier and compressors. Then a novel multi-objective algorithm was developed that was based on decomposition and optimization of the operating parameters. The final optimal energy efficiency obtained was 79% and the output power was 8.04 kW (Chen et al. 2017c). Sohn et al. (2017)

performed similarly optimized the oxygen diffusion in the cathode catalyst layer by numerically generating two cathode catalyst layers. It was based on the agglomerate models to examine the experimental results obtained for two membrane electrode assembly samples with different properties. This was done because the diffusion of oxygen in the cathode layer of the cell is very crucial to ensure high performance of the PEFC. This is especially in higher current densities including the concentration loss regions (Chen and Huang 2017). However, the difficulties of handling gaseous hydrogen have shifted the focus from PEFC to DMFC.

13.2.6 Direct Methanol Fuel Cell

DMFC is one of the ideal fuel cells. DMFC produces electricity by the direct conversion of the methanol fuel at the cell anode. This concept is more attractive than the conventional hydrogen fuel cells particularly for transportation applications, which relies on bulky and often unresponsive reformer system that converts methanol or any other hydrocarbon fuels to hydrogen. However, the commercialization of the technology is effected by the inferior performance of the cell in comparison to a hydrogen-air-operated PEFC. The major limitation is anode performance that requires highly efficient methanol oxidation catalysts (Hogarth and Hards 1996):



$$\Delta G_0 = -698.2 \times 10^3 \text{ J mol}^{-1}; \Delta E_0 = 1.21 \text{ V}$$

The performance of the DMFC can be improved by using high methanol concentration. However, the methanol crossover causes a mixed potential at the Pt cathode catalyst thereby reducing the overall cell efficiency. In a study, carbon-supported 30% Pd-based catalyst was prepared by the sulphite complex route and physico-chemically characterized by X-ray diffraction (XRD), transmission electron microscopy (TEM), energy-dispersive X-ray spectroscopy (EDX) and X-ray photoelectron spectroscopy (XPS) methods. The results showed that Pd and Pd-Co alloy-based electrocatalysts exhibit high methanol tolerance properties that lead to single cell performance enhancement (Vecchio et al. 2018). Despite not requiring a separate hydrogen generation system, the limiting factor for the cost-effective performance of the system is the catalytic activity of the electrodes and in particular the anode. The single most active anode material available is platinum. It is usually dispersed on a high surface area carbon support, and it is found that that addition of small amounts

of metals like lead, rhenium and tin to the platinum can produce a significant increase in activity. The best is a mixture of platinum and ruthenium (Cameron et al. 1987).

For enhancing the discharge performance and perfecting the activation mechanism of a DMFC, a gradient activation method was proposed initially. This method consisted of four steps: proton activation, activity recovery activation, H₂-O₂ mode activation and forced discharging activation. The result of the proposed study proved that the proposed gradient method has realized replenishment of water and protons, recovery of catalytic activity of the catalyst and establishment of transfer in turn. The overall discharge performance was improved to more than 1.9 times higher than that of the original, under 7.5 h (Liu et al. 2017a). The CO₂ emergence from the anode outlet in DMFC should be efficiently discharged, or else it will choke the channels. The CO₂ behaviour inside the anode of a DMFC was studied by using the volume of the fluid method by tracking at the gas-liquid interface. It was found that firstly the CO₂ bubbles emerge near the outlet of the anode and gradually accumulate separately under the rib inside the gas diffusion layer (GDL). In case of the emergence of CO₂ in the flow channels, they expand and merge into the gas slugs (Kang et al. 2017).

In order to enhance the under rib reactant mass transport, a new serpentine flow field design of DMFCs has been developed. This is done without affecting the electronic conductivity to boost up the fuel utilization and to increase the fuel efficiency. The main criteria that the floor design is based on include the number of paths, the length of the ribs as well as the flow path patterning the channels (El-Zoheiry et al. 2017). For the replacement of cathode materials with other cost-effective materials, the study was done to test non-precious metal catalysts like Fe/Co-N-C. Nanosized graphene-derived Fe/Co-N-C catalyst was tested and found that it is capable of tolerating a highly concentrated methanol feed up to 10 M and the power density was 32 mW/cm² (Park and Choi 2017). In another study, a high-performance DMFC was developed with thin electrolyte membrane. The power density was 320 mW/cm² at peak. The study also revealed that the increased anode half-cell performance with temperature contributes primarily to the enhanced results at the elevated temperatures (Wan 2017). In another research, a simple hot-mould-modifying method was introduced in order to lower the methanol crossover and the volume swelling degree. The results of the research showed that when compared to the normal membrane, the modified Nafion membrane with regular spindle-type groove array seems to possess higher proton conductivity and higher methanol diffusion resistance with 31.9% better dimensional stability. It was due to its larger electrical double-layer capacitance coming from the higher contact area between electron-electrode and ion electrolyte and more compact internal structure (Wang et al. 2017a).

In a study to replace platinum with phthalocyanine/carbon-tungsten oxide nanowires, it was seen that it had similar characteristics to platinum. This was done because platinum was expensive and it reduces the active sites for the oxygen reduction reaction (Karim et al. 2017). For the high concentration operations, large methanol concentration gradient across the transport path from the fuel reservoir to the catalyst layer is required. The path includes the fuel reservoir, current collector

and interface, backing layer and the microporous layer. The performance test by lowering the porosity using nanosized carbon powder was done and showed the use of high concentration fuel up to 10.0 M without increasing methanol crossover rate (Yan et al. 2017).

In another study, an ultrasound atomization-based fuel supply system was proposed for methanol crossover alleviation. When compared to the traditional liquid feed cell, it was found that the new proposed system significantly reduces the crossover as the DMFC reaches a large stable OCV. In addition, the polarization performance does not differ much. With a supply of high concentration methanol of 4–8 M, the peak power density reached was 6.05–12.94% higher than liquid-fed systems (Wu et al. 2017).

13.3 Medium-Temperature Fuel Cell

13.3.1 Molten Carbonate Fuel Cell

The molten carbonate fuel cell (MCFC) is a unique fuel cell that uses molten carbonate salts of alkali metals as electrolyte and operates at around 650 °C. The device has generated more power commercially than any other fuel cell before 2016 (Cassir et al. 1996). However, the CO_3^{2-} ions in the electrolyte are consumed in the anode reactions and require replenishment of it by injecting CO_2 at the cathode. However, this CO_2 can be recycled after consumption at the cathode side electrochemical reaction, and it is transported as a pure gas after properly dehumidifying. Therefore, MCFC can also be used to remove CO_2 from the flue gas of other conventional fossil fuel powerplants. It has also been observed that using flue gas contaminated with SO_2 in a MCFC increased the cell voltage (Milewski et al. 2016). The higher operating temperature of MCFC has made it more suitable for commercialization. The prominent features of MCFC that distinguish it from other cells are (Milewski et al. 2017):

1. High energy efficiency.
2. High operating voltage.
3. Higher operating temperature and less prone to contamination.
4. Use of nickel as the catalyst instead of platinum.
5. Liquid molten carbonate electrolyte is easier to manufacture.
6. MCFC can be used as CO_2 separator due to its ability to capture CO_2 from the cathode side.

Due to the matter of convenience of measuring, the impedance measurements have been used extensively in the studies of the performance of MCFC. In such a study, the AC (alternating current) impedance analysis was carried out with 100 cm² class MCFCs (Lee 2016). The simulation was based on an equivalent circuit model, and the kinematic parameters of the MCFC were calculated. The simulation results

clearly showed that the liquid phase mass transfer was due to the concentration of active species in the cathode, while the gas phase mass transfer was mostly due to the gas flow rate in the anode. The polarization curves and electrochemical impedance spectroscopy of a state-of-the-art MCFC were analysed in fuel cell mode and electrolyser mode (Hu et al. 2014). The results of the analysis showed that it is feasible to run a reversible molten carbonate fuel cell and that the cell exhibits lower polarization in the electrolysis mode. The polarization of the Ni hydrogen electrode turned to be slightly higher in the electrolysis mode for all the operating temperature range. The NiO oxygen electrode showed lower polarization loss in the electrolysis cell mode in the range on 600–675 °C.

Kim et al. (2017a, b) as well as Kim and Lee (2017a) have studied the thermal performance of external and internal reforming in an MCFC. They reported that the heat transfer rate towards the anode side was slightly higher than the cathode side in external reforming. Most of the internally generated heat was transferred to the anode side due to the highly intensive endothermic process occurring in the internal reforming. The power consumption of the internal reforming came to be lower than the external reforming. In another study, the anode reaction characteristics in the MCFC have been investigated (Lee 2017). The study was carried out in a 100 cm² single cell by recording its overpotential at different operating temperature. The range of temperature taken was 823–973 K under atmospheric conditions. The result of the investigation showed anodic overpotential at the very extreme temperatures. It was found that enlarged mass transfer resistance of the reaction species, H₂, CO₂ and H₂O, was responsible for the increase in the overpotential at the aforementioned higher temperatures.

The mechanical strength of a conventional MCFC matrix is poor. It is susceptible to thermal shocks and cracks under stress that accelerates cell performance degradation. Thus, a stable and rigid long-term cell operation matrix was suggested in a study to strengthen the mechanical properties of the cell components. The proposed structure was Al foam-reinforced α -LiAlO₂ matrix (Lee et al. 2017). It has significantly strong mechanical strength due to the 3D network structure of aluminium foam and can take the form of hardened alumina skin layer during the cell operation.

Hybridization of MCFC with that of the thermophotovoltaic cell was done in a study to analyse the performance of enhancements in design and optimization (Yang et al. 2016b). The design was based on a simple mechanism where the heat flows from the MCFC to the emitter and from the photovoltaic cell to the environment. The MCFC was operated at 600–700 °C range. The evaluation of the performance of the system showed that the maximum power density of the hybrid system was obtained around 2813 W/m², which is approximately 1.51 times that of an unhybridized single MCFC.

13.3.2 Other Medium-Temperature Fuel Cells

Instead of operating based on gaseous fuel, the direct carbon fuel cell (DCFC) uses solid carbon as fuel. The solid carbon is directly inserted into the anode

compartment. There the carbon gets electro-oxidized to CO_2 at high temperature and produced electrical power. The reason to use molten carbonates in some DCFC is that they are highly conductive and have good stability in the presence of CO_2 . The first DCFC was demonstrated by William Jacques who used molten NaOH as an electrolyte. However, later in the run, molten NaOH was rejected because they seem to react with CO_2 that is produced by the carbon oxidation to form carbonates (Cao et al. 2007).

The hunt for alternative fuel for fuel cells leads people to the development of DCFC. To find such an alternative fuel for the anode side of DCFC, three carbon sources, viz. carbon black, bamboo fibre and waste paper, were tested by Hao et al. (2014). The results showed that the waste paper carbon was more abundant in calcite and kaolinite and thus showed higher thermal reactivity in the intermediate temperature range as compared to the other two sources taken. The testing of the cell performance was done at 650°C in a hybrid single cell. The cell fed with waste paper carbon showed that the highest performance with peak power density as 225 W/cm^2 was achieved. In another attempt to look for alternative fuel, Ca-loaded activated carbon is used as fuel for the DCFC that is operating without any carrier gas and liquid medium (Cai et al. 2017). The loading is done through impregnation technique in the form of CaO that exhibits excellent catalytic activity. This significantly promotes the output performance of the fuel cell. However, Cao et al. (2017) reported that the presence of SnO_2 block film deposits on the anode-electrolyte interface during operation degrades the performance of a DCFC. To mitigate this problem, the researchers introduced carbonate of Li-K on the anode composition. It was seen that the composite anode with 2 mol% molten carbonate demonstrated highest power density as well as stable performance. The fuel cell's performance, as well as the stability, increased further by mixing carbon black with the liquid composite anode.

A study was done to investigate the properties that are catalytic for metallic species commonly present in brown coal towards Boudouard gasification (Rady et al. 2016). This was done by individually doping carbon black with these species and then examining their electrochemical performances in a DCFC. The relative catalytic activities of the dopants were found to be increasing in the order from $\text{Mn} < \text{Fe} < \text{Ca}$ in the presence of oxygen. The final result showed that the catalytic dopants that were added to the carbon fuel had an effect on the equilibrium oxygen partial pressure in the $\text{C}/\text{CO}/\text{CO}_2$ system and the OCV. The major potholes in the development of direct carbon fuel cell are the anode performance, long-term stability and cell scalability in addition to fuel feed mechanism. In a study, lanthanum strontium cobalt ferrite-silver composite anode was evaluated in a bed of carbon powder. Silver was added to increase the lateral conductivity of the anode and also to reduce the ohmic losses (Gil et al. 2017).

When Victorian brown coal is used as fuel for DCFC, the peak power density reached was 65 and 67 W/m^2 for demineralized coal char and carbon black, respectively, at 800°C . On the other hand, when raw coal char is used, power density achieved is 89 W/m^2 (Rady et al. 2014, 2015). In another study, bituminous coal was tested as fuel for the DCFC. The results showed that in the temperature range of

650–850 °C, it is a viable option to other conventional fuel for the cell (Liu et al. 2016a). Biochar that is obtained from the pyrolysis of corn cob is also tested for fuel alternative in DCFC. The results gave a maximum power density of 185 mW/cm² at a current density of 340 mA/cm². The cell was operating at 750 °C and was employing a composite electrolyte composed of samarium-doped ceria and a eutectic carbonate phase (Yu et al. 2014). Another fuel substitute that was tested was Tunisian olive wood charcoal in planar DCFC. It was seen that the fuel gave good power density of 105 mW/cm² and the current density 550 mA/cm² at 700 °C (Elleuch et al. 2015). The nickel-modified Ce_{0.6}Mn_{0.3}Fe_{0.1}O₂ (Ni-CMF) material was evaluated as an anode material. The case was studied in consideration for a hybrid DCFC. The temperature-programmed reaction and gas chromatography tests showed that the Ni additive significantly promotes the carbon oxidation. This also consequently accelerates the formation rate of CO. Moreover the Ni-CMF was seen to have high electrical conductivity compared to pure CMF. The power density was 580.7 mW/cm², and the current density was 50 mA/cm² at 800 and 750 °C, respectively (Liu et al. 2017b).

The study of hybridization of DCFC is a widespread practice to enhance the overall output of the fuel cell system. In one such study, the direct conversion of coal to heat and electricity by a hybrid DCFC is deemed highly efficient and cleaner than conventional combustion power plants (Gil et al. 2017). The DCFC is also seen as the combination of an SOFC and the MCFC. This investigation is based on cathode-supported cells as an alternative configuration for the hybrid cell with better catalytic activity and overall performance. The maximum power density of the cathode-supported cell was reported as double that of an anode-supported cell.

13.4 High-Temperature Fuel Cell

13.4.1 Solid Oxide Fuel Cell (SOFC)

The main characterized identification of a solid oxide fuel cell (SOFC) is the presence of a solid ceramic electrolyte, which is a metallic oxide. The basic components of the SOFC are, namely, the cathode, the anode and the electrolyte. In the cathode, oxygen is reduced to oxide ions and is passed through the solid electrolyte under electrical load. At the anode, they react with the fuel and produce water and carbon dioxide with electricity and heat. The hydrocarbon fuel actually gets converted catalytically into CO and H₂ first and is then electrochemically oxidized to CO₂ and H₂O at the anode (Ormerod 2003).

Though the conventional Ni-based anode exhibits excellent catalytic activity towards the hydrocarbon fuels, the carbon deposition occurs at the anode of an SOFC. These deposited carbons deactivated the anode irreversibly and degrade the cell performance. Studies have been going on to find a solution. In one such solution, the anode structure was modified by the addition of Cu and Ceria in the Ni-YSZ matrix (Cu/CeO₂/Ni/YSZ) to increase coking resistance of the cell under methane fuel (Akdeniz et al. 2016). Such a ceria-based catalytic layer deposited onto the

anode was also studied in an SOFC with direct ethanol as fuel. It was seen that the catalytic layer prevents carbon deposition along with promoting steam reforming reactions of the ethanol with output performance similar to that of hydrogen fuel usage (Steil et al. 2017). Ahn et al. (2017) studied cathode modifications by using nanofibre-based composite cathodes for intermediate temperature SOFC. They show specific solid area cathode resistance value of $0.024 \Omega/\text{cm}^2$ at 650°C . The nanofibre is hollow and porous and is fabricated by electrospinning. Then it is sintered at low temperatures to preserve the high specific surface area for facial oxygen surface exchange reactions to occur.

There are several conditions that appear during the actual field testing of the solid oxide fuel cells (SOFC). One severe problem is the large temperature gradient and generation of local hotspots within the stacks of the cells. The major degradation mechanism that is accelerated by the increase in the temperature is identified in a study as the Sr diffusion from the cathode to the electrolyte while coarsening the constituent particles in the composite electrode (Kim et al. 2017b). Meanwhile, there is crack formation at the anode-electrolyte interface and Cr poisoning. A study was done to understand the effects of temperature and thermal stress in a planar SOFC (Kim and Lee 2017b). The simulations showed that the electrolyte is the weakest component and has the maximum stress. It was due to being the thinnest and the having highest Young modulus of the electrolyte.

Cobalt-containing cathode in an SOFC is very well established to work in very high-temperature applications of the cell. But in case of moderate conditions, these cathodes lead to a mismatch in the thermal expansion coefficient between the cathode and the developed electrolyte material. Therefore, intermittent temperature and low temperature proposes a cobalt-free cathode to work in that temperature range. These novel cobalt-free cathodes are present in powder forms and are prepared by perovskite-structured materials like strontium ferrite oxide, etc. as the main components along with dopants (Baharuddin et al. 2017).

In a study, it was proved that the solvent is the key factor to affect the anode substrate microstructure (Liu et al. 2017c). In those experiments, *N*-methyl-2-pyrrolidone was chosen as the solvent, and a dual-layered anode substrate was achieved that had hierarchically oriented pores. On the other hand, a sponge-like homogeneous anode substrate was obtained using dimethyl sulfoxide as the solvent. The SOFC showed better performance with the dual-layered microstructure anode than that with the sponge-layered anode. A similar study with dual-layered cathode was also performed by Fan et al. (2017) to decrease the contact resistance and reported significant improvement in it. The double-layered cathode was composed of a coarse-particle outer layer that makes the cathode fully contact with the silver current collecting layer and a fine-particle inner layer. The fine-particle inner layer alleviates the structural difference between the coarse and porous cathode and the dense and smooth electrolyte. The performance of SOFC with gadolinium-doped ceria layer was investigated as the diffusion barrier for SOFC by Szymczewska et al. (2017). The layer was fabricated by spray pyrolysis. It was deposited between the cathode and the yttria-stabilized zirconia electrolyte to mitigate harmful

interdiffusion of elements. The result of the study showed that the application of 800 nm thick barrier effectively hindered the negative reactions. On the other hand, a 400 nm thick layer was sufficient to prevent degradation of the ohmic resistance.

13.5 Applications of Fuel Cell

13.5.1 Transportation

The advantages of a fuel cell application in the field of transport services can be ruled to the fact that unlike conventional batteries fuel cell does not take substantial time to cool before reuse and fuel cell does not need to be recharged. Unlike batteries, there is a continuous power delivery by the fuel cells as long as fuel is supplied. Also, fuel cell-embedded vehicle produces zero emissions and a better power to wheel efficiency (Ortiz-Rivera et al. 2007). The start-up time is short, and due to dynamic load demand in the propulsion system of vehicles, use of fuel cells is rising in the transportation sector. However, only the solid state and the PEFC are being considered until now due to heckles related to other types of fuel cells including the spillage of fuels and the electrolytes as well as the type of fuel being used like methanol, liquefied petroleum gas, gasoline, etc. Fuel cells have been targeted to be used in several modes of transportations including the cars, buses, trains and even lifters and heavy machineries. The application targets also include motorcycles and small to medium vehicle ships.

Passenger cars with embedded fuel cells have been in demonstration since 2004. Toyota, Honda and Hyundai have launched their fuel cell electric vehicle models recently in 2015. The latest fuel cell vehicles in the consumer car segment available in the market are offered by Toyota as 'Mirai', Honda as 'Clarity' and Hyundai as 'Tucson ix35' (Yoshida and Kojima 2015; Matsunaga et al. 2009; Burns 2013). In 2012 London Olympic, a few numbers of hydrogen-powered fuel cell – Lithium-polymer battery hybrid black cabs were showcased by Lotus in collaboration with Intelligent Energy, UK (Lucas 2010; Warburton et al. 2013). However, in comparison to cars, buses have been in the long run since the early 1990s. In 1994/1998 methanol-fuelled transit buses have been demonstrated in Georgetown University (Wimmer 1997). Since then London, Aberdeen, Perth, Beijing and Iceland have shown practical demonstrations in the following years for fuel cell-embedded buses. Another promising area for fuel cells' practical application in transportation is seen in the material handling sector. Forklifts are a key target for fuel cell applications. A company known as Plug Power has offered PEFC system for different trucks and lifters of 3–14 kW range. The demonstration is initiated by the United States followed by Europe in the form of HyLIFT-DEMO and HyLIFT-EUROPE projects (Garche and Jürissen 2015).

An attempt was made to use the fuel cell in a motorcycle by Yamaha in 2005 named as 'Yamaha FC-me' (Muramatsu et al. 2007). The attempt to use fuel cells in ships started from 2000. But the most enthusiastic approaches for making a fuel cell-based vehicle are seen in the sector of racing vehicles. Recently a hybrid

PEFC-powered vehicle was developed that consisted of 3 kW cell, PV arrays, secondary battery sets and a chemical hydrogen generation set (Wang and Fang 2017). Effective system performance was evaluated and found that it is viable with some further modifications.

13.5.2 Portable Devices

Another aspect of using the fuel cell is using it as a portable power source. Some of the main advantages of replacing the battery packs with new fuel cell technologies include modularity and high energy density, instant recharging ability and longer lifespan. They are preferred for applications including that of charging of consumer electronics, auxiliary power units and toys. One of the major impacts of using the fuel cells' portability aspect is in the military fields (Patil et al. 2004). The portability and the instant rechargeable ability are of immense importance in a military operation. A typical example of that will be a prototype 30 W portable fuel cell power system that was delivered by Millennium Cell and Protonex Inc. to the Air Force. The system weighs only 15 lb. and was able to provide power for tactical missions for as long as 72 h, reportedly (Agnolucci 2007).

The most common portable fuel cells used are PEFC and DMFC. DMFC finds application as portable sources where there is more emphasis on power density and energy over efficiency (Narayan and Valdez 2008). Fuel cells have been demonstrated to be used for charging battery banks and mobiles as well as laptops. In a demonstration by Toshiba, NEC, Hitachi, Panasonic, Samsung, Sanyo and LG, 10–7 W methanol fuel cells were used for notebook applications. A company known as SFC Energy AG has been in the business of selling fuel cells for portable applications ranging from 40 to 105 W applications. In addition, for relatively larger portable applications like caravans, small sailing boats, etc., high-temperature PEFCs are used that are in the range of 500 W.

13.5.3 Stand-Alone Applications

For the stationary applications of fuel cells, any kind of fuel cell can be used as long as it meets the demand requirement of the site. The application field of the fuel cell in stationary mode can be divided into three types, namely, industrial, residential and backup power. The industrial application requires the most power and thus higher capacity cells are preferred. Among all others, High Temperature Fuel Cell (HT-FC), MCFCs and SOFCs are the prime contenders due to their higher electrical efficiencies for industrial systems. PAFCs, AFCs and PEFCs are declining in usage recently. This is due to the fact that HT-FCs are able to use biogas as its fuel. MCFC-based company in the United States with its subsidiary, FuelCell Energy Solutions in Germany, and having close relations with POSCO, South Korea, is the main player in the market since 2007 (Garche and Jürissen 2015). They are operational in over 65 countries, and the maximum capacity that is on their list is

of 122 MW in Hwasung City, South Korea. Natural gas is the primary fuel used for residential-type fuel cell applications. Both PEFCs and SOFCs are used here. The most successful programme of the world till the date of using residential fuel cell is listed as the Japanese ENE-FARM programme (Maiyalagan and Saji 2017).

For the backup-type application of fuel cell, the storage is not required to be very large as the only function of the cell will be to provide power during short breaks of the main supply. Thus, the storage differs from region to region depending upon the power cut times and demands. A typical example of a backup system by a fuel cell is the telecom application that ranges from 2 to 10 kW. The commercial players use PEFCs for backup supplies, and the major players are Axane, Ballard, Heliocentris, Horizon, Hydrogenics, Intelligent Energy and ReliOn-Plug Power.

Japan, with its tremendous rate of fuel cell installations in the stationary field, is expected to be the largest user that meets its target of 1.4 million micro-CHP (combined heat and power) fuel cell systems by 2020 and a 5.3 million cell systems by 2030 (Wilberforce et al. 2016). Due to the operating mode of stationary fuel cell systems, it is possible to incorporate other forms of energy like renewable sources as wind and solar, in conjugation with the fuel cell parts. These systems can replace the other forms of peak energy supply systems on demand like (diesel generator) DG sets (Colleen 2017). The stationary fuel cell generation can either be central generation or distributed generation types depending upon the distance and the load variations. The advantage of the distributed generation over the central generation is that the power can be produced on the required site and the heat produced can be used as combined heating and power.

The commercial PAFC was developed back in the United States. Target plan in 1967 and PAFC for on-site use was commercialized in 1995. It was proven that PAFC was the only plant with a durability of more than 40,000 h (Okumura 2013). The first pilot-scale application of wastewater treatment with the help of MFC is of 1 m³ brewery wastewater treatment plant in Queensland, Australia (Logan 2010). In another stationary application attempt, it was proven that MFC with biocathodes can be used for electricity production from dairy manure as fuel (Zhang et al. 2012). MFC also acts as a promising method for remediation of toxic vanadium from a contaminated environment. Synergistically electrochemical and microbial reductions result in the complete removal of vanadium (v) within 7 days of operation with a dosage of 200 mg/L (Qiu et al. 2017).

13.5.4 Space Application

The most demanding application of the fuel cells can be seen in space and extra-terrestrial sector. The space applications require a lightweight power source that can provide all the required power and that too at a constant energy density. The technology of fuel cells was used in space applications since before the Apollo missions. The first fuel cell usage is described in the Gemini programme in August 21, 1962. The cell used was a PEFC. Later, Apollo-manned flights used the alkaline

electrolyte FC that contains potassium hydroxide electrolyte, held in asbestos. In recent space applications, much more complicated and modern technologies of fuel cells are used (Halpert et al. 1999).

In the current scenario, NASA is experimenting upon the PEM and SOFC technologies to build solid reliable and compact high-energy power sources for space applications. The main focus is on close cycle regenerative PEM cells. The targeted system will be of around 10 kW range and the runtime will be estimated to around 10 k h. Tests are also being conducted to use PEFC in the space rovers and other vehicles for short terms as well as for the spacecraft itself by NASDA. The experiments under simulated conditions showed that the oxygen was recycled and the hydrogen was dead-ended (Sone et al. 2004).

Yet another field of recent advancement of fuel cell application is in the medical field. Devices have been developed that use fuel cells of microorganisms, enzymes and precious metals as catalysts. Even testers that are needed to be put inside the bodies of humans are tested to be functioning perfectly by using fuel cells of minuscular scales (Xu et al. 2017). The first implanted abiotic glucose fuel cell was developed in the 1970s. They used noble metals, alloys or activated carbon as the catalyst for oxygen reduction and glucose oxidation. In 2010 surgical implantation of GFC in the retroperitoneal space of a Wistar rat was done. In another case, a needle bio-anode was pierced into a rabbit's ear while using an air-breathing biocathode (Cosnier et al. 2014). The applications of fuel cells are even tested for unmanned machines such as robots. Eco-bot-I was declared as the first robot that was powered solely by MFCs (Ieropoulos et al. 2003).

13.6 Conclusions

The fuel cells have proven to be one of the main developing energy conversion technologies in the present scenario. Its advantages and ease to handle have made it as one of the attractive technology to work at. The fuel cells have made valuable contributions in the applications of both stationary and mobile devices such as vehicles, portable power, distributed power, medical, space and cogeneration. Depending upon the requirement at the point of application, the fuel cell of different types and operating temperatures from low to high can be applied. The efficiency of the fuel cells is comparable or better than other conventional energy conversion devices. Moreover, it is quite flexible enough to design to fulfil the change in power requirement by changing the number of modules. Due to its increasing demand and commercial interest, lot of researchers have been currently working on it to overcome technical barriers and thus making it more efficient, durable and affordable. Looking through all its development, flexibility and compatibility, it would not be wrong to predict that fuel cell will be one of the major additions in the energy market in the near future.

References

- Acres GJK (2001) Recent advances in fuel cell technology and its applications. *J Power Sources* 100:60–66
- Agnozzucci P (2007) Economics and market prospects of portable fuel cells. *Int J Hydrog Energy* 32:4319–4328
- Ahn S, Tatarchuk BJ (1997) Fibrous metal-carbon compos struct as gas diffusion electrodes for use in alkaline electrolyte. *J Appl Electrochem* 27:9–17
- Ahn M, Lee J, Lee W (2017) Nanofiber-based composite cathodes for intermediate temperature solid oxide fuel cells. *J Power Sources* 353:176–182
- Akdeniz Y, Timurkutluk B, Timurkutluk C (2016) Development of anodes for direct oxidation of methane fuel in solid oxide fuel cells. *Int J Hydrog Energy* 41:10021–10029
- Allen RM, Bennetto HP (1993) Microbial fuel-cells – electricity production from carbohydrates. *Appl Biochem Biotechnol* 39:27–40
- Al-Saleh MA, Gültekin S, Al-Zakri AS, Celiker H (1994) Effect of carbon dioxide on the performance of Ni/PTFE and Ag/PTFE electrodes in an alkaline fuel cell. *J Appl Electrochem* 24:575–580
- Al-Saleh MA, Gultekin S, Al-Zakri A, Khan A (1996) Steady state performance of copper impregnated Ni/PTFE gas diffusion electrode in alkaline fuel cell. *Int J Hydrog Energy* 21:657–661
- Al-Saleh M, Al-Zakri A, Gultekin S (1997) Preparation of Raney–Ni gas diffusion electrode by filtration method for alkaline fuel cells. *J Appl Electrochem* 27:215–220
- Ansari Y, Tucker TG, Angell CA (2013) A novel, easily synthesized, anhydrous derivative of phosphoric acid for use in electrolyte with phosphoric acid-based fuel cells. *J Power Sources* 237:47–51
- Aragane J, Murahashi T, Odaka T (1988) Change of Pt distribution in the active components of phosphoric acid fuel cell. *J Electrochem Soc* 135:844–850
- Asghari S, Akhgar H, Imani BF (2011) Design of thermal management subsystem for a 5kW polymer electrolyte membrane fuel cell system. *J Power Sources* 196:3141–3148
- Asri NF, Husaini T, Sulong AB, Majlan EH, Daud WRW (2017) Coating of stainless steel and titanium bipolar plates for anticorrosion in PEMFC: a review. *Int J Hydrog Energy* 42 (14):9135–9148
- Bagotsky VS (2012) *Fuel cells: problems and solutions*, vol 56. Wiley, Hoboken
- Baharuddin NA, Muchtar A, Somalu MR (2017) Short review on cobalt-free cathodes for solid oxide fuel cells. *Int J Hydrog Energy* 42:9149–9155
- Bao C, Ouyang M, Yi B (2006) Analysis of the water and thermal management in proton exchange membrane fuel cell systems. *Int J Hydrog Energy* 31:1040–1057
- Baranton S, Chiwata M, Lankiang S, Coutanceau C (2015) Pt, Pd, Au binary and ternary catalysts for the oxygen reduction reaction. *Electrochem Soc Meet Abstr* 37:1371
- Basu D, Basu S (2010) A study on direct glucose and fructose alkaline fuel cell. *Electrochim Acta* 55(20):5775–5779
- Basu D, Basu S (2011a) Synthesis and characterization of Pt-Au/C catalyst for glucose electro-oxidation for the application in direct glucose fuel cell. *Int J Hydrog Energy* 36:14923–14929
- Basu D, Basu S (2011b) Synthesis, characterization and application of platinum based bi-metallic catalysts for direct glucose alkaline fuel cell. *Electrochim Acta* 56:6106–6113
- Basu D, Basu S (2012) Performance studies of Pd-Pt and Pt-Pd-Au catalyst for electro-oxidation of glucose in direct glucose fuel cell. *Int J Hydrog Energy* 37:4678–4684
- Belousov VV (2017) Next-generation electrochemical energy materials for intermediate temperature molten oxide fuel cells and ion transport molten oxide membranes. *Acc Chem Res* 50:273–280
- Bennetto H, Delaney G, Mason J, Roller S, Stirling J, Thurston C (1985) The sucrose fuel cell: efficient biomass conversion using a microbial catalyst. *Biotechnol Lett* 7:699–704

- Besmann TM, Klett JW, Henry JJ, Lara-Curzio E (2000) Carbon/carbon composite bipolar plate for proton exchange membrane fuel cells. *J Electrochem Soc* 147:4083–4086
- Bindra P, Clouser SJ, Yeager E (1979) Platinum dissolution in concentrated phosphoric acid. *J Electrochem Soc* 126:1631–1632
- Borole AP, Reguera G, Ringeisen B, Wang Z-W, Feng Y, Kim BH (2011) Electroactive biofilms: current status and future research needs. *Energy Environ Sci* 4:4813–4834
- Brankovic S, Wang J, Adžić R (2001) Pt submonolayers on Ru nanoparticles: a novel low Pt loading, high CO tolerance fuel cell electrocatalyst. *Electrochem Solid-State Lett* 4:A217–A220
- Burns LD (2013) Sustainable mobility: a vision of our transport future. *Nature* 497:181–182
- Cai W, Liu J, Yu F, Zhou Q, Zhang Y, Wang X, Liu M, Ni M (2017) A high performance direct carbon solid oxide fuel cell fueled by Ca-loaded activated carbon. *Int J Hydrog Energy* 42:21167–21176
- Cameron D, Hards G, Harrison B, Potter R (1987) Direct methanol fuel cells. *Platin Met Rev* 31:173–181
- Cao D, Sun Y, Wang G (2007) Direct carbon fuel cell: fundamentals and recent developments. *J Power Sources* 167:250–257
- Cao XX, Huang X, Liang P, Xiao K, Zhou YJ, Zhang XY, Logan BE (2009) A new method for water desalination using microbial desalination cells. *Environ Sci Technol* 43:7148–7152
- Cao T, Song P, Shi Y, Cai N (2017) Carbonate-tin composite liquid anode for solid oxide direct carbon fuel cell. *Int J Hydrog Energy* 42:6324–6331
- Carrette L, Friedrich KA, Stimming U (2000) Fuel cells: principles, types, fuels, and applications. *Chem Phys Chem* 1:162–193
- Carrette L, Friedrich K, Huber M, Stimming U (2001a) Improvement of CO tolerance of proton exchange membrane (PEM) fuel cells by a pulsing technique. *Phys Chem Chem Phys* 3:320–324
- Carrette L, Friedrich K, Stimming U (2001b) Fuel cells—fundamentals and applications. *Fuel Cells* 1:5–39
- Cassir M, Malinowska B, Canevet C, Sportouch L, Devynck J (1996) Molten carbonate fuel cells: contribution to the study of cathode behaviour and oxygen reduction in molten Li_2CO_3 - K_2CO_3 at 650° C. *J Power Sources* 61:149–153
- Chabot J, Lecomte J, Grumet C, Sannier J (1988) Fuel clean-up system: poisoning of palladium-silver membranes by gaseous impurities. *Fusion Technol* 14:614–618
- Chen C-Y, Huang K-P (2017) Performance and transient behavior of the kW-grade PEMFC stack with the PtRu catalyst under CO-contained diluted hydrogen. *Int J Hydrog Energy* 42:22250–22258
- Chen JY, Zhao CX, Zhi MM, Wang KW, Deng LL, Xu G (2012) Alkaline direct oxidation glucose fuel cell system using silver/nickel foams as electrodes. *Electrochim Acta* 66:133–138
- Chen XH, Wang Y, Cai L, Zhou YH (2015) Maximum power output and load matching of a phosphoric acid fuel cell-thermoelectric generator hybrid system. *J Power Sources* 294:430–436
- Chen J, Hu Y, Tan X, Zhang L, Huang W, Sun J (2017a) Enhanced performance of microbial fuel cell with in situ preparing dual graphene modified bioelectrode. *Bioresour Technol* 241:735–742
- Chen J, Zhang L, Hu Y, Huang W, Niu Z, Sun J (2017b) Bacterial community shift and incurred performance in response to in situ microbial self-assembly graphene and polarity reversion in microbial fuel cell. *Bioresour Technol* 241:220–227
- Chen X, Li W, Gong G, Wan Z, Tu Z (2017c) Parametric analysis and optimization of PEMFC system for maximum power and efficiency using MOEA/D. *Appl Therm Eng* 121:400–409
- Cho E, Jeon U-S, Hong S-A, Oh I-H, Kang S-G (2005) Performance of a 1kW-class PEMFC stack using TiN-coated 316 stainless steel bipolar plates. *J Power Sources* 142:177–183
- Chu H, Wang C, Liao W, Yan W (2006) Transient behavior of CO poisoning of the anode catalyst layer of a PEM fuel cell. *J Power Sources* 159:1071–1077
- Cohen B (1931) The bacteria culture as an electrical half-cell. *J Bacteriol* 21:18–19

- Colleen S (2017) Introduction to fuel cell Applications. <http://www.fuelcellstore.com/blog-section/intro-fuel-cell-applications>. Accessed 01 Nov 2017
- Cooper CD, Burk JJ, Taylor CP, Buratto SK (2017) Ultra-low Pt loading catalyst layers prepared by pulse electrochemical deposition for PEM fuel cells. *J Appl Electrochem* 47:699–709
- Cosnier S, Le Goff A, Holzinger M (2014) Towards glucose biofuel cells implanted in human body for powering artificial organs: review. *Electrochem Commun* 38:19–23
- Daud W, Rosli R, Majlan E, Hamid S, Mohamed R, Husaini T (2017) PEM fuel cell system control: a review. *Renew Energy* 113:620–638
- Delord B, Neri W, Bertaux K, Derre A, Ly I, Mano N, Poulin P (2017) Carbon nanotube fiber mats for microbial fuel cell electrodes. *Bioresour Technol* 243:1227–1231
- Dhar H, Christner L, Kush A, Maru H (1986) Performance study of a fuel cell Pt-on-C anode in presence of CO and CO₂, and calculation of adsorption parameters for CO poisoning. *J Electrochem Soc* 133:1574–1582
- Dundar F, Dur E, Mahabunphachai S, Koc M (2010) Corrosion resistance characteristics of stamped and hydroformed proton exchange membrane fuel cell metallic bipolar plates. *J Power Sources* 195:3546–3552
- Elleuch A, Halouani K, Li Y (2015) Investigation of chemical and electrochemical reactions mechanisms in a direct carbon fuel cell using olive wood charcoal as sustainable fuel. *J Power Sources* 281:350–361
- Elmore GV, Tanner HA (1961) Intermediate Temperature Fuel Cells. *J Electrochem Soc* 108(7):669–671
- El-Zoheiry RM, Ookawara S, Ahmed M (2017) Efficient fuel utilization by enhancing the under-rib mass transport using new serpentine flow field designs of direct methanol fuel cells. *Energy Convers Manag* 144:88–103
- Escalona-Villalpando RA, Dector A, Dector D, Moreno-Zuria A, Duron-Torres SM, Galvan-Valencia M, Arriaga LG, Ledesma-Garcia J (2016) Glucose microfluidic fuel cell using air as oxidant. *Int J Hydrog Energy* 41:23394–23400
- Esmailifar A, Rowshanzamir S, Eikani M, Ghazanfari E (2010) Synthesis methods of low-Pt-loading electrocatalysts for proton exchange membrane fuel cell systems. *Energy* 35:3941–3957
- Fan B, Yu F, Ren X, Yan J, Guo F, Cong Y (2017) The influence of double-layered cathode on contact resistance and electrical performance of solid oxide fuel cells self-supported by anodes. *Solid State Ionics* 304:20–26
- Fuller TF, Newman J (1993) Water and thermal management in solid-polymer-electrolyte fuel cells. *J Electrochem Soc* 140:1218–1225
- Garche J, Jürissen L (2015) Applications of fuel cell technology: status and perspectives. *Electrochem Soc Interface* 24:39–43
- Gil V, Gurauskis J, Deleebeeck L, Stamate E, Hansen KK (2017) Cathode-supported hybrid direct carbon fuel cells. *Int J Hydrog Energy* 42:4311–4319
- Gottesfeld S (1990) Preventing CO poisoning in fuel cells. Patent Number: US4910099A. US Department of Energy
- Götz M, Wendt H (1998) Binary and ternary anode catalyst formulations including the elements W, Sn and Mo for PEMFCs operated on methanol or reformat gas. *Electrochim Acta* 43:3637–3644
- Halpert G, Frank H, Surampudi S (1999) Batteries and fuel cells in space. *Electrochem Soc Interface*:25–30
- Halseid R, Vie PJ, Tunold R (2006) Effect of ammonia on the performance of polymer electrolyte membrane fuel cells. *J Power Sources* 154:343–350
- Hao W, He X, Mi Y (2014) Achieving high performance in intermediate temperature direct carbon fuel cells with renewable carbon as a fuel source. *Appl Energy* 135:174–181
- He Z, Minter SD, Angenent LT (2005) Electricity generation from artificial wastewater using an upflow microbial fuel cell. *Environ Sci Technol* 39:5262–5267
- Hogarth M, Hards G (1996) Direct methanol fuel cells. *Platin Met Rev* 40:150–159

- Honji A, Mori T, Tamura K, Hishinuma Y (1988) Agglomeration of platinum particles supported on carbon in phosphoric acid. *J Electrochem Soc* 135:355–359
- Hu L, Rexed I, Lindbergh G, Lagergren C (2014) Electrochemical performance of reversible molten carbonate fuel cells. *Int J Hydrog Energy* 39:12323–12329
- Ieropoulos I, Melhuish C, Greenman J (2003) Artificial metabolism: towards true energetic autonomy in artificial life. *Lect Notes Artif Int* 2801:792–799
- Im SJ (2015) Device and method for controlling operation of fuel cell system. Patent Number: US20160380281A1. Hyundai Motor Co
- Iraivaninia M, Azizi S, Rowshanzamir S (2017) A comprehensive study on the stability and ion transport in cross-linked anion exchange membranes based on polysulfone for solid alkaline fuel cells. *Int J Hydrog Energy* 42:17229–17241
- Jing F, Hou M, Shi W, Fu J, Yu H, Ming P, Yi B (2007) The effect of ambient contamination on PEMFC performance. *J Power Sources* 166:172–176
- Kahraman H, Cevik I, Dündar F, Ficici F (2016) The corrosion resistance behaviors of metallic bipolar plates for PEMFC coated with physical vapor deposition (PVD): an experimental study. *Arab J Sci Eng* 41:1961–1968
- Kakati BK, Kucernak ARJ (2014) Gas phase recovery of hydrogen sulfide contaminated polymer electrolyte membrane fuel cells. *J Power Sources* 252:317–326
- Kakati BK, Ghosh A, Verma A (2011) Graphene reinforced composite bipolar plate for polymer electrolyte membrane fuel cell. In: ASME 2011 9th international conference on fuel cell science, engineering and technology collocated with ASME 2011 5th international conference on energy sustainability. American Society of Mechanical Engineers, 301–307
- Kakati BK, Kucernak ARJ, Fahy KF (2016a) Using corrosion-like processes to remove poisons from electrocatalysts: a viable strategy to chemically regenerate irreversibly poisoned polymer electrolyte fuel cells. *Electrochim Acta* 222:888–897
- Kakati BK, Unnikrishnan A, Rajalakshmi N, Jafri RI, Dhathathreyan KS, Kucernak ARJ (2016b) Recovery of polymer electrolyte fuel cell exposed to sulphur dioxide. *Int J Hydrog Energy* 41:5598–5604
- Kang S, Zhou B, Jiang M (2017) Bubble behaviors in direct methanol fuel cell anode with parallel design. *Int J Hydrog Energy* 42:20201–20215
- Karim N, Kamarudin S, Loh K (2017) Performance of a novel non-platinum cathode catalyst for direct methanol fuel cells. *Energy Convers Manag* 145:293–307
- Kim YJ, Lee MC (2017a) Comparison of thermal performances of external and internal reforming molten carbonate fuel cells using numerical analyses. *Int J Hydrog Energy* 42:3510–3520
- Kim YJ, Lee MC (2017b) Numerical investigation of flow/heat transfer and structural stress in a planar solid oxide fuel cell. *Int J Hydrog Energy* 42:18504–18513
- Kim S, Yang S, Kim D (2017a) Poly(arylene ether ketone) with pendant pyridinium groups for alkaline fuel cell membranes. *Int J Hydrog Energy* 42:12496–12506
- Kim SJ, Choi M-B, Park M, Kim H, Son J-W, Lee J-H, Kim B-K, Lee H-W, Kim S-G, Yoon KJ (2017b) Acceleration tests: degradation of anode-supported planar solid oxide fuel cells at elevated operating temperatures. *J Power Sources* 360:284–293
- Kumar V, Wati L, Nigam P, Banat IM, Yadav BS, Singh D, Marchant R (1998) Decolorization and biodegradation of anaerobically digested sugarcane molasses spent wash effluent from biomethanation plants by white-rot fungi. *Process Biochem* 33:83–88
- Larrosa-Guerrero A, Scott K, Head IM, Mateo F, Ginesta A, Godinez C (2010) Effect of temperature on the performance of microbial fuel cells. *Fuel* 89:3985–3994
- Lee C-G (2016) Analysis of impedance in a molten carbonate fuel cell. *J Electroanal Chem* 776:162–169
- Lee C-G (2017) Influence of temperature on the anode reaction in a molten carbonate fuel cell. *J Electroanal Chem* 785:152–158
- Lee D, Lim JW (2017) Cathode/anode integrated composite bipolar plate for high-temperature PEMFC. *Compos Struct* 167:144–151

- Lee S-J, Huang C-H, Chen Y-P (2003) Investigation of PVD coating on corrosion resistance of metallic bipolar plates in PEM fuel cell. *J Mater Process Technol* 140:688–693
- Lee M, Lee C-W, Ham H-C, Han J, Yoon SP, Lee KB (2017) Mechanical strength improvement of aluminum foam-reinforced matrix for molten carbonate fuel cells. *Int J Hydrog Energy* 42:16235–16243
- Li X, Horita K (2000) Electrochemical characterization of carbon black subjected to RF oxygen plasma. *Carbon* 38:133–138
- Li M-Q, Shao Z-G, Scott K (2008) A high conductivity $\text{Cs}_{2.5}\text{H}_{0.5}\text{PMo}_{12}\text{O}_{40}$ /polybenzimidazole (PBI)/ H_3PO_4 composite membrane for proton-exchange membrane fuel cells operating at high temperature. *J Power Sources* 183:69–75
- Li Q, Jensen JO, Savinell RF, Bjerrum NJ (2009) High temperature proton exchange membranes based on polybenzimidazoles for fuel cells. *Prog Polym Sci* 34:449–477
- Li F, Sharma Y, Lei Y, Li B, Zhou Q (2010) Microbial fuel cells: the effects of configurations, electrolyte solutions, and electrode materials on power generation. *Appl Biochem Biotechnol* 160:168–181
- Li H, Wang H, Qian W, Zhang S, Wessel S, Cheng TT, Shen J, Wu S (2011) Chloride contamination effects on proton exchange membrane fuel cell performance and durability. *J Power Sources* 196:6249–6255
- Li L, Scott K, Yu EH (2013) A direct glucose alkaline fuel cell using MnO_2 -carbon nanocomposite supported gold catalyst for anode glucose oxidation. *J Power Sources* 221:1–5
- Li X, Lu YB, Luo HP, Liu GL, Zhang RD (2017) Microbial stratification structure within cathodic biofilm of the microbial fuel cell using the freezing microtome method. *Bioresour Technol* 241:384–390
- Liu Z (2013) Effects of fuel and air impurities on PEFC performance. In: Franco AA (ed) *Polymer electrolyte fuel cells: science, applications, and challenges*. CRC Press, Florida, pp 427–485
- Liu H, Grot S, Logan BE (2005) Electrochemically assisted microbial production of hydrogen from acetate. *Environ Sci Technol* 39:4317–4320
- Liu G, Zhang H, Hu J, Zhai Y, Xu D, Shao Z-g (2006) Studies of performance degradation of a high temperature PEMFC based on H₃PO₄-doped PBI. *J Power Sources* 162:547–552
- Liu J, Feng Y, Wang X, Shi X, Yang Q, Lee H, Zhang Z, Ren N (2011) The use of double-sided cloth without diffusion layers as air-cathode in microbial fuel cells. *J Power Sources* 196:8409–8412
- Liu M, Zhang R, Chen W (2014) Graphene-supported nanoelectrocatalysts for fuel cells: synthesis, properties, and applications. *Chem Rev* 114:5117–5160
- Liu S, Liu X, Wang Y, Zhang P (2016) Electricity generation from macroalgae *Enteromorpha prolifera* hydrolysates using an alkaline fuel cell. *Bioresour Technol* 222:226–231
- Liu G, Zhou A, Qiu J, Zhang Y, Cai J, Dang Y (2016a) Utilization of bituminous coal in a direct carbon fuel cell. *Int J Hydrog Energy* 41:8576–8582
- Liu SS, Liu XH, Wang Y, Zhang PP (2016b) Electricity generation from macroalgae *Enteromorpha prolifera* hydrolysates using an alkaline fuel cell. *Bioresour Technol* 222:226–231
- Liu XH, Li Z, Yang YL, Liu P, Zhang PP (2016c) Electricity generation from a refuelable glucose alkaline fuel cell with a methyl viologen-immobilized activated carbon anode. *Electrochim Acta* 222:1430–1437
- Liu G, Yang Z, Halim M, Li X, Wang M, Kim JY, Mei Q, Wang X, Lee JK (2017a) A gradient activation method for direct methanol fuel cells. *Energy Convers Manag* 138:54–60
- Liu J, Qiao J, Yuan H, Feng J, Sui C, Wang Z, Sun W, Sun K (2017b) Ni modified Ce (Mn, Fe) O₂ cermet anode for high-performance direct carbon fuel cell. *Electrochim Acta* 232:174–181
- Liu T, Ren C, Zhang Y, Wang Y, Lei L, Chen F (2017c) Solvent effects on the morphology and performance of the anode substrates for solid oxide fuel cells. *J Power Sources* 363:304–310
- Lobato J, Canizares P, Rodrigo MA, Linares JJ, Manjavacas G (2006) Synthesis and characterisation of poly [2, 2-(m-phenylene)-5, 5-benzimidazole] as polymer electrolyte membrane for high temperature PEMFCs. *J Membr Sci* 280:351–362

- Lobato J, Canizares P, Rodrigo M, Linares J, Aguilar J (2007) Improved polybenzimidazole films for H₃ PO 4-doped PBI-based high temperature PEMFC. *J Membr Sci* 306:47–55
- Logan BE (2010) Scaling up microbial fuel cells and other bioelectrochemical systems. *Appl Microbiol Biotechnol* 85:1665–1671
- Lu ZJ, Rath C, Zhang GS, Kandlikar SG (2011) Water management studies in PEM fuel cells, part IV: effects of channel surface wettability, geometry and orientation on the two-phase flow in parallel gas channels. *Int J Hydrog Energy* 36:9864–9875
- Lucas L (2010) Fuel cell hybrid taxi unveiled in London. *Fuel Cells Bull* 2010:2
- Maiyalagan T, Saji VS (2017) Electrocatalysts for low temperature fuel cells: fundamentals and recent trends. Wiley, New Jersey
- Matsunaga M, Fukushima T, Ojima K (2009) Powertrain system of Honda FCX clarity fuel cell vehicle. *World Elec Vehicle J* 3:1–10
- McBreen J, Taylor EJ, Kordesch KV, Kissel G, Kulesa F, Srinivasan S (1979) Development of fuel cell technology for vehicular applications. Annual report, October 1, 1977–September 30, 1978. Brookhaven National Lab, Upton
- McLean G, Niet T, Prince-Richard S, Djilali N (2002) An assessment of alkaline fuel cell technology. *Int J Hydrog Energy* 27:507–526
- Mehta V, Cooper JS (2003) Review and analysis of PEM fuel cell design and manufacturing. *J Power Sources* 114:32–53
- Merle G, Wessling M, Nijmeijer K (2011) Anion exchange membranes for alkaline fuel cells: a review. *J Membr Sci* 377:1–35
- Milewski J, Futyma K, Szczęśniak A (2016) Molten carbonate fuel cell operation under high concentrations of SO₂ on the cathode side. *Int J Hydrog Energy* 41:18769–18777
- Milewski J, Wejrzanowski T, Fung K-Z, Szabłowski Ł, Baron R, Tang J-Y, Szczęśniak A, Ni C-T (2017) Temperature influence on six layers samaria doped ceria matrix impregnated by lithium/potassium electrolyte for molten carbonate fuel cells. *Int J Hydrog Energy* 43:474–482
- Mirza Z (2011) Development of a thermal and water management system for PEM fuel cell. Honeywell Aerospace. Project No. FC066. https://hydrogenendoev.nrel.gov/pdfs/review10/fc066_mirza_2010_p_web.pdf
- Mohtadi R, Lee W-K, Cowan S, Van Zee J, Murthy M (2003) Effects of hydrogen sulfide on the performance of a PEMFC. *Electrochem Solid-State Lett* 6:A272–A274
- Mukerjee S, Lee S, Ticianelli E, McBreen J, Grgur B, Markovic N, Ross P, Giallombardo J, De Castro E (1999) Investigation of enhanced CO tolerance in proton exchange membrane fuel cells by carbon supported PtMo alloy catalyst. *Electrochem Solid-State Lett* 2:12–15
- Muramatsu Y, Furukawa K, Adachi S (2007) Evaluation of direct methanol fuel cell systems for two-wheeled vehicles. SAE International. Paper number 2007-32-0112
- Narayan S, Valdez TI (2008) High-energy portable fuel cell power sources. *Electrochem Soc Interface* 17:40–45
- Nie YJ, Gao JX, Wang ED, Jiang LH, An L, Wang XY (2017) An effective hybrid organic/inorganic inhibitor for alkaline aluminum-air fuel cells. *Electrochim Acta* 248:478–485
- Oh SH, Sinkevitch RM (1993) Carbon monoxide removal from hydrogen-rich fuel cell feedstreams by selective catalytic oxidation. *J Catal* 142:254–262
- Oh M, Yoon Y, Park S (2004) The electrical and physical properties of alternative material bipolar plate for PEM fuel cell system. *Electrochim Acta* 50:777–780
- Okamoto T, Hayashi H, Ryu T, Yoshida T, Yamada Y (2017) Solid oxide fuel cell. US Patent 9620805
- Okumura M (2013) Fuel cells-phosphoric acid fuel cells: systems. In: Garche J, Dyer CK, Moseley PT, Ogumi Z, Rand DA, Scrosati B (eds) Reference module in chemistry, molecular sciences and chemical engineering. Elsevier
- Ong B, Kamarudin SK, Masdar M, Hasran UA (2017) Applications of graphene nano-sheets as anode diffusion layers in passive direct methanol fuel cells (DMFC). *Int J Hydrog Energy* 42:9252–9261
- Ormerod RM (2003) Solid oxide fuel cells. *Chem Soc Rev* 32:17–28

- Ortiz-Rivera EI, Reyes-Hernandez AL, Febo RA (2007) Understanding the history of fuel cells. In: Electric power IEEE conference on the history of, 2007. IEEE, pp 117–122
- Palmore GTR, Bertschy H, Bergens SH, Whitesides GM (1998) A methanol/dioxygen biofuel cell that uses NAD⁺-dependent dehydrogenases as catalysts: application of an electro-enzymatic method to regenerate nicotinamide adenine dinucleotide at low overpotentials. *J Electroanal Chem* 443:155–161
- Park JC, Choi CH (2017) Graphene-derived Fe/Co-NC catalyst in direct methanol fuel cells: effects of the methanol concentration and ionomer content on cell performance. *J Power Sources* 358:76–84
- Passalacqua E, Lufrano F, Squadrito G, Patti A, Giorgi L (1998) Influence of the structure in low-Pt loading electrodes for polymer electrolyte fuel cells. *Electrochim Acta* 43:3665–3673
- Patil AS, Dubois TG, Sifer N, Bostic E, Gardner K, Quah M, Bolton C (2004) Portable fuel cell systems for America's army: technology transition to the field. *J Power Sources* 136:220–225
- Paul T, Seal M, Banerjee D, Ganguly S, Kargupta K, Sandilya P (2014) Analysis of drying and dilution in phosphoric acid fuel cell (PAFC) using galvanometric study and electrochemical impedance spectroscopy. *J Fuel Cell Sci Tech* 11:041001
- Potter MC (1911) Electrical effects accompanying the decomposition of organic compounds. *P Roy Soc B-Biol Sci* 84:260–276
- Qi Z, Kaufman A (2003) Low Pt loading high performance cathodes for PEM fuel cells. *J Power Sources* 113:37–43
- Qiu R, Zhang BG, Li JX, Lv Q, Wang S, Gu Q (2017) Enhanced vanadium (V) reduction and bioelectricity generation in microbial fuel cells with biocathode. *J Power Sources* 359:379–383
- Rady AC, Giddey S, Kulkarni A, Badwal SP, Bhattacharya S, Ladewig BP (2014) Direct carbon fuel cell operation on brown coal. *Appl Energy* 120:56–64
- Rady AC, Giddey S, Kulkarni A, Badwal SP, Bhattacharya S (2015) Direct carbon fuel cell operation on brown coal with a Ni-GDC-YSZ anode. *Electrochim Acta* 178:721–731
- Rady AC, Giddey S, Kulkarni A, Badwal SP, Bhattacharya S (2016) Catalytic gasification of carbon in a direct carbon fuel cell. *Fuel* 180:270–277
- Ramachandran R, Chen SM, Kumar GPG (2015) Enhancement of different fabricated electrode materials for microbial fuel cell applications: an overview. *Int J Electrochem Sci* 10:7111–7137
- Rao JR, Richter GJ, Von Sturm F, Weidlich E (1976) The performance of glucose electrodes and the characteristics of different biofuel cell constructions. *Bioelectrochem Bioenerg* 3:139–150
- Rapoport BI, Kedzierski JT, Sarpeshkar R (2012) A glucose fuel cell for implantable brain-machine interfaces. *PLoS One* 7:e38436
- Reddy EH, Jayanti S (2012) Thermal management strategies for a 1 kWe stack of a high temperature proton exchange membrane fuel cell. *Appl Therm Eng* 48:465–475
- Reguera G, McCarthy KD, Mehta T, Nicoll JS, Tuominen MT, Lovley DR (2005) Extracellular electron transfer via microbial nanowires. *Nature* 435:1098–1101
- Reiser CA, Sawyer RD (1988) Solid polymer electrolyte fuel cell stack water management system. US4769297A. UTC Power LLC
- Ross P Jr (1985) Deactivation and poisoning of fuel cell catalysts. In: Proceedings of 3rd international symposium on catalyst deactivation and poisoning, University of California Berkeley, USA
- Ross AJ, Schoenhoff RL, Aleem M (1968) Electron transport and coupled phosphorylation in the chemoautotroph *Thiobacillus neapolitanus*. *Biochem Biophys Res Commun* 32:301–306
- Sammes N, Bove R, Stahl K (2004) Phosphoric acid fuel cells: fundamentals and applications. *Curr Opin Solid St M* 8:372–378
- Sánchez M, Pierna A, Lorenzo A, Del Val J (2016) Effect of cocatalyst and composition on catalytic performance of amorphous alloys for ethanol electrooxidation and PEMFCs. *Int J Hydrog Energy* 41:19749–19755
- Santoro C, Arbizzani C, Erable B, Ieropoulos I (2017) Microbial fuel cells: from fundamentals to applications. A review. *J Power Sources* 356:225–244

- Seo A, Lee J, Han K, Kim H (2006) Performance and stability of Pt-based ternary alloy catalysts for PEMFC. *Electrochim Acta* 52:1603–1611
- Shi Z, Song D, Li H, Fatih K, Tang Y, Zhang J, Wang Z, Wu S, Liu Z-S, Wang H (2009) A general model for air-side proton exchange membrane fuel cell contamination. *J Power Sources* 186:435–445
- Simonsson D (1997) Electrochemistry for a cleaner environment. *Chem Soc Rev* 26:181–189
- Sisler FD (1962) Electrical energy from microbiological processes. *J Wash Acad Sci* 52:181–187
- Sohn Y-J, Yim S-D, Park G-G, Kim M, Cha S-W, Kim K (2017) PEMFC modeling based on characterization of effective diffusivity in simulated cathode catalyst layer. *Int J Hydrog Energy* 42:13226–13233
- Sone Y, Ueno M, Kuwajima S (2004) Fuel cell development for space applications: fuel cell system in a closed environment. *J Power Sources* 137:269–276
- Song B-Y, Li Y-S, He Y-L, Cheng Z-D (2014) Anode structure design for the high-performance anion-exchange membrane direct glucose fuel cell. *Energy Procedia* 61:2118–2122
- Steil M, Nobrega S, Georges S, Gelin P, Uhlenbruck S, Fonseca F (2017) Durable direct ethanol anode-supported solid oxide fuel cell. *Appl Energy* 199:180–186
- Stonehart P (1990) Development of advanced noble metal-alloy electrocatalysts for phosphoric acid fuel-cells (Pafc). *Ber Bunsen Phys Chem* 94:913–921
- Strahl S, Husar A, Puleston P, Riera J (2014) Performance improvement by temperature control of an open-cathode PEM fuel cell system. *Fuel Cells* 14:466–478
- Swette L, Giner J (1988) Oxygen electrodes for rechargeable alkaline fuel cells. *J Power Sources* 22:399–408
- Szymczewska D, Chrzan A, Karczewski J, Molin S, Jasinski P (2017) Spray pyrolysis of doped-ceria barrier layers for solid oxide fuel cells. *Surf Coat Technol* 313:168–176
- Tanaka S, Hirose N, Tanaki T (2000) Evaluation of Raney-nickel cathodes prepared with aluminum powder and tin powder. *Int J Hydrog Energy* 25:481–485
- Tee PF, Abdullah MO, Tan IAW, Amin MAM, Nolasco-Hipolito C, Bujang K (2017) Effects of temperature on wastewater treatment in an affordable microbial fuel cell-adsorption hybrid system. *J Environ Chem Eng* 5:178–188
- Ticianelli EA, Derouin CR, Srinivasan S (1988) Localization of platinum in low catalyst loading electrodes to attain high power densities in SPE fuel cells. *J Electroanal Chem Interfacial Electrochem* 251:275–295
- Tremouli A, Martinos M, Lyberatos G (2016) The effects of salinity, pH and temperature on the performance of a microbial fuel cell. *Waste Biomass Valori* 8:2037–2043
- Tsang CHA, Leung DYC (2017) Pd-Pt loaded graphene aerogel on nickel foam composite as binder-free anode for a direct glucose fuel cell unit. *Solid State Sci* 71:123–129
- Uribe FA, Gottesfeld S, Zawodzinski TA (2002) Effect of ammonia as potential fuel impurity on proton exchange membrane fuel cell performance. *J Electrochem Soc* 149:A293–A296
- Vecchio CL, Sebastián D, Alegre C, Aricò AS, Baglio V (2018) Carbon-supported Pd and Pd-Co cathode catalysts for direct methanol fuel cells (DMFCs) operating with high methanol concentration. *J Electroanal Chem* 808:464–473
- Wan N (2017) High performance direct methanol fuel cell with thin electrolyte membrane. *J Power Sources* 354:167–171
- Wang FC, Fang WH (2017) The development of a PEMFC hybrid power electric vehicle with automatic sodium borohydride hydrogen generation. *Int J Hydrog Energy* 42(15):10376–10389
- Wang M, Liu G, Tian Z, Shao Y, Wang L, Ye F, Tran MX, Yun Y, Lee JK (2017a) Microstructure-modified proton exchange membranes for high-performance direct methanol fuel cells. *Energy Convers Manag* 148:753–758
- Wang ZQ, Zeng YC, Sun SC, Shao ZG, Yi B (2017b) Improvement of PEMFC water management by employing water transport plate as bipolar plate. *Int J Hydrog Energy* 42:21922–21929
- Warburton A, Mossop D, Burslem B, Rama P, Adcock P, Cole J, Edwards J, Ninan D, Provost M (2013) Development of an evaporatively cooled hydrogen fuel cell system and its vehicle application. *SAE Technical Papers*. Paper Number: 2013-01-0475

- Watanabe M, Tsurumi K, Mizukami T, Nakamura T, Stonehart P (1994) Activity and stability of ordered and disordered Co-Pt alloys for phosphoric-acid fuel-cells. *J Electrochem Soc* 141:2659–2668
- Weber AZ, Newman J (2006) Coupled thermal and water management in polymer electrolyte fuel cells. *J Electrochem Soc* 153:A2205–A2214
- Wilberforce T, Alaswad A, Palumbo A, Dassisti M, Olabi AG (2016) Advances in stationary and portable fuel cell applications. *Int J Hydrog Energy* 41:16509–16522
- Wilson MS, Gottesfeld S (1992) High performance catalyzed membranes of ultra-low Pt loadings for polymer electrolyte fuel cells. *J Electrochem Soc* 139:L28–L30
- Wimmer RR (1997) Fuel cell transit bus testing and development at Georgetown University. In: Energy conversion engineering conference. IECEC-97, Proceedings of the 32nd Intersociety, 1997. IEEE, pp 825–830
- Winfield J, Chambers LD, Rossiter J, Ieropoulos I (2013) Comparing the short and long term stability of biodegradable, ceramic and cation exchange membranes in microbial fuel cells. *Bioresour Technol* 148:480–486
- Woodman A, Jayne K, Anderson E, Kimble MC (1999) Development of corrosion-resistant coatings for fuel cell bipolar plates. In: Aesf Sur Fin-proceedings. American Electroplaters and Surface Finishers Society, pp 717–726
- Wu C, Liu L, Tang K, Chen T (2017) Studies on an ultrasonic atomization feed direct methanol fuel cell. *Ultrason Sonochem* 34:60–66
- Xiong L, Manthiram A (2005) High performance membrane-electrode assemblies with ultra-low Pt loading for proton exchange membrane fuel cells. *Electrochim Acta* 50:3200–3204
- Xu Q, Zhang FH, Xu L, Leung PK, Yang CZ, Li HM (2017) The applications and prospect of fuel cells in medical field: a review. *Renew Sust Energy Rev* 67:574–580
- Yan X, Gao P, Zhao G, Shi L, Xu J, Zhao T (2017) Transport of highly concentrated fuel in direct methanol fuel cells. *Appl Therm Eng* 126:290–295
- Yang Z, Nie H, Chen X, Chen X, Huang S (2013) Recent progress in doped carbon nanomaterials as effective cathode catalysts for fuel cell oxygen reduction reaction. *J Power Sources* 236:238–249
- Yang YL, Liu XH, Hao MQ, Zhang PP (2015) Performance of a low-cost direct glucose fuel cell with an anion-exchange membrane. *Int J Hydrog Energy* 40:10979–10984
- Yang PQ, Zhang HC, Hu ZY (2016a) Parametric study of a hybrid system integrating a phosphoric acid fuel cell with an absorption refrigerator for cooling purposes. *Int J Hydrog Energy* 41:3579–3590
- Yang Z, Liao T, Zhou Y, Lin G, Chen J (2016b) Performance evaluation and parametric optimum design of a molten carbonate fuel cell-thermophotovoltaic cell hybrid system. *Energy Convers Manag* 128:28–33
- Yoon W, Huang X, Fazzino P, Reifsnider KL, Akkaoui MA (2008) Evaluation of coated metallic bipolar plates for polymer electrolyte membrane fuel cells. *J Power Sources* 179:265–273
- Yoshida T, Kojima K (2015) Toyota MIRAI fuel cell vehicle and progress toward a future hydrogen society. *Electrochem Soc Interface* 24:45–49
- You S-J, Wang X-H, Zhang J-N, Wang J-Y, Ren N-Q, Gong X-B (2011) Fabrication of stainless steel mesh gas diffusion electrode for power generation in microbial fuel cell. *Biosens Bioelectron* 26:2142–2146
- Yu X, Ye S (2007a) Recent advances in activity and durability enhancement of Pt/C catalytic cathode in PEMFC: part I. Physico-chemical and electronic interaction between Pt and carbon support, and activity enhancement of Pt/C catalyst. *J Power Sources* 172:133–144
- Yu X, Ye S (2007b) Recent advances in activity and durability enhancement of Pt/C catalytic cathode in PEMFC: part II: degradation mechanism and durability enhancement of carbon supported platinum catalyst. *J Power Sources* 172:145–154
- Yu X, Zhou B, Sobiesiak A (2005) Water and thermal management for Ballard PEM fuel cell stack. *J Power Sources* 147:184–195

- Yu J, Zhao Y, Li Y (2014) Utilization of corn cob biochar in a direct carbon fuel cell. *J Power Sources* 270:312–317
- Yuan H, Hou Y, Wen Z, Guo X, Chen J, He Z (2015) Porous carbon nanosheets codoped with nitrogen and sulfur for oxygen reduction reaction in microbial fuel cells. *ACS Appl Mat Inter* 7:18672–18678
- Zeikus J (1979) Thermophilic bacteria: ecology, physiology and technology. *Enzym Microb Technol* 1:243–252
- Zhang GD, Zhao QL, Jiao Y, Wang K, Lee DJ, Ren NQ (2012) Biocathode microbial fuel cell for efficient electricity recovery from dairy manure. *Biosens Bioelectron* 31:537–543
- Zhang H, Chen L, Zhang J, Chen J (2014) Performance analysis of a direct carbon fuel cell with molten carbonate electrolyte. *Energy* 68:292–300



Techno-economic Assessment of Thermochemical Biomass Conversion Technologies

14

Tapas Kumar Patra and Pratik N. Sheth

Abstract

This book chapter presents a comprehensive overview of the techno-economic analysis of various thermochemical biomass conversion technologies for the production of fuels, chemicals and electricity. In the first part of the chapter, a brief introduction on the importance of alternative energy sources and the need for the techno-economic analysis for thermochemical conversion processes are discussed. In the next part, various thermochemical routes for biomass conversion processes are described. The reactor configurations, operating parameters and product composition for each of these processes are also discussed. The third section of the chapter focuses on the techno-economic analysis methodology and different steps involved in carrying out the feasibility of biomass conversion processes. Different process modelling tools and cost estimation methods are also discussed in this section. While in the fourth section, different techno-economic studies carried out by various researchers for the production of fuels, chemicals and electricity through thermochemical conversion routes are discussed in terms of process description, and the results are reported. In the final section, two case studies are discussed in details for techno-economic analysis. One case study is of fast pyrolysis for transportation fuel production, and the second one is for dimethyl ether (DME) production through gasification of biomass. This chapter will be helpful for understanding different techno-economic studies available and comparison of different thermochemical conversion routes to get the desired end product at the minimum cost.

T. K. Patra · P. N. Sheth (✉)

Department of Chemical Engineering, Birla Institute of Technology and Science, Pilani, Rajasthan, India

e-mail: pratik@pilani.bits-pilani.ac.in

© Springer Nature Singapore Pte Ltd. 2018

P. K. Sarangi et al. (eds.), *Recent Advancements in Biofuels and Bioenergy Utilization*, https://doi.org/10.1007/978-981-13-1307-3_14

339

Keywords

Biomass · Thermochemical conversion · Techno-economic analysis · Pyrolysis · Gasification

14.1 Introduction

Driven by the rapid economic development in the developing countries, the global energy demand is shifting to the new emerging markets from the traditional developed countries. According to the International Energy Outlook 2017, the total world energy demand is to increase by 28% from 575 quadrillions BTU in 2015 to 736 quadrillions BTU in 2040. With growing concerns about the environment and depletion of fossil fuel sources, the demand for renewable energy sources is increasing at an exponential rate. The report of BP Energy Outlook (2017) projects that the demand for oil and gas along with coal set to decline from 86% of the total energy supply in 2015 to 75% in 2035. The report also predicted the renewable sector as the fastest-growing fuel source at a growth rate of 7.6% per year. The reasons for such rapid growth in renewable energy sector are mainly due to the availability of fossil fuel in selected regions of the world and the growing geopolitical tension in those regions, which led the other countries to look for renewable options to ensure energy security, address environmental concerns and air pollution and reduce the foreign expenditure.

There are a number of different renewable energy sources like solar, wind, biomass, geothermal and hydropower which are being explored for finding an alternate to the conventional resources. According to REN 21's 2016 Annual report, 19.2% of the total global energy consumption comes from renewable energy sources (REN 21 Annual Report 2016). Out of this, 8.9% of the energy consumed comes from traditional biomass sources; 4.2% utilized as heat energy from renewable sources like solar, geothermal and modern biomass sources; 3.9% as hydroelectricity; and the rest 2.2% utilized in the form of electricity from solar, wind, biomass, etc. Out of all these energy sources, biomass is the most economical and clean source as compared to solar, wind and others. Moreover, sources like solar and wind are mainly used for electricity generation, whereas biomass can be used for producing various products such as chemicals, fuels along with electricity and heat. Biomass can be converted to energy broadly by two different pathways, namely, biochemical and thermochemical. In biochemical pathways, biomass is degraded using biological methods such as anaerobic digestion, fermentation and enzymatic hydrolysis processes to give different products such as biogas, ethanol and various chemicals. In thermochemical conversion process as the name suggests, heat is used as the driving force to degrade biomass. In this process, the chemical energy of the biomass is converted in the form of a mixture of combustible fuels. There are a number of different processes being proposed for the production of different

chemicals and fuels using thermochemical biomass conversion process. All these processes need to be assessed for its technical and economic feasibility for sustainable production. Hence, every new chemical/fuel production process needs to be analysed for its potential of production in terms of key technological aspects as well as the cost associated with the production process. In order to carry out this, different methods and tools are used by various researchers. First of all, a process model is developed using process simulators like Aspen Plus which includes all the equipment; key production parameters in terms of temperature, pressure and flow rate are defined. Simulations are performed at different plant configurations and at various operating conditions to find the best process for production. Then cost estimation of the proposed production pathway is carried out by taking into account various investments for the plant and the associated production cost of the process. Finally, the best suitable process for minimum production cost is recommended.

14.2 Thermochemical Biomass Conversion Processes

Due to rapid demand of biomass-based energy production process, much of the focus is now shifted to different pathways for biomass conversion to chemicals, fuels, electricity, etc. Biomass conversion pathways broadly divided into biochemical and thermochemical pathways. In a thermo-chemical process, the heat is used as the energy source to degrade the biomass components into combustible fuel mixtures. The thermochemical conversion of biomass is further divided into six different processes based on the methods, reactor configuration, reaction chemistry, operating conditions and desired end product or application. In Table 14.1, various thermochemical processes, reactor configurations, operating conditions and product compositions are discussed in detail.

14.2.1 Combustion

Combustion is the simplest and the most commonly used biomass conversion process. It is the well-established technology for converting biomass to heat and electricity. Biomass combustion accounts for about 90% of the total energy generated from various biomass conversion technologies. During combustion, biomass fuel is supplied with excess amount of air in order to ensure complete conversion of biomass. In the initial stage, the combustible gases/vapours from the biomass are released due to the burning of solid biomass, which in turn burn as flames to generate the heat that can be utilized for further downstream applications. The hot combustion gases can be directly used for drying. However, it is normally used in a heat exchanger to extract its heat to produce hot air, hot water or steam.

Table 14.1 Various thermochemical biomass conversion technologies

Conversion process	Reactor configuration	Operating conditions	Product composition			References
			Gas (wt%)	Liquid (wt%)	Solid (wt%)	
Slow pyrolysis	Fixed-bed reactor, bubbling fluidized bed reactor, tubular reactor ablative pyrolyser, auger reactor, cyclone reactor, rotating cones reactor	Lower heating rate, reaction temperature between 350 and 750 °C, longer residence time, atmospheric pressure	15–30	30–50	36–60	Williams and Besler (1996) and Nachenius et al. (2013)
Fast pyrolysis		High heating rate, reaction temperature 400–550 °C, atmospheric pressure, short residence time (0.5–2 s)	13–25	65–75	12–19	Iribarren et al. (2012) and Isahak et al. (2012)
Flash pyrolysis		Rapid heating, residence time <0.5 s, reaction temperature 400–1000 °C, very small particle size	10–15	60–70	15–25	Maggi and Delmon (1994) and Home and Williams (1996)
Hydrothermal gasification	Fixed-bed gasifier, fluidized bed gasifier and entrained flow gasifier	Reaction temperature 600–1200 °C, small particle size, gasifying agent	1–2.6 m ³ /kg of biomass	–	–	Zhou et al. (2009), Alauddin et al. (2010) and Parthasarathy and Narayanan (2014)
Combustion	Fixed-bed combustor, fluidized bed combustor, entrained flow bed combustor	Reaction temperature 800–1300 °C, excess air supply	Electricity and thermal heat			Arce et al. (2013)
Hydrothermal liquefaction	Parr high-pressure reactor	Reaction temperature 250–550 °C, reactor pressure 5–25 MPa, heating rate 5–140 °C, solvent	15–20	60–75	8–20	Zhang et al. (2009)
Carbonization	Stainless steel box inside a furnace	Reaction temperature 400–1200 °C, heating rate 4–5 °C/min	–	–	20–35	Kumar et al. (1992)
Co-firing	Boiler	5–20% of biomass and rest coal	Electricity and heat			Sebastián et al. (2011)

14.2.2 Pyrolysis

Pyrolysis is the most basic and important of all biomass thermochemical conversion processes. In pyrolysis, biomass material is degraded into its constituent elements by application of heat in the absence of oxygen. The products of pyrolysis are bio-oil, non-condensable gaseous mixture and biochar. The composition of the product from the pyrolysis process depends on various operating parameters such as reactor configuration, operating temperature, heating rate and biomass particle size. Based on the operating conditions, pyrolysis process can be divided into various processes such as fast pyrolysis, slow pyrolysis, flash pyrolysis, etc.

14.2.3 Gasification

Gasification is the process of converting biomass into a combustible gaseous known as synthesis gas. The process is complex in nature, and broadly it can be divided into two parts: in the first part, the biomass is partially combusted by the supply of around 25% of the stoichiometric amount of oxygen to form producer gas and char. In the later part, CO₂ and H₂O produced in partial oxidation process are reduced by the charcoal to form a mixture rich in CO and H₂. The typical composition of the producer gas generated from the air gasification process is around 15–18% of CO and H₂, 8–10% of CO₂, 3–5% CH₄ and the rest is N₂. There are different designs of gasifiers based on the reactor configuration such as fixed bed, moving bed, fluidized bed and entrained flow. Based on the heating mechanism, the gasifiers are classified into two types that are directly heated or indirectly heated gasifiers. Inside the gasifier different zones are formed, i.e. drying, pyrolysis, combustion and gasification, and each zone can be distinguished from the other based on the temperature profile. Gasification process occurs at temperatures around 800–1000 °C and is operated at atmospheric pressure or higher. A much less calorific value syngas, i.e. less than 5.6 MJ/m³, is generated from biomass gasification process in comparison with natural gas with a calorific value of 38 MJ/m³.

14.2.4 Liquefaction

Liquefaction is a process of converting biomass into liquid fuels. The process occurs at a lower temperature than pyrolysis process, i.e. 250–450 °C, and at a higher pressure in the range of 50–150 atm. The process involves disintegration of large biomass molecules into small molecules which further polymerises to form bio-oil. This process is also known as hydrothermal liquefaction since water acts as a catalyst during the process of breaking down larger hydrocarbon molecules to smaller ones. Higher-pressure requirements and higher time duration of the process make liquefaction an expensive process; however, flexibility of biomass moisture content for the process makes it more preferable over pyrolysis and gasification

(Zhang et al. 2009). Moreover, the bio-oil obtained from liquefaction process contains lesser amount of oxygen, i.e. 12–14%, as compared to the bio-oil obtained from pyrolysis process.

14.2.5 Carbonization

Carbonization is the process of converting organic material into carbon through controlled heating. In this process, the moisture present in the biomass gets evaporated which leads to reduction of hydrogen and oxygen content of biomass and accumulation of carbon molecules. The process occurs in three temperature stages between 100 and 170 °C when the moisture present in the biomass is evaporated. From 170 to 270 °C, mixtures of condensable vapours are released, which in turn condense to form bio-oil. In the final stage between 270 and 280 °C, the biomass starts to burn, which is confirmed by the release of heat during the process. The carbonization process can be divided into three broad categories based on the process of heating such as by controlled combustion of the biomass, by supplying external heat to fossil fuel or wood and by using the hot gas from the retort from different chemical production processes.

14.2.6 Co-firing

Co-firing refers to co-feeding of a renewable or residual fuel together with the conventional fossil fuel-based system. This concept came into picture due to increasing price of fossil fuels and to reduce greenhouse gas emissions. This method is adopted in place of conventional gasification and pyrolysis process. Co-gasification of biomass has several advantages over coal and biomass gasification, which include reduction of sulphur content in the syngas and the amount of tar that is substantially reduced by blending biomass with coal for gasification. Similarly, co-pyrolysis has advantages like the higher yield of bio-oil as compared to coal pyrolysis, which is due to the high H/C ratio in biomass. In addition, higher content of volatile matter in biomass helps in better conversion and production of high-quality liquid fuel. Hence, co-firing is a preferable choice over coal or biomass conversion in order to achieve better resource utilization and reduce the environmental pollution.

14.3 Standard Methodologies for Techno-economic Analysis

The techno-economic assessment (TEA) is a tool to evaluate the viability of a project by comparing different costs and benefits associated with the project. These assessments include various steps such as:

1. Evaluation of a particular project in terms of its economic viability
2. Identification of various finance-related problems over the period of the project

3. Study on different available technologies for achieving the desired product
4. Comparison of costs associated with the available technologies

Techno-economic analysis is generally carried out for a variety of purposes and for a wide range of processes. There is no such fixed method; it varies from process to process based on the purpose of the assessment. However, the approach is somewhat similar in most of the cases; it involves cost assessment, benefit assessment, risk assessment and finally the techno-economic method.

Cost assessment is of two types: investment cost and operational cost. Investment cost includes initial investment, which further includes planning cost, consulting cost, administration cost, annual insurance cost and infrastructure cost. Similarly, operational cost comprises fuel cost, labour cost, maintenance cost and any other additional cost. Benefit assessment refers to the different source of income from the project. It can be from the selling of the product, electricity, any government benefits, carbon credits, etc. The risk assessment is one of the major steps that are normally done before starting the other two steps. It includes factors such as financial risk, environmental risk, technical risk and social risk. Different methods are being followed in order to evaluate the cost of a specific project such as:

1. Assessment of static cost–benefit method
2. Annuity method
3. Net cash flow method
4. Net present value (NPV) method
5. Internal rate of return method

The German Aerospace Center (DLR) had launched a project named ‘future fuels’ to study the economic feasibility of alternative fuels by evaluating key economic performance parameters like capital investment cost and the production cost. By comparing and analysing the existing techno-economic studies on alternative fuels, the team developed a stepwise-standardized methodology for the estimation of net production cost for alternative fuels as shown in Fig. 14.1. The methodology comprises six steps and each step decides the future of the next step. The first step of the method is the literature survey pertaining to the fuel production path. The focus of this step is to find the technologies and process concepts available in the literature along with the economic and technical data from various industrial and research institutions. In the second step, the simulation of the best process selected from the literature survey is carried out using Aspen Plus process simulator. The developed process model helps in obtaining the interdependency of various subprocesses in the fuel production plant in terms of temperature and pressure and also its cost-saving potential. Pinch analysis method is applied to the process model for the heat integration of the model which is useful in minimizing the cost due to external heating and cooling demand. The next step is the most crucial which evaluates the net present cost of the fuel production cost. The simulated model from the second step is integrated with techno-economic process evaluation tool (TEPET) by using the Aspen Simulation Workbook. The parameters calculated for

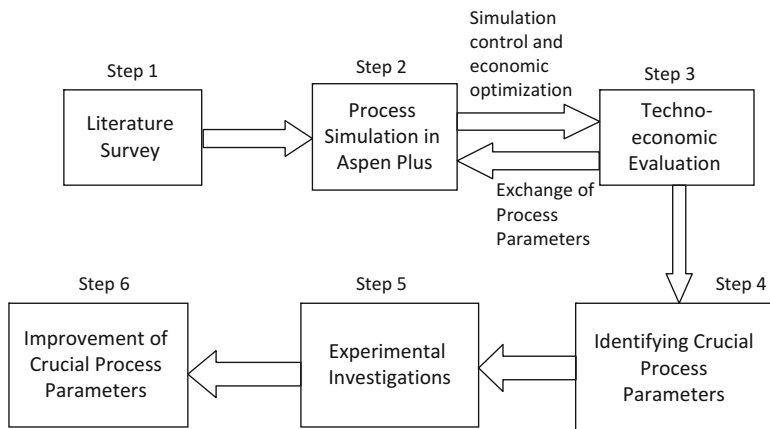


Fig. 14.1 Deutsches Zentrum für Luft- und Raumfahrt (DLR) methodology for techno-economic analysis (Albrecht et al. 2017)

the cost calculations include total capital expenditures (CAPEX), operational expenditures (OPEX) and also the net production costs (NPC) of the fuel. Based on the results of techno-economic evaluation, changes are made in the process simulation model in order to minimize the net production cost. From the first three steps, the best production process with minimum production cost is obtained. In the fourth step, the important subprocesses in the fuel production plant are identified, and in the fifth step, an experimental investigation of the chosen process with the obtained process conditions is carried out. The results of the experiments are then compared with the model predictions, and the necessary improvements are made in the process conditions.

14.4 Techno-economic Analysis of Different Thermochemical Processes

With the increasing interest in biomass thermochemical conversion process, there have been numerous studies for establishing the technology for commercial production of fuels and chemicals. As a result, various researchers have carried out techno-economic analysis for different pathways for biomass to fuels and chemical production processes. A comparison of various thermochemical conversion methods for production of different chemical/fuels and electricity has been described in Tables 14.2 and 14.3, respectively. Recently, Sara et al. (2016) carried out techno-economic analysis of small-scale (100 KW_{th}) biomass gasification-based hydrogen production plant. A block diagram of the production process is given in Fig. 14.2. The process plant consists of a circulating fluidized bed gasifier, a portable purification system (PPS), which includes catalytic candle filter, water gas shift and pressure swing absorption reactors. The study focuses on the relation between hydrogen

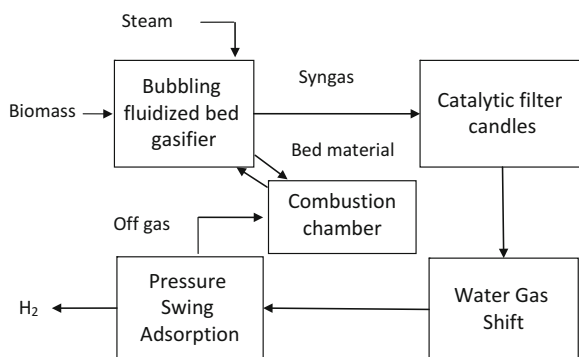
Table 14.2 Comparison of different biomass thermochemical conversion technologies based on costs of production for chemicals and fuels

End product	Biomass feedstock	Process technology	Plant capacity (tonnes/day)	Year	Production cost	Country	References
Methanol	Forest-based residues	Gasification under atmospheric pressure conditions	2000	2008	\$0.33/kg L \$16.31/GJ	Canada	Sarkar et al. (2011)
Methanol	Maize residue	Gasification with methanol synthesis using super converter	10–2000 MW _{th}	2008	\$34.24–94.26/GJ	South Africa	Amigun et al. (2010)
Ethanol	Agricultural biomass	Circulating fluidized bed gasification using air and steam	2140	2010	\$1.03/kg	Spain	Valle et al. (2013)
Dimethyl ether	Forest-based residues	Gasification under atmospheric pressure conditions	2000	2008	\$0.53/kg L \$18.40/GJ	Canada	Sarkar et al. (2011)
Ethylene	Lignocellulosic biomass	Gasification—dimethyl ether—ethylene	—	2010	\$2.24–2.30/kg	Karlsruhe, Germany	Haro et al. (2013)
Ammonia	Forest-based residues	Gasification under atmospheric pressure conditions	2000	2008	\$2.35/kg L \$124.73/GJ	Canada	Sarkar et al. (2011)
Bio-oil	Energy-based crops	Fast pyrolysis	100–800	2009	\$13.18–28.56/GJb	UK	Rogers and Brammer (2012)
Biochar	Pinewood	Slow pyrolysis	—	2012	\$0.23–0.29/kg	USA	Shabangu et al. (2014)
Hydrogen	Forest-based residues	BCL gasifier	4000	2008	\$1.32/kg \$10.98/GJ	Canada	Sarkar and Kumar (2010a, b)
Hydrogen	Forest-based residues	Fast pyrolysis with steam reforming	2000	2008	\$3.38/kg \$28.15/GJ	Canada	Sarkar and Kumar (2010a, b)
Gasoline	Woody biomass	Gasification syngas to methanol to gasoline	2000	2007	\$0.60/L \$18.07/GJ	USA	Phillips et al. (2011)
Gasoline + diesel	Stover	Fast pyrolysis with hydro-processing	2000	2011	\$0.72/L	USA	Brown et al. (2013)

Table 14.3 Comparison of different biomass thermochemical conversion technologies based on the cost of electricity production

Biomass feedstock	Process technology	Power output (MWe)	Year	Production cost (\$/MWh in 2014 USD)	Country	References
Energy crop	Biomass gasification (downdraft gasifier) based on CHP system	0.15	2013	104.04–116.30	UK	Huang et al. (2013)
Woody biomass	Subcritical CFB boiler	250	2011	173.82–318.68	Netherlands	Santos (2011)
Torrefied biomass	IGCC with CO ₂ capture	–	2008	141.89–197.19	Netherlands	Meerman et al. (2013)
Biomass	Fast pyrolysis, diesel engine	1–20	2002	88.78–177.56	UK	Bridgwater et al. (2002)
Biomass	Biomass sole plant	24	2003	166.87	Brazil	Rodrigues et al. (2003)

IGCC integrated gasification combined cycle, *CHP* combined heat and power, *CFB* circulating fluidized bed

Fig. 14.2 Schematic diagram of hydrogen production process plant

production cost with hydrogen production efficiency and cost of the purification system. The authors found that purification system cost plays an important role in reducing the overall production. The improvement in system efficiency has the least impact on reducing the cost of hydrogen production. A 50% reduction in PPS system cost and improvement of steam to biomass ratio for 1–1.5 reduced the cost of hydrogen production from 12.75 to 9.5 €/kg.

Shabangu et al. (2014) compared the feasibility of methanol and biochar production from three different systems, i.e. slow pyrolysis at 300 °C, slow pyrolysis at 450 °C and gasification at 800 °C. A simplified process description for slow pyrolysis at 300 °C and 450 °C is shown in Fig. 14.3, while Fig. 14.4 describes gasification of biomass at 800 °C. After these initial processes, the syngas from the process undergoes tar cracking, cleaning, compression, optional water gas shift and

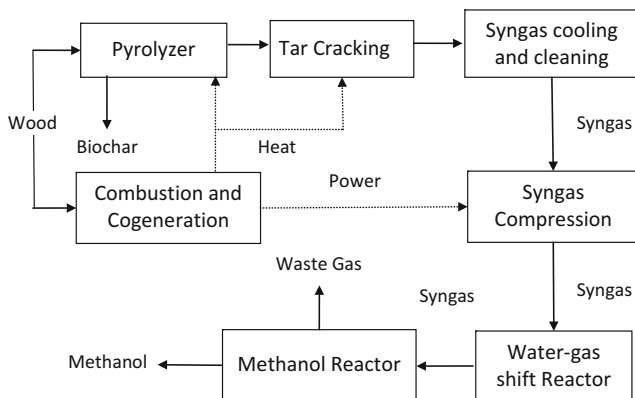


Fig. 14.3 Biomass to methanol production through pyrolysis process (Shabangu et al. 2014)

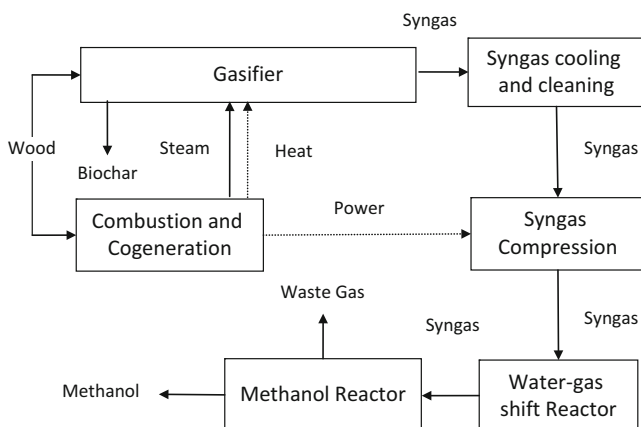


Fig. 14.4 Biomass to methanol production through gasification process (Shabangu et al. 2014)

finally the catalytic methanol production process. The results suggest that methanol production from gasification at 800 °C is more cost-effective as compared to the slow pyrolysis process. Moreover, gasification process was able to produce methanol at a lower cost compared to the methanol production from fossil fuels, which was \$ 422/tonne. The slow pyrolysis processes were cost-effective if the biomass selling cost was above \$220/tonne for slow pyrolysis at 300 °C and \$280/tonne for slow pyrolysis at 450 °C.

Andersson and Lundgren (2014) studied the techno-economic feasibility of ammonia production from a biomass gasification unit integrated with a pulp and paper mill and compared the results with a stand-alone gasification system. The schematic layout of the complete ammonia production process is given in Fig. 14.5. In this study, a pressurized entrained flow gasifier is integrated with an existing pulp and paper mill for the supply of the biomass feed. The syngas from the gasifier then

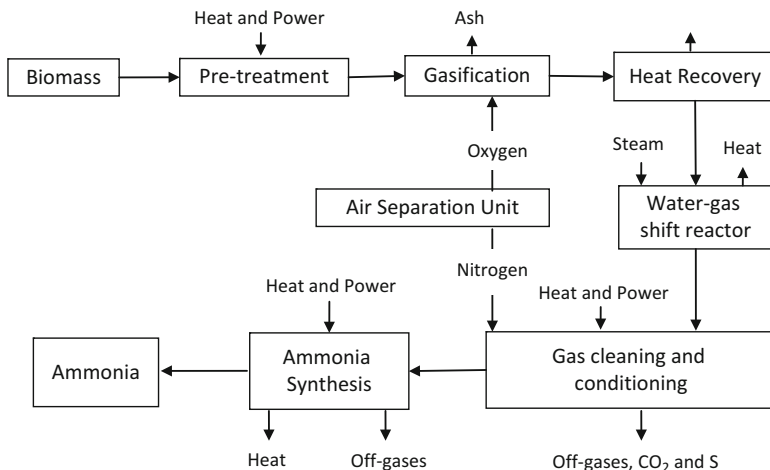


Fig. 14.5 Block diagram for gasification-based ammonia production process (Andersson and Lundgren 2014)

passed through water gas shift reactor to adjust the ratio of H_2/CO suitable for ammonia production. The cleaning and conditioning section includes an acid gas removal (AGR) unit to remove the sulphur-containing contaminants and CO_2 from the process. Finally, the syngas stream was pressurized and fed to the ammonia synthesis reactor. The study reported a higher selling price for ammonia than the current market price is required to make the process economically feasible. For the integrated gasification unit, the suggested ammonia selling price was in the range \$ 509–774/tonne to receive an internal rate of return from 10% to 20%. The study also found that larger production capacity systems might be more economically feasible as compared to small-capacity plants since the ammonia synthesis loop cost is about 45% of the total cost of the system.

Trippe et al. (2011) investigated the techno-economic feasibility of a pressurized entrained flow gasification of slurry derived from the fast pyrolysis process in a biomass-to-liquid production plant. A simple block diagram for the overall production process is shown in Fig. 14.6. The study focuses the cost of syngas production from the slurry gasification unit by varying the process conditions like operating pressure, gasifying agent, the ratio of CO and H_2 in the syngas and co-feeding of coal with biomass slurry. Aspen Plus process simulator was used for the mass and energy balance calculation for various process conditions, and cost estimation was done from literature data as well as from quotation from various suppliers. Based on the study the authors found that increasing the pressure of the system, decreasing the steam supply to the gasifier and co-feeding of 10% of biomass slurry with 90% coal substantially reduced the syngas production cost. The authors also suggested utilization of the excess heat generated from the process and selling of the nitrogen from the air separation unit for a 4–8% reduction in production cost in both cases.

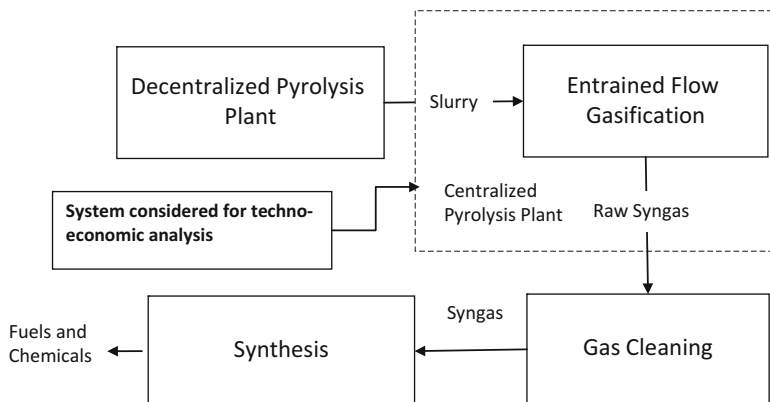


Fig. 14.6 Schematic layout for biomass to liquid fuels and chemical production through slurry gasification process (Trippe et al. 2011)

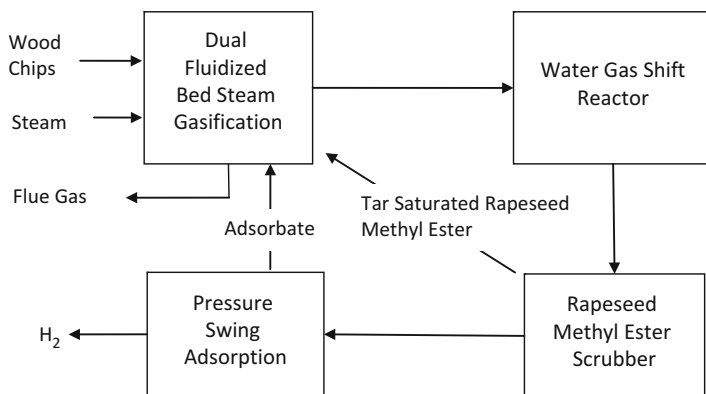


Fig. 14.7 Dual fluidized bed (DFB) biomass steam gasification process for hydrogen production (Yao et al. 2017)

Yao et al. (2017) compared the techno-economic feasibility of hydrogen production through three different processes. The processes considered for the study are dual fluidized bed (DFB) biomass steam gasification, biogas steam reforming (BSR) and alkaline electrolysis (AEL) with the downstream separation and purification systems. The process flow diagrams for all these processes are given in Figs. 14.7, 14.8 and 14.9. The techno-economic study was carried out for an imaginary business unit with capacity 90 kg/h or 1000 m³/h hydrogen. The results of the analysis reported that DFB gasification has the highest investment cost of 12.2 million Euros followed by BSR and AEL processes with investment costs of 9.9 and 4.4 million Euros, respectively, although AEL process has the minimum investment cost. However, the production cost for this process which is determined by the electricity price is very high compared to the DFB and BSR processes. The after-tax

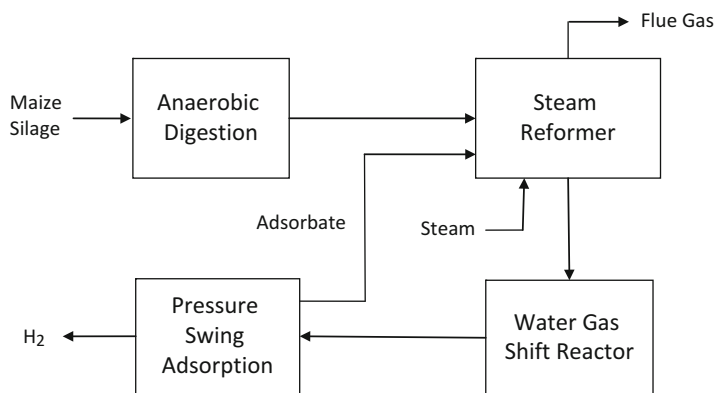
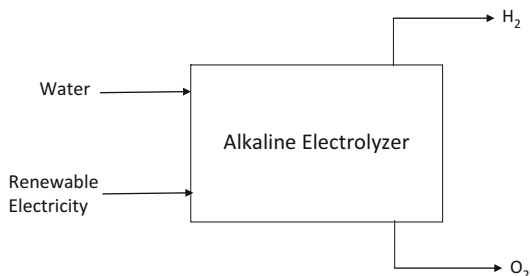


Fig. 14.8 Biogas steam reforming (BSR) process for hydrogen production (Yao et al. 2017)

Fig. 14.9 Alkaline electrolysis (AEL) process for hydrogen production (Yao et al. 2017)



break-even price (BEP) for H_2 production is the lowest for DFB biomass gasification process compared to the other two processes, whereas the before-tax BEP is the lowest for the H_2 production from the BSR process.

14.5 A Few Notable Case Studies Relating to Techno-economic Analysis in Biorefineries

14.5.1 Case Study 1

Wright et al. (2010) have presented a techno-economic case study for the production of transportation fuel (naphtha and diesel range stock) from biomass fast pyrolysis followed by hydro-processing of bio-oil. Two scenarios are developed by authors based on the hydrogen requirement fulfilment. One scenario considers the on-site hydrogen production from a fraction of bio-oil generated via reforming, while the second scenario assumes the direct purchase from the market. Brown et al. (2013) extended the techno-economic analysis carried out by Wright et al. (2010) to include the updated data from the commercial-scale fast pyrolysis facilities. Brown et al. (2013) reported that the minimum fuel selling price of gasoline and diesel fuel

produced via fast pyrolysis and hydro-processing to be \$2.57/gal in comparison to the \$2.11–\$3.09/gal of fuel product value reported by Wright et al. (2010). The salient features of this case study are incorporated here.

14.5.1.1 Process Description

The biomass considered in this study is corn stover with a plant processing capacity of 2000 dry tonnes per day. The study considers all major processing steps including pretreatment of biomass, fast pyrolysis, pyrolysis product separation and oil upgradation using hydro-processing. The processing steps are represented in Fig. 14.10.

The pretreatment steps involve drying and size reduction. The raw biomass is dried from 25% moisture content to 7% and ground to 3 mm diameter. The pyrolyser is of fluidized bed type and operating at 480 °C and at atmospheric pressure. Four pyrolysers of 500 tonnes per day in parallel mode are considered in the design. The flue gas (1.6 kg of gas per kg of dry biomass) coming out from the combustor unit is used as a fluidizing agent. The pyrolysis product distribution is adapted from the literature and adjusted to achieve mole balance.

The assumed values of the pyrolysis bio-oil and non-condensable gas composition per kg of biomass pyrolysed are reported in Table 14.4. The product separation unit includes cyclone to remove char and indirect contact heat exchanger to condense the bio-oil vapours. The condenser produces about 8000 tonnes per day of saturated steam. The non-condensable gases leaving cyclones are passed through an electrostatic precipitator to remove the aerosols and sent to the combustor for burning. The collected char from parallel cyclone section is sent to combustion unit for process heat generation. About one-third of the char produced is required to burn for meeting heat requirements. The heat generated from char and non-condensable gas combustion is used to maintain the temperature in the pyrolyser and also for drying. The bio-oil is hydro-processed to remove the undesirable oxygenated compounds and to convert large hydrocarbon molecules to

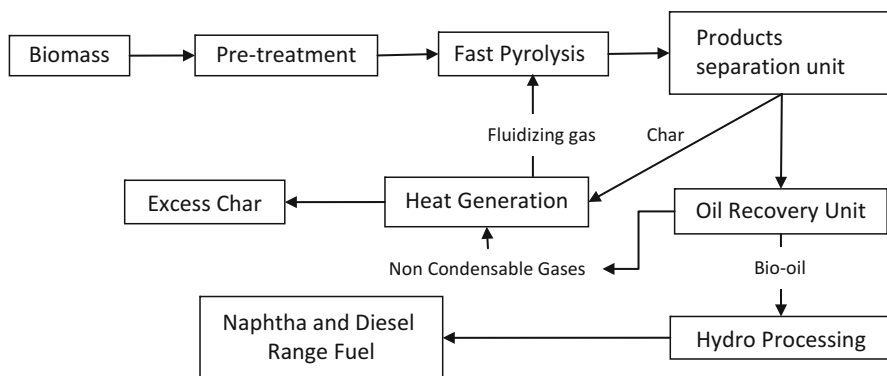


Fig. 14.10 Block diagram representing the biomass to transportation fuel process (Wright et al. 2010)

Table 14.4 Pyrolysis products (bio-oil and non-condensable gas) distribution assumptions (Wright et al. 2010)

Composition (kg/100 kg of dry biomass)					
Gas compounds		Bio-oil compounds			
CO ₂	5.42	Acetic acid	5.93	Toluene	2.27
CO	6.56	Propionic acid	7.31	Furfural	18.98
CH ₄	0.035	Methoxyphenol	0.61	Benzene	0.77
C ₂ H ₆	0.142	Ethyl phenol	3.80	Other compounds	
H ₂	0.588	Formic acid	3.41		
Propene	0.152	Propyl benzoate	16.36	Water	10.8
NH ₃	0.0121	Phenol	0.46	Char/Ash	16.39

naphtha- and diesel-range products. Hydro-treating followed by hydrocracking is employed to convert the bio-oil to transportation fuel. To fulfil the hydrogen requirement, two scenarios are discussed as briefed earlier. On-site hydrogen production utilizes the 38% of the single-phase bio-oil and upon reforming produces requisite hydrogen.

14.5.1.2 Process Economics

Wright et al. (2010) estimated the project capital expenditure using Aspen Icarus software and Peters and Timmerhaus investment factors. To calculate the product value, a modified NREL discounted cash flow rate of return (DCFRROR) analysis is used. The data used in the economic analysis is reported in Table 14.5. The authors compared the two scenarios, i.e. on-site hydrogen production and direct hydrogen purchase. The results suggest that the direct hydrogen purchase (at \$1.5 per kg) requires less capital investment (\$200 million) in comparison with on-site production total cost (\$287 million). However, the annual operating cost of the on-site production hydrogen scenario is significantly lower (\$109 million vs \$183 million). The authors reported based on the analysis that naphtha- and diesel-range products can be produced from biomass at a competitive price. It is also reported that purchasing merchant hydrogen increases higher annual cost but results in increased fuel output and lower fuel cost. The authors of this book chapter are of the opinion that the hydrogen purchase from the market does not necessarily from renewable resources. Moreover, sensitivity analysis also shows that hydrogen fuel price has a significant impact on the product value of the fuel.

14.5.1.3 Extension of the Techno-economic Analysis Presented Above

Figure 14.11 represents the block diagram of the process analysed by Brown et al. (2013). It can be compared with the Fig. 14.10. The reader may notice that there is no excess char stream. All the char produced is combusted, and excess process heat is used in waste heat boiler to produce steam and subsequently to drive a turbine to produce electricity. Another major change in the plant design is the recovery of

Table 14.5 Important design and capacity data used in the economic analysis (Wright et al. 2010)

Variable/parameters	Method/value	Remarks
Plant design method	<i>n</i> th plant design	Current state of technology
Plant life	20 years	–
Capital cost	\$287 million (higher cost due to additional equipment required)	Hydrogen production scenario
	\$200 million	Hydrogen purchase scenario
Annual operating cost	\$109 million	Hydrogen production scenario
	\$183 million	Hydrogen purchase scenario
Biomass consumption rate	2000 dry tonnes per day	–
Liquid fuel production rate	134 million litres per year	Hydrogen production scenario
	220 million litres per year	Hydrogen purchase scenario
Online time	329 days per year	90% capacity factor
Construction time	24 months	–
Start-up period	6 months	25% of construction time
Working capital	15% of the total capital investment	–
Annual maintenance materials	2% of the total installed equipment cost	–
Discounted cash flow rate of return	10%	–
Hydrogen purchase cost	\$1.5 per kg	–
Feedstock cost	\$83 per dry tonne	Includes delivery cost
Electricity cost	\$0.054 kWh	–
Catalyst replacement cost	\$1.77 million per year	Based on cost of crude oil processing

hydrogen from the off-gases leaving hydro-processing unit by pressure swing adsorption. The recovered hydrogen is compressed and recycled back in the process and unrecovered off-gases are fed to waste heat boiler.

Brown et al. (2013) estimated the capital cost using the data reported by KiOR (2011) for its Columbus, Mississippi-based plant (454 mt per day) scaled up to accommodate a 2000 mt per day commercial facility. The estimated capital cost of the plant is \$429 million due to the addition of many equipments such as large waste heat boiler, turbine and electricity generation units, pressure swing adsorption unit and compressor. The minimum fuel selling price of gasoline and diesel fuel produced via fast pyrolysis and hydro-processing to be \$2.57/gal.

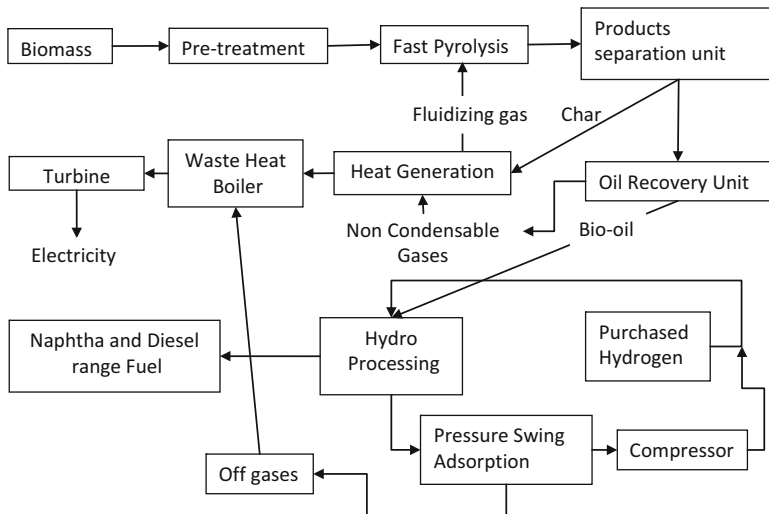


Fig. 14.11 Block diagram representing advanced process of the biomass to transportation fuel (Brown et al. 2013)

14.5.2 Case Study 2

Clausen et al. (2010) studied the techno-economics of dimethyl ether (DME) production using syngas generated from gasification of torrefied wood pellets. Two different DME production plants, namely, recycle (RC) and once-through (OT), are considered for the study. The RC plant recycles the syngas to the DME production reactor for maximizing its production, whereas in OT the unconverted syngas is sent to a combined cycle for electricity production. Both the plants include CO₂ capture system (CCS) for reducing the CO₂ emission during the DME production process. The focus of the study is to process model both the configurations using DNA (dynamic network analysis—a thermal energy system simulator) and Aspen Plus software and analyse the thermodynamic and economic performance both of the DME production plants.

14.5.2.1 Process Description

A simple block diagram for the DME synthesis process is given in Fig. 14.12. Torrefied wood was used in the process to comply with the properties of coal, and existing commercial technology was used to carry out the torrefaction and pretreatment of wood. The torrefied wood pellets are then ground and fed to the gasifier at high pressure. An entrained flow gasifier pressurized to 45 bars was used for the syngas production of wood pellets. The downstream processing of syngas from the gasifier includes a sour gas shift reactor, which maintains the H₂/CO ratio to 1 or 1.6 for the recycle (RC) and once-through (OT) plants, respectively. Thereafter,

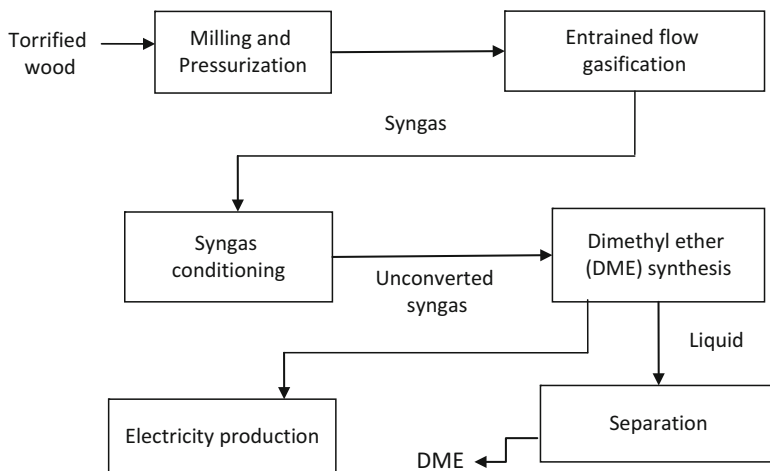


Fig. 14.12 Block diagram for dimethyl ether (DME) production process (Clausen et al. 2010)

the gas gets cooled to 30 °C followed by passing through an acid gas removal (AGR) reactor for removing the sulphur content in the gas. Then the gas at 55–60 bars of pressure is sent to the DME synthesis reactor. The operating temperature for the synthesis process is 280 °C and is maintained by passing saturated steam at 270 °C and 55 bars. The product gas stream temperatures for both recycle and once-through plants are maintained at 37 °C and 50 °C in order to remove the excess CO₂ of the DME liquid, and a gas–liquid separator is used to separate the unconverted syngas from the product stream. In case of a recycling plant, about 95% of the unconverted syngas is sent back to the synthesis reactor, and the remaining part is used for electricity production, whereas in a once-through plant, the unconverted syngas stream is sent to a combined cycle. In order to obtain high-purity DME, the liquid stream from the gas–liquid separator is passed through a two-stage fractional distillation column.

14.5.2.2 Cost Estimation

1. Plant investments

The cost estimates for both recycle and once-through plants are given in Table 14.6. It is clearly seen the major part of the cost, around 38–41% of the total investment, is for the gasification section of the plant. In addition, the plant's operating cost is slightly higher as compared to the recycling plant, which is mainly due to the higher maintenance cost of the gas turbines and heat recovery steam generators (HRSG). The savings in the DME synthesis section could not cover the cost.

2. Levelized cost calculation

The cost calculations for both the DME production plants is done by considering 20-year levelized cost calculation with a capacity factor of 90%

Table 14.6 Investment estimates for plant areas and components in the DME plants (Clausen et al. 2010)

Plant component	Size	Cost (million 2007 \$)	Scaling exponent	Overall installation factor
Air separation unit	52.0 kg-O ₂ /s	141	0.5	1
Gasification island	68.5 kg-feed/s	395	0.7	1
Water gas shift reactor	815 MW _{LHV} biomass	3.36	0.67	1.16
Acid gas removal (Rectisol)	2.48 kmol/s feed gas	28.8	0.63	1.55
CO ₂ compression to 150 bar	13 MWe	9.52	0.67	1.32
CO ₂ transport and storage	113 kg-CO ₂ /s	110	0.66	1.32
Compressors	10 MWe	6.3	0.67	1.32
DME reactor	2.91 kmol/s feed gas	21	0.65	1.52
Cooling plant	3.3 MWe	1.7	0.7	1.32
Distillation	6.75 kg/s DME	28.4	0.65	1.52
Steam turbines and condensers	275 MWe	66.7	0.67	1.16
Heat exchangers	355 MWth	52	1	1.49
Off gas boiler	355 MWth	52	1	1.49
Gas turbine	266 MWe	73.2	0.75	1.27

Table 14.7 Twenty-year leveled production costs for DME (Clausen et al. 2010)

Item	Price	Levelized cost in \$/GJ-DME	
		RC	OT
Capital charges	15.4% of plant investment	4.9	7.2
Observations and Measurements (O&M)	4% of plant investment	1.3	1.9
Torrefied biomass pellets	436 \$/GJ _{LHV}	6.9	9.3
Electricity sales	At 60 \$/MWh	-1.2	-5.4
Credit for bio-CO ₂ storage	-	0	0
DME (\$/GJ _{LHV})	-	11.9	12.9

and no credit for the storage of CO₂. From the calculations, it is reported that the cost of RC plant is less than that of the OT plant (Table 14.7). The literature data for DME production plants without CO₂ storage are \$16.9/GJ_{LHV} for OT plant and \$13.8/GJ_{LHV} for the RC plant. However, if a credit for the CO₂ storage is at \$100/ton-CO₂, the costs of DME production change to \$5.4/GJ_{LHV} for the RC plant and \$3.1/GJ_{LHV} for the OT plant.

14.6 Conclusions

In this book chapter, various thermochemical biomass treatment methods for the production of different fuels and chemicals are discussed comprehensively. The techno-economic analysis is found to be the most essential tool in order to decide the technical and economic viability of any process. However, there are very few methodologies reported for conducting the techno-economic analysis of thermochemical conversion processes of biomass. Therefore, a generic and robust methodology needs to be proposed to carry out the techno-economic analysis of various biomass conversion pathways. Additionally, most of the techno-economic studies focused on a particular process for the production of fuel or chemical rather than considering all the alternative methods which will be helpful in deciding the best combination of different subprocesses. Techno-economic analysis of any process depends mainly on three parameters, i.e. feedstock, process technology and location of the plant, so the techno-economic study must be carried out by taking into account all the possible options available and integrating them all in the study.

Many of the techno-economic analysis studies are focused on the pyrolysis of biomass, so there is enough scope to explore the much-advanced processes for production electricity from biomass such as integrated gasification combined cycle (IGCC), biomass gasification integrated with diesel engine or gas turbine, etc. Liquefaction and carbonization processes are almost neglected in terms of availability of the techno-economic studies; hence more studies need to be carried out on these processes as well. Biomass co-firing is the most attractive alternative to increase the production capacity and to reduce the environmental concerns for existing fossil fuel-based plants. Hence, more techno-economic analysis studies are required for different co-firing options. One of the major concerns for the techno-economic analysis is the availability and access to reliable and transparent plant data. This needs to be addressed by choosing suitable cost range for a particular product through comparison of various production processes. The calibration of results from the techno-economic analysis in the actual plant needs to be given utmost priority to decide the validity of the results. In a short-term goal, more focus should be given to the techno-economic analysis of already existing plants to improve their conversion efficiency, reduce the cost of production and expand their production capacity.

References

- Alauddin ZABZ, Lahijani P, Mohammadi M, Mohamed AR (2010) Gasification of lignocellulosic biomass in fluidized beds for renewable energy development: a review. *Renew Sust Energy Rev* 14:2852–2862
- Albrecht FG, König DH, Baucks N, Dietrich RU (2017) A standardized methodology for the techno-economic evaluation of alternative fuels – a case study. *Fuel* 194:511–526

- Amigun B, Gorgens J, Knoetze H (2010) Biomethanol production from gasification of non-woody plant in South Africa: optimum scale and economic performance. *Energy Policy* 38:312–322
- Andersson J, Lundgren J (2014) Techno-economic analysis of ammonia production via integrated biomass gasification. *Appl Energy* 130:484–490
- Arce M, Saavedra Á, Míguez J, Granada E, Cacabelos A (2013) Biomass fuel and combustion conditions selection in a fixed bed combustor. *Energies* 6:5973–5989
- BP Energy Outlook (2017) 2017 Edition
- Bridgwater AV, Toft AJ, Brammer JG (2002) A techno-economic comparison of power production by biomass fast pyrolysis with gasification and combustion. *Renew Sust Energ Rev* 6:181–246
- Brown TR, Thilakarathne R, Brown RC, Hu G (2013) Techno-economic analysis of biomass to transportation fuels and electricity via fast pyrolysis and hydroprocessing. *Fuel* 106:463–469
- Clausen LR, Elmegaard B, Houbak N (2010) Technoeconomic analysis of a low CO₂ emission dimethyl ether (DME) plant based on gasification of torrefied biomass. *Energy* 35:4831–4842
- Haro P, Trippe F, Stahl R, Henrich E (2013) Bio-syngas to gasoline and olefins via DME – a comprehensive techno-economic assessment. *Appl Energy* 108:54–65
- Horne PA, Williams PT (1996) Influence of temperature on the products from the flash pyrolysis of biomass. *Fuel* 75:1051–1059
- Huang Y, McIlveen-Wright DR, Rezvani S, Huang MJ, Wang YD, Roskilly AP, Hewitt NJ (2013) Comparative techno-economic analysis of biomass fuelled combined heat and power for commercial buildings. *Appl Energy* 112:518–525
- Iribarren D, Peters JF, Dufour J (2012) Life cycle assessment of transportation fuels from biomass pyrolysis. *Fuel* 97:812–821
- Isahak WNRW, Hisham MWM, Yarmo MA, Yun Hin TY (2012) A review on bio-oil production from biomass by using pyrolysis method. *Renew Sust Energ Rev* 16:5910–5923
- KiOR (2011) In: Commission S.A.E (ed) Form 10-Q quarterly report. KiOR, Washington, DC
- Kumar M, Gupta RC, Sharma T (1992) Effects of carbonisation conditions on the yield and chemical composition of Acacia and Eucalyptus wood chars. *Biomass Bioenergy* 3:411–417
- Maggi R, Delmon B (1994) Comparison between ‘slow’ and ‘flash’ pyrolysis oils from biomass. *Fuel* 73:671–677
- Meerman JC, Knoope MMJ, Ramírez A, Turkenburg WC, Faaij APC (2013) Technical and economic prospects of coal- and biomass-fired integrated gasification facilities equipped with CCS over time. *Int J Greenh Gas Control* 16:311–323
- Nachenius RW, Ronse F, Venderbosch RH, Prins W (2013) Biomass pyrolysis. In: Murzin DY (ed) *Advances in chemical engineering*. Academic, Burlington, pp 75–139
- Parthasarathy P, Narayanan KS (2014) Hydrogen production from steam gasification of biomass: influence of process parameters on hydrogen yield – a review. *Renew Energ* 66:570–579
- Phillips SD, Tarud JK, Bidy ML, Dutta A (2011) Gasoline from woody biomass via thermochemical gasification, methanol synthesis, and methanol-to-gasoline technologies: a technoeconomic analysis. *Ind Eng Chem Res* 50:11734–11745
- REN21 Annual Report (2016) 2016 Edition
- Rodrigues M, Faaij APC, Walter A (2003) Techno-economic analysis of co-fired biomass integrated gasification/combined cycle systems with inclusion of economies of scale. *Energy* 28:1229–1258
- Rogers JG, Brammer JG (2012) Estimation of the production cost of fast pyrolysis bio-oil. *Biomass Bioenergy* 36:208–217
- Santos S (2011) Techno-economic evaluation of biomass fired or co-fired power plant with post-combustion capture. Regional workshop for the Baltic Sea and Central & Eastern European countries. Vilnius, Lithuania. http://www.ieaghg.org/docs/General_Docs/IEAGHG_Presentations/S_Santos_-_CGS_CO2_East_Net_Mtg_Biomass_CCS.pdf
- Sara HR, Enrico B, Mauro V, Andrea DC, Vincenzo N (2016) Techno-economic analysis of hydrogen production using biomass gasification – a small scale power plant study. *Energy Proc* 101:806–813

- Sarkar S, Kumar A (2010a) Biohydrogen production from forest and agricultural residues for upgrading of bitumen from oil sands. *Energy* 35:582–591
- Sarkar S, Kumar A (2010b) Large-scale biohydrogen production from bio-oil. *Bioresour Technol* 101:7350–7361
- Sarkar S, Kumar A, Sultana A (2011) Biofuels and biochemicals production from forest biomass in Western Canada. *Energy* 36:6251–6262
- Sebastián F, Royo J, Gómez M (2011) Cofiring versus biomass-fired power plants: GHG (Greenhouse Gases) emissions savings comparison by means of LCA (Life Cycle Assessment) methodology. *Energy* 36:2029–2037
- Shabangu S, Woolf D, Fisher EM, Angenent LT, Lehmann J (2014) Techno-economic assessment of biomass slow pyrolysis into different biochar and methanol concepts. *Fuel* 117:742–748
- Trippe F, Fröhling M, Schultmann F, Stahl R, Henrich E (2011) Techno-economic assessment of gasification as a process step within biomass-to-liquid (BtL) fuel and chemicals production. *Fuel Process Technol* 92:2169–2184
- Valle CR, Perales ALV, Vidal-Barrero F, Gómez-Barea A (2013) Techno-economic assessment of biomass-to-ethanol by indirect fluidized bed gasification: impact of reforming technologies and comparison with entrained flow gasification. *Appl Energy* 109:254–266
- Williams PT, Besler S (1996) The influence of temperature and heating rate on the slow pyrolysis of biomass. *Renew Energy* 7:233–250
- Wright MM, Daugaard DE, Satrio JA, Brown RC (2010) Techno-economic analysis of biomass fast pyrolysis to transportation fuels. *Fuel* 89:S2–S10
- Yao J, Kraussler M, Benedikt F, Hofbauer H (2017) Techno-economic assessment of hydrogen production based on dual fluidized bed biomass steam gasification, biogas steam reforming, and alkaline water electrolysis processes. *Energy Convers Manag* 145:278–292
- Zhang B, von Keitz M, Valentas K (2009) Thermochemical liquefaction of high-diversity grassland perennials. *J Anal Appl Pyrolysis* 84:18–24
- Zhou J, Chen Q, Zhao H, Cao X, Mei Q, Luo Z, Cen K (2009) Biomass–oxygen gasification in a high-temperature entrained-flow gasifier. *Biotechnol Adv* 27:606–611



An Overview of Techno-economic Analysis and Life-Cycle Assessment of Thermochemical Conversion of Lignocellulosic Biomass

15

Ranjeet Kumar Mishra and Kaustubha Mohanty

Abstract

Energy derived from biomass provides a promising alternative source that reduces dependence on fossil fuels along with the emission of greenhouse gases (GHG). The production of heat, electricity, power, fuels, and various chemicals from the biomass can be achieved via thermochemical conversion technologies. This chapter summarizes the techno-economic analysis and life-cycle assessment of lignocellulosic biomass via thermochemical conversion routes such as combustion, pyrolysis, gasification, liquefaction, (hydrothermal) and co-firing. Specific indicators such as production costs, techno-economic analysis, functional units, and environmental impacts in a life-cycle analysis for different techniques were compared. Finally, the research lacunae and possible future trends in biomass conversion via thermochemical conversion techniques have been discussed, which may positively impact the future of research related to techno-economic and environmental benefits of bioenergy.

Keywords

Biomass · Thermochemical techniques · Techno-economic analysis · Life cycle assessments

R. K. Mishra · K. Mohanty (✉)

Department of Chemical Engineering, Indian Institute of Technology Guwahati, Guwahati, Assam, India

e-mail: kmohanty@iitg.ernet.in

© Springer Nature Singapore Pte Ltd. 2018

P. K. Sarangi et al. (eds.), *Recent Advancements in Biofuels and Bioenergy Utilization*, https://doi.org/10.1007/978-981-13-1307-3_15

363

Abbreviations

AAS	Acid-acid synthesis
BCB	Bubbling circulating bed
CHP	Catalytic fast pyrolysis and hydroprocessing
COE	Cost of electricity
COS	Carbonyl sulfide
DME	Dimethyl ether
FTS	Fischer-Tropsch synthesis
GHG	Greenhouse gas emissions
HCN	Hydrogen cyanide
HPH	Hydropyrolysis and hydroprocessing
IGCC	Integrated gasification combined cycle
kWh	Kilowatt hour
LCA	Life-cycle assessment
MAG	Methanol-to-gasoline
MAS	Mixed alcohol synthesis
MJ	Megajoule
MTE	Methanol-to-ethanol
MW	Megawatt
MWe	Megawatt electric
MWh	Megawatt hour
ORC	Organic Rankine cycle
PC	Pulverized coal-fired
RFS2	Revised renewable fuel standard
RME	Rapeseed methyl ester
S2D	Syngas-to-distillates
SF	Syngas fermentation
SNG	Synthetic natural gas
TEA	Techno-economic analysis

15.1 Introduction

Biomass has garnered considerable attention as a viable resource for the production of fuel, value-added chemicals, power, and electricity. In addition, the biomass-derived fuels have a definite advantage over fossil fuel in terms of emission such as CO, CO₂, SO_x, and NO_x gases. Currently, fossil fuels are the principal sources of energy for the entire world. However, the use of fossil fuel emits a high amount of greenhouse gases (GHG) and particulate matter in the environment, which adversely impact the environment. Additionally, the rapid depletion of fossil fuel resources has forced researchers to develop new technologies and strategies. Energy from the

renewable sources is the best alternative to fossil fuel. In 2007, the US Congress set new revised renewable fuel standard (RFS2) in which biofuel was used as an alternative fuel to reduce the consumption of petroleum fuel from domestic uses (Brown 2015). The RFS2 issued an official order to increase the blending volume of biofuel with petroleum fuels such as diesel and gasoline for retail use (Brown 2015).

Among all the renewable energy sources such as solar, geothermal, wind, hydrogen and fuel cell, hydrothermal, tidal, biomass, etc., biomass has the potential to produce energy as well as different types of value-added products. The thermochemical conversion technology is the best route to convert biomass into end products in solid, liquid, and gaseous forms. Further, the efficiency of thermochemical technology depends on the types of biomass to produce different kinds of value-added products (Demirbas 2001).

There are many thermochemical conversion technologies, which produce various value-added products and energy such as combustion, pyrolysis, gasification, liquefaction (hydrothermal), carbonization, and co-firing. Among all the available thermochemical conversion technologies, pyrolysis can convert biomass into solid, liquid, and gas without consuming oxygen. Liquid fuel and gaseous products are the two major products of thermochemical technology which can be further upgraded into the various valuable forms of energy such as transportation fuel, electricity, and value-added chemicals. The significant advantage of lignocellulosic biomass over other feedstocks is that they can be sourced from the nonedible parts of food crops. Thus, their production does not deplete resources meant for food crops nor do they cause a food crisis. However, the crops specifically cultivated for energy production may compete with conventional crops for the use of land (area for cultivation), particularly when the former get subsidies for cultivating the energy crops (Rathmann et al. 2010), although in some cases, energy crops are grown in marginal lands (Liu et al. 2011) and do not compete with other conventional crops for land. The use of biomass for the production of power and energy has been around since the nineteenth century; it was the widespread adoption of thermochemical technology in 2012 that made it a significant player in the energy sector. Thus, when the USA sets up a commercial-scale biorefinery plant, the catalytic fast pyrolysis and hydroprocessing (CHP) yielded 10 million gallons/year of bio-based gasoline and diesel, produced from the yellow pine feedstock (Lane 2013).

Though the viability of setting up more such biorefineries is dependent on the techno-economic analysis (TEA) and life-cycle assessment (LCA) of lignocellulosic biomass, there is a clear paucity of available data. Bridgwater et al. (2002) reported a comparative study of techno-economical assessment of biomass pyrolysis, combustion, and gasification for production of electricity. The same source reported that combining a diesel engine with fast pyrolysis is a significant option for electricity production, with the promise of long-term profits. The report of Gnansounou and Dauriat (2010) on techno-economic analysis of lignocellulosic biomass singled out the high cost of biomass feedstock, as the main factor that must be brought down, to reduce the overall production cost of lignocellulosic bioethanol. The production of biofuel (second generation) from the lignocellulosic biomass by using thermochemical process (fast pyrolysis) was reported by Damartzis and Zabaniotou

(2011). They also focused the possible opportunity and future challenges in process integration applications. Muench and Guenther (2013) have carried out life-cycle assessment on conversion of biomass into heat and electricity, through thermochemical technologies. Menten et al. (2013) reviewed the generation of greenhouse gas (GHG) emission via the thermochemical processes by using meta-regression analysis model.

This present study is focused on the techno-economic analysis and life-cycle assessment of lignocellulosic biomass using thermochemical conversion technology. Life-cycle analysis is an important tool to estimate the potential of environmental impact on end products through various processes in the complete life cycle. Life-cycle analysis is a systemic tool used to evaluate the materials and inputs and output parameters where the generation of emission and subsequent environmental impact of the products is estimated during biomass life cycle. Life-cycle analysis has been done using the ISO series 14040, but the calculation is less proficient by this method because this method was based on data-intensive process. The ISO series 14040 stated that life-cycle assessment has been categorized into four stages. The first stage deals with the selection of the goals, scopes, and boundary definitions. The second stage is characterized by life-cycle inventory analysis. The third stage is distinguished by life-cycle impact and assessment, and the fourth stage is earmarked for result interpretation (Schenk 2009). Four major and cardinal parameters, the feedstocks, system boundaries, functional unit, and environmental impact, determine the life-cycle assessment analysis. By evaluating the techno-economic analysis of different kinds of thermochemical conversion technologies, the most economical route can be identified.

15.2 Biomass to Energy Conversion Technologies

Biomass feedstocks, environment, and economic considerations are the three major parameters which are known to directly influence conversion of biomass into fuel and energy. Conversion of biomass to energy products can be achieved via three main processes such as biochemical process, thermochemical process, and mechanical extraction. Thermochemical and biochemical technologies are widely adopted, whereas mechanical extraction is used for the production of fuel from biomass from sources like rapeseed methyl ester (RME). However, mechanical extraction is not used extensively because of lower yield. Biochemical technology is associated with aerobic and anaerobic digestion, whereas thermochemical process includes combustion, gasification, pyrolysis, and liquefaction (Demirbas 2007). The detailed schemes of conversion of biomass are presented in Fig. 15.1.

15.2.1 Biochemical Conversion of Biomass

Conversion of biomass into value-added products through the biochemical process is an ancient technology. For example, India and China were using this technology for

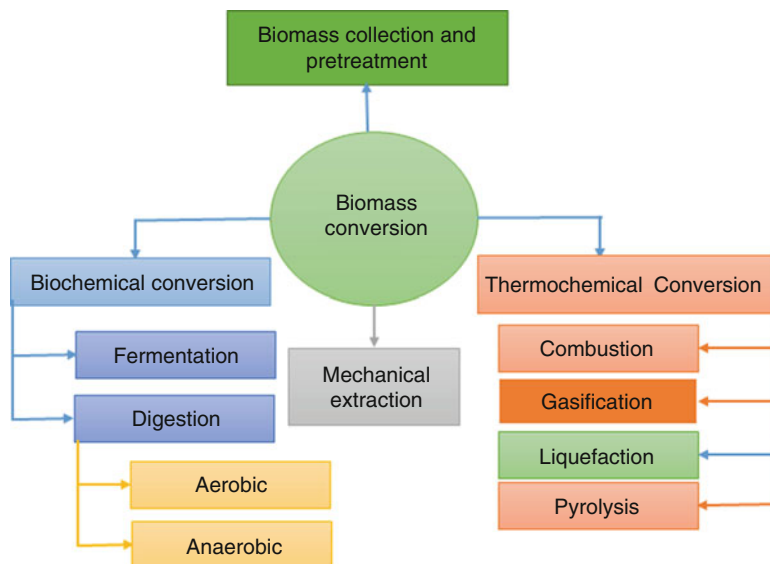


Fig. 15.1 General schemes of biomass to energy conversion routes

a long time for the production of methane gas via anaerobic microbial digestion using animal waste as raw material. Recently, biochemical techniques have been used for the production of automotive fuel (ethanol) through the fermentation process. During biochemical conversion of biomass, higher molecular weight compounds break down into smaller molecular weight compounds by the use of bacteria or enzyme. Among the available technologies, the biochemical conversion method stands out for its significantly low energy requirement; it is handicapped by the long incubation period required for conversion of materials into products. The major routes of the biochemical process are digestion (aerobic and anaerobic), fermentation, and enzymatic or acid hydrolysis.

Anaerobic digestion is a process in which microorganisms break down biodegradable materials in the absence of oxygen. Methane and carbon dioxide are the final products of anaerobic digestion along with some solid residue. Bacteria consume the carbon present within the biomass and break down into smaller compounds. The aerobic process uses oxygen from the outside of the biomass to break down the biomass into smaller compounds. The fermentation process is a biochemical process in which biomass is converted into sugars by use of acid or enzyme. Furthermore, sugar is converted into ethanol or other various value-added chemicals. Lignin is left as residue due to its higher thermal stability. However, production of ethanol from starch- and sugar-based feedstocks via fermentation process has been commercialized. Lignocellulosic biomass requires acid, enzymatic, or hydrothermal treatment to break down the cellulose and hemicellulose into simple sugars, which in turn are carried out by bacteria, yeast, and enzymes.

15.2.2 Thermochemical Conversion of Biomass

In the thermochemical process, heat is supplied for breaking higher molecular weight compounds into smaller molecular weight compounds. During thermochemical conversion, biomass is converted into gases which are later synthesized into desired products or used directly in engine and boilers. Synthesis of syngas into liquid fuel via Fischer-Tropsch is the best example of thermochemical conversion. Energy from the biomass can be extracted by six routes such as combustion, pyrolysis, gasification, liquefaction, carbonization, and co-firing.

15.2.2.1 Combustion

Burning of biomass in the existence of air or O_2 is known as combustion. It is the simplest of all thermochemical techniques. This process includes homogeneous and heterogeneous reactions. The stored chemical energy in biomass is converted into heat energy, power, electricity mechanical energy, and several other products by using the different types of devices such as furnaces, stoves, steam turbines, boilers, etc., during combustion. Further, the advantage of combustion over other process is that it has the potential to burn any biomass, but in practice, biomass having less than 50% moisture is more efficient unless biomass is pre-dried. If biomass contains more than 50% moisture, then the biological process is more proficient (Sharma et al. 1999). However, it was reported that hydrothermal liquefaction is a cost-effective thermochemical technique which can handle biomass with any level of moisture content (Akhtar and Amin 2011). There are several applications of combustion such as domestic heating, cooking, and large-scale industries (100–1300 MW power production). To increase the combustion efficiency, co-combustion (biomass with coal) is an attractive option/route. Total conversion efficiencies achieved were 22–40% through biomass combustion. Meanwhile, higher combustion efficiency can be reached via co-combustion or when the plant is more than 100 MWe (Kumar et al. 2015). Stirling cycle is used for combustion to deliver shaft power directly, but it is limited only to small outputs. Due to the higher emission of NO_x , carbon dioxide, particulate matter, and formation of higher ash content make this process unfeasible (Kumar et al. 2003a).

15.2.2.2 Gasification

Gasification is the thermochemical process where biomass is converted into a mixture of gases with the presence of oxygen, steam, or air at the higher temperature (>700 °C). Pyrolysis and gasification are known as an extension of combustion in which gaseous products are enhanced as compared with solid (biochar). However, the gaseous products are further being condensed and liquid fuel formed. Further, using oxygen gas as the gasifying agent rather than air improved the calorific value of product gas and removed nitrogen. There are many controlling parameters such as rate of heating, the design of the reactor, and post-processing of gases which produced a clean and high quality of gas through gasification. Gas with lower calorific value can be achieved through direct burning which can be used as a fuel for the gas engine and gas turbine. On the other side, production of methanol from

these gases is the best example of gasification (Ganesh and Banerjee 2001). Biomass integrated gasification is one of the promising routes where gaseous fuel is converted into electricity through higher efficiency turbines. Biomass integrated gasification process has various advantages over the other processes, attributed to its lower equipment cost and production of clean gas. About 40–50% net conversion efficiencies can be achieved by gasification for 30–60 MW plant capacity (Kumar et al. 2015). The produced syngas from the gasification was used for the production of potential fuels such as methanol and hydrogen, which are used in transport vehicles. It was observed that indirect gasification or blown oxygen is preferred for the production of methanol.

Over the time, various gasification routes have been developed for the production of syngas. These processes are used for the conversion of biomass into fuel such as ethanol- and hydrocarbon-based fuel by catalytic treatment. Among all the developed routes, acid-acid synthesis (AAS), Fischer-Tropsch synthesis (FTS), mixed alcohol synthesis (MAS), methanol-to-gasoline (MAG), methanol-to-ethanol (MTE), syngas-to-distillates (S2D), and syngas fermentation (SF) are the popular routes. All the gasification routes, which are used for upgradation of syngas, employ different kinds of catalysts. These catalysts may have certain negative impacts such as the presence of contaminants in the raw syngas such as H_2S , carbonyl sulfide (COS), NH_3 , hydrogen cyanide (HCN), HCl, tar, and different types of particulate matter. Therefore, the syngas requires cleaning before upgradation (Woolcock and Brown 2013). The catalysts such as ZnO and CuO are used for the production of methanol via acid-acid synthesis (AAS) technology. However, iodide- and iridium-based catalysts were used for the production of acetic acid from methanol (Zhu and Jones 2009). Furthermore, the produced acetic acid was upgraded with hydrogenation process and produced a mixture of ethanol and water. After separation of water from the mixture, fuel grade ethanol was produced. Methanol-to-ethanol, methanol-to-gasoline synthesis, and syngas-to-distillates pathways also produced methanol by converting syngas at the initial stages. All the pathways reacted with methanol over dehydration catalysts and produced dimethyl ether (DME) in the methanol-to-ethanol (MTE) pathway.

Dimethyl ether (DME) is converted into methyl acetate through heterogeneous catalytic carbonylation. Further methyl acetate is again hydrogenated to produce methanol. However, in case of MTG pathway, dimethyl ether (DME) reacts with the zeolite catalyst and yields alkenes and a blend of aromatics, which have the boiling points equivalent to gasoline (Phillips et al. 2011). The methanol dehydration and hydrocarbon synthesis phases are combined with syngas-to-distillates (S2D) pathways by the reaction of methanol with appropriate catalysts in a single reactor. The syngas is then compressed before combining with methanol and reacting over as metal sulfide catalysts to produce mixed alcohol stream during methanol-to-gasoline (MAS) route. The mixed stream is then separated into individual components such as ethanol, methanol, and alcohols. Further, the produced methanol is recycled, while ethanol is upgraded by distillation process to produce a high-quality fuel. During Fischer-Tropsch synthesis (FTS), the syngas reacts with metal catalysts such as cobalt, iron, and ruthenium catalysts to produce alkanes and hydrocarbons waxes.

Syngas fermentation (SF) routes ferment the cleaned syngas (not cleaned with catalysts) with *Clostridium* bacterium (Abubackar et al. 2011). The use of biocatalyst combines the carbon dioxide and hydrogen gas in the syngas to yield ethanol. Upgradation of syngas through biochemical routes has several advantages over catalytic synthesis process such as high selectivity, consolidation of process steps, and lower operational pressure and reduced the sensitivity of biocatalysts to sulfur and nitrogen contaminants in syngas compared with the metal catalyst. However, lower mass transfer between gaseous feedstock and the microorganism is the major disadvantage (Koroneos et al. 2008).

15.2.2.3 Pyrolysis

The cracking of biomass or organic materials in the absence or partial presence of oxygen at moderate temperature (400–700 °C) is known as pyrolysis. Brown (2015) reported that thermal decomposition of biomass at temperature range 300–700 °C to produce solid, liquid, and gases is known as pyrolysis. Among all the thermochemical techniques, pyrolysis can produce solid, liquid, and gas products. The production of liquid fuel is a major consideration through pyrolysis which can be further upgraded for extraction of various value-added chemicals. However, recently pyrolysis is used for the production of biochar which can be used as an excellent biochar for various applications such as adsorption of toxic gases, soil abetments and fertilizers, and water and wastewater (Mohan et al. 2014). Various process parameters such as heating rate, temperature, particle size, feed composition, types of reactor, sweeping gas flow rate, and composition of biomass affected pyrolysis. Temperature, heating rate, and residence time are the major parameters that influenced pyrolysis. Further, particle size also affected pyrolysis product yields (Graham et al. 1984).

Based on the process conditions, pyrolysis is grouped into six subcategories and presented in Table 15.1. However, based on the application of pyrolytic liquid as a transportation fuel, pyrolysis is divided into four major categories. The slow pyrolysis and upgrading of syngas are considered as the first type; fast pyrolysis and hydroprocessing (FPH) is the second type; catalytic pyrolysis and hydroprocessing (CPH) is the third, while hydropyrolysis and hydroprocessing (HPH) are considered as forth type of pyrolysis. Slow pyrolysis has the lower temperature and lower residence time (5–45 min). Hence, decomposition occurred over the long period. Slow pyrolysis is operated at lower temperature <400 °C (mostly), which yields a higher amount of char along with lower yield of liquid, which is the complex mixture of acids (acetic acids, formic acids, carboxylic acid) and water.

Slow pyrolysis is used for a long time for cooking purposes, but recently it has been used for the production of potential fuel such as methanol and for fertilizer production (Shabangu et al. 2014). During fast pyrolysis, biomass is decomposed at a much higher temperature (500 °C) and higher heating rate, which converts biomass into fuel and chemicals within a few seconds. During fast pyrolysis, the liquid yield is higher compared with biochar and syngas. Biochar and syngas are low value-added products that are used for combustion for getting heat and power. In fast

Table 15.1 The summary of a few biomass thermochemical technologies

Conversion technology	Process condition	Reactor types	Product yield	References
Fast pyrolysis	Smaller particle size (<3 mm); short residence time (0.5–2 s); moderate temperature (400–600 °C) in the absence of oxygen; atmospheric pressure	Fixed bed reactor, tubular reactor, bubbling fluidized bed reactor, auger reactor, rotating cone reactor, ablative pyrolyzer, cyclone reactor, Py-GC/MS	Liquid: 65–75 wt%	Isahak et al. (2012), Carlson et al. (2009), Jones et al. (2009), Xianwen et al. (2000), Thangalazhy-Gopakumar et al. (2010), and Lu et al. (2011)
			Gas: 13–25 wt%	
			Solid: 12–19 wt%	
Slow pyrolysis	Slow heating rate; moderate temperature (350–750 °C); atmospheric pressure or desired pressure; long residence time; presence of nitrogen and absence of oxygen gas	Batch reactor, semi-batch reactor, static batch reactor	Liquid: 30–50 wt%	Williams and Besler (1993, 1996), Shadangi and Singh (2012), Sinağ et al. (2004), and Shadangi and Mohanty (2014a, b)
			Gas: 15–30 wt%	
			Solid: 30–60 wt%	
Intermediate pyrolysis	Moderate temperature (<500 °C); moderate vapor residence time (4–10 s); atmospheric pressure	–	Liquid: 45–55 wt%	Kebelmann et al. (2013)
			Gas: 25–35 wt%	
			Solid: 15–25 wt%	
Flash pyrolysis	Rapid heating (<0.5 s); smaller particle sizes (<0.5 mm); higher temperature (400–1000 °C)	–	Liquid: 60–70 wt%	Scott et al. (1985), Scott and Piskorz (1984), Liden et al. (1988), and Samolada and Vasalos (1991)
			Gas: 10–15 wt%	
			Solid: 15–25 wt%	
Vacuum pyrolysis	Moderate temperature (300–600 °C); pressure: <50 kPa	–	Liquid: 45–60 wt%	Xu et al. (2009), Patel et al. (2011), and Boucher et al. (2000)
			Gas: 17–27 wt%	
			Solid: 19–27 wt%	
Ablative pyrolysis	Moderate temperature (450–600 °C); atmospheric pressure; particle size: 1.4–3.5 mm;	–	Liquid: 60–80 wt%	Peacocke (1994) and Lédé (2003)
			Gas: 6–10 wt%	
			Solid: 12–20 wt%	

(continued)

Table 15.1 (continued)

Conversion technology	Process condition	Reactor types	Product yield	References
	slightly higher residence time			
Hydrothermal gasification	High temperature (600–1200 °C); presence/absence of catalyst; small particle size; gasifying agents	Fixed bed, moving bed, fluidized bed, and entrained flow gasifier	Gas: 1–2.6 m ³ /kg	Parthasarathy and Narayanan (2014), Zhou et al. (2009), and Alauddin et al. (2010)
Combustion	High temperature, 740–1300 °C; air mass flow, 0.1–0.5 kg/m ² .s	Fixed bed, fluidized bed, circulating bed, and entrained flow bed combustor, drop tube furnace	Power and heat	Arce et al. (2013), Nussbaumer (2003), and Wang et al. (2014)
Co-combustion	Higher temperature: 700–1100 °C	Boiler	Power and heat	Hein and Bemtgen (1998), Spliethoff and Hein (1998), and Nussbaumer (2003)
Hydrothermal/thermochemical liquefaction	Moderate to high temperature, 250–550 °C; pressure, 5–25 MPa; heating rate, 5–140 °C/min; solvent required	Parr high-pressure reactor	Liquid: 60–75 wt%	Zhang et al. (2009)
			Gas: 15–20 wt%	
			Solid: 8–20 wt%	
Carbonization	Low to high temperature, 400–1200 °C; heating rate, 4–5 °C/min	Stainless steel container inside a furnace, hydrothermal carbonization	Solid: 20–35 wt%	Kumar et al. (1992)
Hydrothermal carbonization	Temperature, 250 °C; pressure, 4 MPa; particle size, 1–10 μm	–	Biochar: 40–60 wt. %	Sevilla et al. (2011) and Reza et al. (2014)
Co-firing	Biomass: 5–20 wt%	Boiler	Power and heat	Sebastián et al. (2011), Savolainen (2003), and Zuwala and Sciazko (2010)

pyrolysis, smaller particle size (<1.0 mm), moderate temperature (500–700 °C), and lower residence time (2–5 s) were used for enhancing liquid yield (Bridgwater et al. 1999).

Liquid fuel obtained from pyrolysis is associated with several disadvantages such as higher oxygen content, which is further upgraded by hydroprocessing process and results in hydrocarbons and aromatics. The hydroprocessing process is divided into two types: the first type is known as hydrotreating, while the second type is known as hydrocracking. The treatment of organic compounds in the presence of pressurized hydrogen is known as hydrotreating in which oxygen is removed along with nitrogen, sulfur, and chlorine (heteroatoms). However, hydrotreating is a carbon-efficient process because water is used for removal of oxygen, but it requires a large amount of hydrogen (Brown and Brown 2013). During hydrocracking, hydrogen is reacted under more complex conditions to fragment higher modules into fuel range molecules. Further removal of oxygen can be done by catalytic pyrolysis or hydroprocessing (CHP) technology. Zeolite catalysts are usually used and homogeneously mixed with the biomass, which is placed at the downstream of the reactor to remove the CO and CO₂ in the absence of H₂. Hydropyrolysis and hydroprocessing (HPH) are carried out with pressurized hydrogen and catalysts, and the resultant product could be used as fuel because the high amount of oxygen content is removed. It was also observed that HPH process is more carbon efficient than CHP process. The HPH process produced fine grade fuel without any separate hydrocracking units.

15.2.2.4 Liquefaction

Liquefaction is the process in which water plays a significant role in thermochemical conversion. The water is used as a catalyst and reactant at a higher temperature, which results in separating all the organic material into individual compounds. Liquefaction is advantageous over gasification and pyrolysis because it does not require dry biomass (Zhang et al. 2009) and it reduced the number of unit operation required for conversion of biomass into liquid fuel. In this process, biomass is directly converted into fuel and chemicals.

15.2.2.5 Carbonization

Carbonization is known as an extension of pyrolysis, which is operated at a slower heating rate and produces a higher yield of solid products compared with liquid and gas. The production of solid biochar via carbonization is dependent on the operating temperature (generally lower temperature) (Strezov et al. 2007). Carbonization was used to produce biochar, which is also used for combustion and cooking purposes.

15.2.2.6 Co-firing

Co-firing is the clean and low-cost technology in which biomass is converted into electricity efficiently by adding biomass as a partial substitute for fuel in the boiler (Agbor et al. 2014). Co-firing is also used for improving combustion of fuel with low energy content. Biomass co-firing varied between 5 and 20 wt.% depending on boiler capacities and efficiencies (Sebastián et al. 2011). Co-firing technology has a

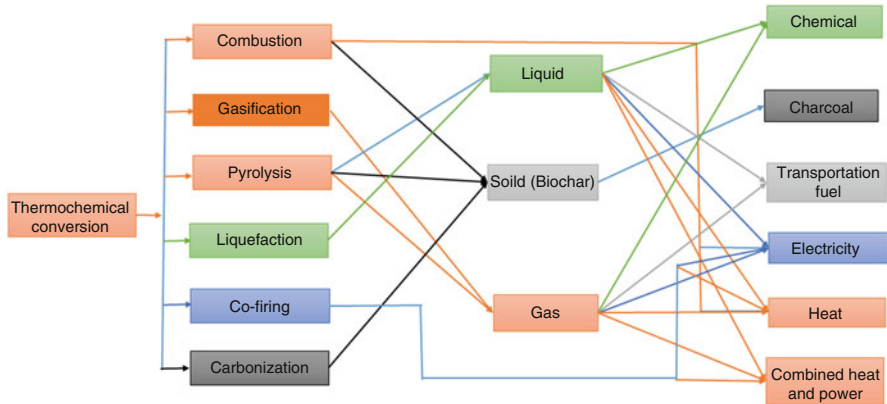


Fig. 15.2 End products produced from thermochemical conversion. (Redrawn based on Patel et al. 2016)

positive impact on the environment by reducing the consumption of fossil fuels. Co-firing of coal or biomass with natural gas improves heat content of the fuel, combustion efficiencies, and equipment performances.

15.2.2.7 Process End Products

The primary products such as solid, liquid, and gas obtained from the six thermochemical conversion technologies are presented in Fig. 15.2. The produced liquid fuel from pyrolysis can be used as alternative fuel after suitable upgradation and directly in the boiler and turbine for power generation. Hydroprocessing unit is mostly used for the upgradation of the pyrolytic liquid. Hydroprocessing process provides upgraded fuel with the presence of catalysts and hydrogen. Various value-added chemicals can be reformed from the liquid fuel. On the other hand, product gas can be used directly into boiler or turbine for the production of heat and electricity. It is also interesting that a range of chemicals can be extracted from product gas (Patel et al. 2016). During gasification, product gases are associated with the higher calorific value. Therefore, they can be converted into transportation fuel and power generation (Parthasarathy and Narayanan 2014). Furthermore, the solid biochar produced through carbonization and slow pyrolysis is used as soil conditioner, insulation, catalysts, beauty products, and fertilizers, besides having the potential to reduce global warming emission.

15.3 Techno-economic Assessment

Biomass is considered as carbon neutral source due to complete recycling of carbon. The quality of biomass has made it more attractive for production of power and energy in recent years. The fossil fuel has more potential as compared to biomass-derived fuel and energy, but biomass seemed more cost competitive compared with

fossil fuel worldwide due to its inherent advantages. Therefore, techno-economic analysis of biomass and biomass-derived fuel through thermochemical process becomes essential for improved efficiency and commercialization. Also, prediction of cost for producing fuels and chemicals is the major outcome of the techno-economic analysis.

Bridgwater et al. (2002) studied techno-economic analysis of thermochemical conversion technologies such as combustion, pyrolysis, and gasification for power generation. In addition, they derived standard equations for calculation of capital and operating costs for each of these technologies. For assessing economic assessment of specific processes, these equations provide useful information. Various products such as biofuel, energy, biochemicals, and electricity can be derived from biomass through thermochemical conversion. Economic analyses of thermochemical conversion products were derived, which helped in evaluating the production cost of each product. The production cost of the various biomass-derived products such as biofuel, power, electricity, and biochemical depends on the thermochemical process adopted. The data reported in this chapter was adopted based on 2014 US \$ value, and 2% inflation was used. The comparisons of the production cost of different biofuels are shown in Tables 15.2 and 15.3.

15.3.1 Gasification

Gasification is used to convert carbonaceous products into liquid transportation fuel at a commercial scale. The process helps to overcome prevailing shortage of petroleum products that resulted in turning coal into diesel for jet fuel application through the gasification pathway by using Fischer-Tropsch synthesis. Over the time, the gasification process was upgraded and employed for generation of various products. Acetic acid synthesis (AAS), which is used for generation of ethanol from cellulose through gasification (Zhu and Jones 2009), methanol-to-ethanol (MTE) also used for ethanol production, methanol-to-gasoline synthesis (MTG), mixed alcohol synthesis (MAS), syngas-to-distillates (S2D), and syngas fermentation (SF) are the main products. During gasification, materials decomposed at the high temperature (1500 °C) and formed the mixture of gases such as CO, CH₄, H₂, CO₂, and light hydrocarbons. The products obtained from the gasification is known as syngas, which was further converted into generation of power and electricity through either combustion or upgrading via catalysts into transportation fuel such as ethanol (Zhu and Jones 2009), methanol (Phillips et al. 2011), gasoline (Swanson et al. 2010), diesel, and jet fuel (Zhu et al. 2012). In addition, a novel *Clostridium* bacterium has the potential to convert switch grass-based syngas into ethanol via syngas fermentation (Piccolo and Bezzo 2009), thereby combining thermochemical and biochemical processes to yield cellulose biofuel. Syngas is the product output from gasification, which can yield high-quality fuel directly or in combination with catalysts. Furthermore, gasification-derived syngas can be used for the production of power by using advanced turbines.

Table 15.2 Comparison of the production cost of fuel and chemical from different biomass thermochemical conversion technologies

Bio-product	Feedstock	Location	Technology	Capacity (dry tonnes/day)	Base year	Production cost (2014 USD)	References
Methanol	Forest residue	Western Canada	Atmospheric pressure gasification + upgrading	2000	2008	\$0.33/kg \$0.26/L \$16.31/GJ	Sarkar et al. (2011)
	Forest residue	Western Canada	Pressurized gasification + upgrading	2000	2008	\$0.51/kg \$0.41/L \$25.53/GJ	Sarkar et al. (2011)
	Forest residue	Western Canada	Atmospheric pressure gasification + upgrading	3000	2008	\$0.32/kg	Sarkar et al. (2011)
	Maize residue	South Africa	Gasification + methanol synthesis using super converter	10–2000 MW (thermal)	2008	\$34.24–94.26/GJ	Amigun et al. (2010)
	Pine	Ithaca, USA	Gasification at 800 °C + methanol synthesis	500–9600	2012	\$15.61–33.29/GJ	Shabangu et al. (2014)
	Pine	Ithaca, USA	Pyrolysis at 450 °C + methanol synthesis	500–9600	2012	\$26.01–49.94/GJ	Shabangu et al. (2014)
	Pine	Ithaca, USA	Pyrolysis at 300 °C + methanol synthesis	500–9600	2012	\$57.22–109.24/GJ	Shabangu et al. (2014)
	Agricultural biomass	Almeria, Spain	Steam–air indirect circulating fluidized bed gasification + upgrading	2140	2010	\$1.03/kg	Valle et al. (2013)
	Agricultural biomass	Karlsruhe, Germany	Fast pyrolysis + gasification + upgrading	600	2008	\$16.22/GJ	Trippe et al. (2010)
	Natural gas	Karlsruhe, Germany		–	2008	\$10.20/GJ	Trippe et al. (2010)
Ethanol	Coal	Karlsruhe, Germany		–	2008	\$6.96/GJ	Trippe et al. (2010)

Dimethyl ether	Forest residue	Western Canada	Atmospheric pressure gasification + upgrading	2000	2008	\$0.53/kg	Sarkar et al. (2011)
						\$0.35/L	
						\$18.40/GJ	
	Forest residue	Western Canada	Pressurized gasification + upgrading	2000	2008	\$0.78/kg	Sarkar et al. (2011)
						\$0.51/L	
						\$26.70/GJ	
Ethylene	Forest residue	Western Canada	Atmospheric pressure gasification + upgrading	3500	2008	\$0.50/kg	Sarkar et al. (2011)
Propylene	Lignocellulosic biomass	Karlsruhe, Germany	Gasification syngas-DME-ethylene	-	2010	\$2.24–2.30/kg	Haro et al. (2013)
Ammonia	Lignocellulosic biomass	Karlsruhe, Germany	Gasification syngas-DME-propylene	-	2010	\$2.20–2.26/kg	Haro et al. (2013)
	Forest residue	Western Canada	Atmospheric pressure gasification + upgrading	2000	2008	\$2.35/kg	Sarkar et al. (2011)
						\$1.60/L	
						\$124.73/GJ	
	Forest residue	Western Canada	Pressurized gasification + upgrading	2000	2008	\$3.06/kg	Sarkar et al. (2011)
						\$2.09/L	
						\$111.01/GJ	
Bio-oil	Forest residue	Western Canada	Atmospheric pressure gasification + upgrading	3000	2008	\$2.32/kg	Sarkar et al. (2011)
Biochar	Energy crops	UK	Fast pyrolysis	100–800	2009	\$13.18–28.56/GJ	Rogers and Brammer (2012)
	Pine	Ithaca, USA	Slow pyrolysis	-	2012	\$0.23–0.29/kg	Shabangu et al. (2014)

(continued)

Table 15.2 (continued)

Bio-product	Feedstock	Location	Technology	Capacity (dry tonnes/day)	Base year	Production cost (2014 USD)	References
Fischer-Tropsch fuel	Forest residue	Western Canada	Atmospheric pressure gasification + upgrading	2000	2008	\$1.09/kg \$0.88/L \$24.54/GJ	Sarkar et al. (2011)
	Forest residue	Western Canada	Pressurized gasification + upgrading	2000	2008	\$1.72/kg \$1.37/L \$38.38/GJ	Sarkar et al. (2011)
	Forest residue	Western Canada	Atmospheric pressure gasification + upgrading	4000	2008	\$1.06/kg	Sarkar et al. (2011)
Hydrogen	Forest residue	Western Canada	Battelle Columbus Laboratory (BCL) gasifier	2000	2008	\$1.32/kg \$10.98/GJ	Sarkar and Kumar (2010a)
	Straw	Western Canada	Battelle Columbus Laboratory (BCL) gasifier	2000	2008	\$1.45/kg \$12.11/GJ	Sarkar and Kumar (2010a)
	Forest residue	Western Canada	Gas Technology Institute (GTI) gasifier	2000	2008	\$1.46/kg \$12.30/GJ	Sarkar and Kumar (2010a)
	Straw	Western Canada	Gas Technology Institute (GTI) gasifier	2000	2008	\$1.50/kg \$12.43/GJ	Sarkar and Kumar (2010a)
Hydrogen	Whole tree	Western Canada	Gas Technology Institute (GTI) gasifier	2000	2008	\$1.49/kg \$12.39/GJ	Sarkar and Kumar (2010b)
	Whole tree	Western Canada	Fast pyrolysis + steam reforming	2000	2008	\$2.70/kg \$22.52/GJ	Sarkar and Kumar (2010b)
	Forest residue	Western Canada	Fast pyrolysis + steam reforming	2000	2008	\$3.38/kg \$28.15/GJ	Sarkar and Kumar (2010b)
	Forest residue	Western Canada	Fast pyrolysis + steam reforming	2000	2008	\$3.38/kg \$28.15/GJ	Sarkar and Kumar (2010b)

	Straw	Western Canada	Fast pyrolysis + steam reforming	2000	2008	\$5.12/kg \$42.79/GJ	Sarkar and Kumar (2010b)
Gasoline	Lignocellulosic biomass	Karlsruhe, Germany	Gasification syngas-DME-gasoline	-	2010	\$1.57-1.62/L \$57.18-58.05/GJ	Trippe et al. (2013)
	Coal	Karlsruhe, Germany	Gasification syngas-DME-gasoline	-	2010	\$1.05/L	Trippe et al. (2013)
Liquefied petroleum gas (LPG)	Lignocellulosic biomass	Karlsruhe, Germany	Gasification syngas-FT synthesis-gasoline	-	2010	\$1.72-1.77/L	Trippe et al. (2013)
	Coal	Karlsruhe, Germany	Gasification syngas-FT synthesis-gasoline	-	2010	\$1.13/L	Trippe et al. (2013)
	Woody biomass	Golden, USA	Gasification syngas-methanol-gasoline	2000	2007	\$0.60/L \$18.07/GJ	Phillips et al. (2011)
	Woody biomass	Golden, USA	Gasification syngas-methanol-LPG	2000	2007	\$0.46/L \$18.07/GJ	Phillips et al. (2011)
Diesel	Lignocellulosic biomass	Karlsruhe, Germany	Gasification syngas-FT synthesis-diesel	-	2010	\$1.72-1.77/L	Trippe et al. (2013)
	Coal	Karlsruhe, Germany	Gasification syngas-FT synthesis-diesel	-	2010	\$1.09/L	Trippe et al. (2013)

(continued)

Table 15.2 (continued)

Bio-product	Feedstock	Location	Technology	Capacity (dry tonnes/day)	Base year	Production cost (2014 USD)	References
Gasoline and diesel	Woody biomass	Ames, USA	Mild catalyst pyrolysis	2000	2011	\$1.03/L	Thilakarathne et al. (2014)
	Woody biomass	Ames, USA	Mild catalyst pyrolysis with cogeneration of electricity and hydrogen	2000	2011	\$0.85/L	Thilakarathne et al. (2014)
	Stover	Ames, USA	Fast pyrolysis + hydroprocessing	2000	2011	\$0.72/L	Brown et al. (2013)
Naphtha and diesel	Corn Stover	Ames, USA	Gasification + Fischer-Tropsch synthesis and hydroprocessing	2000	2007	\$1.22–1.52/L	Swanson et al. (2010)
	Corn Stover	Ames, USA	Fast pyrolysis + upgrading, with hydrogen generation on-site	2000	2007	\$0.94/L	Wright et al. (2010)
	Corn Stover	Ames, USA	Fast pyrolysis + upgrading, with merchant hydrogen	2000	2007	\$0.64/L	Wright et al. (2010)

Source: Adapted from Patel et al. (2016)

Table 15.3 Comparison of the production cost of electricity from different biomass thermochemical conversion technologies

Feedstock	Location	Technology	Power output (MW)	Base year	Production cost (\$/MWh in 2014 USD)	References
Energy crop	UK	Organic Rankine cycle based CHP system	0.15	2013	48–60.2	Huang et al. (2013)
Energy crop	UK	Biomass gasification (downdraft gasifier) based CHP system	0.15	2013	104.04–116.30	Huang et al. (2013)
Woody biomass + coal	The Netherlands	Supercritical pulverized coal-fired (PC) boiler	500	2011	86.91–133.30	Domenichini et al. (2011)
Woody biomass + coal	The Netherlands	Supercritical circulating fluidized bed (CFB) boiler	500	2011	89.77–146.34	Domenichini et al. (2011)
Woody biomass	The Netherlands	Subcritical CFB boiler	250	2011	173.82–318.68	Domenichini et al. (2011)
Woody biomass	The Netherlands	Subcritical bubbling circulating bed (BFB) boiler	75	2011	246.20–434.56	Domenichini et al. (2011)
Torrefied biomass	The Netherlands	IGCC without CO ₂ capture	–	2008	99.78–144.26	Meerman et al. (2013)
Torrefied biomass	The Netherlands	IGCC with CO ₂ capture	–	2008	141.89–197.19	Meerman et al. (2013)
Coal	The Netherlands	IGCC without CO ₂ capture	–	2008	93.8	Meerman et al. (2013)
Coal	The Netherlands	IGCC with CO ₂ capture	–	2008	129.84	Meerman et al. (2013)
Biomass	UK	Fast pyrolysis, diesel engine	1–20	2002	88.78–177.56	Bridgwater et al. (2002)
Biomass + natural gas	Brazil	Indirect co-firing of biomass-derived gas with natural gas	150	2003	73.36	Rodrigues et al. (2003)
Biomass	Brazil	Biomass sole plant	24	2003	166.87	Rodrigues et al. (2003)

Adapted from Patel et al. (2016)

Fischer and Pigneri (2011) estimated the techno-economics study of power generation from gasification pathway in Vanuatu and reported that small-scale gasifiers with readily available raw material supply could be more economical, than similar-sized diesel engine for power generation. Generally, gasifiers are operated at higher pressure or sometimes at normal atmospheric pressures as well. The production cost of the various products such as methanol fuel, ethanol fuel, Fischer-Tropsch fuel, and NH_3 has been presented in Table 15.2, which is derived from pressurized or atmospheric gasifiers. From Table 15.2, it can be concluded that the atmospheric-based gasifier plant is more economical than the high pressurized gasifier-based plant (Sarkar et al. 2011). The production costs of methanol operated at atmospheric and pressurized gasifiers are \$0.29/kg and \$0.45/kg, respectively, with a 2000 dry tonnes per day capacity. It was also observed that production cost of dimethyl ether (DME), NH_3 , and Fischer-Tropsch fuel displayed the similar trend. The capital costs of pressurized equipment are much higher than atmospheric equipment and are one of the possible reasons for the higher price.

According to Bridgwater (1995), the pressurized systems are four times higher than atmospheric systems for a power plant with a capacity of 20 MW. The capital cost of the atmospheric gasifier is much lower than pressurized gasifiers which may be one of the possible reasons for the higher price. The pressurized systems are fourth times higher than atmospheric systems for 20 MW capacities of power plants (Bridgwater 1995). Due to the complex feeding section, higher feeding cost is another possible reason for the higher production cost of pressurized systems. At higher capacities of plants, the atmospheric system is more prominent than pressurized systems.

The lignocellulosic biomass such as agricultural residue, forest waste, woody biomass, and various energy crops are the major feedstocks for gasification. Therefore, the economics related to gasification are associated with the types of biomass. Thus the production of hydrogen fuel from agricultural residue has the higher production cost of about \$1.29–1.33 per kg, while forestry biomass has a lower production cost of about \$1.17–1.13 per kg, showing a direct correlation with biomass feedstocks used. Huang and McIlveen-Wright (2006) reported that mixing of biomass with coal (co-gasification) seems a most promising approach because the volatile content of biomass enables the autothermal gasification. Cormos (2013) studied on co-gasification (biomass and solid waste with coal) in a polygenerated-based integrated gasification combined cycle (IGCC) with carbon capture and concluded that the product produced from IGCC contains H_2 , synthetic natural gas (SNG), and liquid fuel. By increasing co-production cost with power directly affected the plant payback period. Further, the payback period can be controlled by producing a higher yield of SNG and Fischer-Tropsch fuel with power.

15.3.2 Combustion

Different types of the boiler can be used for generation of power from biomass through combustion. Supplying biomass as feedstock in pulverized coal-fired (PC) boiler provides the lower electricity cost compared with fluidized bed boilers

(Table 15.3). Comparison of different fluidized bed boilers indicates that circulating fluidized bed boilers produce electricity at a lower cost than the bubbling circulating bed (BCB) boilers. Moreover, cost of electricity (COE) produced from subcritical boilers is more costly than that from supercritical boilers (PC and CFB). The comparison with various fluidized bed boilers and circulating fluidized bed boilers produced the electricity or power at a reduced cost than bubbling fluidized bed boilers. The higher cost of biomass transportation results in increased cost of electricity produced from solely biomass-based power plants. Since coal transportation is comparatively cheaper, the co-firing of biomass with coal could reduce the production cost of electricity (Table 15.3). Due to higher installation cost of the conventional power generation plant, the biomass has higher breakeven electricity selling price than the cogeneration plant. Production of power and heat by cogeneration gives the more economical solution. An analysis of biomass-based combined heat and power (CHP) showed that higher cost of electricity could be adjusted by a production of heat (Huang et al. 2013). The production cost of organic Rankine cycle (ORC)-based combined heat power plant has the higher initial capital cost compared with gasification-based combined heat and power plant (Patel et al. 2016). However, organic Rankine cycle (ORC)-based combined heat power (CHP) plant agrees with economic profits such as lower electricity price compared with gasification-based combined heat and power unit. The higher amount of production of heat from organic Rankine cycle (ORC)-based combined heat power (CHP) plant is the possible reason which helps improving economic performance significantly (Huang et al. 2013).

15.3.3 Pyrolysis

Fast pyrolysis produced several types of products and by-products from the biomass such as pyrolytic liquid, which can be further synthesized into transportation fuels or several other value-added chemicals. In addition, fast pyrolysis is used for power generation with the combined diesel engine (Patel et al. 2016). Rogers and Brammer (2012) evaluated production cost of bio-oil from the energy crop such as *Miscanthus* and willow through fast pyrolysis and found to be \$12–26/GJ with variable feed-stock and plant size. Consumption of electricity and surplus char selling are the two major factors that strongly affected production cost of pyrolytic liquid from pyrolysis. All the processing and handling of biomass is carried out by using electricity which increases the production cost. It was studied that the produced pyrolytic liquid can be used in a diesel engine for power production in the plant, which in turn reduced the dependence on fossil fuel. The study also confirmed that about 18% of produced pyrolytic liquid would be consumed (Patel et al. 2016). The selling of solid residue (biochar) is the best possible solution to reduce the overall production cost up to 18%, but the selling price of the biochar is market dependent.

The product output obtained from the fast pyrolysis (pyrolytic liquid) and hydroprocessing (upgraded fuel such as transportation fuel) has been studied by several researchers. These studies were based on the initial production cost of

pyrolytic liquid derived from biomass, through pyrolysis and improvement in cost of pyrolytic liquid for upgraded fuel, such as transportation fuel by adding hydrogen and catalysts. Wright et al. (2010) evaluated production cost of naphtha and diesel fuel produced from the pyrolytic liquid and reported that the production cost of upgraded fuel would be \$0.56–0.82 per liter, with 2000 dry tonnes per day plant capacity (Table 15.2). However, the alteration in production cost depends on hydrogen price and cost of catalysts. The production cost of hydrogen from outside the system is much cheaper than that produced from the process itself. The production cost of transportation fuel is critically affected by two main factors, i.e., price of biomass and rate of conversion yield. Brown et al. (2013) studied that production cost of upgraded fuel (gasoline and diesel produced from fast pyrolysis and hydroprocessing) was \$0.68 per liter with 2000 dry tonnes per day of plant capacity. This also falls within the range proposed by Anex et al. (2010). It was found that production of electricity for the fast pyrolysis and diesel engines seemed to be a realistic option. The electricity production costs of a fast pyrolysis and diesel engine system range from around \$0.14/kW h (base year 2002) at 1 MWe to around \$0.07/kW h (base year 2002) at 20 MWe (Bridgwater et al. 2002). However, this is higher than in an established combustion system and lower than any other novel biomass power generation system (Bridgwater et al. 2002). The fast pyrolysis process and diesel system are not sufficient and capable of production in higher capacities. The lower rate of conversion of feedstock into liquid fuel which results in higher electricity production cost and grinding of biomass which results in higher consumption of electricity are two main reasons for the lower efficiencies.

However, disposable products obtained from process, produced heat, several other by-products, selling of solid residue (biochar, coal), produced water, or cogeneration of various value-added chemicals along with power are the other potential solutions which can improve the economy of generation of power from biomass fast pyrolysis and diesel engines (Gnansounou and Dauriat 2010). In addition, system decoupling (more than one engine added in series) is another potential possible solution for improving the economy of the power generation from biomass fast pyrolysis and diesel engine. The production cost of electricity through decoupling system is more proficient than traditional closed coupled systems because of economic benefits of pyrolysis plant (Gnansounou and Dauriat 2010). On the other hand, the decoupling system has the potential to fulfil the requirements of power load at all times because both processes are operated independently.

Slow pyrolysis of biomass results in the solid residue (charcoal) and liquid (methanol) (Shabangu et al. 2014). Production of solid residue from slow pyrolysis is dependent on the temperature. However, lower temperature reduced the production cost. Furthermore, biochar production cost affected the cogeneration plants' profits at the lower temperature due to higher char yield. Shabangu et al. (2014) estimated that selling of biochar provided 70% of the plant revenue, while 30% revenue came from methanol at the lower temperature (300 °C). However, in case of 450 °C, it was the opposite. Gasification of biomass is another possible

solution for cogeneration of biochar. Price of char does not affect the revenue in gasification process because char yield is lower than slow pyrolysis.

15.3.4 Liquefaction

Conversion of biomass into fuel and energy can be done through thermochemical means such as pyrolysis, combustion, liquefaction, and gasification. Pyrolysis is being used along with hydroprocessing (for upgradation of fuel), while gasification is being used with Fischer-Tropsch synthesis and hydroprocessing. The biochemical process is being used with various types of bacteria and enzymes. Anex et al. (2010) estimated that production cost of liquid fuel ranged from \$0.53/L to \$1.45/L of gasoline (based on 2007) with 2000 dry tonnes per day capacity plant, while it was assumed that price of biomass feedstock is \$82.7 tonnes per day. Some specific process parameter such as temperature, heating rates, oxygen feed flow rate, and types of gasification system does not seriously affect the production cost through different pathways. In addition, implementation of different pathways significantly affected the production cost of various products. Due to lower initial capital investment, direct liquefaction has the lower cost (\$0.56–0.975/L) compared to gasification and biochemical pathways. Production of liquid fuel from bio-oil through direct liquefaction via fast pyrolysis by adding hydrogen showed lower production cost as compared to direct production of hydrogen by pyrolysis. However, upgradation of bio-oil to transportation fuel produced from pyrolysis is not well defined; therefore, it is relatively less popular and less used. However, it has potential to replace the fossil fuel completely or partially if used properly such as blending with fossil fuel. Hence, before large-scale implementation, this process requires further development. Upgradation of liquid fuel produced from gasification increases production cost (\$0.53–1.64 per liter compared with pyrolysis).

Trippe et al. (2013) studied straw biomass for production of gasoline by dimethyl ether (DME) synthesis and production of diesel by Fischer-Tropsch synthesis. Based on the techno-economic analysis, they concluded that 38% and 39% of total energy efficiencies were required for biomass to the final product. The production cost of gasoline produced from DME synthesis is \$0.82/L, while diesel and gasoline through Fischer-Tropsch synthesis are \$0.88/L. The capital cost of the liquefaction through pyrolysis and biochemical routes is more economical than gasification route at the lower and the higher temperature situations. Furthermore, the production cost of liquid fuel via biochemical route is relatively higher than gasification route, which offers lower operating cost.

Swanson et al. (2010) have compared the production cost of transportation fuel with two gasification situations with equal syngas synthesis process. The low temperature was being used as the first scenario in the fluidized bed gasifier, and the higher temperature was being used in an entrained flow gasifier. Based on the product yield of products, it was concluded that high-temperature route has the lower production cost compared with lower temperature route; however, capital cost is more at higher temperature condition. The conversion of lignocellulosic biomass

through liquefaction pathways yet needs to be commercialized. It is important to mention that the production cost of a pioneer plant is 60–90% higher than those of nth plant, while capital cost of a nth plant is much lower (double of nth plant) than pioneer plant (Swanson et al. 2010). Biosyncrude is another intermediate for conversion of biomass into biofuel or pyrolytic liquid; however, it is still under research (Patel et al. 2016). It will take some time to compete with existing literature. Biosyncrude is a mixture of liquid and biochar (solid residue) produced from fast pyrolysis. In Germany, they investigated the first-time production of biosyncrude at an estimated production cost of \$14.4/GJ with 600 tonnes per day capacity plant. However, the production cost of biosyncrude in Germany is higher than other fuels such as natural gas (\$9.06/GJ) and conventional fuel such as coal (\$6.18/GJ) (Patel et al. 2016).

15.3.5 Co-firing

Due to environmental benefits, co-firing of biomass with coal or natural gas could be one of the interesting thermochemical technologies compared with the combustion of only coal (Agbor et al. 2014). Co-firing of coal with biomass or plastic waste in fluidized bed technology can be a good route due to fuel flexibility nature. The effect of blending (biomass or plastic waste) up to 20% in a co-firing system (circulating fluidized bed reactor) is found to be negligible for the performance of the co-firing system when blending of biomass or plastic equated with systems fueled by coal (McIlveen-Wright et al. 2006). The techno-economic analysis of biomass-based co-firing plants with coal-fired plants confirms that the capital cost and operating cost are the two major factors to be considered while co-firing biomass with coal or plastic waste. De and Assadi (2009) evaluated economic analysis of biomass co-firing with various parameters like biomass-to-waste ratio, the price of feedstocks, total plant capacity, and distribution of biomass density around the plant. They reported that when the cost of biomass is higher than coal, co-firing cost will increase due to increase in the rate of co-firing; therefore, electricity cost also increases.

15.4 Comparison of the Economics of Different Technologies

The economy of biomass-based fuels is attributed to the end products, which are produced by using different conversion pathways. Production of hydrogen via pyrolysis and gasification followed by steam reforming is one of the best examples. The production cost of gasified hydrogen is more economical than the hydrogen produced from pyrolysis and steam reforming. The comparative study confirmed that power generation from fast pyrolysis with diesel engines is more economical than electricity and power produced through the gasification process. Various researchers have compared the production cost of hydrogen through gasification and steam reforming process. It was confirmed that pyrolytic liquid or bio-oil

gasification process is not as economical as the bio-oil reforming processes (Zhang et al. 2013). The bio-oil gasification capital cost is higher than reforming pathways due to the higher cost of the gasifier (entrained flow). However, the lower capital cost is observed between reformers and air separation. Furthermore, cleaning of gases become more complicated in gasification when compared with the reforming system (Zhang et al. 2013). McIlveen-Wright et al. (2006) studied the techno-economic analysis of generation of electricity from the supercritical boiler by combustion and gasification. They reported that supercritical gasification boiler is more economical (46.5%) compared to the supercritical combustion system. Supercritical boiler gasification system required lower investment cost of production of electricity than combustion system. Supercritical boiler combustion has the investment of \$2150–2400 per kW, and supercritical boiler gasification system has \$1350–1450 per kW. Electricity production cost from combustion system is reported to be \$68–78/MWh, while for gasification system \$49–54/MWh (McIlveen-Wright et al. 2006).

The gasification technology combined with fermentation process was compared with conventional enzymatic hydrolysis – combined with fermentation process for the production of high-grade fuel (ethanol). It was noticed that gasification with combined fermentation technology required higher ethanol production cost than ethanol produced from enzymatic hydrolysis with fermentation process (Piccolo and Bezzo 2009). Higher capital cost, high energy recovery expense, and moderate ethanol yield are the major issues responsible for the higher cost. However, there is a much better application for the broad range of production of ethanol via gasification and fermentation technologies.

15.5 Life-Cycle Assessment (LCA)

Biomass-derived end product produced from the thermochemical process has the potential to mitigate generation of greenhouse gas emission which comes from various sources such as transportation and industries. LCA is a useful tool to explain various impacts which are categorized quantitatively and qualitatively throughout the life cycle of the end products. There are three significant global system boundaries for conversion of biomass into fuel or power via thermochemical process biomass into useful products (end product), which are:

1. Phase 1: Planting of biomass, harvesting, and transportation
2. Phase 2: Plant site operation and upgradation of fuel if required
3. Phase 3: Demolition of plant and recycling of the plant

Based on the availability of data, Phase 1 and Phase 2 have been studied extensively by the various researchers. Life-cycle assessment of fast pyrolysis, gasification, combustion, and co-firing process is extensively available. However, there is lack of literature on liquefaction and carbonization. A number of the analytical tool such as greenhouse gases, regulated emissions, and energy use in transportation

(GREET), SigmaPro, GHGenius, Tools for Environmental Analysis and Management (TEAM), etc. were used by various researchers for collection of data (Mann and Spath 2001; Hsu 2012; Roberts et al. 2009). Two software, Eco-indicator 95/99 and CML (Centre for Environmental Studies, Leiden University, Netherlands), are widely used to evaluate the environmental impacts of various feedstocks based on the system boundary (Faix et al. 2010). In this study, the life-cycle analysis was done on conversion of lignocellulosic biomass into end products via thermochemical technologies. Among all the existing thermochemical technology, life-cycle analysis on pyrolysis was done by several authors. During the life-cycle assessment of biomass, three significant parameters such as system boundary, functional units, and environmental impact are considered.

15.5.1 Feedstocks

Type of feedstock is an important parameter during conversion of biomass via thermochemical technology. Biomass comprises mainly of hemicellulose, cellulose, and lignin; however, based on the type of feedstocks, their concentrations of these components vary. The higher percentage of cellulose in biomass and the lower percentage of lignin are suitable for this process. There are many reported works, where the potential of some of the popular biomass such as energy crops, forest residues, and agricultural residues was carried out to find out their efficiency of conversion. Furthermore, depending on the cultivation and collection methods, a specific feedstock has the specific environmental impact.

Energy crops are classified under third-generation biomass and are developed in such a way to produce useful and lower energy supply source. The advantage of these crops is that these can be genetically modified to increase their property which can result in higher fuel yield (López-Bellido et al. 2014). However, the use of various herbicides and pesticides are the major drawbacks of these types of agriculture crops which could result in resistant weeds and insects that may be more unsafe for nongenetically modified agriculture crops (Maggi and Delmon 1994). Forest residue is another important source for thermochemical conversion of biomass which is produced from harvesting of timber extraction operations, wood waste from lumber mills, or from dead wood. Concerning heating value and moisture content, forest residue is equivalent to wood, though they differ in their ash content.

Agriculture residue is the third lignocellulosic biomass which comes from the unused portions of wheat, corn, rice, bagasse, etc. after they are harvested. Some biomass such as corn stover, wheat straw, and rice husk have been in use for a long time due to their lower moisture and higher heating value. Due to the seasonal availability of the biomass, their cost increases because some of the crop residues are used for cattle fodder and composting. By addition of certain portions of these wastes into soil, level of groundwater and quality of the soil were improved (Nguyen et al. 2013). Thus, life-cycle analyses of these biomass feedstocks become essential for the production of fuel and chemicals.

15.5.2 Phase Involved in the System Boundary

The numbers of phases that are involved with system boundaries are based on the end products. Conversion of lignocellulosic biomass via thermochemical process has three major phases. The requirement of input and output feedstock of biomass is shown in Fig. 15.3. Life-cycle analyses of Phase 1 and Phase 2 are the major interests of several researchers. However, some researchers reported from the cradle to the grave at all phases in the system boundary. The first phase of system boundary involves collection or cultivation of biomass flowed by transportation of biomass to the plant site. Change in use of land, application of fertilizers and pesticides, carbon sequestration, removal of biomass residue from the soil, and transportation distance from the storage site to plant site are the major aspects. Change in land use has greater effects (direct and indirect) on the environment. Direct change in land use comprises conversion of forest or grassland into cropland for biofuel or power production, while the indirect use of change in land comprised when non-croplands were converted into cropland because existing cropland was used for power and biofuel production (Lange 2011). Most of the studies on life-cycle analysis do not include land change, which results in the change in carbon content in the changed land (cultivated area) for the feedstock.

Kimming et al. (2011) proposed the use of set-aside land for harvesting purpose for energy crops as maintaining carbon stocks on soil is not good due to legislative and practical reasons. Conventional crops have lower greenhouse gas emission compared with energy crops due to the application of fertilizer and pesticides.

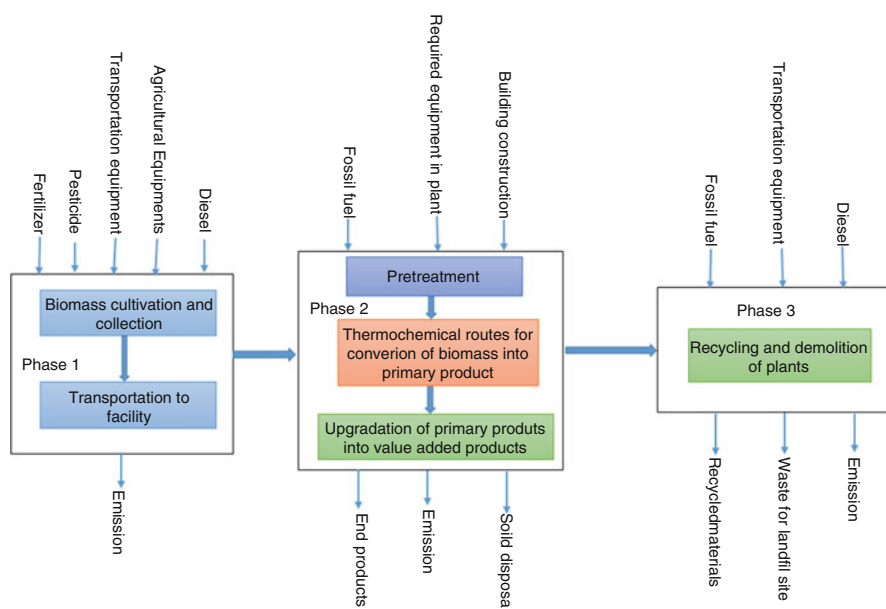


Fig. 15.3 General layout schemes of the system boundary (Redrawn based on Patel et al. 2016)

Skowrońska and Filipek (2014) suggested that production of 1 kg of NPK (nitrogen, phosphorus, and potassium) required 9.91 MJ of energy. However, most of the energy is required for nitrogen production. The production of fertilizer facility leads to the formation of nitrogen oxide, methane, and carbon dioxide emissions which put an extra burden on the environment (Skowrońska and Filipek 2014). To overcome the issues of food scarcity, use of agrochemical (chemicals and fertilizers) increases the production rate of crops within the same land. The use of frequent fertilizer and chemicals degrades the quality of the soil as well as atmosphere. Skowrońska and Filipek (2014) again suggested that replacement of chemical fertilizers with organic fertilizers such as compost is an excellent alternative.

Extraction of the biomass residue from the soil leads various types of pollution and also degrades the quality of the soil. The biomass residues contain lots of mineral matter and nutrients which have the positive effect on the quality of the soil. Gabrielle and Gagnaire (2008) reported that significant extraction of biomass residue (agricultural residue or energy crops) from agriculture soil reduces the ability of volatilization of NH_3 due to significant drops of immobilization of mineral fertilizer. Hence, straw management is essential for the production of fuel, chemicals, and power; therefore, the life-cycle analysis of biomass straw is essential (Gabrielle and Gagnaire 2008). The transportation of biomass from husbandry site or forestry site to plant site is an important characteristic of system boundary. In most of the cases, it was assumed to be carried out near the plant which reduced transportation cost and environmental impacts. About 30–200 km distance was considered in this study. Mostly distance depends on the biomass size facility. Therefore, it is essential to estimate overall life-cycle assessment of greenhouse gas emission of a conversion pathway.

The second phase of system boundary comprises biomass pre-treatment such as crushing, chipping, grinding, and drying. However pre-treatment process varies from process to process. The distribution of particle size of biomass and water molecules depends on the type of thermochemical conversion process. Thus, type of conversion technology also has an adverse effect on the overall variation of environmental impacts. Combustion, gasification, pyrolysis, and co-firing technologies are preferred majorly due to the availability of data. In addition construction materials used for equipments depend on various process conditions such as temperature, pressure, the rate of heating, etc. For example, highly viscous, corrosive, and polar nature of bio-oil makes it mandatory to store it in the stainless steel vessel. The extraction of iron ore and manufacture process of these types of vessels results in the higher emission of greenhouses gases (Martínez et al. 2009). Thus, reduction of greenhouse gas emission of this phase become essentially challenging.

15.5.3 The Functional Units

The functional unit is one of the most critical parts of the life-cycle assessment analysis and required clear and exact definition. It does not measure physical products but measures function of end products. The selection of the functional

units is very crucial because it works as the locus point of all evaluated environmental impacts. In addition, selection of appropriate functional unit is not direct, and variation in functional unit conceives the problem during the life-cycle inventory. Depending on the scope and aim of the work, various researchers have used different functional units. The calorific value of end product, transportation distance, the weight of the feedstock, and the area used for the cultivation of the feedstock was chosen widely by different researchers. Also, based on the system boundary, authors have chosen functional units. Comparing the various units is a very difficult task, but it is possible if all units can be converted into the same unit and provided the same boundary condition is maintained for all life-cycle analysis (Singh et al. 2010).

15.6 Environmental Impact Assessment

Environmental impact assessment (EIA) is one of the utmost difficult tasks executed after defining all the system boundaries and inventory requirement of products or processes. For the calculation of its multiple impacts on ecosystem, human health, and resource depletion, Eco-indicator 99 and Eco-indicator 95 are usually used. These impacts are further categorized into different types of environmental effects. Global warming potential, acidification and eutrophication, ozone layer depletion, human health into smog and toxic substances (heavy metals, carcinogens, and pesticides), and resource diminution into solid waste and energy consumption are the main subdivided ecosystems. Environmental impacts evaluated by the different researchers are presented in Table 15.4. Global warming potential is one of the major study areas, while human health and resource diminution have less importance when compared with the ecosystem. The potential of global warming is reported pursuantly CO₂ equivalent which includes CH₄, N₂O, and CO₂ emissions. Similarly, acidification and eutrophication are evaluated in kg SO₂ equivalent and kg PO₂ equivalent, respectively. Sebastián et al. (2011) suggested that production of fertilizers has significant greenhouse gas emission compared with biomass planting because at the time of cultivation of biomass, net emission of CO₂ is zero due to photosynthesis.

Pre-treatment of biomass is an energy-intensive process and completely connected with the types of thermochemical pathways. Crushing, grinding, chipping, making of pellet, and drying are the major pre-treatment steps. Agriculture residue contains 10–20 wt. % moisture which is lower than forest residue and whole forest (40–50 wt. %) (Kumar et al. 2003b). Hence, consumption of energy differs with the moisture content of the types of feedstock. Iribarren et al. (2012) reported that pre-treatment of the poplar biomass had the utmost environmental impact compared to other unit operations used in fast pyrolysis system because of direct use of the conventional fuel. Distribution of the particle size varies on the process requirement. In fast pyrolysis lower particle size is preferred due to higher heat and mass transfer, while the use of higher particle size reduced liquid yield and increases biochar yield (Iribarren et al. 2012). Royo et al. (2004) estimated that size reduction of 25 mm to 3 mm biomass required 443 MJ per dry tonne energy consumption,

Table 15.4 Summary of the life-cycle assessment of different thermochemical conversion technologies

Process	Feedstock	End product	Boundary	Functional unit	Environmental impact categories	Comments	References
Co-firing	Rice straw	Power	Phases 1 and 2	1 MWh	Acidification, global warming potential (GWP), eutrophication, human toxicity	Significant reduction in impact categories at 5% biomass co-firing condition	Shafie et al. (2013)
Co-firing	Willow	Electricity	Phases 1 and 2	1 MWh	Net energy ratio and net global warming potential	Net energy ratio increased by 9% and net global warming potential decreased by 7–10% at 10% co-firing. GWP: 910 kg CO ₂ eq/MWh	Heller et al. (2004)
Co-firing	Wood residue	Electricity	Phases 1, 2, and 3	1 kWh	Global warming potential	GWP: 894.3 g CO ₂ eq/kWh at 15% co-firing – 1002.9 g CO ₂ eq/kWh at 5% co-firing	Mann and Spath (2001)
Co-firing	Energy crop and wheat straw	Electricity	Phases 1, 2, and 3	1TJ	Global warming potential	GWP: 298 tonnes CO ₂ eq/TJ 10% direct co-firing GWP: 300 tonnes CO ₂ eq/TJ 10% indirect co-firing	Sebastián et al. (2011)
Fast pyrolysis	Corn Stover	Bio-gasoline	Phases 1 and 2	1 ha	Global warming potential	Coal boiler efficiency and biomass treatment are important parameters GWP: 7.65 tonne CO ₂ eq/ha	Kaufman et al. (2011)
Fast pyrolysis	Short rotation poplar	Gasoline, diesel, and char	Phases 1 and 2	1 MJ	Cumulative energy demand, global warming, ozone layer depletion, photochemical	Corn stover removal rate is the sensitive parameter that affects the biochar and bio-oil yield GWP: -50.54 kg CO ₂ eq/MJ Biomass pretreatment, pyrolysis, and steam	Iribarren et al. (2012)

Fast pyrolysis	Forest residue	Gasoline and diesel	Phases 1 and 2	1 km	oxidant formation, land competition, acidification, eutrophication	Global warming potential and net energy value (NEV)	reforming are the main contributors in the environmental impact categories	Hsu (2012)
							GWP: 98–117 g CO ₂ eq/km NEV: 0.92–1.09 MJ/km GWP and NER are lower than the conventional gasoline and diesel	
Fast pyrolysis	Corn Stover	Gasoline	Phases 1 and 2	1 MJ	Global warming potential	Global warming potential	During upgrading of biofuel by hydroprocessing: GHG emissions reduction is maximized when hydrogen is produced from bio-oil reforming	Han et al. (2013)
Fast pyrolysis	Logging residue, hybrid poplar, willow, and waste wood	Electricity	Phases 1 and 2	1 kWh	Global warming potential	Global warming potential	Depending on the feedstock type, life-cycle GHG savings of 77–99% estimated for power generation from pyrolysis oil to fossil fuel combustion	Fan et al. (2011)
Ablative pyrolysis	Wood chip	Electricity	Phases 1 and 2	1 kWh	Global warming, ozone depletion, photochemical ozone creation potential, acidification, eutrophication	Global warming, ozone depletion, photochemical ozone creation potential, acidification, eutrophication	All impact categories are significantly decreased except eutrophication potential due to use of fertilizer during cultivation	Faix et al. (2010)
Slow pyrolysis	Corn stover and switchgrass	Biochar	Phases 1 and 2	1 tonne of dry biomass	Global warming potential	Global warming potential	GWP for corn stover: –	Roberts et al. (2009)
							864 kg CO ₂ eq/tonne of dry biomass GWP for switchgrass: +36 kg CO ₂ eq/tonne of dry biomass	

(continued)

Table 15.4 (continued)

Process	Feedstock	End product	Boundary	Functional unit	Environmental impact categories	Comments	References
Flash pyrolysis	Wood waste	Biofuel and power	Phases 1 and 2		Global warming, ozone layer depletion, photochemical smog, acidification, eutrophication, ecotoxicity, human toxicity	Emission from combustion of bio-oil affects GWP, acidification, human toxicity, and eutrophication	Zhong et al. (2010)
Gasification	Forest residue	Heat and power	Phases 1 and 2	1 MJ	Global warming, ozone layer depletion, photochemical oxidization, acidification, eutrophication, toxicity, abiotic depletion	GWP: 8.8–10.5 g CO ₂ eq/MJ environmental impacts are significant for the biomass procurement and plant operation	Guest et al. (2011)
Gasification	Poplar energy crop	Electricity	Phase 1, 2, and 3	1 MWh	Global warming, ozone layer depletion, smog, acidification, eutrophication, solid waste, energy consumption	Most negative environmental effects are caused by the use of chemicals and fertilizer	Rafaschieri et al. (1999)
Gasification	Willow biomass	Heat and power	Phases 1 and 2	1 MWh	Fossil energy requirement, primary energy requirement, land use, global warming potential, acidification	Significant reduction in GHG emissions from willow biomass to the fossil fuel based systems	Kimming et al. (2011)

Gasification	Biomass	Hydrogen	Phases 1, 2 and 3	1 MJ	Global warming, smog, acidification, eutrophication, carcinogenesis, heavy metals, smog	Among life-cycle studies for two pathways of hydrogen production, biomass gasification-steam reforming-PSA route is the energy efficient one, and biomass- gasification- electricity-electrolysis has better environmental performance	Koroneos et al. (2008)
Combustion	Birchwood	Heat	Phases 1 and 2	1 kWh	Global warming, photochemical oxidation, acidification, eutrophication	GWP: 80–110 g CO ₂ eq/kWh Comparing the life-cycle analysis of new stove technology to old one, the former has the better environmental impact	Solli et al. (2009)
Combustion	Rice Husk	Electricity	Phases 1 and 2	1 MWh	Global warming, acidification, eutrophication, ecotoxicity	GWP: 217.33 kg CO ₂ eq/MWh	Shafie et al. (2012)
Combustion	Forest residue	Power	Phases 1, 2 and 3	1 kWh	Global warming	GWP: 11–14 g CO ₂ eq/kWh Emission and energy consumption depends on the moisture content and the heating value of biomass	Thakur et al. (2014)
Combustion	Wood waste	Electricity	Phases 1 and 2	1 MJ	Global warming, respiratory effect, photo-oxidant formation, acidification, eutrophication	Inventory data collection is the major factor for life-cycle analysis	Pérlillon et al. (2012)

Adapted from Patel et al. (2016)

while size reduction of 300 mm to 25 mm of biomass required 157.5 MJ per dry tonne energy. Environmental impact assessment is subjected to the types of the operating conditions like temperature, heating rate, feed composition, type of reactor, etc. In addition, a material is used for the plant construction and manufacturing of equipment related to greenhouse gas emission. During co-firing, increase in the percentage of biomass reduced environmental impact. However, it decreases the overall efficiency of the boiler in the production of power and electricity (Sebastián et al. 2011). Rafaschieri et al. (1999) studied poplar energy crops in a pressurized fluid bed gasifier at various gasification conditions and reported that replacing oxygen by air as an oxidizer reduced environmental impacts. This is why consumption of electricity was higher for the separation of oxygen and results in the generation of greenhouse gases.

15.7 Conclusions

Since techno-economic analysis of different types of biomass via thermochemical conversion technology has been started recently, most of the study focused on the specific product series for one product. There is a lack of integrated techno-economic analysis for multiple pathways of product cogeneration. Hence, this gap can be filled by studying techno-economic assessment of different types of biomass via thermochemical conversion technology in the near future. However, it is noticed that techno-economic analysis of pyrolysis technology has been studied extensively, but upgradation of pyrolytic liquid for transportation fuels or other purposes still needs more detailed study. The production of fuels through pyrolysis seems the best possible pathway of future research as it has the economic and environmental benefits. The production of power and energy for different types of biomass looked for more advanced techno-economic assessment. There are a large number of studies done for techno-economic analysis of fast pyrolysis, combustion, gasification, and co-firing, but advanced research is still required for economic analysis. It was also found that numerous studies were conducted on co-firing to explain the stoichiometric ratio of biomass along with the plant capacity, but there is a lack of techno-economic analysis on carbonization process.

In the last few years, life-cycle assessment through thermochemical technology on lignocellulosic biomass has been studied; still there is enough scope to carry out more study in this area. Among all pyrolysis technology, fast pyrolysis of lignocellulosic biomass was reported extensively. Furthermore, there is a deficiency of the comparative analysis of diverse pathways based on environmental metrics, which is the major constraint of life-cycle assessment studies. The data availability and life-cycle assessment framework from start to end are the main reasons for varying the system boundaries. A number of programs are available for life-cycle assessment; however, their database varies on location to location, climate, and types of process. Hence, for meaningful life-cycle assessment, a standardized approach is needed. Environmental impact categories (human health, resource depletion and threats to the ecosystem, and global warming potential) are the most emphasized areas of

research. Furthermore, direct change of land was studied by very few researchers, but the indirect changes in the land were completely absent in the literature. Thus, more study is needed on the indirect changes in land in the near future. Production of fertilizers and its application are the main contributors to global warming. Therefore, there is a need to develop plant species that require low maintenance and chemicals. Recently, various policies are implemented for use of biofuel in order to reduce environmental pollution in place of fossil fuel. An appropriate and common method is required which provides the comparative analysis of end products and types of the pathways. It was also notable that selection of types of pathways is mainly dependent on the types of feedstocks, ends products, and geographical condition. Therefore, more techno-economic analyses were required to investigate the formation of single products by different types of pathways.

References

- Abubackar HN, Veiga MC, Kennes C (2011) Biological conversion of carbon monoxide: rich syngas or waste gases to bioethanol. *Biofuels Bioprod Biorefin* 5:93–114
- Agbor E, Zhang X, Kumar A (2014) A review of biomass co-firing in North America. *Renew Sust Energ Rev* 40:930–943
- Akhtar J, Amin NAS (2011) A review on process conditions for optimum bio-oil yield in hydrothermal liquefaction of biomass. *Renew Sust Energ Rev* 15(3):1615–1624
- Alauddin ZABZ, Lahijani P, Mohammadi M, Mohamed AR (2010) Gasification of lignocellulosic biomass in fluidized beds for renewable energy development: a review. *Renew Sust Energ Rev* 14:2852–2862
- Amigun B, Gorgens J, Knoetze H (2010) Biomethanol production from gasification of non-woody plant in South Africa: optimum scale and economic performance. *Energy Policy* 38:312–322
- Anex RP, Aden A, Kazi FK, Fortman J, Swanson RM, Wright MM, Satrio JA, Brown RC, Daugaard DE, Platon A, Kothandaraman G, Hsu DD, Dutta A (2010) Techno-economic comparison of biomass-to-transportation fuels via pyrolysis, gasification, and biochemical pathways. *Fuel* 89:S29–S35
- Arce ME, Saavedra Á, Míguez JL, Granada E, Cacabelos A (2013) Biomass fuel and combustion conditions selection in a fixed bed combustor. *Energies* 6(11):5973–5989
- Boucher M, Chaala A, Pakdel H, Roy C (2000) Bio-oils obtained by vacuum pyrolysis of softwood bark as a liquid fuel for gas turbines. Part II: stability and ageing of bio-oil and its blends with methanol and a pyrolytic aqueous phase. *Biomass Bioenergy* 19:351–361
- Bridgwater A (1995) The technical and economic feasibility of biomass gasification for power generation. *Fuel* 74(5):631–653
- Bridgwater AV, Meier D, Radlein D (1999) An overview of fast pyrolysis of biomass. *Org Geochem* 30(12):1479–1493
- Bridgwater A, Toft A, Brammer J (2002) A techno-economic comparison of power production by biomass fast pyrolysis with gasification and combustion. *Renew Sust Energ Rev* 6(3):181–246
- Brown TR (2015) A techno-economic review of thermochemical cellulosic biofuel pathways. *Bioresour Technol* 178:166–176
- Brown RC, Brown TR (2013) *Biorenewable resources: engineering new products from agriculture*. Wiley, Hoboken
- Brown TR, Thilakarathne R, Brown RC, Hu G (2013) Techno-economic analysis of biomass to transportation fuels and electricity via fast pyrolysis and hydroprocessing. *Fuel* 106:463–469
- Carlson TR, Tompsett GA, Conner WC, Huber GW (2009) Aromatic production from catalytic fast pyrolysis of biomass-derived feedstocks. *Top Catal* 52:241–252

- Cormos C-C (2013) Assessment of flexible energy vectors poly-generation based on coal and biomass/solid wastes co-gasification with carbon capture. *Int J Hydrog Energy* 38:7855–7866
- Damartzis T, Zabaniotou A (2011) Thermochemical conversion of biomass to second generation biofuels through integrated process design—a review. *Renew Sust Energ Rev* 15(1):366–378
- De S, Assadi M (2009) Impact of cofiring biomass with coal in power plants—a techno-economic assessment. *Biomass Bioenergy* 33:283–293
- Demirbas A (2001) Biomass resource facilities and biomass conversion. Elsevier, Amsterdam
- Demirbas A (2007) Producing bio-oil from olive cake by fast pyrolysis. *Energy Sources A* 30:38–44
- Domenichini R, Gasparini F, Cotone P, Santos S (2011) Techno-economic evaluation of biomass fired or co-fired power plants with post combustion CO₂ capture. *Energy Proc* 4:1851–1860
- Faix A, Schweinle J, Schöll S, Becker G, Meier D (2010) (GTI-tcbiomass) life-cycle assessment of the BTO®-process (biomass-to-oil) with combined heat and power generation. *Environ Prog Sustain Energy* 29:193–202
- Fan J, Kalnes TN, Alward M, Klinger J, Sadehvandi A, Shonnard DR (2011) Life cycle assessment of electricity generation using fast pyrolysis bio-oil. *Renew Energy* 36:632–641
- Fischer B, Pigneri A (2011) Potential for electrification from biomass gasification in Vanuatu. *Energy* 36(3):1640–1651
- Gabrielle B, Gagnaire N (2008) Life-cycle assessment of straw use in bio-ethanol production: a case study based on biophysical modelling. *Biomass Bioenergy* 32:431–441
- Ganesh A, Banerjee R (2001) Biomass pyrolysis for power generation—a potential technology. *Renew Energy* 22:9–14
- Gnansounou E, Dauriat A (2010) Techno-economic analysis of lignocellulosic ethanol: a review. *Bioresour Technol* 101:4980–4991
- Graham R, Bergougnou M, Overend R (1984) Fast pyrolysis of biomass. *J Anal Appl Pyrolysis* 6:95–135
- Guest G, Bright RM, Cherubini F, Michelsen O, Strømman AH (2011) Life cycle assessment of biomass-based combined heat and power plants. *J Ind Ecol* 15:908–921
- Han J, Elgowainy A, Dunn JB, Wang MQ (2013) Life cycle analysis of fuel production from fast pyrolysis of biomass. *Bioresour Technol* 133:421–428
- Haro P, Trippe F, Stahl R, Henrich E (2013) Bio-syngas to gasoline and olefins via DME—a comprehensive techno-economic assessment. *Appl Energy* 108:54–65
- Hein K, Bemtgen J (1998) EU clean coal technology—co-combustion of coal and biomass. *Fuel Process Technol* 54:159–169
- Heller MC, Keoleian GA, Mann MK, Volk TA (2004) Life cycle energy and environmental benefits of generating electricity from willow biomass. *Renew Energy* 29:1023–1042
- Hsu DD (2012) Life cycle assessment of gasoline and diesel produced via fast pyrolysis and hydroprocessing. *Biomass Bioenergy* 45:41–47
- Huang Y, McIlveen-Wright D (2006) Biomass co-firing in a PFBC combined cycle power plant: a techno-environmental assessment based on computational simulations. *Fuel Process Technol* 87:927–934
- Huang Y, McIlveen-Wright D, Rezvani S, Huang M, Wang Y, Roskilly A, Hewitt N (2013) Comparative techno-economic analysis of biomass fuelled combined heat and power for commercial buildings. *Appl Energy* 112:518–525
- Iribarren D, Peters JF, Dufour J (2012) Life cycle assessment of transportation fuels from biomass pyrolysis. *Fuel* 97:812–821
- Isahak WNRW, Hisham MW, Yarmo MA, Hin T-YY (2012) A review on bio-oil production from biomass by using pyrolysis method. *Renew Sust Energ Rev* 16:5910–5923
- Jones SB, Valkenburt C, Walton CW, Elliott DC, Holladay JE, Stevens DJ, Kinchin C, Czernik S (2009) Production of gasoline and diesel from biomass via fast pyrolysis, hydrotreating and hydrocracking: a design case. Pacific Northwest National Laboratory (PNNL), Richland
- Kauffman N, Hayes D, Brown R (2011) A life cycle assessment of advanced biofuel production from a hectare of corn. *Fuel* 90:3306–3314

- Kebelmann K, Hornung A, Karsten U, Griffiths G (2013) Intermediate pyrolysis and product identification by TGA and Py-GC/MS of green microalgae and their extracted protein and lipid components. *Biomass Bioenergy* 49:38–48
- Kimming M, Sundberg C, Nordberg Å, Baky A, Bernesson S, Norén O, Hansson P-A (2011) Biomass from agriculture in small-scale combined heat and power plants—a comparative life cycle assessment. *Biomass Bioenergy* 35:1572–1581
- Koroneos C, Dompros A, Roumbas G (2008) Hydrogen production via biomass gasification—a life cycle assessment approach. *Chem Eng Process:Process Intens* 47:1261–1268
- Kumar M, Gupta R, Sharma T (1992) Effects of carbonisation conditions on the yield and chemical composition of Acacia and Eucalyptus wood chars. *Biomass Bioenergy* 3:411–417
- Kumar A, Bhattacharya SC, Pham H-L (2003a) Greenhouse gas mitigation potential of biomass energy technologies in Vietnam using the long range energy alternative planning system model. *Energy* 28:627–654
- Kumar A, Cameron JB, Flynn PC (2003b) Biomass power cost and optimum plant size in western Canada. *Biomass Bioenergy* 24:445–464
- Kumar A, Kumar N, Baredar P, Shukla A (2015) A review on biomass energy resources, potential, conversion and policy in India. *Renew Sust Energ Rev* 45:530–539
- Lane J (2013) Gusher! KiOR starts production of US cellulosic biofuels at scale. *Biofuel Digest*. <http://www.biofuelsdigest.com/bdigest/2012/11/09/gusher-kior-starts-production-of-us-cellulosic-biofuels-at-scale/>
- Lange M (2011) The GHG balance of biofuels taking into account land use change. *Energy Policy* 39(5):2373–2385
- Lédé J (2003) Comparison of contact and radiant ablative pyrolysis of biomass. *J Anal Appl Pyrolysis* 70:601–618
- Liden A, Berruti F, Scott D (1988) A kinetic model for the production of liquids from the flash pyrolysis of biomass. *Chem Eng Commun* 65:207–221
- Liu T, McConkey B, Ma Z, Liu Z, Li X, Cheng L (2011) Strengths, weakness, opportunities and threats analysis of bioenergy production on marginal land. *Energy Proc* 5:2378–2386
- López-Bellido L, Wery J, López-Bellido RJ (2014) Energy crops: prospects in the context of sustainable agriculture. *Eur J Agron* 60:1–12
- Lu Q, Dong C-Q, Zhang X-M, Tian H-Y, Yang Y-P, Zhu X-F (2011) Selective fast pyrolysis of biomass impregnated with ZnCl₂ to produce furfural: analytical Py-GC/MS study. *J Anal Appl Pyrolysis* 90:204–212
- Maggi R, Delmon B (1994) Comparison between ‘slow’ and ‘flash’ pyrolysis oils from biomass. *Fuel* 73:671–677
- Mann M, Spath P (2001) A life cycle assessment of biomass cofiring in a coal-fired power plant. *Clean Technol Environ Pol* 3:81–91
- Martínez E, Sanz F, Pellegrini S, Jiménez E, Blanco J (2009) Life cycle assessment of a multi-megawatt wind turbine. *Renew Energy* 34:667–673
- McIlveen-Wright D, Pinto F, Armesto L, Caballero M, Aznar M, Cabanillas A, Huang Y, Franco C, Gulyurtlu I, McMullan J (2006) A comparison of circulating fluidised bed combustion and gasification power plant technologies for processing mixtures of coal, biomass and plastic waste. *Fuel Process Technol* 87:793–801
- Meerman J, Knoope M, Ramírez A, Turkenburg W, Faaij A (2013) Technical and economic prospects of coal-and biomass-fired integrated gasification facilities equipped with CCS over time. *Int J Greenh Gas Cont* 16:311–323
- Menten F, Chèze B, Patouillard L, Bouvart F (2013) A review of LCA greenhouse gas emissions results for advanced biofuels: the use of meta-regression analysis. *Renew Sust Energ Rev* 26:108–134
- Mohan D et al (2014) Organic and inorganic contaminants removal from water with biochar, a renewable, low cost and sustainable adsorbent—a critical review. *Bioresour Technol* 160:191–202
- Muench S, Guenther E (2013) A systematic review of bioenergy life cycle assessments. *Appl Energy* 112:257–273

- Nguyen TLT, Hermansen JE, Mogensen L (2013) Environmental performance of crop residues as an energy source for electricity production: the case of wheat straw in Denmark. *Appl Energy* 104:633–641
- Nussbaumer T (2003) Combustion and co-combustion of biomass: fundamentals, technologies, and primary measures for emission reduction. *Energy Fuel* 17:1510–1521
- Parthasarathy P, Narayanan KS (2014) Hydrogen production from steam gasification of biomass: influence of process parameters on hydrogen yield—a review. *Renew Energy* 66:570–579
- Patel RN, Bandyopadhyay S, Ganesh A (2011) Extraction of cardanol and phenol from bio-oils obtained through vacuum pyrolysis of biomass using supercritical fluid extraction. *Energy* 36:1535–1542
- Patel M, Zhang X, Kumar A (2016) Techno-economic and life cycle assessment on lignocellulosic biomass thermochemical conversion technologies: a review. *Renew Sust Energy Rev* 53:1486–1499
- Peacocke GV (1994) Ablative pyrolysis of biomass. PhD thesis, Aston University, UK
- Pérlhion C, Alkadee D, Descombes G, Lacour S (2012) Life cycle assessment applied to electricity generation from renewable biomass. *Energy Proc* 18:165–176
- Phillips SD, Tarud JK, Bidy MJ, Dutta A (2011) Gasoline from woody biomass via thermochemical gasification, methanol synthesis, and methanol-to-gasoline technologies: a technoeconomic analysis. *Ind Eng Chem Res* 50:11734–11745
- Piccolo C, Bezzo F (2009) A techno-economic comparison between two technologies for bioethanol production from lignocellulose. *Biomass Bioenergy* 33:478–491
- Rafaschieri A, Rapaccini M, Manfrida G (1999) Life cycle assessment of electricity production from poplar energy crops compared with conventional fossil fuels. *Energy Convers Manag* 40:1477–1493
- Rathmann R, Szklo A, Schaeffer R (2010) Land use competition for production of food and liquid biofuels: an analysis of the arguments in the current debate. *Renew Energy* 35:14–22
- Reza MT, Andert J, Wirth B, Busch D, Pielert J, Lynam JG, Mumme J (2014) Hydrothermal carbonization of biomass for energy and crop production. *Appl Bioenerg* 1:11–29
- Roberts KG, Gloy BA, Joseph S, Scott NR, Lehmann J (2009) Life cycle assessment of biochar systems: estimating the energetic, economic, and climate change potential. *Environ Sci Technol* 44:827–833
- Rodrigues M, Faaij AP, Walter A (2003) Techno-economic analysis of co-fired biomass integrated gasification/combined cycle systems with inclusion of economies of scale. *Energy* 28:1229–1258
- Rogers J, Brammer JG (2012) Estimation of the production cost of fast pyrolysis bio-oil. *Biomass Bioenergy* 36:208–217
- Royo J, Sebastián F, Canalís P, Rodríguez N (2004) The torsional chamber as an alternative to the technologies usually employed in biomass co-firing. In: *Proceedings of power gen Europe*
- Samolada M, Vasalos I (1991) A kinetic approach to the flash pyrolysis of biomass in a fluidized bed reactor. *Fuel* 70:883–889
- Sarkar S, Kumar A (2010a) Biohydrogen production from forest and agricultural residues for upgrading of bitumen from oil sands. *Energy* 35:582–591
- Sarkar S, Kumar A (2010b) Large-scale biohydrogen production from bio-oil. *Bioresour Technol* 101:7350–7361
- Sarkar S, Kumar A, Sultana A (2011) Biofuels and biochemicals production from forest biomass in Western Canada. *Energy* 36:6251–6262
- Savolainen K (2003) Co-firing of biomass in coal-fired utility boilers. *Appl Energy* 74:369–381
- Schenk R (2009) Introduction to lifecycle assessment scoping & inventory. US EPA Region X, American Center for Lifecycle Assessment, Washington, DC
- Scott DS, Piskorz J (1984) The continuous flash pyrolysis of biomass. *Can J Chem Eng* 62:404–412
- Scott DS, Piskorz J, Radlein D (1985) Liquid products from the continuous flash pyrolysis of biomass. *Ind Eng Chem Process Des Dev* 24:581–588

- Sebastián F, Royo J, Gómez M (2011) Cofiring versus biomass-fired power plants: GHG (Greenhouse Gases) emissions savings comparison by means of LCA (Life Cycle Assessment) methodology. *Energy* 36:2029–2037
- Sevilla M, Macia-Agullo JA, Fuertes AB (2011) Hydrothermal carbonization of biomass as a route for the sequestration of CO₂: chemical and structural properties of the carbonized products. *Biomass Bioenergy* 35:3152–3159
- Shabangu S, Woolf D, Fisher EM, Angenent LT, Lehmann J (2014) Techno-economic assessment of biomass slow pyrolysis into different biochar and methanol concepts. *Fuel* 117:742–748
- Shadangi KP, Mohanty K (2014a) Comparison of yield and fuel properties of thermal and catalytic Mahua seed pyrolytic oil. *Fuel* 117:372–380
- Shadangi KP, Mohanty K (2014b) Thermal and catalytic pyrolysis of Karanja seed to produce liquid fuel. *Fuel* 115:434–442
- Shadangi KP, Singh RK (2012) Thermolysis of polanga seed cake to bio-oil using semi batch reactor. *Fuel* 97:450–456
- Shafie S, Mahlia T, Masjuki H, Rismanchi B (2012) Life cycle assessment (LCA) of electricity generation from rice husk in Malaysia. *Energy Proc* 14:499–504
- Shafie S, Mahlia T, Masjuki H (2013) Life cycle assessment of rice straw co-firing with coal power generation in Malaysia. *Energy* 57:284–294
- Sharma A, Unni BG, Singh HD (1999) A novel fed-batch digestion system for biomethanation of plant biomasses. *J Biosci Bioeng* 87:678–682
- Sinağ A, Kruse A, Rathert J (2004) Influence of the heating rate and the type of catalyst on the formation of key intermediates and on the generation of gases during hydrolysis of glucose in supercritical water in a batch reactor. *Ind Eng Chem Res* 43:502–508
- Singh A, Pant D, Korres NE, Nizami A-S, Prasad S, Murphy JD (2010) Key issues in life cycle assessment of ethanol production from lignocellulosic biomass: challenges and perspectives. *Bioresour Technol* 101:5003–5012
- Skowrońska M, Filipek T (2014) Life cycle assessment of fertilizers: a review. *Int Agrophysics* 28:101–110
- Solli C, Reenaas M, Strømman AH, Hertwich EG (2009) Life cycle assessment of wood-based heating in Norway. *Int J Life Cycle Assess* 14:517–528
- Splithoff H, Hein K (1998) Effect of co-combustion of biomass on emissions in pulverized fuel furnaces. *Fuel Process Technol* 54:189–205
- Strezov V, Patterson M, Zymła V, Fisher K, Evans TJ, Nelson PF (2007) Fundamental aspects of biomass carbonisation. *J Anal Appl Pyrolysis* 79:91–100
- Swanson RM, Platon A, Satrio JA, Brown RC (2010) Techno-economic analysis of biomass-to-liquids production based on gasification. *Fuel* 89:S11–S19
- Thakur A, Canter CE, Kumar A (2014) Life-cycle energy and emission analysis of power generation from forest biomass. *Appl Energy* 128:246–253
- Thangalazhy-Gopakumar S, Adhikari S, Ravindran H, Gupta RB, Fasina O, Tu M, Fernando SD (2010) Physicochemical properties of bio-oil produced at various temperatures from pine wood using an auger reactor. *Bioresour Technol* 101:8389–8395
- Thilakarathne R, Brown T, Li Y, Hu G, Brown R (2014) Mild catalytic pyrolysis of biomass for production of transportation fuels: a techno-economic analysis. *Green Chem* 16:627–636
- Trippe F, Fröhling M, Schultmann F, Stahl R, Henrich E (2010) Techno-economic analysis of fast pyrolysis as a process step within biomass-to-liquid fuel production. *Waste Biomass Valor* 1:415–430
- Trippe F, Fröhling M, Schultmann F, Stahl R, Henrich E, Dalai A (2013) Comprehensive techno-economic assessment of dimethyl ether (DME) synthesis and Fischer–Tropsch synthesis as alternative process steps within biomass-to-liquid production. *Fuel Process Technol* 106:577–586
- Valle CR, Perales AV, Vidal-Barrero F, Gómez-Barea A (2013) Techno-economic assessment of biomass-to-ethanol by indirect fluidized bed gasification: impact of reforming technologies and comparison with entrained flow gasification. *Appl Energy* 109:254–266

- Wang G, Silva R, Azevedo J, Martins-Dias S, Costa M (2014) Evaluation of the combustion behaviour and ash characteristics of biomass waste derived fuels, pine and coal in a drop tube furnace. *Fuel* 117:809–824
- Williams PT, Besler S (1993) The pyrolysis of rice husks in a thermogravimetric analyser and static batch reactor. *Fuel* 72:151–159
- Williams PT, Besler S (1996) The influence of temperature and heating rate on the slow pyrolysis of biomass. *Renew Energ* 7:233–250
- Woolcock PJ, Brown RC (2013) A review of cleaning technologies for biomass-derived syngas. *Biomass Bioenergy* 52:54–84
- Wright MM, Daugaard DE, Satrio JA, Brown RC (2010) Techno-economic analysis of biomass fast pyrolysis to transportation fuels. *Fuel* 89:S2–S10
- Xianwen D, Chuangzhi W, Haibin L, Yong C (2000) The fast pyrolysis of biomass in CFB reactor. *Energy Fuel* 14:552–557
- Xu Y, Wang T, Ma L, Zhang Q, Wang L (2009) Upgrading of liquid fuel from the vacuum pyrolysis of biomass over the Mo–Ni/ γ -Al₂O₃ catalysts. *Biomass Bioenergy* 33:1030–1036
- Zhang B, von Keitz M, Valentas K (2009) Thermochemical liquefaction of high-diversity grassland perennials. *J Anal Appl Pyrolysis* 84:18–24
- Zhang Y, Brown TR, Hu G, Brown RC (2013) Comparative techno-economic analysis of biohydrogen production via bio-oil gasification and bio-oil reforming. *Biomass Bioenergy* 51:99–108
- Zhong Z, Song B, Zaki M (2010) Life-cycle assessment of flash pyrolysis of wood waste. *J Clean Prod* 18:1177–1183
- Zhou J, Chen Q, Zhao H, Cao X, Mei Q, Luo Z, Cen K (2009) Biomass–oxygen gasification in a high-temperature entrained-flow gasifier. *Biotechnol Adv* 27:606–611
- Zhu Y, Jones SB (2009) Techno-economic analysis for the thermochemical conversion of lignocellulosic biomass to ethanol via acetic acid synthesis. Pacific Northwest National Laboratory (PNNL), Richland
- Zhu Y, Jones SB, Biddy MJ, Dagle RA, Palo DR (2012) Single-step syngas-to-distillates (S2D) process based on biomass-derived syngas—a techno-economic analysis. *Bioresour Technol* 117:341–351
- Zuwala J, Sciazko M (2010) Full-scale co-firing trial tests of sawdust and bio-waste in pulverized coal-fired 230t/h steam boiler. *Biomass Bioenergy* 34:1165–1174